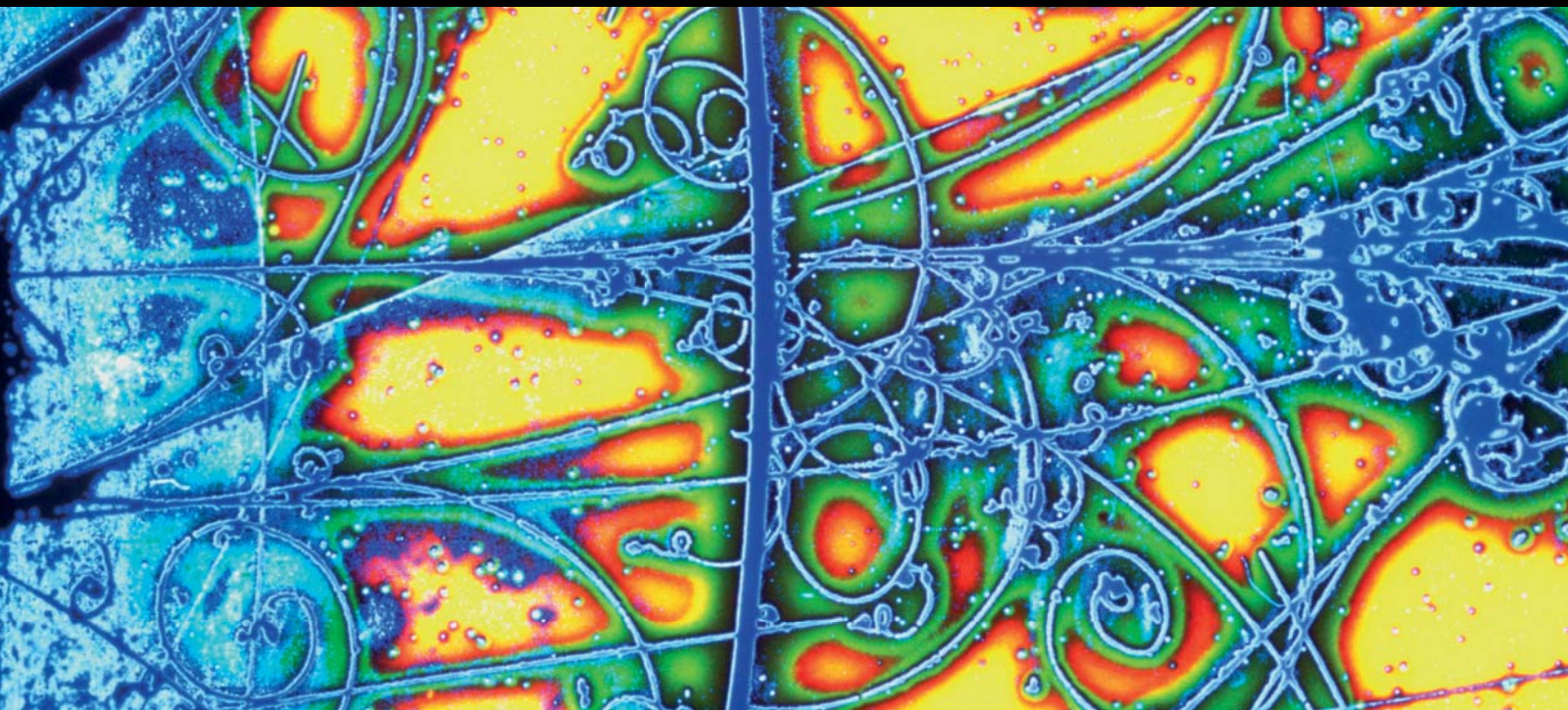


ADVANCES IN HIGH ENERGY PHYSICS

COMPUTATIONAL ALGEBRAIC GEOMETRY IN STRING AND GAUGE THEORY

GUEST EDITORS: YANG-HUI HE, PHILIP CANDELAS, AMIHAY HANANY,
ANDRE LUKAS, AND BURT OVRUT





Computational Algebraic Geometry in String and Gauge Theory

Advances in High Energy Physics

**Computational Algebraic Geometry in
String and Gauge Theory**

**Guest Editors: Yang-Hui He, Philip Candelas, Amihay Hanany, Andre Lukas,
and Burt Ovrut**



Copyright © 2012 Hindawi Publishing Corporation. All rights reserved.

This is a special issue published in "Advances in High Energy Physics." All articles are open access articles distributed under the Creative Commons Attribution License, which permits unrestricted use, distribution, and reproduction in any medium, provided the original work is properly cited.

Editorial Board

Botio Betev, Switzerland
P. J. Bussey, UK
Duncan L. Carlsmith, USA
Kingman Cheung, Taiwan
S. H. Dong, Mexico
Edmond Craig Dukes, USA
Paula Eerola, Sweden
Amir H. Fatollahi, Iran
Thomas Ferbel, USA
F. Filthaut, The Netherlands
Joseph Formaggio, USA
C. Q. Geng, Taiwan
Cecilia Gerber, USA

J. Gracey, UK
Hong-Jian He, China
Ian Jack, UK
Ashutosh V. Kotwal, USA
Pietro Musumeci, USA
John W. Norbury, USA
Dugan O'Neil, Canada
Seog H. Oh, USA
Sandip Pakvasa, USA
Manfred Paulini, USA
Anastasios Petkou, Greece
A. Petrov, USA
Ira Rothstein, USA

Kate Scholberg, USA
Frederik G. Scholtz, South Africa
George Siopsis, USA
Terry Sloan, UK
Neil Spooner, UK
Luca Stanco, Italy
Richard J. Szabo, UK
Elias C. Vagenas, Greece
Nikos Varelas, USA
Kadayam S. Viswanathan, Canada
Yau W. Wah, USA

Contents

Computational Algebraic Geometry in String and Gauge Theory, Yang-Hui He, Philip Candelas, Amihay Hanany, Andre Lukas, and Burt Ovrut
Volume 2012, Article ID 431898, 4 pages

Calabi-Yau Threefolds in Weighted Flag Varieties, Muhammad Imran Qureshi and Balázs Szendrői
Volume 2012, Article ID 547317, 14 pages

Bell's Inequalities, Superquantum Correlations, and String Theory, Lay Nam Chang, Zachary Lewis, Djordje Minic, Tatsu Takeuchi, and Chia-Hsiung Tze
Volume 2011, Article ID 593423, 11 pages

On the Minimal Length Uncertainty Relation and the Foundations of String Theory, Lay Nam Chang, Zachary Lewis, Djordje Minic, and Tatsu Takeuchi
Volume 2011, Article ID 493514, 30 pages

Numerical Polynomial Homotopy Continuation Method and String Vacua, Dhagash Mehta
Volume 2011, Article ID 263937, 15 pages

Non-Supersymmetric CS-Matter Theories with Known AdS Duals, Davide Forcella and Alberto Zaffaroni
Volume 2011, Article ID 393645, 15 pages

On \mathcal{R}^4 Terms and MHV Amplitudes in $\mathcal{N} = 5, 6$ Supergravity Vacua of Type II Superstrings, Massimo Bianchi
Volume 2011, Article ID 479038, 18 pages

Discrete Wilson Lines in F-Theory, Volker Braun
Volume 2011, Article ID 404691, 18 pages

BPS States, Crystals, and Matrices, Piotr Suikowski
Volume 2011, Article ID 357016, 52 pages

Combinatorics in $\mathcal{N} = 1$ Heterotic Vacua, Seung-Joo Lee
Volume 2011, Article ID 397895, 11 pages


Computational Tools for Cohomology of Toric Varieties, Ralph Blumenhagen, Benjamin Jurke, and Thorsten Rahn
Volume 2011, Article ID 152749, 15 pages

The Expanding Zoo of Calabi-Yau Threefolds, Rhys Davies
Volume 2011, Article ID 901898, 18 pages

Chern-Simons: Fano and Calabi-Yau, Amihay Hanany and Yang-Hui He
Volume 2011, Article ID 204576, 14 pages

Polynomial Roots and Calabi-Yau Geometries, Yang-Hui He
Volume 2011, Article ID 719672, 15 pages

Toric Methods in F-Theory Model Building, Johanna Knapp and Maximilian Kreuzer
Volume 2011, Article ID 513436, 18 pages



Baryonic Symmetries in AdS_4/CFT_3 : An Overview, Diego Rodriguez-Gomez
Volume 2011, Article ID 235710, 21 pages

A Simple Introduction to Gröbner Basis Methods in String Phenomenology, James Gray
Volume 2011, Article ID 217035, 12 pages

Del Pezzo Singularities and SUSY Breaking, Dmitry Malyshev
Volume 2011, Article ID 630892, 30 pages

Editorial

Computational Algebraic Geometry in String and Gauge Theory

**Yang-Hui He,^{1,2,3} Philip Candelas,⁴ Amihay Hanany,⁵
Andre Lukas,⁶ and Burt Ovrut⁷**

¹ Department of Mathematics, City University London, London EC1V 0HB, UK

² School of Physics, Nan Kai University, Tianjin 300071, China

³ Merton College, University of Oxford, Oxford OX1 4JD, UK

⁴ Mathematical Institute, University of Oxford, 24-29 St Giles', Oxford OX1 3LB, UK

⁵ Department of Physics, Imperial College, London SW7 2AZ, UK

⁶ Rudolf Peierls Centre for Theoretical Physics, University of Oxford, 1 Keble Road,
Oxford OX1 3NP, UK

⁷ Department of Physics and Astronomy, University of Pennsylvania, Philadelphia, PA 191046395, USA

Correspondence should be addressed to Yang-Hui He, hey@maths.ox.ac.uk

Received 23 November 2011; Accepted 23 November 2011

Copyright © 2012 Yang-Hui He et al. This is an open access article distributed under the Creative Commons Attribution License, which permits unrestricted use, distribution, and reproduction in any medium, provided the original work is properly cited.

The last few years have witnessed a rapid development in algebraic geometry, computer algebra, and string and field theory, as well as fruitful cross-fertilization amongst them. The dialogue between geometry and gauge theory is, of course, an old and rich one, leading to tools crucial to both. The introduction of algorithmic and computational algebraic geometry, however, is relatively new and is tremendously facilitated by the rapid progress in hardware, software as well as theory. Applications of once specialized mathematical topics such as Gröbner bases, sheaf cohomology, scheme theory, and Hilbert series are quickly becoming indispensable tools in theoretical physics, from topics ranging from AdS/CFT to string phenomenology, from supersymmetric gauge theory to Calabi-Yau compactifications, and so forth. In this special issue, we have invited many international experts, culminating in 17 papers on related subjects, which we order below alphabetically according to title.

The paper “A simple Introduction to Gröbner basis methods in string phenomenology” by J. Gray is a review on the most important subject in computational and algorithmic algebraic geometry: the Gröbner basis. It illustrates how this can be used in string phenomenology and gives some concrete examples ranging from flux parameter to vacuum spaces.

The paper “*Baryonic symmetries in AdS4/CFT3: an overview*” by D. Rodriguez-Gomez is an overview of global baryon-like symmetries in the AdS/CFT context. On the gravity side, these are vector fields in AdS arising from Kaluza-Klein reductions of supergravity p -form potentials. The paper focuses on the AdS4/CFT3 case and uses the computation of a noncompact Calabi-Yau fourfold, namely, the cone over the Q^{111} , as an explicit example.

The paper “*Bell’s inequalities, superquantum correlations and string theory*” by L. N. Chang et al. is on a more fundamental and philosophical issue in quantum mechanics. It argues that string theory, viewed as a quantum theory with two deformation parameters, the string tension and the string coupling constant, is a superquantum theory which transgresses the usual quantum violations of Bell’s inequalities. The norms in the theory generalize from the ℓ^2 norm in functional analysis to an ℓ^p norm, in application to quantum correlators.

The paper “*BPS states, crystals, and matrices*” by P. Sułkowski is a review on certain representations of wall-crossing phenomena for toric Calabi-Yau spaces, in relation to free fermions, melting crystal, and matrix models. These have been crucial to the understanding of the BPS spectrum of D-brane theories, in particular D2- and D0-branes bound to a D6-brane. The partition functions which do the counting are intimately related to Donaldson-Thomas invariants and to topological string amplitudes.

The paper “*Calabi-Yau threefolds in weighted flag varieties*” by M. I. Qureshi and B. Szendrői is on the pure mathematical problem of constructing a large class of Calabi-Yau threefolds as projective varieties. In particular, it considers them as quasilinear sections in weighted flag varieties, generalizing the more familiar cases of the ambient spaces being weighted \mathbb{P}^4 . Certain vector bundles, called tautological orbibundles, on these manifolds are also constructed; these may be of interest to model building in heterotic string theory, when using “general embedding” with such stable bundles.

The paper “*Chern-Simons: Fano and Calabi-Yau*” by A. Hanany and Y.-H. He returns to the subject of noncompact, toric, Calabi-Yau fourfolds in the context of AdS4/CFT3. It presents the complete classification of smooth toric Fano threefolds, known to the algebraic geometry literature, and performs some preliminary analyses in the context of brane tilings and Chern-Simons theory on M2-branes probing Calabi-Yau fourfold singularities as cones over these Fano threefolds. Emphasis is placed on the fact that these 18 spaces should be as intensely studied as their well-known two complex dimensional counterparts: the del Pezzo surfaces.

The paper “*Combinatorics in $N = 1$ heterotic vacua*” by S.-J. Lee is on constructing bundles over large sets of Calabi-Yau threefolds. It briefly reviews an algorithmic and systematic strategy to explore the landscape of heterotic $E_8 \times E_8$ vacua, in the context of compactifying smooth Calabi-Yau threefolds with vector bundles. The Calabi-Yau threefolds are algebraically realized as hypersurfaces in toric varieties, and a large class of vector bundles is constructed thereon as so-called monad bundles. In the spirit of searching for standard-like heterotic vacua, the focus is on the integer combinatorics of the model-building programme.

The paper “*Computational tools for cohomology of toric varieties*” by R. Blumenhagen et al. is closely related to the seventh. It addresses a novel computational algorithm for the determination of the dimension of line-bundle-valued cohomology groups on toric varieties. This is clearly useful and can also serve as a first step toward the enormous database of vector bundles on Calabi-Yau hypersurfaces in toric fourfolds. Applications to the computation of chiral massless matter spectra in string compactifications are discussed and the software package “*cohomCalg*” is advertized.

The paper *“Del Pezzo singularities and SUSY breaking”* by D. Malyshev is on del Pezzo singularities in Calabi-Yau threefolds. Singularities of such a type can facilitate dynamical supersymmetry breaking using the Intriligator-Seiberg-Shih technique. An illustrative example is given for the famous quintic manifolds, with its explicit del Pezzo 6 and conifold singularities pointed out. The more general case of complete intersection manifolds is investigated, particularly on the complex deformation of the singularities.

The paper *“Discrete Wilson lines in F-theory”* by V. Braun is on elliptically fibered Calabi-Yau fourfolds to F-theory constructions. Recent works by Heckmann, Vafa et al. have realized the GUT group from sevenbranes wrapping contractible del Pezzo surfaces in the fourfold. However, this makes breaking to the Standard Model group difficult since the del Pezzo surfaces have trivial fundamental group. The paper shows how one may use non-trivial cycles, such as the Enriques surface, and use Wilson lines to break the GUT gauge group.

The paper *“Non-supersymmetric CS-matter theories with known AdS duals”* by D. Forcella and A. Zaffaroni is related to the second and sixth and studies M2-branes probing Calabi-Yau fourfold cones. The dual supergravity solutions of Freund-Rubin type are found while the world-volume field theories are stable and non-supersymmetric. Careful analyses for the theory associated to the cone over the quotient S^7/\mathbb{Z}_k are carried out, giving the Kaluza-Klein spectrum and candidate dual gauge theory.

The paper *“Numerical polynomial homotopy continuation method and string vacua”* by D. Mehta forms a nice contrast with the first and focuses on algebraic geometry without using the Gröbner basis which is known to be quite expensive computationally. Instead, it shows how one may sometimes obtain relevant information, exemplified by various models taken from string and M-theory as well as lattice gauge theory, by using numerical algebraic geometry. Emphasis is paid on the so-called homotopy continuation method.

The paper *“On R^4 terms and MHV amplitudes in $N = 5, 6$ supergravity vacua of type II superstrings”* by M. Bianchi is on $\mathcal{N} = 5$ and 6 supergravity vacua of type II superstring theory. It computes the one-loop threshold corrections to the 4th power of curvature terms as well as nonperturbative corrections of D-brane instantons. The generating functions for maximally helicity violating amplitudes at tree level are also derived.

The paper *“On the minimal length uncertainty relation and the foundations of string theory”* by L. N. Chang et al. echoes the third and reviews the work on minimal length uncertainty as suggested by string theory, in particular what happens to quantum mechanics when a fundamental length scale such as the string length is introduced. The implications of this to the vacuum energy and to a dynamical energy-momentum space are discussed.

The paper *“Polynomial roots and Calabi-Yau geometries”* by Y.-H. He is a numerical and algorithmic experiment, inspired by the fractal nature of the roots of large sets of polynomials with certain constrained coefficients. It looks at the space of Poincaré polynomials (a generalization of Euler number) of all known compact Calabi-Yau threefolds and fourfolds and studies the structure exhibited by their conglomerate roots.

The paper *“The expanding zoo of Calabi-Yau threefolds”* by R. Davies is on the algorithmic search for new Calabi-Yau threefolds with special properties. It reviews the recent constructions of the manifolds of small Hodge number and/or nontrivial fundamental group, which are useful to heterotic model building. The techniques used are topological transitions and quotienting from known manifold by discrete group actions. A first example of a Calabi-Yau threefold with the fundamental group S_3 is given.

The paper "*Toric methods in F-theory model building*" by J. Knapp and M. Kreuzer is related to the seventh, eighth, and the tenth. It reviews how the construction of F-theory models calls for large databases of Calabi-Yau fourfolds which are elliptically fibered. Furthermore, one needs to look for a divisor which is a nonnegatively curved threefold serving as the base and, further still, a divisor inside the base which is a del Pezzo surface. The paper shows how one may do this search algorithmically and explicitly demonstrates this with the powerful computer package "PALP."

Yang-Hui He
Philip Candelas
Amihay Hanany
Andre Lukas
Burt Ovrut

Review Article

Calabi-Yau Threefolds in Weighted Flag Varieties

Muhammad Imran Qureshi and Balázs Szendrői

Mathematical Institute, University of Oxford, 24-29 St Giles', Oxford OX1 3LB, UK

Correspondence should be addressed to Muhammad Imran Qureshi, qureshi@maths.ox.ac.uk

Received 22 May 2011; Accepted 12 October 2011

Academic Editor: Yang-Hui He

Copyright © 2012 M. I. Qureshi and B. Szendrői. This is an open access article distributed under the Creative Commons Attribution License, which permits unrestricted use, distribution, and reproduction in any medium, provided the original work is properly cited.

We review the construction of families of projective varieties, in particular Calabi-Yau threefolds, as quasilinear sections in weighted flag varieties. We also describe a construction of tautological orbibundles on these varieties, which may be of interest in heterotic model building.

1. Introduction

The classical flag varieties $\Sigma = G/P$ are projective varieties which are homogeneous spaces under complex reductive Lie groups G ; the stabilizer P of a point in Σ is a parabolic subgroup P of G . The simplest example is projective space \mathbb{P}^n itself, which is a homogeneous space under the complex Lie group $GL(n+1)$. Weighted flag varieties $w\Sigma$, which are the analogues of weighted projective space in this more general context, were defined by Corti and Reid [1] following unpublished work of Grojnowski. They admit a Plücker-style embedding

$$w\Sigma \subset \mathbb{P}[w_0, \dots, w_n] \quad (1.1)$$

into a weighted projective space. In this paper, we review the construction of Calabi-Yau threefolds X that arise as complete intersections within $w\Sigma$ of some hypersurfaces of weighted projective space [1–3]:

$$X \subset w\Sigma \subset \mathbb{P}[w_0, \dots, w_n]. \quad (1.2)$$

To be more precise, our examples are going to be quasilinear sections in $w\Sigma$, where the degree of each equation agrees with one of the w_i . The varieties X will have standard

threefold singularities similar to complete intersections in weighted projective spaces; they have crepant desingularizations $Y \rightarrow X$ by standard theory.

We start by computing the Hilbert series of a weighted flag variety $w\Sigma$ of a given type. By numerical considerations, we get candidate degrees for possible Calabi-Yau complete intersection families. To prove the existence of a particular family, in particular to check that general members of the family only have mild quotient singularities, we need equations for the Plücker style embedding. It turns out that the equations of $w\Sigma$ in the weighted projective space, which are the same as the equations of the straight flag variety Σ in its natural embedding, can be computed relatively easily using computer algebra [2].

The smooth Calabi-Yau models Y that arise from this method may be new, though it is probably difficult to tell. One problem we do not treat in general is the determination of topological invariants such as Betti and Hodge numbers of Y . Some Hodge number calculations for varieties constructed using a related method are performed in [4], via explicit birational maps to complete intersections in weighted projective spaces; the Hodge numbers of such varieties can be computed by standard methods. Such maps are hard to construct in general. A better route would be to first compute the Hodge structure of $w\Sigma$ then deduce the invariants of their quasilinear sections X and finally their resolutions Y . See, for example, [5] for analogous work for hypersurfaces in toric varieties. We leave the development of such an approach for future work.

We conclude our paper with the outline of a possible application of our construction: by its definition, the weighted flag variety $w\Sigma$ and thus its quasilinear section X carry natural orbibundles; these are the analogues of $\mathcal{O}(1)$ on (weighted) projective space. It is possible that these can be used to construct interesting bundles on the resolution Y which may be relevant in heterotic compactifications. Again, we have no conclusive results.

2. Weighted Flag Varieties

2.1. The Main Definition

We start by recalling the notion of weighted flag variety due to Corti and Reid [1]. Fix a reductive Lie group G and a highest weight $\lambda \in \Lambda_W$ in the weight lattice of G , the lattice of characters of the maximal torus T of G . Then we have a corresponding parabolic subgroup P_λ , well defined up to conjugation. The quotient $\Sigma = G/P_\lambda$ is a homogeneous variety called a (*generalized*) *flag variety*, a projective subvariety of $\mathbb{P}V_\lambda$, where V_λ is the irreducible representation of G with highest weight λ .

Let Λ_W^* denote the lattice of one-parameter subgroups of T , dual to the weight lattice Λ_W . Choose $\mu \in \Lambda_W^*$ and an integer $u \in \mathbb{Z}$ such that

$$\langle w\lambda, \mu \rangle + u > 0 \quad (2.1)$$

for all elements w of the Weyl group of the Lie group G , where \langle, \rangle denotes the perfect pairing between Λ_W and Λ_W^* .

Consider the affine cone $\widetilde{\Sigma} \subset V_\lambda$ of the embedding $\Sigma \hookrightarrow \mathbb{P}V_\lambda$. There is a \mathbb{C}^* -action on $V_\lambda \setminus \{0\}$ given by

$$(\varepsilon \in \mathbb{C}^*) \mapsto (v \mapsto \varepsilon^u (\mu(\varepsilon) \circ v)) \quad (2.2)$$

which induces an action on $\tilde{\Sigma}$. Inequality (2.1) ensures that all the \mathbb{C}^* -weights on V_λ are positive, leading to a well-defined quotient

$$w\mathbb{P}V_\lambda = V_\lambda \setminus \{0\} / \mathbb{C}^*. \quad (2.3)$$

This weighted projective space has weights

$$\{\langle \alpha, \mu \rangle + u \mid \alpha \in \nabla(V_\lambda)\}, \quad (2.4)$$

where $\nabla(V_\lambda)$ denotes the set of weights (understood with multiplicities) appearing in the weight space decomposition of the representation V_λ . Inside this weighted projective space, we consider the projective quotient

$$w\Sigma = \tilde{\Sigma} \setminus \{0\} / \mathbb{C}^* \subset w\mathbb{P}V_\lambda. \quad (2.5)$$

We call $w\Sigma$ a *weighted flag variety*. By definition, $w\Sigma$ quasismooth, that is, its affine cone $\tilde{\Sigma}$ is nonsingular outside its vertex $\underline{0}$. Hence it only has finite quotient singularities.

The weighted flag variety $w\Sigma$ is called *well formed* [6], if no $(n-1)$ of weights w_i have a common factor, and moreover $w\Sigma$ does not contain any codimension $c+1$ singular stratum of $w\mathbb{P}V_\lambda$, where c is the codimension of $w\Sigma$.

2.2. The Hilbert Series of a Weighted Flag Variety

Consider the embedding $w\Sigma \subset w\mathbb{P}V_\lambda$. The restriction of the line (orbi)bundle of degree one Weil divisors $\mathcal{O}_{w\mathbb{P}V_\lambda}(1)$ gives a polarization $\mathcal{O}_{w\Sigma}(1)$ on $w\Sigma$, a \mathbb{Q} -ample line orbundle some tensor power of which is a very ample line bundle. Powers of $\mathcal{O}_{w\Sigma}(1)$ have well-defined spaces of sections $H^0(w\Sigma, \mathcal{O}_{w\Sigma}(m))$. The *Hilbert series* of the pair $(w\Sigma, \mathcal{O}_{w\Sigma}(1))$ is the power series given by

$$P_{w\Sigma}(t) = \sum_{m \geq 0} \dim H^0(w\Sigma, \mathcal{O}_{w\Sigma}(m)) t^m. \quad (2.6)$$

Theorem 2.1 (see [2, Theorem 3.1]). *The Hilbert series $P_{w\Sigma}(t)$ has the closed form*

$$P_{w\Sigma}(t) = \frac{\sum_{w \in W} (-1)^w (t^{\langle w\rho, \mu \rangle} / (1 - t^{\langle w\lambda, \mu \rangle + u}))}{\sum_{w \in W} (-1)^w t^{\langle w\rho, \mu \rangle}}. \quad (2.7)$$

Here ρ is the Weyl vector, half the sum of the positive roots of G , and $(-1)^w = 1$ or -1 depending on whether w consists of an even or odd number of simple reflections in the Weyl group W .

The right hand side of (2.7) can be converted into a form

$$P_{w\Sigma}(t) = \frac{N(t)}{\prod_{\alpha \in \nabla(V_\lambda)} (1 - t^{\langle \alpha, \mu \rangle + u})}, \quad (2.8)$$

where, as before, $\nabla(V_\lambda)$ denotes the set of weights of the representation V_λ . The numerator is a polynomial $N(t)$, the *Hilbert numerator*. Since (2.7) involves summing over the Weyl group, it is best to use a computer algebra system for explicit computations.

A well-formed weighted flag variety is *projectively Gorenstein*, which means that

- (i) $H^i(\omega\Sigma, \mathcal{O}_{\omega\Sigma}(m)) = 0$ for all m and $0 < i < \dim(\omega\Sigma)$;
- (ii) the Hilbert numerator $N(t)$ is a palindromic symmetric polynomial of degree q , called the *adjunction number* of $\omega\Sigma$;
- (iii) the canonical divisor of $\omega\Sigma$ is given by

$$K_{\omega\Sigma} \sim \mathcal{O}_{\omega\Sigma}\left(q - \sum w_i\right), \quad (2.9)$$

where, as above, the w_i are the weights of the projective space $w\mathbb{P}V_\lambda$; the integer $k = q - \sum w_i$ is called the *canonical weight*.

2.3. Equations of Flag Varieties

The flag variety $\Sigma = G/P \hookrightarrow \mathbb{P}V_\lambda$ is defined by an ideal $I = \langle Q \rangle$ of quadratic equations generating a linear subspace $Q \subset Z = S^2V_\lambda^*$ of the second symmetric power of the contragredient representation V_λ^* . The G -representation Z has a decomposition

$$Z = V_{2\nu} \oplus V_1 \oplus \cdots \oplus V_n \quad (2.10)$$

into irreducible direct summands, with ν being the highest weight of the representation V_λ^* . As discussed in [7, 2.1], the subspace Q in fact consists of all the summands except $V_{2\nu}$. The equations of $\omega\Sigma$ can be readily computed from this information using computer algebra [2].

2.4. Constructing Calabi-Yau Threefolds

We recall the different steps in the construction of Calabi-Yau threefolds as quasilinear sections of weighted flag varieties.

(1) Choose Embedding

We choose a reductive Lie group G and a G -representation V_λ of dimension n with highest weight λ . We get a straight flag variety $\Sigma = G/P_\lambda \hookrightarrow \mathbb{P}V_\lambda$ of computable dimension d and codimension $c = n - 1 - d$. We choose $\mu \in \Lambda_W^*$ and $u \in \mathbb{Z}$ to get an embedding $\omega\Sigma \hookrightarrow w\mathbb{P}V_\lambda = \mathbb{P}^{n-1}[\langle \alpha_i, \mu \rangle + u]$, with $\alpha_i \in \nabla(V_\lambda)$ being the weights of the representation V_λ . The equations, the Hilbert series, and the canonical class of $\omega\Sigma \subset w\mathbb{P}$ can be found as described above.

(2) Take Threefold Calabi-Yau Section of $\omega\Sigma$

We take a quasilinear complete intersection

$$X = \omega\Sigma \cap (w_{i_1}) \cap \cdots \cap (w_{i_r}) \quad (2.11)$$

of l generic hypersurfaces of degrees equal to some of the weights w_i . We choose values so that $\dim(X) = d - l = 3$ and $k + \sum_{j=1}^l w_{i_j} = 0$, thus $K_X \sim \mathcal{O}_X$. After relabelling the weights, this gives an embedding $X \hookrightarrow \mathbb{P}^s[w_0, \dots, w_s]$, with $s = n - l - 1$, of codimension c , polarized by the ample \mathbb{Q} -Cartier divisor D with $\mathcal{O}_X(D) = \mathcal{O}_{w\Sigma}(1)|_X$. More generally, as in [1], we can take complete intersections inside projective cones over $w\Sigma$, adding weight one variables to the coordinate ring which are not involved in any relation.

(3) Check Singularities

We are interested in quasismooth Calabi-Yau threefolds, subvarieties of $w\Sigma$ all of whose singularities are induced by the weights of $\mathbb{P}^s[w_i]$. Singular strata S of $\mathbb{P}^s[w_i]$ correspond to sets of weights w_{i_0}, \dots, w_{i_p} with

$$\gcd(w_{i_0}, \dots, w_{i_p}) = r \quad (2.12)$$

nontrivial. If the intersection $X \cap S$ is nonempty, it has to be a singular point $P \in X$ or a curve $C \subset X$ of quotient singularities, and we need to find local coordinates in a neighbourhood of the point of P , respectively of points of C , to check the local transversal structure. Since we are interested in Calabi-Yau varieties which admit crepant resolutions, singular points P have to be quotient singularities of the form $(1/r)(a, b, c)$ with $a + b + c$ divisible by r , whereas the transversal singularity along a singular curve C has to be of the form $(1/r)(a, r - a)$ of type A_{r-1} .

(4) Find Projective Invariants and Check Consistency

The orbifold Riemann-Roch formula of [4, Section 3] determines the Hilbert series of a polarized Calabi-Yau threefold (X, D) with quotient singularities in terms of the projective invariants D^3 and $D \cdot c_2(X)$, as well as for each curve, the degree $\deg D|_C$ of the polarization, and an extra invariant γ_C related to the normal bundle of C in X . Using the Riemann-Roch formula, we can determine the invariants of a given family from the first few values of $h^0(nD)$ and verify that the same Hilbert series can be recovered.

2.5. Explicit Examples

In the next two sections, we find families of Calabi-Yau threefolds admitting crepant resolutions using this programme. We illustrate the method using two embeddings, corresponding to the Lie groups of type G_2 and A_5 , leading to Calabi-Yau families of codimension 8, 6, respectively. Further examples for the Lie groups of type C_3 and A_3 , in codimensions 7 and 9, are discussed in [3].

3. The Codimension Eight Weighted Flag Variety

3.1. Generalities

Consider the simple Lie group of type G_2 . Denote by $\alpha_1, \alpha_2 \in \Lambda_W$ a pair of simple roots of the root system ∇ of G_2 , taking α_1 to be the short simple root and α_2 the long one.

The fundamental weights are $\omega_1 = 2\alpha_1 + \alpha_2$ and $\omega_2 = 3\alpha_1 + 2\alpha_2$. The sum of the fundamental weights, which is equal to half the sum of the positive roots, is $\rho = 5\alpha_1 + 3\alpha_2$. We partition the set of roots into long and short roots as $\nabla = \nabla_l \cup \nabla_s \subset \Lambda_W$. Let $\{\beta_1, \beta_2\}$ be the basis of the lattice Λ_W^* dual to $\{\alpha_1, \alpha_2\}$.

We consider the G_2 -representation with highest weight $\lambda = \omega_2 = 3\alpha_1 + 2\alpha_2$. The dimension of V_λ is 14 [8, Chapter 22]. The homogeneous variety $\Sigma \subset \mathbb{P}V_\lambda$ is five-dimensional, so we have an embedding $\Sigma^5 \hookrightarrow \mathbb{P}^{13}$ of codimension 8. To work out the weighted version in this case, take $\mu = a\beta_1 + b\beta_2 \in \Lambda_W^*$ and $u \in \mathbb{Z}$.

Proposition 3.1. *The Hilbert series of the codimension eight weighted G_2 flag variety is given by*

$$P_{w\Sigma}(t) = \frac{1 - (4 + 2\sum_{\alpha \in \nabla_s} t^{(\alpha, \mu)} + \sum_{\alpha \in \nabla_s} t^{2(\alpha, \mu)} + \sum_{\alpha \in \nabla_l} t^{(\alpha, \mu)})t^{2u} + \dots + t^{11u}}{(1 - t^u)^2 \prod_{\alpha \in \nabla} (1 - t^{(\alpha, \mu) + u})}. \quad (3.1)$$

Moreover, if $w\Sigma$ is well-formed, then the canonical bundle is $K_{w\Sigma} \sim \mathcal{O}_{w\Sigma}(-3u)$.

The Hilbert series of the straight flag variety $\Sigma \hookrightarrow \mathbb{P}^{13}$ can be computed to be

$$P_\Sigma(t) = \frac{1 - 28t^2 + 105t^3 - \dots + 105t^8 - 28t^9 - t^{11}}{(1 - t)^{14}}. \quad (3.2)$$

The image is defined by 28 quadratic equations, listed in the appendix of [2].

3.2. Examples

Example 3.2. Consider the following initial data.

- (i) Input: $\mu = (-1, 1), u = 3$.
- (ii) Plücker embedding: $w\Sigma \subset \mathbb{P}^{13}[1, 2^4, 3^4, 4^4, 5]$.
- (iii) Hilbert numerator: $1 - 3t^4 - 6t^5 - 8t^6 + 6t^7 + 21t^8 + \dots + 6t^{26} - 8t^{27} - 6t^{28} - 3t^{29} + t^{33}$.
- (iv) Canonical divisor: $K_{w\Sigma} \sim \mathcal{O}_{w\Sigma}(33 - \sum_i w_i) = \mathcal{O}(-9)$, as $w\Sigma$ is well formed.
- (v) Variables on weighted projective space together with their weights x_i :

$$\begin{array}{cccccccccccccccc} \text{Variables} & x_1 & x_2 & x_3 & x_4 & x_5 & x_6 & x_7 & x_8 & x_9 & x_{10} & x_{11} & x_{12} & x_{13} & x_{14} \\ \text{Weights} & 2 & 4 & 3 & 2 & 1 & 2 & 4 & 2 & 3 & 4 & 5 & 4 & 3 & 3 \end{array} \quad (3.3)$$

The reason for the curious ordering of the variables is that these variables are exactly those appearing in the defining equations of this weighted flag variety given in [2, Appendix].

Consider the threefold quasilinear section

$$X = w\Sigma \cap \{f_4(x_i) = 0\} \cap \{g_5(x_i) = 0\} \subset \mathbb{P}^{11}[1, 2^4, 3^4, 4^3], \quad (3.4)$$

where the intersection is taken with general forms f_4, g_5 of degrees four and five, respectively. The canonical divisor class of X is

$$K_X \sim \mathcal{O}_X(-9 + (5 + 4)) = \mathcal{O}_X. \quad (3.5)$$

To determine the singularities of the general threefold X , we need to consider sets of variables whose weights have a greatest common divisor greater than one.

- (i) $1/4$ singularities: this singular stratum is defined by setting those variables to zero whose degrees are not divisible by 4. We also have the equations of [2, Appendix]; only (A5), (A23), and (A24) from that list survive to give

$$S = \left\{ \begin{array}{l} \frac{1}{9}x_7x_{10} + x_2x_{12} = 0 \\ -\frac{1}{3}x_{10}^2 + x_7x_{12} = 0 \\ \frac{1}{3}x_7^2 + x_2x_{10} = 0 \end{array} \right\} \subset \mathbb{P}_{x_2, x_7, x_{10}, x_{12}}^3. \quad (3.6)$$

In this case, it is easy to see by hand (or certainly using Macaulay) that $S \subset \mathbb{P}^3$ is in fact a twisted cubic curve isomorphic to \mathbb{P}^1 . We then need to intersect this with the general X ; the quintic equation will not give anything new, since x_2, x_7, x_{10}, x_{12} are degree 4 variables, but the quartic equation will give a linear relation between them. Thus $S \cap X$ consists of three points, the three points of $1/4$ singularities. A little further work gives that they are all of type $(1/4)(3, 3, 2)$.

- (ii) $1/3$ singularities: the general X does not intersect this singular stratum; the equations from [2, Appendix] in the degree three variables give the empty locus; this is easiest to check by Macaulay.
- (iii) $1/2$ singularities: the intersection of X with this singular stratum is a rational curve $C \subset X$ containing the $1/4$ singular points; again, Macaulay computes this without difficulty. At each other point of the curve we can check that the transverse singularity is $(1/2)(1, 1)$.

Thus (X, D) is a Calabi-Yau threefold with three singular points of type $(1/4)(3, 3, 2)$ and a rational curve C of singularities of type $(1/2)(1, 1)$ containing them. Comparing with the orbifold Riemann-Roch formula of [4, Section 3], feeding in the first few known values of $h^0(X, nD)$ from the Hilbert series gives that the projective invariants of this family are

$$D^3 = \frac{9}{8}, \quad D \cdot c_2(X) = 21, \quad \deg D|_C = \frac{9}{4}, \quad \gamma_C = 1. \quad (3.7)$$

Example 3.3. In this example, we consider the same initial data as in Example 3.2. To construct a new family of Calabi-Yau threefolds, we take a projective cone over $\omega\Sigma$. Therefore we get the embedding

$$C\omega\Sigma \subset \mathbb{P}^{14} [1^2, 2^4, 3^4, 4^4, 5]. \quad (3.8)$$

The canonical divisor class of $\mathcal{C}w\Sigma$ is $K_{\mathcal{C}w\Sigma} \sim \mathcal{O}_{\mathcal{C}w\Sigma}(-10)$. Consider the threefold quasilinear section

$$X = \mathcal{C}w\Sigma \cap (5) \cap (3) \cap (2) \subset \mathbb{P}^{11} [1^2, 2^3, 3^3, 4^4, 5] \quad (3.9)$$

with $K_X \sim \mathcal{O}_X$; brackets (w_i) denote a general hypersurface of degree w_i .

- (i) 1/4 singularities: since there is no quartic equation this time, the whole twisted cubic curve $C \subset \mathbb{P}^3[x_2, x_7, x_{10}, x_{12}]$, found above, is contained in the general X and is a rational curve of singularities of type $(1/4)(1, 3)$.
- (ii) 1/3 singularities: the general X does not intersect this singular stratum.
- (iii) 1/2 singularities: the intersection of X with this singular strata defines a further rational curve E of singularities. On each point of the curve we check that local transverse parameters have odd weight. Therefore E is a curve of type $(1/2)(1, 1)$.

Thus (X, D) is a Calabi-Yau threefold with two disjoint rational curves of singularities C and E of type $(1/4)(1, 3)$ and $(1/2)(1, 1)$, respectively. The rest of the invariants of this family are

$$D^3 = \frac{27}{16}, \quad D \cdot c_2(X) = 21, \quad \deg D|_C = \frac{3}{4}, \quad \gamma_C = 2, \quad \deg D|_E = \frac{3}{4}, \quad \gamma_E = 1. \quad (3.10)$$

Example 3.4. The next example is obtained by a slight generalization of the method described so far. The computation of the canonical class $K_{w\Sigma}$, as the basic line bundle $\mathcal{O}_{w\Sigma}(1)$ raised to the power equal to the difference of the adjunction number and the sum of the weights on $w\mathbb{P}^n$, only works if $w\Sigma$ is well formed. In this example, we will make our ambient weighted homogeneous variety not well formed. We then turn it into a well formed variety by taking projective cones over it. We finally take a quasilinear section to construct a Calabi-Yau threefold (X, D) .

- (i) Input: $\mu = (0, 0)$, $u = 2$.
- (ii) Plücker embedding: $w\Sigma \subset \mathbb{P}^{13}[2^{14}]$, not well formed.
- (iii) Hilbert numerator: $1 - 28t^4 + 105t^6 - 162t^8 + 84t^{10} + 84t^{12} - 162t^{14} + 105t^{16} - 28t^{18} + t^{22}$.

We take a double projective cone over $w\Sigma$, by introducing two new variables x_{15} and x_{16} of weight one, which are not involved in any of the defining equations of $w\Sigma$. We get a seven-dimensional well-formed and quasismooth variety

$$\mathcal{C}\mathcal{C}w\Sigma \subset \mathbb{P}^{15} [1^2, 2^{14}] \quad (3.11)$$

with canonical class $K_{\mathcal{C}\mathcal{C}w\Sigma} \sim \mathcal{O}_{\mathcal{C}\mathcal{C}w\Sigma}(-8)$.

Consider the threefold quasilinear section

$$X = \mathcal{C}\mathcal{C}w\Sigma \cap (2)^4 \subset \mathbb{P}^{11} [1^2, 2^{10}]. \quad (3.12)$$

The canonical class K_X becomes trivial. Since $w\Sigma$ is a five-dimensional variety and we are taking a complete intersection with four generic hypersurfaces of degree two inside $\mathbb{P}^{15}[1^2, 2^{14}]$, the singular locus defined by weight two variables defines a curve in $\mathbb{P}^{11}[1^2, 2^{10}]$. Thus (X, D) is a Calabi-Yau threefold with a curve of singularities of type $(1/2)(1, 1)$. The rest of the invariants of (X, D) are given as follows:

$$D^3 = \frac{9}{2}, \quad D \cdot c_2(X) = 42, \quad \deg D|_C = 9, \quad \gamma_C = 1. \quad (3.13)$$

Example 3.5. Our final initial data in this section consists of the following.

- (i) Input: $\mu = (-1, 1)$, $u = 5$.
- (ii) Plücker embedding: $w\Sigma \subset \mathbb{P}^{13}[3, 4^4, 5^4, 6^4, 7]$.
- (iii) Hilbert numerator: $1 - 3t^8 - 6t^9 - 10t^{10} - 6t^{11} - t^{12} + 12t^{13} + \dots + t^{55}$.
- (iv) Canonical class: $K_{w\Sigma} \sim \mathcal{O}_{w\Sigma}(-15)$, as $w\Sigma$ is well formed.

We take a projective cone over $w\Sigma$ to get the embedding

$$Cw\Sigma \subset \mathbb{P}^{14}[1, 3, 4^4, 5^4, 6^4, 7] \quad (3.14)$$

with $K_{Cw\Sigma} \sim \mathcal{O}_{Cw\Sigma}(-16)$. We take a complete intersection inside $Cw\Sigma$, with three general forms of degree seven, five, and four in $w\mathbb{P}^{14}$. Therefore we get a threefold

$$X = Cw\Sigma \cap (7) \cap (5) \cap (4) \hookrightarrow \mathbb{P}^{11}[1, 3, 4^3, 5^3, 6^4], \quad (3.15)$$

with trivial canonical divisor class. To work out the singularities, we work through the singular strata to find that (X, D) is a polarised Calabi-Yau threefold containing three dissident singular points of type $(1/4)(1, 1, 2)$, a rational curve of singularities C of type $(1/6)(1, 5)$ containing them, and a further isolated singular point of type $(1/3)(1, 1, 1)$. The rest of the invariants are

$$D^3 = \frac{5}{24}, \quad D \cdot c_2(X) = 17, \quad \deg D|_C = \frac{5}{4}, \quad \gamma_C = 9. \quad (3.16)$$

4. The Codimension 6 Weighted Grassmannian Variety

4.1. The Weighted Flag Variety

We take G to be the reductive Lie group of type $\mathrm{GL}(6, \mathbb{C})$. The five simple roots are $\alpha_i = e_i - e_{i+1} \in \Lambda_W$, the weight lattice with basis e_1, \dots, e_6 . The Weyl vector can be taken to be

$$\rho = 5e_1 + 4e_2 + 3e_3 + 2e_4 + e_5. \quad (4.1)$$

Consider the irreducible G -representation V_λ , with $\lambda = e_1 + e_2$. Then V_λ is 15-dimensional, and all of the weights appear with multiplicity one. The highest weight orbit space

$\Sigma = G/P_\lambda \subset \mathbb{P}V_\lambda = \mathbb{P}^{14}$ is eight-dimensional. This flag variety can be identified with the Grassmannian of 2-planes in a 6-dimensional vector space, a codimension 6 variety

$$\Sigma^8 = \text{Gr}(2, 6) \hookrightarrow \mathbb{P}V_\lambda = \mathbb{P}^{14}. \quad (4.2)$$

Let $\{f_i, 1 \leq i \leq 6\}$ be the dual basis of the dual lattice Λ_W^* . We choose

$$\mu = \sum_{i=1}^6 a_i f_i \in \Lambda_W^*, \quad (4.3)$$

$u \in \mathbb{Z}$, to get the weighted version of $\text{Gr}(2, 6)$,

$$w\Sigma(\mu, u) = w \text{Gr}(2, 6)_{(\mu, u)} \hookrightarrow w\mathbb{P}^{14}. \quad (4.4)$$

The set of weights on our projective space is $\{\langle \lambda_i, \mu \rangle + u\}$, where λ_i are weights appearing in the G -representation V_λ . As a convention we will write an element of dual lattice as row vector, that is, $\mu = (a_1, a_2, \dots, a_6)$.

We expand formula (2.7) for the given values of λ, μ to get the following formula for the Hilbert series of $w \text{Gr}(2, 6)$:

$$P_{w\text{Gr}(2,6)}(t) = \frac{1 - Q_1(t)t^{2u} + Q_2(t)t^{3u} - Q_3(t)t^{4u} - Q_4(t)t^{5u} + Q_5(t)t^{6u} - Q_6(t)t^{7u} + t^{3s+9u}}{\prod_{1 \leq i < j \leq 6} (1 - t^{a_i+a_j+u})}. \quad (4.5)$$

Here

$$\begin{aligned} Q_1(t) &= \sum_{1 \leq i < j \leq 6} t^{s-(a_i+a_j)}, \\ Q_2(t) &= \sum_{1 \leq (i,j) \leq 6} t^{s+(a_i-a_j)} - t^s, \\ Q_3(t) &= \sum_{1 \leq i \leq j \leq 6} t^{s+(a_i+a_j)}, \\ Q_4(t) &= \sum_{1 \leq i \leq j \leq 6} t^{2s-(a_i+a_j)}, \\ Q_5(t) &= \sum_{1 \leq (i,j) \leq 6} t^{2s+(a_i-a_j)} - t^{2s}, \\ Q_6(t) &= \sum_{1 \leq i \leq j \leq 6} t^{2s+(a_i+a_j)}. \end{aligned} \quad (4.6)$$

In particular, if $w \text{Gr}(2, 6) \hookrightarrow \mathbb{P}^{14}[\langle w_i, \mu \rangle + u]$ is well formed, then its canonical bundle is $K_{w\text{Gr}(2,6)} \sim \mathcal{O}_{w\text{Gr}(2,6)}(-2s - 6u)$, with $s = \sum_{i=1}^6 a_i$.

The defining equations for $\text{Gr}(2,6) \subset \mathbb{P}^{14}$ are well known to be the 4×4 Pfaffians obtained by deleting two rows and the corresponding columns of the 6×6 skew symmetric matrix

$$A = \begin{bmatrix} 0 & x_1 & x_2 & x_3 & x_4 & x_5 \\ & 0 & x_6 & x_7 & x_8 & x_9 \\ & & 0 & x_{10} & x_{11} & x_{12} \\ & & & 0 & x_{13} & x_{14} \\ & & & & 0 & x_{15} \\ & & & & & 0 \end{bmatrix}. \quad (4.7)$$

4.2. Examples

Example 4.1. Consider the following data.

- (i) Input: $\mu = (2, 1, 0, 0, -1, -2)$, $u = 4$.
- (ii) Plücker embedding: $w \text{Gr}(2,6) \subset \mathbb{P}^{14}[1, 2^2, 3^3, 4^3, 5^3, 6^2, 7]$.
- (iii) Hilbert numerator: $1 - t^5 - 2t^6 - 3t^7 - 2t^8 - t^9 + \dots + t^{36}$.
- (iv) Canonical class: $K_{w \text{Gr}(2,6)} \sim \mathcal{O}_{w \text{Gr}(2,6)}(-24)$.

Consider the threefold quasilinear section

$$X = w \text{Gr}(2,6) \cap (7) \cap (6) \cap (5) \cap (4) \cap (2) \subset \mathbb{P}^9[1, 2, 3^3, 4^2, 5^2, 6]. \quad (4.8)$$

Then K_X is trivial, and X is a Calabi-Yau 3-fold with a singular point of type $(1/6)(5, 4, 3)$, lying on the intersection of two curves, C of type $(1/3)(1, 2)$ and E of type $(1/2)(1, 1)$. There is an additional isolated singular point of type $(1/5)(4, 3, 3)$. The rest of the invariants of this variety are

$$D^3 = \frac{11}{30}, \quad D \cdot c_2(X) = \frac{68}{5}, \quad \deg D|_C = \frac{1}{3}, \quad \gamma_C = \frac{-15}{2}, \quad \deg D|_E = \frac{1}{2}, \quad \gamma_E = 1. \quad (4.9)$$

Example 4.2. We take the following.

- (i) Input: $\mu = (2, 1, 1, 1, 1, 0)$, $u = 0$.
- (ii) Plücker embedding: $w \text{Gr}(2,6) \subset \mathbb{P}^{14}[1^4, 2^7, 3^4]$.
- (iii) Hilbert numerator: $1 - 4t^3 - 6t^4 + 4t^5 + \dots + t^{18}$.
- (iv) Canonical class: $K_{w \text{Gr}(2,6)} \sim \mathcal{O}_{w \text{Gr}(2,6)}(-12)$, as $w\Sigma$ is well formed.

Consider the quasilinear section

$$X = w \text{Gr}(2,6) \cap (3)^2 \cap (2)^3 \subset \mathbb{P}^9[1^4, 2^4, 3^2], \quad (4.10)$$

then

$$K_X = \mathcal{O}_X(-12 + (2 \times 3 + 3 \times 2)) = \mathcal{O}_X. \quad (4.11)$$

The variety (X, D) is a well-formed and quasismooth Calabi-Yau 3-fold. Its singularities consist of two rational curves C and E of singularities of type $(1/3)(1, 2)$ and $(1/2)(1, 1)$, respectively. The rest of the invariants are

$$D^3 = \frac{97}{18}, \quad D \cdot c_2(X) = 42, \quad \deg D|_C = \frac{1}{3}, \quad \gamma_C = 2, \quad \deg D|_E = 1, \quad \gamma_E = 1. \quad (4.12)$$

5. Tautological (Orbi)bundles

5.1. The Classical Story

Let $\Sigma = G/P$ be a flag variety. A representation V of the parabolic subgroup P gives rise to a vector bundle \mathcal{E} on Σ as follows:

$$\begin{array}{ccc} \mathcal{E} = G \times_P V & & \\ \downarrow & & (5.1) \\ \Sigma = G/P. & & \end{array}$$

In other words, the total space of \mathcal{E} consists of pairs $(g, e) \in G \times V$ modulo the equivalence

$$(gp, e) \sim (g, pe), \quad \text{for } p \in P. \quad (5.2)$$

The fiber of \mathcal{E} over each point Σ is isomorphic to the vector space underlying V .

Example 5.1. The simplest example is $\Sigma = \mathbb{P}^{n-1}$, a homogeneous variety G/P with $G = \text{GL}(n)$ and P the parabolic subgroup consisting of matrices of the form

$$A = \begin{pmatrix} \alpha & * & \cdots & * \\ 0 & & & \\ \vdots & & B & \\ 0 & & & \end{pmatrix}. \quad (5.3)$$

We obtain a one-dimensional representation of P by mapping A to α . The associated line bundle is just the tautological line bundle on \mathbb{P}^{n-1} , the dual of the hyperplane bundle $\mathcal{O}_{\mathbb{P}^{n-1}}(1)$.

Example 5.2. More generally, consider $\Sigma = \text{Gr}(k, n)$, the Grassmannian of k -planes in \mathbb{C}^n . Then $G = \text{GL}(n)$ and the corresponding parabolic is the subgroup of matrices of the form

$$A = \begin{pmatrix} B_1 & * \\ 0 & B_2 \end{pmatrix}, \quad (5.4)$$

with B_1, B_2 of size $k \times k$ and $(n - k) \times (n - k)$, respectively. The representations of P defined by $A \mapsto B_1, A \mapsto B_2$, respectively, give the standard tautological sub- and quotient bundles \mathcal{S} and \mathcal{Q} on the Grassmannian $\text{Gr}(k, n)$, fitting into the exact sequence

$$0 \longrightarrow \mathcal{S} \longrightarrow \mathcal{O}_{\text{Gr}(k,n)}^{\oplus n} \longrightarrow \mathcal{Q} \longrightarrow 0. \quad (5.5)$$

Example 5.3. Finally consider the G_2 -variety $\Sigma = G/P$ studied in Section 3. The smallest representations of the corresponding P have dimensions 2 and 5. The corresponding tautological bundles are easiest to describe using an embedding $\Sigma \hookrightarrow \text{Gr}(2, 7)$, mapping the G_2 flag variety into the Grassmannian of 2-planes in a 7-dimensional vector space, the space $\text{Im } \mathbb{O}$ of imaginary octonions. Then the tautological bundles on the G_2 -variety Σ are the restrictions of the tautological sub- and quotient bundle from $\text{Gr}(2, 7)$.

5.2. Orbibundles on Calabi-Yau Sections

Recall that weighted flag varieties are constructed by first considering the \mathbb{C}^* -covering $\tilde{\Sigma} \setminus \{0\} \rightarrow \Sigma$ and then dividing $\tilde{\Sigma} \setminus \{0\}$ by a different \mathbb{C}^* -action given by the weights. A tautological vector bundle \mathcal{E} on Σ pulls back to a vector bundle $\tilde{\mathcal{E}}$ on $\tilde{\Sigma} \setminus \{0\}$. This can then be pushed forward to a weighted flag variety $w\Sigma$ along the quotient map $\tilde{\Sigma} \setminus \{0\} \rightarrow w\Sigma$. Because of the finite stabilizers that exist under this second action, the resulting object $w\mathcal{E}$ is not a vector bundle, but an orbibundle [9, Section 4.2], which trivializes on local orbifold covers with compatible transition maps. If X is a Calabi-Yau threefold inside $w\Sigma$, then we can define an orbi-bundle on X by restricting $w\mathcal{E}$ to X .

In the constructions of Sections 3 and 4, the Calabi-Yau sections therefore carry possibly interesting orbibundles of ranks 2 and 5, respectively 4. We have not investigated the question whether these orbibundles can be pulled back to vector bundles on a resolution $Y \rightarrow X$, but this seems to be of some interest. If so, stability properties of the resulting vector bundles may deserve some investigation, in view of their possible use in heterotic model building [10, 11].

Acknowledgment

The first author has been supported by a grant from the Higher Education Commission (HEC) of Pakistan.

References

- [1] A. Corti and M. Reid, "Weighted Grassmannians," in *Algebraic Geometry, A Volume in Memory of Paolo Francia*, M. C. Beltrametti, F. Catanese, C. Ciliberto, A. Lanteri, and C. Pedrini, Eds., pp. 141–163, de Gruyter, Berlin, Germany, 2002.

- [2] M. I. Qureshi and B. Szendrői, "Constructing projective varieties in weighted flag varieties," *Bulletin of the London Mathematical Society*, vol. 43, no. 4, pp. 786–798, 2011.
- [3] M. I. Qureshi, *Families of polarized varieties in weighted flag varieties*, Ph.D. thesis, University of Oxford, 2011.
- [4] A. Buckley and B. Szendrői, "Orbifold Riemann-Roch for threefolds with an application to Calabi-Yau geometry," *Journal of Algebraic Geometry*, vol. 14, no. 4, pp. 601–622, 2005.
- [5] V. V. Batyrev and D. A. Cox, "On the Hodge structure of projective hypersurfaces in toric varieties," *Duke Mathematical Journal*, vol. 75, pp. 293–338, 1994.
- [6] A. R. Fletcher, "Working with weighted complete intersections," in *Explicit birational geometry of 3-Folds*, A. Corti and M. Reid, Eds., London Mathematical Society Lecture Note Series no. 281, pp. 101–173, Cambridge University Press, Cambridge, UK, 2000.
- [7] A. L. Gorodentsev, A. S. Khoroshkin, and A. N. Rudakov, "On syzygies of highest weight orbits," in *Moscow Seminar on Mathematical Physics. II*, V. I. Arnold, S. G. Gindikin, and V. P. Maslov, Eds., vol. 221 of *American Mathematical Society Translations: Series 2*, pp. 79–120, American Mathematical Society, 2007.
- [8] W. Fulton and J. Harris, *Representation Theory, A First Course, GTM 129*, Springer, 1991.
- [9] C. P. Boyer and K. Galicki, *Sasakian Geometry*, Oxford Mathematical Monographs, Oxford University Press, Oxford, UK, 2008.
- [10] M. Green, J. Schwarz, and E. Witten, *Superstring Theory: Volume 2*, CUP, 1998.
- [11] R. Donagi, Y.-H. He, B. A. Ovrut, and R. Reinbacher, "The particle spectrum of heterotic compactifications," *Journal of High Energy Physics*, vol. 8, no. 12, pp. 1229–1294, 2004.

Research Article

Bell's Inequalities, Superquantum Correlations, and String Theory

Lay Nam Chang, Zachary Lewis, Djordje Minic, Tatsu Takeuchi, and Chia-Hsiung Tze

Department of Physics, Virginia Tech, Blacksburg, VA 24061, USA

Correspondence should be addressed to Djordje Minic, dminic@vt.edu

Received 18 April 2011; Accepted 7 October 2011

Academic Editor: Yang-Hui He

Copyright © 2011 Lay Nam Chang et al. This is an open access article distributed under the Creative Commons Attribution License, which permits unrestricted use, distribution, and reproduction in any medium, provided the original work is properly cited.

We offer an interpretation of superquantum correlations in terms of a “doubly” quantum theory. We argue that string theory, viewed as a quantum theory with two deformation parameters, the string tension α' , and the string coupling constant g_s , is such a superquantum theory that transgresses the usual quantum violations of Bell's inequalities. We also discuss the $\hbar \rightarrow \infty$ limit of quantum mechanics in this context. As a superquantum theory, string theory should display distinct experimentally observable supercorrelations of entangled stringy states.

1. Introduction

In this paper, we present an observation relating two fields of physics which are ostensibly quite remote, namely, the study of the foundations of quantum mechanics (QM) centered around the violation of the celebrated Bell inequalities [1–3] and string theory (ST) [4–6]. As is well known, the Bell inequalities, based on the assumption of classical local realism, are violated by the correlations of canonical QM [7–11]. This remarkable feature of QM is often called “quantum nonlocality,” though perhaps a misnomer. However, even quantum correlations, with their apparent “nonlocality,” are bounded and satisfy another inequality discovered by Cirel'son (Also spelled Tsirelson) [12]; see also [13]. The natural question that arises is as follows: do “super” quantum theories exist which predict correlations that transcend those of QM and thereby violate the Cirel'son bound? Popescu and Rohrlich have demonstrated that such “super” correlations can be consistent with relativistic causality (aka the no-signaling principle) [14]. But what theory would predict them? In the following, we give heuristic arguments which suggest that nonperturbative ST may precisely be such a “superquantum” theory.

2. Bell's Inequality, the Cirel'son Bound, and Beyond

Consider two classical variables A and B , which represent the outcomes of measurements performed on some isolated physical system by detectors 1 and 2 placed at two causally disconnected spacetime locations. Assume that the only possible values of both A and B are ± 1 . Denote the state of detector 1 by a and that of detector 2 by b . "Local realism" demands that A depend only on a and B depend only on b . They can also depend on some hidden, but shared, information, λ . The correlation between $A(a, \lambda)$ and $B(b, \lambda)$ is then

$$P(a, b) = \int d\lambda \rho(\lambda) A(a, \lambda) B(b, \lambda), \quad \int d\lambda \rho(\lambda) = 1, \quad (2.1)$$

where $\rho(\lambda)$ is the probability density of the hidden information λ . This classical correlation is bounded by the following form of Bell's inequality [1, 2] as formulated by Clauser, Horne, Shimony, and Holt (CHSH) [3]:

$$|P(a, b) + P(a, b') + P(a', b) - P(a', b')| \leq X, \quad \text{where } X = X_{\text{Bell}} = 2. \quad (2.2)$$

The quantum versions of these correlations violate this bound but are themselves bounded by a similar inequality obtained by replacing the value of X on the right-hand side with $X_{\text{QM}} = 2\sqrt{2}$. This is the famous Cirel'son bound [12, 13], the extra factor of $\sqrt{2}$ being determined by the Hilbert space structure of QM. The same Cirel'son bound has been shown to apply for quantum field theoretic (QFT) correlations also [15, 16].

Let us briefly review the simplest routes to these bounds. Following [12, 13, 17], consider 4 classical stochastic variables $A, A', B,$ and B' , each of which takes values of $+1$ or -1 . Obviously, the quantity

$$C \equiv AB + AB' + A'B - A'B' = A(B + B') + A'(B - B') \quad (2.3)$$

can be only $+2$ or -2 , and thus, the absolute value of its expectation value is bounded by 2

$$|\langle C \rangle| = |\langle AB + AB' + A'B - A'B' \rangle| \leq 2. \quad (2.4)$$

This is the classical Bell bound. For the quantum case, we replace the classical stochastic variables with hermitian operators acting on a Hilbert space. Following [12, 13], we find that if $\hat{A}^2 = \hat{A}'^2 = \hat{B}^2 = \hat{B}'^2 = 1$ and $[\hat{A}, \hat{B}] = [\hat{A}, \hat{B}'] = [\hat{A}', \hat{B}] = [\hat{A}', \hat{B}'] = 0$, then C is replaced by

$$\hat{C} = \hat{A}\hat{B} + \hat{A}\hat{B}' + \hat{A}'\hat{B} - \hat{A}'\hat{B}', \quad (2.5)$$

from which we find

$$\hat{C}^2 = 4 - [\hat{A}, \hat{A}'] \cdot [\hat{B}, \hat{B}']. \quad (2.6)$$

When the commutators are zero, we recover the classical bound of 2. If they are not, we can use the uncertainty relations $|\langle i[\hat{A}, \hat{A}'] \rangle| \leq 2\|\hat{A}\| \cdot \|\hat{A}'\|$ and $|\langle i[\hat{B}, \hat{B}'] \rangle| \leq 2\|\hat{B}\| \cdot \|\hat{B}'\|$ to obtain

$$\langle \hat{C}^2 \rangle \leq 4 + 4 \|\hat{A}\| \cdot \|\hat{A}'\| \cdot \|\hat{B}\| \cdot \|\hat{B}'\| = 8 \rightarrow |\langle \hat{C} \rangle| \leq \sqrt{\langle \hat{C}^2 \rangle} \leq 2\sqrt{2}, \quad (2.7)$$

which is the Cirel'son bound. Alternatively, we can follow [17] and let $\hat{A}|\psi\rangle = |A\rangle$, $\hat{B}|\psi\rangle = |B\rangle$, $\hat{A}'|\psi\rangle = |A'\rangle$, and $\hat{B}'|\psi\rangle = |B'\rangle$. These 4 vectors all have unit norms and

$$|\langle \hat{C} \rangle| = |\langle \psi | \hat{C} | \psi \rangle| = |\langle A | B + B' \rangle + \langle A' | B - B' \rangle| \leq \| |B\rangle + |B'\rangle \| + \| |B\rangle - |B'\rangle \|, \quad (2.8)$$

which implies

$$|\langle \hat{C} \rangle| \leq \sqrt{2(1 + \text{Re}\langle B | B' \rangle)} + \sqrt{2(1 - \text{Re}\langle B | B' \rangle)} \leq 2\sqrt{2}. \quad (2.9)$$

This second proof suggests that the Cirel'son bound is actually independent of the requirement of relativistic causality. If relativistic causality is broken, then the \hat{A} 's and \hat{B} 's will not commute. Then, \hat{C} must be symmetrized as

$$\hat{C} = \frac{1}{2} \left[(\hat{A}\hat{B} + \hat{B}\hat{A}) + (\hat{A}\hat{B}' + \hat{B}'\hat{A}) + (\hat{A}'\hat{B} + \hat{B}\hat{A}') - (\hat{A}'\hat{B}' + \hat{B}'\hat{A}') \right], \quad (2.10)$$

to make it hermitian, and its expectation value will be

$$\langle \hat{C} \rangle = \text{Re}[\langle A | B + B' \rangle + \langle A' | B - B' \rangle], \quad (2.11)$$

which is clearly subject to the same bound as before. So, it is the Hilbert space structure of QM alone which determines this bound.

Indeed, Popescu and Rohrlich have demonstrated that one can concoct superquantum correlations which violate the Cirel'son bound, while still maintaining consistency with relativistic causality [14]. However, such superquantum correlations are also bounded, the value of X in (2.2) being replaced not by $X_{\text{QM}} = 2\sqrt{2}$ but by $X = 4$

$$|P(a, b) + P(a, b') + P(a', b) - P(a', b')| \leq 4. \quad (2.12)$$

Note, though, that this is not a "bound" per se, the value of 4 being the absolute maximum that the left-hand side can possibly be, since each of the 4 terms has its absolute value bounded by one. If the four correlations represented by these 4 terms were completely independent, then, in principle, there seems to be no reason why this bound cannot be saturated.

But what type of theory would predict such correlations? It has been speculated that a specific superquantum theory could essentially be derived from the two requirements of relativistic causality and the saturation of the $X = 4$ bound, in effect elevating these

requirements to the status of “axioms” which define the theory [14]. On the other hand, it has also been proposed that relativistic causality and locality would demand the Cirel’son bound, and thus QM would be uniquely derived [18, 19]. This would imply the necessity of nonlocality to achieve $X = 4$. However, to our knowledge, no concrete realization of either of these programs has thus far emerged.

A related development has been the proof by van Dam that superquantum correlations which saturate the $X = 4$ bound can be used to render all communication complexity problems trivial [20, 21]. Subsequently, Brassard et al. discovered a protocol utilizing correlations with $X > X_{cc} = 4\sqrt{2}/3$, which solves communication complexity problems trivially in a probabilistic manner [22]. Due to this, it has been speculated that nature somehow disfavors superquantum theories and that superquantum correlations, especially those with $X > X_{cc}$, should not exist [23–26]. However, the argument obviously does not preclude the existence of superquantum theories itself.

One proposal for a superquantum theory discussed in the literature uses a formal mathematical redefinition of the norms of vectors from the usual ℓ^2 norm to the more general ℓ^p norm [27]. In a 2D vector space with basis vectors $\{\mathbf{e}_1, \mathbf{e}_2\}$, the ℓ^p norm is

$$\|\alpha\mathbf{e}_1 + \beta\mathbf{e}_2\|_p = \sqrt[p]{\alpha^p + \beta^p}. \quad (2.13)$$

If one identifies $|B\rangle = \mathbf{e}_1$ and $|B'\rangle = \mathbf{e}_2$, then

$$\||B\rangle \pm |B'\rangle\|_p = 2^{1/p}. \quad (2.14)$$

Equation (2.12) would then be saturated for the $p = 1$ case. (The ℓ^1 norm and ℓ^∞ norm are equivalent in 2D, requiring a mere 45° rotation of the coordinate axes to get from one to the other.) Unfortunately, it is unclear how one can construct a physical theory based on this proposal in which dynamical variables evolve in time while preserving total probability.

At this point, we make the very simple observation that it is the procedure of “quantization,” which takes us from classical mechanics to QM, that increases the bound from the Bell/CHSH value of 2 to the Cirel’son value of $2\sqrt{2}$. That is, “quantization” increases the bound by a factor of $\sqrt{2}$. Thus, if one could perform another step of “quantization” onto QM, would it not lead to the increase of the bound by another factor of $\sqrt{2}$, thereby take us from the Cirel’son value of $2\sqrt{2}$ to the ultimate 4? This is the main conjecture of this paper, that is, a “doubly” quantized theory would lead to the violation of the Cirel’son bound.

In the following, we will clarify which “quantization” procedure we have in mind, and how it can be applied for a second time onto QM, leading to a “doubly quantized” theory. We then argue that a physical realization of such a theory may be offered by nonperturbative open string field theory (OSFT).

3. “Double” Quantization and Open String Field Theory

Before going into the “double quantization” procedure, let us first observe that from the point of view of general mathematical deformation theory [28, 29], QM is a theory with one deformation parameter \hbar , while ST is a theory with two: the first deformation parameter of ST is the world-sheet coupling constant α' , which measures the essential nonlocality of the string, and is responsible for the organization of perturbative ST. The second deformation parameter

of ST is the string coupling constant g_s , which controls the nonperturbative aspects of ST, such as D-branes and related membrane-like solitonic excitations and the general nonperturbative string field theory (SFT) [4–6]. Therefore, ST can be expected to be more “quantum” in some sense than canonical QM, given the presence of the second deformation parameter.

Second, superquantum correlations point to a nonlocality, which is more nonlocal, so to speak, than the aforementioned “quantum nonlocality” of QM and QFT. However, QFT’s are actually local theories, and true nonlocality is expected only in theories of quantum gravity. That quantum gravity must be nonlocal stems from the requirement of diffeomorphism invariance, as has been known from the pioneering days of that field [30, 31]. Thus, quantum gravity, for which ST is a concrete example, can naturally be expected to lead to correlations more nonlocal than those in QM/QFT.

Third, the web of dualities discovered in ST [4–6], which points to the unification of QFTs in various dimensions, can themselves be considered a type of “correlation” which transcends the barriers of QFT Lagrangians and spacetime dimensions. Again, the evidence suggests “super” correlations, perhaps much more “super” than envisioned above, in the context of ST.

What follows is a heuristic attempt to make these expectations physically concrete. Our essential observation is as follows: the “quantization” procedure responsible for turning the classical Bell bound of 2 into the quantum Cirel’son bound of $2\sqrt{2}$ is given by the path integral over the classical dynamical variables, which we collectively denote as x . That is, given a classical action $S(x)$, functions of x are replaced by their expectation values defined via the path integral

$$f(x) \longrightarrow \langle f(\hat{x}) \rangle = \int Dx f(x) \exp\left[\frac{i}{\hbar} S(x)\right], \quad (3.1)$$

up to a normalization constant. In particular, the correlation between two observables $\hat{A}(a)$ and $\hat{B}(b)$ will be given by

$$\langle \hat{A}(a)\hat{B}(b) \rangle = \int Dx A(a, x)B(b, x) \exp\left[\frac{i}{\hbar} S(x)\right] \equiv A(a) \star B(b) \quad (3.2)$$

(cf. (2.1)). In a similar fashion, we can envision taking a collection of quantum operators, which we will collectively denote by $\hat{\phi}$, for which a “quantum” action $\tilde{S}(\hat{\phi})$ is given and define another path integral over the quantum operators $\hat{\phi}$

$$F(\hat{\phi}) \longrightarrow \langle\langle F(\hat{\phi}) \rangle\rangle = \int D\hat{\phi} F(\hat{\phi}) \exp\left[\frac{i}{\hbar} \tilde{S}(\hat{\phi})\right], \quad (3.3)$$

and the correlation between two “super” observables will be

$$\langle\langle \hat{A}(a)\hat{B}(b) \rangle\rangle = \int D\hat{\phi} \hat{A}(a, \hat{\phi})\hat{B}(b, \hat{\phi}) \exp\left[\frac{i}{\hbar} \tilde{S}(\hat{\phi})\right]. \quad (3.4)$$

Note that the expectation values here, denoted $\langle\langle *\rangle\rangle$, are not numbers but operators themselves. To further reduce it to a number, we must calculate its expectation value in the usual way

$$\langle\langle\langle\hat{A}(a)\hat{B}(b)\rangle\rangle\rangle \rightarrow \langle\langle\langle\langle\hat{A}(a)\hat{B}(b)\rangle\rangle\rangle\rangle = \left\langle \int D\hat{\phi} \hat{A}(a, \hat{\phi}) \hat{B}(b, \hat{\phi}) \exp\left[\frac{i}{\tilde{\hbar}} \tilde{S}(\hat{\phi})\right] \right\rangle, \quad (3.5)$$

which would amount to replacing all the products of operators on the right-hand side with their first-quantized expectation values, or equivalently, replacing the operators with “classical” variables except with their products defined via (3.2).

This defines our “double quantization” procedure, through which two deformation parameters, \hbar and $\tilde{\hbar}$, are introduced. We would like to emphasize that the $\hat{\phi}$ in the above expressions is already a quantum entity, depending on the first deformation parameter \hbar . Thus, the “double quantization” procedure proposed here is quite distinct from the “second quantization” procedure used in QFT, which, being a single quantization procedure of a classical field, is a misnomer to begin with. The caveats to our definition are, of course, the difficulty in precisely defining the path integral over the quantum operator $\hat{\phi}$, and thus doing any actual calculations with it, and imposing a physical interpretation on what is meant by the quantum operators themselves being probabilistically determined.

At this point, we make the observation that a “doubly quantized” theory may already be available in the form of Witten’s open string field theory (OSFT) [32]. Our “double” quantization procedure can be mapped onto ST as follows: in the first step, the classical action $S(x)$ can be identified with the world-sheet Polyakov action and the first deformation parameter \hbar with the world-sheet coupling α' [4–6]. In the second step, the quantum action $\tilde{S}(\hat{\phi})$ can be identified with Witten’s OSFT action [32] and the second deformation parameter $\tilde{\hbar}$ with the string coupling g_s .

The doubly deformed nature of the theory is explicit in the Witten action for the “classical” open string field Φ , an action of an abstract Chern-Simons type

$$S_W(\Phi) = \int \Phi \star Q_{\text{BRST}} \Phi + \Phi \star \Phi \star \Phi, \quad (3.6)$$

where Q_{BRST} is the open string theory BRST cohomology operator ($Q_{\text{BRST}}^2 = 0$) and the star product is determined via the world-sheet Polyakov action

$$S_P(X) = \frac{1}{2} \int d^2\sigma \sqrt{g} g^{ab} \partial_a X^i \partial_b X^j G_{ij} + \dots, \quad (3.7)$$

and the corresponding world-sheet path integral

$$F \star G = \int DX F(X) G(X) \exp\left[\frac{i}{\alpha'} S_P(X)\right]. \quad (3.8)$$

The fully quantum OSFT is then in principle defined by yet another path integral in the infinite dimensional space of the open string field Φ ; that is,

$$\int D\Phi \exp\left[\frac{i}{g_s} S_W(\Phi)\right], \quad (3.9)$$

with all products defined via the star-product.

In addition to its manifestly “doubly” quantized path integral, OSFT has as massless modes the ordinary photons, which are used in the experimental verification of the violation of Bell’s inequalities [7–11], and it also contains gravity (closed strings) as demanded by unitarity. (The open/closed string theory duality is nicely illustrated by the AdS/CFT duality [4–6]. It is interesting to contemplate the Bell bound and its violations, both quantum and super-quantum, in this well-defined context. Similarly, it would be interesting, even though experimentally prohibitive, to contemplate the superquantum correlations for the QCD string, perhaps in the studies of the quark-gluon plasma.) Thus, our heuristic reasoning suggests that OSFT may precisely be an example of a super-quantum theory, which violates the Cirel’son bound.

We close this section with a caveat and a speculation. In the above reasoning, the two quantizations were taken to be independent with two independent deformation parameters. In the case of OSFT, they were α' and g_s . However, from the point of view of M-theory, we would generically expect that α' and g_s are both of order one (in natural units) and that both are dynamically generated [33]. Thus, the two parameters are not completely independent, and it may not be correct to view OSFT as a fully “doubly quantized” theory. Would this mean that OSFT/M-theory correlations would not saturate the ultimate $X = 4$ bound? Would its CHSH bound be situated somewhere between $X_{QM} = 2\sqrt{2}$ and $X = 4$, perhaps below the communication complexity bound of $X_{cc} = 4\sqrt{2/3}$? If M-theory is indeed unique, it may be natural to expect that its correlations would also be unique from the point of view of communication complexity, and that they would saturate this communication complexity bound. Of course, this conjecture would be testable only in a very precise proposal for M-theory (perhaps along the lines of [34–38]).

4. The $\hbar \rightarrow \infty$ Limit

Given that a superquantum theory is supposedly more “quantum” than QM, let us now consider the the extreme quantum limit of QM, $\hbar \rightarrow \infty$. Though QM is not “doubly quantized,” could it still exhibit certain superquantum behavior in that limit? Taking a deformation parameter to infinity can be naturally performed in ST, either $\alpha' \rightarrow \infty$ or $g_s \rightarrow \infty$, and one can still retain sensible physics. Therefore, the $\hbar \rightarrow \infty$ limit of QM may also be a sensible theory but at the same time quite different from QM. After all, if the $\hbar \rightarrow 0$ limit is to recover classical mechanics, with the Bell bound of $X_{Bell} = 2$, and apparently quite different from QM, it may not be too farfetched to conjecture that the $\hbar \rightarrow \infty$ limit would flow to a superquantum theory, with the superquantum bound of $X = 4$. If this were indeed the case, it may provide us with an opportunity to explore superquantum behavior in the absence of a solution to OSFT/M-theory.

What would the $\hbar \rightarrow \infty$ limit mean from the point of view of the path integral? Given that the path-integral measure is $e^{iS/\hbar}$, in the $\hbar \rightarrow \infty$ limit this measure will be unity for any S , and all histories in the path integral contribute with equal unit weight. Similarly all phases,

measured by $e^{iS/\hbar}$, will be washed out (this immediately raises other issues, such as the meaning of quantum statistics). Because the phases are washed out, we cannot distinguish between $|B\rangle + |B'\rangle$ and $|B\rangle - |B'\rangle$ (note that $-1 = e^{i\pi}$ and that sign can be absorbed into a phase of $|B'\rangle$). This suggests that

$$\| |B\rangle \pm |B'\rangle \| = \| |B\rangle \| + \| |B'\rangle \|, \quad (4.1)$$

which, if applied to the proof of the Cirel'son bound given earlier, leads to the superquantum bound of 4. This property is similar to what was obtained by replacing the ℓ^2 norm with an ℓ^1 (or ℓ^∞) norm, *cf.* (2.14), but presumably, unlike the change of norm, this relation is independent of the choice of basis. This argument seems to suggest that the $\hbar \rightarrow \infty$ limit is indeed superquantum.

However, this observation is perhaps a bit naïve, since the proof of the Cirel'son bound itself may no longer be valid under the wash-out of all phases. Let us invoke here an optical-mechanical analogy: geometric optics is the zero wavelength limit of electromagnetism, which would correspond to the $\hbar \rightarrow 0$ limit of QM. The $\hbar \rightarrow \infty$ limit of QM would, therefore, correspond to the extreme near field limit of electromagnetism, and in that case, the superposition of waves is washed out (we thank Jean Heremans for discussions of this point). Note also that from a geometric point of view, the holomorphic sectional curvature $2/\hbar$ of the projective Hilbert space CP^N of canonical QM goes to zero as $\hbar \rightarrow \infty$, and CP^N becomes just C^N . (For a general discussion of the geometry of quantum theory and its relevance for quantum gravity and string theory, see [34–38].) From these observations, it is clear that the usual Born rule to obtain probabilities will no longer apply.

But before we ask what rule should replace that of Born, let us confront the obvious problem that in the limit $\hbar \rightarrow \infty$, only the ground state of the Hamiltonian will remain in the physical spectrum and the theory will be rendered trivial (if the system has a non-trivial topology, it could allow for degeneracies in the ground state, and thus lead to a non-trivial theory even in the $\hbar \rightarrow \infty$ limit). This can also be argued via the general Feynman-Schwinger formulation of QM [39]

$$\delta S\psi = i\hbar \delta\psi. \quad (4.2)$$

By taking the $\hbar \rightarrow \infty$ limit, we eliminate the classical part δS so that we are left only with $\delta\psi = 0$, and thus, ψ must be a constant $\psi \equiv |\psi|$, a trivial result.

Could the $\hbar \rightarrow \infty$ limit of QM be made less than trivial? Consider the corresponding $\alpha' \rightarrow \infty$ and $g_s \rightarrow \infty$ limits in ST. In the $\alpha' \rightarrow \infty$ of ST, as opposed to the usual $\alpha' \rightarrow 0$ field theory limit, one seemingly ends up with an infinite number of fields and a nontrivial higher spin theory [40, 41]. Recently, such a theory was considered from a holographically dual point of view, and the dual of such a higher spin theory in AdS space was identified to be a free field theory [42]. The $g_s \rightarrow \infty$ limit of ST appears in the context of M-theory, one of whose avatars arises in the $g_s \rightarrow \infty$ limit of type-IIA ST [4–6]. Neither the high spin theory, nor the avatars of M-theory are trivial, as the presence of the tunable second deformation parameter saves them from triviality. Thus, the introduction of a second tunable parameter into QM, for example, Newton's gravitational constant G_N , may be necessary for the limit $\hbar \rightarrow \infty$ to be nontrivial.

Another issue here is that of interpretation: in the classical ($\hbar \rightarrow 0$) case, we have one trajectory, and one event (position, for example) at one point in time. One could speculate that the superquantum ($\hbar \rightarrow \infty$) limit would correspond to the complement of all other virtual trajectories. A general linear map relating virtual and classical trajectories is presumably non-symmetric (there are in principle more possibilities than actual events). Very naïvely, one would then expect that if we impose the condition that all possible events can be “mapped” to actual events, we could end up with a symmetric linear map corresponding to quantum theory ($\hbar \sim 1$), with a natural “map” between the actual events and possibilities, presumably realized by the Born probability rule. Note that according to this scenario, the superquantum theory would correspond essentially to a theory of possibilities and without actual events, which would be an interesting lesson for the foundations of ST.

5. Possible Experimental Signatures

Finally we offer some comments on possible experimental observations of such superquantum violations of Bell’s inequalities. The usual setup involves entangled photons [7–11]. In open ST, photons are the lowest lying massless states, but there is also an entire Regge trajectory associated with them. So, the obvious experimental suggestion would be to observe entangled Reggeized photons. Such an experiment is, of course, forbidding at present, given its Planckian nature.

Superquantum correlations could also be observable in cosmology. The current understanding of the large-scale structure of the universe, that is, the distribution of galaxies and galaxy clusters, is that they are seeded by quantum fluctuations. In standard calculations, it is assumed that the quantum correlations of these fluctuations are Gaussian (non-Gaussian correlations have also been considered). If the correlations were, in fact, superquantum, however, their signature could appear as characteristic deviations from the predicted large-scale structure based on Gaussian correlations. Such superquantum correlations would presumably be generated in the quantum gravity phase, and thus should be enhanced by the expansion of the universe at the largest possible scales. It would be interesting to look for evidence of such large-scale superquantum correlations in the existing WMAP [43] or the upcoming Planck [44, 45] data.

We conclude with a few words regarding a new experimental “knob” needed to test our doubly quantized approach to superquantum correlations. In the classic experimental tests of the violation of Bell’s inequalities [7–11], such a “knob” is represented by the relative angle between polarization vectors of entangled photons. If we have another quantization, there should be, in principle, another angle-like “knob.” Thus, the usual one-dimensional data plot [7–11] should be replaced by a two dimensional surface. By cutting this surface at various values of the new, second angle, we should be able to obtain one dimensional cuts for which the value of the CHSH bound varies depending on the cut, exceeding $2\sqrt{2}$ in some cases, and perhaps not exceeding 2 in others. Thus, the second “knob” may very well allow us to interpolate between the classical, quantum, and superquantum cases. The physical meaning of such an extra “knob” is not clear at the moment. It would be natural to associate this second “knob” with the extended nature of entangled Reggeized photons. However, we must admit that the measure of such nonlocality is not as obvious as the canonical measure of polarization of entangled photons in the standard setup [7–11].

In this paper, we have obviously only scratched the surface of a possible superquantum theory, and many probing questions remain to be answered and understood. We hope to address some of them in future works.

Acknowledgments

The authors thank V. Balasubramanian, J. de Boer, J. Heremans, S. Mathur, K. Park, J. Polchinski, R. Raghavan, D. Rohrlich, V. Scarola, J. Simon, and A. Staples for helpful comments, interesting discussions, and salient questions. D. Minic acknowledges the hospitality of the Mathematics Institute at Oxford University and Merton College, Oxford, and his respective hosts, Philip Candelas and Yang-Hui He. D. Minic also thanks the Galileo Galilei Institute for Theoretical Physics, Florence, for the hospitality and the INFN for partial support. Z. Lewis, D. Minic, and T. Takeuchi are supported in part by the U.S. Department of Energy Grant no. DE-FG05-92ER40677, task A.

References

- [1] J. S. Bell, "On the Einstein Podolsky Rosen paradox," *Physics*, vol. 1, no. 3, pp. 195–200, 1964.
- [2] J. S. Bell, *Speakable and Unspeakable in Quantum Mechanics*, Cambridge University Press, 1987.
- [3] J. F. Clauser, M. A. Horne, A. Shimony, and R. A. Holt, "Proposed experiment to test local hidden-variable theories," *Physical Review Letters*, vol. 23, no. 15, pp. 880–884, 1969.
- [4] J. Polchinski, *String Theory*, vol. 2, Cambridge University Press, 1998.
- [5] K. Becker, M. Becker, and J. H. Schwarz, *String Theory and M-Theory: A Modern Introduction*, Cambridge University Press, 2007.
- [6] M. B. Green, J. H. Schwarz, and E. Witten, *Superstring Theory*, vol. 1, Cambridge University Press, 1988, where it was suggested that string field theory can be viewed as a generalization of quantum theory.
- [7] S. J. Freedman and J. F. Clauser, "Experimental test of local hidden-variable theories," *Physical Review Letters*, vol. 28, no. 14, pp. 938–941, 1972.
- [8] J. F. Clauser and M. A. Horne, "Experimental consequences of objective local theories," *Physical Review D*, vol. 10, no. 2, pp. 526–535, 1974.
- [9] A. Aspect, P. Grangier, G. Roger et al., "Experimental tests of realistic local theories via Bell's theorem," *Physical Review Letters*, vol. 47, no. 7, pp. 460–463, 1981.
- [10] A. Aspect, P. Grangier, G. Roger et al., "Experimental realization of Einstein-Podolsky-Rosen-Bohm gedankenexperiment: a new violation of Bell's inequalities," *Physical Review Letters*, vol. 49, no. 2, pp. 91–94, 1982.
- [11] A. Aspect, J. Dalibard, G. Roger et al., "Experimental test of Bell's inequalities using time-varying analyzers," *Physical Review Letters*, vol. 49, no. 25, pp. 1804–1807, 1982.
- [12] B. S. Cirel'son, "Quantum generalizations of Bell's inequality," *Letters in Mathematical Physics*, vol. 4, no. 2, pp. 93–100, 1980.
- [13] L. J. Landau, "On the violation of Bell's inequality in quantum theory," *Physics Letters A*, vol. 120, no. 2, pp. 54–56, 1987.
- [14] S. Popescu and D. Rohrlich, "Quantum nonlocality as an axiom," *Foundations of Physics*, vol. 24, no. 3, pp. 379–385, 1994.
- [15] S. J. Summers and R. Werner, "Maximal violation of Bell's inequalities is generic in quantum field theory," *Communications in Mathematical Physics*, vol. 110, no. 2, pp. 247–259, 1987.
- [16] S. J. Summers and R. Werner, "Bell's inequalities and quantum field theory. I. General setting," *Journal of Mathematical Physics*, vol. 28, no. 10, pp. 2440–2448, 1987.
- [17] D. Dieks, "Inequalities that test locality in quantum mechanics," <http://arxiv.org/abs/quant-ph/0206172>.
- [18] Y. Aharonov and D. Rohrlich, *Quantum Paradoxes: Quantum Theory for the Perplexed*, Wiley-VCH, 2005.
- [19] D. Rohrlich, "Three attempts at two axioms for quantum mechanics," <http://arxiv.org/abs/1011.5322>.
- [20] W. van Dam, *Nonlocality and communication complexity*, D.Phil. thesis, Department of Physics, University of Oxford, 2000.
- [21] W. Van Dam, "Implausible consequences of superstrong nonlocality," <http://arxiv.org/abs/quant-ph/0501159>.
- [22] G. Brassard, H. Buhrman, N. Linden, A. A. Méthot, A. Tapp, and F. Unger, "Limit on nonlocality in any world in which communication complexity is not trivial," *Physical Review Letters*, vol. 96, no. 25, Article ID 250401, 2006.

- [23] G. Brassard, "Is information the key?" *Nature Physics*, vol. 1, pp. 2–4, 2005.
- [24] S. Popescu, "Quantum mechanics: why isn't nature more non-local?" *Nature Physics*, vol. 2, no. 8, pp. 507–508, 2006.
- [25] J. Barrett, "Information processing in generalized probabilistic theories," *Physical Review A*, vol. 75, Article ID 032304, 2007.
- [26] N. Brunner and P. Skrzypczyk, "Nonlocality distillation and postquantum theories with trivial communication complexity," *Physical Review Letters*, vol. 102, no. 16, Article ID 160403, 4 pages, 2009.
- [27] G. Ver Steeg and S. Wehner, http://arxiv.org/PS_cache/arxiv/pdf/0811/0811.3771v2.pdf.
- [28] L. D. Faddeev, "On the Relationship between Mathematics and Physics," *Asia-Pacific Physics News*, vol. 3, pp. 21–22, June-July, 1988.
- [29] L. D. Faddeev, "Frontiers in physics, high technology and mathematics," in *Proceedings of the 25th Anniversary Conference*, H. A. Cerdeira and S. Lundqvist, Eds., pp. 238–246, World Scientific, Trieste, Italy, 1989.
- [30] B. S. Dewitt, "Quantum theory of gravity. I. the canonical theory," *Physical Review*, vol. 160, no. 5, pp. 1113–1148, 1967.
- [31] W. S. Bickel, "Mean lives of some excited states in multiply ionized oxygen and neon," *Physical Review*, vol. 162, no. 1, pp. 7–11, 1967.
- [32] E. Witten, "Non-commutative geometry and string field theory," *Nuclear Physics B*, vol. 268, no. 2, pp. 253–294, 1986.
- [33] R. Dijkgraaf, "The mathematics of M-theory," in *Proceedings of the 3rd European Congress of Mathematics*, Progress in Mathematics, Birkhuser, Barcelona, Spain, 2000.
- [34] D. Minic and H. C. Tze, "Background independent quantum mechanics and gravity," *Physical Review D*, vol. 68, no. 6, Article ID 061501, 5 pages, 2003.
- [35] D. Minic and C. H. Tze, "A general theory of quantum relativity," *Physics Letters B*, vol. 581, no. 1-2, pp. 111–118, 2004.
- [36] V. Jejjala, M. Kavic, and D. Minic, "Time and M-theory," *International Journal of Modern Physics A*, vol. 22, no. 20, pp. 3317–3405, 2007.
- [37] V. Jejjala, M. Kavic, D. Minic, and C. H. Tze, http://arxiv.org/PS_cache/arxiv/pdf/0804/0804.3598v1.pdf.
- [38] V. Jejjala, M. Kavic, D. Minic, and C. H. Tze, "On the origin of time and the universe," *International Journal of Modern Physics D*, vol. 25, no. 12, pp. 2515–2523, 2010.
- [39] L. M. Brown, Ed., *Feynman's Thesis: A New Approach to Quantum Theory*, World Scientific, 2005.
- [40] M. A. Vasiliev, http://arxiv.org/PS_cache/hep-th/pdf/9910/9910096v1.pdf.
- [41] X. Bekaert, S. Cnockaert, C. Iazeolla, and M. A. Vasiliev, http://arxiv.org/PS_cache/hep-th/pdf/0503/0503128v2.pdf.
- [42] M. R. Douglas, L. Mazzucato, and S. S. Razamat, http://arxiv.org/PS_cache/arxiv/pdf/1011/1011.4926v2.pdf.
- [43] E. Komatsu, K. M. Smith, J. Dunkley et al., "Seven-year wilkinson microwave anisotropy probe (Wmap) observations: cosmological interpretation," *Astrophysical Journal Supplement Series*, vol. 192, no. 2, article 18, 2011.
- [44] G. Efstathiou, C. Lawrence, and J. Tauber, Eds., Planck Collaboration, astro-ph/0604069.
- [45] P. A. R. Ade, N. Aghanim, M. Arnaud et al., Planck Collaboration, http://arxiv.org/PS_cache/arxiv/pdf/1101/1101.2022v2.pdf.

Review Article

On the Minimal Length Uncertainty Relation and the Foundations of String Theory

**Lay Nam Chang, Zachary Lewis, Djordje Minic,
and Tatsu Takeuchi**

Department of Physics, Virginia Tech, Blacksburg, VA 24061, USA

Correspondence should be addressed to Djordje Minic, dminic@vt.edu

Received 1 June 2011; Accepted 9 August 2011

Academic Editor: Yang-Hui He

Copyright © 2011 Lay Nam Chang et al. This is an open access article distributed under the Creative Commons Attribution License, which permits unrestricted use, distribution, and reproduction in any medium, provided the original work is properly cited.

We review our work on the minimal length uncertainty relation as suggested by perturbative string theory. We discuss simple phenomenological implications of the minimal length uncertainty relation and then argue that the combination of the principles of quantum theory and general relativity allow for a dynamical energy-momentum space. We discuss the implication of this for the problem of vacuum energy and the foundations of nonperturbative string theory.

1. Introduction

One of the unequivocal characteristics of string theory [1–3] is its possession of a fundamental length scale which determines the typical spacetime extension of a fundamental string. This is $\ell_s = \sqrt{\alpha'}$, where $\hbar c/\alpha'$ is the string tension. Such a feature is to be expected of any candidate theory of quantum gravity, since gravity itself is characterized by the Planck length $\ell_P = \sqrt{\hbar G_N/c^3}$. Moreover, $\ell_P \sim \ell_s$ is understood to be the *minimal length* below which spacetime distances cannot be resolved [4–7]

$$\delta s \gtrsim \ell_P \sim \ell_s. \quad (1.1)$$

Quantum theory, on the other hand, is completely oblivious to the presence of such a scale, despite its being the putative infrared limit of string theory. A natural question to ask is, therefore, whether the formalism of quantum theory can be deformed or extended in such a way as to consistently incorporate the minimal length. If it is at all possible, the precise manner in which quantum theory must be modified may point to solutions of yet unresolved

mysteries such as the cosmological constant problem [8–12], which is quantum gravitational in its origin. It should also illuminate the nature of string theory [13], whence quantum theory must emerge [14].

The idea of introducing a minimal length into quantum theory has a fascinating and long history. It was used by Heisenberg in 1930 [15, 16] to address the infinities of the newly formulated theory of quantum electrodynamics [17]. Over the years, the idea has been picked up by many authors in a plethora of contexts, for example, [18–42] to list just a few. Various ways to deform or extend quantum theory have also been suggested [43–47]. In this paper, we focus our attention on how a minimal length can be introduced into quantum mechanics by modifying its algebraic structure [48–50].

The starting point of our analysis is the minimal length uncertainty relation (MLUR) [51, 52],

$$\delta x \sim \left(\frac{\hbar}{\delta p} + \alpha' \frac{\delta p}{\hbar} \right), \quad (1.2)$$

which is suggested by a resummed perturbation expansion of the string-string scattering amplitude in a flat spacetime background [53–56]. This is essentially a Heisenberg microscope argument [57] in the S -matrix language [58–61] with fundamental strings used to probe fundamental strings. The first term inside the parentheses on the right-hand side is the usual Heisenberg term coming from the shortening of the probe wavelength as momentum is increased, while the second term can be understood as due to the lengthening of the probe string as more energy is pumped into it

$$\delta p = \frac{\delta E}{c} \sim \frac{\hbar}{\alpha'} \delta x. \quad (1.3)$$

Equation (1.2) implies that the uncertainty in position, δx , is bounded from below by the string length scale,

$$\delta x \gtrsim \sqrt{\alpha'} = \ell_s, \quad (1.4)$$

where the minimum occurs at

$$\delta p \sim \frac{\hbar}{\sqrt{\alpha'}} = \frac{\hbar}{\ell_s} \equiv \mu_s. \quad (1.5)$$

Thus, ℓ_s is the minimal length below which spatial distances cannot be resolved, consistent with (1.1). In fact, the MLUR can be motivated by fairly elementary general relativistic considerations independent of string theory, which suggests that it is a universal feature of quantum gravity [4–7].

Note that in the trans-Planckian momentum region $\delta p \gg \mu_s$, the MLUR is dominated by the behavior of (1.3), which implies that large δp (UV) corresponds to large δx (IR), and that there exists a correspondence between UV and IR physics. Such UV/IR relations have been observed in various string dualities [1–3], and in the context of AdS/CFT correspondence [62, 63] (albeit between the bulk and boundary theories). Thus, the MLUR captures another distinguishing feature of string theory.

In addition to the MLUR, another uncertainty relation has been pointed out by Yoneya as characteristic of string theory. This is the so-called spacetime uncertainty relation (STUR)

$$\delta x \delta t \sim \frac{\ell_s^2}{c}, \quad (1.6)$$

which can be motivated in a somewhat hand-waving manner by combining the usual energy-time uncertainty relation $\delta E \delta t \sim \hbar$ [64–66] with (1.3). However, it can also be supported via an analysis of D0-brane scattering in certain backgrounds in which δx can be made arbitrary small at the expense of making the duration of the interaction δt arbitrary large [67–73]. While the MLUR pertains to dynamics of a particle in a nondynamic spacetime, the STUR can be interpreted to pertain to the dynamics of spacetime itself in which the size of a quantized spacetime cell is preserved.

In the following, we discuss how the MLUR and STUR may be incorporated into quantum mechanics via a deformation and/or extension of its algebraic structure. In Section 2, we introduce a deformation of the canonical commutation relation between \hat{x} and \hat{p} which leads to the MLUR and discuss its phenomenological consequences. In Section 3, we take the classical limit by replacing commutation relations with Poisson brackets and derive the analogue of Liouville’s theorem in the deformed mechanics. We then discuss the effect this has on the density of states in phase space. In Section 4, we discuss the implications of the MLUR on the cosmological constant problem. We conclude in Section 5 with some speculations on how the STUR may be incorporated via a Nambu triple bracket and comment on the lessons for the foundations of string theory and on the question “What is string theory?”

2. Quantum Mechanical Model of the Minimal Length

2.1. Deformed Commutation Relations

To place the MLUR, (1.2), on firmer ground, we begin by rewriting it as

$$\delta x \delta p \geq \frac{\hbar}{2} (1 + \beta \delta p^2), \quad (2.1)$$

where we have introduced the parameter $\beta = \alpha' / \hbar^2$. The minimum value of δx as a function of δp is plotted in Figure 1. This uncertainty relation can be reproduced by deforming the canonical commutation relation between \hat{x} and \hat{p} to

$$\frac{1}{i\hbar} [\hat{x}, \hat{p}] = 1 \longrightarrow \frac{1}{i\hbar} [\hat{x}, \hat{p}] = A(\hat{p}^2), \quad (2.2)$$

with $A(p^2) = 1 + \beta p^2$. Indeed, we find

$$\delta x \delta p \geq \frac{1}{2} |\langle [\hat{x}, \hat{p}] \rangle| = \frac{\hbar}{2} (1 + \beta \langle \hat{p}^2 \rangle) \geq \frac{\hbar}{2} (1 + \beta \delta p^2), \quad (2.3)$$

since $\delta p^2 = \langle \hat{p}^2 \rangle - \langle \hat{p} \rangle^2$. The function $A(p^2)$ can actually be more generic, with βp^2 being the linear term in its expansion in p^2 .

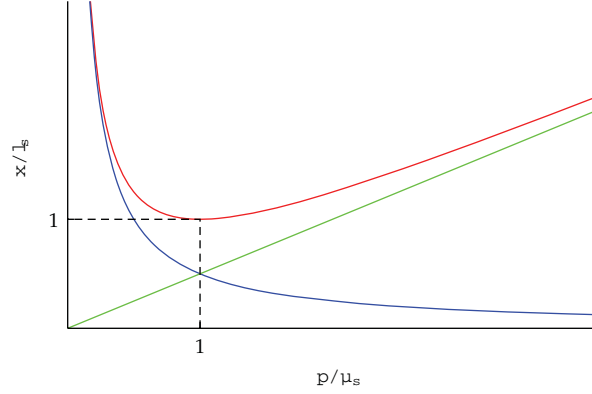


Figure 1: The δp -dependence of the lower bound of δx under the minimal length uncertainty relation (2.1) (red curve). The bound for the usual Heisenberg relation $\delta x \geq \hbar/(2\delta p)$ is shown in blue, and the linear bound $\delta x \geq (\hbar\beta/2)\delta p$ is shown in green.

When we have more than one spatial dimension, the above commutation relation can be generalized to

$$\frac{1}{i\hbar} [\hat{x}_i, \hat{p}_j] = A(\hat{\mathbf{p}}^2) \delta_{ij} + B(\hat{\mathbf{p}}^2) \hat{p}_i \hat{p}_j, \quad (2.4)$$

where $\hat{\mathbf{p}}^2 = \sum_i \hat{p}_i^2$. The right-hand side is the most general form that depends only on the momentum and respects rotational symmetry. Assuming that the components of the momentum commute among themselves,

$$[\hat{p}_i, \hat{p}_j] = 0, \quad (2.5)$$

the Jacobi identity demands that

$$\frac{1}{i\hbar} [\hat{x}_i, \hat{x}_j] = -\left\{ 2(\hat{A} + \hat{B}\hat{\mathbf{p}}^2) \hat{A}' - \hat{A}\hat{B} \right\} \hat{L}_{ij}, \quad (2.6)$$

where we have used the shorthand $\hat{A} = A(\hat{\mathbf{p}}^2)$, $\hat{A}' = (dA/d\mathbf{p}^2)(\hat{\mathbf{p}}^2)$, $\hat{B} = B(\hat{\mathbf{p}}^2)$, and $\hat{L}_{ij} = (\hat{x}_i \hat{p}_j - \hat{x}_j \hat{p}_i) / \hat{A}$. That \hat{L}_{ij} generates rotations can be seen from the following:

$$\begin{aligned} \frac{1}{i\hbar} [\hat{L}_{ij} \hat{x}_k] &= \delta_{ik} \hat{x}_j - \delta_{jk} \hat{x}_i, \\ \frac{1}{i\hbar} [\hat{L}_{ij} \hat{p}_k] &= \delta_{ik} \hat{p}_j - \delta_{jk} \hat{p}_i, \\ \frac{1}{i\hbar} [\hat{L}_{ij} \hat{L}_{k\ell}] &= \delta_{ik} \hat{L}_{j\ell} - \delta_{i\ell} \hat{L}_{jk} + \delta_{j\ell} \hat{L}_{ik} - \delta_{jk} \hat{L}_{i\ell}. \end{aligned} \quad (2.7)$$

Note that the noncommutativity of the components of position can be interpreted as a reflection of the dynamic nature of space itself, as would be expected in quantum gravity.

Various choices for the functions $A(\mathbf{p}^2)$ and $B(\mathbf{p}^2)$ have been considered in the literature. Maggiore [48, 49] proposed that

$$A(\mathbf{p}^2) = \sqrt{1 + 2\beta\mathbf{p}^2}, \quad B(\mathbf{p}^2) = 0, \quad \frac{1}{i\hbar} [\hat{x}_i, \hat{x}_j] = -2\beta\hat{L}_{ij}, \quad (2.8)$$

while Kempf et al. [50] assumed that

$$A(\mathbf{p}^2) = 1 + \beta\mathbf{p}^2, \quad B(\mathbf{p}^2) = \beta' = \text{constant}, \quad (2.9)$$

in which case

$$\frac{1}{i\hbar} [\hat{x}_i, \hat{x}_j] = -\left\{ (2\beta - \beta') + \beta(2\beta + \beta')\hat{\mathbf{p}}^2 \right\} \hat{L}_{ij}. \quad (2.10)$$

Kempf's choice encompasses the algebra of Snyder [19, 20]

$$A(\mathbf{p}^2) = 1, \quad B(\mathbf{p}^2) = \beta', \quad \frac{1}{i\hbar} [\hat{x}_i, \hat{x}_j] = \beta'\hat{L}_{ij}, \quad (2.11)$$

and that of Brau and Buisseret [74, 75]

$$A(\mathbf{p}^2) = 1 + \beta\mathbf{p}^2, \quad B(\mathbf{p}^2) = 2\beta, \quad \frac{1}{i\hbar} [\hat{x}_i, \hat{x}_j] = O(\beta^2), \quad (2.12)$$

for which the components of the position approximately commute. In our treatment, we follow Kempf and use (2.9).

2.2. Shifts in the Energy Levels

Let us see whether the above deformed commutation relations led to a reasonable quantum mechanics, with well-defined energy eigenvalues and eigenstates. Given a Hamiltonian in terms of the deformed position and momentum operators, $H(\hat{\mathbf{x}}, \hat{\mathbf{p}})$, we would like to solve the time-independent Schrödinger equation

$$H(\hat{\mathbf{x}}, \hat{\mathbf{p}})|E\rangle = E|E\rangle. \quad (2.13)$$

The operators which satisfy (2.4), (2.5), and (2.6), subject to the choice (2.9), can be represented using operators which obey the canonical commutation relation $[\hat{q}_i, \hat{p}_j] = i\hbar\delta_{ij}$ as [50, 76]

$$\hat{x}_i = \hat{q}_i + \beta \frac{\hat{p}^2 \hat{q}_i + \hat{q}_i \hat{p}^2}{2} + \beta' \frac{\hat{p}_i (\hat{\mathbf{p}} \cdot \hat{\mathbf{q}}) + (\hat{\mathbf{q}} \cdot \hat{\mathbf{p}}) \hat{p}_i}{2}, \quad (2.14)$$

$$\hat{p}_i = \hat{p}_i.$$

The β and β' terms are symmetrized to ensure the hermiticity of \hat{x}_i . Note that this representation allows us to write the Hamiltonian in terms of canonical \hat{q}_i 's and \hat{p}_i 's

$$H'(\hat{\mathbf{q}}, \hat{\mathbf{p}}) \equiv H(\hat{\mathbf{x}}(\hat{\mathbf{q}}, \hat{\mathbf{p}}), \hat{\mathbf{p}}). \quad (2.15)$$

Thus, our deformation of the canonical commutation relations is mathematically equivalent to a deformation of the Hamiltonian. (In this work, we do not address the question of whether the dependence of the Hamiltonian on the position and momentum operators also need be modified in the presence of a minimal length. Lacking in any guideline to do so, we simply keep them fixed to their standard forms.)

By the standard replacements

$$\hat{q}_i = q_i, \quad \hat{p}_i = \frac{\hbar}{i} \frac{\partial}{\partial q_i}, \quad \text{or } \hat{q}_i = i\hbar \frac{\partial}{\partial p_i}, \quad \hat{p}_i = p_i, \quad (2.16)$$

\hat{x}_i and \hat{p}_j can be represented as differential operators acting on a Hilbert space of L^2 functions in either the q_i 's or the p_i 's, and one can write down a Schrödinger equation for a given Hamiltonian in either q -space or p -space to solve for the energy eigenvalues. Note, however, that while the p_i 's are the eigenvalues of the momentum operators \hat{p}_i , the q_i 's are not the eigenvalues of the position operator \hat{x}_i . In fact, the existence of the minimal length implies that \hat{x}_i cannot have any eigenfunctions within either Hilbert spaces. Therefore, the meaning of the wave function in q -space is somewhat ambiguous. Nevertheless, the q -space representation is particularly useful when the Schrödinger equation cannot be solved exactly, since one can treat

$$\Delta H(\hat{\mathbf{q}}, \hat{\mathbf{p}}) = H'(\hat{\mathbf{q}}, \hat{\mathbf{p}}) - H(\hat{\mathbf{q}}, \hat{\mathbf{p}}) \quad (2.17)$$

as a perturbation and calculate the shifts in the energies via perturbation theory in q -space.

In the following, we look at the energy shifts induced by nonzero β and β' in the harmonic oscillator [77, 78], the Hydrogen atom [74, 79], and a particle in a uniform gravitational well [75, 76]. Since detailed derivations can be found in the respective references, we only provide an outline of the results in each case.

2.2.1. Harmonic Oscillator

Consider a D -dimensional isotropic harmonic oscillator. The Hamiltonian is of course

$$\hat{H} = \frac{\hat{\mathbf{P}}^2}{2m} + \frac{1}{2}m\omega^2\hat{\mathbf{x}}^2. \quad (2.18)$$

The p -space representation of the operators is

$$\hat{x}_i = i\hbar \left[\left(1 + \beta p^2\right) \frac{\partial}{\partial p_i} + \beta' p_i p_j \frac{\partial}{\partial p_j} + \left\{ \beta + \beta' \left(\frac{D+1}{2} \right) - \delta(\beta + \beta') \right\} p_i \right], \quad (2.19)$$

$$\hat{p}_i = p_i.$$

Here, δ is an arbitrary real parameter which can be used to simplify the representation of the operator \hat{x}_i at the expense of modifying the definition of the inner product in p -space to

$$\langle f | g \rangle_\delta = \int \frac{d^D \mathbf{p}}{[1 + (\beta + \beta') \mathbf{p}^2]^\delta} f^*(\mathbf{p}) g(\mathbf{p}). \quad (2.20)$$

The introduction of δ is a canonical transformation which does not affect the energy eigenvalues [76]. The choice

$$\delta = \frac{\beta + \beta' ((D + 1)/2)}{\beta + \beta'} \quad (2.21)$$

eliminates the third term in the expression for \hat{x}_i .

The rotational symmetry of the Hamiltonian, (2.18), allows us to write the wave function in p -space as a product of a radial wave-function and a D -dimensional spherical harmonic:

$$\Psi_D(\mathbf{p}) = R(p) Y_{\ell m_{D-2} m_{D-3} \dots m_2 m_1}(\Omega), \quad p \equiv |\mathbf{p}|. \quad (2.22)$$

The radial Schrödinger equation is then

$$\begin{aligned} -m\hbar\omega \left[\left\{ [1 + (\beta + \beta') p^2] \frac{\partial}{\partial p} \right\}^2 + \frac{(D-1)(1 + \beta p^2)[1 + (\beta + \beta') p^2]}{p} \frac{\partial}{\partial p} \right. \\ \left. - \frac{L^2(1 + \beta p^2)^2}{p^2} \right] R(p) + \frac{1}{m\hbar\omega} p^2 R(p) = \frac{2E}{\hbar\omega} R(p), \end{aligned} \quad (2.23)$$

where

$$L^2 = \ell(\ell + D - 2), \quad \ell = 0, 1, 2, \dots \quad (2.24)$$

is the eigenvalue of the angular momentum operator in D dimensions. The solution to (2.23) has been worked out in detail in [78], and the energy eigenvalues are

$$\begin{aligned} E_{n\ell} = \hbar\omega \left[\left(n + \frac{D}{2} \right) \sqrt{1 + \left\{ \beta^2 L^2 + \frac{(D\beta + \beta')^2}{4} \right\} m^2 \hbar^2 \omega^2} \right. \\ \left. + \left\{ (\beta + \beta') \left(n + \frac{D}{2} \right)^2 + (\beta - \beta') \left(L^2 + \frac{D^2}{4} \right) + \beta' \frac{D}{2} \right\} \frac{m\hbar\omega}{2} \right], \end{aligned} \quad (2.25)$$

with eigenfunctions given by

$$R_{n\ell}(p) = (\beta + \beta')^{D/4} \sqrt{\frac{2(2k + a + b + 1)k!\Gamma(k + a + b + 1)}{\Gamma(k + a + 1)\Gamma(k + b + 1)}} \left(\frac{1-z}{2}\right)^{\lambda/2} \left(\frac{1+z}{2}\right)^{\ell/2} P_k^{(a,b)}(z). \quad (2.26)$$

Here, $P_k^{(a,b)}(z)$ is the Jacobi polynomial of order $k = (n - \ell)/2$ with argument

$$z = \frac{(\beta + \beta')p^2 - 1}{(\beta + \beta')p^2 + 1},$$

$$a = \frac{1}{m\hbar\omega(\beta + \beta')} \sqrt{1 + \left\{ \beta^2 L^2 + \frac{(D\beta + \beta')^2}{4} \right\} m^2 \hbar^2 \omega^2}, \quad b = \frac{D}{2} + \ell - 1, \quad (2.27)$$

$$\lambda = \frac{D\beta + \beta'}{2(\beta + \beta')} + a.$$

Note that due to the $(n + D/2)^2$ -dependent term in (2.25), the energy levels are no longer uniformly spaced. Note also that, due to the explicit L^2 dependence, the original

$$\frac{(D + n - 1)!}{(D - 1)!n!} \quad (2.28)$$

fold degeneracy of the n th energy level, which was due to states with different k and ℓ sharing the same $n = 2k + \ell$, is resolved, leaving only the

$$\frac{(D + \ell - 1)!}{(D - 1)!\ell!} - \frac{(D + \ell - 3)!}{(D - 1)!(\ell - 2)!} \quad (2.29)$$

fold degeneracy for each value of ℓ due to rotational symmetry alone [80–82]. For example, in $D = 2$ dimensions, the $(n + 1)$ -fold degeneracy of the n th level breaks down to the 2-fold degeneracies between the pairs of $m = \pm\ell$ states. This is illustrated in Figure 2.

2.2.2. Hydrogen Atom

The introduction of a minimal length to the coulomb potential problem was first discussed by Born in 1933 [18]. There, it was argued that the singularity at $r = 0$ will be blurred out. Here, we find a similar effect. We consider the usual Hydrogen atom Hamiltonian in D dimensions:

$$\widehat{H} = \frac{\widehat{\mathbf{p}}^2}{2m} - \frac{e^2}{\widehat{r}}, \quad (2.30)$$

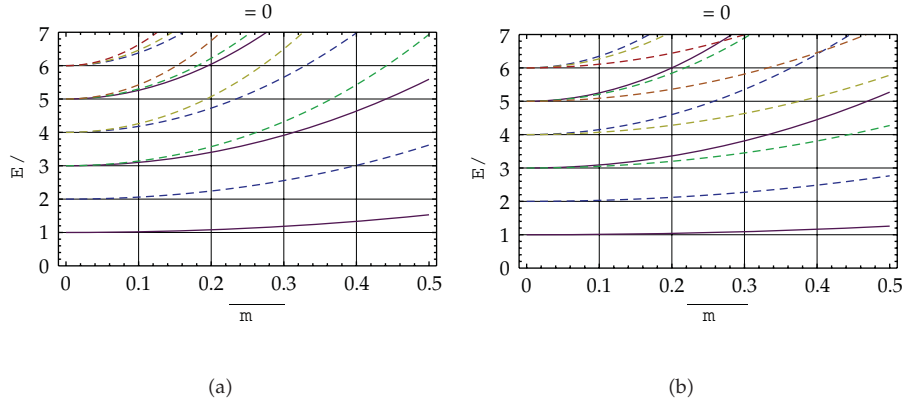


Figure 2: The energy levels of the 2D isotropic harmonic oscillator for the cases $\beta' = 0$ (left) and $\beta = 0$ (right). The purple solid lines indicate s -wave states which are singlets. The dashed lines are doublets with the color indicating that $\ell = 1$ (blue), $\ell = 2$ (green), $\ell = 3$ (yellow), $\ell = 4$ (orange), and $\ell = 5$ (red). $\sqrt{\beta m \hbar \omega}$ is the ratio of the minimal length $\hbar \sqrt{\beta}$ to the characteristic length scale $\sqrt{\hbar/m\omega}$ of the system.

where the operator $1/\hat{r}$ is defined as the inverse of the square root of the operator

$$\hat{r}^2 = \sum_{i=1}^D \hat{x}_i^2. \quad (2.31)$$

$1/\hat{r}$ will be best represented in the basis in which \hat{r}^2 is diagonal. The eigenvalues of \hat{r}^2 can be obtained from those of the harmonic oscillator, (2.25), by taking the limit $m \rightarrow \infty$:

$$\begin{aligned} r_{k\ell}^2 &= \lim_{m \rightarrow \infty} \frac{2E_{n\ell}}{m\omega^2} \\ &= \hbar^2(\beta + \beta') \left[\left\{ \left(2k + \ell + \frac{D}{2} \right) + \frac{1}{\beta + \beta'} \sqrt{\beta^2 L^2 + \frac{(D\beta + \beta')^2}{4}} \right\}^2 - \frac{\beta'}{\beta + \beta'} \left\{ L^2 + \frac{(D-1)^2}{4} \right\} \right]. \end{aligned} \quad (2.32)$$

The corresponding eigenfunctions are given by the same expression as (2.26) except with a replaced with

$$a = \frac{1}{\beta + \beta'} \sqrt{\beta^2 L^2 + \frac{(D\beta + \beta')^2}{4}}. \quad (2.33)$$

Denoting these eigenfunctions as $R_{k\ell}(p)$, we can define

$$\frac{1}{\hat{r}} R_{k\ell}(p) = \frac{1}{r_{k\ell}} R_{k\ell}(p). \quad (2.34)$$

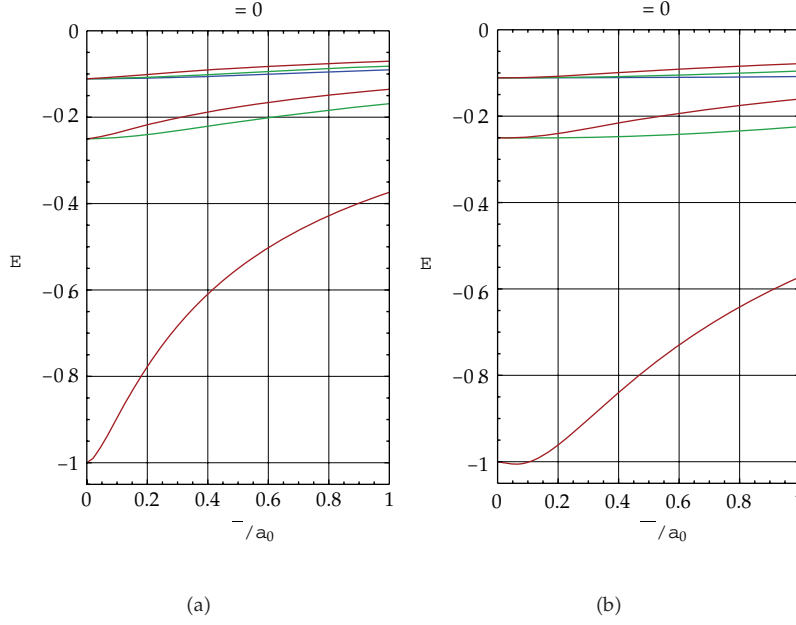


Figure 3: Energy shifts of the $n = 1, 2,$ and 3 states of the Hydrogen atom for the $\beta' = 0$ (left) and $\beta = 0$ (right) cases. $a_0 = \hbar^2/m_e^2$ is the Bohr radius, and the energy is in units of the Rydberg constant $e^2/2a_0$. The color of the lines indicates the orbital angular momentum: s (red), p (green), and d (blue). The s -wave states are affected nonperturbatively even for very small β or β' , indicating their sensitivity to the singularity of the Coulomb potential at the origin.

As in the harmonic oscillator case, the rotational symmetry of the Hamiltonian allows us to write an energy eigenstate wave function as a product of a radial wave function and a spherical harmonic. The radial wave function can then be expressed as a superposition of the \hat{r}^2 eigenfunctions with fixed ℓ :

$$R_\ell(p) = \sum_{k=0}^{\infty} f_k R_{k\ell}(p). \quad (2.35)$$

The radial Schrödinger equation will impose a recursion relation on the coefficients f_n , which can be solved numerically on a computer. The condition that the resulting function be square integrable determines the eigenvalues E . The detailed procedure can be found in [76, 79]. Here, we only display the results for the $D = 3$ case in Figure 3. As can be seen, the degeneracy between difference angular momentum states is lifted, just as in the harmonic oscillator case.

It is also possible to calculate the energy shifts perturbatively using the q -space representation for the cases $D \geq 4$ or $\ell \neq 0$. The unperturbed energy eigenfunctions in D dimensions are

$$R_{n\ell}(q) = \sqrt{\frac{2^{2D}}{a_0^D (2n + D - 3)^{D+1}} \frac{(n - \ell - 1)!}{(n + \ell + D - 3)!}} e^{-\rho/2} \rho^\ell L_{n-\ell-1}^{(2\ell+D-2)}(\rho), \quad (2.36)$$

where $a_0 = \hbar^2/m_e^2$ is the Bohr radius, $L_k^{(\lambda)}(\rho)$ the order k Laguerre polynomial, and

$$\rho = \frac{2q}{a_0(n + ((D-3)/2))}. \quad (2.37)$$

The eigenvalues are

$$E_n = -\frac{e^2}{2a_0(n + ((D-3)/2))^2}, \quad n = 1, 2, 3, \dots \quad (2.38)$$

The operator $1/\hat{r}$ can be expanded in powers of β and β' as [76]

$$\begin{aligned} \frac{1}{\hat{r}} &= \frac{1}{q} + \hbar^2\beta \left(\frac{1}{q} \frac{\partial^2}{\partial q^2} + \frac{D-2}{q^2} \frac{\partial}{\partial q} - \frac{L^2 + D-2}{q^3} \right) + \hbar^2\beta' \left(\frac{1}{q} \frac{\partial^2}{\partial q^2} + \frac{D-2}{q^2} \frac{\partial}{\partial q} + \frac{D^2 - 5D + 8}{4q^3} \right) \\ &+ \dots, \end{aligned} \quad (2.39)$$

and the expectation value of the extra terms converges for $\ell \neq 0$ or $D \geq 4$, yielding

$$\begin{aligned} \Delta E_{n\ell} &= \frac{e^2}{a_0(n + ((D-3)/2))^3} \frac{\hbar^2}{a_0^2} \left[\frac{(D-1)(2\beta - \beta')}{4(\ell + ((D-3)/2))(\ell + ((D-2)/2))(\ell + ((D-1)/2))} \right. \\ &\quad \left. + \frac{(2\beta + \beta')}{(\ell + ((D-2)/2))} - \frac{(\beta + \beta')}{(n + ((D-3)/2))} \right], \end{aligned} \quad (2.40)$$

which agrees very well with the numerical results for all cases to which it is applicable. For $D = 3$, this formula reduces to

$$\Delta E_{n\ell} = \frac{e^2}{a_0 n^3} \frac{\hbar^2}{a_0^2} \left[\frac{(2\beta - \beta')}{2\ell(\ell + (1/2))(\ell + 1)} + \frac{(2\beta + \beta')}{(\ell + (1/2))} - \frac{(\beta + \beta')}{n} \right], \quad (2.41)$$

which is clearly problematic for $\ell = 0$. This is due to the breakdown of the expansion equation (2.39) near $q = 0$ for $D \leq 3$. Physically, this can be interpreted to mean that the s -wave in 3D and lower dimensions is sensitive to the nonperturbative resolution of the singularity at the origin due to the minimal length. Interestingly, in 4D and higher, there are enough spatial dimensions for the wavefunction to spread out around the origin so that even the s -wave is insensitive to the singularity, and the effect of the minimal length becomes perturbative.

2.2.3. Uniform Gravitational Potential

This subsection is based on unpublished material by Benczik in [76]. Consider the 1D motion of a particle in a linear potential

$$V(x) = \begin{cases} mgx & x > 0, \\ \infty & x \leq 0. \end{cases} \quad (2.42)$$

The Hamiltonian is

$$\widehat{H} = \frac{\widehat{p}^2}{2m} + mg\widehat{x}. \quad (2.43)$$

Since \widehat{x} does not have any eigenstates within the Hilbert space, the condition $x > 0$ is replaced with $\langle \widehat{x} \rangle > 0$. In the q -space representation, the operators are given by

$$\begin{aligned} \widehat{x} &= q \left(1 - \hbar^2 \beta \frac{d^2}{dq^2} \right), \\ \widehat{p} &= \frac{\hbar}{i} \frac{d}{dq}, \end{aligned} \quad (2.44)$$

and the Schrödinger equation becomes

$$\widehat{H}\psi = -\frac{\hbar^2}{2m} \frac{d^2\psi}{dq^2} + mgq \left(1 - \hbar^2 \beta \frac{d^2}{dq^2} \right) \psi = E\psi. \quad (2.45)$$

The condition $\langle \widehat{x} \rangle > 0$ can be imposed by restricting the domain of q to $q > 0$ and demanding that the wave function vanish at $q = 0$. The solution to the $\beta = 0$ case is given by the Airy function

$$\psi_n(q) = \frac{1}{|\text{Ai}'(\alpha_n)|} \text{Ai}\left(\frac{q}{a} + \alpha_n\right), \quad a = \left[\frac{\hbar^2}{2m^2g} \right]^{1/3}, \quad (2.46)$$

with eigenvalues

$$\frac{E_n}{mga} = -\alpha_n, \quad (2.47)$$

where

$$\dots < \alpha_3 < \alpha_2 < \alpha_1 < 0 \quad (2.48)$$

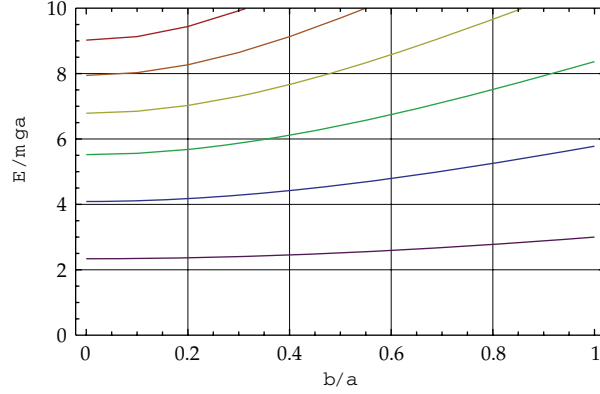


Figure 4: The b dependence of the lowest energy levels of a particle of mass m in a linear gravitational potential $V(x) = mgx$ with $x > 0$. $a = [\hbar^2/2m^2g]^{1/3}$ is the characteristic length scale of the system, and $b = \hbar\sqrt{\beta}$ is the minimal length.

are the zeroes of $\text{Ai}(z)$. The solution to the $\beta \neq 0$ case is given in terms of the confluent hypergeometric function of the second kind [83–85]

$$\psi(q) \propto e^{-q/b} U\left(-\frac{1}{2} \left[\frac{E}{mgb} + \frac{a^3}{b^3} \right]; 0; 2 \left[\frac{a^3}{b^3} + \frac{q}{b} \right] \right), \quad a = \left[\frac{\hbar^2}{2m^2g} \right]^{1/3}, \quad b = \hbar\sqrt{\beta}. \quad (2.49)$$

The energy eigenvalues are determined by the condition

$$U\left(-\frac{1}{2} \left[\frac{E}{mgb} + \frac{a^3}{b^3} \right]; 0; \frac{2a^3}{b^3} \right) = 0, \quad (2.50)$$

which can be solved numerically using Mathematica. In Figure 4, we plot the b dependence of the energies of the lowest lying states. The energies of higher-dimensional cases, in which there are one or more spatial dimensions orthogonal to the potential direction, are discussed in [75, 76].

2.3. Experimental Constraints

As these three examples show, the main effect of the introduction of the minimal length into quantum mechanical systems is the shifts in energy levels which also leads to the breaking of well-known degeneracies. The natural question arises whether these shifts can be used to constrain the minimal length experimentally. Of course, if the minimal length is at the Planck scale, detecting its actual effect would be impossible. However, the exercise is of interest to models of large extra dimensions which possess a much lower effective Planck scale than the 4D value [86–89].

In the case of the harmonic oscillator, actual physical systems are never completely harmonic, so it is difficult to distinguish the shift in energy due to anharmonicity with that due to a possible minimal length. Reference [78] considers using the energy levels of an electron

in a Penning trap to constrain β and finds that even under highly optimistic and unrealistic assumptions, the best bound that can be hoped for is

$$\frac{1}{\sqrt{\beta}} \gtrsim 1 \text{ GeV}/c. \quad (2.51)$$

References [76, 79] consider placing a bound on β using the 1S Lamb shift of the hydrogen atom. The current best experimental value is that given by Schwob et al. in [90]

$$L_{1s}^{\text{exp}} = 8172.837(22) \text{ MHz}. \quad (2.52)$$

This is to be compared with the theoretical value, for which we use that given in [91, 92]

$$L_{1s}^{\text{th}} = 8172.731(40) \text{ MHz}. \quad (2.53)$$

The calculation requires the experimentally determined proton rms charge radius r_p as an input, and the error on L_{1s}^{th} is dominated by the experimental error on r_p . Here, the value of $r_p = 0.862(12) \text{ fm}$ [93] was used. Attributing the entire discrepancy to β ($\beta' = 0$), [76, 79] cite

$$\frac{1}{\sqrt{\beta}} \gtrsim 7 \text{ GeV}/c, \quad (2.54)$$

which is only slightly better than (2.51). There is no bound on β' ($\beta = 0$) since the shift is in the wrong direction as can be seen in Figure 3.

The energy levels of neutrons in a linear gravitational potential have been measured by Nesvizhevsky et al. [94–96]. However, as analyzed by Brau and Buisseret [75], the experimental precision is still very many orders of magnitude above what is necessary to place a meaningful bound on β . The current lower bound on $1/\sqrt{\beta}$ is on the order of $100 \text{ eV}/c$.

3. Classical Limit: The Liouville Theorem and the Density of States

Note that rewriting our 1D-deformed commutator as

$$[\hat{x}, \hat{p}] = i\hbar A(\hat{p}^2) \quad (3.1)$$

suggests that $\hbar A(p^2)$ takes on the role of a momentum-dependent Planck constant. Given that \hbar determines the size of a quantum mechanical state in phase space, a momentum-dependent \hbar would imply that the size of this state must scale according to $A(p^2)$ as it evolves. To see whether this interpretation makes sense, we formally take the naive classical limit by replacing commutators with Poisson brackets,

$$\frac{1}{i\hbar} [\hat{x}, \hat{p}] = A(\hat{p}^2) \longrightarrow \{x, p\} = A(p^2), \quad (3.2)$$

and proceed to derive the analogue of Liouville's theorem [97]. The Poisson brackets among the x_i 's and p_i 's for the multidimensional case are

$$\begin{aligned} \{x_i, p_j\} &= A\delta_{ij} + Bp_i p_j, \\ \{p_i, p_j\} &= 0, \\ \{x_i, x_j\} &= -\left[\frac{2(A + B\mathbf{p}^2)}{A} \frac{dA}{d\mathbf{p}^2} - B\right](x_i p_j - x_j p_i). \end{aligned} \quad (3.3)$$

The generic Poisson bracket of arbitrary functions of the coordinates and momenta can then be defined as

$$\{F, G\} = \left(\frac{\partial F}{\partial x_i} \frac{\partial G}{\partial p_j} - \frac{\partial F}{\partial p_i} \frac{\partial G}{\partial x_j}\right) \{x_i, p_j\} + \frac{\partial F}{\partial x_i} \frac{\partial G}{\partial x_j} \{x_i, x_j\}. \quad (3.4)$$

Here, we use the convention that repeated indices are summed. Assuming that the equations of motion of x_i and p_i are given formally by

$$\begin{aligned} \dot{x}_i &= \{x_i, H\} = \{x_i, p_j\} \frac{\partial H}{\partial p_j} + \{x_i, x_j\} \frac{\partial H}{\partial x_j}, \\ \dot{p}_i &= \{p_i, H\} = -\{x_j, p_i\} \frac{\partial H}{\partial x_j}, \end{aligned} \quad (3.5)$$

the evolution of x_i and p_i during an infinitesimal time interval δt is found to be

$$\begin{aligned} x'_i &= x_i + \dot{x}_i \delta t = x_i + \left[\{x_i, p_j\} \frac{\partial H}{\partial p_j} + \{x_i, x_j\} \frac{\partial H}{\partial x_j} \right] \delta t, \\ p'_i &= p_i + \dot{p}_i \delta t = p_i - \{x_j, p_i\} \frac{\partial H}{\partial x_j} \delta t. \end{aligned} \quad (3.6)$$

To find the change in phase-space volume associated with this evolution, we calculate the Jacobian of the transformation from $(x_1, x_2, \dots, x_D; p_1, p_2, \dots, p_D)$ to $(x'_1, x'_2, \dots, x'_D; p'_1, p'_2, \dots, p'_D)$

$$d^D \mathbf{x}' d^D \mathbf{p}' = \left| \frac{\partial(x'_1, x'_2, \dots, x'_D; p'_1, p'_2, \dots, p'_D)}{\partial(x_1, x_2, \dots, x_D; p_1, p_2, \dots, p_D)} \right| d^D \mathbf{x} d^D \mathbf{p}. \quad (3.7)$$

Since

$$\begin{aligned} \frac{\partial x'_i}{\partial x_j} &= \delta_{ij} + \frac{\partial \dot{x}_i}{\partial x_j} \delta t, & \frac{\partial x'_i}{\partial p_j} &= \frac{\partial \dot{x}_i}{\partial p_j} \delta t, \\ \frac{\partial p'_i}{\partial x_j} &= \frac{\partial \dot{p}_i}{\partial x_j} \delta t, & \frac{\partial p'_i}{\partial p_j} &= \delta_{ij} + \frac{\partial \dot{p}_i}{\partial p_j} \delta t, \end{aligned} \quad (3.8)$$

we find that

$$\left| \frac{\partial(x'_1, x'_2, \dots, x'_D; p'_1, p'_2, \dots, p'_D)}{\partial(x_1, x_2, \dots, x_D; p_1, p_2, \dots, p_D)} \right| = 1 + \left(\frac{\partial \dot{x}_i}{\partial x_i} + \frac{\partial \dot{p}_i}{\partial p_i} \right) \delta t + O(\delta t^2), \quad (3.9)$$

where

$$\begin{aligned} \frac{\partial \dot{x}_i}{\partial x_i} + \frac{\partial \dot{p}_i}{\partial p_i} &= \frac{\partial}{\partial x_i} \left[\{x_i, p_j\} \frac{\partial H}{\partial p_j} + \{x_i, x_j\} \frac{\partial H}{\partial x_j} \right] + \frac{\partial}{\partial p_i} \left[-\{x_j, p_i\} \frac{\partial H}{\partial x_j} \right] \\ &= \frac{\partial}{\partial x_i} [\{x_i, x_j\}] \frac{\partial H}{\partial x_j} - \frac{\partial}{\partial p_i} [\{x_j, p_i\}] \frac{\partial H}{\partial x_j} \\ &= -(D-1) \left[\frac{2(A+B\mathbf{p}^2)}{A} \frac{dA}{d\mathbf{p}^2} - B \right] p_j \frac{\partial H}{\partial x_j} - \left[2 \frac{dA}{d\mathbf{p}^2} + 2 \frac{dB}{d\mathbf{p}^2} \mathbf{p}^2 + (D+1)B \right] p_j \frac{\partial H}{\partial x_j} \\ &= - \left[(D-1) \left(\frac{2(A+B\mathbf{p}^2)}{A} \frac{dA}{d\mathbf{p}^2} \right) + 2 \left(\frac{dA}{d\mathbf{p}^2} + \frac{dB}{d\mathbf{p}^2} \mathbf{p}^2 + B \right) \right] p_j \frac{\partial H}{\partial x_j}. \end{aligned} \quad (3.10)$$

On the other hand, using

$$\delta \mathbf{p}^2 = 2p_i \delta p_i = 2p_i \dot{p}_i \delta t = -2(A+B\mathbf{p}^2) p_j \frac{\partial H}{\partial x_j} \delta t, \quad (3.11)$$

we have

$$\begin{aligned} A' &= A + \frac{dA}{d\mathbf{p}^2} \delta \mathbf{p}^2 \\ &= A \left[1 - \left(\frac{2(A+B\mathbf{p}^2)}{A} \frac{dA}{d\mathbf{p}^2} \right) p_j \frac{\partial H}{\partial x_j} \delta t \right], \\ A' + B' \mathbf{p}'^2 &= (A+B\mathbf{p}^2) + \left(\frac{dA}{d\mathbf{p}^2} + \frac{dB}{d\mathbf{p}^2} \mathbf{p}^2 + B \right) \delta \mathbf{p}^2 \\ &= (A+B\mathbf{p}^2) \left[1 - 2 \left(\frac{dA}{d\mathbf{p}^2} + \frac{dB}{d\mathbf{p}^2} \mathbf{p}^2 + B \right) p_j \frac{\partial H}{\partial x_j} \delta t \right], \end{aligned} \quad (3.12)$$

where we have used the shorthand $A' = A(\mathbf{p}'^2)$ and $B' = B(\mathbf{p}'^2)$. Thus,

$$\begin{aligned} &\frac{(A')^{D-1} (A' + B' \mathbf{p}'^2)}{A^{D-1} (A + B \mathbf{p}^2)} \\ &= \left[1 - \left\{ (D-1) \left(\frac{2(A+B\mathbf{p}^2)}{A} \frac{dA}{d\mathbf{p}^2} \right) + 2 \left(\frac{dA}{d\mathbf{p}^2} + \frac{dB}{d\mathbf{p}^2} \mathbf{p}^2 + B \right) \right\} p_j \frac{\partial H}{\partial x_j} \delta t \right]. \end{aligned} \quad (3.13)$$

Comparing (3.10) and (3.13), it is clear that the ratio

$$\frac{d^D \mathbf{x} d^D \mathbf{p}}{A^{D-1}(A + B\mathbf{p}^2)} \quad (3.14)$$

is invariant under time evolution.

This behavior of the phase space volume can be demonstrated using simple Hamiltonians. In [98], we solve the harmonic oscillator and coulomb potential problems for the case $A = 1 + \beta\mathbf{p}^2$ and $B = \beta'$. There, in addition to the behavior of the phase space, it is found that the orbits of particles in these potentials no longer close on themselves. This is consistent with the breaking of degeneracies observed in the quantum cases which are associated with the conservation of the Runge-Lenz vector.

For the case $B = 0$, (3.14) reduces to $d^D \mathbf{x} d^D \mathbf{p} / A^D$, and our interpretation of $\hbar A(p^2)$ as the momentum dependent Planck constant which determines the size of a unit quantum cell becomes apparent. Integrating (3.14) over space,

$$\frac{1}{V} \int \frac{d^D \mathbf{x} d^D \mathbf{p}}{A^{D-1}(A + B\mathbf{p}^2)} = \frac{d^D \mathbf{p}}{A^{D-1}(A + B\mathbf{p}^2)}, \quad (3.15)$$

we can identify

$$\rho(\mathbf{p}^2) = \frac{1}{A^{D-1}(A + B\mathbf{p}^2)} \quad (3.16)$$

as the density of states in momentum space. At high momentum where A and $B\mathbf{p}^2$ become large, $\rho(\mathbf{p}^2)$ will be suppressed. We look at the impact of this suppression on the cosmological constant problem next.

4. Vacuum Energy and the Minimal Length

4.1. The Cosmological Constant and the Density of States

The origin of the cosmological constant $\Lambda = 3H_0^2\Omega_\Lambda$ remains a mystery, and its understanding presents a major challenge to theoretical physics [8–12]. It is a contentious issue for string theory, notwithstanding its being the leading candidate for quantum gravity, though various hints exist that may point towards its resolution [99, 100]. Furthermore, the problem has recently assumed added urgency due to observations that the cosmological constant is small, positive, and clearly nonzero [101, 102]. In terms of the parameter Ω_Λ , the most-up-to date value is $\Omega_\Lambda \sim 0.73$. With the Hubble parameter $h \sim 0.7$ (the parameter h is defined as $h = H_0 / (100 \text{ km/s/Mpc})$), we obtain as the vacuum energy density

$$\begin{aligned} \frac{c^2 \Lambda}{8\pi G_N} &= c^2 \rho_{\text{crit}} \Omega_\Lambda = \left(\frac{3H_0^2 c^2}{8\pi G_N} \right) \Omega_\Lambda \\ &= (8.096 \times 10^{-47} \text{ GeV}^4 / \hbar^3 c^3) (\Omega_\Lambda h^2) \sim 10^{-47} \text{ GeV}^4 / \hbar^3 c^3. \end{aligned} \quad (4.1)$$

The order of magnitude of this result is set by the dimensionful prefactor in the parentheses which can be expressed in terms of the Planck length $\ell_P = \hbar/\mu_P = \sqrt{\hbar G_N/c^3} \sim 10^{-35}$ m, and the scale of the visible universe $\ell_0 = \hbar/\mu_0 \equiv c/H_0 \sim 10^{26}$ m as

$$\frac{H_0^2 c^2}{G_N} = \frac{c}{\hbar^3 \mu_P^2 \mu_0^2} = \frac{\hbar c}{\ell_P^2 \ell_0^2}. \quad (4.2)$$

In quantum field theory (QFT), the cosmological constant is calculated as the sum of the vacuum fluctuation energies of all momentum states. This is clearly infinite, so the integral is usually cut off at the Planck scale $\mu_P = \hbar/\ell_P$ beyond which spacetime itself is expected to become foamy [4], and the calculation untrustworthy. For a massless particle, we find that

$$\begin{aligned} \frac{1}{(2\pi\hbar)^3} \int^{\mu_P} d^3\mathbf{p} \left[\frac{1}{2} \hbar \omega_p \right] &= \frac{c}{4\pi^2 \hbar^3} \int_0^{\mu_P} dp p^3 = \frac{c}{16\pi^2 \hbar^3} \mu_P^4 \\ &= \frac{\hbar c}{16\pi^2} \frac{1}{\ell_P^4} \sim 10^{74} \text{ GeV}^4 / \hbar^3 c^3, \end{aligned} \quad (4.3)$$

which is about 120 orders of magnitude above the measured value. Note that this difference is essentially a factor of $(\ell_0/\ell_P)^2$, the scale of the visible universe in Planck units squared. The change in the density of states suggested by the MLUR would change this calculation to

$$\frac{1}{(2\pi\hbar)^3} \int_0^\infty d^3\mathbf{p} \rho(\mathbf{p}^2) \left[\frac{1}{2} \hbar \omega_p \right] = \frac{c}{4\pi^2 \hbar^3} \int_0^\infty dp \frac{p^3}{A(p^2)^2 [A(p^2) + p^2 B(p^2)]}. \quad (4.4)$$

For the case $A(p^2) = 1 + \beta p^2$, $B(p^2) = 0$, we find [97] that

$$\frac{c}{4\pi^2 \hbar^3} \int_0^\infty dp \frac{p^3}{(1 + \beta p^2)^3} = \frac{c}{16\pi^2 \hbar^3 \beta^2} = \frac{c}{16\pi^2 \hbar^3 \mu_s^4} = \frac{\hbar c}{16\pi^2} \frac{1}{\ell_s^4}, \quad \ell_s = \frac{\hbar}{\mu_s} = \hbar \sqrt{\beta}. \quad (4.5)$$

The integral is finite, without a UV cutoff, due to the suppression of the contribution of high momentum states. (There is an intriguing similarity here with Planck's resolution of the UV catastrophe of the black body radiation.) However, if we make the identification $\ell_s = \ell_P$, then this result is identical to (4.3), and nothing is gained. Of course, this is not surprising given that ℓ_s is the only scale in the calculation and effectively plays the role of the UV cutoff. To obtain the correct value of the cosmological constant from the above expression, we must choose $\ell_s \sim \sqrt{\ell_P \ell_0} \sim 10^{-5}$ m, which is too large to be the minimal length, or equivalently, $\mu_s = \hbar/\ell_s \sim \sqrt{\mu_P \mu_0} \sim 10^{-3}$ eV/c, which is too small to be the UV cutoff. However, we mention in passing that $\sqrt{\ell_P \ell_0}$ can be considered the uncertainty in measuring ℓ_0 due to the foaminess of spacetime [4, 103, 104] and has been argued as the possible size of a spacetime quantum cell when quantum gravity is properly taken into account [105–114]. At the moment, this point of view seems difficult to reconcile with phenomenological considerations.

We could introduce a second scale into the problem by letting $B(p^2) = \beta' \neq 0$. This leads to

$$\frac{c}{4\pi^2\hbar^3} \int_0^\infty dp \frac{p^3}{(1 + \beta p^2)^2 [1 + (\beta + \beta') p^2]} = \frac{c}{8\pi^2\hbar^3} \frac{1}{\beta\beta'} \left[1 - \frac{\beta}{\beta'} \ln\left(1 + \frac{\beta'}{\beta}\right) \right] \quad (4.6)$$

$$\xrightarrow{\beta' \gg \beta} \frac{c}{8\pi^2\hbar^3} \frac{1}{\beta\beta'} = \frac{c}{8\pi^2\hbar^3} \mu_s^2 \mu_s'^2 = \frac{\hbar c}{8\pi^2} \frac{1}{\ell_s'^2 \ell_s^2} ,$$

where $\ell_s' = \hbar/\mu_s' = \hbar\sqrt{\beta'}$. If we identify $\ell_s = \ell_p$, then we must have $\ell_s' \sim \ell_0$, which is even more problematic than $\sqrt{\ell_p \ell_0}$.

As these considerations show, our simple choice for $A(p^2)$ and $B(p^2)$ succeeds in rendering the cosmological constant finite but does not provide an adequate suppression. Would some other choice of $A(p^2)$ and $B(p^2)$ do better? To this end, let us try to see whether we can reverse engineer these functions so that the correct order of magnitude is obtained. Let us write

$$\epsilon^4 = \int_0^\infty dp \rho(p^2) p^3. \quad (4.7)$$

To generate the correct value for the cosmological constant, we must have $\epsilon \sim \sqrt{\mu_P \mu_0} = 10^{-3} \text{ eV}/c$, as we have seen. At this point, we invoke some numerology and note that if the SUSY breaking scale μ_{SUSY} is on the order of a few TeV/ c , then the seesaw formula,

$$\epsilon \sim \frac{\mu_{\text{SUSY}}^2}{\mu_P} \sim 10^{-3} \text{ eV}/c, \quad (4.8)$$

would give the correct size for ϵ as observed by Banks [115]. This expression is reminiscent of the well-known seesaw mechanism used to explain the smallness of neutrino masses [116–119]. One way to obtain this result is to have the density of states scale as $\rho(p^2) \sim p^4/\mu_P^4$ and place the UV cutoff at μ_{SUSY} , beyond which the bosonic and fermionic contributions cancel. This would yield $\epsilon^4 \sim \mu_{\text{SUSY}}^8/\mu_P^4$. Unfortunately, this density of states is problematic since $p^4/\mu_P^4 \ll 1$ for the entire integration region, so we are effectively suppressing everything. Furthermore, to obtain this suppression, we must have $A(p^2) \sim (\mu_P/p)^{4/3} \gg 1$, making the effective value of \hbar , and thus the size of the quantum cell, huge at low energies in clear contradiction to reality.

In retrospect, this result is not surprising since raising the UV cutoff from $\sqrt{\mu_P \mu_0} \sim 10^{-3} \text{ eV}/c$ to much higher values naturally requires the drastic suppression of contributions from below the cutoff. Thus, it is clear that the modification to the density of states, as suggested by the MLUR, by itself cannot solve the cosmological constant problem.

4.2. Need for a UV/IR Relation and a Dynamical Energy-Momentum Space

In the above discussion of summing over momentum states, the unstated assumption was that states at different momentum scales were independent, and that their total effect on the vacuum energy was the simple sum of their individual contributions. Of course, this

assumption is the basis of the decoupling between small (IR) and large (UV) momentum scales which underlies our use of effective field theories. However, there are hints that this assumption is what needs to be reevaluated in order to solve the cosmological constant problem.

First and foremost, the expression for the vacuum energy density itself, $H_0^2 c^2 / G_N = \hbar c / \ell_p^2 \ell_0^2$, is dependent upon an IR scale ℓ_0 and a UV scale ℓ_p , suggesting that whatever theory that explains its value must be aware of both scales and have some type of dynamical connection between them. Note that effective QFT's are not of this type but string theory is, given the UV/IR mixing relations discovered in several contexts as mentioned in the introduction.

Second, the contributions of the sub-Planckian modes ($p < \mu_p$) independently by themselves are clearly too large, and there is a limit to the tweaking that can be done to the density of states in the IR since those modes undeniably exist. The only way out of the dilemma would be to cancel the contribution of the IR sub-Planckian modes against those of something else, say that coming from the UV trans-Planckian modes ($p > \mu_p$) by introducing a dynamical connection between the two regimes [115].

That the sub-Planckian ($p < \mu_p$) and trans-Planckian ($p > \mu_p$) modes should cancel against each other is also suggested by the following argument: consider how the MLUR, (2.1), would be realized in field theory. The usual Heisenberg relation $\delta x \delta p = \hbar/2$ is a simple consequence of the fact that coordinate and momentum spaces are Fourier transforms of each other. The more one wishes to localize a wave packet in coordinate space (smaller δx), the more momentum states one must superimpose (larger δp). In the usual case, there is no lower bound to δx one may localize the wave packet as much as one likes by simply superimposing states with ever larger momentum, and thus ever shorter wavelength, to cancel out the tails of the coordinate space distributions. On the other hand, the MLUR implies that if one keeps on superimposing states with momenta beyond $\mu_p = 1/\sqrt{\beta}$, then δx ceases to decrease and starts increasing instead. (See Figure 1.) The natural interpretation of such a phenomenon would be that the trans-Planckian modes ($p > \mu_p$) when superimposed with the sub-Planckian ones ($p < \mu_p$) would “jam” the sub-Planckian modes and prevent them from canceling out the tails of the wave-packets effectively. The mechanism we envision here is analogous to the “jamming” behavior seen in nonequilibrium statistical physics, in which systems are found to freeze with increasing temperature [120–123]. In fact, it has been argued that such “freezing by heating” could be characteristic of a background-independent quantum theory of gravity [124–128].

We should also note, that in our calculation presented above, the phase space over which the integration was performed was fixed and flat. Quantum gravity will naturally change the situation, leading to a fluctuating dynamical spacetime background. Furthermore, the MLUR implies that energy-momentum space will be a fluctuating dynamical entity as well [129–134]. First, the necessity of “jamming” between the sub-Planckian and trans-Planckian modes to implement the MLUR in field theory clearly illustrates that momentum space cannot be the simple Fourier transform of coordinate space but must rather be an independent entity. (Introducing a momentum space independent from coordinate space in field theory would make the wave-particle duality more complete in a sense, since for particles, momenta and coordinates are independent until the equation of motion, is imposed [135].) Second, the quantum properties of spacetime geometry may be understood in terms of effective expressions that involve the spacetime uncertainties:

$$g_{ab}(x) dx^a dx^b \longrightarrow g_{ab}(x) \delta x^a \delta x^b. \quad (4.9)$$

The UV/IR relation $\delta x \sim \hbar\beta\delta p$ in the trans-Planckian region implies that this geometry of spacetime uncertainties can be transferred directly to the space of energy-momentum uncertainties, endowing it with a geometry as well:

$$g_{ab}(x)\delta x^a\delta x^b \longrightarrow G_{ab}(p)\delta p^a\delta p^b. \quad (4.10)$$

The usual intuition that local properties in spacetime correspond to non-local features of energy-momentum space (as implied by the canonical uncertainty relations) is obviated by the linear relation between the uncertainties in coordinate space and momentum space.

What would a dynamical energy-momentum space entail? Let us speculate. It has been argued that a dynamical spacetime, with its foamy UV structure [4], would manifest itself in the IR via the uncertainties in the measurements of global spacetime distances as [103–114]

$$\delta\ell \sim \sqrt{\ell\ell_P}, \quad (4.11)$$

a relation which is reminiscent of the famous result for Brownian motion derived by Einstein [136] and is also covariant in 3 + 1 dimensions. Let us assume that a similar “Brownian” relation holds in energy-momentum space due to its “foaminess” [134]

$$\delta\mu \sim \sqrt{\mu\mu_P}. \quad (4.12)$$

If the energy-momentum space has a finite size, a natural UV cutoff, at $\mu_+ \gg \mu_P$, (a maximum energy/momentum is introduced in deformed special relativity [137–140]), then its fluctuation $\delta\mu_+$ will be given by $\delta\mu_+ = \sqrt{\mu_+\mu_P} \gg \mu_P$. The MLUR implies that the mode at this scale must cancel, or “jam,” against another which shares the same δx , namely, the mode with an uncertainty given by $\delta\mu_- = \mu_P^2/\delta\mu_+ = \mu_P\sqrt{\mu_P/\mu_+} = \sqrt{\mu_-\mu_P} \ll \mu_P$, that is,

$$\mu_- = \frac{\mu_P^2}{\mu_+} = \frac{\delta\mu_-^2}{\mu_P} \ll \mu_P. \quad (4.13)$$

All modes between μ_- and μ_+ will “jam.” Therefore, μ_- will be the effective UV cutoff of the momentum integral and not μ_+ , which would yield

$$\epsilon^4 \sim \mu_-^4 \sim \frac{\delta\mu_-^8}{\mu_P^4} \sim \frac{\mu_P^8}{\mu_+^4}. \quad (4.14)$$

This reproduces the seesaw formula, (4.8), and if $\delta\mu_- \sim \text{few TeV}/c$, we obtain the correct cosmological constant.

5. Outlook: What Is String Theory?

In the concluding section, we wish to discuss a few implications of our work for non-perturbative string theory and the question: what is string theory [13]? Our discussion of this difficult question, being limited by the scope of our work on the minimal length, will necessarily be a bit speculative.

Our toy model for the MLUR was essentially algebraic. As such, it raises the possibility that more general algebraic structures may play a key role in nonperturbative string theory. In the introductory section, we mentioned that the MLUR is motivated by the scattering of string-like excitations in first quantized string theory. If one takes into account other objects in nonperturbative string theory, such as D -branes, one is led to the STUR, (1.6), proposed by Yoneya. The STUR generalizes the MLUR, and can be further generalized to a cubic form (motivated by M -theory) [67–73]

$$\delta x \delta y \delta t \sim \ell_p^3 / c. \quad (5.1)$$

Given the usual interpretation of the canonical Heisenberg uncertainty relations in terms of fundamental commutators, one might look for the associated cubic algebraic structures in string theory.

Another hint of cubic algebraic structure appears in the nonperturbative formulation of open string field theory by Witten et al. [141, 142]. The Witten action for the classical open string field, Φ , is of an abstract Chern-Simons type

$$S_o(\Phi) = \int \Phi \star \Phi \star \Phi. \quad (5.2)$$

Here, the star product is defined by the world-sheet path integral,

$$F \star G = \int DX F(X) G(X) \exp \left[\frac{i}{\alpha'} S_P(X) \right], \quad (5.3)$$

which is in turn determined by the world-sheet Polyakov action

$$S_P(X) = \frac{1}{2} \int d^2 \sigma \sqrt{-g} g^{ab} \partial_a X^i \partial_b X^j G_{ij} + \dots. \quad (5.4)$$

The fully quantum open string field theory is then, in principle, defined by yet another path integral in the infinite dimensional space of Φ , that is,

$$\int D\Phi \exp \left[\frac{i}{g_c} S_o(\Phi) \right]. \quad (5.5)$$

A more general, and in principle nonassociative structure, appears in Strominger's formulation of closed string field theory, which is also cubic [143]. Strominger's paper mentions the relevance of the 3-cocycle structure for this formulation of closed string field theory. Very schematically

$$S_c(\Psi) = \int \Psi \times (\Psi \times \Psi), \quad (5.6)$$

where \times is a nonassociative product defined in [143]. (For the role of nonassociativity in the theories of gravity, and a relation between Einstein's gravity and nonassociative Chern-Simons theory, see [144]).

Is there an underlying algebraic structure that could give rise to these cubic structures? In our toy model, the 2-bracket appears quite naturally. Such structures can be naturally generalized into 3-bracket. For example, the usual Lie algebra structure known from gauge theories, $[T_A, T_B] = f_{ABC}T_C$, where the structure constants f_{ABC} satisfy the usual Jacobi identity, seems to be naturally generalized to a triple algebraic structure

$$[T_A, T_B, T_C] = f_{ABCD}T_D, \quad (5.7)$$

where

$$[A_i, A_j, A_k] \equiv \epsilon^{abc} A_a A_b A_c, \quad (5.8)$$

with the structure constants f_{ABCD} satisfying a quartic fundamental identity [145–149]. These structures occur in the context of the theory of N -membranes [150]. They are also present in more elementary examples. Consider a charged particle e of mass m in the external magnetic field \mathbf{B} . As is well known, the velocities \hat{v}_a satisfy the commutation relation

$$[\hat{v}_i, \hat{v}_j] = i \frac{e\hbar}{m^2} \epsilon_{ijk} B_k, \quad (5.9)$$

as well as the triple commutation relation, the associator, given by [151]

$$[\hat{v}_1, [\hat{v}_2, \hat{v}_3]] + [\hat{v}_2, [\hat{v}_3, \hat{v}_1]] + [\hat{v}_3, [\hat{v}_1, \hat{v}_2]] = \frac{e\hbar^2}{m^3} \partial_i B_i. \quad (5.10)$$

This associator is zero, and thus trivial, in the absence of magnetic monopoles: $\partial_i B_i = 0$. Note that the triple bracket defined in (5.8) is “one-half” of the associator since

$$\begin{aligned} [A, \widehat{B}, C] &\equiv \epsilon^{abc} A_a (A_b A_c) = A[B, C] + B[C, A] + C[A, B], \\ [\widehat{A}, B, C] &\equiv \epsilon^{abc} (A_a A_b) A_c = [B, C]A + [C, A]B + [A, B]C. \end{aligned} \quad (5.11)$$

The presence of monopoles is an indicator of a 3-cocycle [151]. The triple commutator has also been encountered in the study of closed string dynamics [156].

What would be the role of such a general algebraic structure for the foundations of string theory? Given the general open-closed string relation (the closed strings being in some sense the bound states of open strings) the noncommutative and nonassociative algebraic structures might be related as in some very general and abstract form of the celebrated AdS/CFT duality [152–155]. We recall that in the AdS/CFT correspondence, one computes the on-shell bulk action S_{bulk} and relates it to the appropriate boundary correlators. The conjecture is that the generating functional of the vacuum correlators of the operator \hat{O} for a d -dimensional conformal field theory (CFT) is given by the partition function $Z(\phi)$ in (Anti-de-Sitter) AdS_{d+1} space

$$\left\langle \exp \left(\int J \hat{O} \right) \right\rangle = Z(\phi) \longrightarrow \exp[-S_{\text{bulk}}(g, \phi, \dots)], \quad (5.12)$$

where, in the semiclassical limit, the partition function becomes $Z = \exp(-S_{\text{bulk}})$. Here g denotes the metric of the AdS_{d+1} space, and the boundary values of the bulk field, ϕ , are given by the sources, J , of the boundary CFT. Essentially, one reinterprets the RG flow of the boundary nongravitational theory in terms of bulk gravitational equations of motion and then rewrites the generating functional of vacuum correlators of the boundary theory in terms of a semiclassical wave function of the bulk “universe” with specific boundary conditions.

In view of our comments on the general algebraic structures in string theory, it is tempting to propose an extension of this duality in a more abstract sense of open and closed string field theory, and the relationship between the non-commutative and nonassociative structures

$$\left\langle \exp\left(\int J\hat{O}(\Phi)\right) \right\rangle_0 = Z(\Psi) \longrightarrow \exp[-S_c(\Psi)]. \quad (5.13)$$

The “boundary” in this abstract case has to be defined algebraically, as a region of the closed string Hilbert space on which the 3-cocycle anomaly vanishes. Inside the region, the 3-cocycle would be nonzero. In this way, we would have more abstract definitions of the “boundary” and “bulk.” In some sense, this relation would look like a generalized Laplace transform of an exponential of a cubic expression giving another exponential of a cubic expression, as with the asymptotics of the Airy function $\int dx \exp(tx - x^3) \sim \exp(-t^3/2)$.

Finally, following our discussion of the vacuum energy problem in the previous section, it seems natural that any more fundamental formulation of string theory would have to work on a curved momentum space. This would mesh nicely with the ideas presented in [124–133]. If curved energy-momentum space is crucial in quantum gravity (and thus string theory) for the solution of the vacuum energy problem, then we are naturally led to question the usual formulation of string theory as a canonical quantum theory. Also, if the vacuum energy can be made small, what physical principle selects such a vacuum? This leads to the question of background independence and vacuum selection. The issue of background independence in string theory is that the fundamental equations should not select a quantum theory the same way Einstein’s gravitational equations do not select any geometry; only asymptotic or symmetry conditions select a geometry. Again, we are back to the questions regarding the role of general quantum theory in the most fundamental formulation of string theory. Note that such discussion of general quantum theory also sheds light on the question of time evolution and the problem of time in string theory [124–128].

Acknowledgments

The authors wish to thank Yang-Hiu He for inviting us to write this review. DM, TT and ZL are supported in part by the U.S. Department of Energy, grant DE-FG05-92ER40677, task A.

References

- [1] M. B. Green, J. H. Schwarz, and E. Witten, *Superstring Theory*, vol. I,II, Cambridge University Press, New York, NY, USA, 1988.
- [2] J. Polchinski, *String Theory*, vol. I,II, Cambridge University Press, New York, NY, USA, 1998.
- [3] K. Becker, M. Becker, and J. H. Schwarz, *String Theory and M-Theory: A Modern Introduction*, Cambridge University Press, New York, NY, USA, 2007.

- [4] J. A. Wheeler, "On the nature of quantum geometrodynamics," *Annals of Physics*, vol. 2, no. 6, pp. 604–614, 1957.
- [5] C. A. Mead, "Possible connection between gravitation and fundamental length," *Physical Review*, vol. 135, no. 3B, pp. B849–B862, 1964.
- [6] M. Maggiore, "A generalized uncertainty principle in quantum gravity," *Physics Letters Section B*, vol. 304, no. 1-2, pp. 65–69, 1993.
- [7] L. J. Garay, "Quantum gravity and minimum length," *International Journal of Modern Physics A*, vol. 10, no. 2, pp. 145–165, 1995.
- [8] S. Weinberger, "The cosmological constant problem," *Reviews of Modern Physics*, vol. 61, no. 1, pp. 1–23, 1989.
- [9] S. M. Carroll, "The cosmological constant," *Living Reviews in Relativity*, vol. 4, article 1, 2001.
- [10] E. Witten, "The cosmological constant from the viewpoint of string theory," . In press, <http://arxiv.org/abs/hep-ph/0002297>.
- [11] N. Straumann, "The history of the cosmological constant problem," . In press, <http://arxiv.org/abs/gr-qc/0208027>.
- [12] S. Nobbenhuis, "Categorizing different approaches to the cosmological constant problem," *Foundations of Physics*, vol. 36, no. 5, pp. 613–680, 2006.
- [13] J. Polchinski, "What is string theory?" . In press, <http://arxiv.org/abs/hep-th/9411028>.
- [14] L. N. Chang, Z. Lewis, D. Minic, T. Takeuchi, and C. H. Tze, "Bell's inequalities, superquantum correlations, and string theory," . In press, <http://arxiv.org/abs/1104.3359>.
- [15] H. Kragh, "Arthur March, Werner Heisenberg, and the search for a smallest length," *Revue d'Histoire des Sciences*, vol. 8, no. 4, pp. 401–434, 1995.
- [16] H. Kragh, "Heisenberg's lattice world: the 1930 theory sketch," *American Journal of Physics*, vol. 63, pp. 595–605, 1995.
- [17] W. Heisenberg and W. Pauli, "Zur Quantendynamik der Wellenfelder," *Zeitschrift für Physik*, vol. 56, no. 1-2, pp. 1–61, 1929.
- [18] M. Born, "Modified field equations with a finite radius of the electron," *Nature*, vol. 132, no. 3329, p. 282, 1933.
- [19] H. S. Snyder, "Quantized space-time," *Physical Review*, vol. 71, no. 1, pp. 38–41, 1947.
- [20] H. S. Snyder, "The electromagnetic field in quantized space-time," *Physical Review*, vol. 72, no. 9, pp. 68–71, 1947.
- [21] C. N. Yang, "On quantized space-time," *Physical Review*, vol. 72, no. 1, p. 874, 1947.
- [22] C. A. Mead, "Observable consequences of fundamental-length hypotheses," *Physical Review*, vol. 143, no. 4, pp. 990–1005, 1966.
- [23] T. G. Pavlopoulos, "Breakdown of Lorentz invariance," *Physical Review*, vol. 159, no. 5, pp. 1106–1110, 1967.
- [24] T. Padmanabhan, "Physical significance of planck length," *Annals of Physics*, vol. 165, no. 1, pp. 38–58, 1985.
- [25] T. Padmanabhan, "Limitations on the operational definition of spacetime events and quantum gravity," *Classical and Quantum Gravity*, vol. 4, article L107, 1987.
- [26] T. Padmanabhan, "Duality and zero-point length of spacetime," *Physical Review Letters*, vol. 78, no. 10, pp. 1854–1857, 1997.
- [27] S. Hossenfelder, M. Bleicher, S. Hofmann, J. Ruppert, S. Scherer, and H. Stöcker, "Signatures in the Planck regime," *Physics Letters Section B*, vol. 575, no. 1-2, pp. 85–99, 2003.
- [28] U. Harbach, S. Hossenfelder, M. Bleicher, and H. Stöcker, "Probing the minimal length scale by precision tests of the muon $g - 2$," *Physics Letters Section B*, vol. 584, no. 1-2, pp. 109–113, 2004.
- [29] U. Harbach and S. Hossenfelder, "The Casimir effect in the presence of a minimal length," *Physics Letters Section B*, vol. 632, no. 2-3, pp. 379–383, 2006.
- [30] S. Hossenfelder, "Running coupling with minimal length," *Physical Review D*, vol. 70, no. 10, Article ID 105003, 2004.
- [31] S. Hossenfelder, "A note on theories with a minimal length," *Classical and Quantum Gravity*, vol. 23, no. 5, pp. 1815–1821, 2006.
- [32] S. Hossenfelder, "Interpretation of quantum field theories with a minimal length scale," *Physical Review D*, vol. 73, no. 10, Article ID 105013, 2006.
- [33] S. Das and E. C. Vagenas, "Universality of quantum gravity corrections," *Physical Review Letters*, vol. 101, no. 22, Article ID 221301, 2008.
- [34] S. Das and E. C. Vagenas, "Phenomenological implications of the generalized uncertainty principle," *Canadian Journal of Physics*, vol. 87, no. 3, pp. 233–240, 2009.

- [35] S. Das and E. C. Vagenas, "Das and Vagenas reply:," *Physical Review Letters*, vol. 104, no. 11, Article ID 119002, 2010.
- [36] A. F. Ali, S. Das, and E. C. Vagenas, "Discreteness of space from the generalized uncertainty principle," *Physics Letters Section B*, vol. 678, no. 5, pp. 497–499, 2009.
- [37] S. Basilakos, S. Das, and E. C. Vagenas, "Quantum gravity corrections and entropy at the planck time," *Journal of Cosmology and Astroparticle Physics*, vol. 2010, no. 9, article 027, 2010.
- [38] S. Das, E. C. Vagenas, and A. F. Ali, "Discreteness of space from GUP II: relativistic wave equations," *Physics Letters Section B*, vol. 690, no. 4, pp. 407–412, 2010.
- [39] S. Das, E. C. Vagenas, and A. Farag Ali, "Erratum to Discreteness of space from GUP II: relativistic wave equations," *Physics Letters Section B*, vol. 692, no. 5, p. 342, 2010.
- [40] B. Bagchi and A. Fring, "Minimal length in quantum mechanics and non-Hermitian Hamiltonian systems," *Physics Letters Section A*, vol. 373, no. 47, pp. 4307–4310, 2009.
- [41] A. Fring, L. Gouba, and F. G. Scholtz, "Strings from position-dependent noncommutativity," *Journal of Physics A*, vol. 43, no. 34, Article ID 345401, 2010.
- [42] A. Fring, L. Gouba, and B. Bagchi, "Minimal areas from q-deformed oscillator algebras," *Journal of Physics A*, vol. 43, no. 42, Article ID 425202, 2010.
- [43] S. Weinberg, "Precision tests of quantum mechanics," *Physical Review Letters*, vol. 62, no. 5, pp. 485–488, 1989.
- [44] S. Weinberg, "Testing quantum mechanics," *Annals of Physics*, vol. 194, no. 2, pp. 336–386, 1989.
- [45] C. M. Bender, D. C. Brody, and H. F. Jones, "Complex extension of quantum mechanics," *eConf*, vol. 617, Article ID C0306234, 2003.
- [46] C. M. Bender, D. C. Brody, and H. F. Jones, "Complex extension of quantum mechanics," *Physical Review Letters*, vol. 89, Article ID 270401, 2002.
- [47] C. M. Bender, D. C. Brody, and H. F. Jones, "Erratum: complex extension of quantum mechanics," *Physical Review Letters*, vol. 92, no. 11, Article ID 119902, 2004.
- [48] M. Maggiore, "Quantum groups, gravity, and the generalized uncertainty principle," *Physical Review D*, vol. 49, no. 10, pp. 5182–5187, 1994.
- [49] M. Maggiore, "The algebraic structure of the generalized uncertainty principle," *Physics Letters Section B*, vol. 319, no. 1–3, pp. 83–86, 1993.
- [50] A. Kempf, G. Mangano, and R. B. Mann, "Hilbert space representation of the minimal length uncertainty relation," *Physical Review D*, vol. 52, no. 2, pp. 1108–1118, 1995.
- [51] D. Amati, M. Ciafaloni, and G. Veneziano, "Can spacetime be probed below the string size?" *Physics Letters B*, vol. 216, no. 1-2, pp. 41–47, 1989.
- [52] E. Witten, "Reflections on the fate of spacetime," *Physics Today*, vol. 49, no. 4, pp. 24–30, 1996.
- [53] D. J. Gross and P. F. Mende, "The high-energy behavior of string scattering amplitudes," *Physics Letters B*, vol. 197, no. 1-2, pp. 129–134, 1987.
- [54] D. J. Gross and P. F. Mende, "String theory beyond the Planck scale," *Nuclear Physics Section B*, vol. 303, no. 3, pp. 407–454, 1988.
- [55] D. Amati, M. Ciafaloni, and G. Veneziano, "Superstring collisions at planckian energies," *Physics Letters B*, vol. 197, no. 1-2, pp. 81–88, 1987.
- [56] D. Amati, M. Ciafaloni, and G. Veneziano, "Classical and quantum gravity effects from Planckian energy superstring collisions," *International Journal of Modern Physics A*, vol. 3, no. 7, pp. 1615–1661, 1988.
- [57] W. Heisenberg, *The Physical Principles of the Quantum Theory*, University of Chicago Press, Dover Publications, 1930.
- [58] J. A. Wheeler, "On the mathematical description of light nuclei by the method of resonating group structure," *Physical Review*, vol. 52, no. 11, pp. 1107–1122, 1937.
- [59] W. Heisenberg, "Die beobachtbaren Größen in der theorie der elementarteilchen," *Zeitschrift für Physik*, vol. 120, no. 7–10, pp. 513–538, 1943.
- [60] W. Heisenberg, "Die beobachtbaren Größen in der theorie der elementarteilchen. II," *Zeitschrift für Physik*, vol. 120, no. 11-12, pp. 673–702, 1943.
- [61] W. Heisenberg, "Die beobachtbaren Größen in der theorie der elementarteilchen. III," *Zeitschrift für Physik*, vol. 123, no. 1-2, pp. 93–112, 1944.
- [62] L. Susskind and E. Witten, "The holographic bound in anti-de sitter space," . In press, <http://arxiv.org/abs/hep-th/9805114>.
- [63] A. W. Peet and J. Polchinski, "UV-IR relations in AdS dynamics," *Physical Review D*, vol. 59, no. 6, pp. 1–5, 1999.

- [64] L. I. Mandelstam and I. E. Tamm, "The uncertainty relation between energy and time in nonrelativistic quantum mechanics," *Journal of Physics-USSR*, vol. 9, pp. 249–254, 1945.
- [65] E. P. Wigner, "On the time–energy uncertainty relation," in *Aspects of Quantum Theory*, A. Salam and E. P. Wigner, Eds., pp. 237–247, Cambridge University Press, New York, NY, USA, 1972.
- [66] M. Bauer and P. A. Mello, "The time-energy uncertainty relation," *Annals of Physics*, vol. 111, no. 1, pp. 38–60, 1978.
- [67] T. Yoneya, "On the interpretation of minimal length in string theories," *Modern Physics Letters A*, vol. 4, no. 16, pp. 1587–1595, 1989.
- [68] T. Yoneya, "Schild action and space-time uncertainty principle in string theory," *Progress of Theoretical Physics*, vol. 97, no. 6, pp. 949–961, 1997.
- [69] T. Yoneya, "String theory and the space-time uncertainty principle," *Progress of Theoretical Physics*, vol. 103, no. 6, pp. 1081–1125, 2000.
- [70] M. Li and T. Yoneya, "Short-distance space-time structure and black holes in string theory: a short review of the present status," *Chaos, Solitons and Fractals*, vol. 10, no. 2, pp. 423–443, 1999.
- [71] A. Jevicki and T. Yoneya, "Space-time uncertainty principle and conformal symmetry in D-particle dynamics," *Nuclear Physics B*, vol. 535, no. 1-2, pp. 335–348, 1998.
- [72] H. Awata, M. Li, D. Minic, and T. Yoneya, "On the quantization of Nambu brackets," *Journal of High Energy Physics*, vol. 5, no. 2, article 013, 2001.
- [73] D. Minic, "On the space-time uncertainty principle and holography," *Physics Letters Section B*, vol. 442, no. 1–4, pp. 102–108, 1998.
- [74] F. Brau, "Minimal length uncertainty relation and the hydrogen atom," *Journal of Physics A*, vol. 32, no. 44, pp. 7691–7696, 1999.
- [75] F. Brau and F. Buisseret, "Minimal length uncertainty relation and gravitational quantum well," *Physical Review D*, vol. 74, no. 3, Article ID 036002, 2006.
- [76] S. Z. Benczik, Ph.D. thesis, Virginia Tech, 2007.
- [77] A. Kempf, "Non-pointlike particles in harmonic oscillators," *Journal of Physics A*, vol. 30, no. 6, pp. 2093–2101, 1997.
- [78] L. N. Chang, D. Minic, N. Okamura, and T. Takeuchi, "Exact solution of the harmonic oscillator in arbitrary dimensions with minimal length uncertainty relations," *Physical Review D*, vol. 65, no. 12, Article ID 125027, 2002.
- [79] S. Benczik, L. N. Chang, D. Minic, and T. Takeuchi, "Hydrogen-atom spectrum under a minimal-length hypothesis," *Physical Review A*, vol. 72, no. 1, Article ID 012104, p. 4, 2005.
- [80] A. Chodos and E. Myers, "Gravitational contribution to the Casimir energy in Kaluza-Klein theories," *Annals of Physics*, vol. 156, no. 2, pp. 412–441, 1984.
- [81] A. Higuchi, "Symmetric tensor spherical harmonics on the N-sphere and their application to the de Sitter group $SO(N,1)$," *Journal of Mathematical Physics*, vol. 28, no. 7, pp. 1553–1566, 1987.
- [82] N. A. Vilenkin, *Special Functions and the Theory of Group Representations*, American Mathematical Society, 1968.
- [83] I. S. Gradshteyn and I. M. Ryzhik, *Table of Integrals, Series and Products*, Academic Press, 2000.
- [84] M. Abramowitz and I. A. Stegun, *Handbook of Mathematical Functions, with Formulas, Graphs, and Mathematical Tables*, Dover Publications, 1965.
- [85] E. W. Weisstein, "Confluent Hypergeometric Function of the Second Kind," <http://mathworld.wolfram.com/ConfluentHypergeometricFunctionoftheSecondKind.html>.
- [86] N. Arkani-Hamed, S. Dimopoulos, and G. Dvali, "The hierarchy problem and new dimensions at a millimeter," *Physics Letters Section B*, vol. 429, no. 3-4, pp. 263–272, 1998.
- [87] K. R. Dienes, E. Dudas, and T. Gherghetta, "Extra spacetime dimensions and unification," *Physics Letters Section B*, vol. 436, no. 1-2, pp. 55–65, 1998.
- [88] T. Han, J. D. Lykken, and R. J. Zhang, "Kaluza-Klein states from large extra dimensions," *Physical Review D*, vol. 59, no. 10, pp. 1–14, 1999.
- [89] T. Appelquist, H.-C. Cheng, and B. A. Dobrescu, "Bounds on universal extra dimensions," *Physical Review D*, vol. 64, no. 3, Article ID 035002, 2001.
- [90] C. Schwob, L. Jozefowski, B. De Beauvoir et al., "Optical frequency measurement of the 2S-12D transitions in hydrogen and deuterium: Rydberg constant and lamb shift determinations," *Physical Review Letters*, vol. 82, no. 25, pp. 4960–4963, 1999.
- [91] S. Mallampalli and J. Sapirstein, "Perturbed orbital contribution to the two-loop lamb shift in hydrogen," *Physical Review Letters*, vol. 80, no. 24, pp. 5297–5300, 1998.
- [92] M. I. Eides, H. Grotch, and V. A. Shelyuto, "Theory of light hydrogenlike atoms," *Physics Report*, vol. 342, no. 2-3, pp. 63–261, 2001.

- [93] G. G. Simon, C. Schmitt, F. Borkowski, and V. H. Walther, "Absolute electron-proton cross sections at low momentum transfer measured with a high pressure gas target system," *Nuclear Physics Section A*, vol. 333, no. 3, pp. 381–391, 1980.
- [94] V. V. Nesvizhevsky, H. G. Börner, A. K. Petukhov et al., "Quantum states of neutrons in the Earth's gravitational field," *Nature*, vol. 415, no. 6869, pp. 297–299, 2002.
- [95] V. V. Nesvizhevsky et al., "Measurement of quantum states of neutrons in the Earth's gravitational field," *Physical Review D*, vol. 67, no. 10, Article ID 102002, 2003.
- [96] V. V. Nesvizhevsky, A. K. Petukhov, H. G. Börner et al., "Study of the neutron quantum states in the gravity field," *European Physical Journal C*, vol. 40, no. 4, pp. 479–491, 2005.
- [97] L. N. Chang, D. Minic, N. Okamura, and T. Takeuchi, "Effect of the minimal length uncertainty relation on the density of states and the cosmological constant problem," *Physical Review D*, vol. 65, no. 12, Article ID 125028, 2002.
- [98] S. Benczik, L. N. Chang, D. Minic, N. Okamura, S. Rayyan, and T. Takeuchi, "Short distance versus long distance physics: the classical limit of the minimal length uncertainty relation," *Physical Review D*, vol. 66, no. 2, Article ID 026003, 2002.
- [99] T. Banks, "The Cosmological Constant Problem," *Physics Today*, vol. 57, no. 3, pp. 46–51, 2004.
- [100] J. Polchinski, "The cosmological constant and the string landscape," . In press, <http://arxiv.org/abs/hep-th/0603249>.
- [101] E. J. Copeland, M. Sami, and S. Tsujikawa, "Dynamics of dark energy," *International Journal of Modern Physics D*, vol. 15, no. 11, pp. 1753–1935, 2006.
- [102] E. Komatsu et al., "Seven-year Wilkinson microwave anisotropy probe (WMAP) observations: cosmological interpretation," *The Astrophysical Journal Supplement*, vol. 192, no. 2, 2011.
- [103] E. P. Wigner, "Relativistic invariance and quantum phenomena," *Reviews of Modern Physics*, vol. 29, no. 3, pp. 255–268, 1957.
- [104] H. Salecker and E. P. Wigner, "Quantum limitations of the measurement of space-time distances," *Physical Review*, vol. 109, no. 2, pp. 571–577, 1958.
- [105] F. Karolyhazy, "Gravitation and quantum mechanics of macroscopic objects," *Nuovo Cimento A*, vol. 42, no. 2, pp. 390–402, 1966.
- [106] Y. J. Ng and H. Van Dam, "Limit to space-time measurement," *Modern Physics Letters A*, vol. 9, no. 4, pp. 335–340, 1994.
- [107] Y. J. Ng and H. Van Dam, "Remarks on gravitational sources," *Modern Physics Letters A*, vol. 10, no. 36, pp. 2801–2808, 1995.
- [108] Y. J. Ng and H. Van Dam, "Measuring the foaminess of space-time with gravity-wave interferometers," *Foundations of Physics*, vol. 30, no. 5, pp. 795–805, 2000.
- [109] Y. J. Ng, "Spacetime foam: from entropy and holography to infinite statistics and nonlocality," *Entropy*, vol. 10, no. 4, pp. 441–461, 2008.
- [110] Non-relativistic space-time foam has more general "turbulent" scaling.
- [111] G. Amelino-Camelia, "Limits on the measurability of space-time distances in (the semiclassical approximation of) quantum gravity," *Modern Physics Letters A*, vol. 9, no. 37, pp. 3415–3422, 1994.
- [112] L. Diósi and B. Lukács, "On the minimum uncertainty of space-time geodesics," *Physics Letters A*, vol. 142, no. 6-7, pp. 331–334, 1989.
- [113] L. Diósi and B. Lukács, "Critique of proposed limit to space-time measurement, based on Wigner's clocks and mirrors," *Europhysics Letters*, vol. 34, no. 7, pp. 479–481, 1996.
- [114] V. Jejjala, D. Minic, Y. J. Ng, and C. H. Tze, "Turbulence and holography," *Classical and Quantum Gravity*, vol. 25, no. 22, Article ID 225012, 2008.
- [115] T. Banks, "Cosmological breaking of supersymmetry?" *International Journal of Modern Physics A*, vol. 16, no. 5, pp. 910–921, 2001.
- [116] M. Gell-Mann, P. Ramond, and R. Slansky, "Complex spinors and unified theories," in *Supergravity*, P. van Nieuwenhuizen and D. Z. Freedman, Eds., North Holland, 1979.
- [117] T. Yanagida, "Horizontal symmetry and masses of neutrinos," *Progress of Theoretical Physics*, vol. 64, no. 3, pp. 1103–1105, 1980.
- [118] R. N. Mohapatra and G. Senjanović, "Neutrino mass and spontaneous parity nonconservation," *Physical Review Letters*, vol. 44, no. 14, pp. 912–915, 1980.
- [119] S. Weinberg, "Varieties of baryon and lepton nonconservation," *Physical Review D*, vol. 22, no. 7, pp. 1694–1700, 1980.
- [120] B. Schmittmann, K. Hwang, and R. K. P. Zia, "Onset of spatial structures in biased diffusion of two species," *Europhysics Letters*, vol. 19, no. 1, article 19, 1992.

- [121] D. Helbing, I. J. Farkas, and T. Vicsek, "Freezing by heating in a driven mesoscopic system," *Physical Review Letters*, vol. 84, no. 6, pp. 1240–1243, 2000.
- [122] D. Helbing, "Traffic and related self-driven many-particle systems," *Reviews of Modern Physics*, vol. 73, no. 4, pp. 1067–1141, 2001.
- [123] R. K. P. Zia, E. L. Praestgaard, and O. G. Mouritsen, "Getting more from pushing less: negative specific heat and conductivity in nonequilibrium steady states," *American Journal of Physics*, vol. 70, no. 4, pp. 384–392, 2002.
- [124] D. Minic and C. H. Tze, "Background independent quantum mechanics and gravity," *Physical Review D*, vol. 68, no. 6, Article ID 061501, 2003.
- [125] D. Minic and C. H. Tze, "A general theory of quantum relativity," *Physics Letters, Section B: Nuclear, Elementary Particle and High-Energy Physics*, vol. 581, no. 1-2, pp. 111–118, 2004.
- [126] V. Jejjala and D. Mimic, "Why there is something so close to nothing: towards a fundamental theory of the cosmological constant," *International Journal of Modern Physics A*, vol. 22, no. 10, pp. 1797–1818, 2007.
- [127] V. Jejjala, M. Kavic, D. Minic, and C. H. Tze, "On the origin of time and the universe," *International Journal of Modern Physics A*, vol. 25, no. 12, pp. 2515–2523, 2010.
- [128] V. Jejjala, M. Kavic, D. Minic, and C. -H. Tze, "The big bang as the ultimate traffic jam," *International Journal of Modern Physics D*, vol. 18, no. 14, pp. 2257–2263, 2009.
- [129] Y. A. Gol'fand, *Soviet Physics JETP*, vol. 10, p. 842, 1960.
- [130] Y. A. Gol'fand, "Quantum field theory in constant curvature p-space," *Soviet Physics JETP*, vol. 16, p. 184, 1963.
- [131] Y. A. Gol'fand, *Soviet Physics JETP*, vol. 37, p. 365, 1966.
- [132] L. Freidel and E. R. Livine, "3D quantum gravity and effective noncommutative quantum field theory," *Physical Review Letters*, vol. 96, no. 22, Article ID 221301, p. 2947, 2006.
- [133] G. Amelino-Camelia, L. Freidel, J. Kowalski-Glikman, and L. Smolin, "The principle of relative locality," . In press, <http://arxiv.org/abs/1101.0931>.
- [134] L. N. Chang, D. Minic, and T. Takeuchi, "Quantum gravity, dynamical energymomentum space and vacuum energy," *Modern Physics Letters A*, vol. 25, no. 35, pp. 2947–2954, 2010.
- [135] I. Bars, "Gauge symmetry in phase space consequences for physics and space-time," *International Journal of Modern Physics A*, vol. 25, no. 9, pp. 5235–5252, 2010.
- [136] A. Einstein, "Investigations on the Theory of the Brownian Movement," 2011, <http://www.bnpublishing.net/>.
- [137] J. Magueijo and L. Smolin, "Lorentz invariance with an invariant energy scale," *Physical Review Letters*, vol. 88, no. 19, Article ID 190403, 2002.
- [138] J. Magueijo and L. Smolin, "Generalized Lorentz invariance with an invariant energy scale," *Physical Review D*, vol. 67, no. 4, Article ID 044017, 2003.
- [139] J. Kowalski-Glikman, "Introduction to doubly special relativity," *Lecture Notes in Physics*, vol. 669, pp. 131–159, 2005.
- [140] F. Girelli and E. R. Livine, "Special relativity as a noncommutative geometry: lessons for deformed special relativity," *Physical Review D*, vol. 81, no. 8, Article ID 085041, 2010.
- [141] E. Witten, "Noncommutative geometry and string field theory," *Nuclear Physics B*, vol. 268, p. 253, 1986.
- [142] G. T. Horowitz, J. Lykken, R. Rohm, and A. Strominger, "Purely cubic action for string field theory," *Physical Review Letters*, vol. 57, no. 3, pp. 283–286, 1986.
- [143] A. Strominger, "Closed string field theory," *Nuclear Physics B*, vol. 294, pp. 93–112, 1987.
- [144] S. Okubo, *Introduction to Octonion and Other Non-Associative Algebras in Physics*, Cambridge University Press, New York, NY, USA, 1995.
- [145] H. Awata, M. Li, D. Minic, and T. Yoneya, "On the quantization of Nambu brackets," *Journal of High Energy Physics*, vol. 5, no. 2, pp. 13–16, 2001.
- [146] Y. Nambu, "Generalized hamiltonian dynamics," *Physical Review D*, vol. 7, no. 8, pp. 2405–2412, 1973.
- [147] L. Takhtajan, "On foundation of the generalized Nambu mechanics," *Communications in Mathematical Physics*, vol. 160, no. 2, pp. 295–315, 1994.
- [148] R. Chatterjee and L. Takhtajan, "Aspects of Classical and Quantum Nambu Mechanics," *Letters in Mathematical Physics*, vol. 37, no. 4, pp. 475–482, 1996.
- [149] G. Dito, M. Flato, D. Sternheimer, and L. Takhtajan, "Deformation quantization and Nambu mechanics," *Communications in Mathematical Physics*, vol. 183, no. 1, pp. 1–22, 1997.
- [150] R. G. Leigh, A. Mauri, D. Minic, and A. C. Petkou, "Gauge fields, membranes, and subdeterminant vector models," *Physical Review Letters*, vol. 104, no. 22, Article ID 221801, 2010.

- [151] R. Jackiw, "Topological investigations of quantized gauge theories," in *Current Algebra and Anomalies*, S. Trieman, R. Jackiw, B. Zumino, and E. Witten, Eds., Princeton, 1985.
- [152] J. M. Maldacena, "The large N limit of superconformal field theories and supergravity," *Advances in Theoretical and Mathematical Physics*, vol. 2, no. 2, pp. 231–252, 1998.
- [153] J. M. Maldacena, "The large N limit of superconformal field theories and supergravity," *International Journal of Theoretical Physics*, vol. 38, no. 4, pp. 1113–1133, 1999.
- [154] S. S. Gubser, I. R. Klebanov, and A. M. Polyakov, "Gauge theory correlators from non-critical string theory," *Physics Letters Section B*, vol. 428, no. 1-2, pp. 105–114, 1998.
- [155] E. Witten, "Anti-de Sitter space and holography," *Advances in Theoretical and Mathematical Physics*, vol. 2, pp. 253–291, 1998.
- [156] R. Blumenhagen and E. Plauschinn, "Nonassociative gravity in string theory?" *Journal of Physics A*, vol. 44, no. 1, Article ID 015401, 2011.

Review Article

Numerical Polynomial Homotopy Continuation Method and String Vacua

Dhagash Mehta

Physics Department, Syracuse University, Syracuse, NY 13244, USA

Correspondence should be addressed to Dhagash Mehta, dbmehta@syr.edu

Received 30 May 2011; Accepted 18 August 2011

Academic Editor: André Lukas

Copyright © 2011 Dhagash Mehta. This is an open access article distributed under the Creative Commons Attribution License, which permits unrestricted use, distribution, and reproduction in any medium, provided the original work is properly cited.

Finding vacua for the four-dimensional effective theories for supergravity which descend from flux compactifications and analyzing them according to their stability is one of the central problems in string phenomenology. Except for some simple toy models, it is, however, difficult to find all the vacua analytically. Recently developed algorithmic methods based on symbolic computer algebra can be of great help in the more realistic models. However, they suffer from serious algorithmic complexities and are limited to small system sizes. In this paper, we review a numerical method called the numerical polynomial homotopy continuation (NPHC) method, first used in the areas of lattice field theories, which by construction finds *all* of the vacua of a given potential that is known to have only isolated solutions. The NPHC method is known to suffer from no major algorithmic complexities and is *embarrassingly parallelizable*, and hence its applicability goes way beyond the existing symbolic methods. We first solve a simple toy model as a warm-up example to demonstrate the NPHC method at work. We then show that all the vacua of a more complicated model of a compactified M theory model, which has an $SU(3)$ structure, can be obtained by using a desktop machine in just about an hour, a feat which was reported to be prohibitively difficult by the existing symbolic methods. Finally, we compare the various technicalities between the two methods.

1. Introduction

A lot of current research in string phenomenology is focused on developing methods to find and analyze vacua of four-dimensional effective theories for supergravity descended from flux compactifications. Stated in explicit terms, one is interested in finding all the vacua (usually, isolated stationary points) of the scalar potential V of such a theory. In particular, given a Kähler potential K and a superpotential W , for uncharged moduli fields, the scalar potential is given by

$$V = e^K \left[K^{A\bar{B}} D_A W D_{\bar{B}} \bar{W} - 3|W|^2 \right], \quad (1.1)$$

where D_A is the Kähler derivative $\partial_A + \partial_A K$ and $K^{A\bar{B}}$ is the inverse of $K_{A\bar{B}} = \partial_A \partial_{\bar{B}} K$. Once the vacua are found, one can then classify them by either using the eigenvalues of the Hessian matrix of V or by introducing further constraints such as $W = 0$.

Finding all the stationary points of a given potential V , amounts to solving the stationary equations, that is, solving the system of equations consisting of the first derivatives of V , with respect to all the fields, equated to zero. The stationary equations for V arising in the string phenomenological models are usually nonlinear. In the perturbative limit, W usually has a polynomial form. This is an important observation since we can then use the algebraic geometry concepts and methods to extract a lot of information about V . Solving systems of nonlinear equations is usually a highly nontrivial task. However, if the system of stationary equations has polynomial-like nonlinearity, then the symbolic methods based on the Gröbner basis technique can be used to solve the system [1]. These symbolic methods ensure that all the stationary points are obtained when the computation finishes. Roughly speaking, for a given system of multivariate polynomial equations, a set of which is called an ideal, the so-called Buchberger Algorithm (BA) or its refined variants can compute a new system of equations, called a Gröbner basis [2]. For the systems known to have only isolated solutions, called 0-dimensional ideals, a Gröbner basis always has at least one univariate equation and the subsequent equations consist of increasing number of variables, that is, it is in a *triangular form* (Note that this is only true for a few specific types of monomial orderings. For other monomial ordering, the new system of equations may not have a triangular form.) The solutions of a Gröbner basis are always the same as the original system, but the former is easier to solve due to its triangular form as the univariate equation can be solved either analytically or numerically quite straightforwardly. Then by back-substituting the solutions in the subsequent equations and continually solving them we can find all the solutions of the system. (Using the Gröbner basis methods, one can also deal with systems which have at least one free variable, called positive dimensional ideals. However, in this paper we only focus on the 0-dimensional ideals.) It should be noted that the BA reduces to Gaussian elimination in the case of linear equations, that is, it is a generalization of the latter. Similarly it is also a generalization of the Euclidean algorithm for the computation of the Greatest Common Divisors of a univariate polynomial. Recently, more efficient variants of the BA have been developed to obtain a Gröbner basis, for example, F4 [3], F5 [4], and Involution Algorithms [5]. Symbolic computation packages such as Mathematica, Maple, and Reduce, have built-in commands to calculate a Gröbner basis. Singular [6], COCOA [7], and MacCaulay2 [8] are specialized packages for Gröbner basis and Computational Algebraic Geometry, available as freeware. MAGMA [9] is also such a specialized package available commercially.

In [10–12], it was shown that one does not need to solve the system using the Gröbner basis techniques, in the usual sense, in order to extract some of the important information such as the dimensionality of the ideal and the number of real roots in the system. But one can indirectly obtain this information by computing the so-called primary decomposition of the ideal (still using the Gröbner basis technique internally). This was a remarkable success as it allowed one to work on nontrivial models and extract a lot of information using a regular desktop machine only. The authors of these papers also made a very helpful computational package, called Stringvacua [11], publicly available. Stringvacua is a Mathematica interface to Singular and has string phenomenology-specific utilities which makes the package quite useful to the users.

However, even with such tricks, there are a few problems with the symbolic methods: the BA is known to suffer from exponential space complexity, that is, the memory (Random Access Memory) required by the machine blows up exponentially with the number of

variables, equations, terms in each polynomial, and so forth. So even for small sized systems, one may not be able to compute a Gröbner basis, nor the related objects such as primary decomposition of the ideal. It is also usually less efficient for systems with irrational coefficients. Another drawback is that the BA is highly sequential, that is, very difficult to efficiently parallelize.

Below we explain a novel numerical method, called the numerical polynomial homotopy continuation (NPHC) method, which overcomes all the shortcomings of the Gröbner basis methods. The method was first introduced in particle physics and condensed matter theory areas in [13–15], where all the stationary points of a multivariate function called the lattice Landau gauge fixing functional [16–19] were found using the NPHC method. Below, we begin by describing the NPHC method for the univariate case before generalizing it to the multivariate case. We then consider a toy model that is used in the Stringvacua manual and also a compactified M theory model. Finding all the vacua using the symbolic methods for both these models is already known to be prohibitively difficult. We briefly describe the models and explain how the corresponding stationary equations can be viewed as having polynomial form. With the help of the NPHC method, we find all the isolated vacua for the model and give a technical comparison between both the symbolic and numerical methods. After mentioning a few other important aspects of the NPHC method in the Frequently Asked Questions section, we conclude the paper.

2. The Numerical Polynomial Homotopy Continuation Method

Here, we explain the numerical polynomial homotopy continuation method. Let us begin by exemplifying the method for the univariate case.

Firstly, we know that for a single-variable equation, $f(x) = \sum_{i=0}^k a_i x^i$, with coefficients a_i and the variable x both defined over \mathbb{C} , the number of solutions is exactly k if $a_k \neq 0$, counting multiplicities. This powerful result comes from the Fundamental Theorem of Algebra. To get all roots of such single-variable polynomials, there exist many numerical methods such as the *companion matrix* trick for low-degree polynomials and the divide-and-conquer techniques for high-degree polynomials. Here we present the Numerical Polynomial Homotopy Continuation (NPHC) by first describing it for the univariate case which can then be extended to the multivariate case in a straightforward manner. We follow [20, 21] throughout this section unless specified otherwise.

The strategy behind the NPHC method is as follows: first write down the equation or system of equations to be solved in a more general parametric form, solve this system at a point in parameter space where its solutions can be easily found, and finally track these solutions from this point in parameter space to the point in parameter space corresponding to the original system/problem. This approach can be applied to many types of equations (e.g., nonalgebraic equations) which exhibit a continuous dependence of the solutions on the parameters, but there exist many difficulties in making this method a primary candidate method to solve a set of nonalgebraic equations. However, for reasons that will be clear below, this method works exceptionally well for polynomial equations.

To clarify how the method works, we first take a univariate polynomial, say $z^2 - 5 = 0$, pretending that we do not know its solutions (i.e., $z = \pm\sqrt{5}$). We then begin by defining the more general parametric family

$$H(z, t) = (1 - t)(z^2 - 1) + t(z^2 - 5) = z^2 - (1 + 4t) = 0, \quad (2.1)$$

where $t \in [0, 1]$ is a parameter. For $t = 0$, we have $z^2 - 1 = 0$ and at $t = 1$ we recover our original problem. The problem of getting all solutions of the original problem now reduces to tracking solutions of $H(z, t) = 0$ from $t = 0$ where we know the solutions, that is, $z = \pm 1$, to $t = 1$. The choice of $z^2 - 1$ in (2.1), called the *start system*, should be clear now: this system has the same number of solutions as the original problem and is easy to solve. For multivariate systems, a clever choice of a start system is essential in reducing the computation, and the discussion about this issue will follow soon. Here, we briefly mention the numerical methods used in path-tracking from $t = 0$ to $t = 1$. One of the ways to track the paths is to solve the differential equation that is satisfied along all solution paths, say $z_i^*(t)$ for the i th solution path,

$$\frac{dH(z_i^*(t), t)}{dt} = \frac{\partial H(z_i^*(t), t)}{\partial z} \frac{dz_i^*(t)}{dt} + \frac{\partial H(z_i^*(t), t)}{\partial t} = 0. \quad (2.2)$$

This equation is called the Davidenko differential equation. Inserting (2.1) in this equation, we have

$$\frac{dz_i^*(t)}{dt} = -\frac{2}{z_i^*(t)}. \quad (2.3)$$

We can solve this initial value problem numerically (again, pretending that an exact solution is hitherto unknown) with the initial conditions as $z_1^*(0) = 1$ and $z_2^*(0) = -1$. The other approach is to use Euler's predictor and Newton's corrector methods. This approach works well too. We do not intend to discuss the actual path tracker algorithm used in practice, but it is important to mention that in these path tracker algorithms, almost all apparent difficulties have been resolved, such as tracking singular solutions, multiple roots, solutions at infinity, and so forth. It is also important to mention here that in the actual path tracker algorithms the homotopy is randomly complexified to avoid singularities, that is, taking

$$H(z, t) = \gamma(1 - t)(z^2 - 1) + t(z^2 - 5) = 0, \quad (2.4)$$

where $\gamma = e^{i\theta}$ with $\theta \in \mathbb{R}$ chosen randomly.

It is shown that for a generic value of the complex γ the paths are well behaved for $t \in [0, 1)$, that is, for the whole path except the endpoint. This makes sure that there is no singularity or bifurcation along the paths. This is a remarkable trick, called the γ -trick, since this is the reason why we can claim that the NPHC method is guaranteed to find *all* solutions. Note that $\gamma = 1$, for example, is not a generic value.

There are several sophisticated numerical packages well equipped with path trackers such as Bertini [22], PHCpack [23], PHoM [24], HOMPACK [25], and HOM4PS2 [26, 27]. They all are available freely from their respective research groups.

In the above example, the PHCpack with its default settings gives the solutions

$$z = \pm 2.23606797749979 \pm i 0.000000000000000. \quad (2.5)$$

Thus, it gives the expected two solutions of the system with a very high numerical precision.

2.1. Multivariate Polynomial Homotopy Continuation

We can now generalize the NPHC method to find all the solutions of a system of multivariate polynomial equations, say $P(x) = 0$, where $P(x) = (p_1(x), \dots, p_m(x))$ and $x = (x_1, \dots, x_m)$, that is *known to have isolated solutions* (i.e., a 0-dimensional ideal). To do so, we first need to have some knowledge about the expected number of solutions of the system. There is a classical result, called the *Classical Bézout Theorem*, that asserts that for a system of m polynomial equations in m variables the maximum number of solutions in \mathbb{C}^m is $\prod_{i=1}^m d_i$, where d_i is the degree of the i th polynomial. This bound, called the Classical Bézout Bound (CBB), is exact for generic values (i.e., roughly speaking, nonzero random values) of coefficients. The *genericity* is well defined, and the interested reader is referred to [21] for details.

Based on the CBB, we can construct a *homotopy*, or a set of problems, similar to the aforementioned one-dimensional case, as

$$H(x, t) = \gamma(1 - t)Q(x) + tP(x) = 0, \quad (2.6)$$

where $Q(x)$ is a system of polynomial equations, $Q(x) = (q_1(x), \dots, q_m(x))$ with the following properties

- (1) The solutions of $Q(x) = H(x, 0) = 0$ are known or can be easily obtained. $Q(x)$ is called the *start system*, and the solutions are called the *start solutions*.
- (2) The number of solutions of $Q(x) = H(x, 0) = 0$ is equal to the CBB for $P(x) = 0$.
- (3) The solution set of $H(x, t) = 0$ for $0 \leq t \leq 1$ consists of a finite number of smooth paths, called homotopy paths, each parametrized by $t \in [0, 1)$.
- (4) Every isolated solution of $H(x, 1) = P(x) = 0$ can be reached by some path originating at a solution of $H(x, 0) = Q(x) = 0$.

We can then track all of the paths corresponding to each solution of $Q(x) = 0$ from $t = 0$ to $t = 1$ and reach $P(x) = 0 = H(x, 1)$. By implementing an efficient path tracker algorithm, we can get all the isolated solutions of a system of multivariate polynomials just as in the univariate case.

The homotopy constructed using the CBB is called the *Total Degree Homotopy*. The start system $Q(x) = 0$ can be taken, for example, as

$$Q(x) = \begin{pmatrix} x_1^{d_1} - 1 \\ x_2^{d_2} - 1 \\ \vdots \\ x_m^{d_m} - 1 \end{pmatrix} = 0, \quad (2.7)$$

where d_i is the degree of the i th polynomial of the original system $P(x) = 0$. Equation (2.7) can be easily solved and its total number of solutions (the start solutions) is $\prod_{i=1}^m d_i$, all of which are nonsingular. The Total Degree Homotopy is a very effective and popular homotopy whose variants are used in the actual path trackers.

For the multivariate case, a solution is a set of numerical values of the variables which satisfies each of the equations within a given tolerance, Δ_{sol} ($\sim 10^{-10}$ in our set up). Since the variables are allowed to take complex values, all the solutions come with real and imaginary parts. A solution is a real solution if the imaginary part of each of the variables is less than or equal to a given tolerance, $\Delta_{\mathbb{R}}$ ($\sim 10^{-7}$ is a suitable choice for the equations we will be dealing with in the next section, below which the number of real solutions does not change). All of these solutions can be further refined to an *arbitrary precision* limited by the machine precision.

The obvious question at this stage would be if the number of real solutions depends on $\Delta_{\mathbb{R}}$. To resolve this issue, we use a recently developed algorithm called alphaCertified which is based on the so-called Smale's α -theory [28]. This algorithm certifies the real nonsingular solutions of polynomial systems using both exact rational arithmetic and arbitrary precision floating point arithmetic. This is a remarkable step, because using alphaCertified we can prove that a solution classified as a real solution is actually a real solution independent of $\Delta_{\mathbb{R}}$, and hence these solutions are as good as the *exact solutions*.

3. A Toy Model

Here, we apply the NPHC method to a toy model from the examples given in the Stringvacua package. The Kähler potential for this model is given as

$$K = -3 \log(T + \bar{T}), \quad (3.1)$$

and the superpotential is given as

$$W = a + bT^8. \quad (3.2)$$

Here, a and b are parameters. Note that the field T comes along with its complex conjugate. So even though they can be treated as different variables by merely relabeling them, they are not actually independent variables. To avoid this problem, we can write them in terms of real and imaginary parts, that is, $T = t + i\tau$ with τ , and t are real. Finally, we get the potential as

$$V = \frac{1}{3t} \left(4b \left(5b(t^2 + \tau^2)^7 - 3a(t^6 - 21t^4\tau^2 + 35t^2\tau^4 - 7\tau^6) \right) \right), \quad (3.3)$$

which has 2 variables. To find the stationary points of V , we need to solve the system of equations consisting of the first-order derivatives of V , with respect to both variables t and τ , equated to zero, that is,

$$\begin{aligned} \frac{\partial V}{\partial t} &= \frac{1}{3t^2} \left(4b \left(5b(13t^2 - \tau^2)(t^2 + \tau^2)^6 - 3a(5t^6 - 63t^4\tau^2 + 35t^2\tau^4 + 7\tau^6) \right) \right) = 0, \\ \frac{\partial V}{\partial \tau} &= \frac{1}{3t} \left(56b\tau \left(5b(t^2 + \tau^2)^6 + a(9t^4 - 30t^2\tau^2 + 9\tau^4) \right) \right) = 0. \end{aligned} \quad (3.4)$$

We also note that the stationary equations in this example involve denominators. Since we are not interested in the solutions for which the denominators are zero, we clear them out by multiplying them with the numerators appropriately.

Using the symbolic methods, this task is known to be difficult for general numerical (i.e., floating points) values of parameters a and b , with the computation continuing indefinitely [1, 12].

Firstly, we used the Stringvacua package to compute the dimension of the ideal which turned out to be 0 for generic values of a and b , that is, the system of equations has only isolated solutions. Note that to actually find the solutions of the system, we have to put some numerical values for a and b . The Gröbner basis techniques, as mentioned above, work much better for the cases where parameters are rational. We first use the same values, $a = 1$ and $b = 1$, as used in the Stringvacua manual. Then, we use the command “NumRoots” which computes the number of real roots of the system, that is, 7 in this case, in less than a minute on a desktop machine.

Let us now turn our attention to solving this system using the NPHC method. Firstly, the CBB for this system is 182. We used both Bertini and HOM4PS2 to track all these paths. Both took around one minute to solve this system: there are 86 complex (including real) finite solutions, out of which 36 solutions are real. Out of the 36 real solutions, six of them are distinct solutions (multiplicity one) and the only other distinct solution $(t, \tau) = (0, 0)$ which comes with multiplicity 30. Thus, there are 7 distinct solutions as expected from the Stringvacua’s “NumRoots” command. However, we should mention that the Stringvacua package does not give any information about the multiplicity of the solutions, as seen in this example, whereas the NPHC method gives all the solutions with its multiplicities making the method already useful for this simple example. Not only that, but the NPHC also gives the infinite solutions (which are the solutions on the projective space but not on the affine space): the running example has 2 infinite solutions both coming with multiplicity 48. Thus, the total number of solutions in this case, $50 + 6 + (1 \times 30) + (2 \times 48)$, is indeed the same as the CBB.

Note that in these equations all the denominators were multiples of t . The condition that none of the denominators is zero can be imposed algebraically by adding a constraint equation as $1 - zt = 0$ with z being an additional variable. Thus there are now 3 equations in 3 variables. Note that in the Stringvacua package the denominators are thrown away by multiplying each equation appropriately, but the additional equation is not included in the final ideal. In the package, one can of course use the “Saturation” command in order to ensure that this equation is properly taken into account.

We can again solve the above system 3 equations in 3 variables using the Bertini and HOM4PS2. The CBB of this new system is 364. In the end, there are 56 finite complex solutions out of which there are six real solutions, all with multiplicity 1. There are no infinite solutions in this case. This should be expected since the only multiple real solution in the previous system was when the denominator was zero. After adding the constraint equation, we have got rid of this solution and hence left with the rest of the six distinct solutions. Finally, the real solutions (throwing the very small imaginary parts out) are

$$\{t, \tau\} = \{ \{-0.5204819146691344, 0.7148265478403096\}, \\ \{0.5204819146691421, -0.7148265478403003\},$$

$$\begin{aligned}
& \{-0.5204819146691322, -0.7148265478403191\}, \\
& \{0.520481914669129, 0.7148265478403104\}, \\
& \{0.8325249117100803, 0\}, \{-0.8325249117100793, 0\}.
\end{aligned} \tag{3.5}$$

Since we have all the real solutions, we can now compute the Hessian of V at these solutions and separate out the physically interesting vacua. Since the purpose of this paper is to introduce the NPHC method only, we refrain from discussing the interesting physics of these solutions here. A detailed analysis of these solutions and the solutions of other systems will be published elsewhere. For now we discuss how the two methods, the symbolic algebra methods and the NPHC, compare with each other.

4. A Model of Compactified M Theory

Here, we take an example of M theory compactified on the coset $(SU(3) \times U(1)) / (U(1) \times U(1))$ from [29] which is also considered in [12]. The coset has $SU(3)$ structure. The corresponding Kähler and superpotential are

$$\begin{aligned}
K &= -4 \log(-i(U - \bar{U})) - \log(-i(T_1 - \bar{T}_1)(T_2 - \bar{T}_2)(T_3 - \bar{T}_3)), \\
W &= \frac{1}{\sqrt{8}}(4U(T_1 + T_2 + T_3) + 2T_2T_3 - T_1T_3 - T_1T_2 + 200).
\end{aligned} \tag{4.1}$$

Here, we use $T_i = -it_i + \tau_i$, for $i = 1, 2, 3$, and $U = -ix + y$. Then the potential is

$$\begin{aligned}
V &= \frac{1}{256t_1t_2t_3x^4} \left(40000 + t_3^2\tau_1^2 - 400\tau_1\tau_2 - 4t_3^2\tau_1\tau_2 + 4t_3^2\tau_2^2 + \tau_1^2\tau_2^2 - 400\tau_1\tau_3 \right. \\
&\quad + 800\tau_2\tau_3 + 2\tau_1^2\tau_2\tau_3 - 4\tau_1\tau_2^2\tau_3 + \tau_1^2\tau_3^2 - 4\tau_1\tau_2\tau_3^2 + 4\tau_2^2\tau_3^2 - 24t_2t_3x^2 \\
&\quad + 4t_3^2x^2 - 24t_1(t_2 + t_3)x^2 + 4\tau_1^2x^2 + 8\tau_1\tau_2x^2 + 4\tau_2^2x^2 + 8\tau_1\tau_3x^2 + 8\tau_2\tau_3x^2 \\
&\quad + 4\tau_3^2x^2 + 1600\tau_1y - 8t_3^2\tau_1y + 1600\tau_2y + 16t_3^2\tau_2y - 8\tau_1^2\tau_2y - 8\tau_1\tau_2^2y \\
&\quad + 1600\tau_3y - 8\tau_1^2\tau_3y + 16\tau_2^2\tau_3y - 8\tau_1\tau_3^2y + 16\tau_2\tau_3^2y + 16t_3^2y^2 + 16\tau_1^2y^2 \\
&\quad + 32\tau_1\tau_2y^2 + 16\tau_2^2y^2 + 32\tau_1\tau_3y^2 + 32\tau_2\tau_3y^2 + 16\tau_3^2y^2 \\
&\quad + t_1^2(t_2^2 + t_3^2 + \tau_2^2 + 2\tau_2\tau_3 + \tau_3^2 + 4x^2 - 8\tau_2y - 8\tau_3y + 16y^2) \\
&\quad \left. + t_2^2(4t_3^2 + \tau_1^2 - 4\tau_1(\tau_3 + 2y) + 4(\tau_3^2 + x^2 + 4\tau_3y + 4y^2)) \right).
\end{aligned} \tag{4.2}$$

We need to solve the stationary equations, that is, the derivatives of V with respect to $t_1, t_2, t_3, \tau_1, \tau_2, \tau_3, x$, and y equated to zero. We also need to add an additional equation $1 - z(t_1t_2t_3x) = 0$ to ensure that none of the denominators of the stationary equations are zero.

Thus, in total there are 9 equations in 9 variables. This system only has isolated solutions, (In [12], this system is reported to have positive dimensional components in its solution space. However, the denominator equation was not included in the analysis there. Once we include the denominator equation in the system, the combined system has no positive dimensional components. Hence, there is no discrepancy here.) The equations are quite complicated, and we avoid writing all of them down here. This system of equations is not only *prohibitively difficult* to be solved completely but also not tractable even using the primary decomposition techniques (except that some information about the solutions may be obtained if one further restricts the system such as taking $y = 0$) [1, 12]. In short, it is not possible to handle this system in its full glory using the available symbolic methods.

Now, let us move to the NPHC method. Firstly, since there are four equations of degree 3, another four equations of degree 4, and one equation of degree 5, the CBB is 103680. This system is actually quite straightforward to solve using the NPHC method. The HOM4PS2 package, for example, solves the full system in around 1 hour on a regular desktop machine: there are 516 total solutions for this system, out of which there are only 12 real solutions. The solutions in the order $\{y, \tau_1, \tau_2, \tau_3, t_2, t_3, x, t_1\}$ are

$$\begin{aligned} & \{ \{-3.3333333333335, 1.3333333333308, 3.333333333331, 3.333333333336, \\ & \quad -6.666666666666705, -6.66666666666667, -6.6666666666667, -2.66666666666603\}, \\ & \{-3.3333333333334, 1.3333333333288, 3.333333333337, 3.333333333335, \\ & \quad 6.666666666667, 6.666666666671, -6.666666666669, 2.6666666666594\}, \\ & \{-3.3333333333344, 1.3333333333324, 3.333333333333, 3.3333333333375, \\ & \quad -6.666666666668, -6.666666666666, 6.666666666667, -2.6666666666634\}, \\ & \{-3.3333333333264, 1.3333333333488, 3.3333333333286, 3.333333333322, \\ & \quad 6.666666666659, 6.666666666666, 6.666666666663, 2.6666666666807\}, \\ & \{3.3333333333338, -1.3333333333228, -3.333333333334, -3.333333333342, \\ & \quad 6.666666666674, 6.666666666669, 6.666666666705, 2.6666666666554\}, \\ & \{3.3333333333286, -1.3333333333406, -3.333333333338, -3.3333333333215, \\ & \quad 6.666666666663, 6.666666666668, -6.666666666665, 2.6666666666714\}, \\ & \{3.3333333333313, -1.3333333333337, -3.3333333333366, -3.3333333333277, \\ & \quad -6.666666666667, -6.6666666666705, 6.666666666668, -2.666666666663\}, \\ & \{3.3333333333313, -1.333333333341, -3.333333333326, -3.333333333335, \\ & \quad -6.6666666666705, -6.666666666671, -6.666666666666, -2.6666666666634\}, \\ & \{0., 0., 0., 0., 7.453559924993, 7.453559924993, -7.453559925, 2.9814239699997\}, \\ & \{0., 0., 0., 0., 7.453559924999, 7.453559924993, 7.453559925, 2.9814239699997\}, \end{aligned}$$

$$\begin{aligned} & \{0., 0., 0., 0., -7.4535599249992, -7.453559925, -7.4535599249992, -2.981423969997\}, \\ & \{0., 0., 0., 0., -7.4535599249993, -7.4535599249992, 7.4535599249, -2.9814239699\}. \end{aligned} \quad (4.3)$$

It is easy to recognize that some of the numbers in the above list of solutions are rational numbers, for example, $3.33333 \approx 10/3$. We can now easily compute the eigenvalues of the Hessian of the potential and other related quantities of all these solutions and hence classify the vacua in terms of physics. However, again we refrain from discussing the interesting physics of these solutions here. The full analysis will be published elsewhere.

5. Comparison between Gröbner Basis Techniques and the NPHC Method

Here, we compare the two different methods. Firstly, the Gröbner basis techniques solve the system symbolically. This is immensely significant since one then has a *proof* for the results and/or the results in closed form. There is caveat here however: if the univariate equation in a Gröbner basis is of degree 5 or higher, then the Abel-Ruffini theorem prevents us from solving it exactly, in general, at least in terms of the radicals of its coefficients (this does not mean that the univariate equation cannot be solved exactly at all). In such a situation, one may end up solving this equation numerically, and hence the above-mentioned feature of the symbolic method no longer applies. The NPHC method is a numerical method. That said, the method by construction gives *all* of the isolated solutions for the system known to have only isolated solutions, up to a numerical precision. The solutions then can be refined to within an arbitrary precision up to the machine precision by the Newton's corrector method or otherwise. Moreover, using the alphaCertified method, we can certify if the real nonsingular solutions obtained by the above packages are actually the real nonsingular solutions of the system independent of the numerical precision used during the computation. Hence, though the solutions cannot be obtained in a closed form using the NPHC method, the solutions are as good as exact solutions for all the practical purposes.

We should emphasize here that using the methods presented in [10–12] one can learn quite a lot about a system without having to necessarily obtain its solutions. In particular, one can use the so-called primary decomposition of the ideal (though making use of the Gröbner basis technique only) to obtain information such as the dimensionality of the solution space and number of isolated real roots. This is indeed a clever way to resolve the above-mentioned issue up to a certain level. However, here, the next difficulty comes in the form of algorithmic complexity. The BA is known to suffer from exponential space complexity, which roughly means that the memory (Random Access Memory) required by the machine blows up exponentially with increasing number of polynomials, variables, monomials, and/or degree of the polynomials involved in the system. Hence, even the computation for the primary decomposition may not finish for large sized systems, whereas the NPHC method is strikingly different from the Gröbner basis techniques in that the algorithm for the former suffers from no known major complexities. Hence one can in principle find all solutions of bigger systems.

The BA is a highly sequential algorithm, that is, each step in the algorithm requires knowledge of the previous one. Thus, although recently there are certain parts of the BA which have been parallelized, in general, it is extremely difficult to parallelize the algorithm.

On the other hand, in the NPHC method, the path tracking is *embarrassingly parallelizable*, because each start solution can be tracked completely independently of the others. This feature along with the rapid progress towards the improvements of the algorithms makes the NPHC well suited for a large class of physical problems arising not only in string phenomenology but in condensed matter theory, lattice QCD, and so forth.

The BA is mainly defined for systems with rational coefficients, while in real-life applications, the systems may have real coefficients. The NPHC method being a purely numerical method by default incorporates floating point coefficients as well.

In conclusion, both the Gröbner basis techniques and the NPHC have advantages and disadvantages. However, for practical purposes, the NPHC method is a far more efficient and promising method for realistic systems.

6. Frequently Asked Questions

In this section, we collect the frequently asked questions and their answers.

- (1) What does the NPHC method tell us about systems which do not have any solutions?

As mentioned above, the NPHC method by construction (in conjunction with the γ -trick) gives all real and complex solutions of a system of multivariate polynomial equations that is known to have only isolated solutions. Hence, we are always sure that we have got all the solutions numerically. This statement is true for all cases such as when the system has no complex solutions and/or no real solutions or no solution at all. One possible issue, as mentioned above, regards the classification of the real solutions independent of the tolerance used. This can be resolved by using, for example, the alphaCertified algorithm which certifies when a solution is a real.

- (2) For many practical problems, only real solutions are required. Thus, when implementing the NPHC, a huge amount of computational effort is wasted in getting the other types of solutions. Would it not be helpful to track only the real solutions?

It would be much more useful if there was a way of getting only real solutions. However, for a number of technical reasons nicely discussed in [21], a path tracker does not know in advance if a given start solution will end up being a real solution of the original system. Moreover, one can wonder if a root count exists only for the real solutions of a system. This would involve obtaining a corresponding fundamental theorem of algebra on the real space for the multivariate case. This, however, has yet to be achieved. Hence, the best way for now is to track all complex (including real paths) solutions and then filter out the real solutions.

- (3) Can the NPHC method be used as a global or local minimization method?

Absolutely, most of the conventional methods used to minimize a function are based on the Newton-Raphson method, where a start solution is guessed and is then refined by successive iterations in the direction of the minima. By performing this algorithm several times on the functions, one can obtain many minima of the given potential. Recently, more efficient methods such as the basin-hopping method are available for local minimization [30]. However, we are never sure if we have got all the minima from any of these methods. For the global minimization, we may

use more efficient methods such as Simulated Annealing and Genetic Algorithm. However, these methods are known to fail for larger systems since it can easily get trapped at a local minimum when trying to find the global minimum. Thus, in addition to the usual error from the numerical precision of the machine, there can be an error of an *unknown* order (i.e., we do not know if the found one is the global minimum!). But if the function has a polynomial-like nonlinearity, in theory the NPHC method can give all the minima since it obtains all the stationary points. So it solves the local minimization problem. Moreover, it is then easy to identify *the* global minimum out of the minima, and hence we are sure that the found one is actually the global minimum.

- (4) As in the example system in this paper, for many systems the number of actual solutions may be well below the CBB. Is there any remedy for this issue?

The main reason why the number of actual solutions is less than the CBB for many systems is that the CBB does not take the sparsity (i.e., very few monomials in each polynomial in the system) of the system into account. There is indeed a tighter upper bound on the number of complex solutions, called the Bernstein-Khovanskii-Kushnirenko (BKK) count [20, 21], which takes this sparsity into account and thus in most cases is much lower than the CBB. In many cases, it is in fact equal to the number of solutions. The BKK bound can thus save a lot of computation time since the number of paths to be tracked is less than the CBB. The details on the BKK count relating to string phenomenology problems will be published elsewhere.

- (5) Are there any alternative/supplementary numerical methods?

There are not many methods to find the stationary points of a multivariate function around, compared to the number of methods to find minima. One of the methods that can find stationary points is the Gradient-minimization method which finds all the minima of an auxiliary function $E = |\nabla V|^2$ whose minima are the stationary points of V provided we further restrict E to be zero [31]. One can find many minima of E using some conventional minimization method such as the Conjugate Gradient method or the Simulated Annealing method. However, it is known that as the system size increases, the number of minima of E that are not the minima of V , that is, $E > 0$, increases rapidly, making the method inefficient [32]. Another method is the Newton-Raphson method (and its sophisticated variants) [30, 32–34]. There, an initial guess is refined iteratively to a given precision. It should be emphasized, however, that no matter how many different random initial guesses are fed into the algorithm, we can never be sure to get all the solutions in the end, unlike the NPHC method. However, these two methods can be supplementary methods for bigger systems to get an idea on what to expect there.

- (6) This paper mainly deals with the potentials having polynomial-like nonlinearity which may be usual in the perturbation limit. What about the fully nonperturbative potentials?

The most interesting application for this method would be in the nonperturbative regime, certainly. This question can be stated in different words: is it possible to translate the stationary equations for the nonperturbative potential (i.e., the potentials which have logarithm and exponential terms), and if so, how? Once we can translate the equations in the polynomial form, we can again use the NPHC method as before. The answer is already available in [10]. In this work, Gray et al.

have already prescribed how to translate the corresponding equations arising in the nonperturbative regime which usually involve logarithms and/or exponentials, by using dummy variables. After that, we can solve the system using algebraic geometry methods, such as the Gröbner basis, or for more complicated cases, the NPHC method presented in this paper. Once we have all the solutions, we can extract the solutions in terms of the original variables which were logarithms and/or exponentials of the fields. This trick makes all the algebraic geometry methods, not only the NPHC method, applicable to finding the vacua of the potentials in the nonperturbative regime.

- (7) This method assumes that one knows that the system under consideration has only isolated solutions. But, in general, one may not know if a given system has only isolated solutions or it contains some positive dimensional components. In that case, do not we need to rely on the Gröbner basis techniques only, at least to check the dimension of the system?

Firstly, in many systems, once we add the constraint equation (i.e., the denominators are never zero), they usually turn out to have only isolated solutions. Thus, there are way too many interesting systems in string phenomenology which only have isolated solutions. Of course, there may be many more systems which would have positive dimensional solution components. To solve such systems, there is a recently developed generalization of the numerical homotopy continuation method, called the Numerical Algebraic Geometry method. This method finds out each of the positive dimensional solution components with its dimensionality. This method is also *embarrassingly parallelizable* and hence goes far beyond the reach of the Gröbner basis methods. The details of this method are much more involved and beyond the scope of the present paper. But, in short, to find out the dimensionality of the system we do not necessarily need to rely on the Gröbner basis methods. The details of this method with applications will be published elsewhere.

7. Summary

In this paper, we have reviewed a novel method, called the numerical polynomial homotopy continuation (NPHC) method, which can find all the string vacua of a given potential. It does not suffer from any major algorithmic complexities compared to the existing symbolic algebra methods based on the Gröbner basis techniques, which are known to suffer from exponential space complexity. Moreover, the NPHC method is *embarrassingly parallelizable*, making it a very efficient alternative to the existing symbolic algebra methods. As an example, we studied a toy model and, using the NPHC method, found all the vacua within less than a minute using a regular desktop machine. Note that this system with the irrational coefficients is already a difficult task using the Gröbner basis techniques. In addition to that, using the NPHC method, with just about an hour of computation on a regular desktop machine, we found all vacua of an M theory model compactified on the coset $(SU(3) \times U(1))/(U(1) \times U(1))$, which has an $SU(3)$ structure. This system was reported to be a prohibitively difficult problem using the symbolic method. Thus, we have already shown how efficiently the NPHC method can solve the problems that are yet far beyond the reach of the traditional symbolic methods. We also emphasize that using the procedure prescribed in [10] to translate the stationary equations arising in the nonperturbative regime, by replacing logarithm and exponential terms of the field variables by dummy variables, into the polynomial form, we can use the NPHC method

to find the vacua for the nonperturbative potentials as well. It is this application of the method which makes it quite promising. With the help of the NPHC method it is thus hoped that we can go far beyond the reach of the existing methods and study realistic models very efficiently.

Acknowledgments

D. Mehta was supported by the US Department of Energy grant under contract no. DE-FG02-85ER40237 and Science Foundation Ireland grant 08/RFP/PHY1462. D. Mehta would like to thank James Gray, Yang-Hui He, and Anton Ilderton for encouraging and helping him throughout in this work.

References

- [1] J. Gray, "A simple introduction to Gröbner basis methods in string phenomenology," *Advances in High Energy Physics*, vol. 2011, Article ID 217035, 12 pages, 2011.
- [2] D. Cox, J. Little, and D. O'Shea, *Ideals, Varieties, and Algorithms: An Introduction to Computational Algebraic Geometry and Commutative Algebra, 3/e*, Undergraduate Texts in Mathematics, Springer, Secaucus, NJ, USA, 3rd edition, 2007.
- [3] J. C. Faugère, "A new efficient algorithm for computing groebner bases (f4)," *Journal of Pure and Applied Algebra*, pp. 75–83, 1999.
- [4] J. C. Faugère, "A new efficient algorithm for computing Gröbner bases without reduction to zero (F5)," in *Proceedings of the International Symposium on Symbolic and Algebraic Computation, (ISSAC '02)*, pp. 75–83, New York, NY, USA, July 2002.
- [5] V. P. Gerdt, "Involutive algorithms for computing groebner bases," <http://arxiv.org/abs/math/0501111>.
- [6] G.-M Pfister, G. S. H. Decker, and W. Greuel, "Singular 3-1-3—a computer algebra system for polynomial computations," 2011, <http://www.singular.uni-kl.de/>.
- [7] CoCoA Team, "CoCoA: a system for doing computations in commutative algebra," <http://cocoa.dima.unige.it/>.
- [8] D. R. Grayson and M. E. Stillman, "Macaulay2, a software system for research in algebraic geometry," <http://www.math.uiuc.edu/Macaulay2/>.
- [9] W. Bosma, J. Cannon, and C. Playoust, "The magma algebra system. I. The user language," *Journal of Symbolic Computation*, vol. 24, no. 3-4, pp. 235–265, 1997.
- [10] J. Gray, Y.-H. He, A. Ilderton, and A. Lukas, "A new method for finding vacua in string phenomenology," *Journal of High Energy Physics*, no. 7, p. 23, 2007.
- [11] J. Gray, Y.-H. He, A. Ilderton, and A. Lukas, "STRINGVACUA. Mathematica package for studying vacuum configurations in string phenomenology," *Computer Physics Communications*, vol. 180, no. 1, pp. 107–119, 2009.
- [12] J. Gray, Y.-H. He, and A. Lukas, "Algorithmic algebraic geometry and flux vacua," *Journal of High Energy Physics*, no. 9, p. 31, 2006.
- [13] D. B. Mehta, A. Sternbeck, L. von Smekal, and A. G. Williams, "Lattice landau gauge and algebraic geometry," in *Proceedings of the International Workshop on QCD Green's Functions, Confinement, and Phenomenology, (QCD-TNT '09)*, vol. 25, ECT, Trento, Italy, 2009.
- [14] D. Mehta, *Lattice vs. Continuum: landau gauge fixing and 't Hooft-Polyakov monopoles*, Ph.D. thesis, The University of Adelaide, Australasian Digital Theses Program, Adelaide, Australia, 2009.
- [15] D. Mehta, "Finding all the stationary points of a potential-energy landscape via numerical polynomial-homotopy-continuation method," *Physical Review E*, vol. 84, no. 2, Article ID 025702, 4 pages, 2011.
- [16] M. Kastner and D. Mehta, "Phase Transitions Detached from Stationary Points of the Energy Landscape," *Physical Review Letters*, vol. 107, no. 16, Article ID 160602, 5 pages, 2011.
- [17] D. Mehta and M. Kastner, "Stationary point analysis of the one-dimensional lattice Landau gauge fixing functional, aka random phase XY Hamiltonian," *Annals of Physics*, vol. 326, no. 6, pp. 1425–1440, 2011.

- [18] L. von Smekal, A. Jorkowski, D. Mehta, and A. Sternbeck, "Lattice Landau gauge via stereographic projection," in *Proceedings of the 8th Conference Quark Confinement and the Hadron Spectrum, (CONFINEMENT '08)*, vol. 8, Mainz, Germany, 2008.
- [19] L. von Smekal, D. Mehta, A. Sternbeck, and A. G. Williams, "Modified lattice landau gauge," *PoS, LAT*, vol. 382, 2007.
- [20] T. Y. Li, "Numerical Solution of Polynomial Systems by Homotopy Continuation Methods," *Handbook of Numerical Analysis*, vol. 11, pp. 209–304, 2003.
- [21] A. J. Sommese and C. W. Wampler, II, *The Numerical Solution of Systems of Polynomials Arising in Engineering and Science*, World Scientific Publishing, Hackensack, NJ, USA, 2005.
- [22] D. J. Bates, J. D. Hauenstein, A. J. Sommese, and C. W. Wampler, <http://www.nd.edu/~sommese/bertini>.
- [23] J. Verschelde, "Algorithm 795: PHCpack: a general-purpose solver for polynomial systems by homotopy continuation," *ACM Transactions on Mathematical Software*, vol. 25, no. 2, pp. 251–276, 1999.
- [24] T. Gunji, S. Kim, M. Kojima, A. Takeda, K. Fujisawa, and T. Mizutani, "PHoM—a polyhedral homotopy continuation method for polynomial systems," *Computing. Archives for Scientific Computing*, vol. 73, no. 1, pp. 57–77, 2004.
- [25] A. P. Morgan, A. J. Sommese, and L. T. Watson, "Finding all isolated solutions to polynomial systems using HOMPACK," *Association for Computing Machinery. Transactions on Mathematical Software*, vol. 15, no. 2, pp. 93–122, 1989.
- [26] T. Gao, T. Y. Li, and M. Wu, "Algorithm 846: mixed vol: a software package for mixed-volume computation," *Association for Computing Machinery. Transactions on Mathematical Software*, vol. 31, no. 4, pp. 555–560, 2005.
- [27] T. L. Lee, T. Y. Li, and C. H. Tsai, "HOM4PS-2.0: a software package for solving polynomial systems by the polyhedral homotopy continuation method," *Computing. Archives for Scientific Computing*, vol. 83, no. 2-3, pp. 109–133, 2008.
- [28] J. D. Hauenstein and F. Sottile, "alphaCertified: certifying solutions to polynomial systems," <http://arxiv.org/abs/1011.1091>.
- [29] A. Micu, E. Palti, and P. M. Saffin, "M-theory on seven-dimensional manifolds with SU(3) structure," *Journal of High Energy Physics*, no. 5, p. 48, 2006.
- [30] D. Wales, *Energy Landscapes : Applications to Clusters, Biomolecules and Glasses (Cambridge Molecular Science)*, Cambridge University Press, New York, NY, USA, 2004.
- [31] K. Broderix, K. K. Bhattacharya, A. Cavagna, A. Zippelius, and I. Giardina, "Energy landscape of a Lennard-Jones liquid: statistics of stationary points," *Physical Review Letters*, vol. 85, no. 25, pp. 5360–5363, 2000.
- [32] J. P. K. Doye and D. J. Wales, "Saddle points and dynamics of Lennard-Jones clusters, solids, and supercooled liquids," *Journal of Chemical Physics*, vol. 116, no. 9, pp. 3777–3788, 2002.
- [33] T. S. Grigera, A. Cavagna, I. Giardina, and G. Parisi, "Geometric approach to the dynamic glass transition," *Physical Review Letters*, vol. 88, no. 5, pp. 555021–555024, 2002.
- [34] D. J. Wales and J. P. K. Doye, "Stationary points and dynamics in high-dimensional systems," *Journal of Chemical Physics*, vol. 119, no. 23, pp. 12409–12416, 2003.

Research Article

Non-Supersymmetric CS-Matter Theories with Known AdS Duals

Davide Forcella¹ and Alberto Zaffaroni^{2,3}

¹ *Physique Théorique et Mathématique and International Solvay Institutes, Université Libre de Bruxelles, C.P. 231, 1050 Bruxelles, Belgium*

² *Dipartimento di Fisica, Università di Milano-Bicocca, 20126 Milano, Italy*

³ *INFN, Sezione di Milano-Bicocca, 20126 Milano, Italy*

Correspondence should be addressed to Alberto Zaffaroni, alberto.zaffaroni@mib.infn.it

Received 15 March 2011; Accepted 16 July 2011

Academic Editor: Amihay Hanany

Copyright © 2011 D. Forcella and A. Zaffaroni. This is an open access article distributed under the Creative Commons Attribution License, which permits unrestricted use, distribution, and reproduction in any medium, provided the original work is properly cited.

We consider three-dimensional conformal field theories living on a stack of N anti-M2 branes at the tip of eight-dimensional supersymmetric cones. The corresponding supergravity solution is obtained by changing sign to the four-form in the Freund-Rubin solution representing M2 branes (“skew-whiffing” transformation) and it is known to be stable. The existence of these non-supersymmetric, stable field theories, at least in the large N limit, is a peculiarity of the $\text{AdS}_4/\text{CFT}_3$ correspondence with respect to the usual $\text{AdS}_5/\text{CFT}_4$, and it is worthwhile to study it. We analyze in detail the KK spectrum of the skew-whiffed solution associated with S^7/\mathbb{Z}_k and we speculate on the natural field content for a candidate non-supersymmetric dual field theory.

1. Introduction

There has been some progress in understanding the conformal field theories living on a stack of N M2 branes at the tip of noncompact eight-dimensional cones. These theories are holographically dual to Freund-Rubin compactifications of M theory of the form $\text{AdS}_4 \times H_7$, where H_7 is the Einstein manifold at the base of the cone. In the case of large supersymmetry, $\mathcal{N} \geq 3$, the conformal field theory has been identified with a Chern-Simons theory in [1–10]. The case where the cone is a Calabi-Yau fourfold corresponds to $\mathcal{N} = 2$ supersymmetry, and a general construction of the dual Chern-Simons theories has been discussed in [11, 12]; a large number of models have been subsequently constructed [13–23]. For the smallest amount of supersymmetry, $\mathcal{N} = 1$, the cone is a $\text{Spin}(7)$ manifold and a generic construction of the dual field theories for orbifolds has been given in [24]. In this paper we are interested in the three-dimensional conformal field theories living on a stack of N anti-M2 branes at the

tip of eight-dimensional cones with at least Spin(7) holonomy. The existence of these non-supersymmetric, stable field theories, at least in the large N limit, is a peculiarity of the AdS₄/CFT₃ correspondence with respect to the usual AdS₅/CFT₄, and it is worthwhile to study it (Previous studies of three-dimensional non-supersymmetric field theories in similar setups can be found in [25, 26].)

The supergravity solutions of N anti-M2 branes at the tip of supersymmetric cones is obtained by changing sign to the four-form in the familiar solutions representing M2 branes. This operation is called “skew-whiffing” in the supergravity literature and it is proven to produce a stable non-supersymmetric background [27]. The KK spectrum of the final theory is obtained from the original spectrum by a reshuffling of states. We will mostly focus on the simple case $H_7 = S^7$ in this paper. In this particular case the skew-whiffing procedure is equivalent to a triality transformation in the isometry group $SO(8)$ and it leaves the theory invariant. However, following the recent results on AdS₄ × CFT₃, we are really interested in $H_7 = S^7/\mathbb{Z}_k$. For $k \geq 2$ the skew-whiffing produces a stable non-supersymmetric background. It is interesting then to find a plausible dual field theory. (In [28] there is a discussion of the effect of the skew-whiffing on the dual field theory for $k = 1$.) In this paper we analyze in detail the KK spectrum of the skew-whiffed theory and we speculate on a candidate for the underlying field theory. Without supersymmetry, it is difficult to make explicit checks of the proposal. We are guided in our search by the attempt of implementing the skew-whiffing procedure to the ABJM theory [6].

The paper is organized as follows. In Section 2 we discuss the skew-whiffing construction. In Section 3 we discuss a natural field content for the skew-whiffing of the ABJM theory. In Section 4 we make some checks of the proposal and in particular we see that the relevant features of the KK spectrum in supergravity are compatible with the operator content of the field theory. In Section 5 we discuss possible generalizations.

2. The Skew-Whiffed Solutions

M-theory has a very natural compactification to four dimensions. (For a comprehensive review see [29].) It comes from the Freund-Rubin ansatz for the 3-form field,

$$F_{\mu\nu\rho\sigma} = 3m\epsilon_{\mu\nu\rho\sigma}, \quad F_{mnpq} = 0, \quad (2.1)$$

where m is a real constant, the greek letters label the four space-time directions, while the latin letters label the internal seven-dimensional space. As a consequence the metric satisfies the equations

$$R_{\mu\nu} = -12m^2 g_{\mu\nu}, \quad R_{mn} = 6m^2 g_{mn} \quad (2.2)$$

and M theory spontaneously compactifies to AdS₄ × H_7 , where H_7 is an Einstein space. If the Einstein manifold H_7 has at least weak G_2 holonomy, then the solution is supersymmetric and hence stable. This solution can indeed be interpreted as the near horizon solution for M2 branes at the tip of the real cone $C(H_7)$. There is another very natural solution that can be obtained sending m to $-m$: the four-form changes sign, while the metric is invariant. This solution can be interpreted as the near horizon solution for anti-M2 branes at the tip of the real cone $C(H_7)$ and it is called the “skew-whiffed” solution.

It is interesting to observe that the skew-whiffed transformation changes the sign of the Page charge $P = 1/\pi^4 \int_{H_7} *F$ and can indeed be equivalently interpreted as a change of orientation for H_7 .

The number of preserved supersymmetries of a solution is the number of independent Killing spinors η solving the equation

$$\left(\nabla_n - \frac{1}{2} m \Gamma_n \right) \eta = 0. \quad (2.3)$$

This supersymmetric condition explicitly depends on m . Indeed it is possible to prove that, with exception of the round sphere S^7 , where both orientations give the maximum supersymmetry $\mathcal{N} = 8$, at most one orientation can have $\mathcal{N} > 0$ [29]. Moreover it is possible to prove that the skew-whiffing of a supersymmetric Freud-Rubin solution is perturbatively stable [27]. Hence, given a supersymmetric Freud-Rubin solution, we can find another non-supersymmetric stable solution, obtained by applying the skew-whiffing transformation. (See [30, 31] for some recent applications of the skew-whiffed solutions.)

These theories are expected to have a well-defined dual non-supersymmetric three-dimensional conformal field theory. In this paper we will discuss a natural field content for these theories.

It is important to observe that the skew-whiffing procedure is somehow peculiar of M theory. Indeed the same transformation could be applied to the five-form in the Freud-Rubin ansatz for type IIB supergravity. However, in this case, the resulting theory would still be supersymmetric.

3. The Skew-Whiffing of the ABJM Theory

When the seven-dimensional Einstein space is a \mathbb{Z}_k quotient of the round sphere, S^7/\mathbb{Z}_k , the dual field theory is the well-known ABJM model [6]. This is an $\mathcal{N} = 6$ three-dimensional $U(N) \times U(N)$ Chern-Simons theory with levels k and $-k$, coupled to four complex bosons X^A and four complex fermions ψ_A transforming in the bifundamental of the gauge group. The global symmetry is $SU(4)_R \times U(1)$, the non-abelian part being the R symmetry group, while the abelian part being the baryonic symmetry. The bifundamental bosons X^A transform in the representation $\mathbf{4}_1$ of the global symmetry group and the bifundamental fermions ψ_A transform in the $\bar{\mathbf{4}}_{-1}$. All fields have canonical dimension: $1/2$ for the bosons and 1 for the fermions.

This specific field content can be understood as the decomposition of the degrees of freedom of the $\mathcal{N} = 8$ conformal theory dual to S^7 under the breaking of the R symmetry group $SO(8) \rightarrow SU(4) \times U(1)$ induced by \mathbb{Z}_k . The natural field content of the theory describing S^7 consists in a scalar Φ_a transforming in the $\mathbf{8}_v$ vectorial representation of $SO(8)$, and a fermion Υ_a transforming in the $\mathbf{8}_s$ spinorial representation of $SO(8)$ (this is the *singleton* representation of the superconformal group); the eight supercharges transform in the $\mathbf{8}_c$ conjugate spinor representation. These are the degrees of freedom that we expect to live on a supersymmetric M2 brane in flat space. The existing $\mathcal{N} = 8$ Chern-Simons theory describing membranes, the BLG model [1–5], have indeed this field content. The $\mathcal{N} = 8$ multiplet decomposes as $\mathbf{8}_v \rightarrow \mathbf{4}_1 + \bar{\mathbf{4}}_{-1}$, $\mathbf{8}_s \rightarrow \mathbf{4}_1 + \bar{\mathbf{4}}_{-1}$ under $SO(8) \rightarrow SU(4) \times U(1)$ and we recover the ABJM matter content describing S^7/\mathbb{Z}_k . The ABJM model has enhanced $\mathcal{N} = 8$

supersymmetry for $k = 1$ but this enhancement is not manifest and it is conjectured to be realized through light monopole operators which become relevant for $k = 1$.

We would like to identify a candidate for the skew-whiffing solution on S^7/\mathbb{Z}_k . As we explained in the previous section, the skew-whiffing procedure can be understood as the change of orientation of S^7 , and hence as a parity transformation on \mathbb{R}^8 . The scalar fields living on the M2 can be seen as the coordinates of the transverse space, and, under parity, an odd number of them change sign, while the associated eight-dimensional spinor changes chirality.

The skew-whiffing procedure can be seen as a map,

$$\text{SW} : (\mathbf{8}_v, \mathbf{8}_s) \longrightarrow (\mathbf{8}_v, \mathbf{8}_c). \quad (3.1)$$

An explicit realization of this map on an $\mathcal{N} = 8$ multiplet is

$$\text{SW} : (\Phi^i, \Phi^8, Y^a) \longrightarrow (\Phi^i, -\Phi^8, (\Gamma^8)_{\dot{a}a} Y^a). \quad (3.2)$$

For $k = 1$, this transformation should be an invariance of the dual-field theory, since S^7 is skew-whiffing invariant. We can test this transformation in the BLG theory [1–5], which is an explicit $\mathcal{N} = 8$ lagrangian theory invariant under the $SO(8)R$ symmetry and describes a pair of membranes. It is an easy exercise to see that the BLG Lagrangian is indeed invariant under the transformation (3.2), as required by the supergravity skew-whiffing transformation. In the ABJM theory with $k = 1$, this transformation is, on the other hand, nonlocally realized.

For generic k , the $SO(8)$ symmetry is broken to $SU(4) \times U(1)$. Under skew whiffing, the $\mathbf{8}_s$ fermions are replaced by $\mathbf{8}_c$ and the fields decompose as $\mathbf{8}_v \rightarrow \mathbf{4}_1 + \bar{\mathbf{4}}_{-1}$, $\mathbf{8}_c \rightarrow \mathbf{1}_2 + \mathbf{6}_0 + \mathbf{1}_{-2}$. The original supersymmetry charges would now transform in the $\mathbf{8}_s \rightarrow \mathbf{4}_1 + \bar{\mathbf{4}}_{-1}$. None is invariant under the $U(1)$ symmetry and hence the theory naturally breaks all the supersymmetries.

It is natural to expect that the dual of the skew-whiffed S^7/\mathbb{Z}_k is a non-supersymmetric three-dimensional Chern-Simons theory with matter. Let us try to understand what is the natural field content. We still expect a gauge group $U(N) \times U(N)$ and a global symmetry $SU(4)$. Comparing with the geometric action of the SW transformation, we introduce complex scalars X^A transforming in the bifundamental of the gauge groups and in the fundamental of the global symmetry $SU(4)$; real fermions Ψ^I transforming in the adjoint of the first gauge group and in the antisymmetric of $SU(4)$; complex fermions ξ transforming in the bifundamental of the $SU(N) \times SU(N)$ gauge group, with charge 2 under the difference of the two $U(1)$ gauge factors and as singlets under the global symmetry $SU(4)$. The matter content of such a theory is summarized in Table 1 below.

As we will see in Section 4, the supergravity KK spectrum predicts the existence of operators with integer dimensions in the dual-field theory. A peculiarity of the skew-whiffing transformation indeed is the fact that it just reshuffles the KK states without changing their dimensions. To match the KK spectrum with the above field content we need to assume that all the fields have canonical dimensions: 1/2 for the scalars and 1 for the fermions. It is then

Table 1: Matter content and charges.

Fields	$SU(N)_1$	$SU(N)_2$	$U(1)_1 - U(1)_2$	$U(1)_1 + U(1)_2$	$SU(4)$
X^A	\mathbf{N}	$\overline{\mathbf{N}}$	$\mathbf{1}$	$\mathbf{0}$	$\mathbf{4}$
Ψ^I	Adj	$\mathbf{0}$	$\mathbf{0}$	$\mathbf{0}$	$\mathbf{6}$
ξ	\mathbf{N}	$\overline{\mathbf{N}}$	$\mathbf{2}$	$\mathbf{0}$	$\mathbf{1}$

tempting to write a classically conformal invariant Lagrangian for the fields X^A, Ψ^I, ξ . The most general Lagrangian we can write is

$$\mathcal{L} = \mathcal{L}_{\text{CS}} + \mathcal{L}_{\text{kin}} + V_{\text{bos}} + V_{\text{fer}}, \quad (3.3)$$

where

$$\begin{aligned} \mathcal{L}_{\text{CS}} &= \frac{k}{4\pi} \text{Tr} \left[e^{\mu\nu\lambda} \left(A_\mu \partial_\nu A_\lambda + \frac{2i}{3} A_\mu A_\nu A_\lambda \right) - e^{\mu\nu\lambda} \left(\tilde{A}_\mu \partial_\nu \tilde{A}_\lambda + \frac{2i}{3} \tilde{A}_\mu \tilde{A}_\nu \tilde{A}_\lambda \right) \right], \\ S_{\text{kin}} &= \text{Tr} \left(-D^\mu X^A D_\mu X_A^\dagger + i \overline{\Psi}^I \gamma^\mu D_\mu \Psi^I + i \bar{\xi}^\dagger \gamma^\mu D_\mu \xi \right), \\ V_{\text{bos}} &= \frac{\pi^2}{12k^2} \text{Tr} \left(X^A X_A^\dagger X^B X_B^\dagger X^C X_C^\dagger + X_A^\dagger X^A X_B^\dagger X^B X_C^\dagger X^C + 4X^A X_B^\dagger X^C X_A^\dagger X^B X_C^\dagger \right. \\ &\quad \left. - 6X^A X_B^\dagger X^B X_A^\dagger X^C X_C^\dagger \right), \\ V_{\text{fer}} &= \frac{i\pi}{2k} \text{Tr} \left(c_1 (\Gamma^{IJ})^B_A X^A X_B^\dagger \Psi^I \Psi^J + c_2 (X^A X_A^\dagger \xi \xi^\dagger - X_A^\dagger X^A \xi^\dagger \xi) \right), \end{aligned} \quad (3.4)$$

where the covariant derivatives act according to Table 1. We keep the same bosonic potential of the ABJM theory, and we introduce two real couplings c_i to parametrize the fermionic potential. The same potential of the ABJM theory guarantees that a probe see $\mathbb{R}^8/\mathbb{Z}_k$ as a moduli space; in the skew-whiffed supergravity background an anti-M2 brane feels no potential, exactly as a M2 brane in the original background. The Lagrangian is scale invariant at classical level. Obviously, without supersymmetry, there is no guarantee that the theory remains conformal invariant at the quantum level and, in general, we expect that the fields acquire anomalous dimensions. It is tempting to speculate that, in the limit where supergravity is valid (large N limit and strong coupling $N/k \gg 1$ in type IIA), the theory becomes conformal with canonical dimensions for the fields.

One could try to impose a relation between the c_i in the fermionic potential by requiring that the scalar BPS operators of the ABJM theory do not acquire anomalous dimensions at weak coupling in the SW ABJM theory. This constraint is suggested by the dimensions of the scalar part of the KK spectrum in supergravity, and the strong assumption that we can extrapolate from strong to weak coupling. The argument goes as follows. Starting from the lagrangian (3.4) it is possible to compute the quantum part of the two loop dilatation operator (mixing matrix) for small values of N/k . The mixing matrix acting on the gauge invariant operators of the field theory gives their anomalous dimensions. The mixing matrix acting on the gauge invariant operators done by contracting only the scalar fields X^A and X_A^\dagger was computed in [32] for the ABJM theory. The computation can be easily repeated for the SW

ABJM theory: the only difference is the contribution coming from the fermions running into the loops, and in particular their contribution to the identity and the trace part of the mixing matrix. By imposing that the scalar mixing matrix of the SW ABJM theory is annihilated by the scalar symmetric traceless operators (4.12) we find a constraint on the c_i . It would be much harder to perform a similar computation with operators with fermionic insertions to see if some of them remain with canonical dimensions with such a choice of c_i .

4. The KK Spectrum

In this section, we discuss in details the KK spectrum of the skew-whiffed M theory solution on S^7/\mathbb{Z}_k and of its reduction to type IIA. The KK states should correspond to the single trace operators of the dual field theory with finite dimensions in the large N and strong coupling limit. It is obviously difficult to predict the spectrum of operators with finite dimensions in a non-supersymmetric theory. However, the distinctive features of the KK spectrum put constraints on the dual field content.

4.1. The Spectrum on S^7

The KK spectrum of the M-theory Freund-Rubin solution on S^7 is well known [33, 34] and reported for completeness in Table 2. The states are classified by the dimension and the representation under $SO(8)$ and are organized in superconformal multiplets specified by an integer number $m \geq 2$. The lowest state in each multiplet is scalar field of dimension $m/2$ transforming in the $[m, 0, 0, 0]$ representation of $SO(8)$. The other states are obtained by acting on the lowest state with the $\mathcal{N} = 8$ supersymmetries transforming as $\mathbf{8}_c = [0, 0, 0, 1]$ under $SO(8)$. The multiplet is short and has spin range equal to two, compared with the spin range of four of a long multiplet. The multiplets $m = 2, 3$ sustain further shortenings; $m = 2$ corresponds to the *massless* multiplet of the $\mathcal{N} = 8$ gauged supergravity. Partition functions encoding the spectrum of S^7 (and of its quotient) in a related context can be found in [35–38].

We can understand the structure of the multiplets by considering a very simple theory of eight free bosons Φ^i and eight free fermions Y^a . These are the expected degrees of freedom living on a membrane in flat space. The lowest state of the m -th KK supermultiplet can be represented by Φ^m , which is a schematic expression for the product of m fields completely symmetrized in their $SO(8)$ indices and with all the traces removed:

$$\Phi^m \equiv \Phi^{(i_1} \dots \Phi^{i_m)} - \text{traces.} \quad (4.1)$$

The other states are obtained by applying the supersymmetry transformations that schematically read

$$\begin{aligned} [Q_{\dot{\alpha}}, \Phi^i] &= i(\tilde{\Gamma}^i)^{\dot{\alpha}a} Y_{\dot{\alpha}}^a, \\ \{Q_{\dot{\alpha}}, Y_{\dot{\beta}}^a\} &= (\Gamma^\mu)_{\dot{\alpha}\dot{\beta}} D_\mu \Phi^i (\Gamma^i)^{\dot{\alpha}\dot{\beta}}. \end{aligned} \quad (4.2)$$

The first spinorial state $(1/2)^{(1)}$ with dimension $(m+1)/2$ reads

$$Y_{\dot{\alpha}}^a \Phi^{m-1}, \quad (4.3)$$

Table 2: The spectrum on S^7 .

Spin	$SO(8)$	Δ
2^+	$[m-2, 0, 0, 0]$	$\frac{m+4}{2}$
$\frac{3}{2}^{(1)}$	$[m-2, 0, 0, 1]$	$\frac{m+3}{2}$
$\frac{3}{2}^{(2)}$	$[m-3, 0, 1, 0]$	$\frac{m+5}{2}$
$1^{-(1)}$	$[m-2, 1, 0, 0]$	$\frac{m+2}{2}$
$1^{+(2)}$	$[m-3, 0, 1, 1]$	$\frac{m+4}{2}$
$1^{-(2)}$	$[m-4, 1, 0, 0]$	$\frac{m+6}{2}$
$\frac{1}{2}^{(1)}$	$[m-1, 0, 1, 0]$	$\frac{m+1}{2}$
$\frac{1}{2}^{(2)}$	$[m-3, 1, 1, 0]$	$\frac{m+3}{2}$
$\frac{1}{2}^{(3)}$	$[m-4, 1, 0, 1]$	$\frac{m+5}{2}$
$\frac{1}{2}^{(4)}$	$[m-4, 0, 0, 1]$	$\frac{m+7}{2}$
$0^{+(1)}$	$[m, 0, 0, 0]$	$\frac{m}{2}$
$0^{-(1)}$	$[m-2, 0, 2, 0]$	$\frac{m+2}{2}$
$0^{+(2)}$	$[m-4, 2, 0, 0]$	$\frac{m+4}{2}$
$0^{-(2)}$	$[m-4, 0, 0, 2]$	$\frac{m+6}{2}$
$0^{+(3)}$	$[m-4, 0, 0, 0]$	$\frac{m+8}{2}$

where, again, Φ^m will represent a fully symmetrized and traceless string of fields Φ^{i_k} . The indices are contracted in such a way that the operator transforms as $[m-1, 0, 1, 0]$. The states with dimension $(m+2)/2$ are obtained by applying two supercharges whose Lorentz indices can be antisymmetrized or symmetrized giving a scalar $0^{-(1)}$ and a vector $1^{-(1)}$ of schematic form

$$Y_{[\alpha}^{[a} Y_{\beta]}^{b]} \Phi^{m-2}, \quad \left(Y_{[\alpha}^{[a} Y_{\beta]}^{b]} + \gamma_{\alpha\beta}^{\mu} \Phi^{[i_1} D_{\mu} \Phi^{i_2]} \right) \Phi^{m-2}. \quad (4.4)$$

The fermionic bilinears transform in the $[0, 0, 2, 0]$ and $[0, 1, 0, 0]$ representation of $SO(8)$, respectively, which can be contracted with $[m-2, 0, 0, 0]$ to give the expected representations

$[m - 2, 0, 2, 0]$ and $[m - 2, 1, 0, 0]$ given in Table 2. The states with dimension $(m + 3)/2$ read schematically

$$\left(Y_a^a Y_\beta^b Y_\gamma^c + \dots \right) \Phi^{m-3}. \quad (4.5)$$

The Lorentz indices can be completely symmetric or with mixed symmetry; we obtain a state $(3/2)^{(1)}$ with three $SO(8)$ indices transforming in the $[1, 0, 0, 1]$ and a state $(1/2)^{(2)}$ with three indices $[0, 1, 1, 0]$, respectively. Combining with the bosonic part we easily recover the representations $[m - 2, 0, 0, 1]$ and $[m - 3, 1, 1, 0]$ reported in Table 2. The states with dimension $(m + 4)/2$ have four fermions whose Lorentz indices can be contracted in order to give a scalar $0^{+(2)}$, a vector $1^{+(2)}$, and a spin two 2^+ . We can write, for example, the schematic form of the spin two operator in the $[m - 2, 0, 0, 0]$ representation of $SO(8)$,

$$D_\mu \Phi^i D_\nu \Phi^j \Phi^{m-2} + Y_{\{\alpha_1}^{[a_1} \dots Y_{\alpha_4]}^{a_4] \Phi^{m-4} + \dots. \quad (4.6)$$

The scalar and vector are obtained with different contraction of the Lorentz indices; it is easy to check that the $SO(8)$ indices then transform as reported in Table 2. The rest of the spectrum can be similarly reconstructed.

The KK spectrum on S^7 should reproduce the full spectrum of short operators with finite dimensions in the large N limit of the field theory dual to $AdS_4 \times S^7$. It is however difficult to write explicit expressions for these multiplets in terms of local operators. The ABJM theory with $k = 1$ is an explicitly scale invariant local Lagrangian dual to $AdS_4 \times S^7$ and its spectrum of single trace chiral operators should match the KK spectrum on S^7 . However, the explicit correspondence is somehow obscured by the fact that the $\mathcal{N} = 8$ supersymmetry of ABJM is not manifest and monopole operators are required to match the spectrum. In the particular case $N = 2$, the ABJM theory with group $SU(2) \times SU(2)$ has manifest $\mathcal{N} = 8$ supersymmetry and $SO(8)$ global symmetry; in fact it coincides with the BLG theory [1–5]. However, even in this case we can only give an explicit representation for the multiplets with even m . Let us discuss briefly how. We use the formulation as a Chern-Simons theory with gauge group $SU(2) \times SU(2)$. The matter content consist of bosonic and fermionic fields Φ^i and Y^a transforming in the bifundamental representation of the gauge group and in the $\mathbf{8}_v$ in the $\mathbf{8}_s$ representation of $SO(8)$, respectively. The fields can be written as two-by-two matrices satisfying the reality condition

$$\Phi_{AA}^i = \epsilon_{AB} \epsilon_{AB} \left(\Phi^{i\dagger} \right)^{BB}, \quad (Y^a)_{AA} = \epsilon_{AB} \epsilon_{AB} \left(Y^{a\dagger} \right)^{BB}. \quad (4.7)$$

The reality conditions ensures that the basic degrees of freedom of an $\mathcal{N} = 8$ multiplet consist in eight real bosons and fermions. Compared with the free theory discussed above, the supersymmetry transformations are modified as

$$\begin{aligned} [Q_{\alpha'}^{\dot{a}}, \Phi^i] &= i \left(\tilde{\Gamma}^i \right)^{\dot{a}a} Y_{\alpha'}^a, \\ \{ Q_{\alpha'}^{\dot{a}}, Y_\beta^a \} &= (\gamma^\mu)_{\alpha\beta} D_\mu \Phi^i \left(\Gamma^i \right)^{\dot{a}a} + \epsilon_{\alpha\beta} \Phi^i \Phi^{j\dagger} \Phi^k \left(\Gamma^{ijk} \right)^{\dot{a}a}. \end{aligned} \quad (4.8)$$

The lowest state of the m th KK supermultiplet is given by $\text{Tr } \Phi^m$ which is schematic expression for a product of m fields Φ^{i_k} or $\Phi^{i_k\dagger}$ completely symmetrized in their $SO(8)$ indices and with all the traces removed

$$\Phi^{[i_1} \Phi^{i_2\dagger} \Phi^{i_3} \Phi^{i_4\dagger} \dots \Phi^{i_m]\dagger} - \text{traces.} \quad (4.9)$$

In order to have a gauge invariant expression m must be even and Φ and Φ^\dagger should be alternated. The other states are obtained, similarly to the free case, by applying the supersymmetry transformations. Let us quote, for example, the schematic form of the scalar $0^{-(1)}$ and the vector $1^{-(1)}$ with dimension $(m+2)/2$

$$\text{Tr} \left(\gamma_{[\alpha}^{[a} \gamma_{\beta]}^{b]} + \Phi^{[i_1} \Phi^{i_2\dagger} \Phi^{i_3} \Phi^{i_4]\dagger} \right) \Phi^{m-2}, \quad \text{Tr} \left(\gamma_{[\alpha}^{[a} \gamma_{\beta]}^{b]} + \gamma_{\alpha\beta}^\mu \Phi^{[i_1} D_\mu \Phi^{i_2]\dagger} \right) \Phi^{m-2}. \quad (4.10)$$

4.2. The SW Spectrum

The KK spectrum of S^7/\mathbb{Z}_k is also known [39]. \mathbb{Z}_k acts by reducing the length of a circle in S^7 and, for large k , the orbifold quotient is equivalent to a type IIA reduction of the theory along this circle. As a result, for large k , the KK spectrum of M theory on S^7/\mathbb{Z}_k is the same as the KK spectrum of type IIA on $\mathbb{C}\mathbb{P}^3$. To obtain the type IIA spectrum we just need to decompose the $SO(8)$ representations under the residual $SU(4) \times U(1)$ group and project out all the states that are not invariant under the $U(1)$ action. This decomposition was exhaustively studied in [39]: the levels with m odd are completely projected out, while the levels labelled by even values of m organize themselves into $\mathcal{N} = 6$ susy multiplets. The resulting spectrum exactly reproduces the set of chiral multiplets of the ABJM theory [6]. (This is strictly correct in the $k \rightarrow \infty$ limit. For finite k , some Fourier modes along the M theory circle survive the projection. These states are D0 branes in type IIA and are realized in the ABJM model with monopole operators. We will not discuss explicitly such states in the paper.)

Consider now the skew-whiffed theory. The skew-whiffing transformation corresponds to a change of chirality for the eight-dimensional fermion: $\mathbf{8}_s \rightarrow \mathbf{8}_c$. This transformation can be easily implemented on the KK spectrum of S^7 given in Table 2. We maintain the dimension Δ invariant while we exchange the spinorial indices in the $SO(8)$ representations: $[a, b, c, d] \rightarrow [a, b, d, c]$. After this transformation, we decompose again the $SO(8)$ representations under the residual $SU(4) \times U(1)$ group and project out all the states that are not invariant under the $U(1)$ action. For odd m we obtain “multiplets” with only fermionic degrees of freedom: all the bosons are projected out; for even m we obtain “multiplets” with only bosonic degrees of freedom: all the fermions are projected out. The result is reported in Tables 3 and 4.

Let us consider now the non-supersymmetric field theory discussed in the previous section. It obviously difficult to predict the spectrum of operators with finite dimensions in a non-supersymmetric theory. However, we should at least be able to construct a gauge invariant operator with the right quantum numbers for each of KK state. We will see now that the proposed field content is compatible with the distinctive features of the KK spectrum.

The dimensions Δ of the KK states are all integers. This is compatible with our assumption that the elementary fields have classical dimensions (1/2 for the bosons and 1 for the fermions) since, with this assumption, all the gauge invariant operators have integer dimensions. Let us see this in detail. Consider a gauge invariant product of m elementary fields. Consider first the case with m even. The bosonic operators have integer dimensions:

Table 3: Bosonic KK spectrum of the SW theory at level $m = 2n$, with $n \geq 1$. The states with negative Dynkin labels should be excluded. In the case $n = 1$ some of the fields are absent, reflecting the fact that the original S^7 multiplet is shorter.

Spin	$SU(4)$	Δ
2^+	$[n-1, 0, n-1]$	$n+2$
$1^{-(1)}$	$[n-1, 0, n-1] + [n, 0, n] + [n, 1, n-2] + [n-2, 1, n]$	$n+1$
1^+	$[n-1, 0, n-1] + [n-1, 0, n-1] + [n+1, 0, n-3] + [n-3, 0, n+1] + [n, 1, n-2] + [n-2, 1, n] + [n-1, 1, n-3] + [n-3, 1, n-1] + [n-2, 2, n-2]$	$n+2$
$1^{-(2)}$	$[n-1, 0, n-1] + [n-2, 0, n-2] + [n-1, 1, n-3] + [n-3, 1, n-1]$	$n+3$
$0^{+(1)}$	$[n, 0, n]$	n
$0^{-(1)}$	$[n-1, 0, n-1] + [n+1, 0, n-3] + [n-3, 0, n+1] + [n, 1, n-2] + [n-2, 1, n] + [n-1, 2, n-1]$	$n+1$
$0^{+(2)}$	$[n-1, 0, n-1] + [n, 0, n] + [n-2, 0, n-2] + [n, 1, n-2] + [n-2, 1, n] + [n-1, 1, n-3] + [n-3, 1, n-1] + [n-2, 2, n-2] + [n, 2, n-4] + [n-4, 2, n]$	$n+2$
$0^{-(2)}$	$[n-1, 0, n-1] + [n+1, 0, n-3] + [n-3, 0, n+1] + [n-1, 1, n-3] + [n-3, 1, n-1] + [n-3, 2, n-3]$	$n+3$
$0^{+(3)}$	$[n-2, 0, n-2]$	$n+4$

Table 4: Fermionic KK spectrum of the SW theory at level $m = 2n + 1$, with $n \geq 1$. The states with negative Dynkin labels should be excluded. In the case $n = 1$ some of the fields are absent, reflecting the fact that the original S^7 multiplet is shorter.

Spin	$SU(4)$	Δ
$\frac{3^{(1)}}{2}$	$[n+1, 0, n-1] + [n-1, 0, n+1] + [n-1, 1, n-1]$	$n+2$
$\frac{3^{(2)}}{2}$	$[n, 0, n-2] + [n-2, 0, n] + [n-1, 1, n-1]$	$n+3$
$\frac{1^{(1)}}{2}$	$[n+1, 0, n-1] + [n-1, 0, n+1] + [n, 1, n]$	$n+1$
$\frac{1^{(2)}}{2}$	$[n+1, 0, n-1] + [n-1, 0, n+1] + [n, 0, n-2] + [n-2, 0, n] + [n, 1, n] + [n-1, 1, n-1] + [n-1, 1, n-1] + [n+1, 1, n-3] + [n-3, 1, n+1] + [n, 2, n-2] + [n-2, 2, n]$	$n+2$
$\frac{1^{(3)}}{2}$	$[n, 0, n-2] + [n-2, 0, n] + [n+1, 0, n-1] + [n-1, 0, n+1] + [n-1, 1, n-1] + [n-1, 1, n-1] + [n-2, 1, n-2] + [n+1, 1, n-3] + [n-3, 1, n+1] + [n-1, 2, n-3] + [n-3, 2, n-1]$	$n+3$
$\frac{1^{(4)}}{2}$	$[n, 0, n-2] + [n-2, 0, n] + [n-2, 1, n-2]$	$n+4$

the dual field theory operators are obtained with an even number of bosonic fields and an even number of fermionic fields; gauge invariant operators of this type are obtained using X^A and Ψ^I , or ξ fields. The fermionic operators would have half-integer dimensions: in fact they would contain an odd number of bosonic fields and odd number of fermionic fields. However, in the proposed field theory it is not possible to build up a gauge invariant operator with such field content. We conclude that for even m there are only bosons in the KK spectrum. Consider now the case with m odd. The fermionic operators have integer dimensions: the dual field theory operators are obtained with an even number of bosonic fields and an odd number of fermionic fields; gauge invariant operators of this type are obtained using X^A and Ψ^I , or ξ fields. The bosonic operators instead would have half-integer dimensions, in fact they would contain an odd number of bosonic fields and an even number of fermionic fields. Such bosonic operators are still forbidden by gauge invariance. We conclude that for odd m there are only fermions in the spectrum.

Let us now check that we can construct at least one field theory operator with the right dimension, Lorentz and $SU(4)$ representation for each KK mode in supergravity. The gauge invariant field theory operators are obtained by contracting the following operators:

$$\left\{ X^A, X_{A'}^\dagger, \xi_{\alpha'}, \xi_{\alpha'}^\dagger, \Psi_{\alpha'}^I, D_\mu \right\}. \quad (4.11)$$

Let us start looking at the generic form of the operators of low dimension for a given n . The first scalar KK modes is $0^{+(1)}$ and the corresponding field theory operator has the schematic form

$$\text{Tr} \left(X^{\{A_1} X_{\{B_1}^\dagger \dots \dots X^{A_n\}} X_{B_n}^\dagger \right), \quad (4.12)$$

where suitable trace subtractions are understood. The first KK spinor mode is $(1/2)^{(1)}$ and the dual operator is

$$\text{Tr} \left(X^{\{A_1} X_{\{B_1}^\dagger \dots \dots X^{A_n\}} X_{B_n}^\dagger \Psi_{\alpha}^I \right). \quad (4.13)$$

The first KK vector mode is $1^{(-1)}$ and the dual operator is

$$\begin{aligned} & \text{Tr} \left(X^{\{A_1} X_{\{B_1}^\dagger \dots \dots X^{A_{n-1}\}} X_{B_{n-1}}^\dagger \Psi_{\{\alpha}^I \Psi_{\beta}^J \right) + \text{Tr} \left(X^{\{A_1} X_{\{B_1}^\dagger \dots \dots X^{A_{n-1}\}} X_{B_{n-1}}^\dagger \xi_{\{\alpha} \xi_{\beta}^\dagger \right) \\ & + \text{Tr} \left(X^{\{A_1} X_{\{B_1}^\dagger \dots \dots X^{A_{n-1}\}} X_{B_{n-1}}^\dagger X^{A_n} D_\mu X_{B_n}^\dagger \right). \end{aligned} \quad (4.14)$$

The first pseudoscalar in the KK spectrum is $0^{(-1)}$ and the dual field operator is schematically

$$\begin{aligned} & \text{Tr} \left(X^{\{A_1} X_{\{B_1}^\dagger \dots \dots X^{A_n\}} X_{B_n}^\dagger \Psi_{[\alpha}^I \Psi_{\beta]}^J \right) + \text{Tr} \left(X^{\{A_1} X_{\{B_1}^\dagger \dots \dots X^{A_{n-1}\}} X_{B_{n-1}}^\dagger \xi_{[\alpha} \xi_{\beta]}^\dagger \right) \\ & + \text{Tr} \left(X^{\{A_1} X_{\{B_1}^\dagger \dots \dots X^{A_n\}} X_{B_n}^\dagger X^{[A} X_{[B}^\dagger X^C] X_{D]}^\dagger \right). \end{aligned} \quad (4.15)$$

Another interesting operator of lower dimension in the KK towers is $(3/2)^{(1)}$ and its dual field operator has the form

$$\begin{aligned} & \text{Tr} \left(X^{\{A_1} X_{\{B_1}^\dagger \dots \dots X^{A_{n-1}\}} X_{B_{n-1}}^\dagger \Psi_{\{\alpha}^I \Psi_{\beta}^J \Psi_{\gamma}^K \right) + \text{Tr} \left(X^{\{A_1} X_{\{B_1}^\dagger \dots \dots X^{A_{n-1}\}} X_{B_{n-1}}^\dagger \Psi_{\{\alpha}^I \xi_{\beta} \xi_{\gamma}^\dagger \right) \\ & + \text{Tr} \left(X^{\{A_1} X_{\{B_1}^\dagger \dots \dots X^{A_n\}} X_{B_n}^\dagger D_\mu \Psi_{\alpha}^I \right). \end{aligned} \quad (4.16)$$

It is easy to verify that the above operators can reproduce the $SU(4)$ representations reported in Tables 3 and 4. The first bosonic level has $m = 2$ and the corresponding operators have the schematic form

$$\begin{aligned}
0^{+(1)} &: \text{Tr}\left(X^A X_B^\dagger\right), \\
0^{-(1)} &: \text{Tr}\left(\Psi_{[\alpha}^{[I} \Psi_{\beta]}^{J]}\right) + \text{Tr}\left(\xi_{[\alpha}^\dagger \xi_{\beta]}^\dagger\right) + \text{Tr}\left(X^{[A} X_{[B}^\dagger X^C] X_{D]}^\dagger\right), \\
1^{-(1)} &: \text{Tr}\left(X^A D_\mu X_B^\dagger\right) + \text{Tr}\left(\xi_{[\alpha}^\dagger \xi_{\beta]}^\dagger\right) + \text{Tr}\left(\Psi_{[\alpha}^{[I} \Psi_{\beta]}^{J]}\right), \\
2^+ &: \text{Tr}\left(D_\mu X^A D_\nu X_A^\dagger\right) + \dots,
\end{aligned} \tag{4.17}$$

where suitable trace subtractions are understood. In the first bosonic level there are two important operators: the part of the $1^{-(1)}$ operator in the $[1, 0, 1]$ representation is the field theory $SU(4)$ global current symmetry $J_\mu^{[IJ]}$ dual to the gauge field $A_\mu^{[IJ]}$ in the adjoint representation of $SU(4)$ propagating in AdS_4 , and the singlet 2^+ operator is the stress-energy tensor dual to the graviton $g_{\mu\nu}$ in AdS_4 . Of course, since the proposed skew-whiffed theory is not supersymmetric, the supercurrent operator dual to the would be $(3/2)^{(1)}$ gravitino is not present in the operator spectrum.

The first fermionic level has $m = 3$ and the corresponding operators are

$$\begin{aligned}
\frac{1}{2}^{(1)} &: \text{Tr}\left(X^A X_B^\dagger \Psi_\alpha^I\right), \\
\frac{1}{2}^{(2)} &: \text{Tr}\left(\Psi_{[\alpha}^{[I} \Psi_{\beta]}^{J]} \Psi_{\gamma]}^{K]}\right) + \text{Tr}\left(\Psi_{[\alpha}^I \xi_{[\beta]}^\dagger \xi_{\gamma]}^\dagger\right) + \text{Tr}\left(X^{[A} X_{[B}^\dagger X^C] X_{D]}^\dagger \Psi_\alpha^I\right), \\
\frac{3}{2}^{(1)} &: \text{Tr}\left(\Psi_{[\alpha}^{[I} \Psi_{\beta]}^{J]} \Psi_{\gamma]}^{K]}\right) + \text{Tr}\left(\Psi_{[\alpha}^I \xi_{\beta]}^\dagger \xi_{\gamma]}^\dagger\right) + \text{Tr}\left(X^A X_B^\dagger D_\mu \Psi^I\right), \\
\frac{3}{2}^{(2)} &: \text{Tr}\left(\xi_{[\alpha}^\dagger \xi_{\beta]}^\dagger D_\mu \Psi_\gamma^I\right) + \dots.
\end{aligned} \tag{4.18}$$

(The operators corresponding $(1/2)^{(2)}$ have a mixed symmetry in the spin and $SU(4)$ indices which is indicated in a somehow imprecise way in the following formula.)

The operators dual to a specific KK modes are, in general, linear combinations of all the gauge invariant operators with the right dimension, Lorentz and $SU(4)$ representation that we can construct. The expectation is that exactly one of these operators will remain with finite dimensions in the large N and strongly coupled regime, while the others will acquire infinite dimension, as standard in the AdS/CFT correspondence.

5. Conclusions

In this paper we discussed general properties of the field theory living on a stack of N anti-M2 branes at the tip of an eight-dimensional real cone with at least one Killing spinor. In particular we focus on the skew-whiffed $\text{AdS}_4 \times S^7/\mathbb{Z}_k$ supergravity solution in M theory (and its reduction to type IIA), which is not supersymmetric but stable. The AdS/CFT

correspondence predicts the existence of a dual non-supersymmetric three-dimensional theory, which should be a unitary conformal field theory at least at large N and strong coupling. Based on an analysis of the KK spectrum of the supergravity theory and on the geometrical action of the skew-whiffing transformation, we speculate on the field content of the dual theory, a skew-whiffed version of the ABJM theory. Due to the fact that the theory is non-supersymmetric, direct checks of any proposal are nontrivial. We identified a field content which is at least compatible with the KK spectrum found in the dual supergravity solution. It is interesting to observe that there is some ambiguity in writing a candidate theory. In particular the SW map and the compatibility with the KK spectrum do not fix unambiguously the representation of the fields under the gauge group; for example, the complex spinor ξ could be either in the bifundamental representation, as we considered in this paper, or in the adjoint representation of one of the gauge group. It would be interesting to see if these various theories are somehow duals. Another observation is that the proposed theory is not really a quiver gauge theory, because the fermions transform in the bifundamental of just the $SU(N)$ part of the full $U(N)$ gauge group. This seems to imply that the theory is a good candidate only in the large N limit, that is exactly, the regime for which the dual supergravity solution is demonstrated to be stable. Further investigations are needed.

We mainly concentrated on the S^7/\mathbb{Z}_k supergravity solution. However, as explained at the very beginning of the paper, there is a SW supergravity solution for any Freund-Rubin solution with at least one Killing spinor and we should be able to find a dual non-supersymmetric Chern-Simons matter theory. There is an infinite set of AdS_4/CFT_3 pairs in the literature and it would be interesting to have a systematic procedure to obtain the SW field theory once the supersymmetric field theory is known. One way to proceed would be to start with orbifolds of the SW ABJM theory. By giving vevs to scalar fields we can flow to other non-supersymmetric Chern-Simons matter field theories. A more efficient way to proceed would be to find the field theory operation dual to the change of orientation of H_7 . We leave this topic for future research.

Acknowledgments

The authors would like to thank J. Gauntlett, N. Halmagyi, A. Hanany, S. Hartnoll, N. Lambert, A. Sen, Y. Tachikawa, J. Troost, K. Zarembo for nice and helpful discussions. The work of D. Forcella is partially supported by IISN—Belgium (Convention 4.4514.08), by the Belgian Federal Science Policy Office through the Interuniversity Attraction Pole P6/11 and by the “Communauté Française de Belgique” through the ARC program. A. Zaffaroni is supported in part by INFN.

References

- [1] J. Bagger and N. Lambert, “Modeling multiple M2-branes,” *Physical Review D*, vol. 75, no. 4, Article ID 045020, 7 pages, 2007.
- [2] A. Gustavsson, “Algebraic structures on parallel M2 branes,” *Nuclear Physics B*, vol. 811, no. 1-2, pp. 66–76, 2009.
- [3] J. Bagger and N. Lambert, “Gauge symmetry and supersymmetry of multiple M2-branes,” *Physical Review D*, vol. 77, no. 6, Article ID 065008, 6 pages, 2008.
- [4] J. Bagger and N. Lambert, “Comments on multiple M2-branes,” *Journal of High Energy Physics*, no. 2, article 105, 15 pages, 2008.
- [5] M. Van Raamsdonk, “Comments on the Bagger-Lambert theory and multiple M2-branes,” *Journal of High Energy Physics*, no. 5, article 105, 9 pages, 2008.

- [6] O. Aharony, O. Bergman, D. L. Jafferis, and J. Maldacena, “ $N = 6$ superconformal Chern-Simons-matter theories, M2-branes and their gravity duals,” *Journal of High Energy Physics*, no. 10, article 091, 2008.
- [7] M. Benna, I. Klebanov, T. Klose, and M. Smedbäck, “Superconformal Chern-Simons theories and AdS_4/CFT_3 correspondence,” *Journal of High Energy Physics*, no. 9, article 072, 2008.
- [8] K. Hosomichi, K.-M. Lee, S. Lee, S. Lee, and J. Park, “ $N = 5, 6$ superconformal Chern-Simons theories and M2-branes on orbifolds,” *Journal of High Energy Physics*, no. 9, article 002, 24 pages, 2008.
- [9] O. Aharony, O. Bergman, and D. L. Jafferis, “Fractional M2-branes,” *Journal of High Energy Physics*, vol. 2008, no. 11, article 043, 2008.
- [10] D. L. Jafferis and A. Tomasiello, “A simple class of $N = 3$ gauge/gravity duals,” *Journal of High Energy Physics*, vol. 2008, no. 10, article 101, 2008.
- [11] D. Martelli and J. Sparks, “Moduli spaces of Chern-Simons quiver gauge theories and $AdS(4)/CFT(3)$,” *Physical Review D*, vol. 78, no. 12, Article ID 126005, 11 pages, 2008.
- [12] A. Hanany and A. Zaffaroni, “Tilings, Chern-Simons theories and M2 branes,” *Journal of High Energy Physics*, vol. 2008, no. 10, article 111, 2008.
- [13] A. Hanany, D. Vegh, and A. Zaffaroni, “Brane tilings and M2 branes,” *Journal of High Energy Physics*, vol. 2009, no. 3, article 012, 2009.
- [14] K. Ueda and M. Yamazaki, “Toric Calabi-Yau four-folds dual to Chern-Simons-matter theories,” *Journal of High Energy Physics*, vol. 2008, no. 12, article 045, 2008.
- [15] Y. Imamura and K. Kimura, “Quiver Chern-Simons theories and crystals,” *Journal of High Energy Physics*, vol. 2008, no. 10, article 114, 2008.
- [16] S. Franco, A. Hanany, J. Park, and D. Rodríguez-Gómez, “Towards M2-brane theories for generic toric singularities,” *Journal of High Energy Physics*, vol. 2008, no. 12, article 110, 2008.
- [17] A. Hanany and Y. H. He, “M2-branes and quiver chern-simons: a taxonomic study,” <http://arxiv.org/abs/0811.4044/>.
- [18] A. Amariti, D. Forcella, L. Girardello, and A. Mariotti, “3D Seiberg-like dualities and M2 branes,” *Journal of High Energy Physics*, vol. 2010, no. 5, article 25, 2010.
- [19] J. Davey, A. Hanany, N. Mekareeya, and G. Torri, “Phases of M2-brane theories,” *Journal of High Energy Physics*, vol. 2009, no. 6, article 025, 2009.
- [20] S. Franco, I. R. Klebanov, and D. Rodríguez-Gómez, “M2-branes on orbifolds of the cone over $Q^{1,1,1}$,” *Journal of High Energy Physics*, vol. 2009, no. 8, article 033, 2009.
- [21] D. Martelli and J. Sparks, “ AdS_4/CFT_3 duals from M2-branes at hypersurface singularities and their deformations,” *Journal of High Energy Physics*, vol. 2009, no. 12, article 017, 2009.
- [22] F. Benini, C. Closset, and S. Cremonesi, “Chiral flavors and M2-branes at toric CY4 singularities,” *Journal of High Energy Physics*, vol. 2010, no. 2, article 036, 2010.
- [23] D. L. Jafferis, “Quantum corrections to $N = 2$ Chern-Simons theories with flavor and their AdS_4 duals,” <http://arxiv.org/abs/0911.4324/>.
- [24] D. Forcella and A. Zaffaroni, “ $N = 1$ Chern-Simons theories, orientifolds and Spin(7) cones,” *Journal of High Energy Physics*, vol. 2010, no. 5, article 045, 2010.
- [25] A. Armoni and A. Naqvi, “A non-supersymmetric large- N 3D CFT and its gravity dual,” *Journal of High Energy Physics*, vol. 2008, no. 9, article 119, 2008.
- [26] K. Narayan, “On nonsupersymmetric C^4/ZN tachyons, terminal singularities and flips,” *Journal of High Energy Physics*, vol. 2010, no. 3, article 019, 2010.
- [27] M. J. Duff, B. E. W. Nilsson, and C. N. Pope, “The criterion for vacuum stability in Kaluza-Klein supergravity,” *Physics Letters B*, vol. 139, no. 3, pp. 154–158, 1984.
- [28] A. Imaanpur and M. Naghdi, “Dual instantons in antimembranes theory,” *Physical Review D*, vol. 83, no. 8, Article ID 085025, 7 pages, 2011.
- [29] M. J. Duff, B. E. W. Nilsson, and C. N. Pope, “Kaluza-Klein supergravity,” *Physics Reports*, vol. 130, no. 1-2, pp. 1–142, 1986.
- [30] F. Denef and S. A. Hartnoll, “Landscape of superconducting membranes,” *Physical Review D*, vol. 79, no. 12, Article ID 126008, 16 pages, 2009.
- [31] J. P. Gauntlett, J. Sonner, and T. Wiseman, “Quantum criticality and holographic superconductors in M-theory,” *Journal of High Energy Physics*, vol. 2010, no. 2, article 060, 2010.
- [32] J. A. Minahan and K. Zarembo, “The Bethe ansatz for superconformal Chern-Simons,” *Journal of High Energy Physics*, vol. 2008, no. 9, article 040, 2008.
- [33] E. Sezgin, “The spectrum of the eleven-dimensional supergravity compactified on the round seven-sphere,” *Physics Letters B*, vol. 138, no. 1–3, pp. 57–62, 1984.

- [34] B. Biran, A. Casher, F. Englert, M. Roman, and P. Spindel, "The fluctuating seven-sphere in eleven-dimensional supergravity," *Physics Letters B*, vol. 134, no. 3-4, pp. 179–183, 1984.
- [35] A. Hanany, N. Mekareeya, and A. Zaffaroni, "Partition functions for membrane theories," *Journal of High Energy Physics*, vol. 2008, no. 9, article 090, 2008.
- [36] A. Hanany and A. Zaffaroni, "The master space of supersymmetric gauge theories," *Advances in High Energy Physics*, vol. 2010, Article ID 427891, 30 pages, 2010.
- [37] M. Bianchi, R. Poghossian, and M. Samsonyan, "Precision spectroscopy and higher spin symmetry in the ABJM model," *Journal of High Energy Physics*, vol. 2010, no. 10, article 021, 2010.
- [38] M. Samsonyan, "Non-perturbative aspects of gauge and string theories and their holographic relations," <http://arxiv.org/abs/1102.1357/>.
- [39] B. E. W. Nilsson and C. N. Pope, "Hopf fibration of eleven-dimensional supergravity," *Classical and Quantum Gravity*, vol. 1, no. 5, pp. 499–515, 1984.

Research Article

On \mathcal{R}^4 Terms and MHV Amplitudes in $\mathcal{N} = 5, 6$ Supergravity Vacua of Type II Superstrings

Massimo Bianchi^{1,2}

¹ *Dipartimento di Fisica, INFN Sezione di Roma "Tor Vergata", Università di Roma "Tor Vergata",
Via della Ricerca Scientifica, 00133 Roma, Italy*

² *Physics Department, Theory Unit, CERN, 1211 Geneva 23, Switzerland*

Correspondence should be addressed to Massimo Bianchi, massimo.bianchi@roma2.infn.it

Received 14 April 2011; Accepted 23 June 2011

Academic Editor: Yang-Hui He

Copyright © 2011 Massimo Bianchi. This is an open access article distributed under the Creative Commons Attribution License, which permits unrestricted use, distribution, and reproduction in any medium, provided the original work is properly cited.

We compute one-loop threshold corrections to \mathcal{R}^4 terms in $\mathcal{N} = 5, 6$ supergravity vacua of Type II superstrings. We then discuss nonperturbative corrections generated by asymmetric D-brane instantons. Finally we derive generating functions for MHV amplitudes at tree level in $\mathcal{N} = 5, 6$ supergravities.

1. Introduction

$\mathcal{N} = 5, 6$ supergravities in $D = 4$ enjoy many of the remarkable properties of $\mathcal{N} = 8$ supergravity. Their massless spectra are unique and consist solely of the supergravity multiplets. Their R -symmetries are not anomalous [1]. Regular BH solutions can be found whereby the scalars are stabilized at the horizon by the attractor mechanism (for a recent review see, e.g., [2]). It is thus tempting to conjecture that if pure $\mathcal{N} = 8$ supergravity turned out to be UV finite [3–7] then $\mathcal{N} = 5, 6$ supergravities should be so, too.

As shown in [8–10], Type II superstrings or M-theory accommodate $\mathcal{N} = 8$ supergravity in such a way as to include nonperturbative states that correspond to singular BH solutions in $D = 4$. The same is true for $\mathcal{N} = 5, 6$ supergravities. While the embedding of $\mathcal{N} = 8$ supergravity corresponds to simple toroidal compactifications, the embedding of $\mathcal{N} = 5, 6$ supergravities, pioneered by Ferrara and Kounnas in [11] and recently reviewed in [12], requires asymmetric orbifolds [13, 14] or free fermion constructions [15–20].

The inclusion of BPS states, whose possible singular behavior from a strict 4D viewpoint is resolved from a higher-dimensional perspective, generates higher derivative corrections to the low-energy effective action. In particular a celebrated \mathcal{R}^4 term appears that spoils the continuous noncompact symmetry of “classical” supergravity. Absence of such a term has been recently shown for pure $\mathcal{N} = 8$ supergravity in [21]. In superstring theory, the \mathcal{R}^4 term receives contribution at tree level, one loop, and from nonperturbative effects associated to D-instantons [22] and other wrapped branes [23]. Proposals for the relevant modular form of the $E_{7(7)}(Z)$ U -duality group have been recently put forward in [24–26] that seem to satisfy all the checks.

In this paper we consider one-loop threshold corrections to the same kind of terms in superstring models with $\mathcal{N} = 5, 6$ supersymmetry in $D = 4$ and $\mathcal{N} = 6$ in $D = 5$. After excluding \mathcal{R}^2 terms (\mathcal{R}^3 terms cannot be supersymmetrized on shell when all particles are in the supergravity multiplet [21]), we will derive formulae for the “perturbative” threshold corrections. In $D = 4$ we will also discuss other MHV amplitudes (for a recent review see, e.g., [27]) that can be obtained by orbifold techniques from the generating function of $\mathcal{N} = 8$ supergravity amplitudes [28].

Aim of the analysis is threefold. First, we would like to show that $\mathcal{N} = 5, 6$ supersymmetric models in $D = 4$ behave very much as their common $\mathcal{N} = 8$ supersymmetric parent. The threshold corrections that we find may be taken as evidence that, as in the $\mathcal{N} = 8$ case, superstring calculations do not reproduce field theory results, where such \mathcal{R}^4 corrections are absent as a result of the unbroken (anomaly free) continuous U -duality symmetry as in the $\mathcal{N} = 8$ case [1]. This is in line with the nondecoupling in Type II superstrings of BPS states that are singular from the strict 4-dimensional supergravity perspective [8–10].

Second, (gauged) $\mathcal{N} = 5, 6$ supergravities have played a crucial role in the recent understanding of M2-brane dynamics [29–32], and nonperturbative tests may be refined by considering the effects of world-sheet instantons in CP^3 [33–36] along the lines of our present (ungauged) analysis. Finally, in addition to world-sheet instantons, D-brane instantons corresponding to Euclidean bound states of “exotic” D-branes should contribute to generalize “standard” D-brane instanton calculus to Left-Right asymmetric backgrounds.

Plan of the paper is as follows. In Section 1, we briefly review $\mathcal{N} = 5, 6$ supergravities in $D = 4, 5$ and their embedding in Type II superstrings. We then pass to consider in Section 2 a 4-graviton amplitude at one loop which allows to derive the “perturbative” threshold corrections to \mathcal{R}^4 terms, thus excluding \mathcal{R}^2 terms. For simplicity, we only give the explicit result for $\mathcal{N} = 6$ in $D = 5$ in Section 3 and sketch how to complete the nonperturbative analysis by including asymmetric D-brane instantons [12] in Section 4. Finally, in Section 5 we consider MHV amplitudes in $\mathcal{N} = 5, 6$ supergravities in $D = 4$ and show how they can be obtained at tree level by orbifold techniques from the generating function for MHV amplitudes in $\mathcal{N} = 8$ supergravity [28]. Section 6 contains a summary of our results and directions for further investigation.

2. Type II Superstring Models with $\mathcal{N} = 5, 6$ in $D = 4, 5$

Let us briefly recall how $\mathcal{N} = 5, 6$ supergravities can be embedded in String Theory. The highest dimension where classical $\mathcal{N} = 6$ supergravity with 24 supercharges can be defined is $D = 6$. However the resulting $\mathcal{N} = (2, 1)$ theory is anomalous and thus inconsistent at the quantum level [37]. So we are led to consider $D = 5$ and then reduce to $D = 4$. $\mathcal{N} = 5$ supergravity with 20 supercharges can only be defined as $D = 4$ and lower. Although we will

only focus on \mathcal{R}^4 terms in $D = 4$ the parent $D = 5$ theory is instrumental to the identification of the relevant BPS instantons.

2.1. $\mathcal{N} = 6 = 2_L + 4_R$ Supergravity in $D = 5$

The simplest way to embed $\mathcal{N} = 6$ in Type II superstrings is to quotient a toroidal compactification $T^5 = T^4 \times S^1$ by a chiral Z_2 twist of the L -movers (T -duality) on four internal directions

$$X_L^i \longrightarrow -X_L^i, \quad \Psi_L^i \longrightarrow -\Psi_L^i, \quad i = 6, 7, 8, 9 \quad (2.1)$$

accompanied by an order-two shift that makes twisted states massive. As a result half of the supersymmetries in the L -moving sector are broken. The perturbative spectrum is coded in the one-loop torus partition function.

In the untwisted sector, one finds

$$\tau_u = \frac{1}{2} \left\{ (Q_o + Q_v) \bar{Q} \Lambda_{5,5} \begin{bmatrix} 0 \\ 0 \end{bmatrix} + (Q_o - Q_v) (X_o - X_v) \bar{Q} \Lambda_{1,5} \begin{bmatrix} 0 \\ 1 \end{bmatrix} \right\}, \quad (2.2)$$

where $X_o - X_v = 4\eta^2/\theta_2^2$ (with η denoting Dedekind's function and $\theta_{1,\dots,4}$ denoting Jacobi's elliptic functions) describes the effect of the Z_2 projection on four internal L -moving bosons, while

$$\Lambda_{l,r} \begin{bmatrix} a \\ b \end{bmatrix} = \sum_{p_L, p_R} e^{i\pi[a_L p_L - a_R p_R]} q^{(1/2)(p_L + (1/2)b_L)^2} \bar{q}^{(1/2)(p_R + (1/2)b_R)^2} \quad (2.3)$$

are (shifted) Lorentzian lattice sums of signature (l, r) and $Q = V_8 - S_8$, $Q_o = V_4 O_4 - S_4 S_4$, $Q_v = O_4 V_4 - C_4 C_4$, with O_n , V_n , S_n , C_n the characters of $SO(n)$ at level $\kappa = 1$ (for n odd S_n coincides with C_n and will be denoted by Σ_n).

At the massless level, in $D = 5$ notation with $SO(3)$ little group, one finds

$$\begin{aligned} & (V_3 + O_3 - 2\Sigma_3) \times (\bar{V}_3 + 5\bar{O}_3 - 4\bar{\Sigma}_3) \\ & \longrightarrow (g + b_2 + \phi)_{\text{NS-NS}} + 6A_{\text{NS-NS}} + 5\phi_{\text{NS-NS}} + 8A_{R-R} + 8\phi_{R-R} - \text{Fermi} \end{aligned} \quad (2.4)$$

that form the $\mathcal{N} = 6$ supergravity multiplet in $D = 5$

$$\text{SG}_{\mathcal{N}=6}^{D=5} = \{g_{\mu\nu}, 6\psi_\mu, 15A_\mu, 20\chi, 14\varphi\}. \quad (2.5)$$

The R -symmetry is $Sp(6)$ while the "hidden" noncompact symmetry is $SU^*(6)$, of dimension 35 and rank 3 generated by 6×6 matrices of the form $Z = (Z_1, Z_2; -\bar{Z}_2, \bar{Z}_1)$ with $\text{Tr}(Z_1 + \bar{Z}_1) = 0$.

For later purposes, let us observe that the 128 massless states of $\mathcal{N} = 6$ supergravity in $D = 5$ are given by the tensor product of the 8 massless states of $\mathcal{N} = 2$ SYM (for the Left-movers) and the 16 massless states of $\mathcal{N} = 4$ SYM (for the Right-movers), namely,

$$\text{SG}_{\mathcal{N}=6}^{D=5} = \text{SYM}_{\mathcal{N}=2}^{D=5} \otimes \text{SYM}_{\mathcal{N}=4}^{D=5} = \{A_\mu, 2\lambda, \phi\}_L \otimes \{\tilde{A}_\nu, 4\tilde{\lambda}, 5\tilde{\phi}\}_R. \quad (2.6)$$

After dualizing all massless 2 forms into vectors, the $\mathbf{15} = 7_{\text{NS-NS}} + 8_{R-R}$ vectors transform according to the antisymmetric tensor of $SU^*(6)$. The $\mathbf{14} = 1_{\text{NS-NS}} + 5_{\text{NS-NS}} + 8_{R-R}$ scalars parameterize the moduli space

$$\mathcal{M}_{\mathcal{N}=6}^{D=5} = \frac{SU^*(6)}{Sp(6)}. \quad (2.7)$$

By world-sheet modular transformations (first S and then T) one finds the contribution of the twisted sector

$$\tau_t = \frac{1}{2} \left\{ (Q_s + Q_c)(X_s + X_c) \bar{Q} \Lambda_{1,5} \begin{bmatrix} 1 \\ 0 \end{bmatrix} + (Q_s - Q_c)(X_s - X_c) \bar{Q} \Lambda_{1,5} \begin{bmatrix} 1 \\ 1 \end{bmatrix} \right\}, \quad (2.8)$$

where $X_s + X_c = 4\eta^2/\theta_4^2$, $X_s - X_c = 4\eta^2/\theta_3^2$, $Q_s = O_4 S_4 - C_4 O_4$ (massless), $Q_c = V_4 C_4 - S_4 V_4$ (massive). Due to the (L - R symmetric) Z_2 shift, the massless spectrum receives no contribution from the twisted sector. Nonperturbative states associated to L - R asymmetric bound states of D-branes were studied in [12]. There are several other ways to embed $\mathcal{N} = 6$ supergravity in Type II superstrings, reviewed in [12].

2.2. $\mathcal{N} = 6$ Supergravities in $D = 4$

Reducing on another circle with or without further shifts yields $\mathcal{N} = 6$ supergravity in $D = 4$ [11].

The massless spectrum is given by

$$\begin{aligned} & (V_2 + 2O_2 - 2S_2 - 2C_2) \times (\bar{V}_2 + 6\bar{O}_2 - 4\bar{S}_2 - 4\bar{C}_2) \\ & \longrightarrow (g + b + \phi)_{\text{NS-NS}} + 8A_{\text{NS-NS}} + 12\phi_{\text{NS-NS}} + 8A_{R-R} + 16\phi_{R-R} - \text{Fermi} \end{aligned} \quad (2.9)$$

and gives rise to the $\mathcal{N} = 6$ supergravity multiplet in $D = 4$

$$\text{SG}_{\mathcal{N}=6}^{D=4} = \{g_{\mu\nu}, 6\psi_\mu, 16A_\mu, 26\chi, 30\varphi\}. \quad (2.10)$$

For later purposes, let us observe that the 128 massless states of $\mathcal{N} = 6$ supergravity in $D = 4$ are given by the tensor product of the 8 massless states of $\mathcal{N} = 2$ SYM (for the Left-movers) and the 16 massless states of $\mathcal{N} = 4$ SYM (for the Right-movers), namely,

$$\text{SG}_{\mathcal{N}=6}^{D=4} = \text{SYM}_{\mathcal{N}=2}^{D=4} \otimes \text{SYM}_{\mathcal{N}=4}^{D=4} = \{A_\mu, 2\lambda, 2\phi\}_L \otimes \{\tilde{A}_\nu, 4\tilde{\lambda}, 6\tilde{\phi}\}_R. \quad (2.11)$$

The hidden noncompact symmetry is $SO^*(12)$, of dimension 66 and rank 3 generated by 12×12 matrices of the form $Z = (Z_1, Z_2; -\bar{Z}_2, \bar{Z}_1)$ with $Z_1 = -Z_1^t$ and Z_2 hermitean. They satisfy $L^\dagger \mathcal{Q} L = \mathcal{Q}$ with $\mathcal{Q} = -\mathcal{Q}^t = -\mathcal{Q}^\dagger$ the symplectic metric in 12D. After dualizing all massless 2 forms into axions, the $30 = 2_{\text{NS-NS}} + 12_{\text{NS-NS}} + 16_{R-R}$ scalar parameterize the moduli space

$$\mathcal{M}_{\mathcal{N}=6}^{D=4} = \frac{SO^*(12)}{U(6)}. \quad (2.12)$$

The $16 = 8_{\text{NS-NS}} + 8_{R-R}$ vectors together with their magnetic duals transform according to the 32-dimensional chiral spinor representation of $SO^*(12)$.

Due to the (L - R symmetric) Z_2 shift, the massless spectrum receives no contribution from the twisted sector. Nonperturbative states associated to L - R asymmetric bound states of D-branes were studied in [12].

2.3. $\mathcal{N} = 5 = 1_L + 4_R$ Supergravity in $D = 4$

The highest dimension where $\mathcal{N} = 5$ supergravity exists is $D = 4$. In $D = 5$ because one cannot impose a symplectic Majorana condition on an odd number of spinors. A simple way to realize $\mathcal{N} = 5 = 1_L + 4_R$ supergravity in $D = 4$ is to combine $Z_2^L \times Z_2^L$ twists, acting by T -duality along T_{6789}^4 and T_{4589}^4 , with order two shifts, that eliminate massless twisted states. In [11], "minimal" $\mathcal{N} = 5$ superstring solutions of this kind have been classified into four classes which correspond to different choices of the basis sets of free fermions or inequivalent choices of shifts in the orbifold language.

Due to the uniqueness of $\mathcal{N} = 5$ supergravity in $D = 4$, all models display the same massless spectrum

$$SG_{\mathcal{N}=5}^{D=4} = \{g_{\mu\nu}, 5\psi_\mu, 10A_\mu, 11\chi, 10\phi\}. \quad (2.13)$$

For later purposes, let us observe that the 64 massless states of $\mathcal{N} = 5$ supergravity in $D = 4$ are given by the tensor product of the 4 massless states of $\mathcal{N} = 1$ SYM (for the Left-movers) and the 16 massless states of $\mathcal{N} = 4$ SYM (for the Right-movers), namely,

$$SG_{\mathcal{N}=5}^{D=4} = \text{SYM}_{\mathcal{N}=1}^{D=4} \otimes \text{SYM}_{\mathcal{N}=4}^{D=4} = \{A_\mu, \lambda\}_L \otimes \{\tilde{A}_\nu, 4\tilde{\lambda}, 6\tilde{\phi}\}_R. \quad (2.14)$$

The massless scalars parameterize the moduli space

$$\mathcal{M}_{\mathcal{N}=5}^{D=4} = \frac{SU(5, 1)}{U(5)}. \quad (2.15)$$

The graviphotons together with their magnetic duals transform according to the 20 complex (3-index totally antisymmetric tensor) representation of $SU(5, 1)$.

3. Four-Graviton One-Loop Amplitude

Since $\mathcal{N} = 5, 6$ supergravities can be obtained as asymmetric orbifolds of tori, tree-level scattering amplitudes of untwisted states such as gravitons are identical to the corresponding amplitudes in the parent $\mathcal{N} = 8$ theory. In particular, denoting by $f_{\mathcal{R}^4}^{\mathcal{N}=5,6}(\varphi)$ the moduli dependent coefficient function of the \mathcal{R}^4 term, one has

$$f_{\mathcal{R}^4}^{\mathcal{N}=5,6} = \frac{2}{n} \zeta(3) \frac{V(\mathbf{T}^d)}{g_s^2 \ell_s^2} + \frac{\mathcal{O}_{d,d}^{\mathcal{N}=8}}{n \ell_s^2} + \dots, \quad (3.1)$$

where n is the order of the orbifold group, that reduces the volume of \mathbf{T}^d with $d = 5, 6$ to the volume of the orbifold, $\ell_s^2 = \alpha'$ and \dots stands for nonperturbative terms. The one-loop threshold integral is given by

$$\mathcal{O}_{d,d}^{\mathcal{N}=8} = (2\pi)^d \int_{\mathcal{F}} \frac{d^2\tau}{\tau_2^2} \left[\tau_2^{d/2} \Gamma_{d,d}(G, B; \tau) - \tau_2^{d/2} \right] = 2\pi^{2-d/2} \Gamma\left(\frac{d}{2} - 1\right) \mathcal{E}_{\mathbf{v}=2\mathbf{d}, s=d/2-1}^{SO(d,d|Z)} \quad (3.2)$$

where

$$\mathcal{E}_{\mathbf{v}=2\mathbf{d}, s=d/2-1}^{SO(d,d|Z)} = \sum_{\vec{m}, \vec{n}: \vec{m} \cdot \vec{n} = 0} \left[(\vec{m} + B\vec{n})^t G^{-1} (\vec{m} + B\vec{n}) + \vec{n}^t G \vec{n} \right]^{-d+2} \quad (3.3)$$

is a constrained Epstein series that encodes the contribution of perturbative 1/2 BPS, states that is, those satisfying $\vec{m} \cdot \vec{n} = 0$. The subtraction eliminates IR divergences, that is the terms with $\vec{m} = \vec{n} = 0$. For $\mathcal{N} = 5, 6$ the contribution of the $(r, s) = (0, 0)$ “untwisted” sector is up to a factor $1/n$ the same as in toroidal Type II compactifications with restricted metric G_{ij} and antisymmetric tensor B_{ij} .

In the following we will focus on the contribution of the “twisted” sectors (we write “twisted” in quotes, since the terminology includes projections of the untwisted sector, i.e., amplitudes with $r = 0$ and $s = 1, \dots, n-1$) with $(r, s) \neq (0, 0)$.

Recall that the partition function reads

$$\mathcal{Z} = \frac{1}{n} \sum_{r,s}^{0,n-1} \sum_{\alpha} \frac{\theta_{\alpha}(0)}{\eta^3} \prod_{I=1}^3 \frac{\theta_{\alpha}(u_{rs}^I)}{\theta_1(u_{rs}^I)} \Gamma \left[\begin{matrix} r \\ s \end{matrix} \right], \quad (3.4)$$

where u_{rs}^I encode the effect of the Left-moving twist on the three complex internal directions, while $\Gamma \left[\begin{matrix} r \\ s \end{matrix} \right]$ denote the twisted and shifted lattice sums.

Following the analysis in [38] for one-loop scattering of vector bosons in unoriented D-brane worlds and exploiting the “factorization” of world-sheet correlation functions one has

$$\mathcal{A}_{4h} = \frac{1}{n} \sum_{r,s}^{0,n-1} \int \frac{d^2\tau}{\tau_2^2} \Gamma \left[\begin{matrix} r \\ s \end{matrix} \right] C_{4v}^L C_{4v}^R. \quad (3.5)$$

Since in both $\mathcal{N} = 5, 6$ cases the orbifold projection only acts by a shift of the lattice on the Left-movers, that is, preserves all four space-time supersymmetries, their contribution is simply

$$\mathcal{C}_{4v}^L = \text{const} \quad (3.6)$$

after summing over spin structures. In the terminology of [38] only terms with 4 fermion pairs contribute. Recall that the graviton vertex in the $q = 0$ superghost picture reads

$$V_h = h_{\mu\nu} (\partial X^\mu + ik\psi\psi^\mu) (\bar{\partial}\tilde{X}^\nu + ik\tilde{\psi}\tilde{\psi}^\nu) e^{ikX}, \quad (3.7)$$

and, for fixed graviton helicity (henceforth we use $D = 4$ notation but the analysis is valid in $D = 5$ too), one can exploit ‘‘factorization’’ of the physical polarization tensor

$$h_{\mu\nu}^{(2\sigma)} = a_\mu^{(\sigma)} a_\nu^{(\sigma)} \quad (3.8)$$

in terms of photon polarization vectors.

In the R -moving sector however, the orbifold projection breaks 1/2 ($\mathcal{N} = 6$) or 3/4 ($\mathcal{N} = 5$) of the original four space-time supersymmetries. Correlation functions of two and three fermion bilinears will be nonvanishing, too.

For two fermion bilinears one has [38]

$$\langle \partial X^{\mu_1} \partial X^{\mu_2} k_3 \psi \psi^{\mu_3} k_4 \psi \psi^{\mu_4} \rangle \left[\eta^{\mu_1 \mu_2} \partial_1 \partial_2 \mathcal{G}_{12} - \sum_{i \neq 1} k_i^{\mu_1} \partial_1 \mathcal{G}_{1i} \sum_{j \neq 2} k_j^{\mu_2} \partial_2 \mathcal{G}_{1j} \right] = \left[k_3 k_4 \eta^{\mu_3 \mu_4} - k_3^{\mu_4} k_4^{\mu_3} \right], \quad (3.9)$$

where \mathcal{G}_{ij} denotes the scalar propagator on the torus (with $\alpha' = 2$)

$$\mathcal{G}_{z,w} = -\log \frac{|\theta_1(z-w)|}{|\theta_1'(0)|} - \pi \frac{\text{Im}(z-w)^2}{\text{Im} \tau}. \quad (3.10)$$

Similarly, for three fermion bilinears, one finds [38]

$$\langle \partial X^{\mu_1} k_2 \psi \psi^{\mu_2} k_3 \psi \psi^{\mu_3} k_4 \psi \psi^{\mu_4} \rangle = \sum_{i \neq 1} k_i^{\mu_1} \partial_1 \mathcal{G}_{1i} \left[k_2 k_3 k_4^{\mu_2} \eta^{\mu_3 \mu_4} - \dots \right] \omega_{234} \quad (3.11)$$

with $\omega_{234} = \partial \log \theta_1(z_{23}) + \partial \log \theta_1(z_{34}) + \partial \log \theta_1(z_{42})$.

For four fermion bilinears, disconnected contractions yield [38]

$$\begin{aligned} \langle k_1 \psi \psi^{\mu_1} k_2 \psi \psi^{\mu_2} k_3 \psi \psi^{\mu_3} k_4 \psi \psi^{\mu_4} \rangle_{\text{disc}} = & \left\{ \left[k_1 k_2 \eta^{\mu_1 \mu_2} - k_1^{\mu_2} k_2^{\mu_1} \right] \left[k_3 k_4 \eta^{\mu_3 \mu_4} - k_3^{\mu_4} k_4^{\mu_3} \right] \right. \\ & \left. \times (\wp_{12} + \wp_{34} - \Delta_{rs}) + \dots \right\}, \end{aligned} \quad (3.12)$$

where \wp is Weierstrass function

$$\begin{aligned}\wp(z) &= \frac{1}{z^2} + \sum'_{m,n} \frac{1}{(z+n+m\tau)^2} - \frac{1}{(n+m\tau)^2} \\ &= -\partial_z^2 \log \theta_1(z) - 2\eta_1 = -2\partial_z^2 \mathcal{G}(z, \bar{z}) - \frac{\pi^2}{3} \hat{E}_2\end{aligned}\quad (3.13)$$

with $\eta_1 = -\theta_1'''/6\theta_1'$ and \hat{E}_2 the nonholomorphic modular form of weight 2 (Eisenstein series). Weierstrass function satisfies $\wp(1/2) = e_1$, $\wp(\tau/2) = e_2$, $\wp(1/2 + \tau/2) = e_3$ with $e_1 + e_2 + e_3 = 0$.

Finally, connected contractions of four fermion bilinears yield [38]

$$\langle k_1 \psi \psi^{\mu_1} k_2 \psi \psi^{\mu_2} k_3 \psi \psi^{\mu_3} k_4 \psi \psi^{\mu_4} \rangle_{\text{conn}} = \left[k_1^{\mu_4} k_2^{\mu_1} k_3^{\mu_2} k_4^{\mu_3} \pm \dots \right] (\wp_{13} - \omega_{123} \omega_{143} + \Delta_{rs}), \quad (3.14)$$

where, for $\mathcal{N} = 6$,

$$\Delta_{rs} = \wp(u_{rs}) \quad (3.15)$$

while, for $\mathcal{N} = 5$,

$$\Delta_{rs} = 3\eta_1 + \frac{1}{6} \frac{\mathcal{L}'''(u_{rs})}{\mathcal{L}'(u_{rs})} \quad (3.16)$$

with $\mathcal{L}'/\mathcal{L} = \sum_I \partial \log \theta_1(u_{rs}^I)$, which is clearly moduli independent, since no NS-NS moduli survive except for the axio-dilaton. Dependence on R - R moduli and the axio-dilaton is expected to be generated by L - R asymmetric bound states of Euclidean D-branes and NS5-branes.

3.1. World-Sheet Integrations

Worldsheet integrations can be performed with the help of $\int d^2 z \partial_z \mathcal{G}_{zw} = 0 = \int d^2 z \partial_z^2 \mathcal{G}_{zw}$ as well as of

$$\begin{aligned}\int d^2 z d^2 w (\partial_z \mathcal{G}_{zw})^2 &= -\tau_2 \hat{E}_2 \frac{\pi^2}{3}, \\ \int d^2 z d^2 w \left[\eta^{\mu_1 \mu_2} \partial_1 \partial_2 \mathcal{G}_{12} k_1 k_2 \mathcal{G}_{12} - \sum_{i \neq 1} k_i^{\mu_1} \partial_1 \mathcal{G}_{1i} \sum_{j \neq 2} k_j^{\mu_2} \partial_2 \mathcal{G}_{1j} \right] &= -\tau_2 \hat{E}_2 \frac{\pi^2}{3} \left[\eta^{\mu_1 \mu_2} k_1 k_2 - k_1^{\mu_2} k_2^{\mu_1} \right].\end{aligned}\quad (3.17)$$

For $\mathcal{N} = 6 = 4_L + 2_R$, setting $f_{\mu\nu}^{L/R} = k_\mu a_\nu^{L/R} - k_\nu a_\mu^{L/R}$, one has

$$\begin{aligned} \mathcal{L}_{\text{eff}}^{\text{twist}} &= \frac{1}{n} \sum'_{r,s} \int d^2\tau \Gamma \left[\begin{matrix} r \\ s \end{matrix} \right] \langle f_1 f_2 f_3 f_4 \rangle_L^{\text{MHV}} \\ &\quad \times \left\{ 4[(f_1 f_2)(f_3 f_4) + \dots]_R \frac{\pi^2}{3} \hat{E}_2 \right. \\ &\quad \left. + [(f_1 f_2)(f_3 f_4) + \dots]_R \left(-2 \frac{\pi^2}{3} \hat{E}_2 + \wp(u_{rs}) \right) \right. \\ &\quad \left. + [(f_1 f_2 f_3 f_4) + \dots]_R \left(-2 \frac{\pi^2}{3} \hat{E}_2 - \wp(u_{rs}) \right) \right\}, \end{aligned} \quad (3.18)$$

where, including all permutations,

$$\begin{aligned} \langle f_1 f_2 f_3 f_4 \rangle^{\text{MHV}} &= (f_1 f_2 f_3 f_4) + (f_1 f_3 f_4 f_2) + (f_1 f_4 f_2 f_3) \\ &\quad - 2(f_1 f_2)(f_3 f_4) - 2(f_1 f_3)(f_4 f_2) - 2(f_1 f_4)(f_2 f_3) \end{aligned} \quad (3.19)$$

is the structure that appears in 4-pt vector boson amplitudes, that are necessarily MHV (Maximally Helicity Violating) in $D = 4$ (in $D = 5$ there is more than one ‘‘helicity,’’ but the tensor structure has the same form [39, 40]).

Combining the R -moving contributions one eventually finds

$$\mathcal{L}_{\text{eff}}^{\text{twist}} = \langle \mathcal{R}_1 \mathcal{R}_2 \mathcal{R}_3 \mathcal{R}_4 \rangle^{\text{MHV}} \frac{1}{n} \sum'_{r,s} \int d^2\tau \Gamma \left[\begin{matrix} r \\ s \end{matrix} \right] \left(+2 \frac{\pi^2}{3} \hat{E}_2 - \wp(u_{rs}) \right), \quad (3.20)$$

where \mathcal{R}_i denote the linearized Riemann tensors of the four gravitons and

$$\langle \mathcal{R}_1 \mathcal{R}_2 \mathcal{R}_3 \mathcal{R}_4 \rangle^{\text{MHV}} = \langle f_1 f_2 f_3 f_4 \rangle_L^{\text{MHV}} \langle f_1 f_2 f_3 f_4 \rangle_R^{\text{MHV}} \quad (3.21)$$

reproduces the expected \mathcal{R}^4 structure, which is MHV in $D = 4$, and no lower derivative \mathcal{R}^2 and/or \mathcal{R}^3 terms [21].

For $\mathcal{N} = 5 = 4_L + 1_R$ in $D = 4$ one gets similar results with $\mathcal{E}_{\mathcal{N}=2_R} = \Gamma \left[\begin{matrix} r \\ s \end{matrix} \right]$ replaced by $\mathcal{E}_{\mathcal{N}=1_R} = \mathcal{O}_{ab} \mathcal{H}' / \mathcal{H}(\alpha' \tau_2)^{-2}$ which is moduli independent.

Henceforth we will focus on the $\mathcal{N} = 6 = 4_L + 2_R$ case and explore NS-NS moduli dependence of the one-loop threshold in $D = 5$.

4. One-Loop Threshold Integrals

One-loop threshold integrals for toroidal compactifications have been briefly reviewed above and shown to represent the contribution of the $(r, s) \neq (0, 0)$ untwisted sector. For $(r, s) \neq (0, 0)$ the threshold integrals involve shifted lattice sums as in heterotic strings with Wilson lines [41–45].

For simplicity let us discuss here the case of $\mathcal{N} = 6$ in $D = 5$. For definiteness we consider $n = 2$ (Z_2 shift orbifold) and start at the special point in the moduli space where $\mathbf{T}^5 = \mathbf{T}_{SO(8)}^4 \times \mathbf{S}^1$. Later on we will include off-diagonal moduli that effectively behave as Wilson lines.

In the ‘‘twisted’’ $[1]_1^0$ sector, the relevant threshold integral is of the form

$$\begin{aligned} \mathcal{D}_{1,5}^{\mathcal{N}=6} \begin{bmatrix} 0 \\ 1 \end{bmatrix} &= (2\pi)^5 \int_{\mathfrak{F}} \frac{d^2\tau}{\tau_2} \tau_2^{5/2} \Gamma_{1,1} \begin{bmatrix} 0 \\ 1 \end{bmatrix} (R) \overline{O}_8 \left[\frac{2\pi^2}{3} \hat{E}_2 + \wp \left(\frac{1}{2} \right) \right] \\ &= (2\pi)^5 \int_{\mathfrak{F}} \frac{d^2\tau}{\tau_2} \tau_2^2 \frac{R}{\sqrt{\alpha'}} \sum_{m,n} e^{-2m+(2n+1)\tau^2\pi R^2/4\alpha'\tau_2} \overline{O}_8 \left[\frac{2\pi^2}{3} \hat{E}_2 + \wp \left(\frac{1}{2} \right) \right]. \end{aligned} \quad (4.1)$$

Setting $(2m, 2n+1) = (2\ell+1)(2m', 2n'+1)$ and using invariance of \overline{O}_8 under $\tau \rightarrow \tau+2$ allow to unfold the integral to the double strip

$$(2\pi)^5 \frac{R}{\sqrt{\alpha'}} \int_{-1}^{+1} d\tau_1 \int_0^\infty d\tau_2 \sum_{\ell} e^{-(2\ell+1)^2\pi R^2/4\alpha'\tau_2} \sum_{N,\overline{N}} d_{\overline{N}} \overline{q}^{\overline{N}} c_N q^N, \quad (4.2)$$

where $\overline{O}_8 = \sum_{N=|\tau|^2/2} d_N \overline{q}^N$ and $(2\pi^2/3)\hat{E}_2 + \wp(1/2) = \sum_N c_N q^N$. Performing the trivial integral over τ_1 (level matching $\overline{N} = N$) and the less trivial integral over τ_2 by means of

$$\int_0^\infty dy y^{v-1} e^{-cy-b/y} = \left(\frac{b}{c} \right)^{v/2} K_v(\sqrt{bc}), \quad (4.3)$$

where $K_\nu(z)$ is a Bessel function of second kind, finally yields

$$\mathcal{D}_{1,5}^{\mathcal{N}=6} \begin{bmatrix} 0 \\ 1 \end{bmatrix} (R, A_i = 0) = (2\pi)^5 \left(\frac{R}{\sqrt{\alpha'}} \right)^{3/2} \sum_{\ell=0}^\infty \sum_{N=1}^\infty (2\ell+1) \sqrt{N} d_N \sigma_1(N) K_1 \left(4\pi(2\ell+1) \sqrt{\frac{NR}{\alpha'}} \right), \quad (4.4)$$

where

$$\sigma_1(N) = \sum_{d|N} = \psi(N) - \psi(1) = \frac{c_N}{N} \quad (4.5)$$

from the expansion of \hat{E}_2 in powers of q .

The result can be easily generalized to the other sectors of the Z_2 orbifold under consideration as well as to different (orbifold) constructions that give rise to different shifted lattice sums. Manifest $SO(1,5 | Z)$ symmetry can be achieved turning on off-diagonal

components of B and G (subject to restrictions). Denoting by $2A_i = G_{i5} + B_{i5}$ and observing that $G_{i5} - B_{i5} = 0$ by construction, one finds

$$\begin{aligned}
\mathcal{D}_{1,5}^{\mathcal{N}=6} \left[\begin{matrix} r \\ s \end{matrix} \right] (R, A_i) &= (2\pi)^5 \frac{R}{2\sqrt{\alpha'}} \sum_{\ell=0}^{\infty} \sum_{\vec{w} \in \Gamma_s} \frac{c_{\vec{w}^2}}{2} \int_0^{\infty} dy (2\ell + 1) e^{-(2\ell+1)^2 \pi R^2 / 4\alpha' y - 2\pi i \vec{w} \cdot \vec{w} + 2\pi i \vec{w} \cdot \vec{A}} \\
&= (2\pi)^5 \left(\frac{R}{\sqrt{\alpha'}} \right)^{3/2} \sum_{\ell=0}^{\infty} \sum_{\vec{w} \in \Gamma_s} \sigma_1 \left(\frac{\vec{w}^2}{2} \right) (2\ell + 1) \\
&\quad \times \sqrt{\frac{\vec{w}^2}{2}} e^{2\pi i \vec{r} \cdot \vec{A}} K_1 \left(4\pi (2\ell + 1) \sqrt{\frac{\vec{w}^2 R}{2\sqrt{\alpha'}}} \right).
\end{aligned} \tag{4.6}$$

Summing up the contributions of the various sectors, that is, various shifted lattice sums, yields the complete one-loop threshold correction to the \mathcal{R}^4 terms for $\mathcal{N} = 6$ superstring vacua in $D = 5$. Clearly only NS-NS moduli (except the dilaton) appear that expose $SO(1,5)$ T -duality symmetry.

The analysis is rather more involved in $D = 4$ where one-loop threshold integrals receive contribution from trivial, degenerate, and nondegenerate orbits [46, 47]. Alternative methods for unfolding the integrals over the fundamental domain have been proposed [48, 49].

Explicit computation is beyond the scope of the present investigation. It proceeds along the lines above and presents close analogy with threshold computations in $\mathcal{N} = 2$ heterotic strings sectors in the presence of Wilson lines [41, 42, 44] or, equivalently, $\mathcal{N} = 4$ heterotic strings in $D = 8$ [50]. Rather than focussing on this interesting but rather technical aspect of the problem, let us turn our attention onto the nonperturbative dependence on the other R - R moduli as well as dilaton. This is brought about by the inclusion of asymmetric D-brane instantons.

5. Low-Energy Action and U -Duality

In [12] the conserved charges coupling to the surviving R - R and NS-NS graviphotons were identified as combinations of those appearing in toroidal compactifications. In the case of maximal $\mathcal{N} = 8$ supergravity, the 12 NS-NS graviphotons couple to windings and KK momenta. Their magnetic duals couple to wrapped NS5-branes (H-monopoles) and KK monopoles. The 32 R - R graviphotons (including magnetic duals) couple to 6 D1-, 6 D5-, and 20 D3-branes in Type IIB and to 1 D0-, 15 D2-, 15 D4-, and 1 D6-branes in Type IIA.

An analogous statement applies to Euclidean branes inducing instanton effects. In toroidal compactifications with $\mathcal{N} = 8$ supersymmetry, one has 15 kinds of worldsheet instantons (EF1), 1 D(-1), 15 ED1, 15 ED3 and one each of EN5, ED5, EKK5 for Type IIB. For Type IIA superstrings one finds 6 ED0, 20 ED2, 6 ED4 and one each of EN5 and EKK5.

In a series of papers [24, 25], a natural proposal has been made for the nonperturbative completion of the modular form of $E_{d+1}(Z)$ that represent the scalar dependence of the \mathcal{R}^4

and higher derivative terms in $\mathcal{N} = 8$ superstring vacua. The explicit formulae are rather simple and elegant. In particular

$$f_{\mathcal{R}^4}^{\mathcal{N}=8}(\Phi) = \mathcal{E}_{[10^d]_{3/2}}^{E(d+1|Z)}(\Phi), \quad (5.1)$$

where $\mathcal{E}_{[10^d]_{3/2}}^{E(d+1|Z)}(\Phi)$ is an Einstein series of the relevant U -duality group. The above proposal satisfies a number of consistency checks including perturbative string limit that is small string coupling in which $E(d+1|Z) \rightarrow SO(d, d|Z)$ and $[10 \cdots 0] \rightarrow \mathbf{2d}$, large radius limit in which $E(d+1|Z) \rightarrow E(d|Z)$ and $[10 \cdots 0] \rightarrow [10 \cdots 0]$, and M-theory limit in which $E(d+1|Z) \rightarrow SL(d+1|Z)$ and $[10 \cdots 0] \rightarrow [10 \cdots 0]'$. Moreover $f_{\mathcal{R}^4}$ only receives contribution from 1/2 BPS states as expected for a supersymmetric invariant that can be written as an integral over half of (on-shell) superspace.

An independent but not necessarily inequivalent proposal has been made in [26].

We expect similar results for \mathcal{R}^4 terms in $\mathcal{N} = 5, 6$ superstring vacua with the following caveats. First, in $\mathcal{N} = 5, 6$ superspace \mathcal{R}^4 terms are 1/5 and 1/3 BPS, respectively, since they require integrations over 16 Grassman variables. Indeed we have explicitly seen that one-loop threshold correction involves the left-moving sector, in which supersymmetry is partially broken, in an essential way. Second, the U -duality group is not of maximal rank, and the same applies to the T -duality subgroup, present in the $\mathcal{N} = 6$ case. Third, $\mathcal{N} = 5, 6$ only exist in $D \leq 5$ or $D \leq 4$. Some decompactification limits should produce $\mathcal{N} = 8$ vacua in $D = 10$.

Let us try and identify the relevant 1/3 or 1/5 BPS Euclidean D-brane bound states.

5.1. $\mathcal{N} = 6$ ED-Branes

In the Type IIB description, the chiral Z_2 projection (T -duality) from $\mathcal{N} = 8$ to $\mathcal{N} = 6$ yields the Euclidean D-brane bound states of the form

$$\begin{aligned} D(-1) + ED3_{\hat{T}^4}, \quad ED1_{T^2} + ED5_{T^2 \times \hat{T}^4}, \quad ED1_{S^1 \times \hat{S}^1} + ED3_{S^1 \times \hat{T}^3}, \\ ED1_{\hat{T}^2} + ED1_{\hat{T}^2}, \quad ED3_{T^2 \times \hat{T}^2} + ED3_{T^2 \times \hat{T}^2}. \end{aligned} \quad (5.2)$$

The above bound states of Euclidean D-branes are 1/3 BPS since they preserve 8 supercharges out of the 24 supercharges present in the background.

A similar analysis applies to world-sheet and ENS5 instantons.

There are several other superstring realizations of $\mathcal{N} = 6$ supergravity in $D = 4$. Given the uniqueness of the low-energy theory, they all share the same massless spectrum but the massive spectrum and the relevant (Euclidean) D-brane bound-states depend on the choice of model.

5.2. Nonperturbative Threshold Corrections

By analogy with $\mathcal{N} = 8$ one would expect $f_{\mathcal{R}^4} = \Theta_G$, that is, an automorphic form of the U -duality group G , that is, $G = SO^*(12)$ ($SU^*(6)$) for $\mathcal{N} = 6$ in $D = 4$ ($D = 5$) and $G = SU(5, 1)$ for $\mathcal{N} = 5$ in $D = 4$. The relevant ‘‘instantons’’ should be associated to BPS particles in one higher dimension (when possible).

For $\mathcal{N} = 6$, in the decompactification limit the relevant decomposition under $SO^*(12) \rightarrow SU(5, 1) \times R^+$ is

$$\mathbf{66} \longrightarrow \mathbf{35}_0 + \mathbf{1}_0 + \mathbf{15}_{+2} + \mathbf{15}'_{-2} \quad (5.3)$$

so that the 15 particle charges in $D = 6$ satisfy 15 1/3 BPS ‘‘purity’’ conditions in $D = 5$

$$\frac{\partial \mathcal{D}_3}{\partial Q^{[ij]}} = 0, \quad (5.4)$$

where $\mathcal{D}_3^{\mathcal{N}=6, D=5} = \varepsilon_{ijklmn} Q^{[ij]} Q^{[kl]} Q^{[mn]}$. The moduli space decomposes according to

$$\frac{SO^*(12)}{U(6)} \supset \frac{SU(5, 1)}{Sp(6)} \times R^{15} \times R^+. \quad (5.5)$$

More precisely the 15 charges decompose under $SO(1, 5)$ into a 15-dim irrep. The ‘‘purity’’ conditions include $\det Q = 0$, viewed as a 6×6 antisymmetric matrix.

For $\mathcal{N} = 6$, in the string theory limit the relevant decomposition under $SO^*(12) \rightarrow SO(2, 6) \times SL(2)_S$ is

$$\mathbf{32} \longrightarrow (\mathbf{8}_v, \mathbf{2})_{NS-NS} + (\mathbf{8}_s, \mathbf{1})_{R-R} + (\mathbf{8}_c, \mathbf{1})_{R-R} \quad (5.6)$$

that yields

$$\mathbf{66} \longrightarrow (\mathbf{28}, \mathbf{1}) + (\mathbf{1}, \mathbf{3}) + (\mathbf{8}_s, \mathbf{2}) + (\mathbf{8}_c, \mathbf{2}) + 3(\mathbf{1}, \mathbf{1}). \quad (5.7)$$

The moduli space decomposes according to

$$\frac{SO^*(12)}{U(6)} \supset \frac{SO(6, 2)}{SO(6) \times SO(2)} \times \frac{SL(2)}{U(1)} \times R^{16}. \quad (5.8)$$

Further decomposition under $SL(2)_T \times SL(2)_U \times SL(2)_S$ should allow to get the ‘‘non-Abelian’’ part of the automorphic from from the ‘‘Abelian’’ one by means of $SL(2)_{U=\tau} \equiv SL(2)_B$. In particular the action for a (T -duality invariant) bound state of ED5 and three ED1’s into the action of EN5 and EF1’s, while the action of (T -duality invariant) bound state of ED(-1) and three ED3’s is invariant (singlet). Clearly further detailed analysis is necessary.

5.3. $\mathcal{N} = 5$ ED-Branes

In the Type IIB description, the two chiral Z_2 projections (“ T -duality” on T_{1234}^4 and T_{3456}^4) from $\mathcal{N} = 8$ to $\mathcal{N} = 5$ yield Euclidean D-brane bound states of the form

$$\begin{aligned}
& D(-1) + ED3_{\widehat{T}_{1234}^4} + ED3_{\widehat{T}_{3456}^4} + ED3_{\widehat{T}_{1256}^4}, \\
& ED(-1)_{12} + ED5_{123456} + ED1_{34} + ED1_{56}, \\
& ED1_{i_1 i_2} + ED3_{i_1 j_2 k_3 l_3} + ED3_{j_1 i_2 k_3 l_3} + ED1_{j_1 j_2}, \\
& ED1_{i_1 i_3} + ED3_{i_1 j_2 k_2 l_3} + ED3_{j_1 j_2 k_2 k_3} + ED1_{j_1 k_3}, \\
& ED1_{i_2 i_3} + ED1_{j_2 j_3} + ED3_{i_1 j_1 j_2 i_3} + ED3_{i_1 j_1 i_2 j_3}.
\end{aligned} \tag{5.9}$$

Bound states of Euclidean D-branes carrying the above charges are 1/5 BPS since they preserve 4 supercharges out of the 20 supercharges present in the background.

As in the $\mathcal{N} = 6$ case, a different analysis applies to BPS states carrying KK momenta or windings or their magnetic duals. However, at variant with the $\mathcal{N} = 6$, the three massive gravitini cannot form a single complex 2/5 BPS multiplet. One of them, together with its superpartners, should combine with string states which are degenerate in mass at the special rational point in the moduli space where the chiral $Z_2 \times Z_2$ projection is allowed.

6. Generating MHV Amplitudes in $\mathcal{N} = 5, 6$ SG’s

Very much like, tree-level amplitudes in $\mathcal{N} = 8$ supergravity in $D = 4$ can be identified with “squares” of tree-level amplitudes in $\mathcal{N} = 4$ SYM theory [3, 4], tree-level amplitudes in $\mathcal{N} = 5, 6$ supergravity in $D = 4$ can be identified with “products” of tree-level amplitudes in $\mathcal{N} = 4$ and $\mathcal{N} = 1, 2$ SYM theory.

As previously observed, a first step in this direction is to show that the spectra of $\mathcal{N} = 5, 6$ supergravity are simply the tensor products of the spectra of $\mathcal{N} = 4$ and $\mathcal{N} = 1, 2$ SYM theory.

The second step is to work in the helicity basis and focus on MHV amplitudes (for a recent review see, e.g., [27]). In $\mathcal{N} = 4$ SYM the generating function for (colour-ordered) n -point MHV amplitudes is given by [51]

$$\mathcal{F}_{\text{MHV}}^{\mathcal{N}=4 \text{ SYM}}(\eta_i^a, u_i^\alpha) = \frac{\delta^8(\sum_i \eta_i^a u_i^\alpha)}{\langle u_1 u_2 \rangle \langle u_2 u_3 \rangle \cdots \langle u_n u_1 \rangle}, \tag{6.1}$$

where η_i^a with $i = 1, \dots, n$ and $a = 1, \dots, 4$ are auxiliary Grassmann variables and u_i are commuting left-handed spinors, such that $p_i = u_i \bar{u}_i$.

Individual amplitudes are obtained by taking derivatives with respect to the Grassman variables η ’s according to the rules

$$A^+ \longrightarrow 1, \quad \lambda_a^+ \longrightarrow \frac{\partial}{\partial \eta^a}, \dots, \quad A^- \longrightarrow \frac{1}{4!} \varepsilon^{abcd} \frac{\partial^4}{\partial \eta^a \cdots \partial \eta^d}. \tag{6.2}$$

The intermediate derivatives representing scalars ($\varphi \sim \partial^2/\partial\eta^2$) and right-handed gaugini ($\lambda^- \sim \partial^3/\partial\eta^3$).

One can reconstruct all tree-level amplitudes, be they MHV or not, from MHV amplitudes using factorization, recursion relation or otherwise, see for example [27].

One can easily derive (super)gravity MHV amplitudes by simply taking the product of the generating functions for SYM amplitudes

$$\mathcal{G}_{\text{MHV}}^{\mathcal{N}=8 \text{ SG}}(\eta_i^A, u_i^\alpha) = \frac{\mathcal{C}(u_i) \delta^{16}(\sum_i \eta_i^A u_i^\alpha)}{\langle u_1 u_2 \rangle^2 \langle u_2 u_3 \rangle^2 \cdots \langle u_n u_1 \rangle^2} = \mathcal{C}(u_i) \mathcal{F}_{\text{MHV,L}}^{\mathcal{N}=4 \text{ SYM}}(\eta_i^{a_L}, u_i^\alpha) \mathcal{F}_{\text{MHV,R}}^{\mathcal{N}=4 \text{ SYM}}(\eta_i^{a_R}, u_i^\alpha), \quad (6.3)$$

where $\eta^A = (\eta_i^{a_L}, \eta_i^{a_R})$ with $A = 1, \dots, 8$ and the correction factor $\mathcal{C}(u_i)$ is only a function of the spinors u_i , actually of the massless momenta $p_i = u_i \bar{u}_i$ [28].

The relevant dictionary would read

$$h^+ \longrightarrow 1, \quad \psi_A^+ \longrightarrow \frac{\partial}{\partial \eta^A}, \dots, h^- \longrightarrow \frac{1}{\mathcal{N}!} \frac{\partial^8}{\partial \eta^8}. \quad (6.4)$$

In principle one can reconstruct all tree-level amplitudes, be they MHV or not, from MHV amplitudes using factorization, recursion relations, or otherwise, see for example [27]. Unitary methods allow to extend the analysis beyond tree level. If all $\mathcal{N} = 8$ supergravity amplitudes were expressible in terms of squares of $\mathcal{N} = 4$ SYM amplitudes, UV finiteness of the latter would imply UV finiteness of the former. Although support to this conjecture at the level of 4-graviton amplitudes, which are necessarily MHV, seems to exclude the presence of \mathcal{R}^4 corrections, which are 1/2 BPS saturated, it would be crucial to explicitly test the absence of $D^8 \mathcal{R}^4$ corrections, the first that are not BPS saturated.

Going back to the problem of expressing MHV amplitudes in $\mathcal{N} = 5, 6$ supergravities in terms of SYM amplitudes, one has to resort to “orbifold” techniques.

In the $\mathcal{N} = 6$ case, half of the 4 η 's (say η_L^3 and η_L^4) of the “left” $\mathcal{N} = 4$ SYM factor are to be projected out, that is, “odd” under a Z_2 involution. As a result the generating function is the same as in $\mathcal{N} = 8$ supergravity but the dictionary gets reduced to

$$h^+ \longrightarrow 1, \quad \psi_{A'}^+ \longrightarrow \frac{\partial}{\partial \eta^{A'}}, \quad A_0^+ = \frac{\partial^2}{\partial \eta_L^3 \partial \eta_L^4}, \quad A_{A'B'}^+ = \frac{\partial^2}{\partial \eta^{A'} \partial \eta^{B'}}, \dots, \quad (6.5)$$

$$h^- = \frac{1}{6!} \varepsilon^{A_1 \dots A_6} \frac{\partial^{2+6}}{\partial \eta_L^3 \partial \eta_L^4 \partial \eta^{A_1} \dots \partial \eta^{A_6}},$$

where $A' = 1, \dots, 6$.

Further reduction is necessary for $\mathcal{N} = 5$ case; 3 of the 4 η 's of the “left” $\mathcal{N} = 4$ SYM factor are to be projected out. For instance, they may acquire a phase $\omega = \exp(i2\pi/3)$ under a Z_3 projection.

The same projections should be implemented on the intermediate states flowing around the loops. Although tree-level amplitudes in $\mathcal{N} = 5, 6$ supergravity are simply a subset of the ones in $\mathcal{N} = 8$ supergravity, naive extension of the argument at loop order does not immediately work [52–54]. Several cancellations are not expected to take place despite the residual supersymmetry of the left SYM factor. However, in view of the recent observations

on the factorization of $\mathcal{N} = 4$ SYM into a kinematical part and a group theory part, where the latter satisfies identities similar to the former [55–57] and can thus be consistently replaced with the former giving rise to consistent and UV finite $\mathcal{N} = 8$ SG amplitudes, it may well be the case that a similar decomposition can be used to produce, possibly UV finite, $\mathcal{N} = 5, 6$ SG amplitudes. Our results on \mathcal{R}^4 lend some support to this viewpoint.

7. Conclusions

Let us summarize our results. We have shown that the first higher derivative corrections to the low-energy effective action around superstring vacua with $\mathcal{N} = 5, 6$ supersymmetry are \mathcal{R}^4 terms as in $\mathcal{N} = 8$. Contrary to $\mathcal{N} \leq 4$, no \mathcal{R}^2 terms appear. In this respect $\mathcal{N} = 5, 6$ supersymmetric models in $D = 4$, having no massless matter multiplets to add, behave similarly to their common $\mathcal{N} = 8$ supersymmetric parent. It is worth stressing again that such nonvanishing threshold corrections confirm that, as in the $\mathcal{N} = 8$ case, superstring calculations do not reproduce field theory results. As in $\mathcal{N} = 8$ supergravity, it is known that \mathcal{R}^4 corrections are absent in $\mathcal{N} = 5, 6$ supergravity due to the anomaly free continuous duality symmetry [1].

Relying on previous results on vector boson scattering at one loop in unoriented D-brane worlds [38], we have studied four graviton scattering amplitudes and derived explicit formulae for the one-loop threshold corrections in asymmetric orbifolds that realize the above vacua. In addition to a term $1/n \times f^{\mathcal{N}=8} \times c\mathcal{R}^4$, coming from the $(0, 0)$ sector, contributions from nontrivial sectors of the orbifold to $f^{\mathcal{N}=5,6} \times c\mathcal{R}^4$ display a close similarity with heterotic threshold corrections in the presence of Wilson lines [41, 42, 44]. For illustrative purposes, we have computed the relevant integrals for $\mathcal{N} = 6$ in $D = 5$ exposing the expected $SO(1, 5)$ T -duality symmetry. The analysis in $D = 4$ is technically more involved and will be performed elsewhere. We have also identified the relevant $1/3$ or $1/5$ BPS bound states of Euclidean D-branes that contribute to the nonperturbative dependence of the thresholds on R - R scalars and on the axio-dilaton. By analogy with $\mathcal{N} = 8$ it is natural to conjecture the possible structure of the automorphic form of the relevant U -duality group. A more detailed analysis of this issue is however necessary. Finally, in view of the potential UV finiteness of $\mathcal{N} = 5, 6$ supergravities, we have discussed how to compute tree-level MHV amplitudes using generating function and orbifolds techniques [28]. All other tree-level amplitudes should follow from factorization and in fact should coincide with $\mathcal{N} = 8$ amplitudes involving only $\mathcal{N} = 5$ or $\mathcal{N} = 6$ supergravity states in the external legs. Loop amplitudes require a separate investigation. In particular no generalization of the KLT relations is known beyond tree level [58].

Acknowledgments

Discussions with C. Bachas, M. Cardella, S. Ferrara, F. Fucito, M. Green, E. Kiritsis, S. Kovacs, L. Lopez, J. F. Morales, N. Obers, R. Poghossyan, R. Richter, M. Samsonyan, and A. V. Santini are kindly acknowledged. This work was partially supported by the ERC Advanced Grant no. 226455 “*Superfields*” and by the Italian MIUR-PRIN Contract 2007-5ATT78 “*Symmetries of the Universe and of the Fundamental Interactions*”.

References

- [1] N. Marcus, “Composite anomalies in supergravity,” *Physics Letters B*, vol. 157, no. 5-6, pp. 383–388, 1985.

- [2] A. Ceresole and S. Ferrara, "Black holes and attractors in supergravity," <http://arxiv.org/abs/1009.4175>.
- [3] Z. Bern, L. J. Dixon, and R. Roiban, "Is $\mathcal{N} = 8$ supergravity ultraviolet finite?" *Physics Letters B*, vol. 644, no. 4, pp. 265–271, 2007.
- [4] Z. Bern, J. J. Carrasco, L. J. Dixon, H. Johansson, and R. Roiban, "Ultraviolet behavior of $\mathcal{N} = 8$ supergravity at four loops," *Physical Review Letters*, vol. 103, no. 8, Article ID 081301, 4 pages, 2009.
- [5] K. S. Stelle, "Is $\mathcal{N} = 8$ supergravity a finite field theory?" *Fortschritte der Physik*, vol. 57, no. 5–7, pp. 446–450, 2009.
- [6] N. Beisert, H. Elvang, D. Z. Freedman, M. Kiermaier, A. Morales, and S. Stieberger, " $E_{7(7)}$ constraints on counterterms in $\mathcal{N} = 8$ supergravity," *Physics Letters B*, vol. 694, no. 3, pp. 265–271, 2010.
- [7] R. Kallosh, "The ultraviolet finiteness $\mathcal{N} = 8$ supergravity," *Journal of High Energy Physics*, vol. 2010, no. 12, 2010.
- [8] M. B. Green, H. Ooguri, and J. H. Schwarz, "Nondecoupling of maximal supergravity from the superstring," *Physical Review Letters*, vol. 99, no. 4, Article ID 041601, 4 pages, 2007.
- [9] M. Bianchi, S. Ferrara, and R. Kallosh, "Perturbative and non-perturbative $\mathcal{N} = 8$ supergravity," *Physics Letters B*, vol. 690, no. 3, pp. 328–331, 2010.
- [10] M. Bianchi, S. Ferrara, and R. Kallosh, "Observations on arithmetic invariants and U-duality orbits in $\mathcal{N} = 8$ supergravity," *Journal of High Energy Physics*, vol. 2010, no. 3, 2010.
- [11] S. Ferrara and C. Kounnas, "Extended supersymmetry in four-dimensional type II strings," *Nuclear Physics B*, vol. 328, no. 2, pp. 406–438, 1989.
- [12] M. Bianchi, "Bound-states of D-branes in L-R asymmetric superstring vacua," *Nuclear Physics B*, vol. 805, no. 1-2, pp. 168–181, 2008.
- [13] K. S. Narain, M. H. Sarmadi, and C. Vafa, "Asymmetric orbifolds," *Nuclear Physics B*, vol. 288, no. 3-4, pp. 551–577, 1987.
- [14] A. Dabholkar and J. A. Harvey, "String islands," *Journal of High Energy Physics*, vol. 3, no. 2, 16 pages, 1999.
- [15] I. Antoniadis, C. P. Bachas, and C. Kounnas, "Four-dimensional superstrings," *Nuclear Physics B*, vol. 289, no. 1, pp. 87–108, 1987.
- [16] I. Antoniadis and C. Bachas, "4d fermionic superstrings with arbitrary twists," *Nuclear Physics B*, vol. 298, no. 3, pp. 586–612, 1988.
- [17] H. Kawai, D. C. Lewellen, and S. H. H. Tye, "Construction of fermionic string models in four dimensions," *Nuclear Physics B*, vol. 288, no. 1, pp. 1–76, 1987.
- [18] H. Kawai, D. C. Lewellen, and S. H. H. Tye, "Classification of closed-fermionic-string models," *Physical Review D*, vol. 34, no. 12, pp. 3794–3804, 1986.
- [19] H. Kawai, D. C. Lewellen, and S. H. H. Tye, "Construction of four-dimensional fermionic string models," *Physical Review Letters*, vol. 57, no. 15, pp. 1832–1835, 1986.
- [20] H. Kawai and D. C. Lewellen, "Erratum: construction of four-dimensional fermionic string models," *Physical Review Letters*, vol. 58, no. 4, p. 429, 1987.
- [21] J. Broedel and L. J. Dixon, " \mathcal{R}^4 counterterm and $E_{7(7)}$ symmetry in maximal supergravity," *Journal of High Energy Physics*, vol. 2010, no. 5, 2010.
- [22] M. B. Green and M. Gutperle, "Effects of D-instantons," *Nuclear Physics B*, vol. 498, no. 1-2, pp. 195–227, 1997.
- [23] K. Becker, M. Becker, and A. Strominger, "Fivebranes, membranes and non-perturbative string theory," *Nuclear Physics B*, vol. 456, no. 1-2, pp. 130–152, 1995.
- [24] M. B. Green, J. G. Russo, and P. Vanhove, "Automorphic properties of low energy string amplitudes in various dimensions," *Physical Review D*, vol. 81, no. 8, Article ID 086008, 49 pages, 2010.
- [25] M. B. Green, S. D. Miller, J. G. Russo, and P. Vanhove, "Eisenstein series for higher-rank groups and string theory amplitudes," <http://arxiv.org/abs/1004.0163>.
- [26] B. Pioline, " \mathcal{R}^4 couplings and automorphic unipotent representations," *Journal of High Energy Physics*, vol. 2010, no. 3, Article ID 116, 2010.
- [27] J. M. Drummond, "Hidden simplicity of gauge theory amplitudes," *Classical and Quantum Gravity*, vol. 27, no. 21, 2010.
- [28] M. Bianchi, H. Elvang, and D. Z. Freedman, "Generating the amplitudes in $\mathcal{N} = 4$ SYM and $\mathcal{N} = 8$ SG," *Journal of High Energy Physics*, vol. 2008, no. 9, 2008.
- [29] J. Bagger and N. Lambert, "Modeling multiple M2-branes," *Physical Review D*, vol. 75, no. 4, Article ID 045020, 7 pages, 2007.
- [30] A. Gustavsson, "Algebraic structures on parallel M2 branes," *Nuclear Physics B*, vol. 811, no. 1-2, pp. 66–76, 2009.

- [31] O. Aharony, O. Bergman, and D. L. Jafferis, "Fractional M2-branes," *Journal of High Energy Physics*, vol. 2008, no. 11, Article ID 043, 27 pages, 2008.
- [32] O. Aharony, O. Bergman, D. L. Jafferis, and J. Maldacena, " $\mathcal{N} = 6$ superconformal Chern-Simons-matter theories, M2-branes and their gravity duals," *Journal of High Energy Physics*, vol. 2008, no. 10, Article ID 091, 38 pages, 2008.
- [33] K. Hosomichi, K. M. Lee, S. Lee, S. Lee, J. Park, and P. Yi, "A nonperturbative test of M2-brane theory," *Journal of High Energy Physics*, vol. 2008, no. 11, 2008.
- [34] A. Cagnazzo, D. Sorokin, and L. Wulff, "String instanton in $\text{AdS}_4 \times \text{CP}^3$," *Journal of High Energy Physics*, vol. 2010, no. 5, 29 pages, 2010.
- [35] M. Bianchi, R. Poghossian, and M. Samsonyan, "Precision spectroscopy and higher spin symmetry in the ABJM model," *Journal of High Energy Physics*, vol. 2010, no. 10, 2010.
- [36] N. Drukker, M. Marino, and P. Putrov, "From weak to strong coupling in ABJM theory," *Communications in Mathematical Physics*, 2011, <http://arxiv.org/abs/1007.3837>.
- [37] R. D'Auria, S. Ferrara, and C. Kounnas, " $\mathcal{N} = (4,2)$ chiral supergravity in six dimensions and solvable Lie algebras," *Physics Letters B*, vol. 420, no. 3-4, pp. 289–299, 1998.
- [38] M. Bianchi and A. V. Santini, "String predictions for near future colliders from one-loop scattering amplitudes around D-brane worlds," *Journal of High Energy Physics*, vol. 2006, no. 12, Article ID 010, 2006.
- [39] M. B. Green, J. H. Schwarz, and E. Witten, *Superstring Theory, vol 2*, Cambridge Monographs on Mathematical Physics, Cambridge University Press, Cambridge, UK, 1987.
- [40] M. B. Green, J. H. Schwarz, and E. Witten, *Superstring theory, vol. 1*, Cambridge Monographs on Mathematical Physics, Cambridge University Press, Cambridge, UK, 1987.
- [41] C. Bachas, C. Fabre, E. Kiritsis, N. A. Obers, and P. Vanhove, "Heterotic/type I duality and D-brane instantons," *Nuclear Physics B*, vol. 509, no. 1-2, pp. 33–52, 1998.
- [42] E. Kiritsis and N. A. Obers, "Heterotic/type-I duality in $D < 10$ dimensions, threshold corrections and D-instantons," *Journal of High Energy Physics*, vol. 1, no. 10, pp. 13–70, 1997.
- [43] M. Bianchi, E. Gava, F. Morales, and K. S. Narain, "D-strings in unconventional type I vacuum configurations," *Nuclear Physics B*, vol. 547, no. 1-2, pp. 96–126, 1999.
- [44] N. A. Obers and B. Pioline, "Exact thresholds and instanton effects in string theory," *Fortschritte der Physik*, vol. 49, no. 4–6, pp. 359–375, 2001.
- [45] M. Bianchi and J. F. Morales, "Unoriented D-brane instantons vs heterotic worldsheet instantons," *Journal of High Energy Physics*, vol. 2008, no. 2, Article ID 073, 27 pages, 2008.
- [46] L. J. Dixon, V. Kaplunovsky, and J. Louis, "Moduli dependence of string loop corrections to gauge coupling constants," *Nuclear Physics B*, vol. 355, no. 3, pp. 649–688, 1991.
- [47] P. Mayr and H. P. Nilles, "String unification and threshold corrections," *Physics Letters B*, vol. 317, no. 1-2, pp. 53–59, 1993.
- [48] M. Trapletti, "On the unfolding of the fundamental region in integrals of modular invariant amplitudes," *Journal of High Energy Physics*, vol. 2003, no. 2, Article ID 012, 20 pages, 2003.
- [49] M. Cardella, "A novel method for computing torus amplitudes for \mathbb{Z}_N orbifolds without the unfolding technique," *Journal of High Energy Physics*, vol. 2009, no. 5, Article ID 010, 16 pages, 2009.
- [50] W. Lerche, S. Stieberger, and N. P. Warner, "Quartic gauge couplings from K3 geometry," *Advances in Theoretical and Mathematical Physics*, vol. 3, no. 5, pp. 1575–1611, 1999.
- [51] V. P. Nair, "A current algebra for some gauge theory amplitudes," *Physics Letters B*, vol. 214, no. 2, pp. 215–218, 1988.
- [52] P. Katsaroumpas, B. Spence, and G. Travaglini, "One-loop $\mathcal{N} = 8$ supergravity coefficients from $\mathcal{N} = 4$ super Yang-Mills," *Journal of High Energy Physics*, vol. 2009, no. 8, Article ID 096, 33 pages, 2009.
- [53] Z. Bern, J. J. M. Carrasco, and H. Johansson, "The structure of multiloop amplitudes in gauge and gravity theories," *Nuclear Physics B*, vol. 205-206, pp. 54–60, 2010.
- [54] J. M. Drummond, P. J. Heslop, and P. S. Howe, "A note on $\mathcal{N} = 8$ counterterms," <http://arxiv.org/abs/1008.4939>.
- [55] H. Tye and Y. Zhang, "Comment on the identities of the gluon tree amplitudes," <http://arxiv.org/abs/1007.0597>.
- [56] S. H. Henry Tye and Y. Zhang, "Dual identities inside the gluon and the graviton scattering amplitudes," *Journal of High Energy Physics*, vol. 2010, no. 6, Article ID 071, 45 pages, 2010.
- [57] Z. Bern, T. Dennen, Y. T. Huang, and M. Kiermaier, "Gravity as the square of gauge theory," *Physical Review D*, vol. 82, no. 6, 2010.
- [58] H. Kawai, D. C. Lewellen, and S. H. H. Tye, "A relation between tree amplitudes of closed and open strings," *Nuclear Physics B*, vol. 269, no. 1, pp. 1–23, 1986.

Research Article

Discrete Wilson Lines in F-Theory

Volker Braun

School of Theoretical Physics, Dublin Institute for Advanced Studies, 10 Burlington Road, Dublin 4, Ireland

Correspondence should be addressed to Volker Braun, vbrown@stp.dias.ie

Received 15 May 2011; Accepted 3 July 2011

Academic Editor: Yang-Hui He

Copyright © 2011 Volker Braun. This is an open access article distributed under the Creative Commons Attribution License, which permits unrestricted use, distribution, and reproduction in any medium, provided the original work is properly cited.

F-theory models are constructed where the 7-brane has a nontrivial fundamental group. The base manifolds used are a toric Fano variety and a smooth toric threefold coming from a reflexive polyhedron. The discriminant locus of the elliptically fibered Calabi-Yau fourfold can be chosen such that one irreducible component is not simply connected (namely, an Enriques surface) and supports a non-Abelian gauge theory.

1. Introduction

F-theory [1] is a way to use geometry as a tool to understand certain compactifications of string theory that are otherwise not entirely geometric [2]. It uses an auxiliary elliptically fibered Calabi-Yau fourfold, not to be confused with the space-time manifold to study string theory in a regime away from any known weakly coupled perturbative description. Recently [3, 4] a particular model building Ansatz has been suggested where the GUT gauge group arises from a 7-brane wrapped on a contractible del Pezzo surface. Various models [5–10] and more have been constructed along these lines.

One key feature of this Ansatz is that the scales of gravity and gauge physics can be decoupled as one can decompactify the Calabi-Yau manifold without changing the del Pezzo surface. However, the price one has to pay for this is that the usual way of GUT symmetry breaking in string theory, namely, the Hosotani mechanism [11, 12] using discrete Wilson lines, no longer works: all del Pezzo surfaces are simply connected. Alternatives have been developed [3, 4, 13], but require one to give a vacuum expectation value to fields locally and not just make global nontrivial identifications. Turning on fields locally then affects the running of the coupling constants and, potentially, defocuses the gauge coupling unification [14, 15].

In this paper I will advocate for a different Ansatz for GUT model building and symmetry breaking in F-theory, namely, by wrapping the GUT 7-brane on a nonsimply

connected divisor in the base of the elliptic fibration. This allows one to choose a globally nontrivial identification of the gauge bundle while keeping it locally trivial, breaking the GUT gauge group by the usual Hosotani mechanism. For what it is worth, this setup also implies that there is no gravity/gauge theory decoupling limit.

Of course this raises the question of whether there are any such divisors in threefolds that are suitable as bases for elliptically fibered Calabi-Yau manifolds. In this paper I will answer this question and work out a rather simple example of an Enriques surface embedded into a toric threefold associated to a reflexive 3-dimensional polytope. There is nothing particularly unique about this example. It just combines the most simple surface with \mathbb{Z}_2 fundamental group and the class of threefolds we are most used to work with. All toric geometry computations used in this paper were done using [16–18].

2. Base Threefold

2.1. Foreword

An Enriques surface is a free quotient of a $K3$ surface by a freely acting holomorphic involution and is probably the best-known example of a complex surface S with fundamental group $\pi_1(S) = \mathbb{Z}_2$. Its first Chern class $c_1(S)$ is the torsion element in $H^2(S, \mathbb{Z}) \simeq \mathbb{Z}^{10} \oplus \mathbb{Z}_2$, so it admits a Ricci-flat metric but has no covariantly constant spinor (equivalently, no covariantly constant $(2,0)$ -form). Some, but not all, $K3$ surfaces can be realized [19] as quartics in \mathbb{P}^3 . Somewhat unfortunately, the locus of quartic $K3$ s and the locus of $K3$ surfaces with an Enriques involution do not intersect in the moduli space of smooth $K3$ surfaces. In other words, no smooth quartic in \mathbb{P}^3 carries an Enriques involution. Therefore, out of necessity one is forced to look at singular (birational) models and then resolve these singularities. This will be the central theme in the following.

To explicitly construct and resolve the singularities, I will make extensive use of toric geometry. However, before delving into these technical details let me first give an overview. The basic idea is to look at the following \mathbb{Z}_4 action on \mathbb{P}^3 :

$$g : \mathbb{P}^3 \rightarrow \mathbb{P}^3, \quad [x_0 : x_1 : x_2 : x_3] \mapsto [x_0 : ix_1 : i^2x_2 : i^3x_3]. \quad (2.1)$$

The fixed point set of g^2 are the two disjoint rational curves

$$\mathbb{P}^1 \cup \mathbb{P}^1 = \{x_0 = x_2 = 0\} \cup \{x_1 = x_3 = 0\}, \quad (2.2)$$

and the fixed points of g are the north and south poles on these (4 points altogether). A sufficiently generic \mathbb{Z}_4 invariant quartic $q(x_0, x_1, x_2, x_3)$ is then a (singular) Enriques surface on the quotient (this construction is rather similar to the way to construct nonsimply connected Calabi-Yau threefolds [20–24], except that I will not be looking at sections of the anticanonical bundle (which would be Calabi-Yau)). The fastest way to see this is to note that the would-be $(2,0)$ -form

$$\Omega^{(2,0)} = \oint \frac{\varepsilon^{ijk\ell} x_i dx_j \wedge dx_k \wedge dx_\ell}{q(x_0, x_1, x_2, x_3)} \quad (2.3)$$

is projected out by g .

Here is where this paper essentially begins, because so far we only have a singular Enriques surface in an even more singular ambient space. Clearly, one wants to resolve the singularities. The first step is to resolve the curves of \mathbb{Z}_2 singularities, for which there is a unique crepant resolution. Then one has to deal with the remaining 4 \mathbb{Z}_4 singularities. By a happy coincidence, the above \mathbb{Z}_4 quotient of \mathbb{P}^3 is itself a toric variety. Hence, the methods of toric geometry can be applied and allow us to construct partial and complete resolutions explicitly as toric varieties.

2.2. Toric Geometry

As a warm-up, I will first review some basic notions of toric geometry. The defining data is a rational polyhedral fan in a lattice $N \simeq \mathbb{Z}^d$, where d is the complex dimension of the variety. A fan Σ is a finite set of cones $\sigma \in \Sigma$, closed under taking faces. Often, the fan will be the cones over the faces of a polytope. This is called the face fan of the polytope.

Amongst the different, but equivalent, ways to define the corresponding complex algebraic variety from the fan data, I will use the Cox homogeneous coordinate [25] description in the following. The basic idea is to associate one complex-valued homogeneous coordinate to each ray (one-dimensional cone) of the fan. Then one has to remove a codimension-2 or higher algebraic subset and mod out generalized homogeneous rescalings. This construction will be reviewed and applied in much more detail in Section 2.4. For now, let us just consider \mathbb{P}^3 as an example. Its fan consists of the cones

$$\begin{aligned} \Sigma_{\mathbb{P}^3} = \{ & \langle 0 \rangle, \langle e_1 \rangle, \langle e_2 \rangle, \langle e_3 \rangle, \langle -\sum e_i \rangle, \langle e_1, e_2 \rangle, \langle e_1, e_3 \rangle, \langle e_1, -\sum e_i \rangle, \\ & \langle e_2, e_3 \rangle, \langle e_2, -\sum e_i \rangle, \langle e_3, -\sum e_i \rangle, \langle e_1, e_2, e_3 \rangle, \langle e_1, e_2, -\sum e_i \rangle, \\ & \langle e_1, e_3, -\sum e_i \rangle, \langle e_2, e_3, -\sum e_i \rangle, \} \end{aligned} \quad (2.4)$$

where e_1, e_2, e_3 are a basis for $N \simeq \mathbb{Z}^3$. There are 4 one-dimensional rays satisfying a unique linear relation, which translates into 4 homogeneous coordinates with the usual identification

$$[x_0 : x_1 : x_2 : x_3] = [\lambda x_0 : \lambda x_1 : \lambda x_2 : \lambda x_3], \quad \lambda \in \mathbb{C}^\times. \quad (2.5)$$

A map of fans is a map of ambient lattices such that every cone of the domain maps into a cone of the range fan. Any such fan morphism defines a morphism of toric varieties in a covariantly functorial way. For the purposes of this paper (except for A), we will only consider the case where the lattice map is the identity. In this case the domain fan is simply a subdivision of the range fan. The toric map corresponding to a subdivision of a cone σ is the blow-up along a toric subvariety of dimension equal to $\text{codim}(\sigma)$.

A toric divisor (all divisors in this paper will be Cartier divisors, even though we will be working with auxiliary singular varieties where not all divisors are Cartier) is a formal linear combination $D = \sum a_i V(x_i)$ of the codimension-one subvarieties

$$V(x_i) = \{x_i = 0\} \quad (2.6)$$

corresponding to the one-dimensional cones of the fan. There are two basic constructions associated to such a toric divisor that will be important in the following.

- (i) Every coefficient a_i can be thought of as the value of a function $f : N \rightarrow \mathbb{Z}$ on the generating lattice point ρ_i of the i -th one-cone. If every cone is simplicial, then there is a uniquely defined continuous function on the fan with the above property. The pull-back of the function on the fan corresponds to the pull-back of the divisor by the toric map.
- (ii) The divisor also defines a polytope

$$P_D = \{m \in M_{\mathbb{R}} \mid \langle m, \rho_i \rangle \geq -a_i\}, \quad (2.7)$$

where $M = N^\vee$ is the dual lattice. The global sections $\Gamma\mathcal{O}(D)$ are in one-to-one correspondence with the integral lattice points $M \cap P_D$ and can easily be counted for any given divisor.

A particularly relevant divisor is the anticanonical divisor $-K = \sum V(x_i)$. Given a lattice polytope $\nabla \in N$, we can construct its face fan and the polytope $\Delta = P_{-K} \subset M$. If Δ is again a lattice polytope, then ∇ is called reflexive.

Finally, note that $H^2(\mathbb{P}^3) = \mathbb{Z}$. Hence, the line bundles on \mathbb{P}^3 are classified by a single integer, their first Chern class. The toric divisors, on the other hand, are defined by 4 integers. Clearly, there is no one-to-one correspondence between divisors D and the isomorphism class of the associated line bundle $\mathcal{O}(D)$. To make this into a bijection, one must mod out *linear equivalence* of divisors. That is, one has to identify the piecewise linear functions modulo linear functions. In particular, one can easily see that

$$D = \sum_{i=0}^3 a_i V(x_i) \sim (a_0 + a_1 + a_2 + a_3)V(x_0) \quad (2.8)$$

on \mathbb{P}^3 .

2.3. Three Birational Models

We now begin with the core of this paper and define the base threefold of the elliptically fibered Calabi-Yau fourfold. In fact, I will choose a smooth toric variety \widehat{B} as the base manifold, containing a nonsimply connected divisor \widehat{D} . However, directly analyzing \widehat{B} will be overly complicated. In particular, \widehat{B} contains exceptional divisors that do not intersect the divisor \widehat{D} we are interested in. Therefore, to better understand $\widehat{D} \subset \widehat{B}$, I will blow down these additional exceptional divisors. This will produce a singular variety B containing the same divisor $D = \widehat{D}$. Finally, I will blow down two more curves in B to obtain a (even more singular) three-dimensional variety \underline{B} . The blown-down divisor $\underline{D} \subset \underline{B}$ is the most suitable one to compute the fundamental groups. To summarize, I am going to define successive blow-ups

$$\widehat{B} \xrightarrow{\widehat{\pi}} B \xrightarrow{\pi} \underline{B} \quad (2.9)$$

of three-dimensional toric varieties. Both of the maps $\hat{\pi}, \underline{\pi}$ are toric morphisms defined in the obvious way by combining cones of the fan into bigger cones, discarding all rays that are no longer part of the more coarse (blown-down) fan.

I now define the fans Σ corresponding to the toric varieties. Let me start by the rays $\Sigma^{(1)}$. The most singular variety has

$$\sum_{\underline{B}}^{(1)} = \{(-3, -2, 4), (0, 1, 0), (1, 0, 0), (2, 1, -4)\}, \quad (2.10)$$

see Figure 1. The convex hull of these four points is a tetrahedron, but not a minimal lattice simplex. In addition to the origin (which is an interior point), it contains the two points $(-1, -1, 2)$ and $(1, 1, -2)$ along two different edges. The variety B will be the maximal crepant partial resolution of \underline{B} , that is, the (in this case unique) maximal triangulation of the convex hull $\text{conv}(\Sigma_{\underline{B}}^{(1)})$. Hence, one must add the additional integral points to the ray generators,

$$\sum_B^{(1)} = \Sigma_{\underline{B}}^{(1)} \cup \{(-1, -1, 2), (1, 1, -2)\}. \quad (2.11)$$

Neither the variety \underline{B} nor its maximal crepant partial resolution B is smooth, related to the fact that the polytope $\text{conv}(\Sigma_B^{(1)}) = \text{conv}(\Sigma_{\underline{B}}^{(1)})$ is not reflexive. One again needs to add rays to resolve all singularities; however these time the generators are necessarily outside of $\text{conv}(\Sigma_{\underline{B}}^{(1)})$. One particular choice I am going to make is the rays generated by the 18 points listed in Table 1.

The 8 facets of the convex hull $\text{conv}(\Sigma_B^{(1)})$ are given by the inequalities

$$(n_x, n_y, n_z) \cdot \begin{pmatrix} -1 & -1 & -1 & -1 & 0 & 1 & 1 & 2 \\ -1 & 0 & 1 & 2 & -1 & -1 & 1 & -1 \\ -1 & -1 & 0 & 0 & 0 & 0 & 1 & 1 \end{pmatrix} \geq (1, 1, 1, 1, 1, 1, 1, 1), \quad (2.12)$$

which is, therefore, a reflexive polytope.

Finally, to completely specify the toric varieties \underline{B} , B , and \hat{B} , let me define the generating cones of the respective fans:

- (i) $\Sigma_{\underline{B}}$ is the face fan of the polytope $\text{conv}(\Sigma_{\underline{B}}^{(1)})$, see Figure 1;
- (ii) Σ_B is the unique maximal subdivision of $\Sigma_{\underline{B}}$;
- (iii) $\Sigma_{\hat{B}}$ is a maximal subdivision of the face fan of the polytope $\text{conv}(\Sigma_B^{(1)})$, see Figure 2.

As there are many different maximal subdivisions of the face fan, this alone does not uniquely specify the fan $\Sigma_{\hat{B}}$. For concreteness, I will fix the one listed in Table 3. Note that not all combinatorial symmetries of the graph in 3 are actually symmetries of the fan.

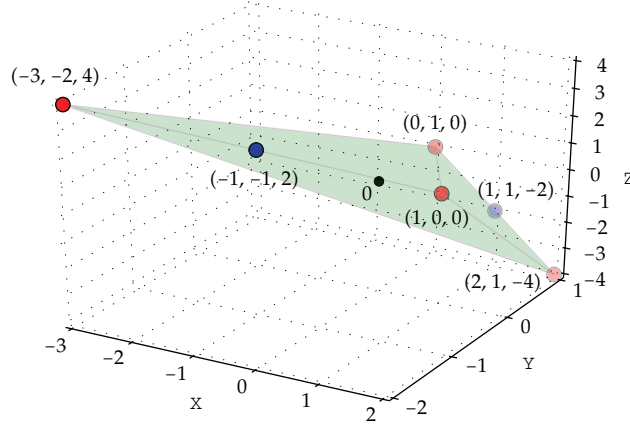


Figure 1: The rays $\Sigma_B^{(1)}$ (red dots) and $\Sigma_B^{(1)}$ (red and blue dots).

Table 1: Ray generators and the associated Cox homogeneous variables.

i	0	1	2	3	4	5	6	7	8	9	10	11	12	13	14	15	16	17
i -th ray	-3	0	1	2	-1	1	-2	-2	-1	-1	-1	0	0	1	1	1	2	2
	-2	1	0	1	-1	1	-1	-1	-1	0	0	0	0	0	0	1	1	1
	4	0	0	-4	2	-2	2	3	1	1	2	-1	1	-2	-1	-1	-3	-2
\underline{B}	\underline{z}_0	\underline{z}_1	\underline{z}_2	\underline{z}_3														
B	z_0	z_1	z_2	z_3	z_4	z_5												
\hat{B}	\hat{z}_0	\hat{z}_1	\hat{z}_2	\hat{z}_3	\hat{z}_4	\hat{z}_5	\hat{z}_6	\hat{z}_7	\hat{z}_8	\hat{z}_9	\hat{z}_{10}	\hat{z}_{11}	\hat{z}_{12}	\hat{z}_{13}	\hat{z}_{14}	\hat{z}_{15}	\hat{z}_{16}	\hat{z}_{17}

2.4. Homogeneous Coordinates

For future reference, let me list the toric Chow groups [26]:

$$A_k(\hat{B}) = \begin{cases} 1 \\ \mathbb{Z}^{15} \\ \mathbb{Z}^{15} \\ 1 \end{cases}, \quad A_k(B) = \begin{cases} 1 \\ \mathbb{Z}^3 \times \mathbb{Z}_2 \\ \mathbb{Z}^3 \times \mathbb{Z}_2^4 \\ 1 \end{cases}, \quad A_k(\underline{B}) = \begin{cases} 1 & k=3 \\ \mathbb{Z} \times \mathbb{Z}_4 & k=2 \\ \mathbb{Z} \times \mathbb{Z}_2^2 & k=1 \\ 1 & k=0 \end{cases}. \quad (2.13)$$

Since all three toric varieties have at most orbifold singularities, the Hodge numbers are $h^{p,p} = \text{rank } A_p$ and $h^{p,q} = 0$ if $p \neq q$.

The appearance of torsion in the Chow group slightly complicates the Cox homogeneous coordinate [25] construction of the toric varieties, so let me spell out the details. In general, a simplicial (that is, with at most orbifold singularities) d -dimensional toric variety X can be written as a geometric quotient

$$X = \frac{\mathbb{C}^{\Sigma_X^{(1)}} - Z}{\text{Hom}(A_{d-1}(X), \mathbb{C}^\times)} \simeq \frac{\mathbb{C}^r - Z}{(\mathbb{C}^*)^{d-r} \times A_{d-1}(X)_{\text{tors}}}, \quad (2.14)$$

where r is the number of rays in the fan Σ_X . The exceptional set Z is the variety defined by the irrelevant ideal. A more catchy way of remembering Z is that it forbids homogeneous

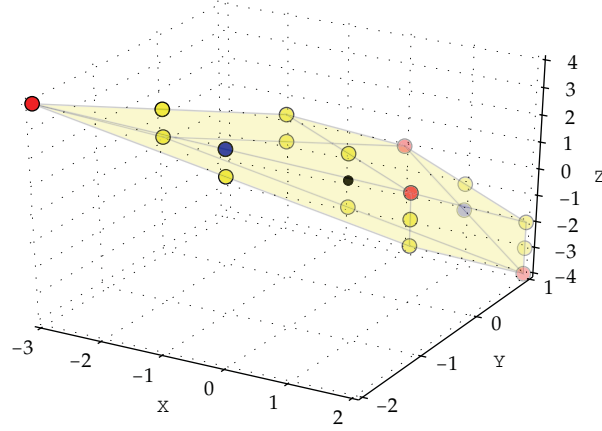


Figure 2: The rays $\Sigma_{\bar{B}}^{(1)}$.

coordinates from vanishing simultaneously if and only if their product is a monomial in the Stanley-Reisner ideal. The latter is

$$\begin{aligned} \text{SR}(\Sigma_B) &= \langle z_0 z_1 z_2 z_3 \rangle, \\ \text{SR}(\Sigma_B) &= \langle z_0 z_2, z_1 z_3, z_4 z_5 \rangle, \\ \text{SR}(\Sigma_{\bar{B}}) &= \langle \cdots 105 \text{ quadric monomials} \cdots \rangle. \end{aligned} \quad (2.15)$$

It remains to describe the groups in the denominator of (2.14). For the most singular variety \underline{B} , one finds

$$\begin{aligned} [z_0 : z_1 : z_2 : z_3] &= [\lambda z_0 : \lambda z_1 : \lambda z_2 : \lambda z_3] \quad \forall \lambda \in \mathbb{C}^\times, \\ [z_0 : z_1 : z_2 : z_3] &= [z_0 : \mu z_1 : \mu^2 z_2 : \mu^3 z_3] \quad \forall \mu \in \{1, i, i^2, i^3\} \simeq \mathbb{Z}_4 \end{aligned} \quad (2.16)$$

and for the intermediate blow-up B

$$\begin{aligned} [z_0 : z_1 : z_2 : z_3 : z_4 : z_5] &= [\lambda z_0 : \lambda z_1 : \lambda z_2 : \lambda z_3 : z_4 : z_5] \quad \forall \lambda \in \mathbb{C}^\times, \\ [z_0 : z_1 : z_2 : z_3 : z_4 : z_5] &= [\lambda z_0 : z_1 : \lambda z_2 : z_3 : \lambda^{-2} z_4 : z_5] \quad \forall \lambda \in \mathbb{C}^\times, \\ [z_0 : z_1 : z_2 : z_3 : z_4 : z_5] &= [z_0 : z_1 : z_2 : z_3 : \lambda z_4 : \lambda z_5] \quad \forall \lambda \in \mathbb{C}^\times, \\ [z_0 : z_1 : z_2 : z_3 : z_4 : z_5] &= [\mu z_0 : \mu z_1 : z_2 : z_3 : \mu z_4 : z_5] \quad \forall \mu \in \{1, -1\} \simeq \mathbb{Z}_2. \end{aligned} \quad (2.17)$$

2.5. A Nonsimply Connected Divisor

I am now going to define a divisor $\underline{D} \subset \underline{B}$ in the same linear system as the toric divisor $(V(\underline{z}_i))$ denotes the toric divisor $\{\underline{z}_i = 0\}$ associated to the i -th ray

$$\underline{D} \sim 4V(\underline{z}_0), \quad (2.18)$$

that is, as the zero set of a sufficiently generic section of the line bundle $\mathcal{O}(\underline{D}) = \mathcal{O}(V(\underline{z}_0))^4$. (By \sim , we will always denote rational equivalence of divisors. That is, $D_1 \sim D_2$ means that there is a one-parameter family of divisors interpolating between D_1 and D_2 . Equivalently, the Chow cycle defined by D_1 and D_2 is the same.) A basis for the sections is

$$H^0(\underline{B}, \mathcal{O}(\underline{D})) = \left\langle \underline{z}_0^4, \underline{z}_2^4, \underline{z}_1^4, \underline{z}_3^4, \underline{z}_1 \underline{z}_2^2 \underline{z}_3, \underline{z}_1^2 \underline{z}_3^2, \underline{z}_0 \underline{z}_2 \underline{z}_3^2, \underline{z}_0 \underline{z}_1^2 \underline{z}_2, \underline{z}_0^2 \underline{z}_2^2, \underline{z}_0^2 \underline{z}_1 \underline{z}_3 \right\rangle, \quad (2.19)$$

corresponding to the points of the polytope

$$P_{\underline{D}} = \text{conv}\{(0, 0, 0), (4, 0, 2), (0, 4, 1), (0, 0, -1)\} \subset M. \quad (2.20)$$

Note that the fan $\Sigma_{\underline{B}}$ is precisely the normal fan of the Newton polytope $P_{\underline{D}}$. In this sense, \underline{B} is the “natural” ambient toric variety for the surface \underline{D} .

For explicitness, let me fix once and for all a linear combination of the monomials as the defining equation of the divisor \underline{D} . I will select the vertices of the Newton polytope and define

$$\underline{D} = \left\{ \underline{z}_0^4 + \underline{z}_1^4 + \underline{z}_2^4 + \underline{z}_3^4 = 0 \right\} \subset \underline{B}. \quad (2.21)$$

This surface is known to be an Enriques surface since it projects out the potential $(2, 0)$ -form as mentioned in Section 2.1. In fact, this example has been known for some time, see Remark 3.6 in [27].

2.6. Kähler Cone and Canonical Divisors

The content of this subsection is not necessary for the understanding of the paper, but I would like to pause for a moment and mention how the “Fermat quartic” in (2.21) fails to define a K3 surface. In other words, how does the divisor $\underline{D} = 4V(\underline{z}_0)$ differ from the anticanonical divisor

$$-K_{\underline{B}} = V(\underline{z}_0) + V(\underline{z}_1) + V(\underline{z}_2) + V(\underline{z}_3) \quad (2.22)$$

of \underline{B} ? Comparing with \mathbb{P}^3 , see (2.8), one might have thought that they were linearly equivalent.

Similarly to the quartic K3 $\subset \mathbb{P}^3$, one can also define a Calabi-Yau variety in \underline{B} as the zero locus of a section of the anticanonical bundle (after resolution of singularities,

the anticanonical divisor will be a smooth 2-dimensional Calabi-Yau manifold, that is, again a K3 surface). The available sections are

$$H^0(\underline{B}, \mathcal{O}(-K_{\underline{B}})) = \langle z_0^2 z_3^2, z_0^3 z_2, z_2^2 z_3^2, z_0 z_2^3, z_1 z_3^3, z_0 z_1 z_2 z_3, z_0^2 z_1^2, z_1^2 z_2^2, z_1^3 z_3 \rangle. \quad (2.23)$$

Note that this differs from the sections of \underline{D} , see (2.19). Therefore, the two divisors are *not* linearly equivalent. Nevertheless, $-K_{\underline{B}}$ and \underline{D} are very close to being linearly equivalent. In fact, it is easy to see that they are in the same rational divisor class since the rational divisor class group is one-dimensional, $\dim(A_2(\underline{B}) \otimes_{\mathbb{Z}} \mathbb{R}) = 1$. (The toric divisor class group of a variety X is often written as $Cl(X)$. I will not use this notation in the following, but opt for $A_{\dim(X)-1}(X)$ instead.) However, their difference is a 2-torsion element in the (integral) divisor class

$$K_{\underline{B}} + \underline{D} \neq 0, \quad 2(K_{\underline{B}} + \underline{D}) = 0 \in A_2(\underline{B}) \simeq \mathbb{Z} \oplus \mathbb{Z}_4. \quad (2.24)$$

The same is true on the crepant partial resolution, where $K_B + D$ is again a 2-torsion element in $A_2(B)$.

On the final smooth resolution \widehat{B} the divisor class group $A_2(\widehat{B}) = \mathbb{Z}^{15}$ is torsion-free. However, the last blow-up $\widehat{\pi} : \widehat{B} \rightarrow B$ is not crepant, so

$$\widehat{\pi}^*(K_B) \neq K_{\widehat{B}}. \quad (2.25)$$

Therefore, the divisors $-K_{\widehat{B}}$ and $\widehat{D} = \widehat{\pi}^*(D)$ are no longer in the same rational equivalence class.

Finally, let me describe the Kähler cones of these varieties. First, let me remind the reader that the Kähler cone of a toric variety is an open rational polyhedral cone in the rational divisor class group corresponding to the cone of convex piecewise linear support functions on the fan. For the two singular varieties, one obtains

$$\begin{aligned} \mathcal{K}(\underline{B}) &= \langle V(z_0) \rangle \subset A_2(\underline{B}) \otimes_{\mathbb{Z}} \mathbb{R} \simeq \mathbb{R} \\ \mathcal{K}(B) &= \langle V(z_0), V(z_1), 2V(z_0) + V(z_4) \rangle \subset A_2(B) \otimes_{\mathbb{Z}} \mathbb{R} \simeq \mathbb{R}^3. \end{aligned} \quad (2.26)$$

As the anticanonical class $-K_{\underline{B}}$ is rationally equivalent to $4V(z_0)$, we see the following.

- (i) \underline{B} is a (singular) Fano variety.
- (ii) B is not Fano, but the anticanonical class is on the boundary of the Kähler cone. In other words, $-K_B$ is nef but not ample.

On the smooth blow-up \widehat{B} , the Kähler cone

$$\mathcal{K}(\widehat{B}) \subset A_2(\widehat{B}) \otimes_{\mathbb{Z}} \mathbb{R} \simeq \mathbb{R}^{15} \quad (2.27)$$

is rather complicated, and we will refrain from listing it explicitly. It is spanned by the origin and 169 rays and has 20 facets (that is, 14-dimensional faces). The anticanonical divisor $-K_{\widehat{B}}$

as well as \widehat{D} sits on the boundary of the Kähler cone, that is, is nef but not ample. However, each satisfies a different subset of 16 out of the 20 facet equations, so they lie on different faces of the Kähler cone.

2.7. Pull-Back Divisors

By the usual dictionary of toric geometry, the toric divisor $4V(z_0) \sim D$ corresponds to a continuous piecewise linear function on $N_{\mathbb{R}} \simeq \mathbb{R}^3$. Explicitly, the function is

$$f(n_x, n_y, n_z) = \begin{cases} n_z & \text{if } \vec{n} \in \langle 0, 1, 2 \rangle, \\ -4n_x - 2n_z & \text{if } \vec{n} \in \langle 0, 1, 3 \rangle, \\ -4n_y - n_z & \text{if } \vec{n} \in \langle 0, 2, 3 \rangle, \\ 0 & \text{if } \vec{n} \in \langle 1, 2, 3 \rangle. \end{cases} \quad (2.28)$$

The pull-back of this toric divisor by the toric morphisms $\underline{\pi}$ and $\underline{\pi} \circ \widehat{\pi}$ is simply given by the pull-back of the piecewise linear function. Therefore,

$$\begin{aligned} \underline{D} &\sim 4V(z_0), \\ D &\sim 4V(z_0) + 2V(z_4), \\ \widehat{D} &\sim 4V(\widehat{z}_0) + 2V(\widehat{z}_4) + 4V(\widehat{z}_6) + 3V(\widehat{z}_7) + 3V(\widehat{z}_8) + 2V(\widehat{z}_9) \\ &\quad + 2V(\widehat{z}_{10}) + 2V(\widehat{z}_{11}) + V(\widehat{z}_{12}) + 2V(\widehat{z}_{13}) + V(\widehat{z}_{14}). \end{aligned} \quad (2.29)$$

What is the exceptional set of the first blow-up $\underline{\pi}$? Recall that it corresponds to the subdivisions along the 2-cones

$$\langle 0, 4 \rangle \cup \langle 2, 4 \rangle \longrightarrow \langle 0, 2 \rangle, \quad \langle 1, 5 \rangle \cup \langle 3, 5 \rangle \longrightarrow \langle 1, 3 \rangle, \quad (2.30)$$

see Figure 1. Therefore, $\underline{\pi}$ is the blow-up along two disjoint rational curves of \mathbb{Z}_2 -singularities in \underline{B} . A standard intersection computation in the Chow group [26] yields that each curve intersects the divisor \underline{D} in two points. Therefore, the proper transform of $D \subset B$ is \underline{D} blown up in four points. The final blow-up $\widehat{\pi} : \widehat{B} \rightarrow B$ does not further subdivide the 2-skeleton $\Sigma_B^{(2)}$ and, therefore, corresponds to the blow-up of points in B . Any sufficiently generic divisor D misses these blow-up points, and, therefore, the surfaces D and \widehat{D} are isomorphic. To summarize,

- (i) \underline{D} is a singular Enriques surface with four \mathbb{Z}_2 -orbifold points;
- (ii) \widehat{D} and D are the same smooth Enriques surface after blowing up the orbifold points;
- (iii) Since the blow-up at a point does not change the fundamental group, we find that

$$\pi_1(\underline{D}) = \pi_1(D) = \pi_1(\widehat{D}) = \mathbb{Z}_2. \quad (2.31)$$

It is important to remember that the actual divisor is a fixed subvariety defined as the zero locus of an equation. To relate this defining equation before and after the blow-up, it is

instructional to write the first blow-up map $\underline{\pi} : B \rightarrow \underline{B}$ explicitly in terms of its action on homogeneous coordinates. One finds

$$\underline{\pi}([z_0 : z_1 : z_2 : z_3 : z_4 : z_5]) = [z_0\sqrt{z_4} : z_1\sqrt{z_5} : z_2\sqrt{z_4} : z_3\sqrt{z_5}]. \quad (2.32)$$

Note that this map is well defined on the equivalence classes (2.17) thanks to the identifications (2.16). One sees that, for example, the section \underline{z}_0^4 corresponds to the section $z_0^4 z_4^2$ under the $\underline{\pi}^*$ pull-back. I leave the analogous expression for $\hat{\pi}$ as an exercise to the reader.

To summarize, the equation for the divisor \underline{D} determines the equation satisfied by the proper transforms D and \hat{D} on the blow-ups. They are

$$\begin{aligned} \underline{D} &= \{z_0^4 + z_1^4 + z_2^4 + z_3^4 = 0\}, \\ D &= \{z_0^4 z_4^2 + z_1^4 z_5^2 + z_2^4 z_4^2 + z_3^4 z_5^2 = 0\}, \\ \hat{D} &= \left\{ \hat{z}_0^4 \hat{z}_4^2 \hat{z}_6^4 \hat{z}_7^3 \hat{z}_8^3 \hat{z}_9^2 \hat{z}_{10}^2 \hat{z}_{11}^2 \hat{z}_{12}^2 \hat{z}_{13}^2 \hat{z}_{14} + \hat{z}_1^4 \hat{z}_5^2 \hat{z}_6^2 \hat{z}_7^3 \hat{z}_9^4 \hat{z}_{10}^4 \hat{z}_{11}^2 \hat{z}_{12}^2 \hat{z}_{15}^3 \hat{z}_{16}^2 \hat{z}_{17}^2 \right. \\ &\quad \left. + \hat{z}_2^4 \hat{z}_4^2 \hat{z}_7 \hat{z}_8 \hat{z}_{10}^2 \hat{z}_{12}^3 \hat{z}_{13}^2 \hat{z}_{14}^2 \hat{z}_{15}^2 \hat{z}_{16}^2 \hat{z}_{17}^4 + \hat{z}_3^4 \hat{z}_5^2 \hat{z}_6^2 \hat{z}_8^2 \hat{z}_9 \hat{z}_{11}^3 \hat{z}_{13}^4 \hat{z}_{14}^2 \hat{z}_{15}^3 \hat{z}_{16}^3 \hat{z}_{17}^2 = 0 \right\}. \end{aligned} \quad (2.33)$$

3. Elliptic Fibration

So far, I have constructed

- (i) a three-dimensional (singular) Fano variety \underline{B} ,
- (ii) a quasismooth divisor \underline{D} in \underline{B} with $\pi_1(\underline{D}) = \mathbb{Z}_2$,
- (iii) a smooth three-dimensional toric variety \hat{B} , corresponding to a maximal subdivision of a reflexive polytope,
- (iv) a smooth divisor \hat{D} in \hat{B} with $\pi_1(\hat{D}) = \mathbb{Z}_2$. This divisor is a smooth Enriques surface.

I will now proceed and construct four-dimensional elliptically fibered Calabi-Yau varieties \underline{Y} , \hat{Y} over \underline{B} and \hat{B} whose discriminant contains \underline{D} and \hat{D} , respectively.

3.1. Weierstrass Models

Ideally, one would like to classify all elliptic fibrations over the base manifold. Unfortunately it is not known how to do so in this generality. It is known, however, that there exists a Weierstrass model (not necessarily over the same base) which is a (in general) different elliptic fibration [28, 29], at least assuming that the base is smooth and the discriminant is a normal crossing divisor. The Weierstrass model and the original elliptic fibration are birational to each other, but apart from that their relationship is arduous at best.

Having said this, let us define the elliptically fibered variety Y in the most unimaginative way possible as a (global) Calabi-Yau Weierstrass model

$$Y = \left\{ y^2 z = x^3 + f(\vec{\xi}) x z^2 + g(\vec{\xi}) z^3 \right\} \subset \mathbb{P}(\mathcal{O} \oplus \mathcal{O}(-2K_Z) \oplus \mathcal{O}(-3K_Z)), \quad (3.1)$$

on a base variety Z with coordinates ζ . The remaining coordinates, z , x , and y , are sections

$$z \in \Gamma\mathcal{O}, \quad x \in \Gamma\mathcal{O}(-2K_Z), \quad y \in \Gamma\mathcal{O}(-3K_Z). \quad (3.2)$$

The defining data of the Weierstrass model is the choice of coefficients in the Weierstrass equation, that is, the choice of sections

$$f \in \Gamma\mathcal{O}(-4K_Z), \quad g \in \Gamma\mathcal{O}(-6K_Z). \quad (3.3)$$

To engineer gauge theories on 7-branes wrapped on a divisor $\{\zeta = 0\} \subset Z$, one needs suitable singularities. In addition, the singularity must be of the correct split or nonsplit type as in Tate's algorithm [30]. For this purpose it is convenient to parametrize the Weierstrass (technically, the singularity appears after blowing down all fiber components of the Weierstrass model not intersecting the zero section, but we will not dwell on this) model by polynomials (that is, sections of suitable line bundles) a_1, a_2, a_3, a_4, a_6 as

$$\begin{aligned} f &= -\frac{1}{48}a_1^4 - \frac{1}{6}a_1^2a_2 + \frac{1}{2}a_1a_3 - \frac{1}{3}a_2^2 + a_4 \\ g &= \frac{1}{864}a_1^6 + \frac{1}{72}a_1^4a_2 - \frac{1}{24}a_1^3a_3 + \frac{1}{18}a_1^2a_2^2 - \frac{1}{12}a_1^2a_4 \\ &\quad - \frac{1}{6}a_1a_2a_3 + \frac{2}{27}a_2^3 - \frac{1}{3}a_2a_4 + \frac{1}{4}a_3^2 + a_6. \end{aligned} \quad (3.4)$$

The degree of vanishing of the $a_\ell(\zeta)$ then determines (except for a few special cases that will be of no relevance for us) the low-energy effective gauge theory, see [31, 32]. For everything to be globally defined, the a_ℓ need to be sections of

$$a_\ell \in \Gamma\mathcal{O}(-\ell K_Z). \quad (3.5)$$

3.2. Weierstrass Model on the Singular Base

To engineer a $SU(5)$ gauge theory coming from a 7-brane wrapped on the divisor \underline{D} , one needs a split A_4 singularity [31]. This translates into a_ℓ vanishing to degree $\ell - 1$ on \underline{D} . In other words, a_ℓ must be divisible by $\underline{d}^{\ell-1} = 0$, where \underline{d} is the defining equation for the divisor \underline{D} as given in (2.33). Put yet differently,

$$\frac{a_\ell}{\underline{d}^{\ell-1}} \in \Gamma\mathcal{O}(-\ell K_{\underline{B}} - (\ell - 1)\underline{D}). \quad (3.6)$$

The number of sections is tabulated in Table 2. Note how the rows repeat with periodicity 2. This again follows from the fact that $K_{\underline{B}}$ and \underline{D} differ by 2-torsion in the divisor class group, see (2.24). Hence, there are plenty sections available for a_1, \dots, a_6 , and one can easily find an elliptic fibration with a split A_4 over \underline{D} .

Table 2: Number of sections of $\mathcal{O}(-\kappa K_{\underline{B}} - \delta \underline{D})$.

$\dim \Gamma \mathcal{O}(-\kappa K_{\underline{B}} - \delta \underline{D})$	$\kappa = 1$	$\kappa = 2$	$\kappa = 3$	$\kappa = 4$	$\kappa = 5$	$\kappa = 6$
$\delta = 0$	9	43	115	245	445	735
$\delta = 1$	0	10	42	116	244	446
$\delta = 2$	0	1	9	43	115	245
$\delta = 3$	0	0	0	10	42	116
$\delta = 4$	0	0	0	1	9	43
$\delta = 5$	0	0	0	0	0	10
$\delta = 6$	0	0	0	0	0	1
$\delta \geq 7$	0	0	0	0	0	0

Table 3: Number of sections of $\mathcal{O}(-\kappa K_{\hat{B}} - \delta \hat{D})$, see also Figure 2.

$\dim \Gamma \mathcal{O}(-\kappa K_{\hat{B}} - \delta \hat{D})$	$\kappa = 1$	$\kappa = 2$	$\kappa = 3$	$\kappa = 4$	$\kappa = 5$	$\kappa = 6$
$\delta = 0$	9	35	91	189	341	559
$\delta = 1$	0	2	18	60	140	270
$\delta = 2$	0	0	0	3	27	85
$\delta = 3$	0	0	0	0	0	4
$\delta \geq 4$	0	0	0	0	0	0

3.3. Weierstrass Model on the Smooth Base

Let me now turn to the smooth threefold \hat{B} and construct a suitable singularity over the smooth divisor \hat{D} . The main difference is that now, after resolving the singularity, the anticanonical divisor is “smaller” than \hat{D} , by which I mean that there are strictly less sections available for the Weierstrass model. See Figure 3 for details. Note that, if one always imposes the maximal degree of vanishing such that there are still nonzero sections, one can at most implement a split A_2 singularity leading to a low-energy $SU(3)$ gauge theory.

Having being dealt this lemon, let me try to make some lemonade. As in the previous subsection, I will write $\hat{D} = \{\hat{d} = 0\}$ for the defining equation, see (2.33). The split A_2 singularity corresponds to a factorized form

$$\begin{aligned}
a_1 &= \alpha_1 & \alpha_1 &\in \Gamma \mathcal{O}(-K_{\hat{B}}), \\
a_2 &= \hat{d} \alpha_2 & \alpha_2 &\in \Gamma \mathcal{O}(-2K_{\hat{B}} - \hat{D}), \\
a_3 &= \hat{d}^2 \alpha_3 & \alpha_3 &\in \Gamma \mathcal{O}(-3K_{\hat{B}} - \hat{D}), \\
a_4 &= \hat{d}^3 \alpha_4 & \alpha_4 &\in \Gamma \mathcal{O}(-4K_{\hat{B}} - 2\hat{D}), \\
a_6 &= \hat{d}^3 \alpha_6 & \alpha_6 &\in \Gamma \mathcal{O}(-6K_{\hat{B}} - 3\hat{D}).
\end{aligned} \tag{3.7}$$

A basis for all sections can, of course, be written as in terms of homogeneous monomials in the 18 homogeneous coordinates $\hat{z}_0, \dots, \hat{z}_{17}$. To save a tree I will now switch to inhomogeneous

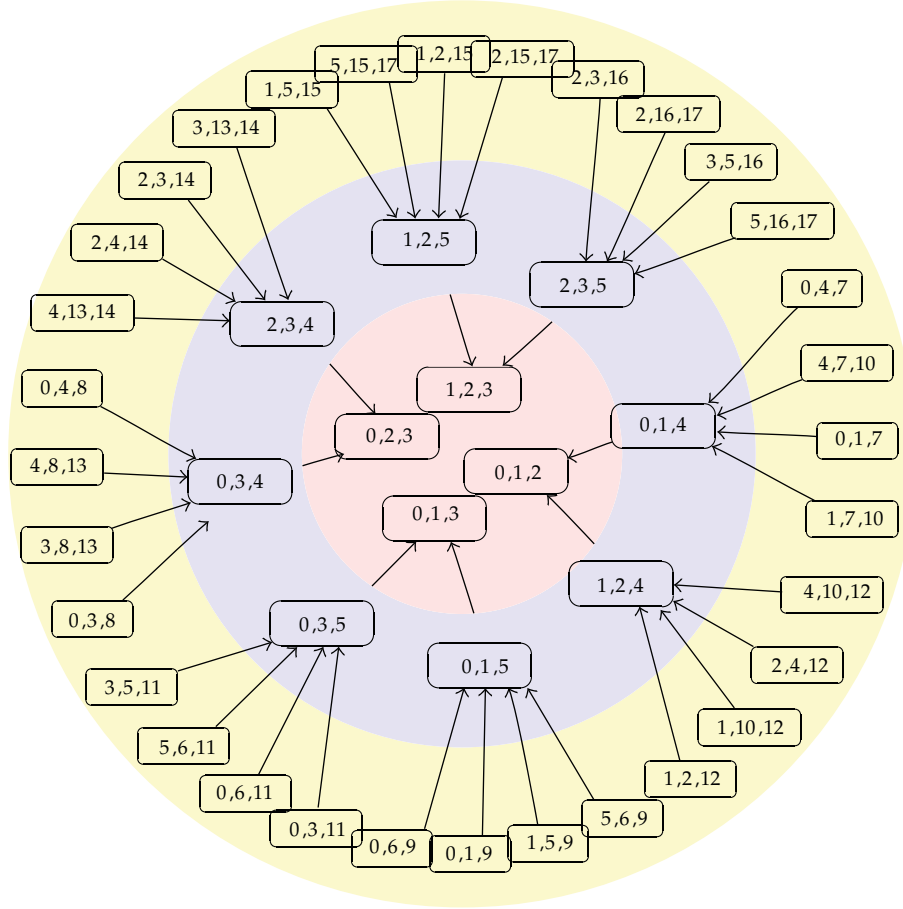


Figure 3: The generating cones of the fan $\Sigma_{\tilde{B}}$ (yellow, outer circle), Σ_B (blue), and Σ_B (red, inner circle). By (i, j, k) we denote the cone spanned by the rays number i, j , and k in 1, and arrows mean “contained in.”

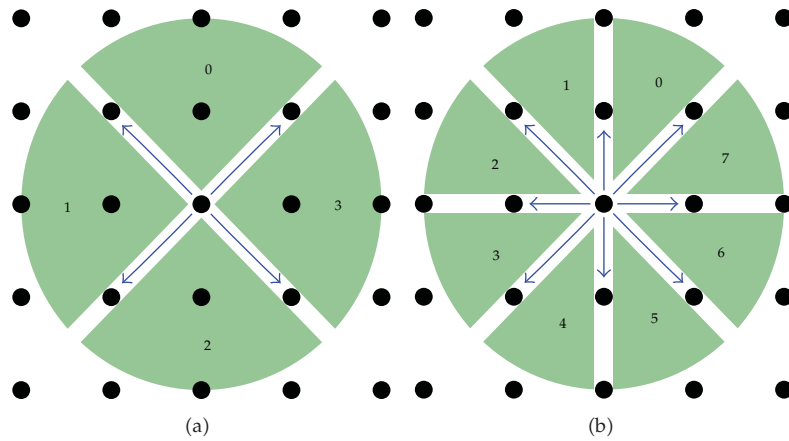


Figure 4: The fan defining the toric variety $S = (\mathbb{P}^1 \times \mathbb{P}^1)/\mathbb{Z}_2$ (a) and its crepant smooth resolution \hat{S} (b).

coordinates $(\xi_0, \xi_1, \xi_2) \in \mathbb{C}^3$ for the coordinate patch, say, corresponding to the cone $\langle 0, 4, 7 \rangle$. This amounts to replacing the homogeneous coordinates with

$$[\widehat{z}_0 : \widehat{z}_1 : \cdots : \widehat{z}_{17}] = [\xi_0 : 1 : 1 : 1 : \xi_1 : 1 : 1 : \xi_2 : 1 : \cdots : 1]. \quad (3.8)$$

In this patch,

$$\widehat{d} = \xi_0^4 \xi_1^2 \xi_2^3 + \xi_1^2 \xi_2 + \xi_2^2 + 1, \quad (3.9)$$

and the sections of the relevant line bundles are

$$\begin{aligned} \Gamma\mathcal{O}(-K_{\widehat{B}}) &= \left\langle 1, \xi_1, \xi_2, \xi_0 \xi_1^2 \xi_2, \xi_1 \xi_2, \xi_0^2 \xi_1 \xi_2, \xi_0^2 \xi_1 \xi_2^2, \xi_0^3 \xi_1^2 \xi_2^2, \xi_0 \xi_1 \xi_2 \right\rangle, \\ \Gamma\mathcal{O}(-2K_{\widehat{B}} - \widehat{D}) &= \left\langle 1, \xi_0^2 \xi_1^2 \xi_2 \right\rangle, \\ \Gamma\mathcal{O}(-3K_{\widehat{B}} - \widehat{D}) &= \left\langle 1, \xi_1, \xi_2, \xi_1 \xi_2, \xi_0^2 \xi_1^3 \xi_2, \xi_0^3 \xi_1^4 \xi_2^2, \xi_0^2 \xi_1^3 \xi_2^2, \xi_0^2 \xi_1 \xi_2, \xi_0^2 \xi_1^2 \xi_2, \xi_0^4 \xi_1^3 \xi_2^2, \right. \\ &\quad \left. \xi_0^4 \xi_1^3 \xi_2^3, \xi_0^5 \xi_1^4 \xi_2^3, \xi_0 \xi_1^2 \xi_2, \xi_0^2 \xi_1^2 \xi_2^2, \xi_0^3 \xi_1^3 \xi_2^2, \xi_0 \xi_1 \xi_2, \xi_0^2 \xi_1^2 \xi_2, \xi_0^3 \xi_1^2 \xi_2^2 \right\rangle, \\ \Gamma\mathcal{O}(-4K_{\widehat{B}} - 2\widehat{D}) &= \left\langle 1, \xi_0^4 \xi_1^4 \xi_2^2, \xi_0^2 \xi_1^2 \xi_2 \right\rangle, \\ \Gamma\mathcal{O}(-6K_{\widehat{B}} - 3\widehat{D}) &= \left\langle 1, \xi_0^6 \xi_1^6 \xi_2^3, \xi_0^2 \xi_1^2 \xi_2, \xi_0^4 \xi_1^4 \xi_2^2 \right\rangle. \end{aligned} \quad (3.10)$$

For simplicity I will choose α_ν to be the sum of the monomials corresponding to the vertices of the Newton polyhedron, that is,

$$\begin{aligned} \alpha_1 &= \xi_0^3 \xi_1^2 \xi_2^2 + \xi_0^2 \xi_1 \xi_2^2 + \xi_0^2 \xi_1 \xi_2 + \xi_0 \xi_1^2 \xi_2 + \xi_1 \xi_2 + \xi_1 + \xi_2 + 1, \\ \alpha_2 &= \xi_0^2 \xi_1^2 \xi_2 + 1, \\ \alpha_3 &= \xi_0^5 \xi_1^4 \xi_2^3 + \xi_0^4 \xi_1^3 \xi_2^3 + \xi_0^4 \xi_1^3 \xi_2^2 + \xi_0^3 \xi_1^4 \xi_2^2 + \xi_0^2 \xi_1^3 \xi_2^2 \\ &\quad + \xi_0^2 \xi_1^3 \xi_2 + \xi_0^2 \xi_1 \xi_2^2 + \xi_0^2 \xi_1 \xi_2 + \xi_1 \xi_2 + \xi_1 + \xi_2 + 1, \\ \alpha_4 &= \xi_0^4 \xi_1^4 \xi_2^2 + 1, \\ \alpha_6 &= \xi_0^6 \xi_1^6 \xi_2^3 + 1. \end{aligned} \quad (3.11)$$

For all purposes in the following, this choice is generic. By construction, the discriminant then factorizes as

$$\Delta = 4f^3 + 27g^2 = \widehat{d}^3 \widehat{r}, \quad (3.12)$$

where the remainder (in fact, \hat{r} is a polynomial consisting of 1083 monomials in ξ_0 , ξ_1 , and ξ_2) defines a new divisor $\hat{R} \stackrel{\text{def}}{=} \{\hat{r} = 0\} \sim -12K_{\hat{B}} - 3\hat{D}$. In particular, the homology class splits as

$$[\Delta] = 3[\hat{D}] + [\hat{R}]. \quad (3.13)$$

Using the explicit equations, one can check [18] that

- (i) \hat{R} is an irreducible divisor;
- (ii) Neither f nor g vanishes at a generic point of \hat{R} . Hence it supports I_0 Kodaira fibers in the Weierstrass model;
- (iii) \hat{D} is smooth;
- (iv) \hat{R} is not smooth, for example, $(\xi_0, \xi_1, \xi_2) = (1, 1, -1)$ is a singular point;
- (v) The curve $\hat{D} \cap \hat{R}$ is not a complete intersection.

Let me further investigate the intersection curve $\hat{D} \cap \hat{R}$. One component (in the $\langle 0, 4, 7 \rangle$ patch) is given by the surprisingly simple expression

$$c : \mathbb{C} \longrightarrow \hat{D} \cap \hat{R}, \quad t \longmapsto (t, 0, i). \quad (3.14)$$

Therefore, (ξ_1, ξ_2) are good normal coordinates. Taylor expanding along the normal directions for a generic point $c(t)$, we see that \hat{D} and \hat{R} share the same tangent plane but do not osculate to any higher degree. Therefore, the degree of vanishing of the discriminant jumps from 5 to 7 along the intersection locus $\hat{D} \cap \hat{R}$, corresponding to worsening of the A_2 singularity to an A_4 singularity.

4. Conclusions

In this paper I have constructed F-theory models with, a priori, SU(5) gauge theory on a singular Fano threefold and a SU(3) gauge theory on the blown-up smooth threefold. In both cases the non-Abelian gauge theory comes from a 7-brane wrapped on an Enriques surface, which has fundamental group \mathbb{Z}_2 . Therefore, in both cases one can switch on a discrete Wilson line and break the gauge group below the compactification scale in the usual manner.

The fact that the only partially resolved base B allows for a higher rank gauge group on the 7-brane than its smooth blow-up is curious: one might be tempted to interpret the Kähler deformation as the usual Higgs mechanism; however the singular points are disjoint from the 7-brane. In any case, there must be further physical degrees of freedom associated to the singularities in the base, and it would be nice to have a more concise F-theory dictionary for them.

Appendix

A. Fibrations of the Base

The base manifolds \underline{B} , B , and \widehat{B} are fibered in an interesting manner which I will describe in this appendix. The map to the 2-dimensional base is given by the N -lattice projection

$$\phi : N^{(3)} \longrightarrow N^{(2)}, \quad \vec{n} \longmapsto \begin{pmatrix} 1 & 1 & 1 \\ -1 & 1 & 0 \end{pmatrix} \vec{n}. \quad (\text{A.1})$$

This defines a toric morphism of toric varieties if and only if every cone of the domain fan is mapped into a cone of the range fan. It is easy to see that the rays $\Sigma_{\underline{B}}^{(1)}$ and $\Sigma_B^{(1)}$ map to the rays of the fan of $S = (\mathbb{P}^1 \times \mathbb{P}^1)/\mathbb{Z}_2$, and the rays $\Sigma_{\widehat{B}}^{(1)}$ map to the crepant resolution \widehat{S} . See Figure 4 for a graphical representation of the fans of S and \widehat{S} .

However, consistently mapping the rays of the fans is not enough to define a toric morphism. Checking all higher-dimensional cones with respect to the lattice homomorphism ϕ , one finds that

- (i) the variety \underline{B} is not fibered;
- (ii) the variety B is a \mathbb{P}^1 -fibrations over S ;
- (iii) the smooth threefold \widehat{B} is a \mathbb{P}^1 -fibration over S , but not over the crepant resolution \widehat{S} .

It is, perhaps, vexing that the resolved threefold \widehat{B} is not a fibration over the resolved base \widehat{S} . However, a closer investigation reveals that one can flop 4 offending curves, corresponding to the 4 bistellar flips

$$\begin{aligned} \{\langle 1, 2, 15 \rangle, \langle 1, 2, 12 \rangle\} &\longmapsto \{\langle 1, 12, 15 \rangle, \langle 2, 12, 15 \rangle\} \\ \{\langle 0, 1, 9 \rangle, \langle 0, 1, 7 \rangle\} &\longmapsto \{\langle 0, 7, 9 \rangle, \langle 1, 7, 9 \rangle\} \\ \{\langle 0, 3, 11 \rangle, \langle 0, 3, 8 \rangle\} &\longmapsto \{\langle 0, 8, 11 \rangle, \langle 3, 8, 11 \rangle\} \\ \{\langle 2, 3, 16 \rangle, \langle 2, 3, 14 \rangle\} &\longmapsto \{\langle 2, 14, 16 \rangle, \langle 3, 14, 16 \rangle\} \end{aligned} \quad (\text{A.2})$$

of the fan $\Sigma_{\widehat{B}}$. The flopped threefold is then a \mathbb{P}^1 fibration over the resolved base \widehat{S} . Of course the flopped threefold is then only birational to B , \underline{B} and no longer a direct blow-up. However, it supports essentially the same elliptic fibration as \widehat{B} as constructed in 3.

References

- [1] C. Vafa, "Evidence for F -theory," *Nuclear Physics B*, vol. 469, no. 3, pp. 403–415, 1996.
- [2] A. Sen, " F -theory and orientifolds," *Nuclear Physics B*, vol. 475, no. 3, pp. 562–578, 1996.
- [3] C. Beasley, J. J. Heckman, and C. Vafa, "GUTs and exceptional branes in F -theory. I," *Journal of High Energy Physics*, vol. 2009, no. 1, article 058, 2009.
- [4] C. Beasley, J. J. Heckman, and C. Vafa, "GUTs and exceptional branes in F -theory. II. Experimental predictions," *Journal of High Energy Physics*, vol. 2009, no. 1, article 059, 2009.
- [5] R. Donagi and M. Wijnholt, "Model building with F -theory," <http://arxiv.org/abs/0802.2969>.

- [6] J. Marsano, N. Saulina, and S. Schäfer-Nameki, “F-theory compactifications for supersymmetric GUTs,” *Journal of High Energy Physics*, vol. 2009, no. 8, article 030, 2009.
- [7] R. Blumenhagen, T. W. Grimm, B. Jurke, and T. Weigand, “Global F-theory GUTs,” *Nuclear Physics B*, vol. 829, no. 1-2, pp. 325–369, 2010.
- [8] C. M. Chen, J. Knapp, M. Kreuzer, and C. Mayrhofer, “Global SO(10) F-theory guts,” *Journal of High Energy Physics*, vol. 2010, no. 10, article 057, 2010.
- [9] C.-M. Chen and Y.-C. Chung, “Flipped SU(5) GUTs from E_8 Singularity in F-theory,” *Journal of High Energy Physics*, vol. 2001, no. 3, article 49, 2011.
- [10] R. Blumenhagen, “Basics of F-theory from the type IIB perspective,” *Fortschritte der Physik*, vol. 58, no. 7-9, pp. 820–826, 2010.
- [11] Y. Hosotani, “Dynamical mass generation by compact extra dimensions,” *Physics Letters B*, vol. 126, no. 5, pp. 309–313, 1983.
- [12] Y. Hosotani, “Dynamics of nonintegrable phases and gauge symmetry breaking,” *Annals of Physics*, vol. 190, no. 2, pp. 233–253, 1989.
- [13] R. Blumenhagen, V. Braun, T. W. Grimm, and T. Weigand, “GUTs in type IIB orientifold compactifications,” *Nuclear Physics B*, vol. 815, no. 1-2, pp. 1–94, 2009.
- [14] R. Donagi and M. Wijnholt, “Breaking GUT groups in F-theory,” <http://arxiv.org/abs/0808.2223>.
- [15] R. Blumenhagen, “Gauge coupling unification in F-theory grand unified theories,” *Physical Review Letters*, vol. 102, no. 7, Article ID 071601, 4 pages, 2009.
- [16] V. Braun and A. Novoseltsev, “Toric geometry in the Sage CAS,” to appear.
- [17] W. Stein et al., “Sage Mathematics Software (Version 4.5.3),” The Sage Development Team, 2010, <http://www.sagemath.org/>.
- [18] G.-M. Greuel, G. Pfister, and H. Schönemann, “Singular 3.0,” a computer algebra system for polynomial computations, Centre for Computer Algebra, University of Kaiserslautern, 2005, <http://www.singular.uni-kl.de/>.
- [19] W. Nahm and K. Wendland, “A hiker’s guide to K . Aspects of $N = (4, 4)$ superconformal field theory with central charge $c = 6$,” *Communications in Mathematical Physics*, vol. 216, no. 1, pp. 85–138, 2001.
- [20] V. Batyrev and M. Kreuzer, “Integral cohomology and mirror symmetry for Calabi-Yau 3-folds,” in *Mirror Symmetry. V*, vol. 38 of *AMS/IP Stud. Adv. Math.*, pp. 255–270, American Mathematical Society, Providence, RI, USA, 2006.
- [21] B. Nill, “Gorenstein toric Fano varieties,” *Manuscripta Mathematica*, vol. 116, no. 2, pp. 183–210, 2005.
- [22] V. Braun, “On free quotients of complete intersection Calabi-Yau manifolds,” *Journal of High Energy Physics*, vol. 2011, no. 4, article 5, 2011.
- [23] V. Braun, P. Candelas, and R. Davies, “A three-generation Calabi-Yau manifold with small Hodge numbers,” *Fortschritte der Physik*, vol. 58, no. 4-5, pp. 467–502, 2010.
- [24] P. Candelas and A. Constantin, “Completing the web of \mathbb{Z}_3 —quotients of complete intersection Calabi-Yau manifolds,” <http://arxiv.org/abs/1010.1878>.
- [25] D. A. Cox, “The homogeneous coordinate ring of a toric variety,” *Journal of Algebraic Geometry*, vol. 4, no. 1, pp. 17–50, 1995.
- [26] W. Fulton, *Introduction to Toric Varieties*, vol. 131 of *Annals of Mathematics Studies*, Princeton University Press, Princeton, NJ, USA, 1993, The William H. Roever Lectures in Geometry.
- [27] M. Oka, “Finiteness of fundamental group of compact convex integral polyhedra,” *Kodai Mathematical Journal*, vol. 16, no. 2, pp. 181–195, 1993.
- [28] N. Nakayama, “Local structure of an elliptic fibration,” in *Higher Dimensional Birational Geometry (Kyoto, 1997)*, vol. 35 of *Adv. Stud. Pure Math.*, pp. 185–295, Math. Soc. Japan, Tokyo, Japan, 2002.
- [29] N. Nakayama, “Global structure of an elliptic fibration,” *Publications of the Research Institute for Mathematical Sciences*, vol. 38, no. 3, pp. 451–649, 2002.
- [30] J. Tate, “Algorithm for determining the type of a singular fiber in an elliptic pencil,” in *Modular Functions of One Variable, IV (Proc. Internat. Summer School, Univ. Antwerp, Antwerp, 1972)*, vol. 476 of *Lecture Notes in Math.*, pp. 33–52, Springer, Berlin, Germany, 1975.
- [31] M. Bershadsky, K. Intriligator, S. Kachru, D. R. Morrison, V. Sadov, and C. Vafa, “Geometric singularities and enhanced gauge symmetries,” *Nuclear Physics B*, vol. 481, no. 1-2, pp. 215–252, 1996.
- [32] K.-S. Choi, “ $SU(3) \times SU(2) \times U(1)$ vacua in F-theory,” *Nuclear Physics B*, vol. 842, no. 1, pp. 1–32, 2011.

Review Article

BPS States, Crystals, and Matrices

Piotr Sułkowski^{1,2}

¹ *California Institute of Technology, Pasadena, CA 91125, USA*

² *Faculty of Physics, University of Warsaw, ul. Hoża 69, 00-681 Warsaw, Poland*

Correspondence should be addressed to Piotr Sułkowski, psulkows@theory.caltech.edu

Received 14 May 2011; Accepted 19 June 2011

Academic Editor: Amihay Hanany

Copyright © 2011 Piotr Sułkowski. This is an open access article distributed under the Creative Commons Attribution License, which permits unrestricted use, distribution, and reproduction in any medium, provided the original work is properly cited.

We review free fermion, melting crystal, and matrix model representations of wall-crossing phenomena on local, toric Calabi-Yau manifolds. We consider both unrefined and refined BPS counting of closed BPS states involving D2- and D0-branes bound to a D6-brane, as well as open BPS states involving open D2-branes ending on an additional D4-brane. Appropriate limit of these constructions provides, among the others, matrix model representation of refined and unrefined topological string amplitudes.

1. Introduction

This paper is devoted to some aspects of counting of BPS states in a system of Dp -branes, with even p , in type IIA string compactifications. The problems of BPS counting span a vast area of research in supersymmetric gauge and string theories. Their important feature is a special, nonconstant character of BPS multiplicities: their values depend on various moduli and jump discontinuously along some special loci in the corresponding moduli space, so called *walls of marginal stability*. The pattern of these jumps follows *wall-crossing formulas*, found from physical perspective by Denef and Moore [1] and, in more general context, formulated mathematically by Kontsevich and Soibelman [2]. The regions of the moduli space in between walls of marginal stability, in which BPS multiplicities are (locally) constant, are called *chambers*.

The BPS states we are interested in, and which we will refer to as *closed BPS states*, arise as bound states of a single D6-brane with arbitrary number of D0 and D2-branes wrapping cycles of a toric Calabi-Yau space. More generally, we will also consider *open BPS states*, which arise when an additional D4-brane spans a Lagrangian submanifold inside the Calabi-Yau space and supports open D2-branes attached to it. The closed and open BPS states give rise, respectively, to single-particle states in the effective four-dimensional and two-dimensional theory (in remaining, space-time filling directions of, resp., D6 and D4-branes). In this context, the character of BPS multiplicities can be understood in much

detail, and it relates to other interesting exactly solvable models: free fermions, crystal, and matrix models. In brief, these connections arise as follows. Firstly, BPS states we consider turn out to be in one-to-one correspondence with configurations of certain statistical models of melting crystals. The structure of these crystals depends on geometry of the underlying Calabi-Yau space, as well as on the chamber one is considering. In consequence, BPS counting functions, upon appropriate identification of parameters, coincide with generating functions of melting crystals. It turns out that the structure of these crystals can be given a free fermion representation. Furthermore, once such free fermion formulation is known, it can also be represented in terms of matrix models. Connection with vast theory of matrix models has many interesting mathematical and physical consequences and allows to shed new light on wall-crossing phenomena. The aim of this paper is to explain these connections.

The BPS generating functions which we consider are intimately related to topological string amplitudes on corresponding Calabi-Yau spaces. This relation is most transparent in the physical derivation discussed in Section 2, which relies on lifting the D-brane system to M-theory. The M-theory viewpoint makes contact with original formulation of closed topological strings by Gopakumar and Vafa [3, 4], and open topological strings by Ooguri and Vafa [5]. In particular, in one specific, so-called *noncommutative chamber*, the BPS-generating function is given as the modulus square of the topological string partition function. In all other chambers, BPS generating functions can be uniquely determined from that noncommutative result. There is also another special, so-called *commutative chamber*, in which BPS generating function coincides (up to the factor of MacMahon function) with the topological string partition function. For toric manifolds which we consider, such topological string amplitudes can be constructed, among the other, by means of the powerful topological vertex formalism [6]. Relation to crystal models was in fact first understood in this topological string chamber [7–9]. One advantage of the formalism presented in this paper is the fact that it allows to construct matrix model representation of all these generating functions (so, in particular, matrix model representation of topological string amplitudes).

In more detail, we will consider generating functions of D2 and D0-branes bound to a single D6-brane of the following form:

$$\mathcal{Z}_{\text{BPS}}(q_s, Q) = \sum_{\alpha, \beta} \Omega(\alpha, \beta) q_s^\alpha Q^\beta, \quad (1.1)$$

where $\alpha \in \mathbb{Z}$ is D0-brane charge and $\beta \in H_2(X, \mathbb{Z})$ is D2-brane charge. Multiplicities $\Omega(\alpha, \beta)$ jump when central charges (which itself are functions of Kähler moduli) of building blocks of a bound state align, and therefore these generating functions are locally constant functions of Kähler moduli. Along the walls of marginal stability, the degeneracies $\Omega(\alpha, \beta)$ change and indeed obey wall-crossing formulas of [1, 2] mentioned above.

If there is an additional D4-brane which spans a Lagrangian submanifold inside the Calabi-Yau space, in addition to the above *closed* BPS states, one can consider also *open* BPS states of D2-branes with boundaries ending on a one-cycle γ on this D4-brane. In this case, the BPS states arise on the remaining two-dimensional world-volume of the D4-brane. The holonomy of the gauge field along γ provides another generating parameter z , so that open BPS-generating functions take form

$$\mathcal{Z}_{\text{BPS}}^{\text{open}}(q_s, Q) = \sum_{\alpha, \beta, \gamma} \Omega(\alpha, \beta) q_s^\alpha Q^\beta z^\gamma. \quad (1.2)$$

As we will show, generating functions of such open BPS states can be identified with integrands of matrix models mentioned above.

One more important aspect of BPS counting is referred to as *refinement*, and amounts to refining BPS counting by introducing one more parameter, customarily denoted β . The refinement can be introduced from several perspectives which give rise to identical results; however, their fundamental common origin is still not fully understood. We will introduce refinement by distinct counting of states with different $SU(2)$ spins inside spacetime $SO(4)$ rotation group in the generating function (1.1). In [10], it was argued that this physical viewpoint should agree with the mathematical counterpart of motivic deformation [2], and also a refined version of a crystal model was constructed. Another notion of refinement arises in Nekrasov partition functions, which are defined in a nontrivial gravitational (so-called Ω -) background parametrized by two parameters ϵ_1 and ϵ_2 [11]. Nekrasov partition functions can also be defined for five-dimensional gauge theories and then they agree with topological string amplitudes. In particular, the formalism of the topological vertex [6] has also been extended to the refined context in [12], and shown to reproduce relevant Nekrasov partition functions. Also BPS generating functions, in the limit of commutative chamber, are known to reproduce refined topological string amplitudes with $\beta = -\epsilon_1/\epsilon_2$ [13]. However, the worldsheet definition of refined topological string amplitudes is not fully understood.

As an exemplary and, hopefully, inspiring application of the entire formalism presented in this paper, in the final Section 6 we derive matrix model representation of the refined topological string partition function for the conifold. The refined matrix model which we find has a standard measure; however, its potential is deformed by β -dependent terms. It is obtained by constructing appropriate refined crystal model and free fermion representation, and subsequently reformulating this representation in matrix model form. Finally, taking the limit of the commutative chamber, we obtain matrix model representation of the refined topological string amplitude. Even though we demonstrate this result in the conifold case, with some technical effort it can be generalized to other toric manifolds which we consider (As we recall in Section 6, refined topological string amplitudes were also postulated to be reproduced by another type of matrix models, so-called β -deformed ones (whose Vandermonde measure is deformed by raising it to power β); however, explicit computations showed that this cannot be the correct representation of refined amplitudes.).

1.1. Short Literature Guide

The literature on the topics presented in this paper is extensive and still growing, and we unavoidably mention just a fraction of important developments. The relation between Donaldson-Thomas invariants for the noncommutative chamber of the conifold was first found by Szendrői [14]. It was generalized to orbifolds of \mathbb{C}^3 , and related to free fermion formalism, by Bryan and Young [15]. The relation to free fermions and crystals was extended to a large class of toric manifolds without compact four-cycles [16, 17]. These developments were accompanied by other mathematical works [18, 19].

In parallel to the above-mentioned mathematical activity, wall-crossing phenomena for local Calabi-Yau manifolds were analyzed from physical viewpoint. The analysis of nontrivial BPS counting for the conifold was described by Jafferis and Moore in [20]. This and more general cases were related to quivers and crystal models in [21, 22]. Derivation of BPS degeneracies from M-theory viewpoint and relation to closed topological strings were discussed in [23], and generalized to open BPS counting in [24–27]. Relations to matrix models, discussed for plane partitions with some other motivation in [28], were extended to other crystal models relevant for BPS counting in [29], and also in [30]. Subsequently, it

was related to open BPS counting in [27]. Refined BPS counting was related to crystal models in [10, 13], and corresponding matrix models were constructed in [31].

Let us also mention some other, related works devoted to crystals and free fermions. The fermionic construction of MacMahon function for \mathbb{C}^3 was originally presented in [7], and its relation to open topological strings and more complicated Calabi-Yau manifolds were discussed in [32–34]. Newer ideas, analyzing more complicated systems involving D4-branes, were presented in [35, 36]. More expository presentations of various aspects described here can be found in [37, 38]. A general introduction to mathematical and physical aspects of mirror symmetry can be found in [39].

1.2. Plan

The plan of this paper is as follows. In Section 2, we introduce BPS generating functions and present one possible derivation of their form, which relies on the M-theory interpretation of a D-brane system, following [23–25, 27]. In Section 3, we provide a little mathematical background and introduce notation pertaining to toric Calabi-Yau manifolds, free fermion formalism, and matrix models. In Section 4, we introduce fermionic formalism for BPS generating functions and present corresponding crystal models, building on earlier ideas of [7, 15] and following [16]. In Section 5, we reformulate the problem of closed BPS counting in terms of matrix models and relate it to open BPS counting [27, 29]. In Section 6, we refine our analysis, present refined BPS generating functions and crystals [10], and construct corresponding refined matrix models [31].

2. BPS Generating Functions

In this section, we introduce generating functions of BPS states of D-branes in toric Calabi-Yau manifolds. Our task in the rest of this paper is to provide interpretation of these generating functions in terms of free fermions, melting crystals, and matrix models. These generating functions can be derived using wall-crossing formulas, as was done first in the unrefined [20] and refined [10] conifold case, and later generalized to arbitrary geometry without compact four-cycles in [18, 19]. On the other hand, we will focus on a simpler physical derivation of BPS generating functions which uses the lift of the D-brane system to M-theory [23]. This also makes contact with M-theory interpretation of topological string theory and allows to express BPS counting functions in terms of topological string amplitudes. Moreover, this M-theory derivation can be extended to the counting of open BPS states, that is, open D2-branes attached to additional D4-brane, which we are also interested in [24, 25, 27].

We start this section by reviewing the M-theory derivation of (unrefined) closed and open BPS generating functions. Then, to get acquainted with a crystal interpretation of these generating functions, we discuss their crystal interpretation in simple cases of \mathbb{C}^3 and conifold. Later, using fermionic interpretation, we will generalize this crystal representation to a large class of toric manifolds without compact four cycles.

2.1. M-Theory Derivation

We start by considering a system of D2 and D0-branes bound to a single D6-brane in type IIA string theory. It can be reinterpreted in M-theory as follows [23]. When additional S^1 is introduced as the eleventh dimension transversely to the D6-brane, then this D6-brane transforms into a geometric background of a Taub-NUT space with unit charge [40]. The

Taub-NUT space is a circle fibration over \mathbb{R}^3 , with a circle S_{TN}^1 attaining a fixed radius R at infinity, and shrinking to a point in the location of the original D6-brane. From M-theory perspective, bound states involving D2 and D0-branes are interpreted as M2-branes with momentum on a circle. Therefore, the counting of original bound states to the D6-brane is reinterpreted as the counting of BPS states of M2-branes in the Taub-NUT space. While in general this is still a nontrivial problem, for the purpose of counting BPS degeneracies we can take advantage of their invariance under continuous deformations of the Taub-NUT space, in particular under deformations of the radius R . We can therefore consider taking this radius to infinity, whereupon BPS counting is reinterpreted in terms of a gas of particles in \mathbb{R}^5 . To make the problem fully tractable, we have to ensure that the particles are noninteracting, which would be the case if moduli of the Calabi-Yau would be tuned so that M2-branes wrapped in various ways would have aligned central charges. This can be achieved when Kähler parameters of the Calabi-Yau space are tuned to zero. However, to avoid generation of massless states, at the same time one has to include nontrivial fluxes of the M-theory three-form field through the two cycles of the Calabi-Yau and S_{TN}^1 . In type IIA, this results in the B -field flux B through two cycles of Calabi-Yau. Finally, to avoid creation of the string states arising from M5-branes wrapping four cycles in Calabi-Yau, we simply restrict considerations to manifolds without compact four cycles. For a state arising from D2-brane wrapping a class β , the central charge then reads

$$Z(l, \beta) = \frac{1}{R}(l + B \cdot \beta), \quad (2.1)$$

where l counts the D0-brane charge, which is taken positive to preserve the same supersymmetry.

Under the above conditions, the counting of D6-D2-D0 bound states is reinterpreted in terms of a gas of particles arising from M2-branes wrapped on cycles β . The excitations of these particles in \mathbb{R}^4 , parametrized by two complex variables z_1, z_2 , are accounted for by the modes of the holomorphic field

$$\Phi(z_1, z_2) = \sum_{l_1, l_2} \alpha_{l_1, l_2} z_1^{l_1} z_2^{l_2}. \quad (2.2)$$

Decomposing the isometry group of \mathbb{R}^4 as $SO(4) = SU(2) \times SU(2)'$, there are $N_\beta^{m, m'}$ five-dimensional BPS states of intrinsic spin (m, m') . We are interested in their net number arising from tracing over $SU(2)'$ spins

$$N_\beta^m = \sum_{m'} (-1)^{m'} N_\beta^{m, m'}. \quad (2.3)$$

The total angular momentum of a given state contributing to the index is $l = l_1 + l_2 + m$. Finally, in a chamber specified by the moduli R and B , the invariant degeneracies can be expressed as the trace over the corresponding Fock space

$$\begin{aligned} \mathcal{Z}_{\text{BPS}} &= \left(\text{Tr}_{\text{Fock}} q_s^{Q_0} Q^{Q_2} \right) \Big|_{\text{chamber}} \\ &= \prod_{\beta, m} \prod_{l_1 + l_2 = l} \left(1 - q_s^{l_1 + l_2 + m} Q^\beta \right)^{N_\beta^m} \Big|_{\text{chamber}} \\ &= \prod_{\beta, m} \prod_{l=1}^{\infty} \left(1 - q_s^{l+m} Q^\beta \right)^{l N_\beta^m} \Big|_{\text{chamber}}, \end{aligned} \quad (2.4)$$

where the subscript chamber denotes restriction to those factors in the above product, which represent states which are mutually BPS

$$Z(l, \beta) > 0 \iff q_s^{l+m} Q^\beta < 1. \quad (2.5)$$

As usual, $Q = e^{-T}$ and $q_s = e^{-g_s}$ above encode, respectively, the Kähler class T and the string coupling g_s (we wish to distinguish carefully q_s which encodes string coupling, from a counting parameter q which will arise in what follows in crystal interpretation). The above condition on central charges is crucial in determining a particular form of the BPS generating functions. If we would restrict products in the formula (2.4) to factors with only positive β , we would get (up to possibly some factor of MacMahon function) the Gopakumar-Vafa representation of the topological string amplitude. With all negative and positive values of β , we would get modulus square of the topological string partition function. Therefore, the upshot of [23] is that in general the above BPS generating function can be expressed in terms of the closed topological string partition function

$$\mathcal{Z}_{\text{BPS}} = \mathcal{Z}_{\text{top}}(Q) \mathcal{Z}_{\text{top}}(Q^{-1}) \Big|_{\text{chamber}}, \quad (2.6)$$

where chamber restriction is to be understood as picking up only those factors in Gopakumar-Vafa product representation of \mathcal{Z}_{top} for which (2.5) is satisfied. In this context, we will often refer to the choice of a chamber as a *closed BPS chamber*. The (instanton part of the) closed topological string partition function entering the above expression is given by [3, 4]

$$\mathcal{Z}_{\text{top}}(Q) = M(q_s)^{\chi/2} \prod_{l=1}^{\infty} \prod_{\beta > 0, m} (1 - Q^\beta q_s^{m+l})^{l N_\beta^m}, \quad (2.7)$$

where $M(q_s) = \prod_l (1 - q_s^l)^{-l}$ is the MacMahon function and χ is the Euler characteristic of the Calabi-Yau manifold.

To be more precise, an identification as a topological string partition function or its square arises if $R > 0$ in (2.1). Because R arises just as a multiplicative factor in (2.1), degeneracies depend only on its sign. Therefore, another extreme case corresponds to negative R and B sufficiently small, when only a single D6-brane contributes to the partition function

$$\tilde{\mathcal{Z}}(R < 0, 0 < B \ll 1) = 1. \quad (2.8)$$

More generally, for $R < 0$, BPS generating functions often (but not always) take finite form.

In what follows we denote BPS generating functions in chambers with positive R by \mathcal{Z} , and in chambers with negative R by $\tilde{\mathcal{Z}}$ (and often omit the subscript BPS). Topological string partition functions will be denoted by \mathcal{Z}_{top} , while generating functions of melting crystals by ordinary Z .

The above structure can be generalized by including in the initial D6-D2-D0 configuration additional D4-branes wrapping Lagrangian cycles in the internal Calabi-Yau manifold and extending in two space-time dimensions [24, 25, 27]. For simplicity, we consider a system with a single D4-brane wrapping a Lagrangian cycle. There are now additional BPS

states in two remaining spacetime dimensions arising from open D2-branes ending on these D4-branes. Their net degeneracies $N_{s,\beta,\gamma}$ are characterized, firstly, by the $SO(2)$ spin s whose origin is most clearly seen from the M-theory perspective [5, 41]. Secondly, they depend on two-cycles β wrapped by open M2-branes, as well as one-cycles γ on which these M2-branes can end (In case of N D4-branes wrapping the same Lagrangian cycle, these states would additionally arise in representations R of $U(N)$ [5]. In case of a single brane, this reduces to $U(1)$, and such a dependence can be reabsorbed into a parameter specifying a choice of γ .)

Lifting this system to M-theory, we obtain a background of the form Taub-NUT \times Calabi-Yau $\times S^1$, with the additional D4-brane promoted to M5-brane. This M5-brane wraps the Lagrangian submanifold L inside Calabi-Yau, the time circle S^1 , and $\mathbb{R}_+ \times S^1_{\text{TN}}$ inside the Taub-NUT space. A part of this Lagrangian L is a torus $T^2 = S^1_{\text{TN}} \times S^1$, which will lead to some modular properties of the BPS counting functions: this modularity will be manifest in one chamber, where the open topological string amplitude will be completed to the product of θ functions. This M5-brane also breaks the $SO(4)$ spatial symmetry down to $SO(2) \times SO(2)'$. We denote the spins associated to both $SO(2)$ factors, respectively, by σ and σ' , and the degeneracies of particles with such spins by $N_{\beta,\gamma}^{\sigma,\sigma'}$. In addition to closed Kähler parameters $Q = e^{-T}$, let us also introduce open ones related to discs wrapped by M2-branes $z = e^{-d}$. The real and imaginary parts of T encode, respectively, the sizes of two-cycles β and the value of the B -field through them. The real and imaginary parts of d encode, respectively, sizes of the discs and holonomies of the gauge fields around them. Similarly as in the closed string case, to get nontrivial ensemble of mutually supersymmetric states, we set the real parts of T and d to zero, and consider nontrivial imaginary parts.

From the M-theory perspective, we are interested in counting the net degeneracies of M2-branes ending on this M5-brane

$$N_{\sigma,\beta,\gamma} = \sum_{\sigma'} (-1)^{\sigma'} N_{\beta,\gamma}^{\sigma,\sigma'}. \quad (2.9)$$

In the remaining three-dimensional space, in the $R \rightarrow \infty$ limit, the M2-branes ending on the M5-brane are represented by a gas of free particles. These particles have excitations in \mathbb{R}^2 which we identify with the z_1 -plane. To each such BPS particle, similarly as in the closed string case discussed above and in [23, 40], we can associate a holomorphic field

$$\Phi(z_1) = \sum_l \alpha_l z_1^l. \quad (2.10)$$

The modes of this field create states with the intrinsic spin s and the orbital momentum l in the \mathbb{R}^2 plane. The derivation of the BPS degeneracies relies on the identification of this total momentum $\sigma + l$ in the $R \rightarrow \infty$ limit, with the Kaluza-Klein modes associated to the rotations along S^1_{TN} for the finite R , following the five-dimensional discussion in [40, 42].

The BPS generating functions we are after are given by a trace over the Fock space built by the oscillators of the second quantized field $\Phi(z_1)$ and restricted to the states which are mutually supersymmetric. In such a trace, each oscillator from (2.10) gives rise to one factor of the form $(1 - q_s^{\sigma+l-1/2} Q^\beta z^\gamma)^{\pm 1}$, where the exponent ± 1 corresponds to the bosonic or fermionic character of the top component of the BPS state,

$$\mathfrak{Z}_{\text{BPS}}^{\text{open}} = \prod_{\sigma,\beta,\gamma} \prod_{l=1}^{\infty} \left(1 - q_s^{\sigma+l-1/2} Q^\beta z^\gamma\right)^{N_{\sigma,\beta,\gamma}} \Big|_{\text{chamber}}, \quad (2.11)$$

where the product is over either both positive or both negative (β, γ) . The parameters q, Q and z specify the chamber structure: the restriction to a given chamber is implemented by imposing the condition on a central charge, analogous to (2.5),

$$q_s^{\sigma+l-1/2} Q^\beta z^\gamma < 1. \quad (2.12)$$

This condition in fact specifies a choice of both *closed* and *open* chambers. The walls of marginal stability between chambers correspond to subspaces where, for some oscillator, the above product becomes 1, and then the contribution from such an oscillator drops out from the BPS generating function.

Similarly as in the closed string case, the above degeneracies can be related to open topological string amplitudes, rewritten in [5] in the form

$$\mathcal{Z}_{\text{top}}^{\text{open}} = \exp \left(\sum_{n=1}^{\infty} \sum_{\sigma} \sum_{\beta, \gamma > 0} N_{\sigma, \beta, \gamma} \frac{q_s^{n\sigma} Q^{n\beta} z^{n\gamma}}{n(q_s^{n/2} - q_s^{-n/2})} \right), \quad (2.13)$$

with integer Ooguri-Vafa invariants $N_{\sigma, \beta, \gamma}$ (In case of N D4-branes wrapping a Lagrangian cycle, this structure is again more complicated, because the states in \mathbb{R}^3 arise in representations of $U(N)$ [5]. This requires replacing the factor $z^{n\gamma}$ by the sum $\sum_R \text{Tr}_R V^n$ of traces in all possible representations R of this $U(N)$ of the matrix V encoding holonomies of the gauge fields. For simplicity we restrict here to the simplest case.). This formula represents in fact a series of quantum dilogarithms

$$L(z, q_s) = \exp \left(\sum_{n>0} \frac{z^n}{n(q_s^{n/2} - q_s^{-n/2})} \right) = \prod_{n=1}^{\infty} (1 - zq_s^{n-1/2}) \quad (2.14)$$

and can be written in the product form

$$\mathcal{Z}_{\text{top}}^{\text{open}}(Q, z) = \prod_{\sigma} \prod_{\beta, \gamma > 0} \prod_{n=1}^{\infty} (1 - Q^\beta z^\gamma q_s^{\sigma+n-1/2})^{N_{\sigma, \beta, \gamma}}. \quad (2.15)$$

Comparing with (2.11) we conclude that the BPS counting functions take form of the modulus square of the open topological string amplitude

$$\mathcal{Z}_{\text{BPS}}^{\text{open}} = \mathcal{Z}_{\text{top}}^{\text{open}}(Q, z) \mathcal{Z}_{\text{top}}^{\text{open}}(Q^{-1}, z^{-1}) \Big|_{\text{chamber}}. \quad (2.16)$$

Similarly as in the closed string case, there are also a few particularly interesting chambers to consider. For example, in the extreme chamber corresponding to $\text{Im } T, \text{Im } d \rightarrow 0$, the trace is performed over the full Fock space and yields the modulus square of the open topological string partition function. In this case, the quantum dilogarithms arise in pairs, which (using the Jacobi triple product identity) combine to the modular function θ_3/η ; in consequence, the total BPS generating function is modular and expressed as a product of such functions.

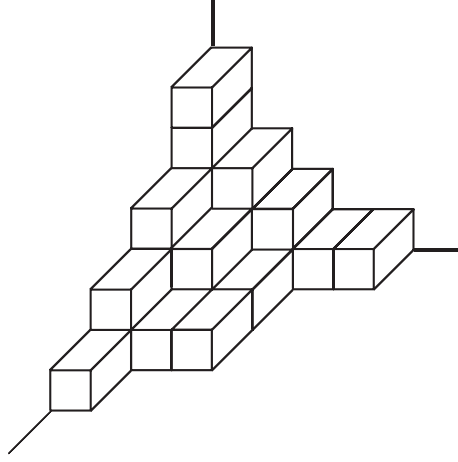


Figure 1: Plane partitions represent melting crystal configurations of \mathbb{C}^3 .

2.2. Crystal Interpretation

Closed BPS generating functions (2.4) turn out to be generating functions of statistical models of crystals, when parameters relevant for both interpretations are appropriately matched. Physical reasons for such relations have been given in [8, 21, 22], and mathematical interpretation arose from works [9, 14, 15]. Such crystal interpretation arises also from the fermionic formulation [16, 17], as we will review below. These crystals, in a more intricate way [27], encode also open BPS generating functions (2.11). However, before discussing details of all these constructions, in this introductory section we present crystal models for two simplest toric Calabi-Yau manifolds, that is, \mathbb{C}^3 and conifold.

\mathbb{C}^3 is the simplest Calabi-Yau manifold. It has no compact two-cycles, so relevant BPS states are bound states of arbitrary number of D0-branes with a single D6-brane wrapping entire \mathbb{C}^3 . Their generating function is therefore expressed in terms of a single parameter $q_s = e^{-g_s}$. There is just a single nonzero Gopakumar-Vafa invariant $N_{\beta=0}^0 = -1$, and as follows from (2.4) this generating function coincides with the so-called MacMahon function

$$\mathcal{Z}_{\text{BPS}} = \prod_{l=1}^{\infty} \frac{1}{(1 - q_s^l)^l} = M(q_s). \quad (2.17)$$

On the other hand, the MacMahon function is a generating function of plane partitions, that is, three-dimensional generalization of Young diagrams. These plane partitions represent the simplest three-dimensional crystal model, namely, they can be identified with stacks of unit cubes filling the positive octant of \mathbb{R}^3 space, as shown in Figure 1. A unit cube located in position (I, J, K) can evaporate from this crystal only if all other cubes with coordinates $(i \leq I, j \leq J, k \leq K)$ are already missing. A plane partition π is weighted by the number of boxes it consists of $|\pi|$, with a weight q associated to a single box, so indeed

$$Z = \sum_{\pi} q^{|\pi|} = \sum_{l=0}^{\infty} p(l) q^l = 1 + q + 3q^2 + 6q^3 + 13q^4 + \dots = M(q), \quad (2.18)$$

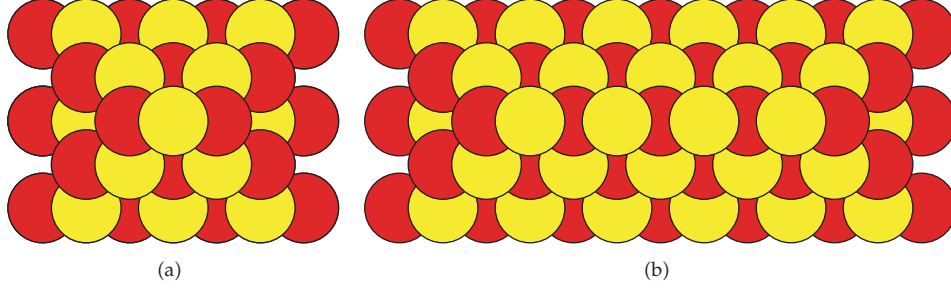


Figure 2: Infinite pyramids with one and four balls in the top row, with generating functions given, respectively, by Z_0^{pyramid} and Z_3^{pyramid} .

where $p(l)$ is the number of plane partitions which consist of l cubes. Therefore, plane partition generating function coincides with the BPS counting function $Z = \mathcal{Z}_{\text{BPS}}$ when a simple identification

$$q_s = q \quad (2.19)$$

is made. From (2.6), it follows that the topological string partition function for \mathbb{C}^3 is given by the square root of the MacMahon function

$$\mathcal{Z}_{\text{top}} = M(q_s)^{1/2}, \quad (2.20)$$

which is indeed true. The relevance of the MacMahon function for \mathbb{C}^3 geometry was noticed for the first time in [3], and a statistical model interpretation of this result was proposed in [7].

The conifold provides another simple, yet nontrivial example of toric Calabi-Yau manifold. It consists of two \mathbb{C}^3 patches glued into $\mathcal{O}(-1) \oplus \mathcal{O}(-1) \rightarrow \mathbb{P}^1$, and it has one Kähler class representing \mathbb{P}^1 , parametrized by $Q = e^{-T}$. This class can be wrapped by D2-branes, which bind with D0-branes to an underlying D6-brane and give rise to BPS states in low energy theory. In this case, there is already a nontrivial structure of chambers and walls, which was analyzed in [14, 18, 20, 21]. This structure is consistent with M-theory derivation discussed in Section 2.1. The generating functions of D6-D2-D0 bound states are parametrized by Q and q_s , and therefore corresponding crystal models consist of two-colored three-dimensional partitions. The Kähler moduli space consists of several infinite countable sets of chambers, and in each chamber relevant crystal configurations take form of so-called pyramid partitions. These partitions are infinite or finite (resp. for positive and negative R in (2.1)) and their size depends on the value of the B -field. This size changes discretely and the pyramid is enlarged when the value of the B -field crosses integer numbers, which changes the chamber in the moduli space, as explained in Section 2.1. Examples of such infinite pyramid partitions are given in Figure 2, and finite ones in Figure 3.

To write down explicitly BPS generating functions for the conifold in various chambers, we can take advantage of their relation to the topological string amplitude (2.6). The topological string partition function in this case reads

$$\mathcal{Z}_{\text{top}}^{\text{conifold}}(Q) = M(q_s) \prod_{k \geq 1} (1 - Qq_s^k)^k, \quad (2.21)$$

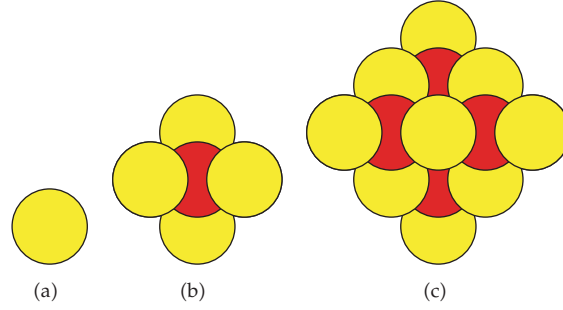


Figure 3: Finite pyramids with $m = 1, 2, 3$ stones in the top row (resp., (a), (b), and (c)), whose generating functions are given by $\tilde{Z}_{m+1}^{\text{pyramid}}$ (note that $\tilde{Z}_1^{\text{pyramid}} = 1$ corresponds to an empty pyramid corresponding to the pure D6-brane).

with the MacMahon function defined in (2.17). From this topological string partition function we can read off Gopakumar-Vafa invariants [3, 4]

$$N_{\beta=0}^0 = -2, \quad N_{\beta=\pm 1}^0 = 1. \quad (2.22)$$

Using the relation (2.6), we can now present conifold closed BPS generating functions in several sets of chambers. In the first set of chambers, we consider $R > 0$ and positive $B \in]n, n + 1[$ (for $n \geq 0$). Firstly, for small B , there is so-called noncommutative chamber discussed first by Szendrői [14], which corresponds to $n = 0$. In this case, the pyramid crystal has just a single ball in the top row, as in Figure 2(a), and the BPS generating function is given by the square of the topological amplitude. On the other hand, for large B , that is $n \rightarrow \infty$, we reach commutative chamber in which the length of the top row extends to infinity. In this case, the BPS generating function agrees, up to a single factor of MacMahon function, with the topological string amplitude. In between, there are chambers with $n + 1$ balls in the top row, for which

$$\mathfrak{Z}_n^{\text{conifold}} = M(q_s)^2 \prod_{k \geq 1} (1 - Qq_s^k)^k \prod_{k \geq n+1} (1 - Q^{-1}q_s^k)^k. \quad (2.23)$$

These BPS generating functions are related to pyramid generating functions with two colors q_0 and q_1 upon the identification (which generalizes (2.19) in \mathbb{C}^3 case)

$$\mathfrak{Z}_n^{\text{conifold}} \text{ chambers : } q_s = q_0 q_1, \quad Q = -q_s^n q_1. \quad (2.24)$$

Indeed, with this identification, the above counting functions agree with those of two-colored pyramid crystals with $n + 1$ yellow balls in its top row

$$Z_n^{\text{pyramid}}(q_0, q_1) = M(q_0 q_1)^2 \prod_{k \geq n+1} (1 + q_0^k q_1^{k+1})^{k-n} \prod_{k \geq 1} (1 + q_0^k q_1^{k-1})^{k+n}. \quad (2.25)$$

In the second set of chambers, we have $R < 0$ and positive $B \in]n - 1, n[$ (for $n \geq 1$). It extends between the core region with a single D6-brane (2.8) and the chamber characterized by so-called Pandharipande-Thomas invariants (for the flopped geometry, or equivalently

for anti-M2-branes). The BPS generating functions read

$$\tilde{\mathcal{Z}}_n^{\text{conifold}} = \prod_{j=1}^{n-1} \left(1 - \frac{q_s^j}{Q}\right)^j. \quad (2.26)$$

The corresponding statistical models were shown in [16, 18, 21] to correspond to finite pyramids with $n - 1$ stones in the top row, as shown in Figure 3. In this case, the generating functions of such partitions are equal to

$$\tilde{\mathcal{Z}}_n^{\text{pyramid}}(q_0, q_1) = \prod_{j=1}^{n-1} \left(1 + q_0^{n-j} q_1^{n-j-1}\right)^j. \quad (2.27)$$

The equality $\tilde{\mathcal{Z}}_n^{\text{conifold}} \equiv \tilde{\mathcal{Z}}_n^{\text{pyramid}}$ arises upon an identification

$$\tilde{\mathcal{Z}}_n^{\text{conifold}} \text{ chambers : } q_s^{-1} = q_0 q_1, \quad Q = -q_s^n q_1. \quad (2.28)$$

There are two other sets of chambers characterized by the negative value of the B -field, for which BPS generating functions are completely analogous to those given above.

Above, we presented just the simplest examples of crystal models. Using fermionic formulation presented below, one can find other crystal models for arbitrary toric geometry without compact four cycles. Let us also mention that those models can be equivalently expressed in terms dimers. In particular, the operation of enlarging the crystal, as in the conifold pyramids, corresponds to so-called *dimer shuffling* [15]. Dimers are also closely related to a formulation using quivers and associated potentials, which underlies physical derivations in [21, 22].

3. A Little Background—Free Fermions and Matrix Models

In this section, we introduce some mathematical background on which the main results presented in this paper rely. In Section 3.1, we start with a brief presentation of toric Calabi-Yau manifolds and introduce the notation which we use in what follows. In Section 3.2, we introduce free fermion formalism. In Section 3.3, we introduce basics of matrix model formalism. Our presentation is necessarily brief, and for more detailed introduction we recommend many excellent reviews on each of those topics.

3.1. Toric Calabi-Yau Threefolds

Some introductory material on toric Calabi-Yau manifolds, from the perspective relevant for mirror symmetry and topological string theory, can be found, for example, in [39]. In this section, our presentation is brief and mainly sets up the notation. Toric Calabi-Yau threefolds arise as the quotient of $\mathbb{C}^{\kappa+3}$, possibly with a discrete set of points deleted, by the action of $(\mathbb{C}^*)^\kappa$ with certain weights. The simplest toric threefold is \mathbb{C}^3 , which corresponds to the trivial choice $\kappa = 0$. The resolved conifold, which we already discussed in Section 2.2, corresponds to $\kappa = 1$ and a choice of weights $(1, 1, -1, -1)$, which represent a local bundle $\mathcal{O}(-1) \oplus \mathcal{O}(-1) \rightarrow \mathbb{P}^1$. The structure of each toric three-fold can be encoded in a two-dimensional diagram

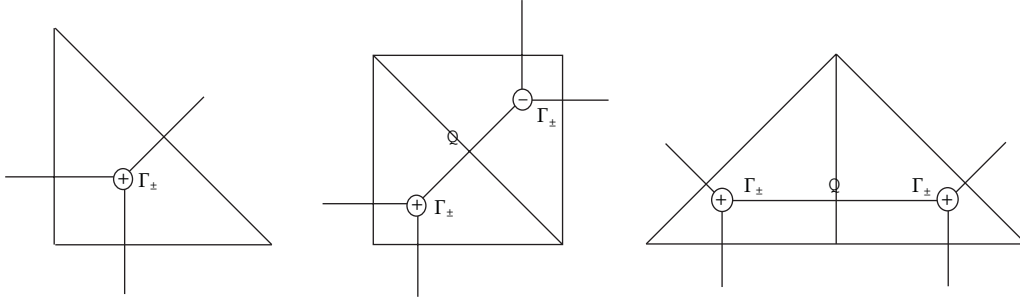


Figure 4: Toric graphs for \mathbb{C}^3 , conifold and resolution of $\mathbb{C}^3/\mathbb{Z}_2$.

built from trivalent vertices. Finite intervals joining two adjacent vertices represent local \mathbb{P}^1 neighborhood inside the manifold. Equivalently, one can consider dual graphs. Examples of toric diagrams and their duals for \mathbb{C}^3 , conifold and resolution of $\mathbb{C}^3/\mathbb{Z}_2$ singularity are given in Figure 4 (the notation Γ_{\pm} at each vertex will be explained in what follows).

A closed loop in a toric diagram represents a compact four cycles in the geometry. As follows from the reasoning in Section 2.1, in the context of BPS counting, we are forced to restrict considerations to manifolds which do not have such four cycles. Apart from a few special cases, there is an infinite class of such geometries whose dual diagrams arise from a triangulation, into triangles of area $1/2$, of a long rectangle or a strip of height 1. A toric diagram arises as a dual graph to such a triangulation. From each vertex in such a toric diagram, one vertical line extends to infinity and crosses either the upper or the lower edge of the strip. Two such consecutive lines can emanate either in the same or in the opposite direction, respectively, when they are the endpoints of an interval representing \mathbb{P}^1 with local $\mathcal{O}(-2) \oplus \mathcal{O}$ or $\mathcal{O}(-1) \oplus \mathcal{O}(-1)$ neighborhood. An example of a generic diagram of this kind is shown in Figure 8.

Let us denote independent \mathbb{P}^1 's, starting from the left end of the strip, from 1 to N , and introduce corresponding Kähler parameters $Q_i = e^{-T_i}$, $i = 1, \dots, N$. Moreover, to each toric vertex we associate a type $t_i = \pm 1$, so that $t_{i+1} = t_i$ if the local neighborhood of \mathbb{P}^1 (represented by an interval between vertices i and $i+1$) is $\mathcal{O}(-2) \oplus \mathcal{O}$; if this neighborhood is of $\mathcal{O}(-1) \oplus \mathcal{O}(-1)$ type, then $t_{i+1} = -t_i$. The type of the first vertex we fix as $t_1 = +1$. In Figures 4 and 8, these types are denoted by \oplus and \ominus . The types t_i will be used much in the construction of fermionic states in Section 4.2.

As explained in Section 2.1, the BPS generating functions can be expressed in terms (the instanton part) of topological string amplitudes. For the above class of geometries, arising from a triangulation of a strip, these amplitudes read

$$\mathcal{Z}_{\text{top}}(Q_i) = M(q_s)^{(N+1)/2} \prod_{l=1}^{\infty} \prod_{1 \leq i < j \leq N+1} \left(1 - q_s^l(Q_i Q_{i+1} \cdots Q_{j-1})\right)^{-(t_i t_j)l}. \quad (3.1)$$

3.2. Free Fermion Formalism

Formalism of free fermions in two dimensions is well known [43, 44] and ubiquitous in literature on topological strings and crystal melting [7, 15, 15, 37, 45]. The main purpose

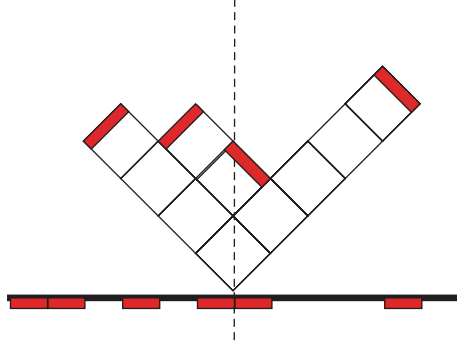


Figure 5: Relation between Young diagrams and states in the Fermi sea.

of this section is therefore to set up the notation which we will follow in the remaining parts of this paper.

The states in the free fermion Fock space are created by the (anticommuting) modes of the fermion field

$$\psi(z) = \sum_{k \in \mathbb{Z}} \psi_{k+1/2} z^{-k-1}, \quad \psi^*(z) = \sum_{k \in \mathbb{Z}} \psi_{k+1/2}^* z^{-k-1}, \quad \{\psi_{k+(1/2)}, \psi_{-l-1/2}^*\} = \delta_{k,l} \quad (3.2)$$

on the vacuum state $|0\rangle$. There is one-to-one map between such fermionic states

$$|\mu\rangle = \prod_{i=1}^d \psi_{-a_i-1/2}^* \psi_{-b_i-1/2} |0\rangle, \quad \text{with } a_i = \mu_i - i, \quad b_i = \mu_i^t - i, \quad (3.3)$$

and two-dimensional partitions $\mu = (\mu_1, \mu_2, \dots, \mu_l)$, as shown in Figure 5. The modes α_m of the bosonized field $\partial\phi =: \psi(z)\psi^*(z) :$ satisfy the Heisenberg algebra $[\alpha_m, \alpha_{-n}] = n\delta_{m,n}$.

We introduce vertex operators

$$\Gamma_{\pm}(x) = e^{\sum_{n>0} (x^n/n) \alpha_{\pm n}}, \quad \Gamma'_{\pm}(x) = e^{\sum_{n>0} ((-1)^{n-1} x^n/n) \alpha_{\pm n}}, \quad (3.4)$$

which act on fermionic states $|\mu\rangle$ corresponding to partitions μ as [15, 43, 44]

$$\Gamma_{-}(x)|\mu\rangle = \sum_{\lambda > \mu} x^{|\lambda|-|\mu|} |\lambda\rangle, \quad \Gamma_{+}(x)|\mu\rangle = \sum_{\lambda < \mu} x^{|\mu|-|\lambda|} |\lambda\rangle, \quad (3.5)$$

$$\Gamma'_{-}(x)|\mu\rangle = \sum_{\lambda^t > \mu^t} x^{|\lambda|-|\mu|} |\lambda\rangle, \quad \Gamma'_{+}(x)|\mu\rangle = \sum_{\lambda^t < \mu^t} x^{|\mu|-|\lambda|} |\lambda\rangle. \quad (3.6)$$

The interlacing relation $<$ between partitions is defined as

$$\lambda > \mu \iff \lambda_1 \geq \mu_1 \geq \lambda_2 \geq \mu_2 \geq \lambda_3 \geq \dots \quad (3.7)$$

The operator Γ' is the inverse of Γ with negative argument. These operators satisfy commutation relations

$$\Gamma_+(x)\Gamma_-(y) = \frac{1}{1-xy}\Gamma_-(y)\Gamma_+(x), \quad (3.8)$$

$$\Gamma'_+(x)\Gamma'_-(y) = \frac{1}{1-xy}\Gamma'_-(y)\Gamma'_+(x), \quad (3.9)$$

$$\Gamma'_+(x)\Gamma_-(y) = (1+xy)\Gamma_-(y)\Gamma'_+(x), \quad (3.10)$$

$$\Gamma_+(x)\Gamma'_-(y) = (1+xy)\Gamma'_-(y)\Gamma_+(x). \quad (3.11)$$

We also introduce various colors q_g and the corresponding operators \widehat{Q}_g (a hat is to distinguish them from Kähler parameters Q_i)

$$\widehat{Q}_g|\lambda\rangle = q_g^{|\lambda|}|\lambda\rangle. \quad (3.12)$$

These operators commute with vertex operators up to rescaling of their arguments

$$\Gamma_+(x)\widehat{Q}_g = \widehat{Q}_g\Gamma_+(xq_g), \quad \Gamma'_+(x)\widehat{Q}_g = \widehat{Q}_g\Gamma'_+(xq_g), \quad (3.13)$$

$$\widehat{Q}_g\Gamma_-(x) = \Gamma_-(xq_g)\widehat{Q}_g, \quad \widehat{Q}_g\Gamma'_-(x) = \Gamma'_-(xq_g)\widehat{Q}_g. \quad (3.14)$$

3.3. Matrix Models

In matrix model theory, or theory of random matrices, one is interested in properties of various ensembles of matrices. Excellent reviews of random matrix theory can be found for example in [46] or, in particular in the context of topological string theory, in [47]. In matrix model theory, one typically considers partition functions of the form

$$Z = \int \mathfrak{D}U \prod_{\alpha} e^{-(1/g_s)\text{Tr}V(U)}, \quad (3.15)$$

where $V = V(U)$ is a matrix potential and $\mathfrak{D}U$ is a measure over a set of matrices of interest U of size N . Typically it is not possible to perform the above integral; however, special techniques allow to determine its formal $1/N$ expansion. These techniques culminated with the formalism of the topological expansion of Eynard and Orantin [48] which, in principle, allows to determine entire $1/N$ expansion of the partition function recursively. This solution is determined by the behavior of matrix eigenvalues, whose distribution among the minima of the potential, in the continuum limit, determines one-dimensional complex curve, so-called spectral curve. The spectral curve is also encoded in the leading $1/N$ expansion of the so-called resolvent, which is defined as the expectation value $\omega(x) = \langle \text{Tr}(1/(x-U)) \rangle$ computed with respect to the measure (3.15).

In the context of BPS counting and topological strings, unitary ensembles of matrices of infinite size arise. In this case, the matrix model simplifies to the integral over eigenvalues u_α , with a measure which takes form of the unitary Vandermonde determinant

$$\mathfrak{D}U = \prod_\alpha du_\alpha \prod_{\alpha < \beta} |z_\alpha - z_\beta|^2, \quad z_\alpha = e^{iu_\alpha}. \quad (3.16)$$

The issue of infinite matrices is a little subtle; however, it can be taken care of by considering matrices of large but finite size N , and subsequently taking $N \rightarrow \infty$ limit. For finite N , one can find the resolvent, and in consequence the spectral curve, using a standard technique of so-called Migdal integral. This requires redefining V to the standard Vandermonde form [29, 47], as well as introducing 't Hooft coupling T

$$V \longrightarrow V + T \log z, \quad T = Ng_s. \quad (3.17)$$

The form of the Migdal integral depends on the number of cuts into which eigenvalues condense in large N limit, and this number of cuts determines the genus of the spectral curve. In our context, only single-cut situations will arise, for which the spectral curve has genus zero. In this case, the Migdal integral determines the resolvent as

$$\omega(p) = \frac{1}{2T} \oint \frac{dz}{2\pi i} \frac{\partial_z V(z)}{p-z} \frac{\sqrt{(p-a)(p-b)}}{\sqrt{(z-a)(z-b)}}, \quad (3.18)$$

so that the integration contour encircles counter-clockwise the endpoints of the cut a and b . A proper asymptotic behavior of the resolvent is imposed by the condition

$$\lim_{p \rightarrow \infty} \omega(p) = \frac{1}{p}. \quad (3.19)$$

Then the spectral curve is determined as a surface on which the resolvent is unambiguously defined, that is, it is given by an (exponential) rational equation automatically satisfied by p and $\omega(p)$. There is also an important consistency condition for the resolvent: when computed on the opposite sides of the cut $\omega(p)_\pm$, it is related to the potential as

$$\omega_+(p) + \omega_-(p) = \frac{\partial_p V(p)}{T}. \quad (3.20)$$

On the other hand, a difference of these values of the resolvent on both sides of the cut provides eigenvalue density

$$\rho(p) = \omega_+(p) - \omega_-(p). \quad (3.21)$$

It has been observed in several contexts that topological strings on toric manifolds can be related to matrix models, whose spectral curves take form of the so-called mirror curves.

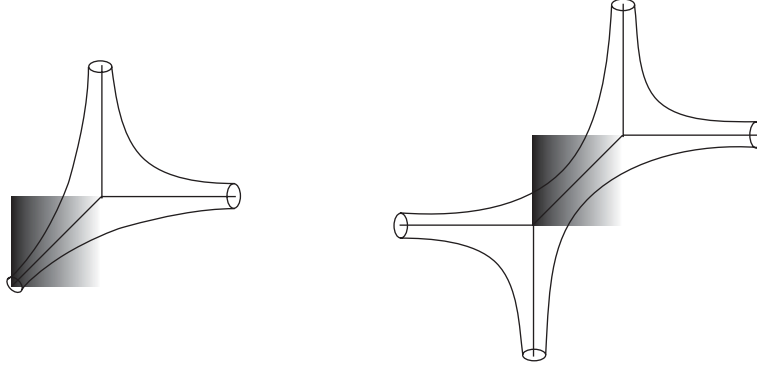


Figure 6: Toric diagrams for \mathbb{C}^3 and conifold and corresponding mirror curves.

Mirror curves arise for manifolds which are mirror to toric Calabi-Yau manifolds [39, 45]. For toric manifolds, their mirror manifolds are determined by the following equation embedded in four-dimensional complex space:

$$z_1 z_2 = H(x, y). \quad (3.22)$$

The mirror curve is the zero locus of $H(x, y)$, that is, it is given as $H(x, y) = 0$. More precisely, x, y are \mathbb{C}^* variables, and it is often convenient to represent them in the exponential form $x = u^u, y = e^v$, with $u, v \in \mathbb{C}$. For example, for \mathbb{C}^3 and the conifold they take the following form:

$$H_{\mathbb{C}^3}(x, y) = x + y + xy = 0, \quad H_{\text{conifold}}(x, y) = x + y + xy + Qx^2 = 0, \quad (3.23)$$

where Q encodes the Kähler parameter of the conifold. Schematically mirror curves arise from thickening edges of the toric graphs, as shown in Figure 6.

One of the first relations between topological strings for toric manifolds and matrix models was encountered in [49, 50], where it was shown that the spectral curve of a unitary matrix model with a Gaussian (i.e., quadratic) potential agrees with the above mirror curve $H_{\text{conifold}}(x, y) = 0$ in (3.23), with 't Hooft coupling $T = g_s N$ encoded in $Q = e^{-T}$. At the same time, it was shown that the matrix model partition function reproduces the topological string partition function. More recently these ideas became important in view of the *remodeling* conjecture [51], which states that the solution to loop equations in the form found by Eynard and Orantin [48], applied to the mirror curve, reproduces topological string partition functions. The method of [48] works for arbitrary curves, not necessarily originating from matrix models. Nonetheless, it is indeed possible to construct matrix models whose partition functions do reproduce topological string amplitudes, and whose spectral curves coincide with appropriate mirror curves [29, 30, 52–56].

One of our aims is to provide matrix model interpretation of BPS counting. It is natural to expect such an interpretation in view of an intimate relation between BPS counting and topological string theory discussed in Section 2.1, and the above-mentioned relations between topological strings and matrix models. As we will see in what follows, there are indeed unitary matrix models which naturally arise in the context of BPS counting and its

fermionic formulation. Among the others, our task will be to analyze them using the above-mentioned Migdal method.

4. Fermionic Formulation of BPS Counting Functions

Having introduced all the ingredients above, we are now ready to present fermionic formulation of BPS counting. To start with, in Section 4.1 we present the idea of such a formulation in the simplest example of \mathbb{C}^3 . In Section 4.2, we introduce a general fermionic formalism, and in Section 4.3 we provide its crystal interpretation. We illustrate the use of our formalism in Section 4.4 revisiting \mathbb{C}^3 example, as well as in explicit case of $\mathbb{C}^3/\mathbb{Z}_N$, and conifold geometry.

4.1. The Idea and \mathbb{C}^3 Example

As explained in Section 2.2, the generating function of bound states of D0-branes to a single D6-brane is given by the MacMahon function, and the corresponding crystal model takes form of the counting of plane partitions [7]. Let us slice each such plane partition by a set of parallel planes, as shown in Figure 7. In this way on each slice, we obtain a two-dimensional partition μ , and it is not hard to see that each two neighboring partitions satisfy the interlacing condition (3.7). Recalling that such a condition arises if we apply $\Gamma_{\pm}(1)$ operators (3.5) to partition states, we conclude that a set of all plane partitions can be built, slice by slice, by acting with infinite sequence of $\Gamma_{\pm}(1)$ on the vacuum. To count each slice μ with appropriate weight $q^{|\mu|}$ we also need to apply weight operator \widehat{Q} defined in (3.12). Therefore, the generating function of plane partitions can be represented as follows

$$\begin{aligned} Z &= \langle \Omega_+ | \Omega_- \rangle \equiv \langle 0 | \cdots \widehat{Q}\Gamma_+(1)\widehat{Q}\Gamma_+(1)\widehat{Q}\Gamma_+(1) | \widehat{Q}\Gamma_-(1)\widehat{Q}\Gamma_-(1)\widehat{Q}\Gamma_-(1)\widehat{Q} \cdots | 0 \rangle \\ &= \langle 0 | \cdots \Gamma_+(q^2)\Gamma_+(q)\Gamma_+(1)\Gamma_-(q)\Gamma_-(q^2)\Gamma_-(q^3) \cdots | 0 \rangle \\ &= \prod_{l_1, l_2=1}^{\infty} \frac{1}{1 - q^{l_1+l_2-1}} = M(q). \end{aligned} \tag{4.1}$$

In the first line, we implicitly introduced two states $\langle \Omega_+ |$ and $| \Omega_- \rangle$, defined by an infinite sequence of Γ_+ (resp. Γ_-) operators, interlaced with weight operators \widehat{Q} and acting on the vacuum. To confirm that this correlator indeed reproduces the MacMahon function, the second line can be reduced to the final infinite product using commutation relations (3.8) and (3.14). We can also represent insertions of $\Gamma_{\pm}(1)$ operators graphically by arrows, so that the above computation can be represented as in Figure 7(b).

In what follows, we present a formalism which allows to generalize this computation to a large class of chambers, for arbitrary toric geometry without compact four cycles.

4.2. Toric Geometry and Quantization

We wish to reformulate BPS counting in the fermionic language in a way in which we associate to each toric manifold a fermionic state, such that the BPS generating function can be expressed as an overlap of two such states, generalizing \mathbb{C}^3 case (4.1). At the same time, the construction of such a fermionic state is supposed to encode the structure of the underlying

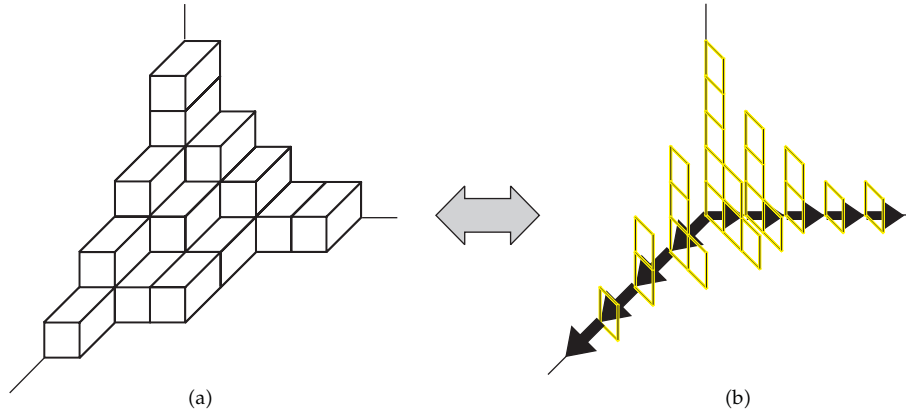


Figure 7: Slicing of a plane partition (a) into a sequence of interlacing two-dimensional partitions (b). A sequence of Γ_{\pm} operators in (4.1) which create two-dimensional partitions is represented by arrows inserted along two axes. Directions of arrows \rightarrow represent interlacing condition $>$ on partitions. We reconsider this example from a new viewpoint in Figure 10.

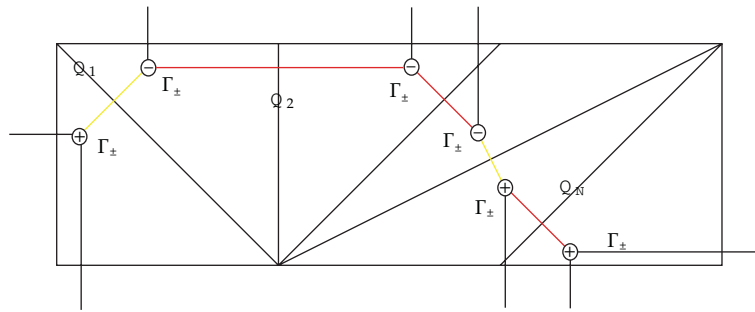


Figure 8: Toric Calabi-Yau manifolds represented by a triangulation of a strip. There are N independent \mathbb{P}^1 's with Kähler parameters $Q_i = e^{-T_i}$, and $N + 1$ vertices to which we associate Γ and Γ' operators represented respectively by \oplus and \ominus signs. Yellow intervals, which connect vertices with opposite signs, represent $\mathcal{O}(-1) \oplus \mathcal{O}(-1) \rightarrow \mathbb{P}^1$ local neighborhoods. Red intervals, which connect vertices with the same signs, represent $\mathcal{O}(-2) \oplus \mathcal{O} \rightarrow \mathbb{P}^1$ local neighborhoods. The first vertex on the left is chosen to be \oplus .

crystal model (generalizing plane partitions in Figure 7). An important difference between \mathbb{C}^3 and other geometries is the existence of many Kähler moduli and correspondingly many chambers, for which BPS generating functions change according to wall-crossing formulas. To take care of these changes in the fermionic formalism, we need to introduce special *wall-crossing* operators.

4.2.1. Toric Geometry and Fermionic Operators

In what follows we use the notation introduced in Section 3.1; in particular to each vertex of the toric diagram we associate its type $t_i = \pm 1$, see also Figure 8. We start with a construction of fermionic states associated to a given toric Calabi-Yau manifold (without compact four-cycles). First we need to introduce several operators which are building blocks of such states. The structure of these operators is encoded in the toric diagram of a given manifold. Namely,

these operators are given by a string of $N + 1$ vertex operators $\Gamma_{\pm}^{t_i}(x)$ (defined in (3.4)) which are associated to the vertices of the toric diagram; the type t_i determines the type of a vertex operator as

$$\Gamma_{\pm}^{t_i=+1}(x) = \Gamma_{\pm}(x), \quad \Gamma_{\pm}^{t_i=-1}(x) = \Gamma'_{\pm}(x). \quad (4.2)$$

In addition the string of operators $\Gamma_{\pm}^{t_i}(x)$ is interlaced with $N + 1$ operators \widehat{Q}_i representing colors q_i , for $i = 0, 1, \dots, N$. Operators $\widehat{Q}_1, \dots, \widehat{Q}_N$ are associated to \mathbb{P}^1 in the toric diagram, and there is an additional \widehat{Q}_0 . We also define

$$\widehat{Q} = \widehat{Q}_0 \widehat{Q}_1 \cdots \widehat{Q}_N, \quad q = q_0 q_1 \cdots q_N. \quad (4.3)$$

Therefore, the upper indices of $\Gamma_{\pm}^{t_i}(x)$ and a choice of colors of the operators which we introduce below are specified by the data of a given toric manifold. As we will see, a sequence of lower indices \pm is determined by the chamber we are going to consider.

Now we can associate several operators to a given toric manifold. Firstly, we define

$$\overline{A}_{\pm}(x) = \Gamma_{\pm}^{t_1}(x) \widehat{Q}_1 \Gamma_{\pm}^{t_2}(x) \widehat{Q}_2 \cdots \Gamma_{\pm}^{t_N}(x) \widehat{Q}_N \Gamma_{\pm}^{t_{N+1}}(x) \widehat{Q}_0. \quad (4.4)$$

Commuting all \widehat{Q}_i 's using (3.14), we also define the following operators:

$$\begin{aligned} A_+(x) &= \widehat{Q}^{-1} \overline{A}_+(x) = \Gamma_+^{t_1}(xq) \Gamma_+^{t_2}\left(\frac{xq}{q_1}\right) \Gamma_+^{t_3}\left(\frac{xq}{q_1 q_2}\right) \cdots \Gamma_+^{t_{N+1}}\left(\frac{xq}{q_1 q_2 \cdots q_N}\right), \\ A_-(x) &= \overline{A}_-(x) \widehat{Q}^{-1} = \Gamma_-^{t_1}(x) \Gamma_-^{t_2}(xq_1) \Gamma_-^{t_3}(xq_1 q_2) \cdots \Gamma_-^{t_{N+1}}(xq_1 q_2 q_N). \end{aligned} \quad (4.5)$$

In addition, we define the above-mentioned *wall-crossing operators*

$$\begin{aligned} \overline{W}_p(x) &= \left(\Gamma_-^{t_1}(x) \widehat{Q}_1 \Gamma_-^{t_2}(x) \widehat{Q}_2 \cdots \Gamma_-^{t_p}(x) \widehat{Q}_p \right) \left(\Gamma_+^{t_{p+1}}(x) \widehat{Q}_{p+1} \cdots \Gamma_+^{t_N}(x) \widehat{Q}_N \Gamma_+^{t_{N+1}}(x) \widehat{Q}_0 \right), \\ \overline{W}'_p(x) &= \left(\Gamma_+^{t_1}(x) \widehat{Q}_1 \Gamma_+^{t_2}(x) \widehat{Q}_2 \cdots \Gamma_+^{t_p}(x) \widehat{Q}_p \right) \left(\Gamma_-^{t_{p+1}}(x) \widehat{Q}_{p+1} \cdots \Gamma_-^{t_N}(x) \widehat{Q}_N \Gamma_-^{t_{N+1}}(x) \widehat{Q}_0 \right). \end{aligned} \quad (4.6)$$

Here the order of Γ and Γ' is the same as for \overline{A}_{\pm} operators, and the difference is that now there are subscripts \mp on first p operators and \pm on the remaining ones.

We often use a simplified notation when the argument of the above operators is $x = 1$

$$\overline{A}_{\pm} \equiv \overline{A}_{\pm}(1), \quad A_{\pm} \equiv A_{\pm}(1), \quad \overline{W}_p \equiv \overline{W}_p(1), \quad \overline{W}'_p \equiv \overline{W}'_p(1). \quad (4.7)$$

4.2.2. Fermionic Formulation and Quantization

Above we associated operators \overline{A}_{\pm} to each toric geometry with a strip-like toric diagram. From these operators, we can build the following states in the Hilbert space of a free fermion \mathcal{H} :

$$|\Omega_{\pm}\rangle \in \mathcal{H}, \quad (4.8)$$

which we define as follows:

$$\begin{aligned} \langle \Omega_+ | &= \langle 0 | \cdots \bar{A}_+(1) \bar{A}_+(1) \bar{A}_+(1) = \langle 0 | \cdots A_+(q^2) A_+(q) A_+(1), \\ |\Omega_- \rangle &= \bar{A}_-(1) \bar{A}_-(1) \bar{A}_-(1) \cdots |0\rangle = A_-(1) A_-(q) A_-(q^2) \cdots |0\rangle. \end{aligned} \quad (4.9)$$

These states encode the full instanton part of the topological string amplitudes. Namely, as shown in [16],

$$Z = \langle \Omega_+ | \Omega_- \rangle \quad (4.10)$$

is equal to the BPS partition function \mathcal{Z} in the noncommutative chamber

$$Z = \mathcal{Z} \equiv |\mathcal{Z}_{\text{top}}|^2 \equiv \mathcal{Z}_{\text{top}}(Q_i) \mathcal{Z}_{\text{top}}(Q_i^{-1}), \quad (4.11)$$

where $\mathcal{Z}_{\text{top}}(Q_i)$ is given in (3.1). The above equality holds under the following identification between q_i parameters (which enter the definition of $|\Omega_{\pm}\rangle$) and physical parameters $Q_i = e^{-T_i}$ and $q_s = e^{-g_s}$:

$$q_i = (t_i t_{i+1}) Q_i, \quad q_s = q \equiv q_0 q_1 \cdots q_N. \quad (4.12)$$

We will provide a proof of (4.10) in Section 6.1.1 in a more general setting of refined invariants.

The states $|\Omega_{\pm}\rangle$ have nontrivial structure and encode the information about the noncommutative chamber. It turns out that the fermionic vacuum $|0\rangle$ itself also encodes some interesting information. We recall that there is another extreme chamber representing just a single BPS state represented by the D6-brane with no other branes bound to it. This multiplicity 1 can be understood as

$$\tilde{\mathcal{Z}} = \tilde{Z} = \langle 0 | 0 \rangle = 1, \quad (4.13)$$

and as we will see below, starting from this expression we can use wall-crossing operators to construct BPS generating functions in an infinite family of other chambers.

4.2.3. Other Chambers and Wall-Crossing Operators

In the previous, section we associated to toric manifolds the states $|\Omega_{\pm}\rangle$, whose overlap reproduces the BPS generating function in the noncommutative chamber (4.10). Now we wish to extend this formalism to other chambers. As discussed in Section 2.1, in a given chamber, the allowed bound states we wish to count must have positive central charge (2.1)

$$Z(R, B) = \frac{1}{R} (n + \beta \cdot B) > 0. \quad (4.14)$$

Firstly, the information about R and B must be encoded in the fermionic states which we wish to construct. It turns out that the choice of positive or negative R is encoded in the choice of the ground state

$$R > 0 \longrightarrow |\Omega_{\pm}\rangle, \quad R < 0 \longrightarrow |0\rangle, \quad (4.15)$$

which generalizes the extreme cases (4.10) and (4.13).

On the other hand, the value of the field B is encoded in the insertion of additional wall-crossing operators, such as those defined in (4.6). In particular, these two types of operators are sufficient if we wish to consider only these chambers, which correspond to a flux of the B -field through only one, but arbitrary \mathbb{P}^1 in the manifold. For simplicity below, we consider only this set of chambers. Denoting this \mathbb{P}^1 as p , it can be shown that insertion of n copies of operators \overline{W}_p or \overline{W}'_p creates, respectively, n positive or negative quanta of the flux through p 'th \mathbb{P}^1 .

Therefore, schematically, the generating functions in chambers with $R > 0$ read

$$Z_n = \langle \Omega_+ | (\overline{W})^n | \Omega_- \rangle, \quad (4.16)$$

and those with $R < 0$ read

$$\tilde{Z}_n = \langle 0 | (\overline{W})^n | 0 \rangle, \quad (4.17)$$

with appropriate form of wall-crossing operators. More precisely, depending on the signs of R and B , we need to consider four possible situations, which we present below. The proofs of all statements below, corresponding to these four situations, can be found in [16].

(i) *Chambers with $R < 0, B > 0$*

Consider a chamber characterized by positive R and positive B -field through p 'th two-cycle

$$R < 0, \quad B \in]n-1, n[, \quad \text{for } 1 \leq n \in \mathbb{Z}. \quad (4.18)$$

The BPS partition function in this chamber contains only those factors which include Q_p and it reads

$$\tilde{\mathcal{Z}}_{n|p} = \prod_{i=1}^{n-1} \prod_{s=1}^p \prod_{r=p+1}^{N+1} \left(1 - \frac{q_s^i}{Q_s Q_{s+1} \cdots Q_{r-1}} \right)^{-t_r t_s i}. \quad (4.19)$$

This can be expressed as the expectation value of n wall-crossing operators \overline{W}_p

$$\tilde{Z}_{n|p} = \langle 0 | (\overline{W}_p)^n | 0 \rangle = \tilde{\mathcal{Z}}_{n|p}, \quad (4.20)$$

under the following identification of variables:

$$Q_p = (t_p t_{p+1}) q_p q_s^n, \quad Q_i = (t_i t_{i+1}) q_i \quad \text{for } i \neq p, \quad q_s = \frac{1}{q}. \quad (4.21)$$

A special case of this result is the trivial generating function (4.13) representing a single D6-brane.

(ii) *Chambers with $R > 0, B > 0$*

In the second case, we consider the positive value of R and the positive flux through p' th \mathbb{P}^1

$$R > 0, \quad B \in]n, n+1[, \quad \text{for } 0 \leq n \in \mathbb{Z}. \quad (4.22)$$

Denote the BPS partition function in this chamber by $\mathcal{Z}_{n|p}$. We find that the expectation value of n wall-crossing operators \overline{W}_p in the background of $|\Omega\rangle$ has the form

$$Z_{n|p} = \langle \Omega_+ | (\overline{W}_p)^n | \Omega_- \rangle = M(1, q)^{N+1} Z_{n|p}^{(0)} Z_{n|p}^{(1)} Z_{n|p}^{(2)}, \quad (4.23)$$

where $Z_{n|p}^{(0)}$ does not contain any factors $(q_s \cdots q_{r-1})^{\pm 1}$ which would include q_p , while $Z_{n|p}^{(1)}$ contains all factors $q_s \cdots q_{r-1}$ which do include q_p , and $Z_{n|p}^{(2)}$ contains all factors $(q_s \cdots q_{r-1})^{-1}$ which also include q_p :

$$\begin{aligned} Z_{n|p}^{(0)} &= \prod_{l=1}^{\infty} \prod_{p \notin s, r+1 \subset \overline{1, N+1}} \left(1 - (t_r t_s) \frac{q^l}{q_s q_{s+1} \cdots q_{r-1}} \right)^{-t_r t_s l} \left(1 - (t_r t_s) q^l q_s q_{s+1} \cdots q_{r-1} \right)^{-t_r t_s l}, \\ Z_{n|p}^{(1)} &= \prod_{l=1}^{\infty} \prod_{p \in s, r+1 \subset \overline{1, N+1}} \left(1 - (t_r t_s) q^{l+n} q_s q_{s+1} \cdots q_{r-1} \right)^{-t_r t_s l}, \\ Z_{n|p}^{(2)} &= \prod_{l=n+1}^{\infty} \prod_{p \in s, r+1 \subset \overline{1, N+1}} \left(1 - (t_r t_s) \frac{q^{l-n}}{q_s q_{s+1} \cdots q_{r-1}} \right)^{-t_r t_s l}. \end{aligned} \quad (4.24)$$

We see that the identification of variables

$$Q_p = (t_p t_{p+1}) q_p q_s^n, \quad Q_i = (t_i t_{i+1}) q_i \quad \text{for } i \neq p, \quad q_s = q \quad (4.25)$$

reproduces the BPS partition function

$$\mathcal{Z}_{n|p} = Z_{n|p}. \quad (4.26)$$

When no wall-crossing operator is inserted the change of variables reduces to (4.12) and we get the noncommutative Donaldson-Thomas partition function (4.11), $Z_{0|p} = \mathcal{Z}$.

(iii) *Chambers with $R < 0, B < 0$*

Now we consider negative R and negative B -field

$$R < 0, \quad B \in]-n-1, -n[\quad \text{for } 0 \leq n \in \mathbb{Z}. \quad (4.27)$$

For such a chamber the BPS partition function reads

$$\tilde{\mathcal{Z}}'_{n|p} = \prod_{i=1}^n \prod_{s=1}^p \prod_{r=p+1}^{N+1} \left(1 - q_s^i Q_s Q_{s+1} \cdots Q_{r-1} \right)^{-t_r t_s^i}. \quad (4.28)$$

Now we find the expectation value of n wall-crossing operators \overline{W}'_p is equal to

$$\tilde{Z}'_{n|p} = \langle 0 | \left(\overline{W}'_p \right)^n | 0 \rangle = \tilde{\mathcal{Z}}'_{n|p}, \quad (4.29)$$

under the change of variables

$$Q_p = (t_p t_{p+1}) q_p q_s^{-n}, \quad Q_i = (t_i t_{i+1}) q_i \quad \text{for } i \neq p, \quad q_s = \frac{1}{q}. \quad (4.30)$$

Now an insertion of \overline{W}'_p has an interpretation of turning on a negative quantum of B -field, and the redefinition of Q_p can be interpreted as effectively reducing t_p by one unit of g_s . As already discussed,

$$\tilde{Z}'_{0|p} = \langle 0 | 0 \rangle = 1 \quad (4.31)$$

represents a chamber with a single D6-brane and no other branes bound to it.

(iv) *Chambers with $R > 0, B < 0$*

In the last case, we consider positive R and negative B

$$R > 0, \quad 0 > B \in]-n, -n+1[, \quad \text{for } 1 \leq n \in \mathbb{Z}. \quad (4.32)$$

We denote the BPS partition function in this chamber by $\mathcal{Z}'_{n|p}$. We find that the expectation value of n operators \overline{W}'_p in the background of $|\Omega_{\pm}\rangle$ has the form

$$Z'_{n|p} = \langle \Omega_+ | \left(\overline{W}'_p \right)^n | \Omega_- \rangle = M(1, q)^{N+1} Z'_{n|p(0)} Z'_{n|p(1)} Z'_{n|p(2)}, \quad (4.33)$$

where $Z'_{n|p}{}^{(0)}$ does not contain any factors $(q_s \cdots q_{r-1})^{\pm 1}$ which would include q_p , $Z'_{n|p}{}^{(1)}$ contains all factors $q_s \cdots q_{r-1}$ which do include q_p , and $Z'_{n|p}{}^{(2)}$ contains all factors $(q_s \cdots q_{r-1})^{-1}$ which also include q_p :

$$\begin{aligned} Z'_{n|p}{}^{(0)} &= \prod_{l=1}^{\infty} \prod_{p \notin \{s, r+1, \dots, N+1\}} \left(1 - (t_r t_s) \frac{q^l}{q_s q_{s+1} \cdots q_{r-1}} \right)^{-t_r t_s l} \left(1 - (t_r t_s) q^l q_s q_{s+1} \cdots q_{r-1} \right)^{-t_r t_s l}, \\ Z'_{n|p}{}^{(1)} &= \prod_{l=n}^{\infty} \prod_{p \in \{s, r+1, \dots, N+1\}} \left(1 - (t_r t_s) q^{l-n} q_s q_{s+1} \cdots q_{r-1} \right)^{-t_r t_s l}, \\ Z'_{n|p}{}^{(2)} &= \prod_{l=1}^{\infty} \prod_{p \in \{s, r+1, \dots, N+1\}} \left(1 - (t_r t_s) \frac{q^{l+n}}{q_s q_{s+1} \cdots q_{r-1}} \right)^{-t_r t_s l}. \end{aligned} \quad (4.34)$$

Under the change of variables,

$$Q_p = (t_p t_{p+1}) q_p q_s^{-n-1}, \quad Q_i = (t_i t_{i+1}) q_i, \quad \text{for } i \neq p, \quad q_s = q. \quad (4.35)$$

This reproduces the BPS partition function

$$\mathcal{Z}'_{n|p} = Z'_{n|p}. \quad (4.36)$$

We note that both $Z'_{1|p}$ with the above change of variables, as well as $Z_{0|p}$ given in (4.23) with a different change of variables in (4.25), lead to the same BPS generating function \mathcal{Z} which corresponds to the noncommutative Donaldson-Thomas invariants.

4.3. Crystal Melting Interpretation

In the previous section, we found a free fermion representation of D6-D2-D0 generating functions. The fermionic correlators which reproduce BPS generating functions automatically provide melting crystal interpretation of these functions [16], generalizing models of plane partitions (for \mathbb{C}^3) or pyramid partitions (for the conifold), presented in Section 2.2. These crystals are also equivalent to those found in [17, 22].

The crystal interpretation is a consequence of the fact that all operators used in the construction of states $|\Omega_{\pm}\rangle$, as well as the wall-crossing operators, are built just from vertex operators Γ_{\pm} and $\tilde{\Gamma}_{\pm}$ with argument 1, and color operators \hat{Q}_i . As follows from (3.5) and (3.6), insertion of these vertex operators is equivalent to the insertion of two-dimensional partitions satisfying interlacing, or transposed interlacing conditions. An infinite sequence of such interlacing partitions effectively builds up a three-dimensional crystal. A relative position of two adjacent slices is determined by a type of two corresponding vertex operators. On the other hand, insertions of color operators have an interpretation of coloring the crystal. The colors \hat{Q}_i appear in the same order in each composite operator, so these colors are always repeated periodically in the full correlators. Therefore, three-dimensional crystals are built of interlacing, periodically colored slices.

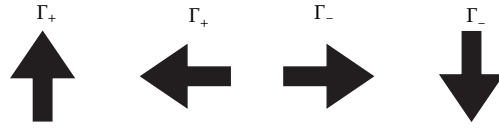


Figure 9: Assignment of arrows.

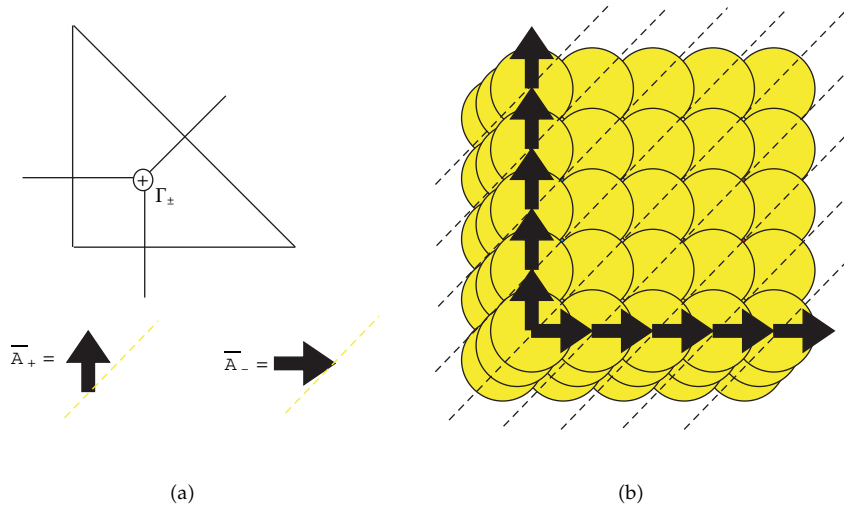


Figure 10: Toric diagram for \mathbb{C}^3 (a) consists of one \oplus vertex. Operators \bar{A}_\pm involve a single Γ_\pm and have a simple arrow (lower part of (a)), as follows from Figure 9. The correlator (4.1) is translated into a sequence of arrows, with rotated dashed lines representing insertions of interlacing two-dimensional partitions. The resulting figure (b) represents plane partitions crystal model, the same as in Figure 7, but now seen from the bottom.

To get more insight about a geometric structure of a crystal, it is convenient to introduce the following graphical representation. We associate various arrows to the vertex operators, as shown in Figure 9. These arrows follow the order of the vertex operators in the fermionic correlators and are drawn from left to right, or up to down (either of these directions is independent of the orientation of the arrow). Following the order of the vertex operators in a given correlator, and drawing a new arrow at the end of the previous one, produces a zig-zag path which represents a shape of the crystal. The coloring of the crystal is taken care of by keeping track of the order of \hat{Q}_i operators, and by drawing at the endpoint of each arrow a (dashed) line, rotated by 45° , colored according to \hat{Q}_i which we come across. These lines represent two-dimensional slices in appropriate colors. In this way, the corners of two-dimensional partitions arising from slicing of the crystal are located at the end-points of the arrows. The orientation of arrows represents the interlacing condition (i.e., arrows point from a larger to smaller partition). The interlacing pattern between two consecutive slices corresponds to the types of two consecutive arrows. Finally, the points from which two arrows point outwards represent those stones in the crystal, which can be removed from the initial, full crystal configuration. In fermionic correlators, these points correspond to $\Gamma_+^{t_i}$ followed by $\Gamma_-^{t_i}$ operators. We illustrate this graphical construction in a few examples in the next section.

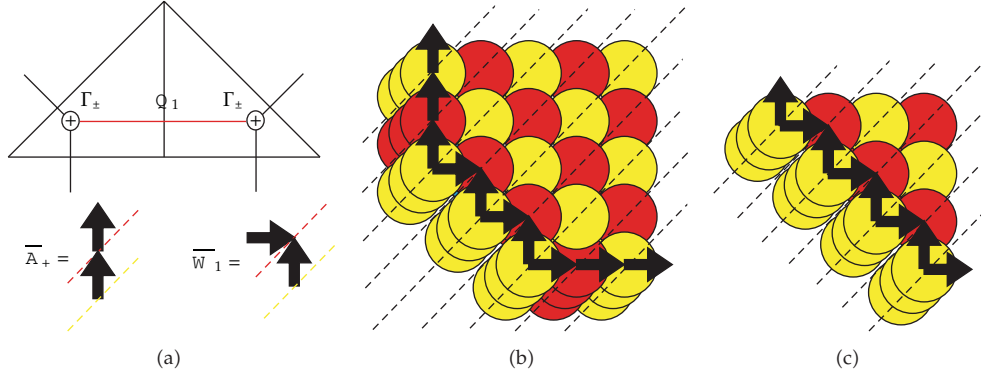


Figure 11: Toric diagram for the resolution of $\mathbb{C}^3/\mathbb{Z}^{N+1}$ geometry has $N + 1$ vertices of the same type \oplus . (a): toric diagram for $N = 1$ and arrow representation of \bar{A}_+ and \bar{W}_1 . In the noncommutative chamber, this leads to the same plane partition crystal as in Figure 10, however colored now in yellow and red. (b): for the chamber with positive R and $2 < B < 3$, the crystal develops two additional corners and its generating function reads $Z_{2|1} = \langle \Omega_+ | (\bar{W}_1)^2 | \Omega_- \rangle$. (c): for negative R and positive $n - 1 < B < n$ the crystal is finite along two axes and develops $n - 1$ yellow corners; its generating function for the case of $n = 5$ shown in the picture reads $\tilde{Z}_{5|1} = \langle 0 | (\bar{W}_1)^5 | 0 \rangle$ (two external arrows, corresponding to Γ_- acting on $\langle 0 |$ and Γ_+ acting on $| 0 \rangle$, are suppressed.).

4.4. Examples

4.4.1. Revisiting \mathbb{C}^3

Let us reconsider \mathbb{C}^3 geometry which motivated our discussion in Section 4.1. In this case, the dual toric diagram consists just of one triangle, see Figure 10(a), so there is just one vertex and only one color $\hat{Q}_0 \equiv \hat{Q}$, and the operators (4.4) take form

$$\bar{A}_\pm = \Gamma_\pm(1)\hat{Q}. \quad (4.37)$$

In consequence, the BPS partition function (4.10) takes exactly the form (4.1).

The crystal structure can be read off from a sequence of arrows associated to \hat{A}_\pm operators, following the rules in Figure 9. This gives rise to the crystal shown in Figure 10(b). This is the same crystal as in Figure 7, which represents plane partitions, however, now seen from the opposite side.

4.4.2. Orbifolds $\mathbb{C}^3/\mathbb{Z}^{N+1}$

Now we consider the resolution of $\mathbb{C}^3/\mathbb{Z}^{N+1}$ orbifold. In this case, the toric diagram takes form of a triangle of area $(N + 1)/2$, see Figure 11(a). There are N independent \mathbb{P}^1 's and $N + 1$ vertices of the same $t_i = +1$, and operators in (4.4) take the form

$$\bar{A}_\pm = \Gamma_\pm(1)\hat{Q}_1\Gamma_\pm(1)\hat{Q}_2 \cdots \Gamma_\pm(1)\hat{Q}_N\Gamma_\pm(1)\hat{Q}_0. \quad (4.38)$$

In the noncommutative chamber, the corresponding crystal consists of plane partitions, however, with slices colored periodically in $N + 1$ colors. The partition function in the noncommutative chamber is given by (4.10).

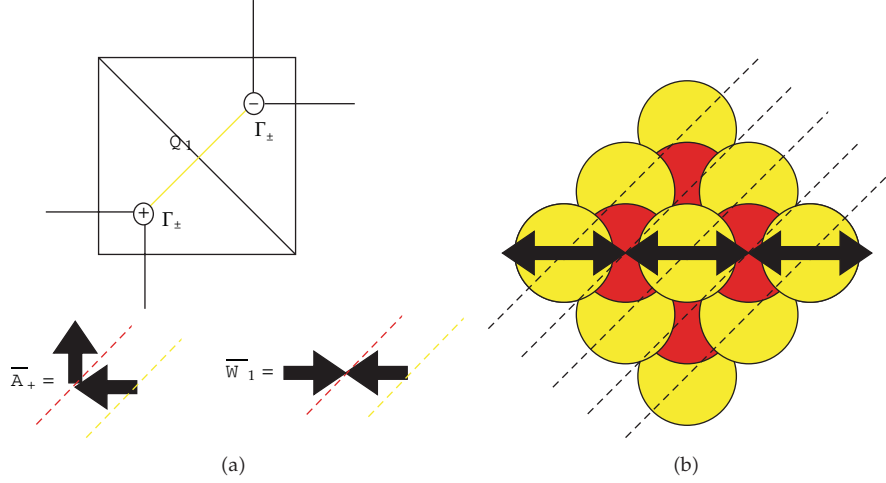


Figure 12: (a): toric diagram for the conifold and arrow representation of \bar{A}_+ and \bar{W}_1 . (b): for chambers with negative R and positive $n - 1 < B < n$ the crystals are given by finite pyramid partitions with $n - 1$ additional corners, represented by $n - 1$ stones in the top row (the figure shows the case $n = 4$). The generating function is given by $\tilde{Z}_{n|1} = \langle 0 | (\bar{W}_1)^n | 0 \rangle$ which reproduces the result (2.27).

If we turn on an arbitrary B -field through a fixed \mathbb{P}^1 , the structure of wall-crossing operators gives rise to modified containers, see for example Figure 11(b). In particular, enlarging the B -field by one unit adds one more yellow corner to the crystal.

The crystals corresponding to $R < 0$ are also easy to find. In the extreme chamber, we get a trivial (empty) crystal, representing a single D6-brane (4.13). Adding wall-crossing operators results in a crystal with several corners, finite along two axis (and extending infinitely along the third axis), as shown in Figure 11(c).

4.4.3. Resolved Conifold

We already presented pyramid crystals for the conifold in Section 2.2. They arise from our formalism as follows. The dual toric diagram for the conifold, see Figure 12(a), consists of two triangles and encodes a single $(N = 1) \mathbb{P}^1$. Two vertices of the toric diagram correspond to two colors \hat{Q}_1 and \hat{Q}_0 , so that

$$\hat{Q} = \hat{Q}_1 \hat{Q}_0, \quad q = q_1 q_0. \quad (4.39)$$

The operators (4.4) in this case read

$$\bar{A}_{\pm}(x) = \Gamma_{\pm}(x) Q_1 \Gamma'_{\pm}(x) Q_0, \quad (4.40)$$

while (4.5) is

$$A_+(x) = \Gamma_+(xq) \Gamma'_+ \left(\frac{xq}{q_1} \right), \quad A_-(x) = \Gamma_-(x) \Gamma'_-(xq_1), \quad (4.41)$$

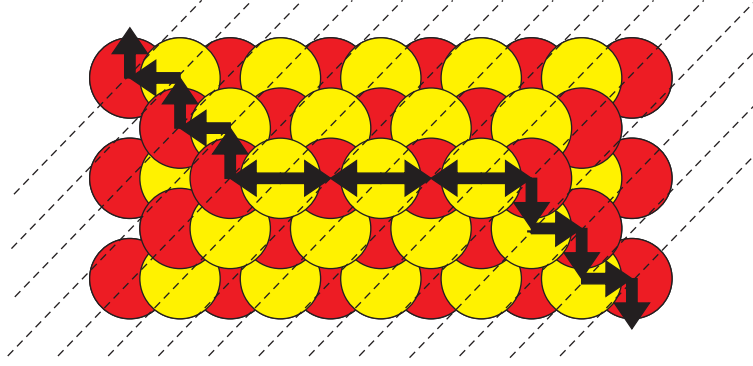


Figure 13: Conifold crystal in the chamber with positive R and $2 < B < 3$ takes form of pyramid partitions with 3 stones in the top row. Its generating function is given by $Z_{2|1} = \langle \Omega_+ | (\overline{W}_1)^2 | \Omega_- \rangle$.

and they satisfy

$$A_+(x)A_-(y) = \frac{(1 + xyq/q_1)(1 + xyqq_1)}{(1 - xyq)^2} A_-(y)A_+(x). \quad (4.42)$$

The quantum states (4.9) take form

$$\begin{aligned} |\Omega_- \rangle &= A_-(1)A_-(q)A_-(q^2) \cdots |0\rangle, \\ \langle \Omega_+ | &= \langle 0 | \cdots A_+(q^2)A_+(q)A_+(1), \end{aligned} \quad (4.43)$$

and the wall-insertion operators (4.6) are

$$W_1(x) = \Gamma_-(x)Q_1\Gamma'_+(x)Q_0, \quad W'_1(x) = \Gamma_+(x)Q_1\Gamma'_-(x)Q_0. \quad (4.44)$$

Therefore, the fermionic correlators take form

$$\begin{aligned} Z_{n|1} &= \langle \Omega_+ | (\overline{W}_1)^n | \Omega_- \rangle, \\ \tilde{Z}_{n|1} &= \langle 0 | (\overline{W}_1)^n | 0 \rangle. \end{aligned} \quad (4.45)$$

and encode generating functions (2.25) and (2.27) introduced in Section 2.2. In the noncommutative chamber, we get the result found first in [14], $Z_{0|1} = \langle \Omega_+ | \Omega_- \rangle$, while a single D6-brane is encoded in $\tilde{Z} = \langle 0 | 0 \rangle = 1$. These crystals are shown in Figures 12(b) and 13.

5. Matrix Models and Open BPS Generating Functions

In this section, we explain how matrix model formalism can be applied to analyze BPS counting functions. In the first part, Section 5.1, we explain how to relate fermionic formalism,

derived in the previous section, to matrix model representation. In Section 5.2, we illustrate how to construct matrix models for the closed noncommutative chamber. In Section 5.3, we analyze in detail BPS generating functions for the conifold for all chambers with $R > 0$, and derive corresponding spectral curves. We discuss how these curves relate to (and generalize) mirror curves, which we find (as we should) in the commutative chamber. In Section 5.4, we reveal that matrix model representation in fact encodes open BPS generating functions, which can be identified with matrix model integrands.

5.1. Matrix Models from Free Fermions

Let us explain how to relate fermionic representation of BPS amplitudes, introduced in Section 4.2, to matrix models. This relies on introducing into fermionic correlators representing BPS generating functions, such as (4.10) or (4.23), a special representation of the identity operator \mathbb{I} . The representation we are interested in also consists of infinite product of vertex operators and arises as follows [29]. Firstly, we can use the representation as a complete set of states $\mathbb{I} = |R\rangle\langle R|$, which represent two-dimensional partitions. Using orthogonality relations of $U(\infty)$ characters χ_R , and the fact that these characters are given in terms of Schur functions $\chi_R = s_R(\vec{z})$ for $\vec{z} = (z_1, z_2, z_3, \dots)$, we can write

$$\begin{aligned} \mathbb{I} &= \sum_R |R\rangle\langle R| = \sum_{P,R} \delta_{P^t R^t} |P\rangle\langle R| \\ &= \int \mathfrak{D}U \sum_{P,R} s_{P^t}(\vec{z}) \overline{s_{R^t}(\vec{z})} |P\rangle\langle R| \\ &= \int \mathfrak{D}U \left(\prod_{\alpha} \Gamma'_{-}(z_{\alpha}) |0\rangle \right) \left(\langle 0 | \prod_{\alpha} \Gamma'_{+}(z_{\alpha}^{-1}) \right). \end{aligned} \quad (5.1)$$

When such a representation of the identity operator is introduced into (4.10) or (4.23) (or any other correlator of similar structure), we can commute away $\Gamma_{\pm}^{t_i}$ operators and get rid of operator expressions. For example, inserting the above identity operator in the string of \overline{A}_+ operators in (4.16) leads to a matrix model with the unitary measure

$$\begin{aligned} Z_n &= \langle 0 | \prod_{i=k}^{\infty} \overline{A}_+(1) | \mathbb{I} | \prod_{j=0}^{k-1} \overline{A}_+(1) | \overline{W}^n | \Omega_- \rangle \\ &= \int \mathfrak{D}U \langle 0 | \prod_{i=k+1}^{\infty} \overline{A}_+(1) | \prod_{\alpha} \Gamma'_{-}(z_{\alpha}) | 0 \rangle \langle 0 | \prod_{\alpha} \Gamma'_{+}(z_{\alpha}^{-1}) | \prod_{j=0}^k \overline{A}_+(1) | \overline{W}^n | \Omega_- \rangle \\ &= f_n^k(q, Q_i) \int \mathfrak{D}U \prod_{\alpha} e^{-(1/g_s) V_n^k(z_{\alpha})}. \end{aligned} \quad (5.2)$$

The product over α represents distinct eigenvalues z_{α} . Note that we have inserted \mathbb{I} at the position k in the string of $\overline{A}_+(1)$ operators. In particular, this affects the form of the resulting potential $V_n^k(z)$. Moreover, apart from matrix integral, we find some overall factors $f_n^k(q, Q_i)$ which take form of various infinite products. They arise, in a generic chamber, from

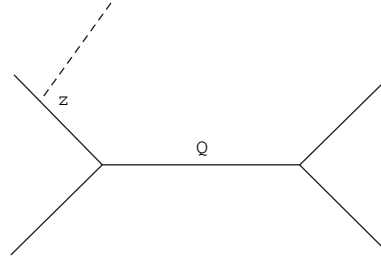


Figure 14: Brane associated to the external leg of a toric diagram (of a conifold in this particular case). Closed string parameter is denoted by Q and open string parameter by z .

commutations between Γ_{\pm} ingredients of wall-crossing operators, and Γ_{\mp} ingredients of $|\Omega_{\mp}\rangle$ states. In the closed noncommutative chamber $n = 0$, these factors are trivial, $f_{n=0}(q, Q_i) = 1$, and they largely simplify in the commutative chamber $n \rightarrow \infty$.

There is a large freedom in choosing the value of k , and it is natural to ask if this choice has some physical interpretation. It was argued in [27] that this is indeed the case, and the choice of k is equivalent to the choice of open BPS chamber (open BPS chambers were introduced in Section 2.1). In particular, it turns out that the open generating parameter can be identified with matrix eigenvalues z_{α} , and the open BPS generating function (2.16) in the open chamber labeled by k can be identified with matrix integrand

$$\mathcal{Z}_{\text{BPS}}^{\text{open}} = e^{-(1/g_s)V_n^k(z)}. \tag{5.3}$$

Even though the overall factors f_n^k in (5.1) may involve closed moduli Q_i , they do not involve open moduli z . In this sense, the matrix integrand is well defined, and up to some simple identification can be identified with open BPS generating function. This identification of parameters amounts to the shift $z \rightarrow -zq^{1/2}$ (to match earlier M-theory convention with half-integer powers of q , to integer powers of q in the fermionic formalism), as well as identification of Kähler parameters considered in M-theory derivation with parameters μ_i introduced below. We also note that the BPS generating function in (2.16) is determined by the open topological string partition function associated to the external axis of the toric diagram, as in Figure 14. As we will also see, the value of the above integral (5.1) can be related to some more general Calabi-Yau geometry Y .

5.2. Matrix Models for the Noncommutative Chamber

In this section, we illustrate the relation between BPS counting and matrix models in case of the noncommutative chamber $n = 0$, and the choice of open chamber also $k = 0$. This corresponds to the insertion of the identity representation (75) exactly in between $|\Omega_{\pm}\rangle$ states in (4.10). In this $n = 0$ case no factor f_n^k in (5.1) arises, and we obtain matrix models with potentials which can be expressed in terms of the following version of the theta function:

$$\Theta(z; q) = \prod_{j=0}^{\infty} \left(1 + zq^j\right) \left(1 + \frac{q^{j+1}}{z}\right). \tag{5.4}$$

For a general geometry of the form shown in Figure 8, with types of vertices given by t_i , corresponding matrix models take form

$$Z = \int dU \prod_{\alpha} e^{-(1/g_s)V(z_{\alpha})} = \int dU \prod_{\alpha} \prod_{l=0}^N \Theta(t_{l+1} z_{\alpha} (q_1 \cdots q_l); q)^{t_{l+1}}, \quad (5.5)$$

where integral is over unitary matrices of infinite size, $N = \infty$. Special cases of this result include

- (i) for \mathbb{C}^3 , the result (5.5) provides a matrix model representation of MacMahon function $Z = M(1) = \prod_{k=1}^{\infty} (1 - q^k)^{-k}$ in terms of a matrix model of the form (5.5) with the integrand

$$e^{-(1/g_s)V(z)} = \prod_{j=0}^{\infty} (1 + zq^j) \left(1 + \frac{q^{j+1}}{z}\right) = \Theta(z; q); \quad (5.6)$$

- (ii) for the conifold, we obtain a representation of the pyramid partition generating function (2.23) (with $n = 0$) in terms of a matrix model with the integrand

$$e^{-(1/g_s)V(z)} = \prod_{j=0}^{\infty} \frac{(1 + zq^j)(1 + q^{j+1}/z)}{(1 + Qzq^j)(1 + (q^{j+1}/Qz))} = \frac{\Theta(z; q)}{\Theta(Qz; q)}; \quad (5.7)$$

- (iii) for $\mathbb{C}^3/\mathbb{Z}^{N+1}$, we have $t_p = +1$ for all p and we find matrix model representation of the BPS generating function in terms of a matrix model with the integrand

$$\begin{aligned} e^{-(1/g_s)V(z)} &= \prod_{j=0}^{\infty} (1 + zq^j) \left(1 + \frac{q^{j+1}}{z}\right) \cdots (1 + (q_1 \cdots q_N)zq^j) \left(1 + \frac{q^{j+1}}{(q_1 \cdots q_N)z}\right) \\ &= \prod_{l=0}^N \Theta((q_1 \cdots q_l)z; q). \end{aligned} \quad (5.8)$$

5.3. Matrix Model for the Conifold Analysis

In this section, we illustrate how matrix model techniques can be used in the context of models which arise for BPS counting. We focus on the conifold matrix model in arbitrary closed BPS chamber n , and fixed $k = 0$. In this case, the result (5.2) takes form (after the redefinition $Q = -q_1 q^n$)

$$\begin{aligned} Z_n &= M(q)^2 \prod_{j=1}^{\infty} (1 - Qq^j)^j (1 - Q^{-1}q^{j+n})^{j+n} \\ &= f_n(q, Q) \int dU \prod_{\alpha} \prod_{j=0}^{\infty} \frac{(1 + z_{\alpha} q^{j+1})(1 + q^j/z_{\alpha})}{(1 + z_{\alpha} q^{j+n+1}/Q)(1 + q^j Q/z_{\alpha})} = f_n(q, Q) Z_{\text{matrix}}, \end{aligned} \quad (5.9)$$

with

$$f_n(q, Q) = M(q) \frac{\prod_{j=1}^{\infty} (1 - q^{n+j}/Q)^n}{M(q^n, q)}, \quad (5.10)$$

with MacMahon function $M(q)$ defined in (2.17), and with the following generalized MacMahon function

$$M(z, q) = \prod_{i=1}^{\infty} \frac{1}{(1 - zq^i)^i}. \quad (5.11)$$

In particular, in the noncommutative chamber $f_0^{\text{conifold}} = 1$, and in the commutative chamber $f_{n \rightarrow \infty}^{\text{conifold}} = M(q)$ which represents topological string degree zero contributions. The result (5.9) implies that the value of the matrix model integral (without the prefactor f_n) is equal to

$$\begin{aligned} Z_{\text{matrix}} &= \frac{Z_n}{f_n(q, Q)} = M(q) \prod_{j=1}^{\infty} \frac{(1 - Qq^j)^j (1 - \mu q^j)^j}{(1 - \mu Qq^j)^j} \\ &= \int dU \prod_{\alpha} \prod_{j=0}^{\infty} \frac{(1 + z_{\alpha} q^{j+1})(1 + q^j/z_{\alpha})}{(1 + z_{\alpha} q^{j+n+1}/Q)(1 + q^j Q/z_{\alpha})}, \end{aligned} \quad (5.12)$$

where $\mu = q^n/Q$.

Now we wish to analyze the matrix model Z_{matrix} . We parametrize the 't Hooft coupling and the chamber dependence, respectively, by

$$T = g_s N, \quad \tau = n g_s. \quad (5.13)$$

As our models correspond to $U(\infty)$ matrices, ultimately we are interested in the limit

$$T \rightarrow \infty, \quad g_s = \text{const}, \quad Q = \text{const}, \quad (5.14)$$

for each fixed chamber (i.e., fixed n and therefore τ). The noncommutative chamber corresponds to $\tau = 0$, while $\tau \rightarrow \infty$ represents the topological string chamber.

Using the expansion of the quantum dilogarithm

$$\log \prod_{i=1}^{\infty} (1 - zq^i) = -\frac{1}{g_s} \sum_{m=0}^{\infty} \text{Li}_{2-m}(z) \frac{B_m g_s^m}{m!}, \quad (5.15)$$

and the redefinition of the unitary measure (3.17) we find, to the leading order in g_s , the following matrix model potential:

$$V_{\tau} = T \log(z) + \text{Li}_2(-z) + \text{Li}_2\left(-\frac{1}{z}\right) - \text{Li}_2\left(-\frac{Q}{z}\right) - \text{Li}_2\left(-\frac{z}{Qe^{\tau}}\right), \quad (5.16)$$

so that

$$\partial_z V_\tau = \frac{T - \log(z + Q) + \log(1 + (z/Qe^\tau))}{z}. \quad (5.17)$$

Now we wish to solve the model (5.9) in the small g_s limit. Firstly, we need to find the resolvent $\omega(p)$, which can be done using the Migdal integral (3.18), and careful derivation is presented in [29]. As we expect one-cut solution of our model, from the Migdal integral we get an expression in terms of the end-points of this cut a and b . The normalization condition (3.19) imposes two constraints, for terms of order p^0 and p^{-1} in the resolvent, which take form

$$\begin{aligned} \frac{\sqrt{a+Q} - \sqrt{b+Q}}{\sqrt{a+Qe^\tau} - \sqrt{b+Qe^\tau}} &= Q^{1/2} e^{(\tau+T)/2}, \\ \frac{\sqrt{(a+Q)b} - \sqrt{(b+Q)a}}{\sqrt{(a+Qe^\tau)b} - \sqrt{(b+Qe^\tau)a}} &= Q^{1/2} e^{-(\tau+T)/2}. \end{aligned} \quad (5.18)$$

These constraints can be solved in the exact form, with result

$$\begin{aligned} a &= -1 + e^2 \frac{(1-\mu)(1-\mu\epsilon^2) + (1-Q)(1+\mu\epsilon^2 - 2\mu)}{(1-\mu\epsilon^2)^2} \\ &\quad + 2i\epsilon \frac{\sqrt{(1-Q)(1-\epsilon^2)(1-\mu)(1-Q\mu\epsilon^2)}}{(1-\mu\epsilon^2)^2}, \\ b &= -1 + e^2 \frac{(1-\mu)(1-\mu\epsilon^2) + (1-Q)(1+\mu\epsilon^2 - 2\mu)}{(1-\mu\epsilon^2)^2} \\ &\quad - 2i\epsilon \frac{\sqrt{(1-Q)(1-\epsilon^2)(1-\mu)(1-Q\mu\epsilon^2)}}{(1-\mu\epsilon^2)^2}, \end{aligned} \quad (5.19)$$

where we introduced

$$\epsilon = e^{-T/2}, \quad \mu = \frac{1}{Qe^\tau}. \quad (5.20)$$

Substituting these end-points back to the formula for the resolvent, we find

$$\omega_\pm(p) = \frac{1}{pT} \log \left(\frac{(1+\mu\epsilon^2)p + (1+Q\epsilon^2) \mp (1-\mu\epsilon^2)\sqrt{(p-a)(p-b)}}{2e^{-T}(p+Q)} \right). \quad (5.21)$$

As a check, this result indeed satisfies the consistency condition (3.20)

$$\omega_+(p) + \omega_-(p) = \frac{\partial_p V_\tau(p)}{T}, \quad (5.22)$$

with V_τ given in (5.16). From the knowledge of the resolvent, we can also determine eigenvalue density along the cut (3.21)

$$\rho(p) = \frac{1}{pT} \log \left(\frac{(1 + \mu\epsilon^2)p + 1 + Q\epsilon^2 - (1 - \mu\epsilon^2)\sqrt{(p-a)(p-b)}}{(1 + \mu\epsilon^2)p + 1 + Q\epsilon^2 + (1 - \mu\epsilon^2)\sqrt{(p-a)(p-b)}} \right), \quad (5.23)$$

as well as the spectral curve. Writing $x = pT\omega(p)$ and $p = e^y$, and after a few simple rescalings, we find that the spectral curve takes form

$$e^{x+y} + e^x + e^y + Q_1 e^{2x} + Q_2 e^{2y} + Q_3 = 0, \quad (5.24)$$

where

$$\begin{aligned} Q_1 &= \epsilon^2 \frac{1 + \mu Q}{(1 + \mu\epsilon^2)(1 + Q\epsilon^2)}, \\ Q_2 &= \mu \frac{1 + Q\epsilon^2}{(1 + \mu Q)(1 + \mu\epsilon^2)}, \\ Q_3 &= Q \frac{1 + \mu\epsilon^2}{(1 + \epsilon^2 Q)(1 + \mu Q)}. \end{aligned} \quad (5.25)$$

The above curve is given by a symmetric function of Q , $\mu = Q^{-1}q^n$ and $\epsilon^2 = e^{-T}$. Apparently this is a mirror curve of the so-called *closed topological vertex* geometry, which is a Calabi-Yau manifold arising from a symmetric resolution of $\mathbb{C}^3/\mathbb{Z}_2 \times \mathbb{Z}_2$ orbifold, see Figure 15. This geometry has three moduli, that is, the original Kähler moduli Q of the resolved conifold, the chamber parameter n (encoded in μ), and the 't Hooft parameter T , which are all unified in a geometric way in our matrix model. Moreover, the fractional coefficients in the curve equation (5.24) encode the correct mirror map for the closed topological vertex geometry (and to the linear order, these coefficients are just Q , μ , and e^{-T}).

In the BPS counting problem we are interested in, as follows from the form of the identity operator (5.1), ultimately we need to consider matrices of infinite size. We also need to keep fixed g_s , so we should consider the limit of $T \rightarrow \infty$, or equivalently $\epsilon \rightarrow 0$. Up to a linear shift of x and y , the (5.24) in this limit becomes

$$\mu e^{2y} + e^{x+y} + e^x + (1 + Q\mu)e^y + Q = 0. \quad (5.26)$$

The manifold corresponding to this curve is the *suspended pinch point* (SPP) geometry, with Q and μ encoding flat coordinates representing sizes of its two \mathbb{P}^1 's. Having found the SPP mirror curve, let us also make the following remarks.

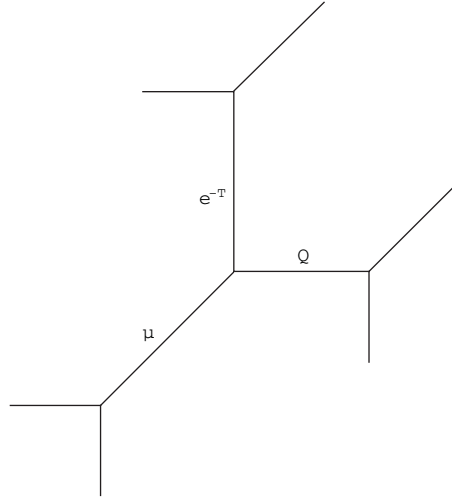


Figure 15: The spectral curve for the conifold matrix model (5.9) in arbitrary closed BPS chamber coincides with the mirror curve of the closed topological vertex geometry, whose toric diagram is shown above. This geometry has three \mathbb{P}^1 moduli, which encode conifold size Q , the closed BPS chamber via μ , and finite 't Hooft coupling via e^{-T} .

Firstly, we see that not only the spectral and mirror curves agree, but moreover the matrix integral (5.9) reproduces (after the identification $q = q_s$) the full topological string partition function of the SPP geometry at finite g_s , which is known to take form

$$\mathcal{Z}_{\text{top}}^{\text{SPP}}(q_s, Q, \mu) = \prod_{k=1}^{\infty} \frac{(1 - Qq_s^k)^k (1 - \mu q_s^k)^k}{(1 - q_s^k)^{3k/2} (1 - \mu Qq_s^k)^k}, \tag{5.27}$$

for Kähler parameters Q and μ . This confirms that our result makes sense, although this also means that the terms in lowest order in g_s in the potential reproduce the full g_s dependence of the partition function. It would be nice to prove rigorously that higher g_s corrections to the potential indeed do not affect the total partition function. This appears to be a very special feature of matrix models integrands which can be expressed—as is the case for (5.12)—in terms of infinite products of the form $\prod_k (1 - xq^k)$. One proof of such statement in a related situation (although in addition taking advantage of a special phenomenon of the *arctic circle*) can be found in [52].

Secondly, it is natural to conjecture that the total partition function of the matrix model, for finite T , should reproduce (at least up to some MacMahon factor) the topological string partition function for the closed topological vertex which reads

$$Z_{\text{matrix}}^{\text{total}}(q, Q, \mu, \epsilon^2) = \prod_{k=1}^{\infty} (1 - q^k)^k \cdot \prod_{k=1}^{\infty} \frac{(1 - Qq^k)^k (1 - \mu q^k)^k (1 - \epsilon^2 q^k)^k (1 - Q\mu\epsilon^2 q^k)^k}{(1 - Q\mu q^k)^k (1 - \mu\epsilon^2 q^k)^k (1 - Q\epsilon^2 q^k)^k}. \tag{5.28}$$

Finally, we also note that in the limit $Q, \mu \rightarrow 0$ our model reduces to the Chern-Simons matrix model discussed in [47, 50]. Indeed, in this limit the potential (5.16) reproduces

Gaussian potential [50]

$$V_{Q \rightarrow 0, n \rightarrow \infty} = -\frac{1}{2}(\log z)^2 = -\frac{1}{2}u^2, \quad (5.29)$$

and the partition function (5.9) correctly reduces to the appropriate Chern-Simons partition function. In this case, the resolvent (5.21) reduces to

$$\omega_{\pm}^{\text{conifold}}(p)_{\mu=Q=0} = \frac{1}{pT} \log \left(\frac{p+1 \mp \sqrt{(p+1)^2 - 4pe^{-T}}}{2pe^{-T}} \right), \quad (5.30)$$

and agrees with the resolvent of the old Chern-Simons matrix model found in [47, 50]. In this case, also the spectral curve reproduces the conifold mirror curve (3.23) of the size given by the 't Hooft coupling

$$x + p + xp + x^2 e^{-T} = 0. \quad (5.31)$$

(Instead of introducing $T \log z$ term to the potential to get the standard Vandermonde determinant, the solution in [47] involves completing the square, which leads to a redefinition $p_{\text{here}} = p_{[47]} e^T$. Due to a different sign of g_s we also need to identify 't Hooft couplings as $T_{\text{here}} = -t_{[47]}$. Taking this rescaling into account, our cut endpoints (5.19) with $Q = \mu = 0$ also coincide with those in [47].)

5.4. Matrix Models and Open BPS Generating Functions

In this section, we finally consider arbitrary closed and open BPS chamber, so that matrix models take most general form. Analyzing the case of \mathbb{C}^3 , conifold and $\mathbb{C}^3/\mathbb{Z}_2$, we illustrate the claim (5.3) that open BPS generating functions can be identified with integrand of matrix models. Also for this reason our analysis is only on the level of these integrands; however, it would also be interesting to understand the corresponding spectral curves.

5.4.1. \mathbb{C}^3

We recall that the open topological string amplitude for a brane in \mathbb{C}^3 is given by the quantum dilogarithm (2.14). The condition for the central charge (2.12) and the general formula (2.16) imply that in the open chamber labeled by k the open BPS generating function reads

$$\mathfrak{Z}_k^{\text{open}} = \prod_{i=1}^{\infty} (1 - zq_s^{i-1/2}) \prod_{j>k}^{\infty} (1 - z^{-1}q_s^{j-1/2}). \quad (5.32)$$

In one extreme chamber $k = 0$, the generating function is equal (up to the overall $q^{1/24}$) to a theta function, and so it is a modular form, as explained in Section 2.1. On the other hand, for $k \rightarrow \infty$, the generating function $Z_{k \rightarrow \infty}$ reduces to the open topological string amplitude (2.15).

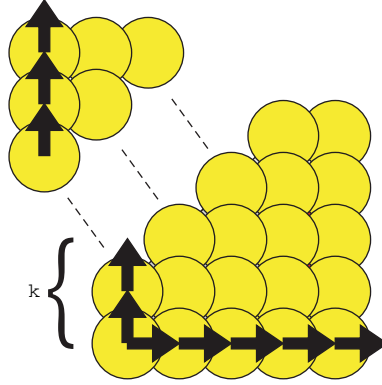


Figure 16: Factorization of \mathbb{C}^3 crystal which leads to open BPS generating functions. The size k encodes the open BPS chamber.

Now we present how the result (5.32) arises from the matrix model viewpoint. To start with, we again consider fermionic representation. Following results of Section 4.4.1, in this case $\bar{A}_+(1) = \Gamma_+(1)\hat{Q}$ and to the geometry of \mathbb{C}^3 , we associate a state

$$|\Omega_-\rangle = \prod_{i=1}^{\infty} \Gamma_-(q^i) |0\rangle, \quad (5.33)$$

and similarly for $\langle\Omega_+$. There is a single closed string chamber in which the generating function $Z = \langle\Omega_+ | \Omega_-\rangle = M(q)$ is given by the MacMahon function. Following the prescription (5.2), we insert the operator \mathbb{I} at the location k (see Figure 16). This gives

$$\begin{aligned} Z = M(q) &= \langle 0 | \prod_{i=k}^{\infty} \bar{A}_+(1) | \mathbb{I} | \prod_{j=0}^{k-1} \bar{A}_+(1) | \Omega_-\rangle \\ &= f^k(q) Z_{\text{matrix}}, \end{aligned} \quad (5.34)$$

where the matrix integral is given by

$$\begin{aligned} Z_{\text{matrix}} &= \int \mathfrak{D}U \prod_{\alpha} \prod_{j=1}^{\infty} (1 + z_{\alpha} q^j) \prod_{i=k}^{\infty} (1 + z_{\alpha}^{-1} q^i), \\ f^k(q) &= \prod_{i=1}^k \prod_{j=0}^{\infty} \frac{1}{1 - q^{i+j}} = \frac{M(1)}{M(q^k, q)}, \end{aligned} \quad (5.35)$$

with the generalized MacMahon function $M(q^k, q)$ defined in (5.11). Matrix model integrand in Z_{matrix} indeed reproduces open BPS generating function (5.32) (up to a redefinition $z \rightarrow -zq^{1/2}$ and identifying $q = q_s$) in a chamber labeled by k .

5.4.2. Conifold

Here we illustrate a relation between matrix models and open BPS generating functions for the conifold, related to a brane associated to the external leg of a toric diagram, as in Figure 14.

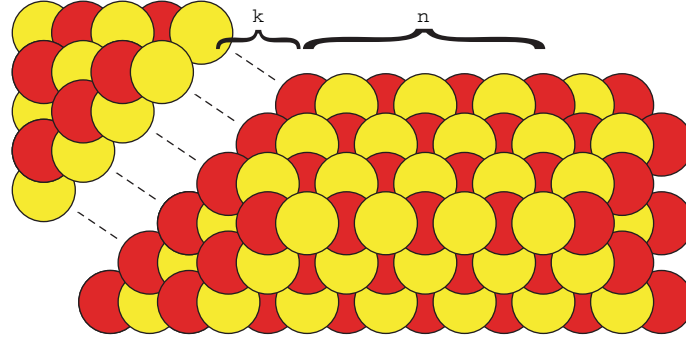


Figure 17: Factorization of the conifold pyramid which leads to open BPS generating functions. The size of the pyramid n represents the closed BPS chamber, while the size k encodes the open BPS chamber.

With appropriate choice of framing, its amplitude reads

$$\mathcal{Z}_{\text{top}}^{\text{open}} = \frac{L(z, q_s)}{L(zQ, q_s)}. \quad (5.36)$$

This also reduces to the modular generating function in the noncommutative chamber $n = k = 0$. More generally, let us consider open BPS counting corresponding to the closed chamber labeled by n , and open chamber labeled by k . From the condition (2.12), after the shift $z \rightarrow -zq^{1/2}$, we get a general generating function of open BPS states

$$\mathcal{Z}_n^{\text{open}, k} = \left| \mathcal{Z}_{\text{top}}^{\text{open}} \right|_{\text{chamber}}^2 = \prod_{l=1}^{\infty} \frac{(1 + zq_s^l)(1 + z^{-1}q_s^{k+l-1})}{(1 + zQq_s^l)(1 + z^{-1}Q^{-1}q_s^{n+k+l-1})}. \quad (5.37)$$

This result arises from matrix model viewpoint as follows. We take advantage of the results of Section 4.4.3, where we determined $\bar{A}_{\pm}(x) = \Gamma_{\pm}(x)\hat{Q}_1\Gamma'_{\pm}(x)\hat{Q}_0$ and $\bar{W} = \Gamma_{-}(1)\hat{Q}_1\Gamma'_{+}(1)\hat{Q}_0$. Inserting the identity operator \mathbb{I} at position k , as represented in Figure 17, leads to

$$Z_n = \langle 0 | \prod_{i=k}^{\infty} \bar{A}_{+}(1) | \mathbb{I} | \prod_{j=0}^{k-1} \bar{A}_{+}(1) | \bar{W}^n | \Omega_{-} \rangle = f_n^k Z_{\text{matrix}}. \quad (5.38)$$

In terms of $\mu = -1/q_1 = Q^{-1}q^n$, the matrix integral takes form

$$Z_{\text{matrix}} = \int \mathfrak{D}U \prod_{\alpha} \prod_{j=1}^{\infty} \frac{(1 + z_{\alpha}q^j)(1 + z_{\alpha}^{-1}q^{k+j-1})}{(1 + z_{\alpha}\mu q^j)(1 + z_{\alpha}^{-1}\mu^{-1}q^{j+n+k-1})}. \quad (5.39)$$

The integrand of this matrix model indeed agrees with (5.37) M-theory (again identifying μ with Kähler parameter used in M-theory derivation, and setting $q = q_s$). In the limit $n \rightarrow \infty$ followed by $\mu \rightarrow 0$, we get the result for \mathbb{C}^3 given in (5.34). On the other hand, for both $n, k \rightarrow \infty$, the integrand reduces to the open topological string amplitude given by a ratio of

two quantum dilogarithms. The prefactor above is found as

$$f_n^k = M(q)^2 \frac{M(\mu q^k, q) M(Q q^k, q)}{M(\mu, q) M(q^k, q) M(Q, q) M(\mu Q q^k, q)} \prod_{j=1}^{\infty} (1 - \mu q^j)^n. \quad (5.40)$$

5.4.3. $\mathbb{C}^3/\mathbb{Z}_2$

As another example, we consider open BPS counting functions for resolved $\mathbb{C}^3/\mathbb{Z}_2$ singularity. In this case, the topological string partition function for a brane on the external leg is

$$Z_{\text{top}}^{\text{ext}} = L(z, q_s) L(zQ, q_s). \quad (5.41)$$

This implies the following BPS generating functions in a closed chamber n and open chamber k (after $z \rightarrow -zq^{1/2}$ shift)

$$\mathcal{Z}_n^{\text{open}, k} = \left| \mathcal{Z}_{\text{top}}^{\text{open}} \right|_{\text{chamber}}^2 = \prod_{l=1}^{\infty} (1 + zq_s^l) (1 + zQq_s^l) (1 + z^{-1}q_s^{k+l-1}) (1 + z^{-1}Q^{-1}q_s^{n+k+l-1}). \quad (5.42)$$

On the other hand, using results of Section 4.4.2, that is, $\overline{A}_{\pm}(x) = \Gamma_{\pm}(x) Q_1 \Gamma_{\pm}(x) Q_0$ and $\overline{W} = \Gamma_{-}(1) \hat{Q}_1 \Gamma_{+}(1) \hat{Q}_0$, and redefining $\mu = 1/q_1 = Q^{-1}q^n$, we obtain

$$\begin{aligned} Z_k^n &= \langle 0 | \prod_{i=k}^{\infty} \overline{A}_{+}(1) | \mathbb{I} | \prod_{j=0}^{k-1} \overline{A}_{+}(1) | \overline{W}^n | \Omega_{-} \rangle = f_n^k Z_{\text{matrix}} \\ &= f_n^k \int \mathfrak{D}U \prod_{\alpha} \prod_{j=1}^{\infty} (1 + z_{\alpha} q^j) (1 + z_{\alpha} \mu q^j) \left(1 + \frac{q^{k+j-1}}{z_{\alpha}} \right) \left(1 + \frac{q^{n+k+j-1}}{z_{\alpha} \mu} \right). \end{aligned} \quad (5.43)$$

The matrix integrand indeed agrees with the M-theory result (when written in terms of the argument μ) above. The prefactor above reads

$$f_n^k = M(q)^2 \frac{M(\mu, q) M(Q, q)}{M(\mu q^k, q) M(q^k, q) M(\mu Q q^k, q) M(Q q^k, q)} \prod_{j=1}^{\infty} (1 - \mu q^j)^{-n}. \quad (5.44)$$

6. Refined Crystals and Matrix Models

In the last section, we turn our attention to so-called refined BPS amplitudes, and explain how to incorporate the effect of such refinement in the fermionic formalism and matrix models, following [31]. To start with, we recall that there are various definitions of refinements, which arise in the context of BPS counting or topological string theory. Here we focus on closed BPS states and consider the following characterization. We introduce an additional parameter y

on which multiplicities of D6-D2-D0 states Ω in the original definition of the generating function (1.1) may depend on

$$Z_n^{\text{ref}}(q_s, Q) = \sum_{\alpha, \gamma} \Omega_{\alpha, \gamma}^{\text{ref}}(n; y) q_s^\alpha Q^\gamma. \quad (6.1)$$

For fixed D0-brane and D2-brane charges α and γ , and a choice of closed BPS chamber n , refined degeneracies are defined as

$$\Omega_{\alpha, \gamma}^{\text{ref}}(n; y) = \text{Tr}_{\mathcal{H}_{\alpha, \gamma}(n)} (-y)^{2J_3}, \quad (6.2)$$

where $\mathcal{H}_{\alpha, \gamma}(n)$ denotes a space of BPS states with given charges α, γ and asymptotic values of moduli corresponding to a chamber n and J_3 represents a generator of the spatial rotation group. For $y = 1$, these degeneracies reduce to those in (1.1). These refined degeneracies are interesting invariants if the underlying Calabi-Yau space does not possess complex structure deformations—and this is indeed the case for noncompact, toric manifolds we are interested in. In [10], it was argued that these invariants agree with motivic Donaldson-Thomas invariants of [2], and in the case of the resolved conifold the corresponding BPS generating functions were derived using the refined wall-crossing formula, and encoded in a refined crystal model. From mathematical viewpoint, this setup was generalized to the whole class of toric manifolds without compact four cycles in [13], and shown therein to agree, in the commutative chamber, with refined topological vertex computations. The refined topological vertex was introduced in [12], see also [57–59]. For other formulations of refinement, see [11, 60, 61].

Our aim in this section is to construct refined crystal and matrix models, which would encode refined BPS generating functions, and in particular (in the commutative chamber) refined topological string amplitudes. We note that an additional motivation to find such models arises from the AGT conjecture [62] and the results of [63], which state that partition functions of Seiberg-Witten theories in the Ω -background (which are related to topological strings by geometric engineering) are reproduced by matrix models with β -deformed measure (i.e., with Vandermonde determinant raised to the power β). Explicit construction of one class of such β -deformed models, however, only to the leading order, was given in [55]; some other works analyzing five-dimensional beta-deformed models include [64, 65]. On the other hand, explicit computations for simpler β -deformed model with Gaussian potential [66, 67] revealed that it does not reproduce refined topological string amplitude for the conifold (even though the unrefined topological string partition function is properly reproduced when $\beta = 1$, see [47, 50]). Nonetheless, the question whether there exist matrix models which reproduce such refined amplitudes remained valid. As we show below (following [31]), such models can indeed be constructed by appropriate deformation of the matrix model potential (rather than the measure). We note that recently another class of matrix models (with different than above deformation of the measure) was proposed [68], which also reproduce refined generating functions.

Let us also note that in this section we consider the same set of walls as in the unrefined case. More general walls, along which only refined BPS states decay, may also exist [10]. They are called *invisible walls* and they do not arise in our analysis.

In this section, we use the following refined notation. The string coupling g_s , related to the D0-brane charge as $q_s = e^{-g_s}$ in the unrefined case, is replaced by two parameters

$$e_1 = \sqrt{\beta} g_s, \quad e_2 = -\frac{g_s}{\sqrt{\beta}}, \quad (6.3)$$

or equivalently $\beta = -\epsilon_1/\epsilon_2$, $\epsilon_1\epsilon_2 = -g_s^2$. We also often use the exponentiated parameters

$$t_1 = e^{-\epsilon_1}, \quad t_2 = e^{\epsilon_2}, \quad (6.4)$$

and introduce

$$g_s B = \epsilon_1 + \epsilon_2 = g_s \left(\sqrt{\beta} - \frac{1}{\sqrt{\beta}} \right). \quad (6.5)$$

The variable y in (6.2) is related to t_1 and t_2 as $y = t_1/q_s = q_s/t_2$, so that $y^2 = t_1/t_2 = q_s^B$. In this notation the unrefined situation $y = 1$ corresponds to $\beta = 1$, for which $\epsilon_1 = -\epsilon_2 = g_s$ and $t_1 = t_2 = q_s$ and $B = 0$.

Let us present now refined BPS generating functions for some Calabi-Yau spaces.

(i) For \mathbb{C}^3 we get the refined MacMahon function [12]

$$Z^{\mathbb{C}^3} = M_{\text{ref}}(t_1, t_2) = \prod_{k,l=0}^{\infty} \frac{1}{1 - t_1^{k+1} t_2^l}. \quad (6.6)$$

In this case, there is no Kähler parameter, and therefore there are no interesting wall-crossing phenomena (In fact, one can consider more general family of refinements parametrized by δ , such that $M_\delta(t_1, t_2) = \prod_{k,l=0}^{\infty} (1 - t_1^{k+1+(\delta-1)/2} t_2^{l-(\delta-1)/2})^{-1}$. In this paper, we fix the value $\delta = 1$ (note that in [10] another choice $\delta = 0$ was made).).

(ii) For the resolved conifold, refined generating functions were computed in [10] using refined wall-crossing formulas. In the closed BPS chamber labeled by $n - 1$, these generating functions read

$$Z_{n-1}^{\text{conifold}} = M_{\text{ref}}(t_1, t_2)^2 \left(\prod_{k,l=0}^{\infty} (1 - Q t_1^{k+1} t_2^l) \right) \left(\prod_{k \geq 1, l \geq 0, k+l \geq n} (1 - Q^{-1} t_1^k t_2^l) \right). \quad (6.7)$$

In the commutative chamber $n \rightarrow \infty$, the terms in the last bracket decouple and the BPS generating function agrees (up to the refined MacMahon factor) with the refined topological string amplitude

$$Z_\infty^{\text{conifold}} = M_{\text{ref}}(t_1, t_2) \mathfrak{Z}_{\text{top}}^{\text{ref}} = M_{\text{ref}}(t_1, t_2) \prod_{k,l=0}^{\infty} (1 - Q t_1^{k+1} t_2^l). \quad (6.8)$$

On the other hand, in the noncommutative chamber $n = 0$ the refined generating function is given by the modulus square of the refined topological string amplitude.

(iii) For a resolution of $\mathbb{C}^3/\mathbb{Z}_2$ singularity, there is also a discrete set of chambers parametrized by an integer n . The corresponding BPS generating functions read

$$Z_{n-1}^{\mathbb{C}^3/\mathbb{Z}_2} = M_{\text{ref}}(t_1, t_2)^2 \left(\prod_{k,l=0}^{\infty} (1 - Q t_1^{k+1} t_2^l)^{-1} \right) \left(\prod_{k \geq 1, l \geq 0, k+l \geq n} (1 - Q^{-1} t_1^k t_2^l)^{-1} \right). \quad (6.9)$$

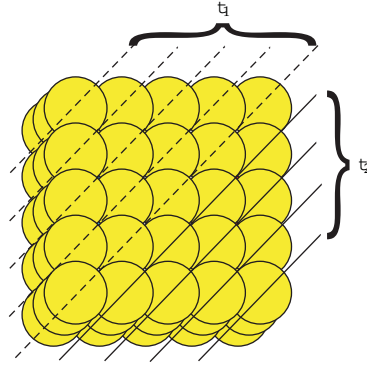


Figure 18: Refined plane partitions which count D6-D0 bound states in \mathbb{C}^3 . In each slice balls, which intersect a dashed or solid line, have, respectively, weight t_1 or t_2 . The resulting generating function is the refined MacMahon function $M_{\text{ref}}(t_1, t_2)$.

- (iv) Generating functions for an arbitrary toric geometry, in for the noncommutative chamber, are given (as in the unrefined case) by the modulus square of the (instanton part of the) refined topological string amplitude

$$Z_0^{\text{ref}} = \left| \mathcal{Z}_{\text{top}}^{\text{ref}} \right|^2 \equiv \mathcal{Z}_{\text{top}}^{\text{ref}}(Q_i) \mathcal{Z}_{\text{top}}^{\text{ref}}(Q_i^{-1}). \quad (6.10)$$

The (instanton part of the) refined topological string amplitude is given by [12, 57]

$$\mathcal{Z}_{\text{top}}^{\text{ref}}(Q_i) = M_{\text{ref}}(t_1, t_2)^{(N+1)/2} \prod_{k,l=0}^{\infty} \prod_{1 \leq i < j \leq N+1} \left(1 - (Q_i Q_{i+1} \cdots Q_{j-1}) t_1^{k+1} t_2^l \right)^{-\tau_i \tau_j}. \quad (6.11)$$

6.1. Refining Free Fermion Representation

In the nonrefined case to a geometry consisting of N \mathbb{P}^1 's, we associated in Section 4 a crystal which can be sliced into layers in $N + 1$ colors, denoted $q_0, q_1, q_2, \dots, q_N$. In that case, parameters q_1, \dots, q_N encode Kähler parameters of the geometry Q_1, \dots, Q_N , while the product $\prod_{i=0}^N q_i$ is mapped to (possibly inverse of) $q_s = e^{-g_s}$. In the refined case, the assignment of colors must take into account a refinement of a single parameter q_s into t_1 and t_2 introduced in (6.4). In particular, in the noncommutative chamber $q_{i \neq 0}$ are mapped (up to a sign, as in the nonrefined case) to Q_i ; however, we will have to replace q_0 by two refined colors $q_0^{(1)}$ or $q_0^{(2)}$, so that $t_i = q_0^{(i)} q_1 \cdots q_N$, for $i = 1, 2$. The simplest case of \mathbb{C}^3 refined plane partitions (discussed also in [12]) is shown in Figure 18. In what follows, we will discuss assignment of colors for other manifolds.

Now we wish to follow the idea of Section 4. Firstly, we wish to construct refined states $|\Omega_{\pm}^{\text{ref}}\rangle$ whose correlators would reproduce refined BPS amplitudes in the noncommutative chamber

$$Z_0^{\text{ref}} = \left\langle \Omega_+^{\text{ref}} \mid \Omega_-^{\text{ref}} \right\rangle. \quad (6.12)$$

Secondly, we wish to construct refined wall-crossing operators $\overline{W}_n^{\text{ref}}$, such that the BPS generating function in n 'th chamber can be written as

$$Z_n^{\text{ref}} = \left\langle \Omega_+^{\text{ref}} \left| \overline{W}_n^{\text{ref}} \right| \Omega_-^{\text{ref}} \right\rangle. \quad (6.13)$$

In Section 6.1.1 below, we construct states $|\Omega_{\pm}^{\text{ref}}\rangle$ for arbitrary manifold in a class of our interest. In Section 6.1.2, we construct states $|\Omega_{\pm}^{\text{ref}}\rangle$ and wall-crossing operators $\overline{W}_n^{\text{ref}}$ for all chambers of the resolved conifold and a resolution of $\mathbb{C}^3/\mathbb{Z}_2$ singularity.

6.1.1. Arbitrary Geometry—Noncommutative Chamber

Here we construct fermionic states $|\Omega_{\pm}^{\text{ref}}\rangle$, which allow to write the BPS generating functions in the noncommutative chamber as in (6.12). As in the nonrefined case, the states $|\Omega_{\pm}^{\text{ref}}\rangle$ are constructed from an interlacing series of vertex operators $\Gamma_{\pm}^{r_i}$ and weight operators. The refinement does not modify the three-dimensional shape of the corresponding crystal; therefore, the assignment of vertex operators is the same as in the nonrefined case (4.2), as explained in Section 4.2.1. However, this is assignment of colors, encoded in the weight operators, which is modified in the refined case. Let us introduce N operators \widehat{Q}_i representing colors q_i , for $i = 1, \dots, N$, and in addition two other colors $q_0^{(1)}$ and $q_0^{(2)}$, which are eigenvalues of $\widehat{Q}_0^{(1)}$ and $\widehat{Q}_0^{(2)}$. Operators $\widehat{Q}_1, \dots, \widehat{Q}_N$, similarly as in Section 4.2.1, are assigned to \mathbb{P}^1 's in the toric diagram, and we introduce

$$\widehat{Q}^{(i)} = \widehat{Q}_0^{(i)} \widehat{Q}_1 \cdots \widehat{Q}_N, \quad t_i = q_0^{(i)} q_1 \cdots q_N, \quad \text{for } i = 1, 2. \quad (6.14)$$

Now we define refined version of \overline{A}_{\pm} operators

$$\begin{aligned} \overline{A}_+(x) &= \Gamma_+^{r_1}(x) \widehat{Q}_1 \Gamma_+^{r_2}(x) \widehat{Q}_2 \cdots \Gamma_+^{r_N}(x) \widehat{Q}_N \Gamma_+^{r_{N+1}}(x) \widehat{Q}_0^{(1)}, \\ \overline{A}_-(x) &= \Gamma_-^{r_1}(x) \widehat{Q}_1 \Gamma_-^{r_2}(x) \widehat{Q}_2 \cdots \Gamma_-^{r_N}(x) \widehat{Q}_N \Gamma_-^{r_{N+1}}(x) \widehat{Q}_0^{(2)}. \end{aligned} \quad (6.15)$$

Commuting all \widehat{Q}_i 's to the left or right, it is convenient to use

$$\begin{aligned} A_+(x) &= \left(\widehat{Q}^{(1)}\right)^{-1} \overline{A}_+(x) = \Gamma_+^{r_1}(xt_1) \Gamma_+^{r_2}\left(\frac{xt_1}{q_1}\right) \Gamma_+^{r_3}\left(\frac{xt_1}{q_1 q_2}\right) \cdots \Gamma_+^{r_{N+1}}\left(\frac{xt_1}{q_1 q_2 \cdots q_N}\right), \\ A_-(x) &= \overline{A}_-(x) \left(\widehat{Q}^{(2)}\right)^{-1} = \Gamma_-^{r_1}(x) \Gamma_-^{r_2}(x q_1) \Gamma_-^{r_3}(x q_1 q_2) \cdots \Gamma_-^{r_{N+1}}(x q_1 q_2 \cdots q_N), \end{aligned} \quad (6.16)$$

and when the argument of these operators is $x = 1$, we often use a simplified notation

$$\overline{A}_{\pm} \equiv \overline{A}_{\pm}(1), \quad A_{\pm} \equiv A_{\pm}(1). \quad (6.17)$$

Finally we associate to a given toric manifold two (refined) states

$$\begin{aligned} \left\langle \Omega_+^{\text{ref}} \right| &= \langle 0 | \cdots \bar{A}_+(1) \bar{A}_+(1) \bar{A}_+(1) = \langle 0 | \cdots A_+(t_1^2) A_+(t_1) A_+(1), \\ \left| \Omega_-^{\text{ref}} \right\rangle &= \bar{A}_-(1) \bar{A}_-(1) \bar{A}_-(1) \cdots |0\rangle = A_-(1) A_-(t_2) A_-(t_2^2) \cdots |0\rangle, \end{aligned} \quad (6.18)$$

where $|0\rangle$ is the fermionic Fock vacuum.

Our claim now is that the refined BPS generating function can be written as

$$Z_0^{\text{ref}} = \left\langle \Omega_+^{\text{ref}} \mid \Omega_-^{\text{ref}} \right\rangle \equiv \mathcal{Z}_{\text{top}}(Q_i) \mathcal{Z}_{\text{top}}(Q_i^{-1}), \quad (6.19)$$

with $\mathcal{Z}_{\text{top}}(Q_i)$ given in (3.1), and if one identifies q_i parameters which enter a definition of $|\Omega_{\pm}^{\text{ref}}\rangle$ and string parameters $Q_i = e^{-T_i}$ (for $i = 1, \dots, N$) as follows:

$$q_i = (\tau_i \tau_{i+1}) Q_i, \quad (6.20)$$

and with refined parameters $t_{1,2}$ identified as in (6.14).

To prove (6.19) for general geometry, we first note that commuting operators $A_+(x)$ with $A_-(y)$

$$A_+(x) A_-(y) = A_-(y) A_+(x) C(x, y) \quad (6.21)$$

gives rise to a factor

$$C(x, y) = \frac{1}{(1 - t_1 x y)^{N+1}} \prod_{1 \leq i < j \leq N+1} \left((1 - (\tau_i \tau_j) x y t_1 (q_i q_{i+1} \cdots q_{j-1})) \left(1 - \frac{(\tau_i \tau_j) x y t_1}{q_i q_{i+1} \cdots q_{j-1}} \right) \right)^{-\tau_i \tau_j}. \quad (6.22)$$

Now we write the states $|\Omega_{\pm}^{\text{ref}}\rangle$ in terms of A_{\pm} operators, and commute Γ_{\pm} within each pair of A_+ and A_- separately

$$Z_0^{\text{ref}} = \left\langle \Omega_+^{\text{ref}} \mid \Omega_-^{\text{ref}} \right\rangle = \langle 0 | \left(\prod_{i=0}^{\infty} A_+(t_1^i) \right) \left(\prod_{j=0}^{\infty} A_-(t_2^j) \right) |0\rangle = \prod_{i,j=0}^{\infty} C(t_1^i, t_2^j). \quad (6.23)$$

This last product reproduces modulus square (6.19) of the refined topological string partition function (6.11) and therefore proves the claim (6.12). Moreover, for the special $\beta = 1$, we automatically obtain the proof of the analogous statement (4.10) in the nonrefined case from Section 4.2.2.

6.1.2. Refined Conifold and $\mathbb{C}^3/\mathbb{Z}_2$

We can now extend the fermionic representation to nontrivial chambers, for simplicity restricting our considerations to the case of a conifold and a resolution of $\mathbb{C}^3/\mathbb{Z}_2$ singularity, which both involve just one Kähler parameter $Q_1 \equiv Q$. Our task amounts to determining

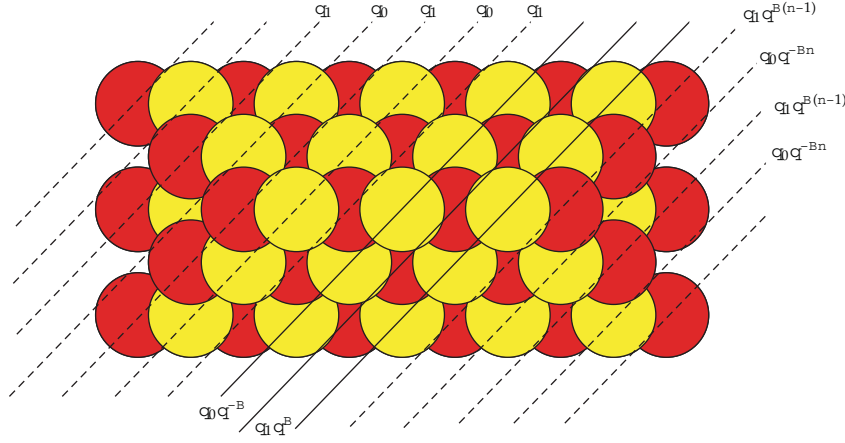


Figure 19: Refined pyramid crystal for the conifold, in the chamber corresponding to n stones in the top row. Along each slice (as indicated by broken or solid lines), all stones have the same color, assigned as follows. On the left side (along broken lines), each light (yellow) and dark (red) slice has color denoted q_0 and q_1 , respectively. Moving to the right, in the intermediate region (along solid lines), a color of each new light or dark slice is modified by, respectively, $q^{\mp B}$ factor (with respect to the previous light or dark slice). On the right side (again along broken lines), each light or dark slice has again the same color, respectively, $q_0 q^{-Bn}$ or $q_1 q^{B(n-1)}$. The assignment of colors in the intermediate region (along solid lines) interpolates between constant assignments on the left and right sides of the pyramid.

appropriate wall-crossing operators, denoted $\overline{W}_{n-1}^{\text{ref}}$, so that in the chamber labeled by $n-1$ the BPS generating function can be written as

$$Z_{n-1}^{\text{ref}} = \left\langle \Omega_+^{\text{ref}} \left| \overline{W}_{n-1}^{\text{ref}} \right| \Omega_-^{\text{ref}} \right\rangle. \quad (6.24)$$

In these both cases, the toric diagram has two vertices, the first one of type $\tau_1 = 1$ and the second one denoted now $\tau \equiv \tau_2$ and $\tau = \mp 1$, respectively, for the conifold and $\mathbb{C}^3/\mathbb{Z}_2$. A crystal associated to the expression (6.24) has n stones in the top row and can be sliced into interlacing single-colored layers. The assignment of colors is analogous as in the pyramid model discussed in [10, 13]. The pyramid crystal for the conifold and $\mathbb{C}^3/\mathbb{Z}_2$ are shown in Figures 19 and 20.

The assignment of colors is determined as follows. All stones on one side of the crystal are encoded in

$$\left\langle \Omega_+^{\text{ref}} \right| = \langle 0 | \cdots \left(\Gamma_+(1) \widehat{Q}_1 \Gamma_+^{\tau}(1) \widehat{Q}_0 \right) \left(\Gamma_+(1) \widehat{Q}_1 \Gamma_+^{\tau}(1) \widehat{Q}_0 \right). \quad (6.25)$$

The Kähler parameter Q , as well as the parameter t_1 , arises as

$$q_1 = \tau Q t_1^{1-n}, \quad q_0 = \tau \frac{t_1^n}{Q}, \quad \text{so that } q_0 q_1 = t_1. \quad (6.26)$$

Now the crystal with $n-1$ additional stones in the top row arises from an insertion of the operator

$$\overline{W}_{n-1}^{\text{ref}} = \left(\Gamma_-(1) \widehat{Q}_1 \Gamma_+^{\tau}(1) \widehat{Q}_0 \widehat{q}^{-B} \right) \left(\Gamma_-(1) \widehat{Q}_1 \widehat{q}^B \Gamma_+^{\tau}(1) \widehat{Q}_0 \widehat{q}^{-2B} \right) \cdots \left(\Gamma_-(1) \widehat{Q}_1 \widehat{q}^{(n-2)B} \Gamma_+^{\tau}(1) \widehat{Q}_0 \widehat{q}^{(1-n)B} \right). \quad (6.27)$$

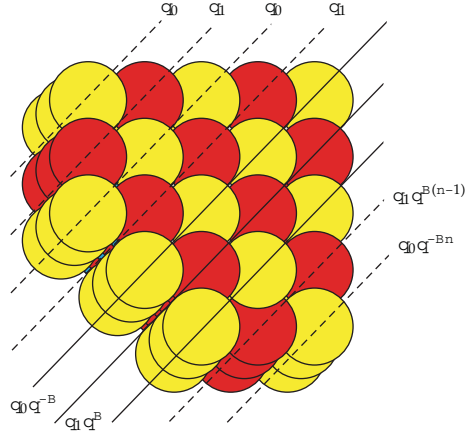


Figure 20: Refined pyramid crystal for the resolution of $\mathbb{C}^3/\mathbb{Z}_2$ singularity, in the chamber corresponding to n stones in the top row, as seen from the bottom (i.e., a negative direction of z -axis). Even though the three-dimensional shape of the crystal is different than in the conifold case, the assignment of colors is the same, see Figure 19.

This operator is made of $n - 1$ terms of the form $(\Gamma_-(1)\widehat{Q}_1 q^{iB}\Gamma_+^T(1)\widehat{Q}_0 q^{-(i+1)B})$ for $i = 0, \dots, n - 2$, where in each subsequent dark or light slice we insert one additional operator $\widehat{q}^{\pm B}$. This additional operator changes the weight of each stone in this slice by $q^{\pm B} = (t_1/t_2)^{\pm 1}$ (with respect to the previous slice of the same light or dark color).

Finally, all stones on the right side of the crystal have again the same light or dark color, so that the corresponding state is

$$|\mathcal{Q}_-^{\text{ref}}\rangle = \left(\Gamma_-(1)\widehat{Q}_1 q^{(n-1)B}\Gamma_-^T(1)\widehat{Q}_0 q^{-nB}\right) \left(\Gamma_-(1)\widehat{Q}_1 q^{(n-1)B}\Gamma_-^T(1)\widehat{Q}_0 q^{-nB}\right) \cdots |0\rangle. \quad (6.28)$$

We see that varying weights in the middle range (along solid lines in Figures 19 and 20) interpolate between fixed weights of light and dark stones on two external sides of a crystal.

We can now commute away all weight operators in the above expressions, using commutation relations from Section 3.2. This results in

$$Z_{n-1}^{\text{ref}} = \langle 0 | \left(\prod_{k=1}^{\infty} \Gamma_+ \left(t_1^k \right) \Gamma_+^T \left(\frac{t_1^k}{q_1} \right) \right) \left(\prod_{i=0}^{n-2} \Gamma_- \left(t_2^i \right) \Gamma_+^T \left(q_1^{-1} t_1^{-i} \right) \right) \left(\prod_{k=0}^{\infty} \Gamma_- \left(t_2^{n-1+k} \right) \Gamma_-^T \left(t Q t_2^k \right) \right) | 0 \rangle. \quad (6.29)$$

To check that this is a correct representation, we commute all vertex operators, and find

$$Z_{n-1}^{\text{ref}} = M_{\text{ref}}(t_1, t_2)^2 \prod_{k=1, l=0}^{\infty} \left(1 - Q t_1^k t_2^l \right)^{-\tau} \prod_{k \geq 1, l \geq 0, k+l \geq n}^{\infty} \left(1 - Q^{-1} t_1^k t_2^l \right)^{-\tau}, \quad (6.30)$$

where $\tau = \mp 1$, respectively, for the conifold and $\mathbb{C}^3/\mathbb{Z}_2$. This result reproduces (6.7) and (6.9), which confirms that the fermionic representation we started with is correct.

6.2. Refined Matrix Models

In the refined case, one can associate matrix models to refined generating functions in the same way as described in Section 5.1, that is, by inserting the representation (5.1) of the identity operator into fermionic representation (6.19) or (6.24). This does not change a unitary character of the matrix model, which is a consequence of the representation (5.1). However, due to more subtle weight assignments, this is matrix potential which gets deformed by β -dependent factors. In general, we will therefore obtain matrix models of the following form:

$$Z_n^{\text{ref}} = f_n \int \mathfrak{D}U \prod_k e^{-(\sqrt{\beta}/g_s)V(z_k;\beta)}, \quad (6.31)$$

where for convenience we introduced a factor $\sqrt{\beta}$ in front of the potential $V(z;\beta)$. We will consider a few examples below.

6.2.1. Noncommutative Chamber

For arbitrary geometry, in the noncommutative chamber, refined matrix model integrand can be expressed in terms of the refined theta function

$$\Theta(z; t_1, t_2) = \prod_{j=0}^{\infty} \left(1 + z t_1^{j+1}\right) \left(1 + \frac{t_2^j}{z}\right). \quad (6.32)$$

Repeating the computation described in Section 5.1, however, starting with the refined representation (6.19), in the noncommutative chamber for general geometry, we find the matrix model

$$Z_0^{\text{ref}} = \int \mathfrak{D}U \prod_k \prod_{l=0}^N \Theta\left(\frac{\tau_{l+1} z_k}{q_1 \cdots q_l}; t_1, t_2\right)^{\tau_{l+1}}, \quad (6.33)$$

that is, we identify $e^{-(\sqrt{\beta}/g_s)V(z;\beta)} \equiv \prod_{l=0}^N \Theta(\tau_{l+1} z (q_1 \cdots q_l)^{-1}; t_1, t_2)^{\tau_{l+1}}$. The product over l runs over all vertices and we identify Kähler parameters Q_p with weights q_p via $q_p = (\tau_p \tau_{p+1}) Q_p$.

6.2.2. Refined \mathbb{C}^3 Matrix Model

We obtain a refined matrix model for \mathbb{C}^3 as the special case of (6.33). For the refined \mathbb{C}^3 , the BPS generating function is a refined MacMahon function $Z^{\text{ref}} = M_{\text{ref}}(t_1, t_2)$ introduced in (6.6), and the corresponding matrix integrand takes form of a refined theta function

$$e^{-(\sqrt{\beta}/g_s)V(z;\beta)} = \prod_{j=0}^{\infty} \left(1 + z t_1^{j+1}\right) \left(1 + \frac{t_2^j}{z}\right) = \Theta(z; t_1, t_2). \quad (6.34)$$

Using the asymptotics (5.15), we find the leading order expansion of the potential

$$e^{-(\sqrt{\beta}/g_s)V(z;\beta)} = e^{-(\sqrt{\beta}/g_s)[-(1/2)(\log z)^2 - (1-\beta^{-1})\text{Li}_2(-z) + \mathcal{O}(g_s, \beta)]}. \quad (6.35)$$

The quadratic term in the potential is the same as in the nonrefined case. The term involving $Li_2(-z)$, as well as all higher-order terms $\mathcal{O}(g_s, \beta)$, arises as deformations which vanish for $\beta = 1$. Therefore, for $\beta = 1$, we obtain a Chern-Simons matrix model which indeed gives rise to MacMahon function in $N \rightarrow \infty$ limit, as we explained in Section 5.3. For arbitrary β , the resolvent $\omega(p)$ can also be found using the Migdal integral (3.18). In principle, one could repeat the computation described in Section 5.3; however, this is technically more involved. Nonetheless, this would lead to β -deformed end-points of the cut (91), and in consequence to the β -deformed spectral curve. This curve would be some β -deformation of the mirror curve given in (3.23). It is still an interesting question to find this curve in the exact form and analyze its properties.

6.2.3. Refined Conifold Matrix Model

Finally we find matrix models for the refined conifold. Starting with the representation (6.29), inserting the identity representation (5.1) and following standard by now computations, we find the following matrix model for the conifold in the n 'th chamber (corresponding to a pyramid with $(n+1)$ stones on top)

$$\begin{aligned} Z_n^{\text{ref}} &= M_{\text{ref}}(t_1, t_2)^2 \prod_{k=1, l=0}^{\infty} (1 - Qt_1^k t_2^l) \prod_{k \geq 1, l \geq 0, k+l \geq n+1}^{\infty} (1 - Q^{-1} t_1^k t_2^l) \\ &= f_n(q, Q) \int \mathfrak{D}U \prod_k \prod_{j=0}^{\infty} \frac{(1 + z_k t_1^{j+1})(1 + t_2^j / z_k)}{(1 + z_k t_1^{j+n+1} / Q)(1 + t_2^j Q / z_k)}, \end{aligned} \quad (6.36)$$

with the prefactor given by

$$f_n(q, Q) = \left(\prod_{i=1}^n \prod_{k=0}^{\infty} \frac{1}{1 - t_1^i t_2^k} \right) \left(\prod_{i=1}^n \prod_{j=n+1-i}^{\infty} \left(1 - \frac{t_1^i t_2^j}{Q} \right) \right). \quad (6.37)$$

In the limit of the commutative chamber, $n \rightarrow \infty$, we get $f_{\infty} = M_{\text{ref}}(t_1, t_2)$. Therefore, in the commutative chamber, we get a matrix model representation of the refined topological string conifold amplitude

$$\begin{aligned} \mathcal{Z}_{\text{top}}^{\text{ref}} &= M_{\text{ref}}(t_1, t_2) \prod_{k, l=0}^{\infty} (1 - Qt_1^{k+1} t_2^l) \\ &= \int \mathfrak{D}U \prod_k \prod_{j=0}^{\infty} \frac{(1 + z_k t_1^{j+1})(1 + t_2^j / z_k)}{(1 + t_2^j Q / z_k)}. \end{aligned} \quad (6.38)$$

In this case, the lowest order potential is a modification of the \mathbb{C}^3 potential (6.35) by a Q -dependent dilogarithm term

$$V(z; \beta) = -\frac{1}{2}(\log z)^2 - (1 - \beta^{-1})Li_2(-z) - Li_2\left(-\frac{Q}{z}\right) + \mathcal{O}(g_s, \beta). \quad (6.39)$$

This is quite an interesting result—as we already explained above, it has been postulated for some time that the refined topological string amplitude for the conifold should have matrix model representation; however, it was not clear how to derive it. Here we find an explicit matrix model representation of this amplitude. The corresponding spectral curve would again be a β -deformation of the conifold mirror curve (3.23). It would be interesting to compare it with other notions of deformed, or quantum mirror curves in the literature. We also note that in the limit $Q \rightarrow 0$ the above topological string partition function becomes just the refined MacMahon function, and the matrix integral consistently reproduces \mathbb{C}^3 result (6.34).

Acknowledgments

The author thanks Robbert Dijkgraaf, Hiroshi Ooguri, Cumrun Vafa, and Masahito Yamazaki for discussions and collaboration on related projects. This research was supported by the DOE Grant DE-FG03-92ER40701FG-02 and the European Commission under the Marie-Curie International Outgoing Fellowship Programme. The contents of this publication reflect only the views of the author and not the views of the funding agencies.

References

- [1] F. Denef and G. Moore, “Split states, entropy enigmas, holes and halos,” . In press, <http://arxiv.org/abs/hep-th/0702146>.
- [2] M. Kontsevich and Y. Soibelman, “Stability structures, motivic Donaldson-Thomas invariants and cluster transformations,” . In press, <http://arxiv.org/abs/0811.2435>.
- [3] R. Gopakumar and C. Vafa, “M-theory and topological strings. I,” . In press, <http://arxiv.org/abs/hep-th/9809187>.
- [4] R. Gopakumar and C. Vafa, “M-theory and topological strings. II,” . In press, <http://arxiv.org/abs/hep-th/9812127>.
- [5] H. Ooguri and C. Vafa, “Knot invariants and topological strings,” *Nuclear Physics B*, vol. 577, no. 3, pp. 419–438, 2000.
- [6] M. Aganagic, A. Klemm, M. Mariño, and C. Vafa, “The topological vertex,” *Communications in Mathematical Physics*, vol. 254, no. 2, pp. 425–478, 2005.
- [7] A. Okounkov, N. Reshetikhin, and C. Vafa, “Quantum Calabi-Yau and classical crystals,” . In press, <http://arxiv.org/abs/hep-th/0309208>.
- [8] A. Iqbal, C. Vafa, N. Nekrasov, and A. Okounkov, “Quantum foam and topological strings,” *Journal of High Energy Physics*, vol. 2008, no. 4, article 011, 2008.
- [9] D. Maulik, N. Nekrasov, A. Okounkov, and R. Pandharipande, “Gromov-Witten theory and Donaldson-Thomas theory, I,” *Compositio Mathematica*, vol. 142, no. 5, pp. 1263–1285, 2006.
- [10] T. Dimofte and S. Gukov, “Refined, motivic, and quantum,” *Letters in Mathematical Physics*, vol. 91, no. 1, pp. 1–27, 2009.
- [11] N. A. Nekrasov, “Seiberg-Witten prepotential from instanton counting,” *Advances in Theoretical and Mathematical Physics*, vol. 7, no. 5, pp. 831–864, 2004.
- [12] A. Iqbal, C. Kozçaz, and C. Vafa, “The refined topological vertex,” *Journal of High Energy Physics*, no. 10, p. 69, 2009.
- [13] K. Nagao, “Refined open noncommutative Donaldson-Thomas invariants for small crepant resolutions,” . In press, <http://arxiv.org/abs/0907.3784>.
- [14] B. Szendrői, “Non-commutative Donaldson-Thomas theory and the conifold,” *Geometry & Topology*, vol. 12, no. 2, pp. 1171–1202, 2008.
- [15] J. Bryan and B. Young, “Generating functions for colored 3D young diagrams and the Donaldson-Thomas invariants of orbifolds,” *Duke Mathematical Journal*, vol. 152, no. 1, pp. 115–153, 2010.
- [16] P. Sułkowski, “Wall-crossing, free fermions and crystal melting,” *Communications in Mathematical Physics*, vol. 301, no. 2, pp. 517–562, 2011.
- [17] K. Nagao, “Noncommutative Donaldson-Thomas theory and vertex operators,” . In press, <http://arxiv.org/abs/0910.5477>.
- [18] K. Nagao and H. Nakajima, “Counting invariant of perverse coherent sheaves and its wallcrossing,” *International Mathematics Research Notices*, vol. 2011, no. 13, 2011.

- [19] K. Nagao, "Derived categories of small toric Calabi-Yau 3-folds and counting invariants," . In press, <http://arxiv.org/abs/0809.2994>.
- [20] D. Jafferis and G. Moore, "Wall crossing in local Calabi Yau manifolds," . In press, <http://arxiv.org/abs/0810.4909>.
- [21] W. Y. Chuang and D. L. Jafferis, "Wall crossing of BPS states on the conifold from Seiberg duality and pyramid partitions," *Communications in Mathematical Physics*, vol. 292, no. 1, pp. 285–301, 2009.
- [22] H. Ooguri and M. Yamazaki, "Crystal melting and toric Calabi-Yau manifolds," *Communications in Mathematical Physics*, vol. 292, no. 1, pp. 179–199, 2009.
- [23] M. Aganagic, H. Ooguri, C. Vafa, and M. Yamazaki, "Wall crossing and M-theory," *Nuclear Physics B*, vol. 47, no. 2, pp. 569–584, 2011.
- [24] M. Aganagic and M. Yamazaki, "Open BPS wall crossing and M-theory," *Nuclear Physics B*, vol. 834, no. 1-2, pp. 258–272, 2010.
- [25] R. Dijkgraaf, P. Sułkowski, and C. Vafa, *unpublished* .
- [26] K. Nagao and M. Yamazaki, "The non-commutative topological vertex and wall crossing phenomena," *Advances in Theoretical and Mathematical Physics*, vol. 14, pp. 1147–1181, 2010.
- [27] P. Sułkowski, "Wall-crossing, open BPS counting and matrix models," *Journal of High Energy Physics*, vol. 2011, no. 3, p. 89, 2011.
- [28] B. Eynard, "A matrix model for plane partitions and TASEP," *Journal of Statistical Mechanics*, no. 10, Article ID P10011, 2009.
- [29] H. Ooguri, P. Sułkowski, and M. Yamazaki, "Wall Crossing As Seen By Matrix Models," *Communications in Mathematical Physics*, 2011.
- [30] R. Szabo and M. Tierz, "Matrix models and stochastic growth in Donaldson-Thomas theory," . In press, <http://arxiv.org/abs/1005.5643>.
- [31] P. Sułkowski, "Refined matrix models from BPS counting," *Physical Review D*, vol. 83, no. 8, Article ID 085021, 12 pages, 2011.
- [32] N. Saulina and C. Vafa, "D-branes as defects in the Calabi-Yau crystal," . In press, <http://arxiv.org/abs/hep-th/0404246>.
- [33] N. Halmagyi, A. Sinkovics, and P. Sułkowski, "Knot invariants and Calabi-Yau crystals," *Journal of High Energy Physics*, no. 1, article 040, p. 32, 2006.
- [34] J. Gomis and T. Okuda, "D-branes as a bubbling Calabi-Yau," *Journal of High Energy Physics*, no. 7, article 005, p. 28, 2007.
- [35] M. Aganagic and K. Schaeffer, "Wall crossing, quivers and crystals," . In press, <http://arxiv.org/abs/1006.2113>.
- [36] T. Nishinaka and S. Yamaguchi, "Wall-crossing of D4-D2-D0 and flop of the conifold," *Journal of High Energy Physics*, vol. 2010, no. 9, 2010.
- [37] P. Sułkowski, "Calabi-Yau crystals in topological string theory," . In press, <http://arxiv.org/abs/0712.2173>.
- [38] M. Yamazaki, "Crystal melting and wall crossing phenomena," *International Journal of Modern Physics A*, vol. 26, no. 7-8, pp. 1097–1228, 2011.
- [39] C. Vafa and E. Zaslow, Eds., *Mirror Symmetry*, CMI/AMS publication.
- [40] R. Dijkgraaf, C. Vafa, and E. Verlinde, "M-theory and a topological string duality," . In press, <http://arxiv.org/abs/hep-th/0602087>.
- [41] J. M. F. Labastida, M. Mariño, and C. Vafa, "Knots, links and branes at large N ," *Journal of High Energy Physics*, no. 11, p. 7, 2000.
- [42] D. Gaiotto, A. Strominger, and X. Yin, "New connections between 4D and 5D black holes," *Journal of High Energy Physics*, no. 2, p. 10, article 024, 2006.
- [43] M. Jimbo and T. Miwa, "Solitons and infinite-dimensional lie algebras," *Kyoto University. Research Institute for Mathematical Sciences. Publications*, vol. 19, no. 3, pp. 943–1001, 1983.
- [44] I. G. Macdonald, *Symmetric Functions and Hall Polynomials*, Oxford Mathematical Monographs, The Clarendon Press Oxford University Press, New York, NY, USA, 2nd edition, 1995.
- [45] M. Aganagic, R. Dijkgraaf, A. Klemm, M. Mariño, and C. Vafa, "Topological strings and integrable hierarchies," *Communications in Mathematical Physics*, vol. 261, no. 2, pp. 451–516, 2006.
- [46] P. Di Francesco, P. Ginsparg, and J. Zinn-Justin, "2D gravity and random matrices," *Physics Reports*, vol. 254, no. 1-2, pp. 1–133, 1995.
- [47] M. Mariño, *Chern-Simons Theory, Matrix Models, And Topological Strings*, vol. 131 of *International Series of Monographs on Physics*, The Clarendon Press Oxford University Press, Oxford, UK, 2005.
- [48] B. Eynard and N. Orantin, "Invariants of algebraic curves and topological expansion," . In press, <http://arxiv.org/abs/math-ph/0702045>.

- [49] M. Mariño, “Chern-Simons theory, matrix integrals, and perturbative three-manifold invariants,” *Communications in Mathematical Physics*, vol. 253, no. 1, pp. 25–49, 2004.
- [50] M. Aganagic, A. Klemm, M. Mariño, and C. Vafa, “Matrix model as a mirror of Chern-Simons theory,” *Journal of High Energy Physics*, no. 2, article 010, p. 46, 2004.
- [51] V. Bouchard, A. Klemm, M. Mariño, and S. Pasquetti, “Remodeling the B-model,” *Communications in Mathematical Physics*, vol. 287, no. 1, pp. 117–178, 2009.
- [52] B. Eynard, “All order asymptotic expansion of large partitions,” *Journal of Statistical Mechanics*, no. 7, Article ID P07023, 2008.
- [53] A. Klemm and P. Sułkowski, “Seiberg-Witten theory and matrix models,” *Nuclear Physics B*, vol. 819, no. 3, pp. 400–430, 2009.
- [54] P. Sułkowski, “Matrix models for 2^* theories,” *Physical Review D*, vol. 80, no. 8, Article ID 086006, 2009.
- [55] P. Sułkowski, “Matrix models for β -ensembles from Nekrasov partition functions,” *Journal of High Energy Physics*, no. 4, article 063, p. 63, 2010.
- [56] B. Eynard, A. K. Kashani-Poor, and O. Marchal, “A matrix model for the topological string I: deriving the matrix model,” . In press, <http://arxiv.org/abs/1003.1737>.
- [57] M. Taki, “Refined topological vertex and instanton counting,” *Journal of High Energy Physics*, no. 3, article 048, p. 48, 2008.
- [58] H. Awata and H. Kanno, “Instanton counting, Macdonald function and the moduli space of D-branes,” *Journal of High Energy Physics*, no. 5, article 039, p. 26, 2005.
- [59] H. Awata and H. Kanno, “Refined BPS state counting from Nekrasov’s formula and Macdonald functions,” *International Journal of Modern Physics A*, vol. 24, no. 12, pp. 2253–2306, 2009.
- [60] I. Antoniadis, S. Hohenegger, K. S. Narain, and T. R. Taylor, “Deformed topological partition function and Nekrasov backgrounds,” *Nuclear Physics B*, vol. 838, no. 3, pp. 253–265, 2010.
- [61] Y. Nakayama, “Refined topological amplitudes in $N = 1$ flux compactification,” *Journal of High Energy Physics*, vol. 2010, no. 11, article 117, pp. 1–14, 2010.
- [62] L. F. Alday, D. Gaiotto, and Y. Tachikawa, “Liouville correlation functions from four-dimensional Gauge theories,” *Letters in Mathematical Physics*, vol. 91, no. 2, pp. 167–197, 2010.
- [63] R. Dijkgraaf and C. Vafa, “Toda theories, matrix models, topological strings, and $N = 2$ Gauge systems,” . In press, <http://arxiv.org/abs/0909.2453>.
- [64] A. Mironov, A. Morozov, and A. Morozov, “Matrix model version of AGT conjecture and generalized Selberg integrals,” *Nuclear Physics B*, vol. 843, no. 2, pp. 534–557, 2011.
- [65] H. Awata and Y. Yamada, “Five-dimensional AGT relation and the deformed beta-ensemble,” *Progress of Theoretical Physics*, vol. 124, no. 2, pp. 227–262, 2010.
- [66] M. Huang and A. Klemm, “Direct integration for general Omega backgrounds,” . In press, <http://arxiv.org/abs/1009.1126>.
- [67] A. Brini, M. Mariño, and S. Stevan, “The uses of the refined matrix model recursion,” *Journal of Mathematical Physics*, vol. 52, no. 5, 2011.
- [68] M. Aganagic and S. Shakirov, “Knot homology from refined Chern-Simons theory,” . In press, <http://arxiv.org/abs/1105.5117>.

Review Article

Combinatorics in $\mathcal{N} = 1$ Heterotic Vacua

Seung-Joo Lee

School of Physics, Korea Institute for Advanced Study, Seoul 130-722, Republic of Korea

Correspondence should be addressed to Seung-Joo Lee, s.lee@kias.re.kr

Received 15 May 2011; Accepted 14 June 2011

Academic Editor: André Lukas

Copyright © 2011 Seung-Joo Lee. This is an open access article distributed under the Creative Commons Attribution License, which permits unrestricted use, distribution, and reproduction in any medium, provided the original work is properly cited.

We briefly review an algorithmic strategy to explore the landscape of heterotic $E_8 \times E_8$ vacua, in the context of compactifying smooth Calabi-Yau threefolds with vector bundles. The Calabi-Yau threefolds are algebraically realised as hypersurfaces in toric varieties, and a large class of vector bundles are constructed thereon as monads. In the spirit of searching for standard-like heterotic vacua, emphasis is placed on the integer combinatorics of the model-building programme.

1. Introduction

Compactifications of $E_8 \times E_8$ heterotic theory [1, 2] and heterotic M-theory [3–7] on smooth Calabi-Yau threefolds provide a simple and compelling way to reach $\mathcal{N} = 1$ supersymmetry at four dimensions. A Calabi-Yau threefold necessarily admits a Ricci-flat metric $g_{\alpha\bar{\beta}}$, where $\alpha, \bar{\beta} = 1, 2, 3$ are, respectively, the holomorphic and antiholomorphic indices. One also turns on an internal gauge field, in a subalgebra \mathcal{G} of the full E_8 , resulting in the reduction of the four-dimensional gauge group down to the commutant \mathcal{H} of $\mathcal{G} \subset E_8$. To preserve supersymmetry, the gauge field should satisfy the Hermitian Yang-Mills equations:

$$F_{\alpha\beta} = F_{\bar{\alpha}\bar{\beta}} = 0, \quad g^{\alpha\bar{\beta}} F_{\alpha\bar{\beta}} = 0, \quad (1.1)$$

where F is the associated field strength. Although these equations cannot be solved analytically, the Donaldson-Uhlenbeck-Yau theorem [8, 9] states that, on a holomorphic (poly) stable bundle, there exists a unique connection that solves (1.1).

So each of the heterotic vacua comes in two pieces: a Calabi-Yau threefold X and a holomorphic stable vector bundle V thereon. Studying the detailed geometry, however, is not an easy task. To begin with, we do not even know the Ricci-flat metrics on Calabi-Yau threefolds. Fortunately, as will be seen shortly, it turns out that the topology of a vacuum already determines many interesting features of the four-dimensional effective theory.

Table 1: A vector bundle V with structure group $\mathcal{G} = SU(4)$ or $SU(5)$, respectively, breaks the E_8 group of the heterotic string into the Grand Unifying group $\mathcal{H} = SO(10)$ or $SU(5)$. The four-dimensional low-energy representation contents of \mathcal{H} arise from the branching of the **248** adjoint of E_8 under $\mathcal{G} \times \mathcal{H} \subset E_8$. The particle spectrum is obtained as various bundle-valued cohomology groups.

\mathcal{G}	\mathcal{H}	Branching of 248 under $\mathcal{G} \times \mathcal{H} \subset E_8$	Particle spectrum
$SU(4)$	$SO(10)$	$(\mathbf{1}, \mathbf{45}) \oplus (\mathbf{4}, \mathbf{16}) \oplus (\bar{\mathbf{4}}, \bar{\mathbf{16}}) \oplus (\mathbf{6}, \mathbf{10}) \oplus (\mathbf{15}, \mathbf{1})$	$n_{16} = h^1(X, V)$
			$n_{\bar{16}} = h^1(X, V^*) = h^2(V)$
			$n_{10} = h^1(X, \wedge^2 V)$
			$n_1 = h^1(X, V \otimes V^*)$
$SU(5)$	$SU(5)$	$(\mathbf{1}, \mathbf{24}) \oplus (\mathbf{5}, \mathbf{10}) \oplus (\bar{\mathbf{5}}, \bar{\mathbf{10}}) \oplus (\mathbf{10}, \bar{\mathbf{5}}) \oplus (\bar{\mathbf{10}}, \mathbf{5}) \oplus (\mathbf{24}, \mathbf{1})$	$n_{10} = h^1(X, V)$
			$n_{\bar{10}} = h^1(X, V^*) = h^2(V)$
			$n_5 = h^1(X, \wedge^2 V^*)$
			$n_{\bar{5}} = h^1(X, \wedge^2 V)$
			$n_1 = h^1(X, V \otimes V^*)$

In order for the heterotic models to be “Standard-like,” they must give rise to the correct gauge group, $SU(3)_C \times SU(2)_L \times U(1)_Y$, possibly with an extra $U(1)_{B-L}$ factor, as well as a correct spectrum for light particles coming in three generations. Firstly, the choices $\mathcal{G} = SU(4)$ and $SU(5)$ for the structure group of V reduce the E_8 to the four-dimensional gauge groups $\mathcal{H} = SO(10)$ and $SU(5)$, respectively, which are desirable in the viewpoint of Grand Unification¹. The light particles then arise from the branching of the adjoint **248** of E_8 into $\mathcal{G} \times \mathcal{H}$, and the spectrum is determined by various bundle-valued cohomologies on the Calabi-Yau threefold [2], as summarised in Table 1. Of course, the gauge group \mathcal{H} should be further broken down to a standard-like one and discrete Wilson-lines are made use of, if there ever exists any, for this second breaking.

In this paper, we will make it clear how the construction of standard-like heterotic vacua turns into the integer combinatorics for a discrete system. Specifically, the Calabi-Yau threefolds will be *torically* constructed and described by the combinatorics of *reflexive* lattice polytopes [10].² Next, *monad* vector bundles [11] will be constructed thereon, equivalent of turning on internal gauge fluxes over the Calabi-Yau threefolds.

The remainder of this paper is structured as follows. In the ensuing two sections, we lay down the foundation by explaining the basic mathematical toolkit for describing $\mathcal{N} = 1$ heterotic vacua. Next, in Section 4, further constraints will be imposed on the internal geometry so that the resulting $\mathcal{N} = 1$ four-dimensional effective theory may mimic the standard model. We will conclude in Section 5 with a summary and outlook.

2. Toric Construction of Calabi-Yau Threefolds

Soon after the famous 7890 Calabi-Yau threefolds were realised as complete intersections of hypersurfaces in multiprojective spaces [12–16], Kreuzer and Skarke have classified the Calabi-Yau threefolds that arise as codimension-one hypersurfaces in toric fourfolds, comprising a much bigger dataset [17–19]. This construction, first proposed by Batyrev [10], involves an extensive usage of toric geometry. Here, we do not intend by any means to give a pedagogical introduction to toric geometry. The readers interested in the details of this subject are referred either to the maths texts [20–23] or to the excellent, introductory reviews for physicists [24, 25].

2.1. Ambient Toric Fourfolds

The Calabi-Yau threefolds X are embedded in toric fourfolds \mathcal{A} as hypersurfaces and, therefore, we will start with the description of these ambient toric varieties. A toric fourfold is described by the combinatorial data called a *fan* in \mathbb{R}^4 , which is a collection of convex *cones* in \mathbb{R}^4 with their common apex at the origin $O = (0, 0, 0, 0)$. For the sake of Calabi-Yau subvarieties, however, every fan is not appropriate. We first define a certain class of convex *polytopes* in \mathbb{R}^4 , of which fans of a special kind are made.

The polytopes considered here must contain the origin O as the unique interior lattice point and all the vertices must lie in the lattice $\mathbb{Z}^4 \subset \mathbb{R}^4$. Such polytopes are called *reflexive*. It can be shown that, for a given reflexive polytope Δ in \mathbb{R}^4 , the *dual* polytope Δ° defined by

$$\Delta^\circ = \left\{ \mathbf{v} \in \mathbb{R}^4 \mid \langle \mathbf{m}, \mathbf{v} \rangle \geq -1 \quad \forall \mathbf{m} \in \Delta \right\} \quad (2.1)$$

also has all its vertices on the lattice \mathbb{Z}^4 , like the original polytope Δ does. To this dual polytope Δ° , we can associate a collection of the convex cones over all its faces, forming the fan for our toric fourfold \mathcal{A} .

Now, as for the construction of toric fourfold from a given fan in \mathbb{R}^4 , several equivalent methods are known. What best suits our purpose amongst them is Cox's homogeneous-coordinate approach [26], where a complex homogeneous coordinate x_ρ is associated to each one-dimensional cone ρ in the fan. Thus, if the fan has k edges, then there are k homogeneous coordinates (x_1, \dots, x_k) for \mathbb{C}^k . The next task is to identify a certain measure zero subset Z of \mathbb{C}^k which should be removed. Let S be a set of edges that do not span any cone in the fan and let $Z(S) \subset \mathbb{C}^k$ be the linear subspace defined by setting $x_\rho = 0$, for all $\rho \in S$. Now, let $Z \subset \mathbb{C}^k$ be the union of the subspaces $Z(S)$ for all such S . Then, the toric fourfold is constructed as a quotient of $\mathbb{C}^k - Z$ by the following $(\mathbb{C}^*)^{k-4}$ action:

$$(x_1, \dots, x_k) \sim (\lambda_r^{\beta_r^1} x_1, \dots, \lambda_r^{\beta_r^k} x_k), \quad \lambda_r \in \mathbb{C}^* \text{ for } r = 1, \dots, k-4, \quad (2.2)$$

where the coefficients β_r^ρ are defined by the linear relations $\sum_{\rho=1}^k \beta_r^\rho x_\rho = 0$ amongst the edges. Hence, β_r^ρ form a $(k-4) \times k$ matrix which is often referred to as a *charge matrix* [27]. The identification rule in (2.2) can be schematically written as

$$\mathcal{A} = \frac{(\mathbb{C}^k - Z)}{(\mathbb{C}^*)^{k-4}}. \quad (2.3)$$

Note that the construction of toric fourfolds in (2.3) naturally generalises that of projective space \mathbb{P}^4 , the simplest toric fourfold, in which case $Z = \{O\}$ and $k = 5$; that is,

$$\mathbb{P}^4 = \frac{(\mathbb{C}^5 - \{O\})}{\mathbb{C}^*}. \quad (2.4)$$

2.2. Calabi-Yau Threefolds

A Calabi-Yau hypersurface X to the toric fourfold \mathcal{A} is constructed in a straightforward manner without requiring any further data: as long as the polytope Δ is reflexive, it also defines $X \subset \mathcal{A}$. Note that, in this case, Δ° is also a reflexive polytope since $(\Delta^\circ)^\circ = \Delta$. To a reflexive polytope Δ in \mathbb{R}^4 , we can associate a family of Calabi-Yau threefolds X defined as

the vanishing loci of the polynomials of the form

$$P_{\{C_m\}}(x_1, \dots, x_k) = \sum_{\mathbf{m} \in \Delta} C_{\mathbf{m}} \prod_{\rho=1}^k x_{\rho}^{\langle \mathbf{m}, \mathbf{v}_{\rho} \rangle + 1}, \quad (2.5)$$

where $x_{\rho=1, \dots, k}$ are the k homogeneous coordinates of \mathcal{A} associated to the lattice vertices $\mathbf{v}_{\rho=1, \dots, k}$ of Δ° and $C_{\mathbf{m}}$ are numerical coefficients parameterising the complex structure of X .

Heterotic compactifications ask for compact Calabi-Yau threefolds that are smooth. However, a toric fourfold \mathcal{A} constructed by (2.3) usually bears singularities and they in general descend to the hypersurfaces X too. In order to make X nonsingular, we partially desingularise \mathcal{A} so that the hypersurfaces may avoid the singularities of the ambient space [10]. This process corresponds to triangulating the (dual) polytope in a special way and is called an *MPCP-triangulation*.³

As for the statistics, a total of 473,800,776 reflexive polytopes in \mathbb{R}^4 have been classified [17–19], each of which gives rise to a toric fourfold \mathcal{A} as well as a family of Calabi-Yau threefolds X . It turns out that only 124 out of them describe smooth manifolds, for which no MPCP-triangulations are required.

3. Monad Construction of Vector Bundles

In the physics literature, especially in the context of heterotic string phenomenology, construction of vector bundles has been attempted in several ways. They include *spectral cover construction* [28–34], *bundle extension* [35–37], and the mixture thereof [38]. In many of them, it was essential for the base threefolds to have a torus-fibration structure. On the other hand, *monad construction* [11] does not assume any extra structure and has proved particularly useful for algorithmically scanning a vast number of vector bundles [39–43].

A *monad* vector bundle is essentially the quotient of two Whitney sums of line bundles. More precisely, a monad bundle V over a Calabi-Yau threefold X is defined by the short exact sequence of the form

$$0 \longrightarrow V \longrightarrow \bigoplus_{i=1}^{r_b} \mathcal{O}_X(\mathbf{b}_i) \xrightarrow{f} \bigoplus_{j=1}^{r_c} \mathcal{O}_X(\mathbf{c}_j) \longrightarrow 0, \quad (3.1)$$

where \mathbf{b}_i and \mathbf{c}_j are integer vectors of length $h^{1,1}(X)$, representing the first Chern classes of the summand line bundles $\mathcal{O}_X(\mathbf{b}_i)$ and $\mathcal{O}_X(\mathbf{c}_j)$. The bundle V is a holomorphic $U(n)$ -bundle, where

$$n = r_b - r_c \quad (3.2)$$

is the rank of V .

From (3.1), one can readily read off the Chern class of V :

$$\begin{aligned} c_1(V) &= \left(\sum_{i=1}^{r_b} b_i^r - \sum_{j=1}^{r_c} c_j^r \right) J_r, \\ c_2(V) &= \frac{1}{2} d_{rst} \left(\sum_{j=1}^{r_c} c_j^s c_j^t - \sum_{i=1}^{r_b} b_i^s b_i^t \right) \mathcal{V}^r, \\ c_3(V) &= \frac{1}{3} d_{rst} \left(\sum_{i=1}^{r_b} b_i^r b_i^s b_i^t - \sum_{j=1}^{r_c} c_j^r c_j^s c_j^t \right), \end{aligned} \quad (3.3)$$

where $J_r \in H^{1,1}(X, \mathbb{R})$ represent the harmonic $(1, 1)$ -forms $c_1(\mathcal{O}_X(\mathbf{e}_r))$, the d_{rst} are the triple intersection numbers defined by

$$d_{rst} = \int_X J_r \wedge J_s \wedge J_t, \quad (3.4)$$

and the ν^r are the 4-forms furnishing the dual basis to the Kähler generators J_r , subject to the duality relation

$$\int_X J_r \wedge \nu^s = \delta_r^s. \quad (3.5)$$

As can be seen from (3.3), the Chern class of V only depends on the integer parameters \mathbf{b}_i and \mathbf{c}_j , as well as the topology of the base manifold X . Choosing an appropriate morphism f in the defining sequence (3.1) corresponds to the tuning of more refined invariants of V .

4. Towards the Standard Model

Sections 2 and 3 have shown that the vacuum topology is essentially described by lattice vertices and integer parameters, both of which are discrete and combinatorial in nature. One can therefore attempt to construct $\mathcal{N} = 1$ heterotic vacua in an algorithmic way. Torically constructed Calabi-Yau threefolds form a dataset of reflexive polytopes represented by the lattice vertices, and monad bundles are explored on each of the base manifolds by varying the integer parameters.

4.1. Phenomenological Constraints on the Vacua

With the geometric constraints so far explained, one would only be able to guarantee the right number of supersymmetry at low energy, that is, $\mathcal{N} = 1$ at $D = 4$. Since the goal of string phenomenology is to obtain (supersymmetric versions of) the standard model, more criteria should further be imposed on the $\mathcal{N} = 1$ vacua. To make things clear, let us emphasize that in this paper the terminology “standard-like” model will imply the following:

- (i) Gauge invariance under $SU(3)_C \times SU(2)_L \times U(1)_Y$, possibly with an extra $U(1)_{B-L}$ factor;
- (ii) three generations of quarks and leptons, and no exotics;
- (iii) cancellation of heterotic anomaly.

Here, we translate the above three phenomenological constraints into the conditions on the vacuum topology.

4.1.1. Gauge Group

As explained in Section 1, the structure group \mathcal{G} of the visible sector bundle sits in E_8 and its commutant \mathcal{H} becomes the low-energy gauge group. In order to obtain $\mathcal{H} = SO(10)$ and $SU(5)$, one must choose $\mathcal{G} = SU(4)$ and $SU(5)$, respectively. In particular, the rank of the bundle should be either 4 or 5 and, hence, by (3.2),

$$r_b - r_c = 4 \text{ or } 5, \quad (4.1)$$

where r_b and r_c are the ranks of the two vector bundles in the defining sequence (3.1) of V . What is more, since the structure group should be “special” unitary, the first Chern class $c_1(V)$ of V is to vanish. By (3.4), this corresponds to

$$\sum_{i=1}^{r_b} \mathbf{b}_i = \sum_{j=1}^{r_c} \mathbf{c}_j, \quad (4.2)$$

where $\mathbf{b}_i = (b_i^1, \dots, b_i^{h^{1,1}})$ and $\mathbf{c}_j = (c_j^1, \dots, c_j^{h^{1,1}})$ are the $h^{1,1}$ -tuples of integers labelling the summand line bundles and, hence, parameterising the monad V .

We still have to break the GUT group further down to a standard-like one, and this second breaking will require $\pi_1(X)$ -Wilson-lines. However, given the observation that most of the torically constructed Calabi-Yau threefolds have a trivial first fundamental group [44], they must be quotiented out by freely-acting discrete symmetries so that we may turn on appropriate Wilson lines. Therefore, we will eventually have to look for a discrete symmetry group G that acts freely on X and make a quotient space $\hat{X} = X/G$, which will then have a nontrivial first fundamental group $\pi_1(\hat{X}) \simeq G$.

4.1.2. Cancellation of Heterotic Anomaly

Heterotic models need to satisfy a well-known anomaly condition. So far, we have only mentioned one holomorphic vector bundle V for the visible sector but the theory has another bundle \tilde{V} for the hidden sector. Heterotic vacua can also have five-branes whose strong-coupling origin is M5-branes. In order to keep the four-dimensional Lorentz symmetry, their world volumes must stretch along the external Minkowski M_4 . The remaining two dimensions should then wrap holomorphic two cycles in X for unbroken supersymmetry. Thus, the homology classes associated with these two cycles must be *effective* and, hence, belong to the Mori cone in $H_2(X, \mathbb{Z})$. In other words, the corresponding four-forms must belong to the corresponding cone in $H^4(X, \mathbb{Z})$.

In this most general setup, heterotic anomaly cancellation imposes a topological constraint relating the Calabi-Yau threefold, the two vector bundles, and the five-brane classes. When $c_1(TX) = c_1(V) = c_1(\tilde{V}) = 0$, the anomaly condition can be expressed, at the level of cohomology, as

$$c_2(TX) - c_2(V) - c_2(\tilde{V}) = W, \quad (4.3)$$

where $W = \sum_i W_i$ is the sum of the five-brane classes. Note that W itself should also belong to the Mori cone of X as all the summands W_i do. In our discussion, however, without mentioning the second bundle \tilde{V} , we presume a trivial bundle for the hidden sector. Thus, the anomaly constraint in (4.3) says that $c_2(TX) - c_2(V)$ is effective.

4.1.3. Particle Spectra

Table 1 shows how the low-energy particle spectra are determined from various bundle-valued cohomology groups. Assuming that V is a stable bundle⁴ implies that $h^0(X, V) = 0 = h^3(X, V)$, and, hence, to obtain three net generations of quarks and leptons, we must have

$$-\frac{1}{2} \int_X c_3(V) = h^1(X, V) - h^2(X, V) = 3|G|, \quad (4.4)$$

Table 2: The list of standard-like constraints on the $\mathcal{N} = 1$ heterotic vacua, each described by a Calabi-Yau threefolds X and a \mathcal{G} -bundle V thereon; the integers b_i^r and c_j^r parameterise the bundle V as in (3.1), where $i = 1, \dots, r_b$, $j = 1, \dots, r_c$, and $r = 1, \dots, h^{1,1}(X)$. The second column states the constraints on the background geometry, and the third column expresses the corresponding algebraic equations that the parameters b_i^r and c_j^r must obey, where $d_{rst} = \int_X J_r \wedge J_s \wedge J_t$ are the intersection numbers for a given basis $\{J_r\}_{1 \leq r \leq h^{1,1}(X)}$ for $H^{1,1}(X, \mathbb{R})$.

Physics origin	Background geometry	Algebraic constraints on \mathbf{b}_i and \mathbf{c}_j
Gauge group	(a) $\mathcal{G} = SU(n)$, for $n = 4, 5$ (b) X has a discrete free action G	(a1) $r_b - r_c = 4$ or 5 (a2) $\sum_{i=1}^{r_b} b_i^r = \sum_{j=1}^{r_c} c_j^r$, for all r
Anomaly	$c_2(TX) - c_2(V)$ is effective	$c_2(TX)_r - (1/2)d_{rst}(\sum_{j=1}^{r_c} c_j^s c_j^t - \sum_{i=1}^{r_b} b_i^s b_i^t) > 0$, for all r
Particle spectra	$(1/2) \int_X c_3(V) = -3 G $	$d_{rst}(\sum_{i=1}^{r_b} b_i^r b_i^s b_i^t - \sum_{j=1}^{r_c} c_j^r c_j^s c_j^t) = -18 G $

where the Aiyah-Singer index theorem [45] has been applied to the differential operator \not{D}_V on X and $|G|$ is the order of the discrete symmetry group G , with which we will have to quotient the ‘‘upstairs’’ threefolds X .

4.2. Discrete System for Standard-Like Vacua

In this subsection, we briefly summarise the model-building requirements that have so far been discussed.

- (i) Calabi-Yau threefold: a reflexive polytope $\Delta \subset \mathbb{R}^4$ describes a Calabi-Yau threefold X . In the computer package PALP [46], by inserting the list of lattice vertices of Δ or, equivalently, the corresponding ‘‘weight system’’ [18], one can obtain all the topological invariants of X relevant to the heterotic compactification.
- (ii) Monad vector bundle: the $r_b + r_c$ integer vectors \mathbf{b}_i and \mathbf{c}_j of length $h^{1,1}(X)$, each labelling a line bundle summand, parameterise our monad bundle V .
- (iii) Standard-like constraints: the internal backgrounds are also constrained by the standard-like phenomenology. It turns out that given a Calabi-Yau threefold X , that is, for a fixed topology of X , the monad parameters \mathbf{b}_i and \mathbf{c}_j must obey the algebraic equations of degree 0, 1, 2, and 3 shown in Table 2.

Note that the integer combinatorics under the algebraic constraints of small degrees has formed a simple discrete system for standard-like heterotic vacua. However, this system of vacua is far from being finite yet. To begin with, there are no upper bounds on r_b and r_c that count the number of monad parameters. Before initiating an exploration of the landscape, one first needs to add more constraints to make the system finite and those extra constraints had better be related to preferred phenomenology. Now, if the line bundle summands in (3.1) are ample or, equivalently, if all the monad parameters b_i^r and c_j^r are positive,⁵ then, by Kodaira’s vanishing theorem [45, 47], the cohomology group $H^2(X, V)$ vanishes and, hence, the low-energy effective theory acquires no antigerations. Of course this is a phenomenologically preferred feature, although not necessary. We call a monad *positive* if it is only parameterised by positive integers and *semipositive* if all its parameters are either positive or zero. Secondly, one can also constrain the relative size of these monad parameters so that each entry of the vector $\mathbf{b}_i - \mathbf{c}_j$ may be nonnegative, for all i and j . In this case, we will call the monad *generic*

since the monad map f in (3.1), thought of as an $r_c \times r_b$ matrix of polynomials, may generically have all the entries nonzero.

4.3. Exploring a Region of the Landscape

As for the first step, one can think of exploring generic, positive monads over a “small” class of Calabi-Yau threefolds. As was mentioned in Section 2.2, the total dataset of torically constructed Calabi-Yau threefolds are way too large to grasp altogether. Therefore, at the initial stage, those in “smooth” ambient spaces have first been considered amongst the total of 500 million [40]. It turns out that over these $O(100)$ manifolds, the generic, positive monads are finite in number under the constraints in Table 2 and the standard-like vacua have indeed been classified, resulting in 61 candidate models.

Based on this experience, one can become more ambitious and extend the vacuum search, both bundle-wise and Calabi-Yau-wise. Firstly, with the positivity condition a bit relaxed, the generic, semipositive monads have been explored over the same $O(100)$ Calabi-Yau threefolds [40]. The standard-like vacua with the monads of this type turn out to form an infinite class, and, hence, they have been explored under an artificial upper bound on the monad parameters, resulting in 85 models. Secondly, the programme has also been extended to include singular ambient manifolds with small $h^{1,1}$ [41]. A total of $O(300)$ torically constructed Calabi-Yau threefolds have the Hodge number $h^{1,1} \leq 3$, and the generic, positive monads have been classified thereon, giving rise to new candidate models.

5. Summary and Outlook

In this paper, we have discussed a systematic approach towards standard-like heterotic vacua. The proposed algorithms have indeed been implemented in a computer package [48]. Simplicity of the integer combinatorics for the $\mathcal{N} = 1$ heterotic vacua was the essential feature that made this approach a tractable programme. It was motivated by the general observation that any carefully chosen single model is likely to fail the detailed structure of the standard model. Thus, the spirit of the programme is to obtain a large number of standard-like models, on which further constraints should be imposed later on to refine the set of candidates, eventually reaching the “genuine” standard model(s).

The combinatorics of toric geometry has been invaluable for constructing toric ambient fourfolds, to which Calabi-Yau threefolds have been embedded as hypersurfaces, and for computing their topological invariants relevant to the four-dimensional phenomenology. Smooth ambient fourfolds have been considered as a starter [40], and general ambient fourfolds have also been dealt with [41] by partially resolving the singularities, if they bear any, so that the smoothness of the hypersurface Calabi-Yau threefolds is guaranteed. In both cases, the generic, positive monads (and some semipositive ones, too, in the former case) have been probed under the standard-like criteria. We have thus obtained a set of candidate models, that are anomaly free and that have a chance to produce three generations of quarks and leptons without any antigerations.

To guarantee the three-generation property of these candidates, further study of discrete symmetries of the manifolds is essential. Braun has recently classified the free group actions on complete intersection Calabi-Yau threefolds in multiprojective spaces [49], and his algorithm can in principle be generalised to toric cases. The line-bundle cohomologies on the torically constructed Calabi-Yau threefolds are also an essential part of the model building. The starting point would be to work out the cohomologies on the ambient toric

varieties, which have already been investigated in the mathematics and physics literatures [23, 50–52]. Practical conversion of this information into the line-bundle cohomologies on the hypersurfaces is a rewarding work along the line of monad bundles and heterotic strings. As for the completion of the detailed particle spectra, the cohomologies of the monads in different representations are also to be revealed.

Acknowledgment

The author is grateful to Yang-Hui He and Andre Lukas for collaborations and to Lara Anderson and James Gray for discussion, on the projects which this paper is based upon. He would especially like to thank Maximilian Kreuzer, who passed away in the middle of collaborations on part of the work reviewed here, for invaluable correspondence and advice.

Endnotes

1. The choice $G = SU(3)$ also gives rise to E_6 GUT models. However, they have an inherent trouble in doublet-triplet splitting of Higgs multiplet (see, for a recent example, [39]) and, hence, we will not address the models of this type here.
2. In algebraic geometry, Calabi-Yau threefolds are, in general, realised as complete intersections of hypersurfaces in toric varieties of dimension greater than or equal to four but this paper will only be dealing with single-hypersurface cases.
3. MPCP is a short for maximal, projective, crepant and partial. A triangulation is said to be *maximal* if all lattice points of the polytope are involved, *projective* if the Kähler cone of the resolved manifold has a nonempty interior, and *crepant* if no points outside the polytope are taken. In practice, all possible MPCP-triangulations of a given reflexive polytope are searched by the computer package PALP [46].
4. Testing the bundle stability is indeed one of the crucial steps for our model construction. However, it is not at all an easy task to check if a given bundle is stable. So, our strategy is first to make use of some consequences of stability and then to check the validity at the very end of the story. In this paper, focusing on the discrete combinatorics for the vacua, we will not say more about the issue of stability.
5. To be precise, the Kodaira vanishing assumes that the vectors \mathbf{b}_i and \mathbf{c}_j lie in the Kähler cone of X . In case the Kähler cone does not coincide with the positive region, one may redefine the standard basis vectors of $H^{1,1}(X, \mathbb{R})$ to be the Kähler cone generators. For this to work, however, the cone generators should form a linearly independent basis and hence, we implicitly restrict ourselves to the Calabi-Yau threefolds of this type.

References

- [1] P. Candelas, G. T. Horowitz, A. Strominger, and E. Witten, "Vacuum configurations for superstrings," *Nuclear Physics B*, vol. 258, pp. 46–74, 1985.
- [2] M. B. Green, J. H. Schwarz, and E. Witten, *Superstring Theory*, vol. 2 of *Cambridge Monographs on Mathematical Physics*, Cambridge University Press, Cambridge, UK, 1987.
- [3] E. Witten, "Strong coupling expansion of Calabi-Yau compactification," *Nuclear Physics B*, vol. 471, no. 1-2, pp. 135–158, 1996.
- [4] A. Lukas, B. A. Ovrut, and D. Waldram, "On the four-dimensional effective action of strongly coupled heterotic string theory," *Nuclear Physics B*, vol. 532, no. 1-2, pp. 43–82, 1998.
- [5] A. Lukas, B. A. Ovrut, K. S. Stelle, and D. Waldram, "The Universe as a domain wall," *Physical Review D*, vol. 59, no. 8, pp. 1–9, 1999.

- [6] A. Lukas, B. A. Ovrut, and D. Waldram, "Non-standard embedding and five-branes in heterotic M theory," *Physical Review D*, vol. 59, no. 10, pp. 1–17, 1999.
- [7] A. Lukas, B. A. Ovrut, K. S. Stelle, and D. Waldram, "Heterotic M-theory in five dimensions," *Nuclear Physics B*, vol. 552, no. 1-2, pp. 246–290, 1999.
- [8] S. K. Donaldson, "Anti self-dual yang-mills connections over complex algebraic surfaces and stable vector bundles," *Proceedings of the London Mathematical Society*, vol. 50, no. 1, pp. 1–26, 1985.
- [9] K. Uhlenbeck and S. T. Yau, "On the existence of hermitian-yang-mills connections in stable vector bundles," *Communications on Pure and Applied Mathematics*, vol. 39, supplement 1, pp. S257–S293, 1986.
- [10] V. V. Batyrev, "Dual polyhedra and mirror symmetry for Calabi-Yau hypersurfaces in toric varieties," *Journal of Algebraic Geometry*, vol. 3, p. 493, 1994.
- [11] C. Okonek, M. Schneider, and H. Spindler, *Vector Bundles on Complex Projective Spaces*, Birkhäuser, 1980.
- [12] P. Candelas, A. M. Dale, C. A. Lütken, and R. Schimmrigk, "Complete intersection Calabi-Yau manifolds," *Nuclear Physics B*, vol. 298, no. 3, pp. 493–525, 1988.
- [13] P. Candelas, C. A. Lütken, and R. Schimmrigk, "Complete intersection Calabi-Yau manifolds (II). Three generation manifolds," *Nuclear Physics B*, vol. 306, no. 1, pp. 113–136, 1988.
- [14] P. S. Green, T. Hübsch, and C. A. Lütken, "All hodge numbers of all complete intersection Calabi-Yau manifolds," *Classical and Quantum Gravity*, vol. 6, no. 2, pp. 105–124, 1989.
- [15] A. He and P. Candelas, "On the number of complete intersection Calabi-Yau manifolds," *Communications in Mathematical Physics*, vol. 135, no. 1, pp. 193–199, 1990.
- [16] M. Gagnon and Q. Ho-Kim, "An exhaustive list of complete intersection Calabi-Yau manifolds," *Modern Physics Letters A*, vol. 9, no. 24, pp. 2235–2243, 1994.
- [17] M. Kreuzer and H. Skarke, "On the classification of reflexive polyhedra," *Communications in Mathematical Physics*, vol. 185, no. 2, pp. 495–508, 1997.
- [18] M. Kreuzer and H. Skarke, "Complete classification of reflexive polyhedra in four dimensions," *Advances in Theoretical and Mathematical Physics*, vol. 4, p. 1209, 2002.
- [19] M. Kreuzer, "Toric geometry and Calabi-Yau compactifications," *Ukrainian Journal of Physics*, vol. 55, no. 5, pp. 613–625, 2010.
- [20] W. Fulton, *Introduction to Toric Varieties*, Princeton University Press, 1993.
- [21] T. Oda, *Convex Bodies and Algebraic Geometry*, Springer, 1988.
- [22] D. Cox, "Recent developments in toric geometry," In press, <http://arxiv.org/abs/alg-geom/9606016>.
- [23] D. Cox, J. Little, and H. Schenck, *Toric Varieties*, American Mathematical Society, 2011.
- [24] B. R. Greene, "String theory on Calabi-Yau manifolds," In press, <http://arxiv.org/abs/hep-th/9702155>.
- [25] V. Bouchard, "Lectures on complex geometry, Calabi-Yau manifolds and toric geometry," In press, <http://arxiv.org/abs/hep-th/0702063>.
- [26] D. Cox, "The homogeneous coordinate ring of a toric variety, revised version," In press, <http://arxiv.org/abs/alg-geom/9210008>.
- [27] K. Hori et al., *Mirror Symmetry*, American Mathematical Society, 2003.
- [28] R. Friedman, J. W. Morgan, and E. Witten, "Vector bundles over elliptic fibrations," *Journal of Algebraic Geometry*, vol. 8, no. 2, pp. 279–401, 1999.
- [29] R. Donagi, A. Lukas, B. A. Ovrut, and D. Waldram, "Non-perturbative vacua and particle physics in M-theory," *Journal of High Energy Physics*, vol. 3, no. 5, article 018, 1999.
- [30] R. Donagi, A. Lukas, B. A. Ovrut, and D. Waldram, "Holomorphic vector bundles and non-perturbative vacua in M-theory," *Journal of High Energy Physics*, vol. 3, no. 6, article 034, 1999.
- [31] D. E. Diaconescu and G. Ionesi, "Spectral covers, charged matter and bundle cohomology," *Journal of High Energy Physics*, vol. 2, no. 12, article 001, 1998.
- [32] B. Andreas, G. Curio, and A. Klemm, "Towards the standard model spectrum from elliptic Calabi-Yau manifolds," *International Journal of Modern Physics A*, vol. 19, no. 12, pp. 1987–2014, 2004.
- [33] B. Andreas and D. Hernandez-Ruiperez, "Comments on $N = 1$ heterotic string vacua," *Advances in Theoretical and Mathematical Physics*, vol. 7, pp. 751–786, 2004.
- [34] G. Curio, "Standard model bundles of the heterotic string," *International Journal of Modern Physics A*, vol. 21, no. 6, pp. 1261–1282, 2006.
- [35] V. Braun, Y. H. He, B. A. Ovrut, and T. Pantev, "A heterotic standard model," *Physics Letters B*, vol. 618, no. 1–4, pp. 252–258, 2005.

- [36] V. Braun, Y. H. He, B. A. Ovrut, and T. Pantev, "A standard model from the $E8 \times E8$ heterotic superstring," *Journal of High Energy Physics*, no. 6, article 039, pp. 897–914, 2005.
- [37] V. Braun, Y. H. He, B. A. Ovrut, and T. Pantev, "Vector bundle extensions, sheaf cohomology, and the heterotic standard model," *Advances in Theoretical and Mathematical Physics*, vol. 10, no. 4, pp. 525–589, 2006.
- [38] R. Donagi, Y. H. He, B. A. Ovrut, and R. Reinbacher, "The spectra of heterotic standard model vacua," *Journal of High Energy Physics*, no. 6, article 070, pp. 1601–1634, 2005.
- [39] L. B. Anderson, J. Gray, Y. H. He, and A. Lukas, "Exploring positive monad bundles and a new heterotic standard model," *Journal of High Energy Physics*, vol. 2010, no. 2, article 054, 2010.
- [40] Y. H. He, S. J. Lee, and A. Lukas, "Heterotic models from vector bundles on toric Calabi-Yau manifolds," *Journal of High Energy Physics*, vol. 2010, no. 5, article 071, 2010.
- [41] Y. H. He, M. Kreuzer, S. J. Lee, and A. Lukas, "Heterotic bundles on Calabi-Yau manifolds with small Picard number," In preparation.
- [42] L. B. Anderson, Y. H. He, and A. Lukas, "Heterotic compactification, an algorithmic approach," *Journal of High Energy Physics*, vol. 2007, no. 7, article 049, 2007.
- [43] L. Anderson, Y. H. He, and A. Lukas, "Monad bundles in heterotic string compactifications," *Journal of High Energy Physics*, vol. 2008, no. 7, article 104, 2008.
- [44] V. Batyrev and M. Kreuzer, "Integral cohomology and mirror symmetry for Calabi-Yau 3-folds," In press, <http://arxiv.org/abs/math/0505432>.
- [45] P. Griffiths and J. Harris, *Principles of Algebraic Geometry*, Wiley, 1978.
- [46] M. Kreuzer and H. Skarke, "Palp: a package for analysing lattice polytopes with applications to toric geometry," *Computer Physics Communications*, vol. 157, no. 1, pp. 87–106, 2004.
- [47] R. Hartshorne, *Algebraic Geometry (Graduate Texts in Mathematics)*, Springer, 1977.
- [48] A. Lukas, L. Anderson, J. Gray, Y. H. He, and S. J. Lee, CICY package, based on methods described in Refs. [15, 47-49].
- [49] V. Braun, "Discrete wilson lines in F-theory," . In press, <http://arxiv.org/abs/1010.2520>.
- [50] R. Blumenhagen, B. Jurke, T. Rahn, and H. Roschy, "Cohomology of line bundles: a computational algorithm," *Journal of Mathematical Physics*, vol. 51, no. 10, article 103525, 2010.
- [51] H. Roschy and T. Rahn, "Cohomology of line bundles: proof of the algorithm," *Journal of Mathematical Physics*, vol. 51, no. 10, article 103520, 2010.
- [52] R. Blumenhagen, B. Jurke, T. Rahn, and H. Roschy, "Cohomology of line bundles: applications," In press, <http://arxiv.org/abs/1010.3717>.

Review Article

Computational Tools for Cohomology of Toric Varieties

Ralph Blumenhagen, Benjamin Jurke, and Thorsten Rahn

Max-Planck-Institut für Physik, Föhringer Ring 6, 80805 München, Germany

Correspondence should be addressed to Thorsten Rahn, rahn@mppmu.mpg.de

Received 15 April 2011; Accepted 27 June 2011

Academic Editor: André Lukas

Copyright © 2011 Ralph Blumenhagen et al. This is an open access article distributed under the Creative Commons Attribution License, which permits unrestricted use, distribution, and reproduction in any medium, provided the original work is properly cited.

Novel nonstandard techniques for the computation of cohomology classes on toric varieties are summarized. After an introduction of the basic definitions and properties of toric geometry, we discuss a specific computational algorithm for the determination of the dimension of line-bundle-valued cohomology groups on toric varieties. Applications to the computation of chiral massless matter spectra in string compactifications are discussed, and using the software package *cohomCalc*, its utility is highlighted on a new target space dual pair of $(0, 2)$ heterotic string models.

1. Introduction

The computation of certain cohomology groups is a critical technical step in string model building, relevant, for example, in determining the (chiral) zero-mode spectrum or parts of the effective four-dimensional theory, like the Yukawa coupling. Common methods often try to relate the computation at hand via a chain of isomorphisms back to known results in order to avoid most of the cumbersome computations from the ground up. Spectral sequences are the established technique to deal with such problems, but often end up to become laborious rather quickly. Having reasonable efficient algorithms to one's avail is therefore a vital requirement to make progress.

Supersymmetry in four dimensions puts strong restrictions on the geometries admissible for string compactifications. In the absence of additional background fluxes (besides a gauge flux), this leads to the class of Calabi-Yau manifolds, where of particular interest for $\mathcal{N} = 1$ supersymmetry are the Calabi-Yau threefolds and fourfolds. Due to the Atiyah-Singer index theorem, chirality is realized by also turning on a nontrivial gauge background, which can be understood as the curvature of a nontrivial holomorphic vector bundle on the manifold. The majority of known Calabi-Yau manifolds are based on toric

geometry. In particular, they are constructed as complete intersections of hypersurfaces in toric varieties. The vector bundle can then be described by different methods, where the three mostly used ones are

- (1) the monad construction, which naturally arises in the $(0,2)$ gauged linear sigma model,
- (2) the spectral cover construction, which gives stable holomorphic vector bundles with structure group $SU(n)$ on elliptically fibered Calabi-Yau threefolds,
- (3) the construction via extensions, which is the natural counterpart of brane recombinations.

All these three constructions have in common that they involve line bundles in one way or the other. For instance, the monad is defined via sequences of the Whitney sums of line bundles, whereas the n -fold spectral cover is equipped in addition with a nontrivial line bundle on it, which via the Fourier-Mukai transform gives an $SU(n)$ vector bundle on the Calabi-Yau manifold. The basis starting point of every cohomology computation is therefore the knowledge of line-bundle-valued cohomology classes on the ambient toric variety.

Using a simple yet powerful algorithm, we can compute the line-bundle-valued cohomology dimensions $h^i(X; L_X) = \dim H^i(X; L_X)$ for any toric variety based on the information contained in the Stanley-Reisner ideal. The Koszul complex then allows to relate the cohomology on the toric variety to the cohomology of a hypersurface or complete intersection. The particular form of the algorithm also allows to easily deal with finite group actions on such geometries, that is, to consider orbifold spaces and twisted string states.

This paper is organized as follows. In Section 2 some basics of toric geometry are introduced, including the Stanley-Reisner ideal and toric fans. Section 3 introduces the computational algorithm for cohomology group dimensions of toric varieties that will be used throughout this paper. Section 4 shows how a finite group action and the resulting quotient space can be handled. In Section 5 the Koszul sequence is introduced, which allows to relate the ambient variety's cohomology to the cohomology of hypersurfaces and complete intersections. Monad bundle constructions and the Euler sequence are introduced in Section 6. In Section 7 we show an example of how to compute the data for a $(2,2)$ model that is dual to a $(0,2)$ model. The paper closes in Section 8 with a brief outlook on potential further applications and developments.

2. Toric Varieties

One of the most important aspects of toric geometry is the ability to understand it in purely combinatorial terms, which is ideally suited to be handled by computers (see [1–4] for introductions into the subject). Toric geometry is also directly related to gauged linear σ -models (GLSMs) in physics [5]. On a more basic notion, a toric variety is a generalization of a projective space, which consists of a set of homogeneous coordinates x_1, \dots, x_n as well as R projective relations

$$(x_1, \dots, x_n) \sim \left(\lambda_r^{Q_1^{(r)}} x_1, \dots, \lambda_r^{Q_n^{(r)}} x_n \right) \quad \text{for } \lambda_r \in \mathbb{C}^\times. \quad (2.1)$$

The $Q_i^{(r)}$ for $r = 1, \dots, R$ and $i = 1, \dots, n$ are GLSM charges, that is, the Abelian $U(1)$ charges in the associated GLSM, and corresponding to the projective weights. In direct comparison to

projective spaces, toric varieties can be characterized as arising due to the usage of multiple projective relations instead of just a single one. The special case of a projective space therefore corresponds to $R = 1$ in the above notation.

The homogeneous coordinates x_i become $\mathcal{N} = (2, 2)$ chiral superfields in the GLSM picture, and the Fayet-Iliopoulos parameters ξ_r of the Abelian symmetries can be interpreted as the Kähler parameters of the geometric space. This parameter space of $\vec{\xi} = (\xi_1, \dots, \xi_R)$ is then split into R -dimensional cones due to the vanishing of the D-terms associated to the GLSM. Within each cone the D-flatness condition can be solved and the cones correspond to the geometrical Kähler cones. Each such cone is often referred to as a geometric phase and can be fully characterized by a set of collections of coordinates

$$\mathcal{S}_\rho = \{x_{\rho_1}, x_{\rho_2}, \dots, x_{\rho_{|\mathcal{S}_\rho|}}\} \quad \text{for } \rho = 1, \dots, N \quad (2.2)$$

which are not allowed to vanish simultaneously. Note that such a collection is often written in product form; that is, the square-free monomial $x_{\rho_1} x_{\rho_2} \cdots x_{\rho_{|\mathcal{S}_\rho|}}$ refers exactly to the same set. All those sets form the Stanley-Reisner ideal

$$\text{SR}(X) = \langle \mathcal{S}_1, \dots, \mathcal{S}_N \rangle, \quad (2.3)$$

which can be equivalently used to uniquely specify a geometric phase. Note that the Stanley-Reisner ideal is Alexander dual to the irrelevant ideal B_Σ used in the mathematical literature.

Given the GLSM charges and the Stanley-Reisner ideal to identify the geometric phase, the toric variety X of dimension $d = n - R$ can be described as the coset space

$$X = \frac{(\mathbb{C}^n - Z)}{(\mathbb{C}^\times)^R}, \quad (2.4)$$

where Z is the set of removed points specified by $\text{SR}(X)$ via

$$Z = \bigcup_{\rho=1}^N \{x_{\rho_1} = x_{\rho_2} = \cdots = x_{\rho_{|\mathcal{S}_\rho|}} = 0\}. \quad (2.5)$$

This set Z can be understood as the toric generalization of the removed origin in a projective space $\mathbb{C}\mathbb{P}^n = (\mathbb{C}^{n+1} - \{0\})/\mathbb{C}^\times$, as the Stanley-Reisner ideal for $\mathbb{C}\mathbb{P}^n$ is just the collection of all coordinates.

The combinatorial perspective on toric geometry mentioned at the start is formulated in terms of toric fans, cones, and triangulations. In this language a geometric phase corresponds to a triangulation of a certain set of lattice vectors ν_i that span the fan Σ_X . The GLSM charges $Q_i^{(r)}$ reappear in the form of R linear relations

$$\sum_{i=1}^n Q_i^{(r)} \nu_i = 0 \quad \text{for } r = 1, \dots, R. \quad (2.6)$$

By associating the lattice vectors ν_i to the homogeneous coordinates x_i , it becomes obvious that the linear relations (2.6) between the lattice vectors encode the projective equivalences

(2.1) between the homogeneous coordinates. In the language of fans the Stanley-Reisner ideal consists of all square-free monomials whose coordinates are not contained in any cone of the toric fan Σ_X .

3. Dimensions of Line-Bundle-Valued Cohomology Groups

Given a toric variety X and a line bundle L_X , a frequent issue is to compute the L_X -valued cohomology group dimensions $h^i(X; L_X)$ for $i = 0, \dots, \dim X$. After a couple of preliminary observations in [6, 7], in [8] a complete novel algorithm for the determination of $h^i(X; L_X)$ was presented. This was subsequently proven in [9] and independently in [10].

The geometric input data for the computational algorithm presented below are the GLSM charges $Q_i^{(r)}$ and the Stanley-Reisner ideal generators $\mathcal{S}_1, \dots, \mathcal{S}_N$. The basic idea of the algorithm is to count the number of monomials, where the total GLSM charge is equal to the divisor class of D , which is the divisor that specifies the line bundle $L_X = \mathcal{O}_X(D)$. The form of those monomials is highly restricted by the Stanley-Reisner ideal, that is, the simpler the structure of $\text{SR}(X)$, the easier the computation.

More precisely, negative integer exponents are only admissible for those coordinates that are contained in subsets of the Stanley-Reisner ideal generators. The most economic way is therefore to determine in a first step the set of square-free monomials Q that arise from unions of the coordinates in any subset of $\text{SR}(X)$. Each Q gives a set of coordinates with negative exponents, and to each Q there is an associated weighting factor $h_i(Q)$ that specifies to which cohomology group's dimension $h^i(X; \mathcal{O}_X(D))$ the number of monomials $\mathcal{N}_D(Q)$ with GLSM charge D contributes. The cohomology group dimension formula can be summarized as

$$\dim H^i(X; \mathcal{O}_X(D)) = \sum_Q \overbrace{h_i(Q)}^{\text{multiplicity factor}} \cdot \underbrace{\mathcal{N}_D(Q)}_{\text{number of monomials}}, \quad (3.1)$$

where the sum ranges over all square-free monomials that can be obtained from unions of Stanley-Reisner ideal generators. In the remainder of this section, both $h_i(Q)$ and $\mathcal{N}_D(Q)$ will be properly defined.

3.1. Computation of Multiplicity Factors

The multiplicity factors are defined by the dimensions of an intermediate relative homology. Let $[N] := \{1, \dots, N\}$ be a set of indices for the N square-free monomials that generate the Stanley-Reisner ideal. Then let, for each subset

$$S_\rho := \{\mathcal{S}_{\rho_1}, \dots, \mathcal{S}_{\rho_k}\} \subset \{\mathcal{S}_1, \dots, \mathcal{S}_N\} \quad (3.2)$$

of generators, $Q(S_\rho)$ be the square-free monomial that arises from the union of all coordinates in each generator \mathcal{S}_{ρ_i} of the subset.

The construction of the relative complex Γ^Q , from which $h_i(Q)$ is defined, goes as follows. From the full simplex on $[N] = \{1, \dots, N\}$, extract only those subsets $\rho \subset [N]$ with $Q(S_\rho) = Q$; that is, one considers all possible combinations of the Stanley-Reisner ideal

generators whose coordinates unify to the same square-free monomial Q . For some fixed $|\rho| = k$, this then defines the set of $(k - 1)$ -dimensional faces $F_{k-1}(Q)$ of the complex Γ^Q , that is,

$$F_k(Q) := \left\{ \rho \subset [N] : \begin{array}{l} |\rho| = k + 1 \\ Q(S_\rho) = Q \end{array} \right\}. \quad (3.3)$$

Furthermore, let $\mathbb{C}^{F_k(Q)}$ be the complex vector space with basis vectors e_ρ for $\rho \in F_k(Q)$. The relative complex

$$\Gamma^Q: 0 \longrightarrow F_{N-1}(Q) \xrightarrow{\phi_{N-1}} \cdots \xrightarrow{\phi_1} F_0(Q) \xrightarrow{\phi_0} F_{-1}(Q) \longrightarrow 0, \quad (3.4)$$

where $F_{-1}(Q) := \{\emptyset\}$ is a face of dimension -1 , is then specified by the chain mappings

$$\begin{aligned} \phi_k: F_k(Q) &\longrightarrow F_{k-1}(Q), \\ e_\rho &\longmapsto \sum_{s \in \rho} \text{sign}(s, \rho) e_{\rho - \{s\}}. \end{aligned} \quad (3.5)$$

A basis vector $e_{\rho - \{s\}}$ vanishes if ρ with the element s removed is not contained in Γ^Q . Furthermore, the signum is defined by $\text{sign}(s, \rho) := (-1)^{\ell-1}$ when s is the ℓ th element of $\rho \subset [N] = \{1, \dots, N\}$ when written in increasing order.

The homology group dimensions

$$h_i(Q) := \dim H_{|Q|-i-1}(\Gamma^Q) \quad (3.6)$$

of the relabeled complex then provide the multiplicity factors that determine to which cohomology group $H^i(X; \mathcal{O}_X(D))$ the monomials associated to Q contribute. It should be emphasized that the $h_i(Q)$ depend only on the geometry (the Stanley-Reisner ideal) of the toric variety X and not on the line bundle $\mathcal{O}_X(D)$, that is, the multiplicity factors only have to be computed once for each geometry.

3.2. Counting Monomials

After computing the multiplicity factors $h_i(Q)$, it remains to count the number of relevant monomials. This second part of the algorithm depends on the GLSM charges of the homogeneous coordinates x_i and the specific line bundle $\mathcal{O}_X(D)$. Let Q again be a square-free monomial. In order to simplify the notation, let $I = (i_1, \dots, i_k, \dots, i_n)$ be an index relabeling such that the product of the first k coordinates gives $Q = x_{i_1} \cdots x_{i_k}$. Then one considers monomials of the form

$$\begin{aligned} R^Q(x_1, \dots, x_n) &:= (x_{i_1})^{-1-a} (x_{i_2})^{-1-b} \cdots (x_{i_k})^{-1-c} (x_{i_{k+1}})^d \cdots (x_{i_n})^e \\ &= \frac{T(x_{i_{k+1}}, \dots, x_{i_n})}{x_{i_1} \cdots x_{i_k} \cdot W(x_{i_1}, \dots, x_{i_k})} \end{aligned} \quad (3.7)$$

Table 1: Toric data for the del Pezzo-1 surface.

Vertices of the polyhedron/fan	Coords.	GLSM charges		Divisor class
		Q^1	Q^2	
$v_1 = (-1, -1)$	x_1	1	0	H
$v_2 = (1, 0)$	x_2	1	0	H
$v_3 = (0, 1)$	x_3	1	1	$H + X$
$v_4 = (0, -1)$	x_4	0	1	X

Intersection form: $HX - X^2$.

$SR(dP_1) = \langle x_1x_2, x_3x_4 \rangle = \langle \mathcal{S}_1, \mathcal{S}_2 \rangle$.

where T and W are monomials (not necessarily square-free) as well as exponents $a, b, c, d, e \in \mathbb{N} \cup \{0\}$. One obviously finds the coordinates of the square-free monomial Q in the denominator, whereas their complements are in the numerator. Based on the particular form of the relevant monomials define

$$\mathcal{N}_D(Q) := \dim \left\{ R^Q : \deg_{\text{GLSM}}(R^Q) = D \right\}, \quad (3.8)$$

which counts the number of relevant monomials that have the same GLSM degree as the divisor D that specified the line bundle $L_X = \mathcal{O}_X(D)$.

3.3. A Step by Step Example: del Pezzo-1 Surface

In order to show the working algorithm in detail, we consider the del Pezzo-1 surface. Its toric data is summarized in Table 1 for the reader's convenience. The two Stanley-Reisner ideal generators yield four possible combinations that become relevant in the computation, namely,

$$Q = 1, \quad x_1x_2, \quad x_3x_4, \quad x_1x_2x_3x_4. \quad (3.9)$$

The computation of the multiplicity factors for those square-free monomials leads to

$$\begin{aligned} \mathfrak{C}_0(1) &= \{\{\emptyset\}\}, & \mathfrak{C}_1(x_1x_2) &= \{\{\mathcal{S}_1\}\}, & \mathfrak{C}_1(x_3x_4) &= \{\{\mathcal{S}_2\}\}, \\ \mathfrak{C}_2(x_1x_2x_3x_4) &= \{\{\mathcal{S}_1, \mathcal{S}_2\}\}, \end{aligned} \quad (3.10)$$

and all other spaces $\mathfrak{C}_i(Q)$ vanishing. After computing the homology, this leads to the following contributions of the monomials (3.7) to the cohomology groups:

$$\begin{aligned} H^0(dP_1; \mathcal{O}(m, n)) &: T(x_1, x_2, x_3, x_4), \\ H^1(dP_1; \mathcal{O}(m, n)) &: \frac{T(x_3, x_4)}{x_1x_2 \cdot W(x_1, x_2)}, \quad \frac{T(x_1, x_2)}{x_3x_4 \cdot W(x_3, x_4)}, \\ H^2(dP_1; \mathcal{O}(m, n)) &: \frac{1}{x_1x_2x_3x_4 \cdot W(x_1, x_2, x_3, x_4)}. \end{aligned} \quad (3.11)$$

Consider computing $h^\bullet(dP_1; \mathcal{O}(-1, -2))$. Since all GLSM charges are positive, there is no contribution to h^0 . Likewise, the denominator monomial of the h^2 contribution already has the GLSM charge $(3, 2)$, which “overshoots” the target values and therefore also gives no contribution. $\deg_{\text{GLSM}}(1/x_1x_2) = (-2, 0)$ is no good either, but $\deg_{\text{GLSM}}(1/x_3x_4) = (-1, -2)$ fits perfectly, such that there is a sole contribution

$$\frac{1}{x_3x_4} \rightsquigarrow h^\bullet(dP_1; \mathcal{O}(-1, -2)) = (0, 1, 0). \quad (3.12)$$

All the aforementioned steps involved in the computation of the cohomology have been conveniently implemented in a high-performance cross-platform package called *cohomCalc* [11].

4. Equivariant Cohomology for Finite Group Actions

Due to the explicit form of the relevant monomials that are counted by the algorithm, one can consider a rather simple generalization that also takes the action of finite groups into account [12, 13]. In orientifold and orbifold settings, the internal part of the space-time is usually specified by a discrete symmetry acting on the “upstairs” geometry. This then induces a corresponding splitting of the cohomology groups

$$H^i(X) = H_{\text{inv}}^i(X) \oplus H_{\text{non-inv}}^i(X) \quad (4.1)$$

as the generating p -cycles can be either invariant or noninvariant under the symmetry. It is also necessary to specify the induced action on the bundle defined on the upstairs geometry.

The so-called equivariant structure uplifts the action on the base geometry to the bundle and preserves the group structure. In fact, for a generic group G , each group element g induces an involution mapping $g : X \rightarrow X$ on the base geometry and has a corresponding uplift $\phi_g : V \rightarrow V$ that has to be compatible with the bundle structure. This makes the diagram

$$\begin{array}{ccc} V & \xrightarrow{g} & V \\ \downarrow & & \downarrow \\ X & \xrightarrow{g} & X \end{array} \rightsquigarrow g = g \quad (4.2)$$

commutative, and the G -structure V is called an equivariant structure if it preserves the group structure, that is, if $\phi_g \circ \phi_h = \phi_{gh}$ holds such that the mapping $g \mapsto \phi_g$ is a group homomorphism.

The choice of an equivariant structure provides the means of how the finite group acts on the relevant monomials (3.7) counted by the algorithm. For a given line bundle $\mathcal{O}_X(D)$, one then has to check for all monomials whether or not they are invariant under the induced action. Consider, for example, the bundle $\mathcal{O}(-6)$ on $\mathbb{C}\mathbb{P}^2$ and the \mathbb{Z}_3 action

$$g_1 : (x_1, x_2, x_3) \mapsto (\alpha x_1, \alpha^2 x_2, x_3) \quad \text{for } \alpha := \sqrt[3]{1} = e^{2\pi i/3} \quad (4.3)$$

on the base coordinates. The same action is used for the monomials, and thus it defines the equivariant structure. The relevant monomials for the algorithm then pick up the following values from the involution:

$$\underbrace{
 \begin{array}{ccccc}
 \frac{1}{u_1^4 u_2 u_3} & \frac{1}{u_1 u_2^4 u_3} & \frac{1}{u_1 u_2 u_3^4} & \frac{1}{u_1^3 u_2^2 u_3} & \frac{1}{u_1^3 u_2 u_3^2} \\
 \underbrace{\hspace{1.5cm}}_{g_1 \rightarrow 1} & \underbrace{\hspace{1.5cm}}_{g_1 \rightarrow 1} & \underbrace{\hspace{1.5cm}}_{g_1 \rightarrow 1} & \underbrace{\hspace{1.5cm}}_{g_1 \rightarrow \alpha} & \underbrace{\hspace{1.5cm}}_{g_1 \rightarrow \alpha^2} \\
 \frac{1}{u_1^2 u_2^3 u_3} & \frac{1}{u_1 u_2^3 u_3^2} & \frac{1}{u_1^2 u_2 u_3^3} & \frac{1}{u_1 u_2^2 u_3^3} & \frac{1}{u_1^2 u_2^2 u_3^2} \\
 \underbrace{\hspace{1.5cm}}_{g_1 \rightarrow \alpha^2} & \underbrace{\hspace{1.5cm}}_{g_1 \rightarrow \alpha} & \underbrace{\hspace{1.5cm}}_{g_1 \rightarrow \alpha} & \underbrace{\hspace{1.5cm}}_{g_1 \rightarrow \alpha^2} & \underbrace{\hspace{1.5cm}}_{g_1 \rightarrow 1}
 \end{array}
 }_{h^2(\mathbb{CP}^2; \mathcal{O}(-6)) = (4_{\text{inv}}, 3_\alpha, 3_{\alpha^2})} , \quad (4.4)$$

such that $h_{\text{inv}}^\bullet(\mathbb{CP}^2; \mathcal{O}(-6)) = (0, 0, 4)$ follows. This gives the cohomology of the quotient space $\mathbb{CP}^2/\mathbb{Z}_3$ as defined by the action in (4.3).

This powerful generalization of the algorithm allows for instance to compute the untwisted matter spectrum in heterotic orbifold models or (parts of) the instanton zero mode spectrum for the Euclidean D-brane instantons in Type II orientifold models (see [14] for concrete applications).

5. The Koszul Complex

In most string theory applications, the geometries of interest are not toric varieties by themselves, but rather defined as subspaces thereof. These are defined as complete intersections of hypersurfaces of certain degrees. In order to relate the cohomology of the toric variety X to the cohomology of a subspace, the Koszul sequence is used.

To make this paper self-contained and because it has been implemented in the *cohomCalc* Koszul extension package, let us briefly describe how this works. Let $D \subset X$ be an irreducible hypersurface, and let $0 \neq \sigma \in H^0(X; \mathcal{O}(D))$ be a global nonzero section of $\mathcal{O}_X(D)$, such that $Z(\sigma) \cong D$. This induces a mapping $\mathcal{O}_X \rightarrow \mathcal{O}_X(D)$ and its dual $\mathcal{O}_X(-D) \hookrightarrow \mathcal{O}_X$, the latter of which can be shown to be injective. Given an effective divisor

$$D := \sum_i a_i H_i \subset X, \quad (5.1)$$

where all $a_i \geq 0$, there is a short exact sequence

$$0 \longrightarrow \mathcal{O}_X(-D) \hookrightarrow \mathcal{O}_X \twoheadrightarrow \mathcal{O}_D \longrightarrow 0, \quad (5.2)$$

called the Koszul sequence. Here \mathcal{O}_D is the quotient of the sheaf \mathcal{O}_X of holomorphic functions on X by all holomorphic functions vanishing at least to order a_i along the irreducible hypersurface $H_i \subset X$. This allows to treat \mathcal{O}_D as the structure sheaf on the divisor D , which effectively identifies the sheaf cohomology $H^i(X; \mathcal{O}_D)$ with $H^i(D; \mathcal{O}_D)$. A proper definition

of the involved mappings, which become quite laborious to work out explicitly, can be found in [15]. In addition of the plain Koszul sequence (5.2), there is also a twisted variant

$$0 \longrightarrow \mathcal{O}_X(T - D) \hookrightarrow \mathcal{O}_X(T) \twoheadrightarrow \mathcal{O}_D(T) \longrightarrow 0 \quad (5.3)$$

that is obtained by tensoring (5.2) with the line bundle $\mathcal{O}_X(T)$. The induced long exact cohomology sequence

$$\begin{aligned} 0 &\longrightarrow H^0(X; \mathcal{O}_X(T - D)) \longrightarrow H^0(X; \mathcal{O}_X(T)) \longrightarrow H^0(D; \mathcal{O}_D(T)) \\ &\longrightarrow H^1(X; \mathcal{O}_X(T - D)) \longrightarrow H^1(X; \mathcal{O}_X(T)) \longrightarrow H^1(D; \mathcal{O}_D(T)) \\ &\longrightarrow H^2(X; \mathcal{O}_X(T - D)) \longrightarrow H^2(X; \mathcal{O}_X(T)) \longrightarrow H^2(D; \mathcal{O}_D(T)) \longrightarrow \dots \end{aligned} \quad (5.4)$$

then allows to relate the cohomology of the toric variety X directly to the cohomology of the hypersurface.

Given a more generic case of several (mutually transverse) hypersurfaces $\{S_1, \dots, S_l\}$, one can compute the cohomology on the complete intersection via the generalized Koszul sequence

$$\begin{aligned} 0 &\longrightarrow \mathcal{O}_X \left(-\sum_{j=1}^l S_j + D \right) \longrightarrow \dots \longrightarrow \bigoplus_{i_1 < i_2} \mathcal{O}_X(-S_{i_1} - S_{i_2} + D) \\ &\longrightarrow \bigoplus_{i_1} \mathcal{O}_X(-S_{i_1} + D) \longrightarrow \mathcal{O}_X(D) \longrightarrow \mathcal{O}_S(D) \longrightarrow 0. \end{aligned} \quad (5.5)$$

In contrast to the hypersurface sequence, this is no longer a short exact sequence and hence does not give rise to a long exact sequence in cohomology. One way to proceed is via the technique of spectral sequences, which inductively allows one to compute the wanted cohomology classes on the complete intersection. However, for our implementation, we decided to take a different approach. We break down this long sequence (5.5) into several short exact sequences using several auxiliary sheaves \mathcal{I}_k :

$$\begin{aligned} 0 &\longrightarrow \mathcal{O}_X \left(-\sum_{j=1}^l S_j + D \right) \longrightarrow \bigoplus_{i_1 < \dots < i_{l-1}} \mathcal{O}_X \left(-\sum_{j=1}^{l-1} S_{i_j} + D \right) \twoheadrightarrow \mathcal{I}_1 \longrightarrow 0, \\ 0 &\longrightarrow \mathcal{I}_1 \hookrightarrow \bigoplus_{i_1 < \dots < i_{l-2}} \mathcal{O}_X \left(-\sum_{j=1}^{l-2} S_{i_j} + D \right) \twoheadrightarrow \mathcal{I}_2 \longrightarrow 0, \\ &\vdots \\ 0 &\longrightarrow \mathcal{I}_{l-2} \hookrightarrow \bigoplus_{i_1} \mathcal{O}_X(-S_{i_1} + D) \twoheadrightarrow \mathcal{I}_{l-1} \longrightarrow 0, \\ 0 &\longrightarrow \mathcal{I}_{l-1} \hookrightarrow \mathcal{O}_X(D) \twoheadrightarrow \mathcal{O}_S(D) \longrightarrow 0. \end{aligned} \quad (5.6)$$

The individually induced long exact sequences of cohomology can then be used for the step-wise computation of $H^\bullet(S; \mathcal{O}_S(D))$, which is the cohomology on the complete intersection $S = \bigcap_{i=1}^l S_i$.

6. Monad Construction of Vector Bundles

Before we come to a concrete application in heterotic string model building, let us present the construction of holomorphic vector bundles via the so-called monad. Such a structure directly arises in the $(0, 2)$ GLSM description and can be regarded as a generalization of the tangent bundle of a complete intersection in a toric variety.

Given the GLSM charges defined in (2.1), the tangent bundle can be defined as the quotient $T_S = \text{Ker}(f) / \text{Im}(g)$ of the sequence

$$0 \longrightarrow \underbrace{\mathcal{O}_S^{\oplus R}}_{\substack{\text{one } \mathcal{O}_S \text{ for each} \\ \text{Picard generator}}} \xrightarrow{g} \underbrace{\bigoplus_{i=1}^n \mathcal{O}_S(Q_i)}_{\substack{\text{one bundle with the GLSM} \\ \text{charges for each coordinate}}} \xrightarrow{f} \underbrace{\bigoplus_{j=1}^l \mathcal{O}_S(S_j)}_{\substack{\text{one bundle with the degree} \\ \text{for each hypersurface}}} \longrightarrow 0, \quad (6.1)$$

where the individual line bundles are restricted to the complete intersection $S = \bigcap_{i=1}^l S_i$. The rank of the resulting vector bundle is given by $\text{rk}(T) = n - l - R$. Using the methods presented so far, it is clear that they allow to compute the dimensions of the cohomology classes $h^i(S; T_S)$, where the initial input data for the set of long exact sequences are the line-bundle-valued cohomology classes on the ambient toric variety.

The $(0, 2)$ GLSM generalizes this in the sense that the bundle the left-moving world-sheet fermions couple to is not any longer the tangent bundle of the Calabi-Yau, but a more general holomorphic (stable) vector bundle V , which is analogously defined via a sequence of the Whitney sums of line bundles

$$0 \longrightarrow \mathcal{O}_S^{\oplus R_V} \xrightarrow{g} \bigoplus_{a=1}^{\delta} \mathcal{O}_S(N_a) \xrightarrow{g} \bigoplus_{l=1}^{\lambda} \mathcal{O}_S(M_l) \longrightarrow 0. \quad (6.2)$$

The rank is $\text{rk}(V) = \delta - \lambda - R_V$. The charges N_a and M_l have to satisfy the anomaly cancellation conditions

$$\begin{aligned} \sum_a N_a^{(\alpha)} &= \sum_l M_l^{(\alpha)}, \quad \forall \alpha, \\ \sum_l M_l^{(\alpha)} M_l^{(\beta)} - \sum_a N_a^{(\alpha)} N_a^{(\beta)} &= \sum_j S_j^{(\alpha)} S_j^{(\beta)} - \sum_i Q_i^{(\alpha)} Q_i^{(\beta)}, \quad \forall \alpha, \beta, \end{aligned} \quad (6.3)$$

where $1 \leq \alpha, \beta \leq R$ denote the components corresponding to the $U(1)$ actions in the GLSM. The most delicate issue for such constructions is the proof of μ -stability. However, it should be clear that besides that the monad construction provides a large set of heterotic $(0, 2)$ backgrounds and that the methods described so far are indeed tailor-made for the

Table 2: Correlation between zero modes in representations of the GUT group H .

Number of zero modes in reps. of H	1	$h_5^1(V)$	$h_5^1(V^*)$	$h_5^1(\Lambda^2 V)$	$h_5^1(\Lambda^2 V^*)$	$h_5^1(V \otimes V^*)$
E_8				248		
\downarrow				\downarrow		
$SU(3) \times E_6$	(1, 78)	\oplus (3, 27)	\oplus ($\bar{3}$, $\bar{27}$)			\oplus (8, 1)
$SU(4) \times SO(10)$	(1, 45)	\oplus (4, 16)	\oplus ($\bar{4}$, $\bar{16}$)	\oplus (6, 10)		\oplus (15, 1)
$SU(5) \times SU(5)$	(1, 24)	\oplus (5, $\bar{10}$)	\oplus ($\bar{5}$, 10)	\oplus (10, 5)	\oplus ($\bar{10}$, $\bar{5}$)	\oplus (24, 1)

determination of the zero-mode spectrum, which is given by the dimensions of vector bundle valued cohomology classes $h^i(S; \Lambda^k V)$.

7. A (2, 2) Model Dual to a (0, 2) Model

Now let us show all this for concrete heterotic (0, 2) models, for which we first recall a couple of issues. The theory is naturally equipped with an $E_8 \times E_8$ gauge theory. One of these E_8 's may be taken to be invisible to the real world, and hence only one E_8 remains. The holomorphic vector bundle now is endowed with a certain structure group G which breaks this E_8 down to some GUT group. The remaining GUT group is then simply the commutant of G in E_8 . Depending on what kind of GUT group we are interested in, we may choose the structure group G to be either $SU(3)$, $SU(4)$, or $SU(5)$ breaking E_8 down to E_6 , $SO(10)$ or $SU(5)$, respectively.

In order to obtain the number of zero modes in different representations of the GUT group, we have to calculate the cohomology classes of bundles involving the holomorphic vector bundle [16]. The precise correlation of vector bundle cohomology and zero modes for all three GUT groups are given in Table 2 (for a nice review on the particle spectrum of heterotic theories, see, i.e., [17]).

The moduli appearing in such a framework are given by possible deformations of the Calabi-Yau manifold, which are counted by the Hodge numbers

$$h^{2,1}(S), \quad h^{1,1}(S) \quad (7.1)$$

and by possible deformations of the bundle, that is, the bundle moduli, which are counted by the dimension of the cohomology of the endomorphism bundle $\text{End}(V)$ of V . Furthermore one can show that

$$H^1(S; \text{End}(V)) \cong H^1(S; V^* \otimes V), \quad (7.2)$$

which simplifies its determination. In case of the standard embedding, the vector bundle is simply the tangent bundle and hence has $SU(3)$ structure and gauge group E_6 . Many vector bundles can be constructed using monads, by defining the vector bundle to be the cohomology of the complex (6.2). Using only this complex, it is possible to construct bundles with the structure groups shown in Table 2, and hence computing all these cohomologies simply boils down to the computation of line bundle cohomology on the complete intersection. This on the other hand can be related, using the Koszul sequence (5.5), to the cohomology of line bundles on the ambient toric variety.

In the following we give an example of a pair of heterotic models which are related by the so-called target space duality [7, 18, 19] and were derived in [20]. The first of those will be a (2,2) model $(M_a, V_a) = (M_a, T_{M_a})$ while the second one, referred to as (M_b, V_b) , is of type (0,2) equipped with an $SU(3)$ -bundle which is assumed to be stable.

Let us start with an example in which we can already see most of the structure but which is not too involved. Consider

$$V_{1,1,1,1,2,2,2}[3,4,3] \rightarrow \mathbb{P}_{1,1,1,1,2,2,2}^6[3,4,3]. \quad (7.3)$$

Since this configuration is singular we have to resolve it by introducing a new coordinate. This yields the smooth configuration shown in Table 3, leading to the following monad for the tangent bundle:

$$\begin{array}{ccccccc} 0 & - & \mathcal{O}_{M_a}^2 & \hookrightarrow & \mathcal{O}_{M_a}(0,1)^4 & \mathcal{O}_{M_a}(1,2)^3 & \mathcal{O}_{M_a}(1,0) \\ & & & & & \downarrow & \\ & & & & & \mathcal{O}_{M_a}(1,3)^2 & \mathcal{O}_{M_a}(2,4) - 0, \end{array} \quad (7.4)$$

where the Koszul sequence (5.3) has to be applied as well. Using *cohomCalc Koszul* extension, we can obtain the number of zero modes of the chiral spectrum in this model as well as the dimension of the moduli space:

$$\begin{aligned} h_{M_a}^\bullet(V_a) &= (0, 68, 2, 0), \\ h_{M_a}^{1,1} + h_{M_a}^{2,1} + h_{M_a}^1(\text{End}(V_a)) &= 2 + 68 + 140 = 210, \end{aligned} \quad (7.5)$$

where the reader should keep in mind that in this case $V_a = T_{M_a}$ is just the tangent bundle. The dual (0,2) model geometry can then be determined to be the data in Table 4, and its monad is specified by the sequence

$$\begin{array}{ccccccc} 0 & - & \mathcal{O}_{M_b}^2 & & & & \\ & & \downarrow & & & & \\ \mathcal{O}_{M_b}(0,0,1)^4 & \mathcal{O}_{M_b}(0,1,2) & \mathcal{O}_{M_b}(1,0,0) & \mathcal{O}_{M_b}(0,2,4) & \mathcal{O}_{M_b}(0,1,0) & & \\ & & \downarrow & & & & \\ & & \mathcal{O}_{M_b}(0,1,3)^2 & \mathcal{O}_{M_b}(1,2,4) & - & 0. \end{array} \quad (7.6)$$

This configuration satisfies conditions (6.3), and we obtain the following topological data:

$$\begin{aligned} h_{M_b}^\bullet(V_b) &= (0, 68, 2, 0), \\ h_{M_b}^{1,1} + h_{M_b}^{2,1} + h_{M_b}^1(\text{End}(V_b)) &= 3 + 51 + 156 = 210. \end{aligned} \quad (7.7)$$

Table 3: Toric data for the smooth (2,2) model 3-fold geometry M_a .

Coordinate GLSM charges								Hypers. degrees			
0	0	0	0	1	1	1	1	1	1	1	2
1	1	1	1	2	2	2	0	3	3		4

Table 4: Toric data for the dual (0,2) model 3-fold geometry M_b .

Coordinate GLSM charges								Hypersurf. degrees				
0	0	0	0	0	0	0	1	1	0	0	1	1
0	0	0	0	1	1	1	1	0	0	1	1	1
1	1	1	1	2	2	2	0	0	0	3	3	2

Comparing to the data (7.5) we can see that the number of zero modes in the chiral spectrum does not change, and even though the individual Hodge numbers as well as their sum are both different, the dimension of the full moduli space stays the same.

This is a manifestation of a so far only very poorly understood perturbative (in g_s) target space duality in the configuration space of heterotic string compactifications with $\mathcal{N} = 1$ supersymmetry in four dimensions.

8. Outlook

So far most implementations of computational methods in string model building have been based on toric geometry [21] and in particular on the combinatorial formulas of Batyrev and Borisov [22–24]. Of course there are also general software tools for algebraic geometry like [25–27]. Clearly, these are very powerful but also have their limitations. First, they only apply in the (2,2) case, where the vector bundle is identified with the tangent bundle. Second, for complete intersections the combinatorial formulas hold only for the so-called nef-partitions which ensure that the corresponding polytopes representing the space are reflexive.

The computational tool reviewed in this paper can also be applied to situations where other packages fail. As explained, the powerful algorithm for the determination of the dimensions of line-bundle-valued cohomology classes is tailor made for dealing also with general complete intersection and for (0,2) models, where the vector bundle is defined via line bundles, for example, the monad construction or the spectral cover construction.

Of course, also the algorithm implementation *cohomCalc* has its limitations. First, in situations where the number of the Picard generators (projective relations, reflected by $h^{1,1}$) becomes large (about the order of ten), the computations become too involved and the program too time consuming. A second drawback is the exponential growth of the computing time with the number of the Stanley-Reisner ideal generators, which at the moment takes several hours for about 40 generators. Third, if there are not enough zeros in the many intermediate long exact sequences, the result is not unique and consequently one has to determine the kernel image of maps by hand.

Note that there is also the Macaulay 2 package [3] which can be used as an alternative to the algorithm presented herein. Preliminary testing indicates that it seems to be able to handle geometries of a high Picard rank and huge numbers of Stanley-Reisner ideal generators, but for simple geometries, *cohomCalc* appears to be faster. Further study is necessary to fully evaluate strengths and weaknesses for the two algorithms implemented in [28] and the algorithm described in Section 3. Also see [29, prop. 4.1].

Acknowledgment

The authors would like to thank Helmut Roschy for his contributions to the original work presented in this paper.

References

- [1] W. Fulton, *Introduction to Toric Varieties*, vol. 131 of *Annals of Mathematics Studies*, Princeton University Press, Princeton, NJ, USA, 1993.
- [2] M. Kreuzer, "Toric geometry and calabi-yau compactifications," *Ukrainian Journal of Physics*, vol. 55, no. 5, pp. 613–625, 2010.
- [3] S. Reffert, "The geometer's toolkit to string compactifications," <http://arxiv.org/abs/0706.1310>.
- [4] D. A. Cox, J. B. Little, and H. Schenck, *Toric Varieties*, American Mathematical Society, 2011, <http://www.cs.amherst.edu/~dac/toric.html>.
- [5] E. Witten, "Phases of $N = 2$ theories in two dimensions," *Nuclear Physics B*, vol. 403, no. 1-2, pp. 159–222, 1993.
- [6] J. Distler, B. R. Greene, and D. R. Morrison, "Resolving singularities in $(0, 2)$ models," *Nuclear Physics B*, vol. 481, no. 1-2, pp. 289–312, 1996.
- [7] R. Blumenhagen, "Target space duality for $(0, 2)$ compactifications," *Nuclear Physics B*, vol. 513, no. 3, pp. 573–590, 1998.
- [8] R. Blumenhagen, B. Jurke, T. Rahn, and H. Roschy, "Cohomology of line bundles: a computational algorithm," *Journal of Mathematical Physics*, vol. 51, no. 10, Article ID 103525, 15 pages, 2010.
- [9] S. Jow, "Cohomology of toric line bundles via simplicial Alexander duality," *Journal of Mathematical Physics*, vol. 52, no. 3, Article ID 033506, 2011.
- [10] H. Roschy and T. Rahn, "Cohomology of line bundles: proof of the algorithm," *Journal of Mathematical Physics*, vol. 51, no. 10, Article ID 103520, 11 pages, 2010.
- [11] cohomCalc package, "High-performance line bundle cohomology computation based on [8]," 2010, <http://wwwth.mpp.mpg.de/members/bjurke/cohomcalc/>.
- [12] M. Cvetič, I. García-Etxebarria, and J. Halverson, "On the computation of non-perturbative effective potentials in the string theory landscape - IIB/F-theory perspective -," *Fortschritte der Physik*, vol. 59, no. 3-4, pp. 243–283, 2011.
- [13] R. Blumenhagen, B. Jurke, T. Rahn, and H. Roschy, "Cohomology of line bundles: applications," <http://arxiv.org/abs/1010.3717>.
- [14] R. Blumenhagen, A. Collinucci, and B. Jurke, "On instanton effects in F-theory," *Journal of High Energy Physics*, vol. 2010, no. 8, article 079, 2010.
- [15] P. Griffiths and J. Harris, *Principles of Algebraic Geometry*, Wiley Classics Library, John Wiley & Sons, New York, NY, USA, 1994.
- [16] E. Witten, "New issues in manifolds of $SU(3)$ holonomy," *Nuclear Physics B*, vol. 268, no. 1, pp. 79–112, 1986.
- [17] R. Donagi, Y.-H. He, B. A. Ovrut, and R. Reinbacher, "The particle spectrum of heterotic compactifications," *Journal of High Energy Physics*, no. 12, article 054, 2004.
- [18] J. Distler and S. Kachru, "Duality of $(0, 2)$ string vacua," *Nuclear Physics B*, vol. 442, no. 1-2, pp. 64–74, 1995.
- [19] T.-M. Chiang, J. Distler, and B. R. Greene, "Some features of $(0, 2)$ moduli space," *Nuclear Physics B*, vol. 496, no. 3, pp. 590–616, 1997.
- [20] R. Blumenhagen and T. Rahn, "Landscape study of target space duality of $(0, 2)$ heterotic string models," <http://arxiv.org/abs/1106.4998>.
- [21] M. Kreuzer and H. Skarke, "PALP: a package for analysing lattice polytopes with applications to toric geometry," *Computer Physics Communications*, vol. 157, no. 1, pp. 87–106, 2004.
- [22] L. Borisov, "Towards the mirror symmetry for Calabi-Yau complete intersections in Gorenstein toric Fano varieties," <http://arxiv.org/abs/alg-geom/9310001>.
- [23] V. V. Batyrev and L. A. Borisov, "Dual cones and mirror symmetry for generalized Calabi-Yau manifolds," in *Mirror Symmetry, II*, vol. 1 of *AMS/IP Studies in Advanced Mathematics*, pp. 71–86, American Mathematical Society, Providence, RI, USA, 1997.
- [24] V. V. Batyrev and L. A. Borisov, "On Calabi-Yau complete intersections in toric varieties," in *Higher-Dimensional Complex Varieties (Trento, 1994)*, pp. 39–65, de Gruyter, Berlin, Germany, 1996.

- [25] J. Rambau, "TOPCOM: triangulations of point configurations and oriented matroids," in *Mathematical Software—ICMS 2002*, A. M. Cohen, X.-S. Gao, and N. Takayama, Eds., pp. 330–340, World Scientific, River Edge, NJ, USA, 2002.
- [26] D. R. Grayson and M. E. Stillman, "Macaulay2, a software system for research in algebraic geometry," <http://www.math.uiuc.edu/Macaulay2/>.
- [27] W. Stein et al., *Sage Mathematics Software*, The Sage Development Team, 2010, <http://www.sagemath.org/>.
- [28] R. Birkner, N. O. Ilten, and L. Petersen, "Computations with equivariant toric vector bundles," *Journal of Software for Algebra and Geometry*, vol. 2, pp. 11–14, 2010.
- [29] L. Borisov and Z. Hua, "On the conjecture of King for smooth toric Deligne-Mumford stacks," *Advances in Mathematics*, vol. 221, no. 1, pp. 277–301, 2009.

Review Article

The Expanding Zoo of Calabi-Yau Threefolds

Rhys Davies

*Mathematical Institute, University of Oxford, 24-29 St Giles, Oxford,
OX1 3LB, UK*

Correspondence should be addressed to Rhys Davies, daviesr@maths.ox.ac.uk

Received 29 March 2011; Accepted 12 April 2011

Academic Editor: Yang-Hui He

Copyright © 2011 Rhys Davies. This is an open access article distributed under the Creative Commons Attribution License, which permits unrestricted use, distribution, and reproduction in any medium, provided the original work is properly cited.

This is a short review of recent constructions of new Calabi-Yau threefolds with small Hodge numbers and/or nontrivial fundamental group, which are of particular interest for model building in the context of heterotic string theory. The two main tools are topological transitions and taking quotients by actions of discrete groups. Both of these techniques can produce new manifolds from existing ones, and they have been used to bring many new specimens to the previously sparse corner of the Calabi-Yau zoo, where both Hodge numbers are small. Two new manifolds are also obtained here from hyperconifold transitions, including the first example with fundamental group S_3 , the smallest non-Abelian group.

1. Introduction

This paper is a short review of recent work on constructing smooth Calabi-Yau threefolds with interesting topological properties, such as small cohomology groups and nontrivial fundamental group. In practice, these two properties often go hand-in-hand, as emphasised in [1, 2].

The majority of known three-dimensional Calabi-Yau manifolds are constructed as complete intersections in higher-dimensional toric varieties [3–8]. Most of the new examples found in recent years are in fact obtained from these via one of two techniques. The first is to take the quotient by a holomorphic action of some finite group. As explained in Section 2, when the group action is fixed-point-free, this is guaranteed to yield another Calabi-Yau manifold, and many Calabi-Yau threefolds with nontrivial fundamental group have been constructed in this way. Several early examples can be found in [9–14], but recent efforts have brought to light many more [2, 15–26], some of which will be discussed later. In the case that the group action has fixed points, it is often possible to resolve the resulting orbifold singularities in such a way as to again obtain a Calabi-Yau manifold. Examples can be found in [27–29]. The second technique is to vary either the complex structure or Kähler moduli of a known space until it becomes singular and then desingularise it by varying the other

type of moduli. Topologically, such a process is a surgery and yields a Calabi-Yau manifold topologically distinct from the original. Two classes of such topological transitions, the conifold and hyperconifold transitions, are discussed in Section 3, and explicit examples of each are given. Conifold transitions have been known for some time to connect many Calabi-Yau threefolds [30–33] and have been used to construct new manifolds in [2, 24, 34, 35]. Hyperconifold transitions were described in [36], and the first examples of new manifolds discovered this way were given in [37]. The examples of Section 3.2 yield two more new manifolds, one of which is the first known with fundamental group S_3 , the smallest non-Abelian group.

The fruit of these labours is that there are now many more known Calabi-Yau threefolds with small Hodge numbers (defined arbitrarily in this paper by $h^{1,1} + h^{2,1} \leq 24$) than were known to the authors of [1]. The number with nontrivial fundamental group has also increased dramatically, thanks largely to Braun’s classification of free group actions on complete intersections in products of projective spaces [23]. (The Hodge numbers of many of these quotients are yet to be calculated, but some are likely to be “small” as defined above.)

The physical motivation for studying such manifolds comes predominantly from heterotic string theory. In this context, a nontrivial fundamental group is necessary to be able to turn on discrete Wilson lines and thus obtain a realistic four-dimensional gauge group. The requirement of small Hodge numbers is not so clear-cut, but it seems advantageous if one wants to appeal to the methods of [38, 39] to stabilise the moduli, and this is currently the only known way to stabilise all (geometric) moduli in heterotic Calabi-Yau backgrounds. Although heterotic model building is not the theme of this review, other recent developments will be mentioned sporadically.

Throughout the paper, an arbitrary Calabi-Yau and its universal cover will be denoted by X and \tilde{X} , respectively, while a particular Calabi-Yau threefold with Hodge numbers $(h^{1,1}, h^{2,1})$ will be denoted by $X^{h^{1,1}, h^{2,1}}$. $X^\#$ will denote a singular member of the family X , and $\hat{X}^\#$ a resolution of such a singular variety.

2. Quotients by Group Actions

2.1. The Calabi-Yau Condition

It is an elementary fact of topology that every manifold X has a simply connected universal covering space \tilde{X} , from which it can be obtained as a quotient by the free action of a group $G \cong \pi_1(X)$. We will write this relationship as $X = \tilde{X}/G$. Although our interest is in (complex) threefolds, we will allow the dimension n of X to be arbitrary through much of this section.

If X is a Calabi-Yau manifold, it is easy to see that its universal cover \tilde{X} is too, by pulling back the complex structure, Kähler form ω , and holomorphic $(n, 0)$ -form Ω under the covering map (for this reason, we will often abuse notation by using the same symbols for these objects on X and \tilde{X}). Only a little more difficult is the converse: under what conditions is $X = \tilde{X}/G$ a Calabi-Yau manifold, given that \tilde{X} is? There are several points to consider (we assume always that G is a finite group).

- (i) X will be a manifold as long as the action of G is fixed-point free. Otherwise, it will have orbifold singularities.
- (ii) It will furthermore be a complex manifold if and only if G acts by biholomorphic maps. In this case, X simply inherits the complex structure of \tilde{X} .

- (iii) To see that X is Kähler, pick any Kähler form ω on \tilde{X} . Now, note that for any element $g \in G$, $g^*\omega$ is also a Kähler form, since $d(g^*\omega) = g^*(d\omega) = 0$, and for any k -dimensional complex submanifold M_k ,

$$\int_{M_k} g^*\omega^k = \int_{g(M_k)} \omega^k > 0. \quad (2.1)$$

We can use this to construct a Kähler form which is invariant under G and, therefore, descends to a Kähler form on X .

$$\omega^G := \frac{1}{|G|} \sum_{g \in G} g^*\omega. \quad (2.2)$$

- (iv) Finally, we must check whether X supports a nowhere-vanishing holomorphic $(n, 0)$ -form. This can only descend from the one on \tilde{X} , so we need to check whether Ω is G -invariant. Note that Ω is the unique (up to scale) element of $H^{n,0}(\tilde{X})$, so since G acts freely, the Atiyah-Bott fixed point formula [40, 41] for any $g \in G \setminus e$ reduces to

$$0 = \sum_{q=0}^n (-1)^q \operatorname{Tr}(H^{n,q}(g)) = \operatorname{Tr}(H^{n,0}(g)) + (-1)^n \operatorname{Tr}(H^{n,n}(g)), \quad (2.3)$$

where $H^*(g)$ denotes the induced action of g on the cohomology H^* . The group $H^{n,n}(\tilde{X})$ is generated by $(\omega^G)^n$, which is invariant, so we conclude that $\operatorname{Tr}(H^{n,0}(g)) = (-1)^{n+1}$, and therefore,

$$g^*\Omega = (-1)^{n+1}\Omega \quad \forall g \in G \setminus e. \quad (2.4)$$

In odd dimensions, therefore, Ω is automatically invariant under free group actions. In even dimensions, on the other hand, this simple calculation shows that there are no multiply-connected Calabi-Yau manifolds.

In summary, if \tilde{X} is a smooth Calabi-Yau threefold, then $X = \tilde{X}/G$ is a Calabi-Yau manifold if and only if G acts freely and holomorphically.

2.1.1. Smoothness

Above, we have simply assumed that the covering space \tilde{X} is smooth. In practice, \tilde{X} usually belongs to a family of spaces of which only a subfamily admits a free G action. It may be the case that although a generic member of \tilde{X} is smooth, members of the symmetric subfamily are all singular, so we never get a smooth quotient. Although this seems to be rare, it does occur for $\mathbb{Z}_8 \times \mathbb{Z}_8$ -symmetric complete intersections of four quadrics in \mathbb{P}^7 [11, 18], $\mathbb{Z}_5 \times \mathbb{Z}_5$ -symmetric complete intersections of five bilinears in $\mathbb{P}^4 \times \mathbb{P}^4$ [2], and a number of other examples, including some found in [23]. The extra condition, that a generic *symmetric* member is smooth, must, therefore, be checked on a case-by-case basis.

Let us start with the special case of complete intersection Calabi-Yau manifolds in smooth ambient spaces. This includes what have traditionally been called the ‘‘CICY’’ manifolds, where the ambient space is a product of projective spaces [3–5] and certain of the

toric hypersurfaces [7, 8]. The complete intersection condition means that if the ambient space has dimension $n + k$, then the Calabi-Yau \tilde{X} is given by the intersection of k hypersurfaces, each given by a single polynomial equation $f_a = 0$. In other words, the number of equations needed to specify \tilde{X} is equal to its codimension. When the ambient space is smooth, it can be covered in affine patches each isomorphic to \mathbb{C}^{n+k} , and the condition for \tilde{X} to be smooth is that $df_1 \wedge \cdots \wedge df_k$ is nonzero at every point on \tilde{X} . This is a very intuitive condition—if it holds, then at any point of \tilde{X} we can choose local coordinates x_1, \dots, x_{n+k} such that $f_a = x_a + \mathcal{O}(x^2)$. Locally, then, \tilde{X} projects biholomorphically onto the linear subspace $x_1 = x_2 = \cdots = x_k = 0$, and is, therefore, smooth. On any affine coordinate patch, the components of the differential form $df_1 \wedge \cdots \wedge df_k$ are just the $k \times k$ minors of the Jacobian matrix $J = (\partial f_a / \partial x_i)$, so the condition is that this matrix has rank k everywhere on \tilde{X} . It is, therefore, necessary to check that there is no simultaneous solution to the equations $f_a = 0$ along with the vanishing of all $k \times k$ minors of J , which is equivalent to the algebraic statement that the ideal generated by the polynomials and the minors is the entire ring $\mathbb{C}[x_1, \dots, x_{n+k}]$. This is checked by calculating a Gröbner basis for the ideal, algorithms for which are implemented in a variety of computer algebra packages [42–44]; a Gröbner basis for the entire ring is just a constant (usually given as 1 or -1 by software).

The more general case of singular ambient spaces or noncomplete intersections is not much harder than the above. Suppose \tilde{X} is not a complete intersection so that it is given by l equations in an $n + k$ -dimensional ambient space, where now we allow $l > k$. (A typical example is the Veronese embedding of \mathbb{P}^2 in \mathbb{P}^5 . If we take homogeneous coordinates z_i for \mathbb{P}^2 , and w_{ij} for \mathbb{P}^5 , where $j \geq i$, then the embedding is given by $w_{ij} = z_i z_j$. The equations needed to specify the image of this map are $w_{ij} w_{kl} - w_{il} w_{kj} = 0$, which amount to six independent equations, whereas the codimension of the embedded surface is only three.) Then, the condition for \tilde{X} to be smooth is still that the rank of the Jacobian be equal to k (the codimension) everywhere on \tilde{X} [45]. The reasoning is the same as before—if this is true, k of the polynomials will provide good local coordinates on the ambient space, allowing us to define a smooth coordinate patch on \tilde{X} .

If some affine patch on the ambient space is singular, it can still be embedded in \mathbb{C}^N for some N , by polynomial equations $F_1 = \cdots = F_K = 0$. The Calabi-Yau is then given by $F_1 = \cdots = F_K = f_1 = \cdots = f_l = 0$, and the condition for smoothness is once again that the Jacobian has rank equal to the codimension, $N - n$, at all points.

For examples of interest, Gröbner basis calculations are often very computationally intensive, since at intermediate stages the number of polynomials, as well as their coefficients, can become extremely large. It is, therefore, convenient to choose integer coefficients for all polynomials and perform the calculation over a finite field \mathbb{F}_p . As explained in [2], if a collection of polynomial equations are inconsistent over \mathbb{F}_p , then they are also inconsistent over \mathbb{C} , so the corresponding variety is smooth.

Note that there does exist a slight variation on the above procedure which still leads to smooth quotient manifolds. It may be the case that although the symmetric manifolds admit a free group action, they are all singular. If, however, these singularities can be resolved in a group-invariant way, the resolved space still admits a free group action, with a smooth quotient. Examples can be found in [15, 18, 21].

The final possibility is that the symmetric manifolds are smooth, but the group action always has fixed points, in which case the quotient space has orbifold singularities. It is frequently possible to resolve these in such a way as to again obtain a Calabi-Yau manifold, but this will not be discussed in detail here.

2.2. Notable Examples

2.2.1. New Three-Generation Manifolds

Calabi-Yau threefolds with Euler number $\chi = \pm 6$ were of particular interest in the early days of string phenomenology, since these give physical models with three generations of fermions via the “standard embedding” compactification of the heterotic string [9]. This typically gives an E_6 grand unified theory, and although the gauge symmetry can be partially broken by Wilson lines, it is impossible to obtain exactly the standard model gauge group in this way [46]. Nevertheless, it was argued by Witten that deformations of the standard embedding, combined with Wilson lines, can give realistic models [47], and this was put on firmer mathematical foundations by Li and Yau [48].

The archetypal example of a three-generation manifold is Yau’s manifold, with fundamental group \mathbb{Z}_3 [10], but recently two new promising three-generation manifolds were constructed in [22]. These are quotients of a manifold $X^{8,44}$ by groups of order twelve, which are the cyclic group \mathbb{Z}_{12} and the non-Abelian group $\text{Dic}_3 \cong \mathbb{Z}_3 \rtimes \mathbb{Z}_4$ (this is generated by two elements, one of order three and one of order four, satisfying $g_4 g_3 g_4^{-1} = g_3^2$), and each has Hodge numbers $(h^{1,1}, h^{2,1}) = (1, 4)$. Unfortunately, it was shown in [49] that the physical model on the non-Abelian quotient does not admit a deformation which yields exactly the field content of the minimal supersymmetric standard model (MSSM) in four dimensions. However, the \mathbb{Z}_{12} quotient allows many more distinct deformations, and the analysis of the corresponding physical models has not been completed.

The covering space $X^{8,44}$ is an anticanonical hypersurface in $dP_6 \times dP_6$, where dP_6 is the del Pezzo surface of degree six, which is \mathbb{P}^2 blown up in three generic points. This surface is rigid and toric, and its fan is shown in Figure 1.

As well as the action of the torus $(\mathbb{C}^*)^2$, dP_6 also admits an action by the dihedral group D_6 , as suggested by its fan. This can be realised as a group of lattice morphisms preserving the fan, generated by an order-six rotation ρ and a reflection σ , with matrix representations

$$\rho = \begin{pmatrix} 1 & -1 \\ 1 & 0 \end{pmatrix}, \quad \sigma = \begin{pmatrix} 0 & 1 \\ 1 & 0 \end{pmatrix}. \quad (2.5)$$

The product $dP_6 \times dP_6$ therefore has symmetry group $(D_6 \times D_6) \rtimes \mathbb{Z}_2$, where the extra \mathbb{Z}_2 factor swaps the two copies of the surface. The quotient groups Dic_3 and \mathbb{Z}_{12} are both order-twelve subgroups of this which act transitively on the vertices of the fan. Many more details can be found in [22].

2.2.2. Quotients of the (19, 19) Manifold

The Euler number of a three-dimensional Calabi-Yau manifold is given by the simple formula $\chi = 2(h^{1,1} - h^{2,1})$. If a group G acts freely, then $\chi(\tilde{X}/G) = \chi(\tilde{X})/|G|$, so this gives a simple necessary condition for the existence of such an action: the order of the group must divide $\chi/2$. This usually gives a fairly strong restriction on the groups which can act freely on any given manifold. The only time it gives no restriction is when $\chi = 0$. In this section, we will look at a particular manifold, $X^{19,19}$, which admits free actions by a number of disparate groups, including groups of order five, eight, and nine. For a Calabi-Yau threefold with $\chi \neq 0$, this would imply $|G| \geq 720$.

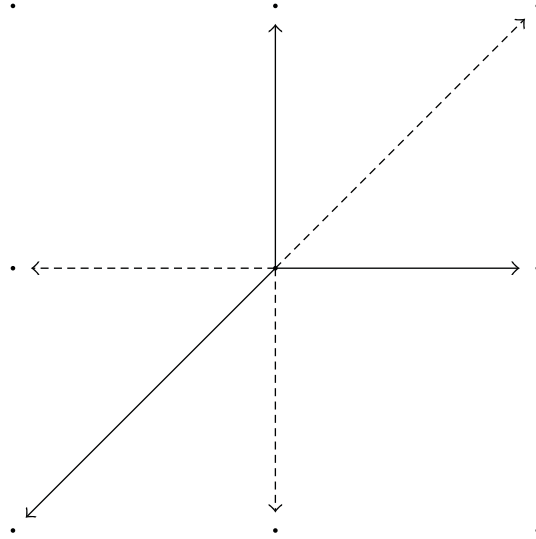


Figure 1: The fan for the toric surface dP_6 . Removing the dashed rays corresponds to the projection to \mathbb{P}^2 . All graphics were produced using [43].

The manifold $X^{19,19}$ can be represented in a number of different ways. Abstractly, it is the fibre product of two rational surfaces, each elliptically fibred over \mathbb{P}^1 [16, 19]. Such a surface is given by blowing up \mathbb{P}^2 at the nine points given by the intersection of two cubic curves; if we take homogeneous coordinates t_0, t_1 on \mathbb{P}^1 and z_0, z_1, z_2 on \mathbb{P}^2 , the corresponding equation is

$$f(z)t_0 + g(z)t_1 = 0, \quad (2.6)$$

where f and g are homogeneous cubic polynomials. We can easily see that this corresponds to \mathbb{P}^2 blown up at the nine points given by $f = g = 0$. Indeed, for any point of \mathbb{P}^2 , where $f \neq 0$ or $g \neq 0$, we get a unique solution for $[t_0 : t_1]$, whereas for $f = g = 0$, the equation is satisfied identically, giving a whole copy of \mathbb{P}^1 . To see that it is also an elliptic fibration over \mathbb{P}^1 , note that for any fixed value of $[t_0 : t_1] \in \mathbb{P}^1$, we get a cubic equation in \mathbb{P}^2 , which defines an elliptic curve.

To get the fibre product of two such surfaces, we introduce another \mathbb{P}^2 , with homogeneous coordinates w_0, w_1, w_2 , and another equation of the form (2.6) over the same \mathbb{P}^1 . The resulting threefold is Calabi-Yau, and has a projection to \mathbb{P}^1 , with typical fibre which is a product of two elliptic curves. In [19], Bouchard and Donagi studied group actions which preserve the elliptic fibration, and found free actions by the groups $\mathbb{Z}_3 \times \mathbb{Z}_3, \mathbb{Z}_4 \times \mathbb{Z}_2, \mathbb{Z}_6 \cong \mathbb{Z}_3 \times \mathbb{Z}_2$ and \mathbb{Z}_5 (as well as all subgroups of these, of course).

Certain of these quotient manifolds have, in fact, played crucial roles in the heterotic string literature. A model with the spectrum of the $U(1)_{B-L}$ -extended supersymmetric standard model was constructed on a quotient by $\mathbb{Z}_3 \times \mathbb{Z}_3$ and studied in [50, 51] (a similar model on the $\mathbb{Z}_3 \times \mathbb{Z}_3$ quotient of the ‘‘bicubic’’, which is related to this manifold by a conifold transition, was found in [52]), while a model with the exact MSSM spectrum exists on a \mathbb{Z}_2 quotient and was described in [53, 54]. In [55, 56], the quotient by a different $\mathbb{Z}_3 \times \mathbb{Z}_3$ action was used as a test case for calculating instanton corrections on manifolds with torsion curves.

Table 1: The Hodge numbers for known quotients of $X^{19,19}$.

$h^{1,1} = h^{2,1}$	Fundamental Group	Reference
11	\mathbb{Z}_2	[2, 19]
7	$\mathbb{Z}_3, \mathbb{Z}_2 \times \mathbb{Z}_2$	[2, 19]
5	\mathbb{Z}_4	[19]
3	$\mathbb{Z}_5, \mathbb{Z}_6, \mathbb{Z}_4 \times \mathbb{Z}_2, Q_8, \mathbb{Z}_3 \times \mathbb{Z}_3$	[2, 19]
2	$\mathbb{Z}_{12}, \text{Dic}_3$	[22, 49]

There are, in fact, further (relatively large) groups which act freely on $X^{19,19}$, which can be easily described using its representation(s) as a CICY. First, we note that the fibre product construction above is equivalent to the rather more prosaic statement that the manifold is a complete intersection of two hypersurfaces in $\mathbb{P}^1 \times \mathbb{P}^2 \times \mathbb{P}^2$, of multi-degrees $(1, 3, 0)$ and $(1, 0, 3)$. In the notation of [3, 4], $X^{19,19}$ can, therefore, be specified by the ‘‘configuration matrix’’

$$\begin{matrix} \mathbb{P}^1 \\ \mathbb{P}^2 \\ \mathbb{P}^2 \end{matrix} \begin{pmatrix} 1 & 1 \\ 3 & 0 \\ 0 & 3 \end{pmatrix} \tag{2.7}$$

By utilising various *splittings* and *contractions* (see, e.g., [2, 4, 30, 31]), and checking that the Euler number remains constant, it is easy to show that $X^{19,19}$ can also be specified by the configuration matrices

$$\begin{matrix} \mathbb{P}^1 \\ \mathbb{P}^1 \\ \mathbb{P}^1 \\ \mathbb{P}^1 \\ \mathbb{P}^1 \end{matrix} \begin{pmatrix} 1 & 1 \\ 2 & 0 \\ 2 & 0 \\ 0 & 2 \\ 0 & 2 \end{pmatrix}, \quad \begin{matrix} \mathbb{P}^1 \\ \mathbb{P}^2 \\ \mathbb{P}^2 \\ \mathbb{P}^2 \\ \mathbb{P}^2 \end{matrix} \begin{pmatrix} 1 & 1 & 0 & 0 & 0 & 0 \\ 1 & 0 & 1 & 1 & 0 & 0 \\ 1 & 0 & 1 & 1 & 0 & 0 \\ 0 & 1 & 0 & 0 & 1 & 1 \\ 0 & 1 & 0 & 0 & 1 & 1 \end{pmatrix}. \tag{2.8}$$

It was shown in [2] that in the first form, $X^{19,19}$ admits a free action of the order-eight quaternion group (denoted in [2] by \mathbb{H} , but more conventionally by Q_8), with elements $\{\pm 1, \pm i, \pm j, \pm k\}$, induced by a linear action of this group on the ambient space.

In the second form, $X^{19,19}$ admits free actions by two groups of order twelve. One is the cyclic group \mathbb{Z}_{12} , and the other is the dicyclic group $\text{Dic}_3 \cong \mathbb{Z}_3 \times \mathbb{Z}_4$ (introduced in Section 2.2.1) [49]. These were in fact discovered via conifold transitions from the corresponding quotients of $X^{8,44}$, an idea reviewed in Section 3.

In summary, $X^{19,19}$ is rather exceptional in that it admits free actions by the groups $\mathbb{Z}_{12}, \text{Dic}_3, \mathbb{Z}_3 \times \mathbb{Z}_3, \mathbb{Z}_4 \times \mathbb{Z}_2, Q_8, \mathbb{Z}_6,$ and \mathbb{Z}_5 . The Hodge numbers for the quotients by all these groups and their subgroups are collected in Table 1.

2.2.3. Manifolds with Hodge Numbers (1,1)

For a long time, the smallest known Hodge numbers of a Calabi-Yau threefold satisfied $h^{1,1} + h^{2,1} = 4$. This record has now been overtaken by Braun’s examples of manifolds with

$(h^{1,1}, h^{2,1}) = (1, 1)$ [25] (as well as Freitag and Salvati Manni's manifold with $(h^{1,1}, h^{2,1}) = (2, 0)$ [29]).

The covering space of Braun's $(1, 1)$ manifolds is a self-mirror manifold $X^{20,20}$. This is realised as an anticanonical hypersurface in the toric fourfold determined by the face fan over the 24-cell, which is a self-dual regular four-dimensional polytope.

There are three different groups of order 24 which act freely on particular smooth one-parameter subfamilies of $X^{20,20}$; these are $\mathbb{Z}_3 \times \mathbb{Z}_8, \mathbb{Z}_3 \times Q_8$, and $SL(2, 3)$. The first two are self-explanatory, while the third is the group of two-by-two matrices of determinant one over the field with three elements. All the groups act via linear transformations on the lattice in which the polytope lives, and act transitively on its vertices. Full details can be found in [25].

2.2.4. Complete Intersections of Four Quadrics in \mathbb{P}^7

A particularly fertile starting point for finding new Calabi-Yau manifolds has been the complete intersection of four quadrics in \mathbb{P}^7 . A smooth member of this family is a Calabi-Yau manifold with Hodge numbers $(h^{1,1}, h^{2,1}) = (1, 65)$. Hua classified free group actions on smooth subfamilies in [18], finding groups of order 2, 4, 8, 16, and 32. The quotients all have $h^{1,1} = 1$, and $h^{2,1} = 33, 17, 9, 5$, and 3, respectively.

Certain nodal families allow free actions of groups of order 64 and, furthermore, have equivariant small resolutions [15, 18]. The resolutions have Hodge numbers $(h^{1,1}, h^{2,1}) = (2, 2)$ and inherit the free group actions. Remarkably, in this case, all the quotients have the same Hodge numbers as the covering space. The quotient by $\mathbb{Z}_8 \times \mathbb{Z}_8$ was investigated as a background for heterotic string theory in [57], but unfortunately, no realistic models were found.

Freitag and Salvati Manni have also constructed a large number of new manifolds by starting with a particular complete intersection $X^\#$ of four quadrics which has 96 nodes and a very large symmetry group [28, 29]. They show that the quotients by many subgroups admit crepant projective resolutions, thereby giving rise to a large number of new Calabi-Yau manifolds. Some of the subgroups of order 2, 4, 8, and 16 act freely on a small resolution of $X^\#$, and the corresponding quotient manifolds are connected to some of Hua's examples by conifold transitions. The manifolds from [29] with small Hodge numbers are listed in the appendix 4, including one with $(h^{1,1}, h^{2,1}) = (2, 0)$, which is, therefore, equal with Braun's manifolds for smallest known Hodge numbers. Note that the theoretical minimum is $(h^{1,1}, h^{2,1}) = (1, 0)$.

3. New Manifolds From Topological Transitions

One fascinating feature of Calabi-Yau threefolds is the interconnectedness of moduli spaces of topologically distinct manifolds. Generally speaking, there are two ways to pass from one smooth Calabi-Yau to another. We may deform the complex structure until a singularity develops and then "resolve" this singularity using the techniques of algebraic geometry, which involves replacing the singular set with new embedded holomorphic curves or surfaces. Alternatively, we may allow certain embedded curves or surfaces to collapse to zero size and then "smooth" the resulting singular space by varying its complex structure. Obviously these two processes are inverses of each other.

Our main interest here is in constructing new smooth Calabi-Yau threefolds via such topological transitions, but first we will indulge in a few comments about the connectedness of the space of all Calabi-Yau threefolds.

The suggestion that all Calabi-Yau threefolds might be connected by topological transitions goes back to [58]. Early work showed that this was true for nearly all examples known at the time [30, 31]. These papers considered conifold transitions, in which the intermediate variety has only nodal singularities; the smoothing process replaces these singular points by three-spheres, while the “small” resolution replaces them by two-spheres (holomorphically embedded). Such singularities were shown to be at finite distance in moduli space [32, 33], and conifold transitions were later shown to be smooth processes in type II string theory [59, 60].

If we wish to connect all Calabi-Yau threefolds, conifold transitions are not sufficient, because they cannot change the fundamental group. To see this, we note that topologically, a conifold transition consists of removing neighbourhoods of some number of copies of S^3 , each with boundary $S^3 \times S^2$, and replacing them with similar neighbourhoods of S^2 . Since all these spaces are simply connected, a simple application of van Kampen’s theorem (see, e.g., [61]) shows that the fundamental group does not change.

There do exist relatively mild topological transitions which can change the fundamental group; these are known as *hyperconifold transitions* and were described by the author in [36, 37]. Here, the singularities of the intermediate variety are finite quotients of a node, and their resolutions are no longer “small”. It is an interesting question whether all Calabi-Yau threefolds can be connected by conifold and hyperconifold transitions.

In the following sections, we will consider these two types of transition separately, mostly through examples. The examples in Section 3.2 actually yield previously unknown manifolds, with Hodge numbers $(h^{1,1}, h^{2,1}) = (2, 5)$ and $(2, 3)$ and fundamental groups \mathbb{Z}_5 and S_3 , respectively.

3.1. Conifold Transitions

In [2, 24], free group actions were followed through conifold transitions, leading to webs of conifold transitions between smooth quotients with the same fundamental group (conifold transitions were also used in [34, 35] to construct new simply connected manifolds). Here, we will just consider a simple example (taken from [2]) which exemplifies the idea.

Consider the well-known family of quintic hypersurfaces in \mathbb{P}^4 , with Hodge numbers $(h^{1,1}, h^{2,1}) = (1, 101)$ and hence Euler number $\chi = -200$. If we take homogeneous coordinates z_0, \dots, z_4 on \mathbb{P}^4 , then an action of \mathbb{Z}_5 can be defined by the generator

$$g_5 : z_i \longrightarrow z_{i+1}. \quad (3.1)$$

Then, there is a smooth family of invariant quintics, given by

$$f = \sum_{ijklm} A_{j-i, k-i, l-i, m-i} z_i z_j z_k z_l z_m = 0. \quad (3.2)$$

For generic coefficients, \mathbb{Z}_5 acts freely, so we get a family of smooth quotients with Hodge numbers $(h^{1,1}, h^{2,1}) = (1, 21)$.

Now, let us consider a nongeneric choice for the coefficients in (3.2) such that f is the determinant of some 5×5 matrix M which is linear in the homogeneous coordinates. If we take the entries of M to be

$$M_{ik} = \sum_j a_{j-i, k-i} z_j, \quad (3.3)$$

then the induced \mathbb{Z}_5 action is $M_{ik} \rightarrow M_{i+1,k+1}$, so the determinant does indeed correspond to an invariant quintic. The action of \mathbb{Z}_5 is still generically fixed-point-free on the family given by $\det M = 0$, but the hypersurfaces are no longer smooth. Indeed, using a computer algebra package, it can be checked that the rank of M drops to three at exactly fifty points on a typical such hypersurface, and that these points are nodes. Furthermore, they fall into ten orbits of five nodes under the \mathbb{Z}_5 action.

We now ask whether these nodes can be resolved in a group-invariant way; if so, the group will still act freely on the resolved manifolds, and we will have constructed a conifold transition between the quotient manifolds. In fact this is easy to do. Introduce a second \mathbb{P}^4 , with homogeneous coordinates w_0, \dots, w_4 , and consider the equations

$$f_i := \sum_k M_{ik} w_k = \sum_{j,k} a_{j-i,k-i} z_j w_k = 0. \quad (3.4)$$

These are five bilinears in $\mathbb{P}^4 \times \mathbb{P}^4$, and it can be checked that they generically define a smooth Calabi-Yau threefold $X^{2,52}$. Since we cannot have $w_i = 0$ for all i , there are only simultaneous solutions to these equations when $\det M = 0$, so this gives a projection from $X^{2,52}$ to nodal members of $X^{1,101}$. At most points, this is one-to-one, but at the fifty points where the rank of M drops to three, we get a whole copy of $\mathbb{P}^1 \subset \mathbb{P}^4$ projecting to a (nodal) point of $X^{1,101}$. In this way we see that we have constructed a conifold transition $X^{1,101} \rightsquigarrow X^{2,52}$.

To see that the free \mathbb{Z}_5 action is preserved by the conifold transition above, it suffices to note that if we extend the action by defining $g_5 : w_i \rightarrow w_{i+1}$, then this induces $f_i \rightarrow f_{i+1}$, implying that the manifolds defined by (3.4) are \mathbb{Z}_5 -invariant. The absence of fixed points follows from the absence of fixed points on the nodal members of $X^{1,101}$ although this can also be checked directly.

Since the conifold transition from $X^{1,101}$ to $X^{2,52}$ can be made \mathbb{Z}_5 -equivariant, it descends to a conifold transition between their quotients, $X^{1,21} \rightsquigarrow X^{2,12}$, where the intermediate variety has ten nodes.

3.2. Hyperconifold Transitions

The conifold transition in the last section illustrates two completely general features of such transitions: the fundamental group does not change, for reasons explained previously, and the intermediate singular variety has multiple nodes [62]. We now turn our attention to a class of transitions for which neither of these statements hold—the so-called hyperconifold transitions introduced in [36]. Here, the intermediate space typically has only one singular point, which is a quotient of a node by some finite cyclic group \mathbb{Z}_N . (Quotients by non-Abelian groups can also occur, but these do not admit a toric description, and their resolutions have not been studied.) These arise naturally when a generically free group action is allowed to develop a fixed point. A \mathbb{Z}_N -hyperconifold transition changes the Hodge numbers according to

$$\delta(h^{1,1}, h^{2,1}) = (N - 1, -1). \quad (3.5)$$

The resolution of a hyperconifold singularity replaces the singular point with a simply connected space, and in this way, we see that the transitions can change the fundamental group. It is worth pausing here to consider this in more detail than has been done in previous papers.

Suppose that we have a smooth quotient $X = \tilde{X}/G$ and deform the complex structure until some order- N element g_N , which generates a subgroup $\langle g_N \rangle \cong \mathbb{Z}_N < G$, develops a fixed point $p \in \tilde{X}$. Then, as described in [36], this point will be singular, and generically a node. In some cases, the group structure implies that other elements will simultaneously develop fixed points, which we can see by taking a group element $g' \in G \setminus \langle g_N \rangle$ and performing an elementary calculation

$$g' g_N g'^{-1} \cdot (g' \cdot p) = g' \cdot (g_N \cdot p) = g' \cdot p. \quad (3.6)$$

So, the point $g' \cdot p \in \tilde{X}$ is fixed by $g' g_N g'^{-1}$. We see that every subgroup conjugate to $\langle g_N \rangle$ also develops a fixed point. All such points are identified by G , so the singular quotient $X^\#$ has only one \mathbb{Z}_N -hyperconifold singularity.

What is the fundamental group of the resolution $\hat{X}^\#$? To calculate this, excise a small ball around each fixed point of $\tilde{X}^\#$ to obtain a smooth space \tilde{X}' on which the whole group G acts freely. We can then quotient by G to obtain X' , with fundamental group G . Finally, we glue in a neighbourhood Σ of the exceptional set of the resolution of the hyperconifold. Σ is simply connected. We now have $\hat{X}^\# = X' \cup \Sigma$, and can use van Kampen's theorem to calculate $\pi_1(\hat{X}^\#)$. Note that the intersection of the two subspaces X' and Σ is homotopy equivalent to $S^3 \times S^2/\mathbb{Z}_N$, since the stabiliser of each point on the covering space was isomorphic to \mathbb{Z}_N . So, we have the data

$$\hat{X}^\# = X' \cup \Sigma, \quad X' \cap \Sigma \stackrel{\text{hom.}}{\cong} S^3 \times S^2/\mathbb{Z}_N, \quad \pi_1(\Sigma) \cong \mathbf{1}, \quad \pi_1(X') \cong G, \quad (3.7)$$

which by van Kampen's theorem immediately implies that $\pi_1(\hat{X}^\#) \cong G/\langle g_N \rangle^G$, where $\langle g_N \rangle^G$ is the smallest normal subgroup of G which contains $\langle g_N \rangle$, usually called the normal closure.

Trivial examples arise when $G = \mathbb{Z}_N \times H$ or $\mathbb{Z}_N \rtimes H$, and the generator of \mathbb{Z}_N develops a fixed point. In this case, the corresponding hyperconifold transition changes the fundamental group from G to H .

3.2.1. Example 1: $X^{1,6} \rightsquigarrow X^{2,5}$

We will first consider an example related to that in Section 3.1. If we demand that the matrix appearing in (3.4) is symmetric, $a_{jk} = a_{kj}$, then the resulting family of threefolds are invariant under a further order-two symmetry, generated by $g_2 : z_i \leftrightarrow w_i$. As shown in [2], this family is still generically smooth, and the entire group $\mathbb{Z}_5 \times \mathbb{Z}_2 \cong \mathbb{Z}_{10}$ acts freely, so we get a smooth quotient family $X^{1,6}$.

Suppose now that we ask for g_2 to develop a fixed point. In the ambient space, it fixes an entire copy of \mathbb{P}^4 , given by $w_i = z_i$ for all i . Choose a single point on this locus (as long as it is not also a fixed point of g_5), say $w_i = z_i = \delta_{i0}$. The evaluation of the defining polynomials at this point is $f_i = c_{-i,-i}$, so it lies on the hypersurface if $c_{i,i} = 0$ for all i . One can check that for arbitrary choices of the other coefficients; this point is a node on the covering space, and there are no other singularities. This, therefore, corresponds to a sub-family of $X^{1,6}$ with an isolated \mathbb{Z}_2 -hyperconifold singularity. Such a singularity has a crepant projective resolution, as described in [36], obtained by a simple blowup of the singular point. This introduces an irreducible exceptional divisor, thus increasing $h^{1,1}$ by one, and since we imposed a single constraint on the complex structure of $X^{1,6}$, (naïvely, it seems that we have imposed five constraints, $c_{i,i} = 0$). However, we had the freedom to choose a generic point on the fixed \mathbb{P}^4 ,

corresponding to a four-parameter choice of possible conditions, so the number of complex structure parameters is actually only reduced by one.) the resolved space has Hodge numbers $(h^{1,1}, h^{2,1}) = (2, 5)$, and its fundamental group is \mathbb{Z}_5 . (Note that this is, in fact, a new “three-generation” manifold, with $\chi = -6$. Unfortunately, \mathbb{Z}_5 -valued Wilson lines cannot perform the symmetry breaking required for a realistic model.)

So we have constructed a \mathbb{Z}_2 -hyperconifold transition $X^{1,6} \xrightarrow{\mathbb{Z}_2} X^{2,5}$, where the fundamental group of the first space is \mathbb{Z}_{10} and that of the second space is \mathbb{Z}_5 .

3.2.2. Example 2: $X^{1,4} \rightsquigarrow X^{2,3}$

For a second example, which will also yield an interesting new manifold, consider the Dic_3 quotient of $X^{8,44}$, described in Section 2.2.1. As shown in [22], there is a codimension-one locus in moduli space, where the unique order-two element of the group develops a fixed point. It is easy to check that on the covering space, this is the only singular point, and is a node. As such, the quotient space $X^{1,4}$ develops a \mathbb{Z}_2 -hyperconifold singularity. Blowing up this point yields a new Calabi-Yau manifold, with Hodge numbers $(h^{1,1}, h^{2,1}) = (2, 3)$, as per the general formula (3.5).

The \mathbb{Z}_2 subgroup of Dic_3 is actually the centre, so it is trivially normal, and the fundamental group of the new manifold $X^{2,3}$ is $\text{Dic}_3/\mathbb{Z}_2$, which is isomorphic to S_3 , the symmetric group on three letters. To see this, recall that Dic_3 is generated by two elements, g_3 and g_4 , of orders three and four, respectively, subject to the relation $g_4 g_3 g_4^{-1} = g_3^2$. So, the \mathbb{Z}_2 subgroup is generated by g_4^2 , meaning that in $\text{Dic}_3/\mathbb{Z}_2$, $g_4^2 \sim e$. To reflect this, we rename g_4 to g_2 and obtain

$$\text{Dic}_3/\mathbb{Z}_2 \cong \langle g_2, g_3 \mid g_2^2 = g_3^3 = e, g_2 g_3 g_2 = g_3^2 \rangle, \quad (3.8)$$

which is the standard presentation of S_3 .

So, in summary, we have constructed a \mathbb{Z}_2 -hyperconifold transition $X^{1,4} \xrightarrow{\mathbb{Z}_2} X^{2,3}$, where the fundamental group of the first space is Dic_3 and that of the second space is S_3 . This is the first known Calabi-Yau threefold with fundamental group S_3 [23].

Appendix

The New-Look Zoo

The techniques reviewed in Sections 2 and 3, along with a few exceptional constructions, have led in recent years to the construction of a relatively large number of new Calabi-Yau threefolds with small Hodge numbers and/or nontrivial fundamental group. A table appeared in [2] of all manifolds known at the time with $h^{1,1} + h^{2,1} \leq 24$. Instead of repeating that list here, only new manifolds discovered since the appearance of [2] are listed in Table 2 and Table 3. Since they are of most relevance for string theory, those with nontrivial fundamental group are listed separately in Table 2, while Table 3 contains new simply connected manifolds and those with fundamental group yet to be calculated. Figure 2 displays the tip of the distribution of manifolds catalogued by their Hodge numbers, showing which values of $(h^{1,1}, h^{2,1})$ satisfying $h^{1,1} + h^{2,1} \leq 24$ are realised by known examples (and their mirrors, which are assumed to exist).

Table 2: Manifolds with small Hodge numbers and $\pi_1 \neq 1$.

(X, Y)	$(h^{1,1}, h^{2,1})$	Manifold	π_1	Reference
(0,24)	(12,12)	$X^{20,20}/\mathbb{Z}_2$	\mathbb{Z}_2	[25]
(-16,18)	(5,13)	(Hypersurface in $\mathbb{P}^1 \times \mathbb{P}^1 \times dP_4)/\mathbb{Z}_2 \times \mathbb{Z}_2$	$\mathbb{Z}_2 \times \mathbb{Z}_2$	[26]
(-20,16)	(3,13)	$\begin{matrix} \mathbb{P}^1 \\ \mathbb{P}^1 \\ \mathbb{P}^1 \\ \mathbb{P}^2 \\ \mathbb{P}^2 \\ \mathbb{P}^2 \end{matrix} \begin{pmatrix} 1 & 0 & 0 & 1 & 0 & 0 \\ 0 & 1 & 0 & 1 & 0 & 0 \\ 0 & 0 & 1 & 1 & 0 & 0 \\ 1 & 0 & 0 & 0 & 1 & 1 \\ 0 & 1 & 0 & 0 & 1 & 1 \\ 0 & 0 & 1 & 0 & 1 & 1 \end{pmatrix} / \mathbb{Z}_3$	\mathbb{Z}_3	[23, 24]
(-12,16)	(5,11)	$\begin{matrix} \mathbb{P}^1 \\ \mathbb{P}^1 \\ \mathbb{P}^1 \\ \mathbb{P}^3 \\ \mathbb{P}^2 \end{matrix} \begin{pmatrix} 1 & 1 & 0 & 0 & 0 \\ 1 & 1 & 0 & 0 & 0 \\ 1 & 1 & 0 & 0 & 0 \\ 0 & 1 & 1 & 1 & 1 \\ 0 & 0 & 1 & 1 & 1 \end{pmatrix} / \mathbb{Z}_3$	\mathbb{Z}_3	[23, 24]
(0,16)	(8,8)	$X^{20,20}/\mathbb{Z}_3$	\mathbb{Z}_3	[25]
(0,16)	(8,8)	(Toric hypersurface $Y^{20,20})/\mathbb{Z}_3$	\mathbb{Z}_3	[37]
(32,16)	(16,0)	$(\widehat{\mathbb{P}^7 [2 \ 2 \ 2 \ 2 \ 2]})/\mathbb{Z}_2$	\mathbb{Z}_2	[29]
(-14,15)	(4,11)	$\begin{matrix} \mathbb{P}^1 \\ \mathbb{P}^1 \\ \mathbb{P}^1 \\ \mathbb{P}^1 \\ \mathbb{P}^2 \\ \mathbb{P}^2 \\ \mathbb{P}^2 \\ \mathbb{P}^2 \end{matrix} \begin{pmatrix} 1 & 0 & 0 & 0 & 0 & 0 & 1 & 0 \\ 0 & 1 & 0 & 0 & 0 & 0 & 1 & 0 \\ 0 & 0 & 1 & 0 & 0 & 0 & 1 & 0 \\ 1 & 0 & 0 & 1 & 0 & 0 & 0 & 1 \\ 0 & 1 & 0 & 0 & 1 & 0 & 0 & 1 \\ 0 & 0 & 1 & 0 & 0 & 1 & 0 & 1 \\ 0 & 0 & 0 & 0 & 1 & 1 & 0 & 0 \end{pmatrix} / \mathbb{Z}_3$	\mathbb{Z}_3	[23, 24]
(-10,15)	(5,10)	$\begin{matrix} \mathbb{P}^1 \\ \mathbb{P}^1 \\ \mathbb{P}^1 \\ \mathbb{P}^1 \\ \mathbb{P}^1 \\ \mathbb{P}^2 \\ \mathbb{P}^2 \\ \mathbb{P}^2 \end{matrix} \begin{pmatrix} 1 & 0 & 0 & 0 & 0 & 0 & 1 & 0 & 0 \\ 0 & 1 & 0 & 0 & 0 & 0 & 1 & 0 & 0 \\ 0 & 0 & 1 & 0 & 0 & 0 & 1 & 0 & 0 \\ 0 & 0 & 0 & 1 & 0 & 0 & 1 & 0 & 0 \\ 0 & 0 & 0 & 0 & 1 & 0 & 0 & 1 & 0 \\ 0 & 0 & 1 & 0 & 0 & 1 & 0 & 0 & 1 \\ 1 & 0 & 0 & 1 & 0 & 0 & 0 & 0 & 1 \\ 0 & 1 & 0 & 0 & 1 & 0 & 0 & 0 & 1 \\ 0 & 0 & 1 & 0 & 0 & 1 & 0 & 0 & 1 \end{pmatrix} / \mathbb{Z}_3$	\mathbb{Z}_3	[23, 24]
(-12,14)	(4,10)	(Toric hypersurface $X^{8,26})/\mathbb{Z}_3$	\mathbb{Z}_3	[37]
(-8,14)	(5,9)	$\begin{matrix} \mathbb{P}^1 \\ \mathbb{P}^1 \\ \mathbb{P}^1 \\ \mathbb{P}^1 \\ \mathbb{P}^2 \\ \mathbb{P}^2 \\ \mathbb{P}^2 \\ \mathbb{P}^2 \end{matrix} \begin{pmatrix} 1 & 0 & 0 & 0 & 0 & 0 & 0 & 0 & 0 & 1 \\ 0 & 1 & 0 & 0 & 0 & 0 & 0 & 0 & 0 & 1 \\ 0 & 0 & 1 & 0 & 0 & 0 & 0 & 0 & 0 & 0 \\ 1 & 0 & 0 & 1 & 0 & 0 & 1 & 0 & 0 & 0 \\ 0 & 1 & 0 & 0 & 1 & 0 & 0 & 1 & 0 & 0 \\ 0 & 0 & 1 & 0 & 0 & 1 & 0 & 0 & 1 & 0 \\ 0 & 0 & 0 & 1 & 1 & 1 & 0 & 0 & 0 & 0 \\ 0 & 0 & 0 & 0 & 0 & 0 & 1 & 1 & 1 & 0 \end{pmatrix} / \mathbb{Z}_3$	\mathbb{Z}_3	[23, 24]
(-4,14)	(6,8)	$\begin{matrix} \mathbb{P}^1 \\ \mathbb{P}^1 \\ \mathbb{P}^1 \\ \mathbb{P}^1 \\ \mathbb{P}^1 \\ \mathbb{P}^2 \\ \mathbb{P}^2 \\ \mathbb{P}^2 \end{matrix} \begin{pmatrix} 1 & 0 & 0 & 0 & 0 & 0 & 0 & 0 & 1 & 0 \\ 0 & 1 & 0 & 0 & 0 & 0 & 0 & 0 & 1 & 0 \\ 0 & 0 & 1 & 0 & 0 & 0 & 0 & 0 & 1 & 0 \\ 0 & 0 & 0 & 1 & 0 & 0 & 0 & 0 & 1 & 0 \\ 0 & 0 & 0 & 0 & 1 & 0 & 0 & 0 & 0 & 1 \\ 0 & 0 & 1 & 0 & 0 & 1 & 0 & 0 & 0 & 1 \\ 1 & 0 & 0 & 1 & 0 & 0 & 0 & 0 & 0 & 0 \\ 0 & 1 & 0 & 0 & 1 & 0 & 1 & 0 & 0 & 0 \\ 0 & 0 & 1 & 0 & 0 & 1 & 0 & 1 & 0 & 0 \\ 0 & 0 & 0 & 0 & 0 & 0 & 1 & 1 & 1 & 0 \end{pmatrix} / \mathbb{Z}_3$	\mathbb{Z}_3	[23, 24]
(0,12)	(6,6)	$X^{20,20}/\mathbb{Z}_4$	\mathbb{Z}_4	[25]
(-10,9)	(2,7)	(Hypersurface in $dP_5 \times dP_5)/\mathbb{Z}_5$	\mathbb{Z}_5	[26]
(2,9)	(5,4)	(Toric hypersurface $X^{21,16})/\mathbb{Z}_5$	\mathbb{Z}_5	[37]
(-4,8)	(3,5)	(Hypersurface in $dP_4 \times dP_4)/\mathbb{Z}_4 \times \mathbb{Z}_2$	$\mathbb{Z}_4 \times \mathbb{Z}_2$	[26]
(0,8)	(4,4)	$X^{20,20}/\mathbb{Z}_6$	\mathbb{Z}_6	[25]

Table 2: Continued.

(χ, y)	$(h^{1,1}, h^{2,1})$	Manifold	π_1	Reference
(16,8)	(8,0)	$(\mathbb{P}^7[2\ 2\ 2\ 2]^\# / \{\mathbb{Z}_2 \times \mathbb{Z}_2, \mathbb{Z}_4\})$	$\mathbb{Z}_2 \times \mathbb{Z}_2, \mathbb{Z}_4$	[29]
(-6,7)	(2,5)	$(X^{2,52} / \mathbb{Z}_{10})^\#$	\mathbb{Z}_5	Section 3.2.1
(-8,6)	(1,5)	(Hypersurface in $(\mathbb{P}^1)^4$) / $\mathbb{Z}_8 \times \mathbb{Z}_2$	$\mathbb{Z}_8 \times \mathbb{Z}_2$	[26]
(0,6)	(3,3)	$X^{20,20} / \{\mathbb{Z}_8, Q_8\}$	\mathbb{Z}_8, Q_8	[25]
(-6,5)	(1,4)	$X^{8,44} / \{\text{Dic}_3, \mathbb{Z}_{12}\}$	$\text{Dic}_3, \mathbb{Z}_{12}$	[22]
(-2,5)	(2,3)	$(X^{8,44} / \text{Dic}_3)^\#$	S_3	Section 3.2.2
(0,4)	(2,2)	$X^{19,19} / \{\text{Dic}_3, \mathbb{Z}_{12}\}$	$\text{Dic}_3, \mathbb{Z}_{12}$	[22, 49]
(0,4)	(2,2)	$X^{20,20} / \mathbb{Z}_{12}$	\mathbb{Z}_{12}	[25]
(8,4)	(4,0)	$(\mathbb{P}^7[2\ 2\ 2\ 2]^\# / G), G = 8$	G	[29]
(0,2)	(1,1)	$X^{20,20} / \{SL(2,3), \mathbb{Z}_3 \rtimes \mathbb{Z}_8, \mathbb{Z}_3 \times Q_8\}$	$SL(2,3), \mathbb{Z}_3 \rtimes \mathbb{Z}_8, \mathbb{Z}_3 \times Q_8$	[25]
(4,2)	(2,0)	$(\mathbb{P}^7[2\ 2\ 2\ 2]^\# / G), G = 16$	G	[29]

This table complements the one in [2], and briefly describes the manifolds which have $y = h^{1,1} + h^{2,1} \leq 24$ and nontrivial fundamental group discovered since that paper appeared in 2008. There should still be a number of other manifolds in this region, including quotients from [23] whose Hodge numbers have not yet been calculated, and manifolds obtained from known quotients by hyperconifold transitions [37], of which only a few have so far been written down explicitly. In the ‘‘Manifold’’ column, $X^{20,20}$ denotes the Calabi-Yau toric hypersurface associated to the 24-cell, discussed in [25] and Section 2.2.3, while $X^{19,19}$ refers to the manifold discussed in Section 2.2.2, and $X^{8,44}$ to that in Section 2.2.1. dP_n is the del Pezzo surface of degree n . Multiple quotient groups indicate different quotients with the same Hodge numbers. $X^\#$ denotes a singular member of a generically smooth family, while \hat{X} denotes a resolution of a singular variety X . The column labelled by π_1 gives the fundamental group. For each manifold listed here there should also be a mirror, which is not listed.

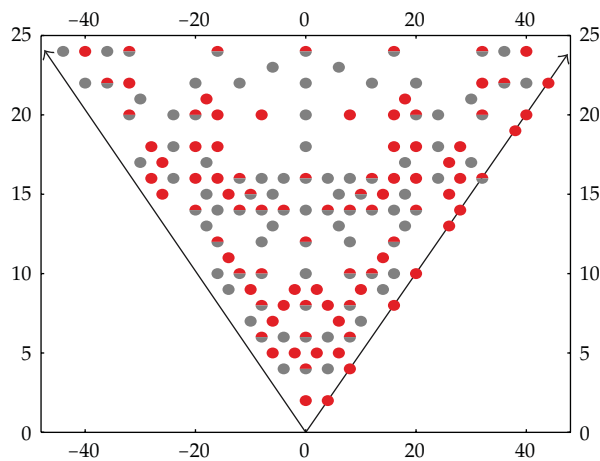


Figure 2: The tip of the distribution of Calabi-Yau threefolds. Grey dots denote manifolds included in [2], while red dots denote newer examples. Split dots indicate multiple occupation of a site. Note that some red and grey dots are also multiply occupied.

Table 3: Other manifolds with small Hodge numbers.

(χ, y)	$(h^{1,1}, h^{2,1})$	Manifold	Reference
(16,24)	(16,8)	—	[29]
(32,24)	(20,4)	—	[29]
(40,24)	(22,2)	—	[29]
(-32, 22)	(3,19)	$(\widehat{\mathbb{P}^4[5]}/D_5)$	[27]
(36,22)	(20,2)	Smoothing of variety obtained by blowing down 18 rational curves on the rigid “Z” manifold.	[35]
(44,22)	(22,0)	—	[29]
(18,21)	(15,6)	Smoothing of variety obtained by blowing down 27 rational curves on the rigid “Z” manifold.	[35]
(-20, 20)	(5,15)	$(\widehat{\mathbb{P}^4[5]}/A_5)$	[27]
(8,20)	(12,8)	—	[29]
(16,20)	(14,6)	—	[29]
(32,20)	(18,2)	—	[29]
(40,20)	(20,0)	—	[29]
(38,19)	(19,0)	—	[29]
(20,18)	(14,4)	—	[29]
(28,18)	(16,2)	—	[29]
(26,17)	(15,2)	—	[29]
(16,16)	(12,4)	—	[29]
(28,16)	(15,1)	—	[29]
(32,16)	(16,0)	—	[29]
(26,15)	(14,1)	—	[29]
(20,14)	(12,2)	—	[29]
(28,14)	(14,0)	—	[29]
(26,13)	(13,0)	—	[29]
(16,12)	(10,2)	—	[29]
(14,11)	(9,2)	—	[29]
(8,10)	(7,3)	—	[29]
(12,10)	(8,2)	—	[29]
(20,10)	(10,0)	—	[29]
(8,8)	(6,2)	—	[29]
(16,8)	(8,0)	—	[29]
(8,4)	(4,0)	—	[29]

This table is the same as that above, except all the manifolds listed either have trivial fundamental group, or a fundamental group which has not been calculated (which is the case for several examples from [29]). The notation is the same as above, and the manifolds with no description are all desingularisations of quotients by various groups of a singular complete intersection of four quadrics in \mathbb{P}^7 [29].

Acknowledgments

The author would like to thank Eberhard Freitag for useful correspondence, and Philip Candelas for helpful comments on a draft of this paper. This work was supported by the Engineering and Physical Sciences Research Council (Grant no. EP/H02672X/1).

References

- [1] P. Candelas, X. de la Ossa, Y.-H. He, and B. Szendroi, "Triadophilia: a special corner in the landscape," *Advances in Theoretical and Mathematical Physics*, vol. 12, no. 2, pp. 429–473, 2008.
- [2] P. Candelas and R. Davies, "New Calabi-Yau manifolds with small hodge numbers," *Fortschritte der Physik*, vol. 58, no. 4-5, pp. 383–466, 2010.
- [3] P. Green and T. Hubsch, "Calabi-Yau manifolds as complete intersections in products of complex projective spaces," *Communications in Mathematical Physics*, vol. 109, no. 1, pp. 99–108, 1987.
- [4] P. Candelas, A. M. Dale, C. A. Lutken, and R. Schimmrigk, "Complete intersection Calabi-Yau manifolds," *Nuclear Physics B*, vol. 298, no. 3, pp. 493–525, 1988.
- [5] P. S. Green, T. Hubsch, and C. A. Lutken, "All the Hodge numbers for all Calabi-Yau complete intersections Calabi-Yau manifolds," *Classical and Quantum Gravity*, vol. 6, no. 2, pp. 105–124, 1989.
- [6] V. Batyrev and L. A. Borisov, "On Calabi-Yau complete intersections in toric varieties," <http://arxiv.org/abs/alg-geom/9412017>.
- [7] M. Kreuzer and H. Skarke, "On the classification of reflexive polyhedra," *Communications in Mathematical Physics*, vol. 185, no. 2, pp. 495–508, 1997.
- [8] M. Kreuzer and H. Skarke, "Complete classification of reflexive polyhedra in four-dimensions," *Advances in Theoretical and Mathematical Physics*, vol. 4, no. 6, pp. 1209–1230, 2000.
- [9] P. Candelas, G. T. Horowitz, A. Strominger, and E. Witten, "Vacuum configurations for superstrings," *Nuclear Physics B*, vol. 258, no. 1, pp. 46–74, 1985.
- [10] S.-T. Yau, "Compact three-dimensional Kähler manifolds with zero Ricci curvature," in *Proceedings of the Argonne-Chicago Symposium on Anomalies, Geometry and Topology*, A. White, Ed., pp. 395–406, World Scientific, 1985.
- [11] A. Strominger and E. Witten, "New manifolds for superstring compactification," *Communications in Mathematical Physics*, vol. 101, no. 3, pp. 341–361, 1985.
- [12] P. Candelas, C. A. Lutken, and R. Schimmrigk, "Complete intersection Calabi-Yau manifolds II: three generation manifolds," *Nuclear Physics B*, vol. 306, no. 1, pp. 113–136, 1988.
- [13] R. Schimmrigk, "A new construction of a three-generation Calabi-Yau manifold," *Physics Letters B*, vol. 193, no. 2-3, pp. 175–180, 1987.
- [14] A. Beauville, "A Calabi-Yau threefold with non-abelian fundamental group," in *New Trends in Algebraic Geometry*, vol. 264 of *London Mathematical Society Lecture Note Series*, pp. 13–17, Cambridge University Press, Cambridge, UK, 1999.
- [15] M. Gross and S. Popescu, "Calabi-Yau threefolds and moduli of abelian surfaces I," *Compositio Mathematica*, vol. 127, no. 2, pp. 169–228, 2001.
- [16] V. Braun, B. A. Ovrut, T. Pantev, and R. Reinbacher, "Elliptic Calabi-Yau threefolds with $\mathbb{Z}_3 \times \mathbb{Z}_3$ Wilson lines," *Journal of High Energy Physics*, vol. 2004, no. 12, article 062, 2004.
- [17] V. Batyrev and M. Kreuzer, "Integral cohomology and mirror symmetry for Calabi-Yau 3-folds," in *Proceedings of "Mirror Symmetry IV"*, *AMS/IP Studies in Advanced Mathematics*, N. Yui, S.-T. Yau, S.-T. Yau, and J. D. Lewis, Eds., 2006, <http://arxiv.org/abs/math/0505432>.
- [18] Z. Hua, "Classification of free actions on complete intersections of four quadrics," <http://arxiv.org/abs/0707.4339>.
- [19] V. Bouchard and R. Donagi, "On a class of non-simply connected Calabi-Yau threefolds," *Communications in Number Theory and Physics*, vol. 2, no. 1, pp. 1–61, 2008.
- [20] L. Borisov and Z. Hua, "On Calabi-Yau threefolds with large nonabelian fundamental groups," *Proceedings of the American Mathematical Society*, vol. 136, no. 5, pp. 1549–1551, 2008.
- [21] M. Gross and S. Popescu, "Calabi-yau three-folds and moduli of abelian surfaces II," *Transactions of the American Mathematical Society*, vol. 363, no. 7, pp. 3573–3599, 2011.
- [22] V. Braun, P. Candelas, and R. Davies, "A three-generation Calabi-Yau manifold with small Hodge numbers," *Fortschritte der Physik*, vol. 58, no. 4-5, pp. 467–502, 2010.
- [23] V. Braun, "On free quotients of complete intersection Calabi-Yau manifolds," *JHEP* 1104 (2011) 005, <http://arxiv.org/abs/1003.3235>.

- [24] P. Candelas and A. Constantin, "Completing the web of Z_3 -quotients of complete intersection Calabi-Yau manifolds," <http://arxiv.org/abs/1010.1878>.
- [25] V. Braun, "The 24-cell and Calabi-Yau threefolds with hodge numbers (1,1)," <http://arxiv.org/abs/1102.4880>.
- [26] G. Bini and F. F. Favale, "Groups acting freely on Calabi-Yau threefolds embedded in a product of del Pezzo surfaces," <http://arxiv.org/abs/1104.0247>.
- [27] A. Stapledon, "New mirror pairs of Calabi-Yau orbifolds," <http://arxiv.org/abs/1011.5006>.
- [28] E. Freitag and R. Salvati Manni, "Some siegel threefolds with a Calabi-Yau model II," <http://arxiv.org/abs/1001.0324>.
- [29] E. Freitag and R. Salvati Manni, "On siegel threefolds with a projective Calabi-Yau model," <http://arxiv.org/abs/1103.2040>.
- [30] P. S. Green and T. Hubsch, "Connecting moduli spaces of Calabi-Yau threefolds," *Communications in Mathematical Physics*, vol. 119, no. 3, pp. 431–441, 1988.
- [31] P. S. Green and T. Hubsch, "Possible phase transitions among Calabi-Yau compactifications," *Physical Review Letters*, vol. 61, no. 10, pp. 1163–1166, 1988.
- [32] P. Candelas, P. S. Green, and T. Hubsch, "Finite distance between distinct Calabi-Yau manifolds," *Physical Review Letters*, vol. 62, no. 17, pp. 1956–1959, 1989.
- [33] P. Candelas, P. S. Green, and T. Hubsch, "Rolling among Calabi-Yau vacua," *Nuclear Physics B*, vol. 330, no. 1, pp. 49–102, 1990.
- [34] V. Batyrev and M. Kreuzer, "Constructing new Calabi-Yau 3-folds and their mirrors via conifold transitions," *Advances in Theoretical and Mathematical Physics*, no. 14, pp. 879–898, 2010, <http://arxiv.org/abs/0802.3376>.
- [35] S. Filippini and V. Garbagnati, "A rigid Calabi—Yau 3-fold," <http://arxiv.org/abs/1102.1854>.
- [36] R. Davies, "Quotients of the conifold in compact Calabi-Yau threefolds, and new topological transitions," *Advances in Theoretical and Mathematical Physics*, no. 14, pp. 965–990, 2010, <http://arxiv.org/abs/0911.0708>.
- [37] R. Davies, "Hyperconifold transitions, mirror symmetry, and string theory," *Nuclear Physics B*, vol. 850, pp. 214–233, 2011, <http://arxiv.org/abs/1102.1428>.
- [38] L. B. Anderson, J. Gray, A. Lukas, and B. Ovrut, "Stabilizing the complex structure in heterotic Calabi-Yau vacua," *Journal of High Energy Physics*, vol. 2011, no. 2, article 88, 2011.
- [39] L. B. Anderson, J. Gray, A. Lukas, and B. Ovrut, "Stabilizing all geometric moduli in heterotic Calabi-Yau vacua," *Physical Review D*, vol. 83, Article ID 106011, 14 pages, 2011.
- [40] M. F. Atiyah and R. Bott, "A Lefschetz fixed point formula for elliptic differential operators," *Bulletin of the American Mathematical Society*, vol. 72, pp. 245–250, 1966.
- [41] M. F. Atiyah and R. Bott, "A Lefschetz fixed point formula for elliptic complexes: II applications," *Annals of Mathematics*, vol. 88, pp. 451–491, 1968.
- [42] W. Decker, G.-M. Greuel, G. Pfister, and H. Schönemann, "Singular 3-1-2—a computer algebra system for polynomial computations," <http://www.singular.uni-kl.de>.
- [43] Wolfram Research, *Mathematica, Version 8.0*, Wolfram Research, 2010.
- [44] J. Gray, Y.-H. He, A. Ilderton, and A. Lukas, "Stringvacua: a mathematica package for studying vacuum configurations in string phenomenology," *Computer Physics Communications*, vol. 180, no. 1, pp. 107–119, 2009.
- [45] R. Hartshorne, *Algebraic Geometry*, Graduate Texts in Mathematics, Springer, New York, NY, USA, 1977.
- [46] B. McInnes, "Group-theoretic aspects of the Hosotani mechanism," *Journal of Physics A*, vol. 22, no. 13, pp. 2309–2328, 1989.
- [47] E. Witten, "New issues in manifolds of $SU(3)$ holonomy," *Nuclear Physics B*, vol. 268, no. 1, pp. 79–112, 1986.
- [48] J. Li and S.-T. Yau, "The existence of supersymmetric string theory with torsion," *Journal of Differential Geometry*, vol. 70, no. 1, pp. 143–181, 2005.
- [49] R. Davies, *Calabi-Yau threefolds and heterotic string compactification*, DPhil thesis, Oxford University, Oxford, UK, 2010, <http://ora.ouls.ox.ac.uk/objects/uuid:be92aac5-6874-431e-95a0-ac61a88ee63d>.
- [50] V. Braun, Y.-H. He, B. A. Ovrut, and T. Pantev, "The exact MSSM spectrum from string theory," *Journal of High Energy Physics*, vol. 2006, no. 5, article 043, 2006.
- [51] V. Braun, Y.-H. He, and B. A. Ovrut, "Yukawa couplings in heterotic standard models," *Journal of High Energy Physics*, vol. 2006, no. 4, article 019, 2006.
- [52] L. B. Anderson, J. Gray, Y.-H. He, and A. Lukas, "Exploring positive monad bundles and a new heterotic standard model," *Journal of High Energy Physics*, vol. 2010, no. 2, article 054, 2010.

- [53] V. Bouchard and R. Donagi, "An SU(5) heterotic standard model," *Physics Letters B*, vol. 633, no. 6, pp. 783–791, 2006.
- [54] V. Bouchard, M. Cvetič, and R. Donagi, "Tri-linear couplings in an heterotic minimal supersymmetric standard model," *Nuclear Physics B*, vol. 745, no. 1-2, pp. 62–83, 2006.
- [55] V. Braun, B. A. Ovrut, M. Kreuzer, and E. Scheidegger, "Worldsheet instantons and torsion curves, part A: direct computation," *Journal of High Energy Physics*, vol. 2007, no. 10, article 022, 2007.
- [56] V. Braun, B. A. Ovrut, M. Kreuzer, and E. Scheidegger, "Worldsheet instantons and torsion curves part B: mirror symmetry," *Journal of High Energy Physics*, vol. 2007, no. 10, article 023, 2007.
- [57] A. Bak, V. Bouchard, and R. Donagi, "Exploring a new peak in the heterotic landscape," *Journal of High Energy Physics*, vol. 2010, no. 6, article 108, 2010.
- [58] M. Reid, "The moduli space of 3-folds with $K = 0$ may nevertheless be irreducible," *Mathematische Annalen*, vol. 278, no. 1–4, pp. 329–334, 1987.
- [59] A. Strominger, "Massless black holes and conifolds in string theory," *Nuclear Physics B*, vol. 451, no. 1-2, pp. 96–108, 1995.
- [60] B. R. Greene, D. R. Morrison, and A. Strominger, "Black hole condensation and the unification of string vacua," *Nuclear Physics B*, vol. 451, no. 1-2, pp. 109–120, 1995.
- [61] A. Hatcher, *Algebraic Topology*, Cambridge University Press, Cambridge, UK, 2002.
- [62] P. Candelas and X. C. de la Ossa, "Comments on conifolds," *Nuclear Physics B*, vol. 342, no. 1, pp. 246–268, 1990.

Research Article

Chern-Simons: Fano and Calabi-Yau

Amihay Hanany^{1,2} and Yang-Hui He^{3,4,5}

¹ *Theoretical Physics Group, Blackett Laboratory, Imperial College, London SW7 2AZ, UK*

² *KITP, University of California, Santa Barbara, CA 93106-4030, USA*

³ *Rudolf Peierls Centre for Theoretical Physics, Oxford University, 1 Keble Road, Oxford OX1 3NP, UK*

⁴ *Collegium Mertonense in Academia Oxoniensi, Merton College, Oxford OX1 4JD, UK*

⁵ *Mathematical Institute, Oxford University, 24-29 St. Giles', Oxford OX1 3LB, UK*

Correspondence should be addressed to Amihay Hanany, a.hanany@imperial.ac.uk

Received 13 October 2010; Accepted 6 March 2011

Academic Editor: André Lukas

Copyright © 2011 A. Hanany and Y.-H. He. This is an open access article distributed under the Creative Commons Attribution License, which permits unrestricted use, distribution, and reproduction in any medium, provided the original work is properly cited.

We present the complete classification of smooth toric Fano threefolds, known to the algebraic geometry literature, and perform some preliminary analyses in the context of brane tilings and Chern-Simons theory on M2-branes probing Calabi-Yau fourfold singularities. We emphasise that these 18 spaces should be as intensely studied as their well-known counterparts: the del Pezzo surfaces.

1. Introduction

A flurry of activity has, since the initial work of Bagger and Lambert [1–3] and Gustavsson [4], rather excited the community for the past two years upon the subject of supersymmetric Chern-Simons theories. It is by now widely believed that the world-volume theory of M2-branes on various backgrounds is given by a $(2+1)$ -dimensional quiver Chern-Simons (QCS) theory [5–26], most conveniently described by a brane tiling.

Even though analogies with the case of D3-branes in Type IIB, whose world-volume theory is a $(3+1)$ -dimensional supersymmetric quiver gauge theory, are very reassuring, the story is much less understood for the M2 case. Much work has been devoted to the understanding of issues such as orbifolding, phases of duality, brane tilings, and dimer/crystal models and so forth. Nevertheless, the role played by the correspondence between the world-volume theory and the underlying Calabi-Yau geometry is of indubitable importance. Indeed, there is a bijection: the vacuum moduli space of the former is, tautologically, the latter, while the geometrical engineering on the latter gives, by construction, the former. This bijection, called, respectively, the “forward” and “inverse” algorithms [27, 28], persists in any dimension and can be succinctly summarised in Table 1.

Table 1: Brane probes and associated world-volume physics in various backgrounds.

Brane probe	Theory	Background	World-volume theory	Vacuum moduli space
D5	Type IIB	$\mathbb{R}^{1,5} \times \text{CY2}$	(5+1)-d $\mathcal{N} = 1$ gauge theory	CY2
D3	Type IIB	$\mathbb{R}^{1,3} \times \text{CY3}$	(3+1)-d $\mathcal{N} = 1$ gauge theory	CY3
M2	M-theory	$\mathbb{R}^{1,2} \times \text{CY4}$	(2+1)-d $\mathcal{N} = 2$ Chern-Simons	CY4

A crucial feature for all the brane embeddings in Table 1 is that in the toric case they are all described by brane tilings. The first case, with CY2, is described by one-dimensional tilings, that is, brane intervals and thus brane constructions following the work in [29]. The second case is the well-established two-dimensional brane tilings which use dimer techniques to study supersymmetric gauge theories [30–32]. The third case is the newly proposed construction [13] of Chern-Simon theories.

It is perhaps naïvely natural to propose three-dimensional tilings for the case of M2-branes probing CY4, but in fact, it turns out not to be as useful as it may initially seem. These three-dimensional tilings have been nicely advocated in the crystal model [33, 34]. The main issue perhaps is the current shortcoming of this model to identify the gauge groups with a simplex as it is done for the tilings in dimensions one and two. In the one-dimensional case for toric CY2, the gauge group is identified with an edge of the tiling, and the matter content with nodes. For the two-dimensional case for toric CY3, the gauge fields, matter fields, and interactions are, respectively, identified with faces, edges, and nodes of the tiling. But for the proposed crystal model, there is no such simple interpretation yet known.

We are thus led, for now, to keep on the path of two-dimensional tilings, while bearing in mind that the data needed to specify a QCS theory is given by gauge groups, matter fields, and interactions, as well as the additional data of the CS levels for the gauge groups. These nicely map, respectively, to tiles, edges, and nodes, while the corresponding CS levels are given by fluxes on the tiles. It would be interesting to check if this correspondence between tilings in one and two dimensions, that is, for toric Calabi-Yau n -folds with $n = 2, 3, 4$, can be extended to possibly higher-dimensional tilings and perhaps higher-dimensional Calabi-Yau spaces.

The cases for Calabi-Yau two- and threefolds are well established over the past decade. These are affine complex cones over base complex curves and surfaces, or real cones over real, compact, Sasaki-Einstein three and five manifolds. Perhaps the most extensively studied are, inspired by phenomenological concerns, D3-branes and Calabi-Yau threefolds and the widest class studied therein is *toric Calabi-Yau cones*. A rather complete picture for both the forward and inverse algorithms, as well as the unifying perspective of brane tilings and dimer models, has emerged over the last decade. Ricci-flat metrics have even been found for infinite families within the class of these noncompact spaces.

Another crucial family of Calabi-Yau threefold cones affords a clear construction, and the world-volume physics has been intensely investigated (cf., e.g., [35–37]). The base surfaces here are so-called *del Pezzo* surfaces which afford positive curvature, so that the appropriate cones over them have just the right behaviour to make the affine threefold have zero Ricci curvature. More precisely, these surfaces are dP_n , which is \mathbb{P}^2 blowup at n equal to zero up to eight generic points, or the zeroth Hirzebruch surface $F_0 := \mathbb{P}^1 \times \mathbb{P}^1$. In fact, the cones over F_0 and $dP_{n=0,1,2,3}$ are toric, whereby making these five del Pezzo members of particular interest. The $(3 + 1)$ -dimensional gauge theories for these were first constructed in [27, 28], giving rise to such interesting phenomena as toric duality and tilings.

Indeed, all toric gauge theories in $(3 + 1)$ dimensions obey a remarkable topological formula: take the number of nodes in the quiver, the number of fields, and the number of terms in the superpotential; their alternating sum vanishes. This is a key for the powerful brane tiling (dimer model) description (cf. review in [32]) of these theories. Interestingly, this relation is still obeyed for the myriad of all known $(2 + 1)$ -dimensional QCS theories to date and suggests that a planar brane tiling may still be the underlying principle behind theories living on M2-branes probing affine Calabi-Yau fourfolds. The richness of the $(3 + 1)$ -dimensional theories beckons for their analogous and extensions to the $(2 + 1)$ -dimensional case.

It is therefore a natural and important question to ask what are the corresponding geometries for Calabi-Yau fourfolds and physically what are the associated $(2 + 1)$ -dimensional QCS theories on the M2-brane world volume, that is, what are the (smooth) toric complex threefolds which admit positive curvature? Based on the ample experience with and the wealth of physics engendered by the aforementioned five del Pezzo cases for threefolds, these fourfolds could hold a key toward understanding QCS and M2 theories.

It is the purpose of the current short note, a prologue to [38], to present the *dramatis personae* onto the stage and to introduce some rudiments of their properties as well as to initiate the first constructions of the QCS physics associated thereto. Indeed, complex manifolds admitting positive curvature are in general called *Fano varieties* of which the del Pezzo surfaces are merely the two-dimensional examples. We will see that a complete and convenient classification exists for the smooth toric Fano threefolds over which Calabi-Yau four-fold cones can be established; we will take advantage of the existing data and use the forward algorithm to explicitly construct the quivers, superpotentials, and Chern-Simons levels for some cases. A companion paper, of substantially more length and in-depth analysis [38], will ensue in the near future. It is our hope that the 18 characters to which we draw your attention will, in due course, become as familiar as the del Pezzo family to the community.

2. Fano Varieties

Fano varieties are of obvious importance; these are varieties which admit an ample anticanonical sheaf; thus, whereas Calabi-Yau varieties are of zero curvature, they are of positive curvature. (Recently, lower bounds on the Ricci curvature of Fano manifolds have been found [39].) Therefore, not only could Fano varieties constitute cycles of positive volume that can shrink inside a Calabi-Yau, but also, could they provide local models of Calabi-Yau of a higher dimension. This second case is perhaps of more interest in the brane-probe scenario where the transverse directions to the branes are affine, noncompact Calabi-Yau spaces. In particular, one could construct an affine complex cone over a Fano n -fold, so as to construct a Calabi-Yau $(n + 1)$ -fold, and the branes then reside at the tip of the cone. This situation has become well known to the AdS/CFT correspondence.

What are explicit examples of Fano varieties? In complex dimension one, there is only \mathbb{P}^1 , the sphere, which obviously has positive curvature. In dimension two, they are called del Pezzo surfaces. In particular, they are \mathbb{P}^2 , as well its blowup dP_n at $n = 1$ up to $n = 8$ generic points thereon, and the zeroth Hirzebruch surface $\mathbb{F}_0 := \mathbb{P}^1 \times \mathbb{P}^1$. Of these 10, \mathbb{P}^2 , \mathbb{F}_0 , and dP_n for $n = 1, 2, 3$ admit a toric description. These have been used extensively in constructing gauge theories on the D3-brane world volume [27–40], and the moduli spaces of these theories are correspondingly local Calabi-Yau threefolds.

We point out that, of course, the aforementioned are *smooth* Fano varieties. Indeed, we can readily construct affine Calabi-Yau spaces which are singular cones. For example, for complex dimension one, we indeed have the smooth \mathbb{P}^1 , leading to the affine Calabi-Yau 2-fold $\mathbb{C}^2/\mathbb{Z}_2$, with the corresponding quiver gauge theory in $(5 + 1)$ dimensions, but we also have any of the famous ADE singularities given by \mathbb{C}^2 quotient by a discrete subgroup of $SU(2)$ which give rise to well-known gauge theories. In complex dimension 2, we have \mathbb{P}^2 , corresponding to the affine Calabi-Yau 3-fold $dP_0 = \mathbb{C}^3/\mathbb{Z}_3$; however, any $\mathbb{C}^3/\mathbb{Z}_n$ is just as good with a singular base Fano 2-fold in a weighted projected space.

Our chief interest lies in the situation of dimension three. These Fano threefolds can give rise to Calabi-Yau fourfolds which can then be probed by M2-branes in order to arrive at quiver Chern-Simons (QCS) theories on their world volume. A classification of the Fano varieties was achieved in the 80s [41–43]; there is a wealth thereof. Our particular interest will once more be on the toric Fano threefolds where such techniques as tilings and dimers will be conducive. Toric Fano threefolds have been studied in [44, 45]. In dimension n , an obvious general class of toric Fano k -folds is $\prod_j \mathbb{P}^{k_j}$ where $\{k_j\}$ is a partition of n , that is, $n = \sum_j k_j$.

With the rapid advance of computer algebra and algorithmic algebraic geometry, especially in applications to physics (cf. [46–48]), even non-smooth Fano varieties can be classified [50]. (Indeed, in any dimension d , it is known that there are a finite number of *smooth* Fano varieties [49].) A convenient database has been established whereby one could readily search within an online depository [51]. (We are grateful to Richard Thomas for revealing this treasure trove to us.)

2.1. Smooth Toric Fano Threefolds

Given the enormity of the number, we were to allow singularities—against which, physically, there need be no prejudice—and being inspired by the 2-fold case of the del Pezzo surfaces all being smooth, we will henceforth restrict our attention to the *smooth* toric Fano threefolds. In the parlance of toric geometry, the corresponding cone is called regular. There is a total of 18 such threefolds, a reasonable set indeed. We will adhere to the standard notation of [45] wherein the family is tabulated and also to the identifier with the database [51] for the sake of canonical reference. This is presented in Table 2.

2.1.1. Toric Data

Some detailed explanation of the nomenclature in Table 2 is in order. The toric data is such that the columns are vectors which generate the cone of the variety; in the D-brane context, this has become known as the G_t matrix. Note that each is a 3-vector, signifying that we are dealing with threefolds. Moreover, the point $(0, 0, 0)$ is always an internal point. This property is equivalent to the Fano condition. Indeed, as we recall from [27, 28], the del Pezzo surfaces all have a single internal point. The explicit topology of each space is also given, following [45].

Indeed, our interest in (compact) Fano threefolds is that the complex cone thereupon is an (noncompact) affine Calabi-Yau fourfold which M2-branes may probe. Going from the data in the table to the fourfold is simple; we only need to add one more dimension, say, a row of 1s to each of the matrices. In such cases, the geometry will be cones over what is reported in the third column. In the physics literature, there have been several cases which

Table 2: The 18 smooth toric Fano threefolds. For full explanation of notation, see the second paragraph of Section 2.1 and those that follow.

	Id of [51]	G_i : toric data	Geometry	(b_2, g, Sym)
\mathbb{P}^3	4	$\begin{pmatrix} 1 & 0 & 0 & -1 & 0 \\ 0 & 1 & 0 & -1 & 0 \\ 0 & 0 & 1 & -1 & 0 \end{pmatrix}$	\mathbb{P}^3	$(1, 33, \mathcal{U}(4))$
\mathcal{B}_1	35	$\begin{pmatrix} 1 & 0 & 1 & -1 & 1 & 0 \\ 0 & 1 & 1 & -1 & 1 & 0 \\ 0 & 0 & 2 & -1 & 1 & 0 \end{pmatrix}$	$\mathbb{P}(\mathcal{O}_{\mathbb{P}^2} \oplus \mathcal{O}_{\mathbb{P}^2}(2))$	$(2, 32, [3, 1^2])$
\mathcal{B}_2	36	$\begin{pmatrix} 1 & 0 & 0 & -1 & -1 & 0 \\ 0 & 1 & 0 & -1 & 0 & 0 \\ 0 & 0 & 1 & -1 & 0 & 0 \end{pmatrix}$	$\mathbb{P}(\mathcal{O}_{\mathbb{P}^2} \oplus \mathcal{O}_{\mathbb{P}^2}(1))$	$(2, 29, [3, 1^2])$
\mathcal{B}_3	37	$\begin{pmatrix} 1 & 0 & 0 & -1 & -1 & 0 \\ 0 & 1 & 0 & -1 & -1 & 0 \\ 0 & 0 & 1 & -1 & 0 & 0 \end{pmatrix}$	$\mathbb{P}(\mathcal{O}_{\mathbb{P}^1} \oplus \mathcal{O}_{\mathbb{P}^1} \oplus \mathcal{O}_{\mathbb{P}^1}(1))$	$(2, 28, [2^2, 1^2])$
\mathcal{B}_4	24	$\begin{pmatrix} 1 & 0 & 0 & -1 & 0 & 0 \\ 0 & 1 & 0 & -1 & 0 & 0 \\ 0 & 0 & 1 & 0 & -1 & 0 \end{pmatrix}$	$\mathbb{P}^2 \times \mathbb{P}^1$	$(2, 28, [3, 2, 1])$
\mathcal{C}_1	105	$\begin{pmatrix} 1 & 0 & 1 & -1 & 0 & 1 & 0 \\ 0 & 1 & 1 & -1 & 0 & 1 & 0 \\ 0 & 0 & 1 & 0 & -1 & 0 & 0 \end{pmatrix}$	$\mathbb{P}(\mathcal{O}_{\mathbb{P}^1 \times \mathbb{P}^1} \oplus \mathcal{O}_{\mathbb{P}^1 \times \mathbb{P}^1}(1, 1))$	$(3, 27, [2^2, 1^2])$
\mathcal{C}_2	136	$\begin{pmatrix} 1 & 0 & 0 & -1 & -1 & -2 & 0 \\ 0 & 1 & 0 & -1 & 0 & -1 & 0 \\ 0 & 0 & 1 & -1 & 0 & -1 & 0 \end{pmatrix}$	$\mathbb{P}(\mathcal{O}_{dP_1} \oplus \mathcal{O}_{dP_1}(\ell)), \quad \ell^2 _{dP_1} = 1$	$(3, 26, [2, 1^3])$
\mathcal{C}_3	62	$\begin{pmatrix} 1 & 0 & 0 & -1 & 0 & 0 & 0 \\ 0 & 1 & 0 & 0 & -1 & 0 & 0 \\ 0 & 0 & 1 & 0 & 0 & -1 & 0 \end{pmatrix}$	$\mathbb{P}^1 \times \mathbb{P}^1 \times \mathbb{P}^1$	$(3, 25, [2^3, 1])$
\mathcal{C}_4	123	$\begin{pmatrix} 1 & 0 & 0 & -1 & 0 & -1 & 0 \\ 0 & 1 & 0 & -1 & 0 & 0 & 0 \\ 0 & 0 & 1 & 0 & -1 & 0 & 0 \end{pmatrix}$	$dP_1 \times \mathbb{P}^1$	$(3, 25, [2^2, 1^2])$
\mathcal{C}_5	68	$\begin{pmatrix} 1 & 0 & 0 & -1 & -1 & 1 & 0 \\ 0 & 1 & 0 & -1 & -1 & 1 & 0 \\ 0 & 0 & 1 & -1 & 0 & 0 & 0 \end{pmatrix}$	$\mathbb{P}(\mathcal{O}_{\mathbb{P}^1 \times \mathbb{P}^1} \oplus \mathcal{O}_{\mathbb{P}^1 \times \mathbb{P}^1}(1, -1))$	$(3, 23, [2^2, 1^2])$
\mathcal{D}_1	131	$\begin{pmatrix} 1 & 0 & 0 & -1 & -1 & -1 & 0 \\ 0 & 1 & 0 & -1 & 0 & -1 & 0 \\ 0 & 0 & 1 & -1 & 0 & 0 & 0 \end{pmatrix}$	\mathbb{P}^1 -blowup of \mathcal{B}_2	$(3, 26, [2, 1^3])$
\mathcal{D}_2	139	$\begin{pmatrix} 1 & 0 & 0 & -1 & -1 & 0 & 0 \\ 0 & 1 & 0 & -1 & 0 & -1 & 0 \\ 0 & 0 & 1 & -1 & 0 & -1 & 0 \end{pmatrix}$	\mathbb{P}^1 -blowup of \mathcal{B}_4	$(3, 24, [2, 1^3])$
\mathcal{E}_1	218	$\begin{pmatrix} 1 & 0 & 0 & -1 & -1 & 0 & -1 & 0 \\ 0 & 1 & 0 & -1 & 0 & 0 & -1 & 0 \\ 0 & 0 & 1 & -1 & 0 & 0 & 0 & 0 \end{pmatrix}$	dP_2 bundle over \mathbb{P}^1	$(4, 24, [2, 1^3])$
\mathcal{E}_2	275	$\begin{pmatrix} 1 & 0 & 0 & -1 & 0 & -1 & -1 & 0 \\ 0 & 1 & 0 & -1 & 0 & 0 & 0 & 0 \\ 0 & 0 & 1 & 0 & -1 & 0 & -1 & 0 \end{pmatrix}$	dP_2 bundle over \mathbb{P}^1	$(4, 23, [2, 1^3])$
\mathcal{E}_3	266	$\begin{pmatrix} 1 & 0 & 0 & -1 & 0 & -1 & 0 & 0 \\ 0 & 1 & 0 & -1 & 0 & 0 & -1 & 0 \\ 0 & 0 & 1 & 0 & -1 & 0 & 0 & 0 \end{pmatrix}$	$dP_2 \times \mathbb{P}^1$	$(4, 22, [2, 1^3])$
\mathcal{E}_4	271	$\begin{pmatrix} 1 & 0 & 0 & -1 & -1 & -1 & 1 & 0 \\ 0 & 1 & 0 & -1 & 0 & -1 & 1 & 0 \\ 0 & 0 & 1 & -1 & 0 & 0 & 0 & 0 \end{pmatrix}$	dP_2 bundle over \mathbb{P}^1	$(4, 21, [2, 1^3])$
\mathcal{F}_1	324	$\begin{pmatrix} 1 & 0 & 0 & -1 & 0 & -1 & 0 & 1 & 0 \\ 0 & 1 & 0 & -1 & 0 & 0 & -1 & 1 & 0 \\ 0 & 0 & 1 & 0 & -1 & 0 & 0 & 0 & 0 \end{pmatrix}$	$dP_3 \times \mathbb{P}^1$	$(5, 19, [2, 1^3])$
\mathcal{F}_2	369	$\begin{pmatrix} 1 & 0 & 0 & -1 & -1 & 0 & -1 & 1 & 0 \\ 0 & 1 & 0 & -1 & 0 & -1 & -1 & 1 & 0 \\ 0 & 0 & 1 & -1 & 0 & 0 & 0 & 0 & 0 \end{pmatrix}$	dP_3 bundle over \mathbb{P}^1	$(5, 19, [2, 1^3])$

have been studied in considerable depth and detail: the cone over \mathbb{P}^3 is the orbifold $\mathbb{C}^4/\mathbb{Z}_4$, the Sasaki-Einstein 7-fold (a homogeneous space which is a circle fibration over the $\mathbb{P}^1 \times \mathbb{P}^2$), which is a *real* cone over \mathcal{B}_4 , is dubbed $M^{1,1,1}$ (see [13]), and the real Sasaki-Einstein cone over \mathcal{C}_3 is called $Q^{1,1,1}/\mathbb{Z}_2$ (cf., e.g., [19, 24, 25]).

2.1.2. Fibrations and Bundles

We, of course, recognise \mathbb{P}^3 (succeeding the sequence of \mathbb{P}^1 in dimension 1 and $\mathbb{P}^2 = dP_0$ in dimension 2) and the natural generalisation $\mathbb{P}^1 \times \mathbb{P}^1 \times \mathbb{P}^1$ of \mathbb{F}_0 . Indeed, in k complex dimensions, \mathbb{P}^k and $(\mathbb{P}^1)^{\times k}$ are always smooth, toric, and Fano. The toric del Pezzo surfaces $dP_{0,1,2,3}$ also appear in Table 2, either in direct product or as various fibers. The notation $\mathbb{P}()$ means projectivisation so as to manufacture a compact project threefold. Indeed, we are primarily interested in the *affine* Calabi-Yau four-fold cone over these Fano threefolds, so the spaces in which we have interest do not need this projectivisation; we have included them for consistency of notation in that we are discussing the Fano threefolds in this section.

Therefore, the cone in a sense undoes the said projectivisation, and the fourfold is simply the total space of the fibration. For example, \mathcal{B}_1 is $\mathbb{P}(\mathcal{O}_{\mathbb{P}^2} \oplus \mathcal{O}_{\mathbb{P}^2}(2))$; here, $\mathcal{O}_{\mathbb{P}^2}(d)$ is a line bundle of degree d over \mathbb{P}^2 , hence the fiber of $\mathcal{O}_{\mathbb{P}^2} \oplus \mathcal{O}_{\mathbb{P}^2}(2)$ is of dimension $1 + 1 = 2$, which together with the base \mathbb{P}^2 dictates the total space as being of dimension $2 + 2 = 4$. (Of course, in line with standard notation \mathcal{O} is the structure sheaf, or the line bundle of degree 0.) Subsequently, the projectivisation is of dimension $4 - 1 = 3$, as required. The actual affine Calabi-Yau fourfold is simply the total space $\mathcal{O}_{\mathbb{P}^2} \oplus \mathcal{O}_{\mathbb{P}^2}(2)$.

2.1.3. Symmetries

One piece of information, obviously of great importance, is the symmetry of the variety, which is encoded in the world-volume physics, either manifestly or as hidden global symmetries [52–55]. Inspecting the toric diagrams, we readily see that our list of Fano threefolds affords the following symmetries. The most symmetric case is, of course, \mathbb{P}^3 , the cone over it has a full $U(4)$, acting as unitary transformations on the four coordinates. Next, both \mathcal{B}_1 and \mathcal{B}_2 have $SU(3) \times U(1)^2$, with $SU(3)$ acting on the base \mathbb{P}^2 and $U(1)$ for each fiber. Similarly, \mathcal{B}_3 has symmetry $SU(2)^2 \times U(1)^2$, with $SU(2)$ for the base \mathbb{P}^1 , another $U(2)$ for the 2 identical line bundles $\mathcal{O}_{\mathbb{P}^1}$, and one more $U(1)$ for $\mathcal{O}(1)_{\mathbb{P}^1}$. Likewise, \mathcal{B}_4 has $SU(3) \times SU(2) \times U(1)$, with the $SU(3)$ and $SU(2)$ for the \mathbb{P}^2 and \mathbb{P}^1 , respectively, and $U(1)$ for the cone which gives the affine Calabi-Yau 4-fold. Proceeding along the same vein, \mathcal{C}_1 , \mathcal{C}_4 , and \mathcal{C}_5 share the symmetry $SU(2)^2 \times U(1)^2$, \mathcal{C}_2 has $SU(2) \times U(1)^3$, and \mathcal{C}_3 has $SU(2)^3 \times U(1)$. All remaining cases, namely, the \mathcal{D} 's, \mathcal{E} 's, and \mathcal{F} 's, are of symmetry $SU(2) \times U(1)^3$.

Note that the rank of the group of symmetries must total to 4 because we are dealing with a toric (affine) Calabi-Yau 4-fold. Indeed, one $U(1)$ factor of the symmetry is the R-symmetry and the remaining rank 3 symmetry, a global mesonic symmetry (cf. [52, 53]), and there could be possible additional $U(1)$ -baryonic symmetries. We have summarised these mesonic symmetries in the last column of Table 2, under the entry *Sym*. Unless explicitly written, we have used the short-hand notation that

$$\left[3^{k_3}, 2^{k_2}, 1^{k_1}\right] := SU(3)^{k_3} \times SU(2)^{k_2} \times U(1)^{k_1}. \quad (2.1)$$

We note that the three cases of there being only a *single* $U(1)$ symmetry, namely, \mathbb{P}^3 (for which $U(4)$ contains the $U(1)$), \mathcal{B}_4 , and \mathcal{C}_3 , are products of projective spaces corresponding to the three partitions of 3. The corresponding QCS theories for these have been already constructed in the literature. This is perhaps unsurprising given the high degree of symmetry for these spaces.

2.1.4. Some Geometrical Data

We have also listed, to the rightmost of the table, some geometrical data, such as topological invariants. In particular, we tabulate the second Betti number b_2 and the genus g . Indeed, $b_2 = E - 3$, where E is the number of external points in the toric diagram, or since there is always a single internal point as discussed above, E is the number of columns of G_t minus 1. Now, recall that in the D3-brane probes on Calabi-Yau threefold case, the external vertices count the conserved anomaly-free global charges of the $(3 + 1)$ -dimensional gauge theory. Each external vertex in the toric diagram is a divisor, and its corresponding charge gives rise to a basis for the set of mesonic, and baryonic charges: one of which is the R-symmetry, three of which are mesonic and the remaining $E - 4$ charges are baryonic.

However, in our present case of M2-branes probing the Calabi-Yau fourfold, the world-volume Chern-Simons theory in $(2 + 1)$ dimensions has no notion of anomaly, and hence there is no distinction between anomalous and anomaly-free baryonic charges. (An exception to this is the parity anomaly where one starts with a theory that has no CS terms, and one-loop perturbation theory generates a nonzero CS term. Since the CS term is odd under parity, one says that parity is conserved in the classical level but broken by a one-loop effect, hence anomalous. This is the only instance in which one can have anomalies in $(2 + 1)$ dimensions. Nevertheless, all the theories we deal with are protected by supersymmetry and, as long as the ranks are equal, the CS levels do not get quantum corrections (cf. [56]).) Thus, b_2 seems to be counting the number of baryonic charges if we extend the analogy from the $(3 + 1)$ -dimensional situation.

On the other hand, a conserved baryonic charge corresponds to a gauge field in AdS. This is counted by the number of 2-cycles in the Sasaki-Einstein 7-fold (SE7), given by the 3-form on each 2-cycle. The number of 2-cycles in the SE7 is equal to the number of 5-cycles by Poincaré duality, which is in turn equal to the number E of external points in the toric diagram subtracted by 4. That is, the baryonic symmetries also afford a nice geometrical interpretation here: the number of columns of G_t is $E + 1$, then the number of baryonic symmetries is $E - 4$, signifying $U(1)^{E-4}$ (cf. of [25, Section 2] and also [23]). Then, since the second Betti number is $E - 3$, we have the number of baryonic symmetries as the topological quantity $b_2 - 1$.

Next, let us discuss the genus g . Note that a polarisation can be chosen as the ample anticanonical sheaf $A = K_X^{-1}$, which, due to its ampleness, can be used to embed into a projective space. It turns out that this embedding is of degree $d = c_1(X)^3$ into \mathbb{P}^{g+1} such that $d = 2g - 2$. Of physical importance is that the $g + 2$ homogeneous coordinates of the ambient \mathbb{P}^{g+1} constitute $g + 2$ gauge invariant chiral operators which parameterise the supersymmetric vacuum moduli space, with the relations satisfied amongst them providing the explicit equation thereof. In short, the number of generators of the moduli space is $g + 2$.

2.1.5. Hilbert Series

Now, it was first pointed out in [57, 58] that the Hilbert series of an algebraic variety is central toward understanding the gauge invariant operators of the gauge theory living on

the branes probing the variety. For our purposes, this is a rational function which is the generating function for counting the spectrum of operators; it could be multivariate, having a number of “chemical potentials,” which we call the refined Hilbert series, or it could depend on a single grading, which we call the unrefined Hilbert series. In particular, cones over the Fano twofolds, that is, the del Pezzo surfaces, have an elegant expression for their unrefined Hilbert series. We recall, [57, Section 3.3.1], that for the n th del Pezzo, of degree $9 - n$, it is $f(t; dP_n) = 1 + ((7 - n)t + t^2 / (1 - t)^3)(n = 0, \dots, 8)$; Note that \mathbb{F}_0 has the same unrefined Hilbert series as that of dP_1 though the refined, multi-variate Hilbert series does differentiate the two.

The unrefined Hilbert series, computed for the canonical embedding stated above, is also presented in [51], though perhaps not of immediate use since they are given as series expansions. We have recomputed these as rational functions. By inspection, a succinct equation, similar to the del Pezzo case, exists

$$f(t; X) = \frac{1 + (g - 2)t + (g - 2)t^2 + t^3}{(1 - t)^4} = \sum_{n=0}^{\infty} \frac{t^n}{6} (2n + 1) \left((g - 1)n^2 + (g - 1)n + 6 \right), \quad (2.2)$$

where g is the genus of X .

In the special cases where the Fano threefold X is the product of dP_n with \mathbb{P}^1 , the genus turns out to be $28 - 3n$. Whence, the number of generators of the moduli space is $30 - 3n = 3(10 - n)$; the 3 corresponds to the \mathbb{P}^1 factor, and the $10 - n$ refers to the dP_n factor.

3. Reconstructing the Vacuum Moduli Space

With a current want of an inverse algorithm, with or without the aid of dimer technology, it is difficult to systematically find the requisite quiver Chern-Simons theories whose moduli spaces are Calabi-Yau cones over the Fano threefolds listed above, a question certainly of considerable interest. Nevertheless, because the forward algorithm is now well established [20], one could explicitly check whether a certain ansatz theory indeed gives the correct moduli space. Therefore, with a combination of inspired guesses and systematic computer scans, one could hope to find some theories.

Nomenclature

In accordance with the notation of [14, 19], and emphasising the intimate relation between the $(3 + 1)$ -dimensional gauge theory and the $(2 + 1)$ -dimensional QCS, we denote the latter as follows: let the superpotential and matter content be that of the D3-brane world-volume theory for the Calabi-Yau threefold X , then we keep the same superpotential and quiver,

but impose Chern-Simons levels \vec{k} , ordered according to a fixed choice for the nodes, while obeying the constraint [19, 20]

$$\sum_i k_i = 0, \quad \text{GCD}(k_i) = 1. \quad (3.1)$$

We subsequently run the forward algorithm, the resulting vacuum moduli space is now a Calabi-Yau fourfold and the QCS theory we will denote as $\tilde{X}_{\vec{k}}$. Note, of course, that the actual 4-fold may be seemingly quite unrelated to X .

Furthermore, as always, we let X_{ij}^a denote the a th bifundamental field between nodes i and j , and let ϕ_i^a signify the a th adjoint field for the i th node.

3.1. Various Candidates

$\widetilde{dP}_{0(1,-2,1)}$ and \mathcal{B}_4

The quiver and superpotential can be readily recalled from, for example, [27, 28] (cf. also this theory as a QCS from [13]); next, we can assign the Chern-Simons levels as $(1, -2, 1)$, which indeed satisfies the constraint (3.1)

$$W = \epsilon_{\alpha\beta\gamma} X_{12}^{(\alpha)} X_{23}^{(\beta)} X_{31}^{(\gamma)},$$

$$\text{CS-levels} = (1, -2, 1).$$

(3.2)

Running through the forward algorithm gives us the following charge matrix Q_t and toric diagram G_t :

$$Q_t = \begin{pmatrix} -1 & -1 & -1 & 1 & 1 & 1 \\ 0 & 0 & 0 & -2 & 1 & 1 \end{pmatrix}, \quad G_t = \begin{pmatrix} -1 & 1 & 0 & 0 & 0 & 0 \\ 0 & -1 & 1 & 0 & 0 & 0 \\ 0 & 0 & 0 & 0 & -1 & 1 \\ 1 & 1 & 1 & 1 & 1 & 1 \end{pmatrix}. \quad (3.3)$$

Now, take \mathcal{B}_4 , or number 24, of the Fano list from Table 2, and consider the affine CY4 cone thereupon, by adding a row of 1s. One can readily check that upto reordering the columns, the two G_t matrices are explicitly related by a $PSL(4; \mathbb{Z})$ transformation. This means that the moduli spaces, as affine toric varieties, are isomorphic.

Phases of F_0

Next, we recall the well-known two phases of the $(3 + 1)$ -dimensional theories for the CY3 over the zeroth Hirzebruch surface

$$\begin{aligned}
 W_{(F_0)_I} &= \epsilon_{ij} \epsilon_{pq} X_{12}^i X_{23}^p X_{34}^j X_{41}^q, \\
 W_{(F_0)_{II}} &= \epsilon_{ij} \epsilon_{mn} X_{12}^i X_{23}^m X_{31}^{jn} - \epsilon_{ij} \epsilon_{mn} X_{14}^i X_{43}^m X_{31}^{jn}.
 \end{aligned}$$

(3.4)

There are two toric phases, the first having 8 fields, and the second 12.

From these progenitors, we can obtain quite a few Calabi-Yau fourfold cones with judicious choices of CS levels. We list these in Table 3, running, in each case, the forward algorithm to the theory. The input is the superpotential and quiver of the indicated phase of F_0 , together with the chosen Chern-Simons levels, and the output, the charge matrix Q_t and toric diagram G_t .

In this table, we have used the notation $\sim Cone(X)$ to mean that it is isomorphic, by an explicit $SL(4; \mathbb{Z})$ transformation of the toric diagrams (upto repetition and permutation of the vertices) G_t to the Calabi-Yau fourfold cone over the Fano threefold X . Note that the last row of G_t is always 1, this is a consequence of the Calabi-Yau condition. Furthermore, note that the second 2 rows for phase I, corresponding to the F-terms, decouple into diagonal form; this reflects the fact that the master space [52, 53] is the direct product of two conifolds. Moreover, the first row of the table, for the theory corresponding to $(\mathbb{P}^1)^{\times 3}$, has been obtained in [25].

\widetilde{dP}_1 and \mathfrak{D}_1

The theory for the cone over the dP_1 surface is again well known. We present it below (note that only two of the three bifundamental fields X_{34} group into an $SU(2)$ multiplet and the third is a singlet). Now, if we took the Chern-Simons levels as $(-1, -1, 0, 2)$, and combining with the standard theory

$$\begin{aligned}
 W &= \epsilon_{ab} X_{13} X_{34}^a X_{41}^b + \epsilon_{ab} X_{42} X_{23}^a X_{34}^b + \epsilon_{ab} X_{34}^3 X_{41}^a X_{12} X_{23}^b, \\
 \text{CS-levels} &= (-1, -1, 0, 2),
 \end{aligned}$$

(3.5)

Table 3: The two phases of the $(3 + 1)$ -dimensional gauge theory for the cone over the zeroth Hirzebruch surface F_0 beget 4 new QCS theories in $(2 + 1)$ dimensions, the moduli spaces for which are cones over 4 different Fano threefolds.

F_0	CS Levels \vec{k}	Q_t	G_t	$\sim \text{Cone}(X)$
I	$(1, 1, -1, -1)$	$\begin{pmatrix} 1 & 1 & -1 & 1 & -1 & -1 & 0 & 0 \\ 1 & 1 & 1 & -1 & 0 & 0 & -1 & -1 \\ 0 & 0 & 0 & 0 & -1 & -1 & 1 & 1 \\ -1 & -1 & 1 & 1 & 0 & 0 & 0 & 0 \end{pmatrix}$	$\begin{pmatrix} 0 & 0 & 0 & 0 & 0 & 0 & -1 & 1 \\ 0 & 0 & 0 & 0 & -1 & 1 & 0 & 0 \\ -1 & 1 & 0 & 0 & 0 & 0 & 0 & 0 \\ 1 & 1 & 1 & 1 & 1 & 1 & 1 & 1 \end{pmatrix}$	\mathcal{C}_3
I	$(-2, 0, 1, 1)$	$\begin{pmatrix} 0 & 0 & 0 & 2 & -1 & -1 & 0 & 0 \\ 0 & 0 & -1 & 0 & 0 & 0 & 1 & 0 \\ 0 & 0 & 0 & 0 & -1 & -1 & 1 & 1 \\ -1 & -1 & 1 & 1 & 0 & 0 & 0 & 0 \end{pmatrix}$	$\begin{pmatrix} 0 & -1 & -1 & 0 & 0 & 0 & -1 & 1 \\ 0 & 0 & 0 & 0 & -1 & 1 & 0 & 0 \\ -1 & 1 & 0 & 0 & 0 & 0 & 0 & 0 \\ 1 & 1 & 1 & 1 & 1 & 1 & 1 & 1 \end{pmatrix}$	\mathcal{C}_4
I	$(-2, 1, 0, 1)$	$\begin{pmatrix} 0 & 0 & 1 & -1 & 0 & 0 & -1 & 1 \\ 0 & 0 & -1 & 0 & 0 & 0 & 0 & 1 \\ 0 & 0 & 0 & 0 & -1 & -1 & 1 & 1 \\ -1 & -1 & 1 & 1 & 0 & 0 & 0 & 0 \end{pmatrix}$	$\begin{pmatrix} -1 & 0 & 0 & -1 & 1 & 0 & 1 & 0 \\ 0 & 0 & 0 & 0 & -1 & 1 & 0 & 0 \\ -1 & 1 & 0 & 0 & 0 & 0 & 0 & 0 \\ 1 & 1 & 1 & 1 & 1 & 1 & 1 & 1 \end{pmatrix}$	\mathcal{C}_5
II	$(-2, 0, 1, 1)$	$\begin{pmatrix} 0 & -2 & 0 & 0 & 1 & 1 & 2 & -2 & 0 \\ 1 & -1 & 0 & 0 & 0 & 0 & 0 & 1 & -1 \\ 0 & 0 & 0 & 0 & 1 & 1 & -1 & 0 & -1 \\ 0 & 0 & 1 & 1 & 0 & 0 & 0 & -1 & -1 \\ 1 & 1 & 0 & 0 & 0 & 0 & -1 & -1 & 0 \end{pmatrix}$	$\begin{pmatrix} 0 & -1 & 1 & 0 & 0 & 0 & -1 & 0 & 1 \\ 0 & 0 & -1 & 1 & 0 & 0 & 0 & 0 & 0 \\ 0 & 0 & 0 & 0 & -1 & 1 & 0 & 0 & 0 \\ 1 & 1 & 1 & 1 & 1 & 1 & 1 & 1 & 1 \end{pmatrix}$	\mathcal{C}_4
II	$(-2, 1, 0, 1)$	$\begin{pmatrix} 0 & 1 & -1 & 0 & 0 & 0 & 0 & 0 & 0 \\ 0 & 0 & 0 & 1 & 0 & 0 & 0 & 0 & -1 \\ 0 & 1 & 0 & 0 & 0 & -1 & -1 & 0 & 1 \\ 0 & 0 & 0 & 0 & 1 & -1 & -1 & 0 & 0 \\ 1 & -1 & -1 & 1 & 0 & 0 & 0 & 0 & 0 \end{pmatrix}$	$\begin{pmatrix} -1 & 0 & 0 & 1 & 1 & 0 & 1 & 0 & 1 \\ 0 & 0 & 0 & -1 & 0 & 0 & 1 & 0 & 0 \\ 1 & 0 & 0 & -1 & 0 & -1 & 0 & -1 & -1 \\ 1 & 1 & 1 & 1 & 1 & 1 & 1 & 1 & 1 \end{pmatrix}$	\mathcal{C}_1

then we find the charge and toric matrices to be

$$Q_t = \begin{pmatrix} 0 & 0 & 1 & 1 & 0 & 0 & 0 & -2 \\ 0 & 0 & 0 & 1 & 0 & 0 & -1 & 0 \\ -1 & -1 & 1 & 1 & 1 & 0 & 0 & -1 \\ 0 & 0 & 0 & 0 & -1 & -1 & 1 & 1 \end{pmatrix}, \quad G_t = \begin{pmatrix} 0 & 0 & -1 & 1 & 0 & 1 & 1 & 0 \\ -1 & 0 & 0 & 0 & -1 & 1 & 0 & 0 \\ -1 & 1 & 0 & 0 & 0 & 0 & 0 & 0 \\ 1 & 1 & 1 & 1 & 1 & 1 & 1 & 1 \end{pmatrix}, \quad (3.6)$$

and resulting moduli space to be \mathfrak{D}_1 .

4. Outlook

In this short note, a prelude to [38], we have initiated the study of Fano threefolds in the context of M2-branes. In particular, we have presented the classification of all smooth toric Fano threefolds, the cones over which are Calabi-Yau fourfold singularities which the M2-branes could probe. We have computed some preliminary geometrical data, including such quantities as Hilbert series and global symmetries which have recently turned out to be important for the physics of these models.

These 18 spaces are direct analogues of the toric del Pezzo surfaces, which have been the subject of much investigation in the past decade in association with the construction of $(3 + 1)$ -dimensional world-volume quiver gauge theories for D3-branes. It is self-evident that these spaces should be central to the study of $(2 + 1)$ -dimensional quiver Chern-Simons theories.

For some of these we have identified, using the forward algorithm, the quiver theories whose mesonic moduli spaces are precisely as desired. Such a *prima facie* scan has produced 6 as moduli spaces of vacua, and they, as with all theories so far produced in the toric M2-brane scenario, obey the planar brane tiling/dimer model condition. It is our hope that

systematically all gauge theories for the 18 spaces can be soon geometrically engineered and the corresponding tiling descriptions prescribed. These and many further details will appear in the companion work of [38].

Acknowledgments

בהקדשה לואלרי ואֵלֶה שמאירות אתחיי, תמיד.

Scientiae et Technologiae Concilio Anglicae, et Ricardo Fitzjames, Episcopo Londiniensis, ceterisque omnibus benefactoribus Collegii Mertonensis Oxoniensis, sed super omnes, pro amore Catharinae Sanctae Alexandriae, lacrimarum Mariae semper Virginis, et ad Maiorem Dei Gloriam hoc opusculum Y.-H. He dedicat. The authors are indebted to John Davey, Kentaro Hori, Noppadol Mekareeya, Richard Thomas, Giuseppe Torri, and Alberto Zaffaroni for enlightening discussions. A. Hanany would like to thank the kind hospitality, during the initiation of this project, of IPMU in Tokyo and is further grateful to the University of Richmond, the Perimeter Institute as well as the KITP in Santa Barbara, during the completion. This research was supported in part by the National Science Foundation under Grant no. PHY05-51164.

References

- [1] J. Bagger and N. Lambert, "Modeling multiple M2-branes," *Physical Review D*, vol. 75, no. 4, Article ID 045020, 2007.
- [2] J. Bagger and N. Lambert, "Gauge symmetry and supersymmetry of multiple M2-branes," *Physical Review D*, vol. 77, no. 6, Article ID 065008, 2008.
- [3] J. Bagger and N. Lambert, "Comments on multiple M2-branes," *Journal of High Energy Physics*, vol. 2008, no. 2, article 105, 2008.
- [4] A. Gustavsson, "Algebraic structures on parallel M2 branes," *Nuclear Physics B*, vol. 811, no. 1-2, pp. 66–76, 2009.
- [5] M. Van Raamsdonk, "Comments on the Bagger-Lambert theory and multiple M2-branes," *Journal of High Energy Physics*, vol. 2008, no. 5, article 105, 2008.
- [6] S. Mukhi and C. Papageorgakis, "M2 to D2," *Journal of High Energy Physics*, vol. 2008, no. 5, article 085, 2008.
- [7] O. Aharony, O. Bergman, D. L. Jafferis, and J. Maldacena, "N = 6 superconformal Chern-Simons-matter theories, M2-branes and their gravity duals," *Journal of High Energy Physics*, vol. 2008, no. 10, article 091, 2008.
- [8] M. Benna, I. Klebanov, T. Klose, and M. Smedbäck, "Superconformal Chern-Simons theories and AdS/CFT correspondence," *Journal of High Energy Physics*, vol. 2008, no. 9, article 072, 2008.
- [9] S. Kim, S. Lee, S. Lee, and J. Park, "M2-brane probe dynamics and toric duality," *Nuclear Physics B*, vol. 797, no. 1-2, pp. 340–370, 2008.
- [10] K. Hosomichi, K.-M. Lee, S. Lee, S. Lee, and J. Park, "N = 5, 6 superconformal Chern-Simons theories and M2-branes on orbifolds," *Journal of High Energy Physics*, vol. 2008, no. 9, article 002, 2008.
- [11] M. Schnabl and Y. Tachikawa, "Classification of N = 6 superconformal theories of ABJM type," *Journal of High Energy Physics*, vol. 2010, no. 9, article 103, 2010.
- [12] D. Martelli and J. Sparks, "Moduli spaces of Chern-Simons quiver gauge theories and AdS₄/CFT₃," *Physical Review D*, vol. 78, no. 12, Article ID 126005, 2008.
- [13] A. Hanany and A. Zaffaroni, "Tilings, Chern-Simons theories and M2 branes," *Journal of High Energy Physics*, vol. 2008, no. 10, article 111, 2008.
- [14] A. Hanany, D. Vegh, and A. Zaffaroni, "Brane tilings and M2 branes," *Journal of High Energy Physics*, vol. 2009, no. 3, article 012, 2009.
- [15] Y. Imamura and K. Kimura, "On the moduli space of elliptic Maxwell-Chern-Simons theories," *Progress of Theoretical Physics*, vol. 120, no. 3, pp. 509–523, 2008.

- [16] Y. Imamura and K. Kimura, "N = 4 Chern-Simons theories with auxiliary vector multiplets," *Journal of High Energy Physics*, vol. 2008, no. 10, article 040, 2008.
- [17] Y. Imamura and K. Kimura, "Quiver Chern-Simons theories and crystals," *Journal of High Energy Physics*, vol. 2008, no. 10, article 114, 2008.
- [18] K. Ueda and M. Yamazaki, "Toric Calabi-Yau four-folds dual to Chern-Simons-matter theories," *Journal of High Energy Physics*, vol. 2008, no. 12, article 045, 2008.
- [19] S. Franco, A. Hanany, J. Park, and D. Rodriguez-Gomez, "Towards M2-brane theories for generic toric singularities," *Journal of High Energy Physics*, vol. 2008, no. 12, article 110, 2008.
- [20] A. Hanany and Y. H. He, "M2-branes and quiver Chern-Simons: a taxonomic study," <http://arxiv.org/abs/0811.4044>.
- [21] O. Aharony, O. Bergman, and D. L. Jafferis, "Fractional M2-branes," *Journal of High Energy Physics*, vol. 2008, no. 11, article 043, 2008.
- [22] C. Krishnan, C. MacCafferri, and H. Singh, "M2-brane flows and the Chern-Simons level," *Journal of High Energy Physics*, vol. 2009, no. 5, article 114, 2009.
- [23] Y. Imamura, "Charges and homologies in AdS₄/CFT₃," <http://arxiv.org/abs/0903.3095>.
- [24] S. Franco, I. R. Klebanov, and D. Rodríguez-Gómez, "M2-branes on orbifolds of the cone over Q^{1,1,1}," *Journal of High Energy Physics*, vol. 2009, no. 8, article 033, 2009.
- [25] J. Davey, A. Hanany, N. Mekareeya, and G. Torri, "Phases of M2-brane theories," *Journal of High Energy Physics*, vol. 2009, no. 6, article 025, 2009.
- [26] A. Amariti, D. Forcella, L. Girardello, and A. Mariotti, "3D Seiberg-like dualities and M2 branes," *Journal of High Energy Physics*, vol. 2010, no. 5, article 025, 2010.
- [27] B.O. Feng, A. Hanany, and Y. H. He, "D-brane gauge theories from toric singularities and toric duality," *Nuclear Physics B*, vol. 595, no. 1-2, pp. 165–200, 2001.
- [28] B. Feng, A. Hanany, and Y. H. He, "Phase structure of D-brane gauge theories and toric duality," *Journal of High Energy Physics*, vol. 5, no. 8, article 040, 2001.
- [29] A. Hanany and E. Witten, "Type IIB superstrings, BPS monopoles, and three-dimensional gauge dynamics," *Nuclear Physics B*, vol. 492, no. 1-2, pp. 152–190, 1997.
- [30] A. Hanany and K. D. Kennaway, "Dimer models and toric diagrams," <http://arxiv.org/abs/hep-th/0503149>.
- [31] S. Franco, A. Hanany, D. Vegh, B. Wecht, and K. D. Kennaway, "Brane dimers and quiver gauge theories," *Journal of High Energy Physics*, no. 1, pp. 2401–2448, 2006.
- [32] K. D. Kennaway, "Brane tilings," *International Journal of Modern Physics A*, vol. 22, no. 18, pp. 2977–3038, 2007.
- [33] S. Lee, "Superconformal field theories from M-theory crystal lattices," *Physical Review D*, vol. 75, no. 10, Article ID 101901, 2007.
- [34] S. Lee, S. Lee, and J. Park, "Toric AdS₄/CFT₃ duals and M-theory crystals," *Journal of High Energy Physics*, vol. 2007, no. 5, 2007.
- [35] B. Feng, A. Hanany, Y. H. He, and A. Iqbal, "Quiver theories, soliton spectra and Picard-Lefschetz transformations," *Journal of High Energy Physics*, vol. 7, no. 2, pp. 1265–1297, 2003.
- [36] B. Feng, S. Franco, A. Hanany, and Y. H. He, "Unhiggsing the del Pezzo," *Journal of High Energy Physics*, vol. 7, no. 8, pp. 1385–1420, 2003.
- [37] M. Wijnholt, "Large volume perspective on branes at singularities," *Advances in Theoretical and Mathematical Physics*, vol. 7, no. 6, pp. 1117–1153, 2003.
- [38] J. Davey et al., "M2 theories from Fano threefolds," to appear.
- [39] G. Székelyhidi, "Greatest lower bounds on the Ricci curvature of Fano manifolds," *Compositio Mathematica*, vol. 147, pp. 319–331, 2011.
- [40] B. Feng, A. Hanany, Y. H. He, and A. M. Uranga, "Toric duality as Seiberg duality and brane diamonds," *Journal of High Energy Physics*, vol. 5, no. 12, article 28, 2001.
- [41] S. Mori and S. Mukai, "Classification of Fano 3-folds with $B_2 \geq 2$, I," in *Algebraic and Topological Theories*, M. Nagata et al., Ed., pp. 496–545, Kinokuniya Company, Tokyo, Japan, 1986.
- [42] J.-P. Murre, "Classification of Fano threefolds according to Fano and Iskovskih," in *Proceedings of the 2nd Session of the Centro Internazionale Matematico Estivo (C.I.M.E.)*, vol. 947 of *Lecture Notes in Mathematics*, pp. 35–92, Varenna, Italy, June 1981.
- [43] S. D. Cutkosky, "On Fano 3-folds," *Manuscripta Mathematica*, vol. 64, no. 2, pp. 189–204, 1989.
- [44] V. V. Batyrev, "Toroidal Fano 3-folds," *Mathematics of the USSR-Izvestiya*, vol. 19, pp. 13–25, 1982.
- [45] V. V. Batyrev, "On the classification of toric Fano 4-folds," *Journal of Mathematical Sciences*, vol. 94, no. 1, pp. 1021–1050, 1999.

- [46] L. B. Anderson, Y.-H. He, and A. Lukas, "Heterotic compactification, an algorithmic approach," *Journal of High Energy Physics*, vol. 2007, no. 7, article 049, 2007.
- [47] J. Gray, Y. H. He, A. Ilderton, and A. Lukas, "STRINGVACUA. A Mathematica package for studying vacuum configurations in string phenomenology," *Computer Physics Communications*, vol. 180, no. 1, pp. 107–119, 2009.
- [48] J. Gray, "A simple introduction to Grobner basis methods in string phenomenology," <http://arxiv.org/abs/0901.1662>.
- [49] J. Kollar, Y. Miyaoka, and S. Mori, "Rational connectedness and boundedness of Fano manifolds," *Journal of Differential Geometry*, vol. 36, no. 3, pp. 765–779, 1992.
- [50] A. M. Kasprzyk, M. Kreuzer, and B. Nill, "On the combinatorial classification of toriclog del Pezzo surfaces," *LMS Journal of Computation and Mathematics*, vol. 13, pp. 33–46, 2010.
- [51] <http://grdb.lboro.ac.uk/>.
- [52] D. Forcella, A. Hanany, Y.-H. He, and A. Zaffaroni, "The master space of $N = 1$ gauge theories," *Journal of High Energy Physics*, vol. 2008, no. 8, article 012, 2008.
- [53] D. Forcella, A. Hanany, Y. H. he, and A. Zaffaroni, "Mastering the master space," *Letters in Mathematical Physics*, vol. 85, no. 2-3, pp. 163–171, 2008.
- [54] B. Feng, S. Franco, A. Hanany, and Y. H. He, "Symmetries of toric duality," *Journal of High Energy Physics*, vol. 6, no. 12, pp. 1769–1798, 2002.
- [55] S. Franco, A. Hanany, and P. Kazakopoulos, "Hidden exceptional global symmetries in 4d CFTs," *Journal of High Energy Physics*, vol. 8, no. 7, pp. 1475–1530, 2004.
- [56] O. Aharony, A. Hanany, K. Intriligator, N. Seiberg, and M. J. Strassler, "Aspects of $N = 2$ supersymmetric gauge theories in three dimensions," *Nuclear Physics B*, vol. 499, no. 1-2, pp. 67–99, 1997.
- [57] S. Benvenuti, B. Feng, A. Hanany, and Y.-H. He, "Counting BPS operators in gauge theories: quivers, syzygies and plethystics," *Journal of High Energy Physics*, vol. 2007, no. 11, article 050, 2007.
- [58] B. Feng, A. Hanany, and Y.-H. He, "Counting gauge invariants: the plethystic program," *Journal of High Energy Physics*, vol. 2007, no. 3, article 090, 2007.

Research Article

Polynomial Roots and Calabi-Yau Geometries

Yang-Hui He^{1, 2, 3}

¹ School of Physics, Nankai University, Tianjin 300071, China

² Department of Mathematics, City University London, Northampton Square, London EC1V 0HB, UK

³ Merton College, University of Oxford, Oxford OX1 4JD, UK

Correspondence should be addressed to Yang-Hui He, hey@maths.ox.ac.uk

Received 13 October 2010; Accepted 27 April 2011

Academic Editor: André Lukas

Copyright © 2011 Yang-Hui He. This is an open access article distributed under the Creative Commons Attribution License, which permits unrestricted use, distribution, and reproduction in any medium, provided the original work is properly cited.

The examination of roots of constrained polynomials dates back at least to Waring and to Littlewood. However, such delicate structures as fractals and holes have only recently been found. We study the space of roots to certain integer polynomials arising naturally in the context of Calabi-Yau spaces, notably Poincaré and Newton polynomials, and observe various salient features and geometrical patterns.

1. Introduction and Summary

The subject of roots of monovariate polynomials is, without doubt, an antique one and has germinated an abundance of fruitful research over the ages. It is, therefore, perhaps surprising that any new statements could at all be made regarding such roots. The advent of computer algebra, chaotic phenomena, and random ensembles has, however, indeed shed new light upon so ancient a metier.

Polynomials with constrained coefficients and form, though permitted to vary randomly, have constituted a vast field itself. As far back as 1782, Edward Waring, in relation to his famous problem on power summands, had shown that for cubic polynomials with random real coefficients, the ratio of the probability of finding nonreal zeros versus that of not finding non-real zeros is less than or equal to 2. Constraining the coefficients to be integers within a fixed range has, too, its own history. It was realised in [1] that a degree n random polynomial $P(z) = 1 + \sum_{k=1}^n a_k z^k$ with $a_k = -1, 0, 1$ distributed evenly, the expected number ν_n of real roots is of order $\mathcal{O}(n^{1/2})$ asymptotically in n . This was furthered by [2] to be essentially independent of the statistics, in that ν_n has the same asymptotics (cf. also [3, 4]), as much for a_k being evenly distributed real numbers, in $[-1, 1]$, or as Gaussian distributed in $(-\infty, \infty)$.

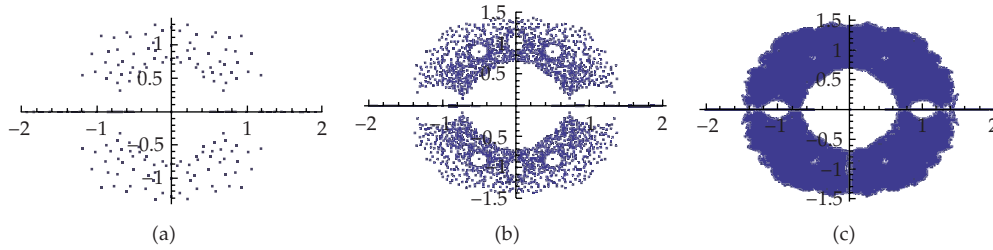


Figure 1: The position, on the complex plane, of the zeros of 50000 random integer polynomials with coefficients $-1, 0, \text{ or } 1$, for degrees up to 4 in part (a), 6 in part (b), and 10 in part (c).

Continual development ensued (q.v. also [5]), notably by Littlewood [6], Erdős and Turán [7], Hammersley [8], and Kac [9]. Indeed, a polynomial with coefficients only taking values as ± 1 has come to be known as a *Littlewood polynomial*, and the *Littlewood Problem* asks for the precise asymptotics, in the degree, of such polynomials taking values, with complex arguments, on the unit circle. The classic work of Montgomery [10] and Odlyzko [11], constituting one of the most famous computer experiments in mathematics (q. v. Section 3.1 of [12] for some recent remarks on the distributions), empirically showed that the distribution of the (normalized) spacings between successive critical zeros of the Riemann zeta function is the same as that of a Gaussian unitary ensemble of random matrices, whereby infusing our subject with issues of uttermost importance.

Subsequently, combining the investigation of zeros and of random polynomials, Odlyzko and Poonen [13] studied the zeros of Littlewood-type polynomials by setting the coefficients to 0 and 1; they provided certain bounds as well as found interesting fractal structures. Thus, inspired and with the rapid advance of computational power, Borwein et al. constructed various plots of zeros of constrained random polynomials and many remarkable features were instantly visible [14, 15]. We can readily demonstrate this with Mathematica [16], as is shown in Figure 1. In the figure, we take a sample of 50000 random polynomials with coefficients $-1, 0, \text{ or } 1$ up to various degrees, and plot, on the complex plane, their zeros. Not only do we see fractal behaviour (cf. discussions in [3, 17] on chaotic dualities in field theories) near the boundaries, the nature of the holes are intimately related [18] to the Lehmer-Mahler Conjecture: that the Mahler measure $M(P) := \exp((1/2\pi) \int_0^{2\pi} \log |P(e^{i\theta})| d\theta)$ of any integral polynomial $P(z)$ (which is not a multiple of cyclotomic polynomials) should be bounded below by that of $z^{10} - z^9 + z^7 - z^6 + z^5 - z^4 + z^3 - z + 1$, which is approximately 1.17.

High resolution variants of Figure 1 have been considered recently by Christensen [19], Jörgenson [20] and Derbyshire and Matson [21], inter alia, and many beautiful pictures can be found (cf. also a nice account in [22]). Particular striking are the coloured density plots in [21].

An interesting query, in somewhat reverse direction to the above line of thought, was posed in [23]: recalling that the Lee-Yang Circle Theorem placed severe constraints on the generating function of the partition function of the Ising Model, the author asked if one could statistically test whether a given Laurent polynomial could, in fact, be the Jones polynomial of a knot. Using a landscape of knots generated by the programme “knotscape” [24], the said work investigated many distribution properties of the zeros of known Jones polynomials.

Enchanted by this motif which has threaded varying developments over the decades while persistently generating new perspectives, a question immediately springs to mind. One of the central topics of both modern mathematics and theoretical physics is undoubtedly that of Calabi-Yau geometries. A key feature is the superabundance thereof. In complex dimension one, there is only the torus; in dimension two, there are the 4-torus and the K3-surface; however, for dimension three and above, no classification is known, and already a plethora has been constructed. The first database was that of the so-called CICYs, or, complete intersection Calabi-Yau threefolds in products of projective spaces [25] as well as hypersurfaces in weighted $\mathbb{C}P^4$ [26], by Candelas et al. Then, over more than a decade, Kreuzer and Skarke formulated and compiled an impressive list of on the order of 10^{10} threefolds as hypersurfaces in toric varieties [27]. Finding new patterns in this vast distribution of manifolds has seen some recent activity [28–30]. Indeed, the multitude of these geometries is at the core of the so-called vacuum degeneracy problem of superstring theory and constitutes a part of the landscape issue [31].

Along a parallel vein, the space of noncompact (singular) Calabi-Yau spaces (as affine varieties) has also been extensively explored, notably by Hanany et al. over the past decade [32–39], especially those which admit a toric description [33]; the discovery of their intimate relation to dimer models and brane tilings [34, 35, 38] has also generated some excitement. These supplant yet another corner in the landscape of geometries and associated supersymmetric vacua.

Thus motivated, many tasks lend themselves to automatic investigation; we here give a precis of some key points. In Section 2, we begin with the compact, smooth Calabi-Yau manifolds. As mentioned above, there had been much effort in classifying and constructing these, especially in complex dimensions three and four. An immediate polynomial, of constrained form and integer coefficients, and yet succinctly encoding some topological information, is the Poincaré polynomial, which can be readily written in terms of the Hodge numbers. We take the “experimental data” of all the known Hodge numbers of the threefolds and fourfolds spanning two decades of work and plot the complex roots of the associated Poincaré polynomials in Figures 4 and 8, respectively.

Much intricate structures are clearly visible. These are then contrasted with a “standard background sample”, namely, the roots of random integer sextic and octic polynomials, with unit leading coefficient and vanishing linear term, drawn in Figures 2 and 7. From such collections are extracted the subclass of those which admit -1 as roots, which, by a theorem from differential geometry, correspond to spaces which have more than one isometry. Interestingly, they correspond to self-mirror threefolds and “quasi-”self-mirror fourfolds. We plot the roots for these in Figures 5 and 10, and see that they furnish certain substrata of the conglomerate plots mentioned above.

Thenceforth, we move on to noncompact Calabi-Yau geometries in Section 3. There, too, is a plenitude of examples, most notably those which are toric. We focus on toric threefolds because these have planar toric diagrams as lattice points in \mathbb{Z}^2 due to the Calabi-Yau condition. Once more, a natural polynomial invites itself: the Newton polynomial. The Riemann surface corresponding to this bivariate polynomial has been a central subject to the gauge and brane theories in the context of string theory. Moreover, the two important projections thereof, namely, the amoeba and alga projections, have provided many beautiful Monte Carlo plots, illustrating deep algebraic geometry as well as gauge theory. Because we are confronted with two complex variables, we need to slightly deviate from our theme of complex roots; instead, we find it expedient to regard the variables as real and consider

the real projection of the Riemann surface. Subsequently, we can study the ensemble of real turning (critical) points of these planar curves.

Again, we resort to “actual data” and focus on the most well-known affine toric threefold geometries—as shown in Figure 11—corresponding to local Calabi-Yau singularities, including, of course, the famous conifold. To each space, we find the collective of critical points in \mathbb{R}^2 as we vary the integer coefficients—commonly known as multiplicities in the dimer model interpretation—of the Newton polynomial, and plot them in Figure 13. We see a sensitive dependence of the emergent subtle structures upon the choice of toric data.

In many respects, we have taken a very pragmatic and empirical approach toward the data accumulated over many years of theoretical research, of quantity large enough to justify experimentation. To this philosophy of “experimental mathematics” we adhere throughout, observe wherever we should, and infer wherever we may. Without much to do, therefore, let us delve into the details of the issues summarized above.

2. Compact Calabi-Yau Manifolds, Poincaré Polynomials, and Complex Roots

An important quantifying polynomial for a smooth compact manifold X is the Poincaré polynomial, which is a generating function for topological invariants of X (say of dimension n):

$$P(t; X) = \sum_{i=0}^n b_i t^i, \quad (2.1)$$

with the b_i being the i th Betti number. Indeed, this seems a more natural candidate for our present studies than some because other famous polynomials such as the Hilbert polynomial or the numerator of the Hilbert series (which of late have been instrumental in counting BPS operators [40–42]) are not topological invariants and depend on the specific projective embedding. Furthermore, by definition, at $t = -1$, the polynomial evaluates to the Euler characteristic; this will be of significance shortly.

The zeros of the Poincaré polynomial have rather remarkable properties. It was conjectured that [43] that if the rank of the manifold X is greater than 1, where rank is defined to be the maximal number of everywhere independent, mutually commuting, vector fields on X , that is, the number of isometries, then -1 is a multiple root of the Poincaré polynomial of X . Unfortunately, this conjecture was shown to be false [44]. Nevertheless, it still holds that the rank of X exceeds unity if and only if -1 is a multiple root of $P(t; X)$.

Moreover, of number theoretic and arithmo-geometric significance is the fact that certain Poincaré polynomials exhibit Riemann Hypothesis behaviour [45, 46], in analogy to the Hasse-Weil zeta local zeta functions. Recently, alignment of zeros of Hilbert polynomials have been studied by [47], in relation to zeta functions.

2.1. Calabi-Yau Threefolds

Our focus will be on (2.1). First, let us study the case of Calabi-Yau threefolds, which have been of the greatest interest, at least historically. Because we are dealing with complex (Kähler) manifolds, Hodge decomposition implies that $b_i(X) = \sum_{p,q} h^{p,q}(X)$, with $h^{p,q}(X) = \dim H_{\bar{0}}^{p,q}(X)$ the dimensions of the Dolbeault cohomology groups. Indeed, for

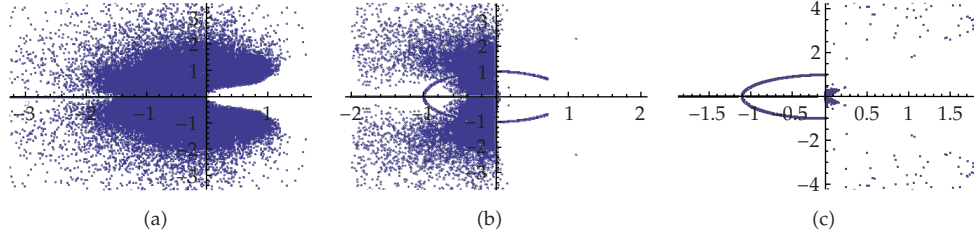


Figure 2: (a) The position, on the complex plane, of the zeros of 50000 random integer degree six polynomials with coefficients between 0 and 1000. (b) The same, but with monic palindromic sextics. (c) Monic palindromic sextics, and with linear term vanishing.

(compact, smooth, connected) Calabi-Yau threefolds, the Hodge diamond, and subsequently the Betti numbers and the Poincaré polynomial, can be written as

$$\begin{array}{cccccc}
 & & & & & 1 \\
 & & & & 0 & \\
 & & 0 & & 0 & \\
 & 0 & h^{1,1} & & 0 & \\
 1 & h^{2,1} & & h^{2,1} & & 1 \\
 & 0 & h^{1,1} & & 0 & \\
 & & 0 & & 0 & \\
 & & & & & 1
 \end{array}
 \quad (b_0 = b_6, b_1 = b_5, b_2 = b_4, b_3) = (1, 0, h^{1,1}, 2 + 2h^{2,1}), \tag{2.2}$$

$$P(t; X) = 1 + h^{1,1}t^2 + (2 + 2h^{2,1})t^3 + h^{1,1}t^4 + t^6.$$

That the Poincaré polynomial is palindromic is obvious and follows from Poincaré duality. Therefore, our first constraint is palindromicity to which we will presently restrict. We recall the roots of a completely random sample of integer polynomials with coefficients in $[-1, 1]$ up to the sextic in part (b) of Figure 1. In Figure 2, we plot, in part (a), a sample of 50000 random integer sextic polynomials with coefficients in $[0, 1000]$ (making sure that the highest coefficient at degree 6 is not 0) as a comparative norm. Next, in part (b), we plot the same, but for monic palindromic sextics, that is, $P(t) = 1 + b_1t + b_2t^2 + b_3t^3 + b_2t^4 + b_1t^5 + t^6$. Then, in (c), we restrict once more, with some foresight, so that the linear term vanishes, that is, $P(t) = 1 + b_2t^2 + b_3t^3 + b_2t^4 + t^6$. We see that upon the condition of palindromicity, there is a marked emergence of roots on the unit circle; this of course arises from the symmetric terms of the form e^{it} combining to give (co)sines whose reality then facilitates the addition to zero. The symmetry about the x -axis is simply that all roots appear in conjugate pairs because our polynomials have real coefficients.

For our amusement, seeing the form of the semiunit-circular shape being prominent, we are reminded of the conformal map $z \rightarrow (z/(z - 1))$ which takes the unit circle to the critical strip of the Riemann Hypothesis, as shown in detail by part (a) of Figure 3. We take the space of roots of monic palindromic sextics with vanishing linear/quintic terms from part (c) of Figure 2, apply the inverse map $z \rightarrow (z/(z+1))$ to map to the critical strip, and redo the plot in part (b) of Figure 3. We see that the plot resembles the zero-free region of the Riemann zeta function inside the critical strip.

Founded upon these above discussions, we are ready to approach “actual data.” We now collect all known Calabi-Yau threefolds, which come from three major databases,

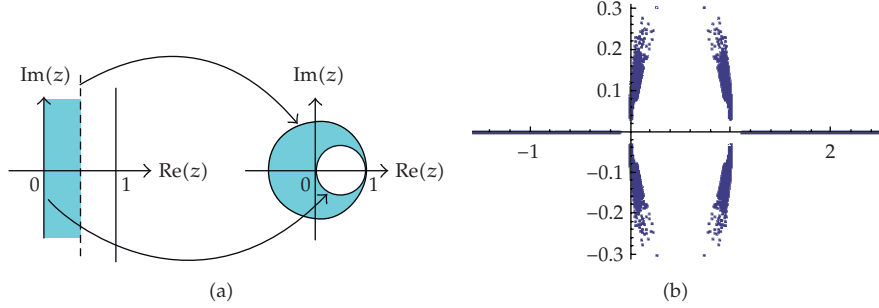


Figure 3: (a) The conformal map $z \rightarrow (z/(z-1))$ takes the left half of the critical strip to the inside of the unit disk, with the boundaries mapped as shown by the arrows. It takes the mirror image, in the right half of the critical strip, to the complement of the unit disk. The inverse map is given by $z \rightarrow (z/(z+1))$. (b) The position of 50000 randomly integer monic palindromic sextic polynomials with vanishing linear/quintic terms and with coefficients ranging in $[0, 1000]$, applying the map $z \rightarrow (z/(z+1))$.

namely, the aforementioned CICYs, the hypersurfaces in toric varieties, as well as the collection of individually tailored ones of small Hodge numbers (cf. [28, 29]). These total, respectively, 30108, 266 and 54 distinct pairs of Hodge numbers $(h^{1,1}(X), h^{2,1}(X))$. In all, there are 30237 distinct pairs (of course, each with much degeneracy) of Hodge numbers; to our present knowledge, these are all the ones circulated in the literature.

We plot (Traditionally, the now-famous plot, first appearing in [26], is done with $\chi = 2(h^{1,1} - h^{2,1})$ as abscissa and $h^{1,1} + h^{2,1}$ as ordinate.) these, with $h^{1,1}$ as the abscissa and $h^{2,1}$, ordinate, in part (a) of Figure 4, the largest amongst these is (491, 11). Note that because of mirror symmetry, there is a symmetry interchanging the two coordinates. It is still an open question whether there exists any Calabi-Yau threefold whose either Hodge number exceeds 491, a bound which has defied constructions so far. This is why in our random standard background sample in Figure 2, we have conveniently selected the largest integer coefficient to be $1000 \sim 2 \cdot (491 + 1)$. In part (b) of the said Figure, we plot, on the complex plane, the roots of the Poincaré polynomials of all these known threefolds. Because we are dealing with polynomials of nonnegative coefficients, there should be many generic roots with negative real parts. Comparing with the random sample in part (c) of Figure 2, we see a beautiful clustering of points in the first quadrant (and, by complex conjugation, the fourth).

Next, let us test for how many Poincaré polynomials -1 is a root; these, as mentioned above, would correspond to manifolds which have more than one isometries. Interestingly, of the some 30000, only 148 pass the test. These turn out to be only the 148 known self-mirror manifolds; we plot their Hodge numbers in Part (a) of Figure 5 (the values of Hodge numbers range from (1, 1) to (251, 251), skipping many high values, as well as the number 13). Indeed, this is a simple consequence of palindromicity as one sees that, upon substituting $t = -1$ into $P(t; X)$ in (2.2), we obtain $P(-1; X) = 2(h^{1,1} - h^{2,1}) = \chi(X)$, the Euler characteristic. In Part (b), we plot all the other roots as well, and see that these constitute a portion of the small crescent around the origin.

2.2. Calabi-Yau Fourfolds

Having explored the space of Calabi-Yau threefolds, it is automatic to proceed onto the space of fourfolds, a relative *terra incognita*. We again resort to the wonderful database compiled by

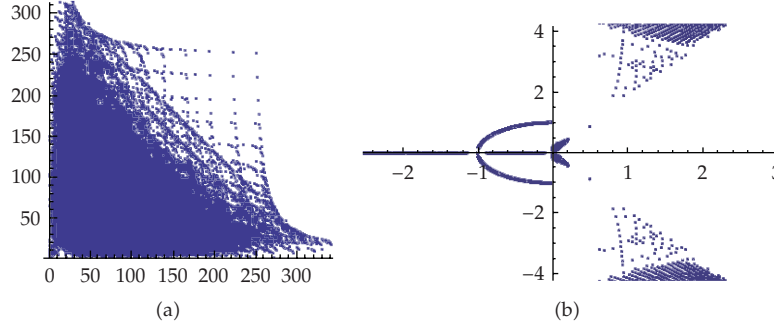


Figure 4: (a) The Hodge numbers, with $h^{1,1}$ as the abscissa and $h^{2,1}$, the ordinate, of all the known Calabi-Yau threefolds. (b) The position, on the complex plane, of the zeros of their Poincaré polynomials.

Kreuzer-Skarke [27, 48]. Now, there are, totaling the hypersurfaces in toric fivefolds, 14598161 manifolds, with 3015056 distinct triplet of Hodge numbers. To explain this triplet notation, we remind the reader of the Hodge diamond of compact, connected, smooth Calabi-Yau fourfolds, adhering to the nomenclature and explanation of [49]

$$\begin{array}{cccccc}
 & & & & & 1 \\
 & & & & & 0 & 0 \\
 & & & & & 0 & h^{1,1} & 0 \\
 & & & & & 0 & h^{2,1} & h^{2,1} & 0 \\
 1 & & h^{3,1} & & h^{2,2} & & h^{3,1} & & 1 \\
 & & 0 & & h^{2,1} & & h^{2,1} & & 0 \\
 & & 0 & & h^{1,1} & & 0 & & \\
 & & 0 & & 0 & & & & \\
 & & & & & & & & 1
 \end{array}
 \quad
 \begin{aligned}
 h^{2,2} &= 44 + 4h^{1,1} - 2h^{2,1} + 4h^{3,1}, \\
 (b_0 = b_8, b_1 = b_7, b_2 = b_6, b_3 = b_5, b_4) \\
 &= (1, 0, ; h^{1,1}, 2h^{2,1}, 2 + 2h^{3,1} + h^{2,2}) \\
 &= (1, 0, h^{1,1}, 2h^{2,1}, 46 + 4h^{1,1} - 2h^{2,1} + 6h^{3,1}).
 \end{aligned}
 \tag{2.3}$$

We note that though seemingly there are four degrees of freedom, owing to topological constraints in complex dimension four or higher, as exhibited by the above relation of $h^{2,2}$ with the others, there are really only three independent Hodge numbers, which we choose as $(h^{1,1}, h^{2,1}, h^{3,1})$; in terms of this triplet, we express the Betti numbers, as shown above. Consequently, we can write the Poincaré polynomial of the fourfold, from the Betti numbers in (2.3), as

$$P(t; X) = 1 + h^{1,1}t^2 + 2h^{2,1}t^3 + (46 + 4h^{1,1} - 2h^{2,1} + 6h^{3,1})t^4 + 2h^{2,1}t^5 + h^{1,1}t^6 + t^8. \tag{2.4}$$

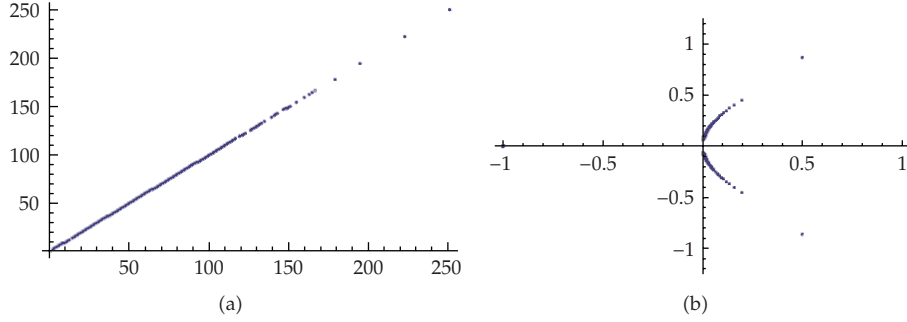


Figure 5: (a) The Hodge number of self-mirror Calabi-Yau threefolds; these have -1 as a root of the Poincaré polynomial. (b) All of the roots of the Poincaré polynomial of these self-mirrors.

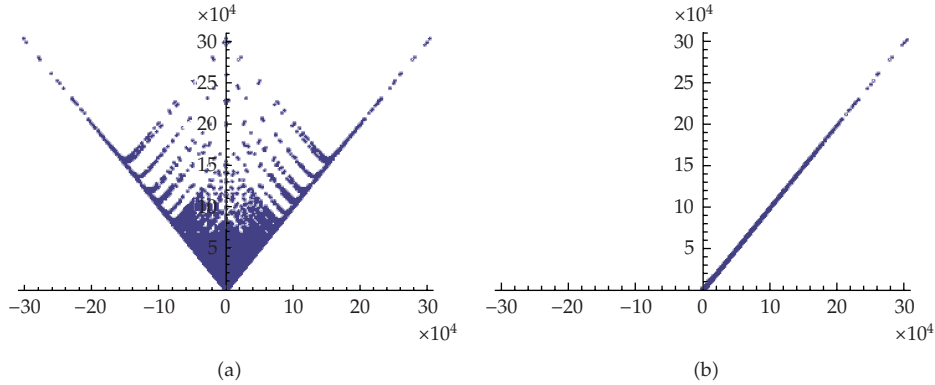


Figure 6: (a) The Hodge numbers, with $h^{1,1} - h^{3,1}$ as the abscissa and $h^{1,1} + h^{3,1}$, the ordinate, of the fourfolds from Kreuzer-Skarke's database. (b) The same, but with $h^{1,1} - h^{2,1}$, as the abscissa and $h^{1,1} + h^{2,1}$ as the ordinate.

Following [49], we plot $h^{1,1} + h^{3,1}$ as ordinate versus $h^{1,1} - h^{3,1}$ as abscissa, which demonstrates mirror-like behaviour. (Though in *cit. ibid.*, only the hypersurfaces in weighted $\mathbb{C}P^5$ were considered, whereas here we plot the entirety of the known fourfolds.) We also plot $h^{1,1} + h^{2,1}$ versus $h^{1,1} - h^{2,1}$, showing that the behaviour in the application direction is rather trivial. These are shown in Figure 6.

We now repeat the experiment undertaken for threefolds. First, we plot the space of generic roots, and present them in Figure 7. In part (a), a sample of 50000 random integer octic polynomials with coefficients in $[0, 2500000]$ (making sure that the highest coefficient at degree 8 is not 0) as a comparative basis: octic, since we will be contrasting with degree 8 Poincaré polynomials, upper bound of 2500000, since we can see from Figure 6 and (2.3), that the Min and Max of the Hodge numbers are, respectively, $(h^{1,1}, h^{2,1}, h^{3,1}) \in ([1, 303148], [0, 2010], [1, 3030148])$, so that the upper bound to the b_4 term is 2425228. Next, in part (b), we plot the same, but for monic palindromic octics, that is, $P(t) = 1 + b_1 t + b_2 t^2 + b_3 t^3 + b_4 t^4 + b_3 t^5 + b_2 t^6 + b_1 t^7 + t^8$. Finally, in (c), we restrict once more, so that the linear term vanishes, that is, $P(t) = 1 + b_2 t^2 + b_3 t^3 + b_4 t^4 + b_3 t^5 + b_2 t^6 + t^8$.

In contradistinction to these generic results, we can now find all the complex roots of the Poincaré polynomials of all known Calabi-Yau fourfolds. The three million or so distinct Hodge data now presents a heavy computational challenge, on which a Quadra-core MacPro

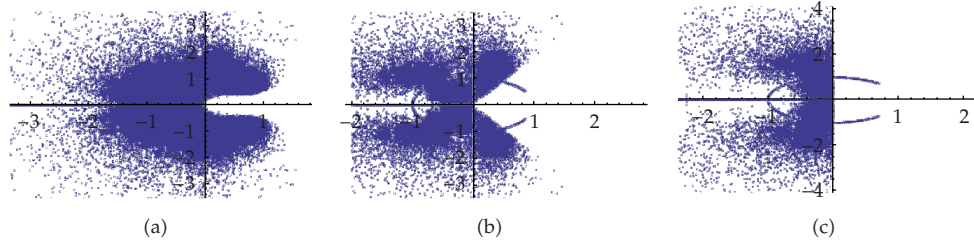


Figure 7: (a) The position, on the complex plane, of the zeros of 50000 random integer polynomials with coefficients between 0 and 2500000. (b) The same, but with monic palindromic octics. (c) Monic palindromic octics, and with linear term vanishing.

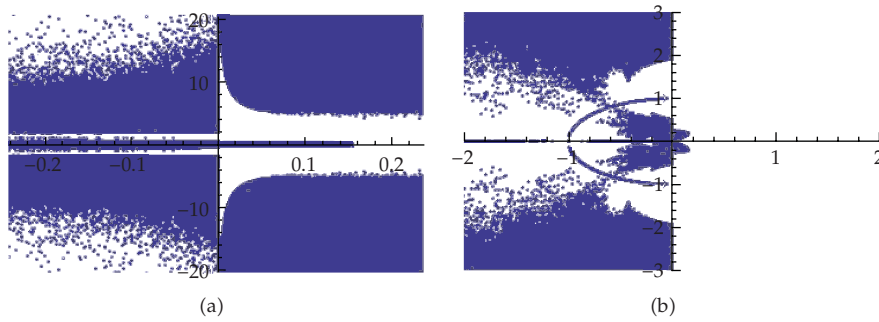


Figure 8: (a) The position, on the complex plane, of the some 23 million zeros of the Poincaré polynomials of the approximately 1 million smooth Calabi-Yau fourfolds arising as hypersurfaces in toric fivefolds. (b) A slightly magnified area emphasizing the ordinate in the range $[-1, 1]$.

with 40 Gb of memory laboured for a week, to produce some 23 million complex roots. We present a scatter plot of these roots in part (a) of Figure 8. In part (b) of the same figure, we magnify it slightly to emphasize the same range as the random plots in Figure 7.

The theorem that -1 being a root of the Poincaré polynomial of X implies X has rank exceeding unity is generally applicable. Hence, we can continue with this analysis. Now, (2.4) implies that (of course, the last equality follows directly for the definition of the the Euler characteristic $\chi(X)$)

$$P(-1, X) = 48 + 6(h^{1,1} - h^{2,1} + h^{3,1}) = \chi(X). \tag{2.5}$$

However, the relation between χ and being self-mirror, or even the concept of the latter, is obviously not as clear in complex dimension greater than three. Be that as it may, we can still examine (2.5) in the the space of fourfolds. Of the some 3 million distinct triplets, there are only 61 with vanishing Euler number, which we demonstrate in Figure 9: in part (a), $h^{1,1} + h^{3,1}$ against $h^{1,1} - h^{3,1}$, and in part (b), $h^{1,1} + h^{2,1}$ against $h^{1,1} - h^{2,1}$. We see that these are all of relatively small Hodge numbers, and in part (b), we see that in spite of the general linear behaviour seen in part (b) of Figure 6, there is some substructure. In part (c), we plot the interesting shape of the roots of the Poincaré polynomials for these 61 members. In retrospect to Figure 6, we see that perhaps the closest notion to mirror symmetry in complex dimension four is the interchange of $h^{1,1}$ and $h^{3,1}$. Of the circa 3 million, we find 5009 which

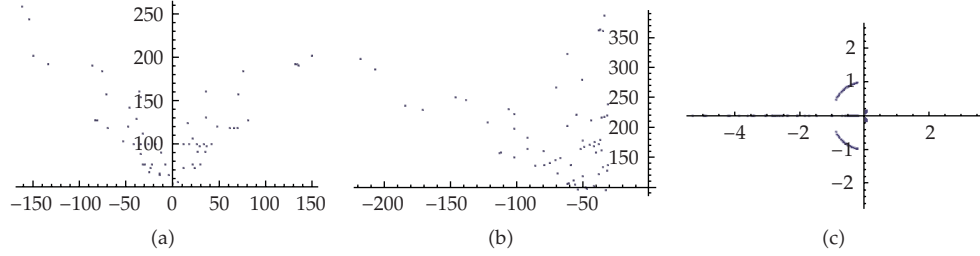


Figure 9: (a) The Hodge numbers, with $h^{1,1} - h^{3,1}$ as the abscissa and $h^{1,1} + h^{3,1}$, the ordinate, of the fourfolds which have vanishing Euler number, and hence rank exceeding unity. (b) The same, but with $h^{1,1} - h^{2,1}$, as the abscissa and $h^{1,1} + h^{2,1}$ as the ordinate. (c) The position of the roots, on the complex plane, of the Poincaré polynomial of these 61 spaces out of the some 3 million.

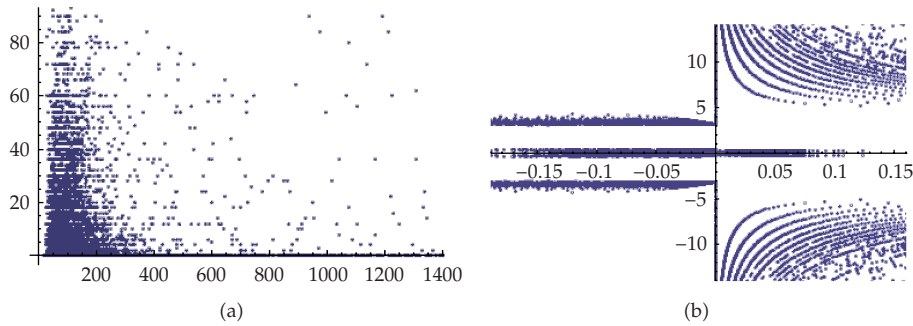


Figure 10: (a) The Hodge numbers, with $h^{1,1} = h^{3,1}$ as the abscissa and $h^{2,1}$, the ordinate, of the “self-mirror” Calabi-Yau fourfolds. (b) The position of the roots of the Poincaré polynomials of these 5009 spaces.

have the property that $h^{1,1} = h^{3,1}$. We plot the pairs $(h^{1,1} = h^{3,1}, h^{2,1})$ in part (a) of Figure 10 and the roots of their Poincaré polynomials in part (b).

3. Noncompact Calabi-Yau Geometries, Toric Diagrams, and Newton Polynomials

Having indulged in an excursion into the space of compact smooth Calabi-Yau threefolds and fourfolds, as well as their Poincaré polynomials, proceeding to the space of noncompact Calabi-Yau geometries is almost a perfunctory next step. These are affine varieties such as flat space \mathbb{C}^d and singularities which locally admit Gorenstein resolutions, and are central to McKay Correspondence and generalizations in mathematics as well as AdS/CFT and branes in string theory. A rich tapestry on this subject has been woven over the past few decades, whereby augmenting the relevance of our present investigation.

The most important family of non-compact Calabi-Yau geometries is indubitably those which afford toric description, as mentioned in the introduction. In complex dimension three, the Calabi-Yau condition compels the toric diagram to be coplanar, whence each is characterized by a (convex) lattice polygon $D = \{v_i\}$, with each $v_i \in \mathbb{Z}^2$. Therefore, a polynomial which instantly springs to mind is the Newton polynomial

$$D = \{(x_i, y_i)\} \implies P(z, w; X) = \sum_i a_i z^{x_i} w^{y_i} \in \mathbb{C}[z, w], \quad (3.1)$$

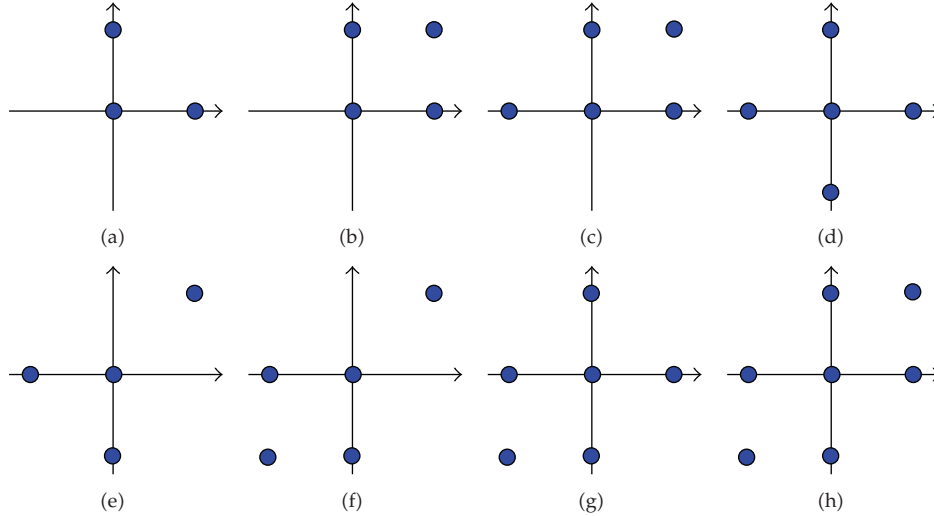


Figure 11: The most popular affine Calabi-Yau threefold toric diagrams, corresponding, respectively, to (a) \mathbb{C}^3 , (b) conifold, (c) SPP, (d) \mathbb{F}_0 , and (e, f, g, h) $dP_{0,1,2,3}$. The end points are at the standard lattice points in \mathbb{Z}^2 .

where we have inserted potential coefficients a_i for generality. This is not a frivolous act; indeed, when $a_i \in \mathbb{Z}_{\geq 0}$, they are the so-called “multiplicities” first defined in [33] and play a vital rôle in comprehending the dimer model/brane tiling interpretation of toric gauge theories [34, 35, 50].

The most famous toric diagrams for affine Calabi-Yau threefolds are depicted in Figure 11, with the endpoints at the self-explanatory lattice points in \mathbb{Z}^2 ; these include the reflexive polytopes in dimension two, and are commonly known as (a) \mathbb{C}^3 , (b) the conifold, (c) the suspended pinched point (SPP), (d) affine cone over the zeroth Hirzebruch surface $\mathbb{F}_0 = \mathbb{P}^1 \times \mathbb{P}^1$, (e) $dP_0 = \mathbb{C}^3/\mathbb{Z}_3$, the affine cone over \mathbb{P}^2 , and (f, g, h) dP_n , cones over, respectively, the first, second, and third del Pezzo surfaces which are \mathbb{P}^2 blown up at $n = 1, 2,$ and 3 generic points.

An immediate difficulty with (3.1) is, of course, that the polynomial is bi-variate, whereby describing, algebraically, Riemann surfaces. Even though such surfaces are crucial in the understanding of the gauge theory constructed on branes probing these affine toric Calabi-Yau spaces (cf. [50] for discussion on a web of inter-relations and various projections and spines of these Riemann surfaces), the notion of zeros is not obvious. We could, for example, set one of the coördinates to a fixed value, and consider the roots of the resulting univariate projection. This, however, does not seem particularly natural. Nevertheless, for illustrative purposes, we include a few examples in Figure 12, wherein we have set z to 1, varied the coefficients a_i randomly and integrally in $[-5, 5]$, and plotted the roots of the resulting polynomial in w for 5000 samples.

A much more natural and, as it turns out, interesting direction to take is to consider (3.1) not as a complex, but as a real curve. For comparative purposes, we should be mindful of the “amoebae” and the so-dubbed “algae” projections proposed in [50], which are, respectively the (natural log of the) real and imaginary projections of the Newton polynomials of the associated toric Calabi-Yau threefold.

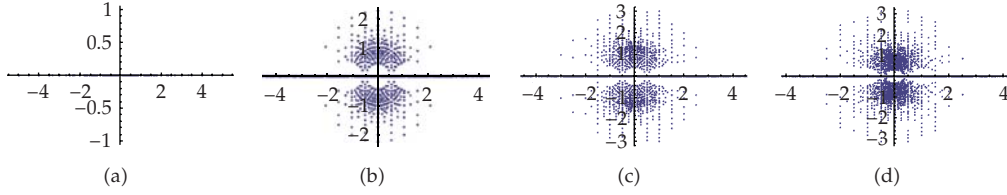


Figure 12: The roots of the Newton polynomials $P(z, w)$ at $z = 1$, for (a) the conifold, (b) \mathbb{F}_0 , (c) dP_1 , and (d) dP_3 .

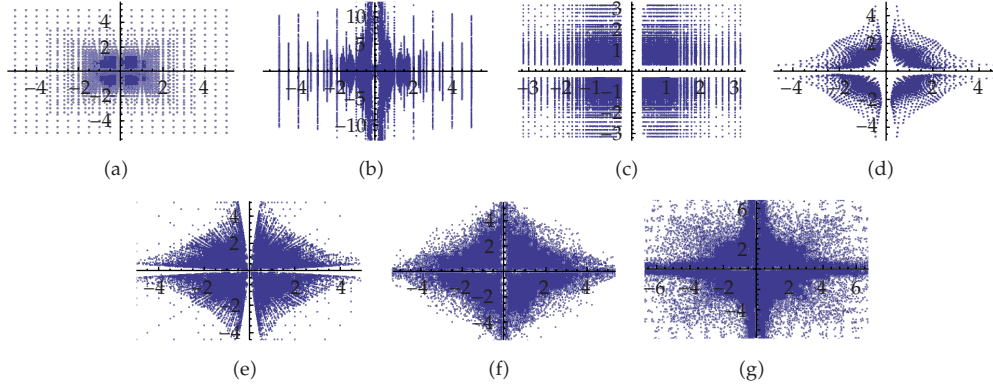


Figure 13: In reference to the toric diagrams in Figure 11, for each Calabi-Yau threefold geometry, we find the corresponding Newton polynomial as a real algebraic curve. We sample over 50000 random integer coefficients in the range $[-10, 10]$, and isolate the real critical points in \mathbb{R}^2 , which are then plotted collectively for (b) conifold, (c) SPP, (d) \mathbb{F}_0 , and (e, f, g, h) $dP_{0,1,2,3}$.

In this regard, perhaps the most significant quantity for our complex Newton polynomials is the set of turning points in \mathbb{R}^2 , namely, the set of real critical points of $P(z, w) \in \mathbb{R}[z, w]$. In other words, we find the simultaneous real solutions to

$$\partial_z P(z, w) = \sum_i a_i x_i z^{x_i-1} w^{y_i} = 0, \quad \partial_w P(z, w) = \sum_i a_i y_i z^{x_i} w^{y_i-1} = 0, \quad (3.2)$$

with a_i randomly sampled and discard the imaginary solutions. This, indeed, brings us back to Waring's original considerations on nonreal roots.

In Figure 13, we take a fixed toric diagram corresponding to a given Calabi-Yau geometry, and consider the Newton Polynomial in (3.1). Then, we sample 50000 random integer coefficients a_i in an appropriate range, here taken to be $[-10, 10]$. For each, we find the real critical points, and collectively plot them. We note that \mathbb{C}^3 does not have any real critical points and is thus left out. This is because the Newton polynomial is simply $a + bz + cw$ for $a, b, c \in \mathbb{Z}$. Thus, (3.2) gives $b = c = 0$, independent of (z, w) coordinates. Similarly, the case of (b), the conifold, can be considered a reference point. The Newton polynomial is $a + bz + cw + dzw$, whence, the critical points are given by the solutions of $b + dw = c + dz = 0$, or, $w_0 = -b/d, z_0 = -c/d$. Hence, given that each of b, c, d is independently randomly evenly distributed, the turning points (z_0, w_0) are then distributed as quotients of even random samples, and whence the clustering nearer to the lower values as seen in the darker region in the figure.

Dedication

To the occasion of the happy Installation of Professor Sir Martin Taylor as the Fiftieth Warden of Merton College, Oxford, on the Second Day of the Month of October, in the Year of Our Lord Two Thousand and Ten, and to the noble retirement of Professor Dame Jessica Rawson, this humble brief note is dedicated. Vivat Custos, vivat Collegium, & Stet Fortuna Domus!

Acknowledgments

Ad Catharinae Sanctae Alexandriae et ad Maiorem Dei Gloriam, cum Universitate Nankai, Universitate Civitate Londiniensis, Scientiae et Technologiae Concilio Anglicae, et Collegio Mertonense Oxoniensis, atque amore Elizabethae Katherinae Hunter, Rosae Hiberniae, multas gratias YHH agit.

References

- [1] A. Bloch and G. Pólya, "On the zeros of certain algebraic equations," *Proceedings London Mathematical Society*, vol. 33, pp. 102–114, 1932.
- [2] J. Littlewood and A. Offord, "On the number of real roots of a random algebraic equation," *Journal London Mathematical Society*, vol. 13, pp. 288–295, 1938.
- [3] J. H. Hannay, "Chaotic analytic zero points: exact statistics for those of a random spin state," *Journal of Physics. A*, vol. 29, no. 5, pp. L101–L105, 1996.
- [4] Y. Peres and B. Virag, "Zeros of the i.i.d. Gaussian power series: a conformally invariant determinantal process," *Journal of Physics A*, vol. 29, no. 5.
- [5] A. T. Bharucha-Reid and M. Sambandham, *Random polynomials*, Probability and Mathematical Statistics, Academic Press, Orlando, Fla, USA, 1986.
- [6] J. Littlewood, "Some problems in real and complex analysis," in *Heath Mathematical Monographs*, Lexington, Mass, USA, 1968.
- [7] P. Erdős and P. Turán, "On the distribution of roots of polynomials," *Annals of Mathematics*, vol. 51, pp. 105–119, 1950.
- [8] J. M. Hammersley, "The zeros of a random polynomial," in *Proceedings of the 3rd Berkeley Symposium on Mathematical Statistics and Probability*, vol. 2, pp. 89–111, University of California Press, Los Angeles, Calif, USA.
- [9] M. Kac, "On the average number of real roots of a random algebraic equation," *Bulletin of the American Mathematical Society*, vol. 49, pp. 314–320, 1943.
- [10] H. Montgomery, "The pair correlation of zeros of the zeta function," in *Proceedings of Symposia in Pure Mathematics*, vol. 24, pp. 181–193, American Mathematical Society, Providence, RI, USA, 1973.
- [11] A. Odlyzko, "10²⁰-th zero of the Riemann zeta function and 70 million of its neighbors," 1989, preprint, A.T.T.
- [12] Y. H. He, V. Jejjala, and D. Minic, "On the physics of the Riemann zeros," In press, <http://arxiv.org/abs/1004.1172>.
- [13] A. M. Odlyzko and B. Poonen, "Zeros of polynomials with 0,1 coefficients," *L'Enseignement Mathématique*, vol. 39, no. 3-4, pp. 317–348, 1993.
- [14] P. Borwein and L. Jörgenson, "Visible structures in number theory," *The American Mathematical Monthly*, vol. 108, no. 10, pp. 897–910, 2001.
- [15] D. Bailey, J. Borwein, N. Calkin, R. Girgensohn, D. Luke, and V. Moll, *Experimental Mathematics in Action*, A. K. Peters Ltd., Wellesley, Mass, USA, 2007.
- [16] "Mathematica Edition: Version 7.0," Wolfram Research.
- [17] S. Franco, Y. H. He, C. Herzog, and J. Walcher, "Chaotic duality in string theory," *Physical Review D*, vol. 70, article 046006, 2004.

- [18] F. Beaucloup, P. Borwein, D. Boyd, and C. Pinner, "Multiple roots of $[[\text{minus}]1, 1]$ power series," *Journal of the London Mathematical Society*, vol. 57, no. 1, pp. 135–147, 1998.
- [19] D. Christensen, <http://jdc.math.uwo.ca/roots/>.
- [20] J. Jörgenson, <http://oldweb.cecm.sfu.ca/personal/loki/Projects/Roots/>.
- [21] S. Derbyshire and J. Matson, "Polynomial plot: simple math expressions yield intricate visual patterns," *Scientific American*, 2009.
- [22] J. Baez, <http://math.ucr.edu/home/baez/roots/>.
- [23] X. S. Lin, "Zeros of the Jones polynomial," <http://math.ucr.edu/~xl/abs-jk.pdf>.
- [24] J. Hoste and M. Thistlethwaite, <http://www.math.utk.edu/~morwen/knotscape.html>.
- [25] P. Candelas, A. M. Dale, C. A. Lütken, and R. Schimmrigk, "Complete intersection Calabi-Yau manifolds," *Nuclear Physics*, vol. 298, no. 3, pp. 493–525, 1988.
- [26] P. Candelas, M. Lynker, and R. Schimmrigk, "Calabi-Yau manifolds in weighted $P(4)$," *Nuclear Physics*, vol. 341, no. 2, pp. 383–402, 1990.
- [27] M. Kreuzer and H. Skarke, "Complete classification of reflexive polyhedra in four dimensions," *Advances in Theoretical and Mathematical Physics*, vol. 4, pp. 1209–1230, 2002.
- [28] P. Candelas, X. de la Ossa, Y. H. He, and B. Szendroi, "Triadophilia: a special corner in the landscape," *Advances in Theoretical and Mathematical Physics*, vol. 12, p. 2, 2008.
- [29] P. Candelas and R. Davies, "New Calabi-Yau manifolds with small Hodge numbers," *Fortschritte der Physik*, vol. 58, p. 383, 2010.
- [30] V. Braun, "On free quotients of complete intersection Calabi-Yau manifolds," In press, <http://arxiv.org/abs/1003.3235>.
- [31] F. Denef and M. R. Douglas, "Computational complexity of the landscape. I," *Annals of Physics*, vol. 322, p. 1096, 2007.
- [32] A. Hanany and Y. H. He, "Non-Abelian finite gauge theories," *Journal of High Energy Physics*, vol. 2, article 013, 1999.
- [33] B. Feng, A. Hanany, and Y. H. He, "D-brane gauge theories from toric singularities and toric duality," *Nuclear Physics*, vol. B595, p. 165, 2001.
- [34] A. Hanany and K. D. Kennaway, "Dimer models and toric diagrams," In press, <http://arxiv.org/abs/hep-th/0503149>.
- [35] S. Franco, A. Hanany, D. Martelli, J. Sparks, D. Vegh, and B. Wecht, "Gauge theories from toric geometry and brane tilings," *Journal of High Energy Physics*, vol. 1, article 128, 2006.
- [36] D. Forcella, A. Hanany, Y. H. He, and A. Zaffaroni, "The master space of $N=1$ Gauge theories," *Journal of High Energy Physics*, vol. 8, article 012, 2008.
- [37] A. Hanany and Y. H. He, "M2-branes and quiver Chern-Simons: a taxonomic study," In press, <http://arxiv.org/abs/0811.4044v2>.
- [38] J. Davey, A. Hanany, N. Mekareeya, and G. Torri, "Brane tilings, M2-branes and Chern-Simons theories," in *Proceedings of the 49th Cracow School of Theoretical Physics: Non-Perturbative Gravity and Quantum Chromodynamics*, Zakopane, Poland, May-June 2009.
- [39] J. Davey, A. Hanany, and R. K. Seong, "Counting orbifolds," *Journal of High Energy Physics*, vol. 6, no. 6, article 010, 2010.
- [40] S. Benvenuti, B. Feng, A. Hanany, and Y. H. He, "Counting BPS operators in gauge theories: quivers, syzygies and plethystics," *Journal of High Energy Physics*, vol. 11, article 050, 2007.
- [41] D. Forcella, "Operators and vacua of $N=1$ field theories," *Nuovo Cimento*, vol. 125, pp. 905–914, 2010.
- [42] A. Hanany, N. Mekareeya, and G. Torri, "The Hilbert series of adjoint SQCD," *Nucl. Phys.*, vol. 825, no. 1-2, pp. 52–97, 2010.
- [43] T. Emery, "Vector fields on manifolds," *Bulletin of the American Mathematical Society*, vol. 75, pp. 643–683, 1969.
- [44] G. E. Bredon, "Counterexamples on the rank of a manifold," *Proceedings of the American Mathematical Society*, vol. 27, no. 3, pp. 592–594, 1971.
- [45] D. Bump, K. K. Choi, P. Kurlberg, and J. Vaaler, "A local Riemann hypothesis. I," *Mathematische Zeitschrift*, vol. 233, no. 1, pp. 1–19, 2000.
- [46] A. Postnikov and R. P. Stanley, "Deformations of Coxeter hyperplane arrangements," *Journal of Combinatorial Theory. Series A*, vol. 91, no. 1-2, pp. 544–597, 2000.
- [47] F. Rodriguez-Villegas, "On the zeros of certain polynomials," *Proceedings of the American Mathematical Society*, vol. 130, no. 8, pp. 2251–2245, 2002.

- [48] M. Kreuzer and H. Skarke, "Calabi-Yau 4-folds and toric fibrations," *Journal of Geometry and Physics*, vol. 26, no. 3-4, pp. 272–290, 1998.
- [49] M. Lynker, R. Schimmrigk, and A. Wisskirchen, "Landau-Ginzburg vacua of string, M-and F-theory at $c = 12$," *Nuclear Physics*, vol. 550, p. 123, 1999.
- [50] B. Feng, Y. H. He, K. D. Kennaway, and C. Vafa, "Dimer models from mirror symmetry and quivering amoebae," *Advances in Theoretical and Mathematical Physics*, vol. 12, p. 3, 2008.

Review Article

Toric Methods in F-Theory Model Building

Johanna Knapp^{1,2} and Maximilian Kreuzer²

¹ *Institute for the Physics and Mathematics of the Universe (IPMU), The University of Tokyo,
5-1-5 Kashiwanoha, Kashiwa 277-8583, Japan*

² *Institut für Theoretische Physik, TU Vienna, Wiedner Hauptstraße 8-10, 1040 Vienna, Austria*

Correspondence should be addressed to Johanna Knapp, johanna.knapp@ipmu.jp

Received 12 March 2011; Accepted 2 April 2011

Academic Editor: Yang-Hui He

Copyright © 2011 J. Knapp and M. Kreuzer. This is an open access article distributed under the Creative Commons Attribution License, which permits unrestricted use, distribution, and reproduction in any medium, provided the original work is properly cited.

We discuss recent constructions of global F-theory GUT models and explain how to make use of toric geometry to do calculations within this framework. After introducing the basic properties of global F-theory GUTs, we give a self-contained review of toric geometry and introduce all the tools that are necessary to construct and analyze global F-theory models. We will explain how to systematically obtain a large class of compact Calabi-Yau fourfolds which can support F-theory GUTs by using the software package PALP.

1. Introduction

Even though it has been around for quite a while [1], F-theory has recently received a lot of new attention as a setup where grand unified theories (GUTs) can be conceived from string theory. Starting with [2–4] the phenomenology of F-theory GUTs has become an active field of research. The basic idea is that the GUT theory is localized on a (p, q) seven-brane S inside a three-dimensional base manifold B of an F-theory compactification on an elliptically fibered Calabi-Yau fourfold. The location of the GUT brane and the gauge group are determined by the degeneration of the elliptic fibration. Chiral matter localizes on curves inside the GUT brane S , where gauge enhancement occurs, and Yukawa couplings sit at points. For many phenomenological applications, it is sufficient to consider the field theory living on the GUT brane without specifying the details of the global F-theory compactification. However, fluxes, monodromies, or consistency constraints such as tadpole cancellation cannot be addressed in a purely local setup. These issues have recently received a lot of attention in the literature [5–25]. Therefore, it is interesting to see whether it is possible to embed the local F-theory GUT into a compactification on a Calabi-Yau fourfold. Most known examples of compact Calabi-Yau manifolds are hypersurfaces or complete intersections in a toric ambient space.

It is thus natural to look for Calabi-Yau fourfolds within this class of examples. A prescription for constructing elliptically fibered Calabi-Yau fourfolds as complete intersections in a six-dimensional toric ambient space has been given in [6, 8]. Before that, complete intersection Calabi-Yau fourfolds in F-theory had already been used in the context of F-theory uplifts of type IIB string theory [26–28]. A similar construction has also been discussed in [10]. It has been shown in examples that it is indeed possible to construct viable F-theory GUTs within this framework.

The construction of [6] is very well-suited for a systematic search of a large class of models. This is interesting for several reasons: one goal is to find particularly nice examples of F-theory compactifications. Even though the known examples have been able to incorporate F-theory models, one usually gets much more than just that. In minimal F-theory GUTs, one typically needs only very few Yukawa points and a small number of moduli on the matter curves. This is not satisfied in most known global models. A related question deals with the genericity of F-theory GUTs. The geometric configurations used for constructing such models are usually quite special, and one may wonder how often they can be realized in elliptically fibered fourfolds. From the point of view of model building, it is useful to have some easy-to-check geometric conditions which makes it possible to select suitable models from a large class of geometries. This will be discussed in more details in the text. From a mathematical point of view it might be interesting to obtain a partial classification of Calabi-Yau fourfolds.

This paper discusses selected topics in toric geometry and F-theory GUTs. The paper is organized as follows: in Section 2, we recall the construction of global F-theory models and discuss the basic requirements we would like to impose. In Section 3, we review several notions in toric geometry which are required in order to perform the F-theory calculations. The geometries one has to deal with are usually quite complicated, and very often, one has to rely on computer support in order to be able to do explicit calculations. Therefore, we discuss how such calculations can be implemented using existing software such as PALP [29]. We will mainly focus on the application of toric geometry in the context of F-theory model building. For a more complete picture on this vast subject of F-theory phenomenology, we refer to other review articles such as [30–32]. For more extensive discussions of toric geometry, we recommend [33–35].

2. Global F-Theory Models

2.1. Setup

In this section, we introduce the basic concepts and notions used in global F-theory models. In the remainder of this paper we will explain the techniques which are necessary to do calculations within this framework. For more details on how the quantities introduced below come about, we refer to the original papers or the recent review article [32].

In [6], it has been proposed to construct Calabi-Yau fourfolds, which are suitable for F-theory model building, as complete intersections of two hypersurfaces in a six-dimensional toric ambient space. The hypersurface equations have the following structure:

$$P_B(y_i, w) = 0, \quad P_W(x, y, z, y_i, w) = 0. \quad (2.1)$$

The first equation only depends on the homogeneous coordinates (y_i, w) of the three-dimensional base B of the elliptically fibered Calabi-Yau fourfold X_4 . Here, we have singled

out one coordinate w , indicating that the divisor given by $w = 0$ defines a seven-brane S which supports a GUT theory of the type introduced in [2–4]. The second equation in (2.1) defines a Weierstrass model, where (x, y, z) are those coordinates of the six-dimensional ambient space that describe the torus fiber. For this type of elliptic fibrations, P_W is of Tate form which is defined as follows:

$$P_W = x^3 - y^2 + xyz a_1 + x^2 z^2 a_2 + y z^3 a_3 + x z^4 a_4 + z^6 a_6. \quad (2.2)$$

The $a_n(y_i, w)$ are sections of K_B^{-n} , where K_B is the canonical bundle of the base manifold. Furthermore, x and y can be viewed as sections of K_B^{-2} and K_B^{-3} , respectively.

The information about the F-theory model is encoded in the Tate equation (2.2). In order to have a nontrivial gauge group on the GUT brane the elliptic fibration must degenerate above S . The gauge group is determined by the structure of the singularity. The elliptic fibration becomes singular at the zero locus of the discriminant Δ . Defining the polynomials $\beta_2 = a_1^2 + 4a_2$, $\beta_4 = a_1 a_3 + 2a_4$ and $\beta_6 = a_3^2 + 4a_6$, the discriminant is given by the following expression:

$$\Delta = -\frac{1}{4}\beta_2^2(\beta_2\beta_6 - \beta_4^2) - 8\beta_4^3 - 27\beta_6^2 + 9\beta_2\beta_4\beta_6. \quad (2.3)$$

According to Kodaira's classification [36] and Tate's algorithm [37], the gauge group can be inferred from the factorization properties of the $a_n(y_i, w)$ with respect to w . Considering, for instance, $SU(5)$ - and $SO(10)$ -models, the factorization looks like this

$$\begin{aligned} SU(5) : a_1 &= b_5 w^0 & a_2 &= b_4 w^1 & a_3 &= b_3 w^2 & a_4 &= b_2 w^3 & a_6 &= b_0 w^5, \\ SO(10) : a_1 &= b_5 w^1 & a_2 &= b_4 w^1 & a_3 &= b_3 w^2 & a_4 &= b_2 w^3 & a_6 &= b_0 w^5. \end{aligned} \quad (2.4)$$

The b_i s are sections of some appropriate line bundle over B that have at least one term independent of w .

In F-theory GUT models, chiral matter localizes on curves on S , where a rank 1 enhancement of the gauge group appears. In $SU(5)$ models, the matter curves are at the following loci inside S :

$$b_3^2 b_4 - b_2 b_3 b_5 + b_0 b_5^2 = 0 \quad \mathbf{5} \text{ matter}, \quad b_5 = 0 \quad \mathbf{10} \text{ matter}. \quad (2.5)$$

The matter curves for the $SO(10)$ models are at

$$b_3 = 0 \quad \mathbf{10} \text{ matter}, \quad b_4 = 0 \quad \mathbf{16} \text{ matter}. \quad (2.6)$$

Yukawa coupling arise at points inside S , where the GUT singularity has an rank 2 enhancement. In $SU(5)$ models, the Yukawa points sit at

$$\begin{aligned} b_4 = 0 \cap b_5 = 0 & \quad \mathbf{10} \mathbf{10} \mathbf{5} \text{ Yukawas} \quad E_6 \text{ enhancement}, \\ b_5 = 0 \cap b_3 = 0 & \quad \mathbf{10} \overline{\mathbf{5}} \overline{\mathbf{5}} \text{ Yukawas} \quad SO(12) \text{ enhancement}. \end{aligned} \quad (2.7)$$

In the $SO(10)$ -case, we have the following Yukawa couplings:

$$\begin{aligned} b_3 = 0 \cap b_4 = 0 & \quad \mathbf{16} \ \mathbf{16} \ \mathbf{10} \text{ Yukawas} \quad E_7 \text{ enhancement,} \\ b_2^2 - 4b_0b_4 = 0 \cap b_3 = 0 & \quad \mathbf{16} \ \mathbf{10} \ \mathbf{10} \text{ Yukawas} \quad SO(14) \text{ enhancement.} \end{aligned} \quad (2.8)$$

Given a complete intersection Calabi-Yau fourfold of the form (2.1), the expressions for matter curves and Yukawa points are globally defined and can be calculated explicitly. Having a global F-theory compactification, we can furthermore calculate the Hodge numbers and the Euler number χ_4 of the Calabi-Yau fourfold X_4 . The latter enters the D3-tadpole cancellation condition,

$$\frac{\chi_4}{24} = N_{D3} + \frac{1}{2} \int_{X_4} G_4 \wedge G_4, \quad (2.9)$$

where G_4 denotes the fourform flux on X_4 and N_{D3} is the number of $D3$ -branes.

2.2. Geometric Data in F-Theory Models

So far, we have summarized the basic structure of a global F-theory GUT. In the present section, we will discuss which properties of the GUT model are encoded in the geometries of the base manifold B and the Calabi-Yau fourfold X_4 . We will not go deeply into the phenomenology of F-theory GUTs but rather focus on the basic geometric properties which should be satisfied in order to obtain a viable GUT model.

2.2.1. Base Manifold

Since the GUT brane S is a divisor in a three-dimensional base manifold B , a large amount of information about the model can be extracted from the geometry of B . The base B is a non-negatively curved manifold of complex dimension three. In our setup, it will be given by a hypersurface in a toric ambient space. Note that Fano threefolds are not a good choice for B due to the lack of a decoupling limit [38]. In Section 3, we discuss a systematic construction of such base manifolds using toric geometry. In order to have a well-defined model, we have to make sure that B is nonsingular. In contrast to Calabi-Yau threefolds, the base manifolds for F-theory GUTs may inherit the singularities of the ambient space. Therefore, checks for the regularity of B have to be implemented.

Having found a suitable base manifold, the next step is to identify divisors inside B that can support GUT models. The most promising candidates for F-theory model building are del Pezzo surfaces. These are Fano twofolds (see, e.g., [39]). Note, however, that del Pezzos are not the only possibility for the construction of GUT models in F-theory. See [40] for a recent discussion. There are several motivations to focus on del Pezzo divisors. In local F-theory GUTs, the del Pezzo property ensures the existence of a decoupling limit [3, 4]. For $SU(5)$ GUT models, the fact that del Pezzos have $h^{0,1} = h^{2,0} = 0$ implies some powerful vanishing theorems which forbid exotic matter after breaking $SU(5)$ to the standard model gauge group [4].

We can identify candidates for del Pezzo divisors inside B by their topological data. Suppose that the base manifold B is embedded in a toric ambient space which has toric

divisors D_i . The D_i give a homology basis of the ambient space. In this setup, the hypersurface is specified by a divisor, which we will by abuse of notation also call B , that is given in terms of a linear combination of the D_i . The total Chern class of a particular divisor S in the ambient space is, after restriction to B (for more details, see Section 3.3)

$$c(S) = \frac{\prod_i (1 + D_i)}{(1 + B)(1 + S)}. \quad (2.10)$$

In order to apply this formula, we have to know the intersection ring of B . As we will discuss in Section 3.3, this can be obtained from the intersection ring of the ambient space.

A necessary condition for a divisor S to be dP_n is that it must have the following topological data:

$$\int_S c_1(S)^2 = 9 - n, \quad \int_S c_2(S) = n + 3 \implies \chi_h = \int_S \text{Td}(S) = 1, \quad (2.11)$$

where $\chi_h = \sum_i (-1)^i h^{0,i}$ is the holomorphic Euler characteristic and Td denotes the Todd class. In the equations above the integration over the four-cycle (representing the divisor) S is equivalent to computing the intersection with S . Since del Pezzos are Fano twofolds, we have a further necessary condition: the intersections of $c_1(S)$ with curves on S have to be positive. In the toric setup, we can only check this for curves which are induced from the divisors on the ambient space. In that case, the condition is

$$D_i \cdot S \cdot c_1(S) > 0 \quad D_i \neq S \quad \forall D_i \cdot S \neq \emptyset. \quad (2.12)$$

In order to make these calculations, we need to know the homology basis of toric divisors and their intersection numbers.

In local F-theory GUTs, the del Pezzo property is sufficient to ensure the existence of a decoupling limit. For global models, further checks are in order. Gravity decouples from the gauge degrees of freedom if the mass ratio $M_{\text{GUT}}/M_{\text{pl}}$ becomes parametrically small. The Planck mass M_{pl} and the mass scale M_{GUT} of the GUT theory are related to the geometry of B and S in the following way:

$$M_{\text{pl}}^2 \sim \frac{M_s^8}{g_s^2} \text{Vol}(B) \quad M_{\text{GUT}} \sim \text{Vol}(S)^{-1/4} \quad \frac{1}{g_{\text{YM}}^2} \sim \frac{M_s^4}{g_s} \text{Vol}(S). \quad (2.13)$$

Therefore, one has

$$\frac{M_{\text{GUT}}}{M_{\text{pl}}} \sim g_{\text{YM}}^2 \frac{\text{Vol}(S)^{3/4}}{\text{Vol}(B)^{1/2}}. \quad (2.14)$$

There are two ways to achieve a small value for $M_{\text{GUT}}/M_{\text{pl}}$, now commonly referred to as the physical and the mathematical decoupling limit. In the physical decoupling limit, the volume of the GUT brane S is kept finite, while $\text{Vol}(B) \rightarrow \infty$. The mathematical decoupling limit takes $\text{Vol}(S) \rightarrow 0$ for finite volume of B . The two limits may not be equivalent in the sense

that they may be implemented by tuning different Kähler parameters. The volumes of B and S can be determined in terms of the Kähler form J of the ambient toric variety restricted to B

$$\text{Vol}(B) = J^3 \quad \text{Vol}(S) = S \cdot J^2. \quad (2.15)$$

In order for the volumes to be positive, we must find a basis of the Kähler cone K_i , where, by definition, J can be written as $J = \sum_i r_i K_i$ with $r_i > 0$. The existence of mathematical and physical decoupling limits can be deduced from the moduli dependence of these volumes.

Having found a suitable base manifold, we can also study matter curves and Yukawa couplings. The curve classes M of the matter curves can be expressed in terms of the toric divisors of the ambient space. The genus of the matter curves can be computed using the first Chern class of the matter curve and the triple intersection numbers

$$c(M) = \frac{\prod_i (1 + D_i)}{(1 + B)(1 + S)(1 + M)}. \quad (2.16)$$

Here, we have assumed that M is irreducible. After expanding this expression to get $c_1(M)$, the Euler number is obtained by the following intersection product:

$$\chi(M) = 2 - 2g(M) = c_1(M) \cdot M \cdot S. \quad (2.17)$$

The genus of a matter curve gives us information about the number of moduli the curve has. Since these moduli have to be stabilized, matter curves of low genus are desirable from a phenomenological point of view. In the generic situation, the equations specifying the Yukawa points can be expressed as classes Y_1, Y_2 in terms of the toric divisors. The number of Yukawa points is then given by the following intersection product:

$$n_{\text{Yukawa}} = S \cdot Y_1 \cdot Y_2. \quad (2.18)$$

In order to account for the standard model Yukawa couplings, only a small number of Yukawa points is needed.

2.2.2. Fourfold

Given a base manifold B , one can construct a Calabi-Yau fourfold X_4 which is an elliptic fibration over B . As described in the next section, this can be done systematically using toric geometry. However, not all of the desirable features of global F-theory models are automatic in this construction. The main requirement on X_4 is that it is a complete intersection of two hypersurfaces. Furthermore, these hypersurfaces must have a specific structure (2.1). In order to be able to use powerful mathematical tools, we, furthermore, have to require that there exists a nef-partition (cf. Section 3.2) which is compatible with the elliptic fibration. When this elementary requirement is satisfied, we can engineer a GUT model. This is done in two steps: first, we have to identify the GUT divisor S , given by the equation $w = 0$ in B within the Calabi-Yau fourfold. The second step is to impose the GUT group. This amounts to explicitly imposing the factorization conditions such as (2.4) on the Tate model. This means that we

have to remove all those monomials in (2.2) which do not satisfy the factorization constraints. This amounts to fixing a number of complex structure moduli of X_4 .

Recently, there has been active discussion in the literature how to globally define fluxes in F-theory models [6–8, 11, 15, 16, 20, 21, 25]. In F-theory, model building fluxes enter at several crucial points. Gauge flux along the matter curve is needed in order to generate chiral matter. Breaking of the GUT group to the standard model gauge group can be achieved by turning on $U(1)$ -flux. Furthermore, in $SU(5)$ F-theory GUTs, we need global $U(1)$ s in order to forbid dimension 4 proton decay operators. In $SO(10)$ F-theory GUTs they are needed in order to obtain chiral matter [13, 41]. A general global description of the fourform flux G_4 is still missing. In [42], an auxiliary construction involving spectral covers that factorize was used to describe fluxes locally in the vicinity of the GUT brane. It has been shown in [14–16] that under certain circumstances, the information captured by the spectral cover can be encoded in the Tate model and is, therefore, global. However, this need not be the case [11]. In [14], it has been shown that a spectral cover which factorizes is generically globally defined for “ $U(1)$ -restricted Tate models”. This is achieved by imposing a global $U(1)_X$ symmetry in the elliptic fibration. In terms of the Tate model, this is achieved by setting $a_6 = 0$.

3. Ingredients and Techniques from Toric Geometry

In the previous section, we have introduced quantities which encode important information about F-theory GUT models in the geometry of the base manifold and the Calabi-Yau fourfold. In this section, we will provide the tools to calculate them. The input data needed for these calculations can be obtained by using toric geometry. After giving the basic definitions, we will discuss how to describe hypersurfaces and complete intersections of hypersurfaces in toric ambient spaces. Then, we explain how to obtain the intersection ring and the Kähler cone, or dually, the Mori cone. Finally, we will discuss how to use the computer program PALP [29] for calculations in toric geometry. This discussion of toric geometry has been compiled with a view towards the applications in F-theory model building. It is by no means an exhaustive description of this vast subject which brings together algebraic geometry and combinatorics.

3.1. Toric Varieties

We start by defining a toric variety X of dimension n as the following quotient:

$$X = \frac{(\mathbb{C}^r - Z)}{((\mathbb{C}^*)^{r-n} \times G)}, \quad (3.1)$$

where G is a finite abelian group, $(\mathbb{C}^*)^{r-n}$ describes the action of an algebraic $(r-n)$ -torus, and $Z \subset \mathbb{C}^r$ is an exceptional set which tells us which combinations of coordinates are not allowed to vanish simultaneously. The simplest example is $\mathbb{C}\mathbb{P}^2$, where the \mathbb{C}^* -action is given by $(z_1, z_2, z_3) \sim (\lambda z_1, \lambda z_2, \lambda z_3)$, $\lambda \in \mathbb{C}^*$, the exceptional set is $Z = \{z_1 = z_2 = z_3 = 0\}$, and G is trivial. Thus, as is well known: $\mathbb{C}\mathbb{P}^2 = (\mathbb{C}^3 - \{z_1 = z_2 = z_3 = 0\}) / ((z_1, z_2, z_3) \sim (\lambda z_1, \lambda z_2, \lambda z_3))$.

The crucial fact about toric geometry is that the geometric data of the toric variety can be described in terms of combinatorics of cones and polytopes in dual pairs of integer lattices.

The information about the toric variety is encoded in a fan Σ , which is a collection of strongly convex rational polyhedral cones, where all the faces and intersections of pairs of cones also belong to the fan. “Strongly convex” means that all the cones of the fan have an apex at the origin, and “rational” means that the rays that span the cone go through points of the lattice. We denote by $\Sigma^{(n)}$ the set of all n -dimensional cones. In order to define the fan, we use the fact that a toric variety X contains an n -torus $T = (\mathbb{C}^*)^n$ as a dense open subset whose action extends to X . Parametrizing T by coordinates (t_1, \dots, t_n) , one defines the character group $M = \{\chi : T \rightarrow \mathbb{C}^*\}$ and the one-parameter subgroups $N = \{\lambda : \mathbb{C}^* \rightarrow T\}$. M and N can be identified with integer lattices that are isomorphic to \mathbb{Z}^n . Given a point $m \in M$, the character is given by $\chi^m(t) = t_1^{m_1} \cdots t_n^{m_n} \equiv t^m$. This is a holomorphic function on T and descends to a rational function on the toric variety X . For every $u \in N$, λ is defined as $\lambda^u(\tau) = (\tau^{u_1}, \dots, \tau^{u_n})$ for $\tau \in \mathbb{C}^*$. The fan Σ and its cones σ are defined on the real extension $N_{\mathbb{R}}$ of N . The lattices M, N are dual due to the composition $(\chi \circ \lambda)(\tau) = \chi(\lambda(\tau)) = \tau^{\langle \chi, \lambda \rangle}$, where $\langle \chi^m, \lambda^u \rangle = m \cdot u$ is the scalar product.

The M -lattice encodes the data about regular monomials in X , the N -lattice captures the information about the divisors. The divisors defined by $\chi^m = 0$ can be decomposed in terms of irreducible divisors D_j : $\text{div}(\chi^m) = \sum_{j=1}^r a_j D_j$. These divisors are principal divisors, that is, divisors of meromorphic function, where D_j correspond to poles or zeros and the a_j are orders of the pole/zero. The coefficients $a_j(m) \in \mathbb{Z}$ are unique, and there exists a map $m \rightarrow a_j(m) = \langle m, v_j \rangle$ with $v_j \in N$. Thus, there is a vector v_j for every irreducible divisor D_j . The v_j are the primitive generators of the one-dimensional cones ρ_j (i.e., rays) in the fan Σ . The convex hull of the v_j defines a polytope $\Delta^* = \text{conv}\{v_j\}$. Locally, we can write the divisors as $D_j = \{z_j = 0\}$, where z_j is regarded as a local section of a line bundle. D_j are called toric divisors. There are linear relations among the $v_j \in \Delta^*$ which translate into linear relations among the toric divisors.

In order to make contact with the definition (3.1) of X , we view the $\{z_j\}$ as global homogeneous coordinates $(z_1 : \cdots : z_r)$. If all z_j are nonzero the coordinates $(\lambda^{q_1} z_1 : \cdots : \lambda^{q_r} z_r) \sim (z_1 : \cdots : z_r)$ with $\lambda \in \mathbb{C}^*$ describe the same point on the torus T if $\sum q_j v_j = 0$ for $v_j \in N$ as above. Since the v_j live in an n -dimensional lattice, they satisfy $r - n$ linear relations. If the v_j do not span the N -lattice, there is a finite abelian group G such that $G \simeq N / (\text{span}\{v_1, \dots, v_r\})$. Identifications coming from the action of G have to be added to the identifications between the homogeneous coordinates coming from the torus action. Having introduced the fan Σ , we are also able to specify the exceptional set Z that tells us where the homogeneous coordinates are not allowed to vanish simultaneously: a subset of coordinates z_j is allowed to vanish simultaneously if and only if there is a cone $\sigma \in \Sigma$ containing all the corresponding rays ρ_j . To be more precise, the exceptional set is the union of sets Z_I with minimal index sets I of rays for which there is no cone that contains them: $Z = \cup_I Z_I$. This is equivalent to the statement that the corresponding divisors D_j intersect in X . Putting the pieces together, we arrive at the definition (3.1).

There are two important properties of the fan Σ which translate into crucial properties of the toric variety X . Firstly, X is compact if and only if the fan is complete, that is, if the support of the fan covers the N -lattice: $|\Sigma| = \cup_{\sigma \in \Sigma} \sigma = N_{\mathbb{R}}$. Secondly, X is non-singular if and only if all cones are simplicial and basic, which means that all cones $\sigma \in \Sigma$ are generated by a subset of a lattice basis of N . Singularities can be removed by blowups, where singular points are replaced by \mathbb{P}^{n-1} s. All the singularities of a toric variety can be resolved by a series of blowups. These correspond to subdivisions of the fan. In order to completely resolve all singularities, one must find a maximal triangulation of the fan. In many cases, it is sufficient to find a maximal triangulation of the polytope Δ^* .

Finally, let us emphasize the significance of the homogeneous weights q_i . In general, there will be a full $(r - n) \times r$ matrix Q_{ij} , called weight matrix, whose $(r - n)$ lines encode the \mathbb{C}^* -actions. Since each of the z_j corresponds to an irreducible divisor in X , the columns of the weight matrix define a homology basis of the divisors D_j . In physics language the weights q_i are the $U(1)$ -charges in the gauged linear sigma model that defines the toric variety X . Note that the weights contain all the information to recover the M - and N -lattice. With the weight matrix as input, this can be done using PALP.

3.2. Hypersurfaces and Complete Intersections

Having defined a toric variety, we go on to discuss hypersurfaces and complete intersections of hypersurfaces in toric varieties. The hypersurface equations are sections of non-trivial line bundles. The information of these bundles can be recovered from their transition functions. In this context, we introduce the notions of Cartier divisors and Weil divisors. A Cartier divisor is given, by definition, by rational equations $f_\alpha = 0$ and regular transition functions f_α / f_β on the overlap of two coordinate patches U_α, U_β . Cartier divisor classes determine the Picard group $\text{Pic}(X)$ of holomorphic line bundles. Weil divisors are finite formal sums of irreducible varieties of codimension 1. On a toric variety, the Chow group $A_{n-1}(X)$ modulo linear equivalence is generated by the T -invariant irreducible divisors D_j modulo the principal divisors $\text{div}(\chi^m)$, $m \in M$. A Weil divisor of the form $D = \sum a_j D_j$ is Cartier if there exists an $m_\sigma \in M$ for each maximal cone $\sigma \in \Sigma^{(n)}$ such that $\langle m_\sigma, v_j \rangle = -a_j$ for all rays $\rho_j \in \sigma$. If X is smooth, then all Weil divisors are Cartier. If X is compact and D is Cartier, then $\mathcal{O}(D)$ is generated by global sections if and only if $\langle m_\sigma, v_j \rangle > -a_j$ for $\sigma \in \Sigma^{(n)}$ and $\rho_j \notin \sigma$. If this is the case for $v \in \sigma$, $\psi_D(v) = \langle m_\sigma, v \rangle$ is a strongly convex support function. With that, we can define a polytope $\Delta_D = \{m \in M_{\mathbb{R}} : \langle m_\sigma, v_j \rangle \geq -a_j\}$. This is a convex lattice polytope in $M_{\mathbb{R}}$ whose lattice points provide global sections of the line bundle $\mathcal{O}(D)$ corresponding to the divisor D . D is generated by global sections if and only if Δ_D is the convex hull of $\{m_\sigma\}$. Furthermore, D is ample if and only if Δ_D is n -dimensional with vertices m_σ for $\sigma \in \Sigma^{(n)}$ and with $m_\sigma \neq m_\tau$ for $\sigma \neq \tau \in \Sigma^{(n)}$. Finally, D is called base point free if and only if $m_\sigma \in \Delta_D$ for all $\sigma \in \Sigma^{(n)}$. Base point freedom is a sufficient condition for a hypersurface defined by D to be regular: Bertini's theorem states that the singular points of D are the base locus and the singular points inherited from the ambient space. The absence of base points implies that D can be deformed transversally in every point and, therefore, generically avoids the singularities of the ambient space. Thus, a base point free D is regular. We emphasize, however, that base point freedom is not a necessary condition for the regularity of D .

Equations for hypersurfaces or complete intersections are sections of line bundles $\mathcal{O}(D)$ given by the following Laurent polynomial:

$$f = \sum_{m \in \Delta_D \cap M} c_m \chi^m = \sum_{m \in \Delta_D \cap M} c_m \prod_j z_j^{\langle m, v_j \rangle}. \quad (3.2)$$

In an affine patch U_σ , the local section $f_\sigma = f / \chi^{m_\sigma}$ is a regular function. Given a polytope $\Delta_D \in M$, we can define the polar polytope Δ_D° by $\Delta_D^\circ = \{y \in N_{\mathbb{R}} : \langle x, y \rangle \geq -1 \forall x \in \Delta_D\}$. It can be shown [43] that the Calabi-Yau condition for hypersurfaces requires that $\Delta_D \subseteq M_{\mathbb{R}}$ is polar to $\Delta^* = \Delta_D^\circ \subseteq N_{\mathbb{R}}$, where Δ^* is the convex hull of the $v_j \in N$ as defined in Section 3.1. A lattice polytope whose polar polytope is again a lattice polytope is called reflexive. For

reflexive polytopes (Δ, Δ°) , there exists a combinatorial formula for the Hodge numbers [43]

$$h_{1,1}(X_\Delta) = h_{\dim \Delta - 2, 1}(X_{\Delta^\circ}) = l(\Delta^\circ) - 1 - \dim \Delta - \sum_{\text{codim}(\theta^\circ)=1} l^*(\theta^\circ) + \sum_{\text{codim}(\theta^\circ)=2} l^*(\theta^\circ) l^*(\theta), \quad (3.3)$$

where θ and θ° is a dual pair of faces of Δ and Δ° . Furthermore, $l(\theta)$ is the number of lattice points of a face θ , and $l^*(\theta)$ is the number of its interior lattice points.

In our discussion of F-theory model building, we also encounter complete intersection Calabi-Yaus. The concept of polar pairs of reflexive lattice polytopes can be generalized as follows:

$$\begin{aligned} \Delta &= \Delta_1 + \cdots + \Delta_r & \Delta^\circ &= \langle \nabla_1, \dots, \nabla_r \rangle_{\text{conv}}, \\ \nabla^\circ &= \langle \Delta_1, \dots, \Delta_r \rangle_{\text{conv}} & \nabla &= \nabla_1 + \cdots + \nabla_r. \end{aligned} \quad (\nabla_n, \Delta_m) \geq -\delta_{nm}, \quad (3.4)$$

Here, r is the codimension of the Calabi-Yau and the defining equations $f_i = 0$ are sections of $\mathcal{O}(\Delta_i)$. The decomposition of the M -lattice polytope $\Delta \subset M_{\mathbb{R}}$ into a Minkowski sum (the Minkowski sum $A + B$ of two sets A, B is defined as follows: $A + B = \{a + b \mid a \in A, b \in B\}$) $\Delta = \Delta_1 + \cdots + \Delta_r$ is dual to a nef (numerically effective) partition of the vertices of a reflexive polytope $\nabla \subset N_{\mathbb{R}}$ such that the convex hulls $\langle \nabla_i \rangle_{\text{conv}}$ of the respective vertices and $0 \in N$ only intersect at the origin. The nef-property means that the restriction of the line bundles associated to the divisors specified by the N -lattice points to any algebraic curve of the variety are nonnegative. There exists a combinatorial formula for the Hodge numbers [44] which has been implemented in PALP.

In many string theory applications, and in particular also in F-theory, the fibration structure of a Calabi-Yau manifold is of great interest. For Calabi-Yaus which can be described in terms of toric geometry, the fibration structure can be deduced from the geometry of the lattice polytopes. If we are looking for toric fibrations where the fibers are Calabi-Yaus of lower dimensions, we have to search for reflexive subpolytopes of Δ° which have appropriate dimension. Given a base b and a fiber f , the fibrations descend from toric morphisms of the ambient spaces corresponding to a map $\phi : \Sigma \rightarrow \Sigma_b$ of fans in N and N_b , where $\phi : N \rightarrow N_b$ is a lattice homomorphism such that for each cone $\sigma \in \Sigma$, there is a cone $\sigma_b \in \Sigma_b$ that contains the image of σ . The lattice N_f for the fiber is the kernel of ϕ in N . The fiber polytope is then defined as follows: $\Delta_f^\circ = \Delta^\circ \cap N_f$. In order to guarantee the existence of a projection, one must find a triangulation of Δ_f° and extend it to a triangulation of Δ° . For each choice of triangulation, the homogeneous coordinates corresponding to the rays in Δ_f° can be interpreted as coordinates of the fiber.

3.3. Intersection Ring and Mori Cone

Two further pieces of data that are necessary in many string theory calculations are the intersection numbers of the toric divisors and the Mori cone, which is the dual of the Kähler cone. Inside the Kähler cone, the volumes such as (2.15) are positive. Thus, in the context of F-theory model, building the Kähler cone is needed in order to make statements about a decoupling limit.

Let us start with discussing the intersection ring. For a compact toric variety X_Σ the intersection ring is of the form $\mathbb{Z}[D_1, \dots, D_r]/\langle I_{\text{lin}} + I_{\text{non-lin}} \rangle$. The two ideals to be divided out take into account linear and nonlinear relations between the divisors. The linear relations have the form $\sum_j \langle m, v_j \rangle D_j$, where $m \in M$ form a set of basis vectors in the M-lattice. The non-linear relations are denoted by $R = \cup R_I$, where the R_I are of the form $R_I = D_{j_1} \dots D_{j_k} = 0$. They come from the exceptional set $Z = \cup Z_I$ defined in Section 3.1, which determines which homogeneous coordinates are not allowed to vanish at the same time. As mentioned before, this is the case when a collection of rays $\rho_{j_1}, \dots, \rho_{j_k} \in N$ is not contained in a single cone. The non-linear relations R generate the ideal $I_{\text{non-lin}}$ which is called Stanley-Reisner ideal. Thus, the intersection ring $A_*(X_\Sigma)$ of a non-singular toric variety has the following form:

$$A_*(X_\Sigma) = \frac{\mathbb{Z}[D_1, \dots, D_r]}{\langle R, \sum_j \langle m, v_j \rangle D_j \rangle}. \quad (3.5)$$

The definition of the intersection ring holds for non-singular toric varieties but may be generalized to the case where X_Σ is simplicial projective. This means that the toric variety may be singular, but still, all the cones of the fan Σ are simplicial. Such a situation may occur, for example, if we choose a nonmaximal triangulation of the polytope Δ^* . In this case, the intersection numbers take values in \mathbb{Q} . To compute the Stanley-Reisner ideal in the non-singular case, one must find a maximal triangulation of the fan Σ or the polytope Δ^* . In order to get intersection numbers, we still have to fix a normalization: for a maximal simplicial cone $\sigma \in \Sigma^{(n)}$ spanned by v_{j_1}, \dots, v_{j_n} , we fix the intersection numbers of the corresponding divisors to be $D_{j_1} \dots D_{j_n} = 1/\text{Vol}(\sigma)$, where $\text{Vol}(\sigma)$ is the lattice volume of σ (i.e., the geometric volume divided by the volume $1/n!$ of a basic simplex). If X is non-singular, the volume is 1. Using the intersection ring, one can compute the total Chern class of the tangent bundle T_X of X which is given by the following formula: $c(T_X) = \prod_{j=1}^r (1 + D_j)$.

So far, we have only discussed the intersection ring of the toric variety X . However in many applications, we rather need the intersection numbers for divisors on a hypersurface given by a divisor D in X . Here, we can make use of the restriction formula that relates the intersection form on the hypersurface divisor to the intersection form on X

$$D_{j_1} \dots D_{j_{n-1}}|_D = D_{j_1} \dots D_{j_{n-1}} \cdot D|_X. \quad (3.6)$$

This allows us to compute the intersection ring of D from the intersection ring of X . In (3.5) restriction to D amounts to computing the ideal quotients of I_{lin} and $I_{\text{non-lin}}$ with the ideal generated by D . By adjunction, the Chern class for the hypersurface specified by D is $c(D) = \prod_{j=1}^r (1 + D_j)/(1 + D)$.

In order to be able to calculate all the quantities defined in Section 2.2, we miss one more ingredient: the Mori cone. By definition, the Mori cone is the dual of the Kähler cone. We need the information about the Kähler cone in order to be able to compute the volumes of divisors. By definition, the volumes will be positive inside the Kähler cone. The Mori cone is generated by $l^{(1)}, \dots, l^{(k)}$, where $k = r - n$ if the fan Σ is simplicial. Otherwise, the number of Mori generators can be larger. The Mori cone L is then defined as follows: $L = \mathbb{R}_{\geq 0} l^{(1)} + \dots + \mathbb{R}_{\geq 0} l^{(k)}$. For the calculation of the Mori cone, we also require a maximal triangulation of Δ^* . Given such a triangulation, the Mori generators can be determined as follows [45]: take every pair of n -dimensional simplices (S_k, S_l) which have a common $n - 1$ -dimensional

simplex $s_{kl} = S_k \cap S_l$. Then, find the unique linear relation $\sum_i l_i^{k,l} v_i = 0$ with $v_i \in S_k \cup S_l$, where the $l_i^{k,l}$ are minimal integers and the coefficients of the points in $(S_k \cup S_l) \setminus (S_k \cap S_l)$ are non-negative. The Mori generators are then the minimal integers $l^{(a)}$ by which every $l^{k,l}$ can be expressed as positive integer linear combinations. There is an equivalent algorithm to determine the Mori generators due to Oda and Park [46] which has been implemented in an unreleased version of PALP [47]. Note that the relations $\sum_{i=1}^r l_i^{(a)} D_i = 0$ define the ideal I_{lin} in (3.5). Assembling the Mori vectors into a $k \times r$ -matrix, the columns of the matrix encode inequalities for the values of the Kähler parameters. Solving these inequalities yields a basis K_i of the Kähler cone such that the Kähler form of X can be written as $J = \sum_i r_i K_i$ with $r_i > 0$. Note that this prescription computes the Kähler cone of the toric variety X . It is often assumed that this is a good approximation for the Kähler cone of a hypersurface in X .

3.4. Toric Calculations Using PALP and Other Software

In string theory and F-theory, we deal with compactifications on Calabi-Yau threefolds and fourfolds. In F-theory model building, the base manifold B is a hypersurface in a four-dimensional toric ambient space. The fourfolds are complete intersections in a six-dimensional toric space. The associated lattice polytopes live in four- and six-dimensional integer lattices and typically have a large number of points. It is in general not possible to do calculations without computer support. There exist several software packages which are useful for particular aspects in toric geometry. In this section, we will mostly focus on the program PALP [29]. Before that, let us mention some other useful programs: Schubert by Katz and Strømme is a Maple package for calculations in intersection theory. TOPCOM [48] computes triangulations of point configurations. Singular [49] is a powerful computer algebra program which is optimized for calculations with polynomial rings such as the intersection ring. A recent addition is cohomCalg [50], which can compute line bundle-valued cohomology classes over toric varieties.

Let us now discuss some features and applications of PALP [29], which stands for “package for analyzing lattice polytopes”. It consists of several programs.

- (i) `poly.x` computes the data of a lattice polytope and its dual if the polytope is reflexive. The input can be either a weight matrix or the points of a polytope in the M -lattice or the N -lattice. Apart from the polytope data, `poly.x` computes Hodge numbers of the associated Calabi-Yau hypersurfaces, information about fibrations, and other data. `poly.x` has been extended with several features that include information about the facets of the polytope, data of Fano varieties and conifold Calabi-Yaus. In [51, 52], this extension of PALP has been used to find new Calabi-Yau manifolds with small $h^{1,1}$ which are obtained from known Calabi-Yau threefolds via conifold transitions. The full set of options in PALP can be obtained with `poly.x -h` and `poly.x -x` for extended options.
- (ii) The program `nef.x` can be used for complete intersection Calabi-Yaus. It takes the same input as `poly.x` and computes the polytope data, nef partitions, and Hodge numbers as well as information about fibrations. There are several extended options which include most notably the data of the Gorenstein cones (cf. [53] for the definition and construction in toric geometry) in the M/N -lattice.
- (iii) `cws.x` creates weight systems and combined weight systems of polytopes of dimension to be specified in the input.

- (iv) `class.x` classifies reflexive polytopes by searching for subpolytopes of a Newton polytope associated to a combined weight system.

Apart from recent applications in F-theory model building, which we will discuss in the next section, PALP has been used in many other contexts. A data base of Calabi-Yau threefolds has been generated by listing all 473 800 776 reflexive polyhedra in four dimensions [54]. In view of the landscape problem in string theory, the statistics of the polytope data is also of interest [55]. Some of the most recent extensions of PALP which we will mention below have already been used in [13, 24, 56].

3.5. Application to F-Theory GUTs

In this section, we make the connection to F-theory model building and discuss how the calculations discussed in Section 2.2 can be carried out explicitly. The approach discussed here is used in [13, 24]. Our aim is a systematic construction of a large class of examples of global F-theory models. The first step is the construction of the base manifold B . In [13], we have obtained a set of geometries by systematically constructing weight matrices associated to point and curve blowups on Fano hypersurfaces in \mathbb{P}_4 . In [24], we have considerably extended this class of models by defining hypersurfaces in a subset of the toric ambient spaces described by the 473 800 776 reflexive polyhedra in four dimensions [54]. Concretely, we have restricted ourselves to configurations, where the N -lattice polytopes have at most nine points. As one can check, for example, at [57], there are 1088 such polytopes. We used PALP to recover the toric data of the ambient space and considered all nonnegatively curved hypersurfaces in these ambient spaces. In order to be able to perform the calculations outlined in Section 2.2 we must compute the intersection ring and the Mori cone. We have achieved this by using an extended version of `poly.x` [47]. The following additional features have been implemented: processing of non-Calabi-Yau hypersurfaces by specifying the hypersurface degrees as input parameters, a calculation of the maximal triangulations of the N -lattice polytope, calculation of the Mori cone and the Stanley-Reisner ideal, and calculation of the intersection ring with the help of Singular. Using this data, we can identify del Pezzo divisors, check the existence of a decoupling limit, and compute the topological properties of matter curves and Yukawa points. In [24], we have analyzed a total number of 569 674 base manifolds. The resulting geometries are available at [58].

The next step in the calculation is to construct the Calabi-Yau fourfold X_4 which is an elliptic fibration over the base B . The toric data of X_4 is obtained by extending the weight matrix of B . Schematically, this looks as follows:

$$\begin{array}{cccccc}
 3 & 2 & 1 & 0 & \cdots & 0 \\
 * & * & 0 & w_{11} & \cdots & w_{1n} \\
 * & * & 0 & \cdots & \cdots & \cdots \\
 * & * & 0 & w_{m1} & \cdots & w_{mn}.
 \end{array} \tag{3.7}$$

Here, the w_{ij} denote the entries of the weight matrix associated to B . The $*$ -entries in the extended weight matrix have to be chosen in such a way that the fiber coordinates x, y are sections of K_B^{-2} and K_B^{-3} , respectively. These entries of the fourfold weight matrix contain

the information about the hypersurface degrees of the base. Not every extended weight system will lead to a Calabi-Yau fourfold of the form (2.1). The calculations can be done using `nef .x`. Several problems can appear: first, there may be no nef partition, and, therefore, our methods do not work. A second conceptual problem is that the polytope corresponding to the extended weight system is not always reflexive. Many of the combinatorial tools used in PALP are only valid for reflexive polytopes. Even though one might have a perfectly fine Calabi-Yau fourfold, we cannot apply our technology to them. The third issue is of a technical nature: due to the complexity of the fourfold polytopes one may reach the software bounds of PALP which results in numerical overflows. For the 569 674 extended weight systems discussed in [24], we find only 27 345 reflexive fourfold polytopes which have at least one nef partition. Furthermore, there are 18 632 reflexive polytopes without a nef partition, 381 232 nonreflexive polytopes, and 142 470 cases with numerical overflow.

Having found a reflexive fourfold polytope with at least one nef partition is not enough to have a good global F-theory model. If we further demand that the base B has at least one del Pezzo divisor with a mathematical or physical decoupling limit, the number of fourfolds decreases significantly. In addition, we should also impose some constraints on the regularity of the base. Demanding that B is Cartier leaves us with 16 011 good models. Imposing the stronger criterion of base point freedom, we are down to 7386 models. Focusing on these 7 386 good geometries, we apply the constraint that the nef partition should be compatible with the elliptic fibration. This information can be extracted from the output of `nef .x`. This further reduces the number of geometries to 3978.

Having found a good Calabi-Yau fourfold, we can construct a GUT model on every (del Pezzo) divisor. A toric description on how to impose a specific GUT group on a Tate model has been given in [6]. The Tate form (2.2) implies that the a_n appear in the monomials which contain z^n . We can isolate these monomials by identifying the vertex v_z in (∇_1, ∇_2) that corresponds to the z -coordinate in the Tate model. All the monomials that contain z^r are then in the following set:

$A_r = \{w_k \in \Delta_m : \langle v_z, w_k \rangle + 1 = r\}$, $v_z \in \nabla_m$, (26) where Δ_m is the dual of ∇_m , which denotes the polytope containing the z -vertex. The polynomials a_r are then given by the following expressions:

$$a_r = \sum_{w_k \in A_r} c_k^m \prod_{n=1}^2 \prod_{v_i \in \nabla_n} y_i^{\langle v_i, w_k \rangle + \delta_{mn}} \Big|_{x=y=z=1}. \quad (3.8)$$

Now, we can remove all the monomials in a_r which do not satisfy the factorization constraints (2.4) of the Tate algorithm. In order to perform this calculation, we have to identify the fiber coordinates (x, y, z) and the GUT coordinate w within the weight matrix of the fourfold. We have applied this procedure to every del Pezzo divisor in the 3978 “good” fourfold geometries. Note that the procedure described above can destroy the reflexivity of the polytope, which happens in about 30% of the examples. For $SU(5)$ -models, we found 11 275 distinct models (since the procedure has been applied to all del Pezzo divisors in a given base geometry not all these models may have a decoupling limit) with reflexive polyhedra, for $SO(10)$ GUTs, there are 10 832. $U(1)$ -restricted GUT models [14] can be engineered along the same lines. It turns out that $U(1)$ -restriction does not put any further constraints on the reflexivity of the polytope.

4. Outlook

In this paper we have discussed how toric geometry can be used to construct a large number of geometries that can support global F-theory GUTs. Using this technology, we could show that elementary consistency constraints greatly reduce the number of possible models. However, due to computational constraints, we did not quite succeed in systematically listing all possible F-theory models within a class of geometries. Such an endeavor would require substantial changes in the computer programs we are using. It is actually quite remarkable that we could make use of PALP for Calabi-Yau fourfolds and non-Calabi-Yau threefolds, since this goes beyond what it was originally designed for.

Let us present a list of suggestions to extend PALP in order to improve the applicability to the current problems in mathematics and physics and to make it more accessible for users. The original purpose of PALP was to solve a classification problem for polytopes. Over the years, it has been adjusted and extended in order to be applied to specific problems. Many of the basic routines that were implemented to tackle some special questions could be used in much more general contexts but cannot be easily accessed. Therefore, a better modularization of the software is necessary in order to have flexible access to these basic routines. Another problem of PALP is that one has to specify several parameters and bounds such as the number of points in a polytope in a given dimension at the compilation of the program. It would be practical to have fully dynamical dimensions in order to work with a precision tailored to the problem at hand without recompiling.

A fundamental change would be to step away from the description of polytopes and instead use the ray representation which has the full data of the cones. This is necessary if one wants to deal with non-reflexive polytopes. A further extension which has already been partially implemented is to include triangulations, intersection rings, and even the calculation of Picard-Fuchs operators needed for mirror symmetry calculations into PALP. The ultimate goal is to have an efficient and versatile program which can be used for toric calculations of all kinds without having to rely on commercial software. Finally, a detailed documentation of all the features of PALP would be helpful [59].

As for the search for F-theory models, an extended version of PALP would hopefully help to overcome the problems of nonreflexivity and overflows we have encountered in [24]. Apart from finding new examples for physics applications, one might also attempt a partial classification of Calabi-Yau fourfolds. Enumerating all toric Calabi-Yau fourfolds may be out of reach or even impossible, but for finding all models of type (2.1), one can at least give a prescription for the construction: take each of the 473 800 776 reflexive polyhedra in four dimensions and put in all nonnegatively curved hypersurfaces that are not Calabi-Yau. Then, construct fourfolds which are elliptic fibrations over these base manifolds. A rough estimate shows that this procedure would yield $\mathcal{O}(10^{11})$ fourfold geometries.

Acknowledgments

In October 2010, M. Kreuzer asked J. Knapp to be the coauthor of this paper. Sadly, he passed away on November 26, 2010, when this work was still in the early stages. J. Knapp is grateful for many years of collaboration with him, as well as for his constant support and encouragement. The author would like to thank her collaborators Ching-Ming Chen, Christoph Mayrhofer, and Nils-Ole Walliser for a pleasant and fruitful collaboration on the projects [13, 24] this paper is based on. Furthermore, she thank Emanuel Scheidegger

for valuable comments on the paper. This work has been supported by World Premier International Research Center Initiative (WPI Initiative), MEXT, Japan.

References

- [1] C. Vafa, "Evidence for F-theory," *Nuclear Physics B*, vol. 469, pp. 403–418, 1996.
- [2] R. Donagi and M. Wijnholt, "Model building with F-theory," <http://arxiv.org/abs/0802.2969>.
- [3] C. Beasley, J. J. Heckman, and C. Vafa, "GUTs and exceptional branes in F-theory—I," *Journal of High Energy Physics*, vol. 2009, no. 1, article 058, 2009.
- [4] C. Beasley, J. J. Heckman, and C. Vafa, "GUTs and exceptional branes in F-theory—II. Experimental predictions," *Journal of High Energy Physics*, vol. 2009, no. 1, article 059, 2009.
- [5] B. Andreas and G. Curio, "From local to global in F-theory model building," *Journal of Geometry and Physics*, vol. 60, no. 9, pp. 1089–1102, 2010.
- [6] R. Blumenhagen, T. W. Grimm, B. Jurke, and T. Weigand, "Global F-theory GUTs," *Nuclear Physics B*, vol. 829, no. 1-2, pp. 325–369, 2010.
- [7] J. Marsano, N. Saulina, and S. Schafer-Nameki, "Compact F-theory GUTs with $U(1)_{PQ}$," *Journal of High Energy Physics*, vol. 2010, no. 4, article 095, 2010.
- [8] W. Grimm, S. Krause, and T. Weigand, "F-theory GUT vacua on compact Calabi-Yau fourfolds thomas," *Journal of High Energy Physics*, vol. 2010, no. 7, article 037, 2010.
- [9] R. Blumenhagen, A. Collinucci, and B. Jurke, "On instanton effects in F-theory," *Journal of High Energy Physics*, vol. 2010, no. 8, article 079, 2010.
- [10] M. Cvetič, I. García-Etxebarria, and J. Halverson, "Global F-theory models: instantons and gauge dynamics," *Journal of High Energy Physics*, vol. 2011, no. 1, article 073, 2011.
- [11] H. Hayashi, T. Kawano, Y. Tsuchiya, and T. Watari, "More on dimension-4 proton decay problem in F-theory. Spectral surface, discriminant locus and monodromy," *Nuclear Physics B*, vol. 840, no. 1-2, pp. 304–348, 2010.
- [12] C.-M. Chen and Y.-C. Chung, "Flipped $SU(5)$ GUTs from E_8 singularities in F-theory," *Journal of High Energy Physics*, vol. 2011, no. 3, article 049, 2011.
- [13] C.-M. Chen, J. Knapp, M. Kreuzer, and C. Mayrhofer, "Global $SO(10)$ F-theory GUTs," *Journal of High Energy Physics*, vol. 2010, no. 10, article 057, 2010.
- [14] T. W. Grimm and T. Weigand, "Abelian gauge symmetries and proton decay in global F-theory GUTs," *Physical Review D*, vol. 82, no. 8, Article ID 086009, 17 pages, 2010.
- [15] J. Marsano, N. Saulina, and S. Schäfer-Nameki, "A note on G-fluxes for F-theory model building," *Journal of High Energy Physics*, vol. 2010, no. 11, article 088, 2010.
- [16] Y.-C. Chung, "On global flipped $SU(5)$ GUTs in F-theory," *Journal of High Energy Physics*, vol. 2011, no. 3, article 126, 2011.
- [17] J. J. Heckman, Y. Tachikawa, C. Vafa, and B. Wecht, " $N = 1$ SCFTs from brane monodromy," *Journal of High Energy Physics*, vol. 2010, no. 11, article 132, 2010.
- [18] M. Cvetič, I. García-Etxebarria, and J. Halverson, "On the computation of non-perturbative effective potentials in the string theory landscape—IIB/F-theory perspective—," *Fortschritte der Physik*, vol. 59, no. 3-4, pp. 243–283, 2011.
- [19] S. Cecotti, C. Cordova, J. J. Heckman, and C. Vafa, "T-branes and monodromy," <http://arxiv.org/abs/1010.5780>.
- [20] J. Marsano, "Hypercharge flux, exotics, and anomaly cancellation in F-theory grand unification," *Physical Review Letters*, vol. 106, no. 8, Article ID 081601, 2011.
- [21] A. Collinucci and R. Savelli, "On flux quantization in F-theory," <http://arxiv.org/abs/1011.6388>.
- [22] C.-C. Chiou, A. E. Faraggi, R. Tatar, and W. Walters, "T-branes and Yukawa couplings," *Journal of High Energy Physics*, vol. 2011, no. 5, article 023, 2011.
- [23] C. Lüdeling, H. P. Nilles, and C. C. Stephan, "The potential fate of local model building," *Physical Review D*, vol. 83, no. 8, Article ID 086008, 14 pages, 2011.
- [24] J. Knapp, M. Kreuzer, C. Mayrhofer, and N.-O. Walliser, "Toric construction of global F-theory GUTs," *Journal of High Energy Physics*, vol. 2011, no. 3, article 188, 2011.
- [25] M. J. Dolan, J. Marsano, N. Saulina, and S. Schafer-Nameki, "F-theory GUTs with $U(1)$ symmetries: generalities and survey," <http://arxiv.org/abs/1102.0290>.
- [26] A. Collinucci, "New F-theory lifts," *Journal of High Energy Physics*, vol. 2009, no. 8, article 076, 2009.
- [27] A. Collinucci, "New F-theory lifts II: permutation orientifolds and enhanced singularities," *Journal of High Energy Physics*, vol. 2010, no. 4, article 076, 2010.

- [28] R. Blumenhagen, T. W. Grimm, B. Jurke, and T. Weigand, "F-theory uplifts and GUTs," *Journal of High Energy Physics*, vol. 2009, no. 9, article 053, 2009.
- [29] M. Kreuzer and H. Skarke, "PALP: a package for analysing lattice polytopes with applications to toric geometry," *Computer Physics Communications*, vol. 157, no. 1, pp. 87–106, 2004.
- [30] F. Denef, "Les Houches lectures on constructing string vacua," <http://arxiv.org/abs/0803.1194>.
- [31] J. J. Heckman, "Particle physics implications of F-theory," *Annual Review of Nuclear and Particle Science*, vol. 60, pp. 237–265, 2010.
- [32] T. Weigand, "Lectures on F-theory compactifications and model building," *Classical and Quantum Gravity*, vol. 27, no. 21, Article ID 214004, 2010.
- [33] W. Fulton, *Introduction to Toric Varieties*, vol. 131 of *Annals of Mathematics Studies*, Princeton University Press, Princeton, NJ, USA, 1993.
- [34] M. Kreuzer, "Toric geometry and Calabi-Yau compactifications," *Ukrainian Journal of Physics*, vol. 55, no. 5, pp. 613–625, 2010.
- [35] D. A. Cox, J. B. Little, and H. Schenck, *Toric Varieties*, American Mathematical Society, 2011, <http://www.cs.amherst.edu/~7Edac/toric.html>.
- [36] K. Kodaira, "On compact analytic surfaces II," *The Annals of Mathematics*, vol. 77, no. 3, pp. 563–626, 1963.
- [37] J. Tate, "Algorithm for determining the type of a singular fiber in an elliptic pencil," in *Modular Functions of One Variable IV (Proc. Internat. Summer School, Univ. Antwerp, Antwerp, 1972)*, vol. 476 of *Lecture Notes in Mathematics*, pp. 33–52, Springer, Berlin, Germany, 1975.
- [38] C. Cordova, "Decoupling gravity in F-theory," <http://arxiv.org/abs/0910.2955>.
- [39] P. Griffiths and J. Harris, *Principles of Algebraic Geometry*, Wiley Classics Library, John Wiley & Sons, New York, NY, USA, 1994.
- [40] V. Braun, "Discrete Wilson lines in F-theory," <http://arxiv.org/abs/1010.2520>.
- [41] C.-M. Chen and Y.-C. Chung, "On F-theory E_6 GUTs," *Journal of High Energy Physics*, vol. 2011, no. 3, article 129, 2011.
- [42] R. Donagi and M. Wijnholt, "Higgs bundles and UV completion in F-theory," <http://arxiv.org/abs/0904.1218>.
- [43] V. V. Batyrev, "Dual polyhedra and mirror symmetry for Calabi-Yau hypersurfaces in toric varieties," *Journal of Algebraic Geometry*, vol. 3, no. 3, pp. 493–535, 1994.
- [44] V. V. Batyrev and L. A. Borisov, "Mirror duality and string-theoretic Hodge numbers," *Inventiones Mathematicae*, vol. 126, no. 1, pp. 183–203, 1996.
- [45] P. Berglund, S. Katz, and A. Klemm, "Mirror symmetry and the moduli space for generic hypersurfaces in toric varieties," *Nuclear Physics B*, vol. 456, no. 1-2, pp. 153–204, 1995.
- [46] T. Oda and H. Park, "Linear Gale transforms and Gel'fand-Kapranov-Zelevinskij decompositions," *The Tohoku Mathematical Journal*, vol. 43, no. 3, pp. 375–399, 1991.
- [47] M. Kreuzer and N.-O. Walliser, work in progress.
- [48] J. Rambau, "TOPCOM: triangulations of point configurations and oriented matroids," in *Mathematical Software (Beijing, 2002)*, A. M. Cohen, X.-S. Gao, and N. Takayama, Eds., pp. 330–340, World Scientific, River Edge, NJ, USA, 2002.
- [49] W. Decker, G.-M. Greuel, G. Pfister, and H. Schönemann, "Singular 3-1-2—a computer algebra system for polynomial computations," <http://www.singular.uni-kl.de>.
- [50] R. Blumenhagen, B. Jurke, T. Rahn, and H. Roschy, "Cohomology of line bundles: a computational algorithm," *Journal of Mathematical Physics*, vol. 51, no. 10, Article ID 103525, 2010.
- [51] V. Batyrev and M. Kreuzer, "Constructing new Calabi-Yau 3-folds and their mirrors via conifold transitions," <http://arxiv.org/abs/0802.3376>.
- [52] M. Kreuzer, "The making of Calabi-Yau spaces: beyond toric hypersurfaces," *Fortschritte der Physik*, vol. 57, no. 5–7, pp. 625–631, 2009.
- [53] V. V. Batyrev and L. A. Borisov, "Dual cones and mirror symmetry for generalized Calabi-Yau manifolds," in *Mirror Symmetry, II*, vol. 1 of *AMS/IP Stud. Adv. Math.*, pp. 71–86, American Mathematical Society, Providence, RI, USA, 1997.
- [54] M. Kreuzer and H. Skarke, "Complete classification of reflexive polyhedra in four dimensions," *Advances in Theoretical and Mathematical Physics*, vol. 4, no. 6, pp. 1209–1230, 2000.
- [55] M. Kreuzer, "On the statistics of lattice polytopes," in *International Conference on Information Theory and Statistical Learning (ITSL '08)*, pp. 119–124, Las Vegas, Nev, USA, July 2008.
- [56] A. Collinucci, M. Kreuzer, C. Mayrhofer, and N. O. Walliser, "Four-modulus "swiss Cheese" chiral models," *Journal of High Energy Physics*, vol. 2009, no. 7, article 074, 2009.
- [57] <http://hep.itp.tuwien.ac.at/~kreuzer/CY/>.

[58] <http://hep.itp.tuwien.ac.at/f-theory/>.

[59] A. Braun and N.-O. Walliser, work in progress.

Review Article

Baryonic Symmetries in AdS_4/CFT_3 : An Overview

Diego Rodriguez-Gomez^{1,2}

¹ Department of Physics, Technion-Israel Institute of Technology, Haifa 3200, Israel

² Department of Mathematics and Physics, University of Haifa at Oranim, Tivon 36006, Israel

Correspondence should be addressed to Diego Rodriguez-Gomez,
drodrigu@physics.technion.ac.il

Received 27 February 2011; Accepted 14 March 2011

Academic Editor: Yang-Hui He

Copyright © 2011 Diego Rodriguez-Gomez. This is an open access article distributed under the Creative Commons Attribution License, which permits unrestricted use, distribution, and reproduction in any medium, provided the original work is properly cited.

Global symmetries play an important role in classifying the spectrum of a gauge theory. In the context of the AdS/CFT duality, global baryon-like symmetries are specially interesting. In the gravity side, they correspond to vector fields in AdS arising from KK reduction of the SUGRA p -form potentials. We concentrate on the AdS_4/CFT_3 case, which presents very interesting characteristic features. Following arXiv:1004.2045, we review aspects of such symmetries, clarifying along the way some arguments in that reference. As a byproduct, and in a slightly unrelated context, we also study \mathcal{Z} minimization, focusing on the HVZ theory.

1. Introduction

Over the last few years there has been considerable progress towards understanding the AdS_4/CFT_3 duality [1]. The maximally supersymmetric example of this duality corresponds to the $AdS_4 \times S^7$ space. This space arises as the near-horizon region of the background sourced by a stack of M2 branes moving in \mathbb{C}^4 . Conversely, standard decoupling limit arguments show that a dual description is given by the CFT_3 on the world volume of the M2 branes. Following on the seminal work in [2, 3], Aharony, Bergman et al. (henceforth ABJM) constructed in [4] what it is by now agreed to be the field theory dual to N M2 branes probing the $\mathbb{C}^4/\mathbb{Z}_k$ singularity, of which the maximally SUSY example is the $k = 1$ case.

Since then, much activity has been devoted to further understand this duality in less supersymmetric cases. While there are purely theoretical reasons for that—as constructing and understanding dual pairs shedding information on both field theoretic and gravitational aspects—, a number of potential applications, in particular in what it has been dubbed the AdS/CMT duality, have been recently considered.

These less supersymmetric examples arise from M2 branes probing more involved singularities, which generically have a rich topological structure. In particular, supergravity p -form potentials can be KK reduced on these topologically nontrivial cycles giving rise to vector fields in AdS . In turn, these are related to global symmetries of the dual CFT_3 . On general grounds, global symmetries play an important role in classifying the spectrum of a theory. Furthermore, they are also expected to be relevant from the point of view of potential applications of AdS/CFT . It is thus important to understand them in the context of the AdS_4/CFT_3 duality.

Of particular interest are the global baryonic symmetries. These are abelian symmetries whose charged states have dimensions $\mathcal{O}(N)$. As such, they cannot correspond to KK states ($\Delta \sim \mathcal{O}(1)$), and must be dual to wrapped branes. Thus, they must be associated to the nontrivial topology of the cone where the M2 move. Indeed, as mentioned, nontrivial topology allows for the supergravity p -forms to wrap on cycles leading to gauge fields in AdS_4 as potential duals to these baryonic symmetries. However, as we will discuss below, following [5] (see also [6]) the fate of these bulk fields and their boundary duals, is remarkably different than the AdS_5 case (see, e.g., [7] and references therein for an account of this case). In this short review we discuss several aspects of these symmetries by extracting as much information as possible from the gravity side of the correspondence. We start in Section 2 with a lightning overview of some relevant facts about the AdS_4/CFT_3 duality. We then turn in Section 3 to the baryonic symmetries of interest. In Section 4 we suggest an application to a particularly interesting geometry, in particular slightly clarifying arguments presented in [5]. As a by-product, in the appendix we apply \mathcal{L} -minimization to the HVZ theory.

2. M2 Branes Probing CY_4 : General Aspects

As discussed in the introduction, the AdS_4/CFT_3 duality arises as the near horizon limit of a stack of M2 branes probing a conical geometry. In fact, the low energy limit of the M2 brane worldvolume theory must supply the CFT side of the correspondence, according to the usual decoupling limit arguments [1].

The best understood case is that of M2 branes in flat space, when the near horizon region is the maximally supersymmetric $AdS_4 \times S^7$ space. In turn, the dual field theory is the $U(N) \times U(N)$ Chern-Simons theory with levels $(1, -1)$ and particular matter content constructed in [4]. This theory arises as a member of a whole family of $\mathcal{N} = 6$ SCFT's with levels $(k, -k)$ [4, 8]. For generic k the moduli space is the orbifold $\mathbb{C}^4/\mathbb{Z}_k|_{(1, 1, -1, -1)}$. It is only for $k = 1, 2$ that there is a quantum-mechanical enhancement to $\mathcal{N} = 8$ due to special properties of monopole operators. Conversely, the gravity side of the duality is provided by the near horizon region of the background sourced by a stack of M2 branes probing this orbifold, namely, $AdS_4 \times S^7/\mathbb{Z}_k$. The \mathbb{Z}_k orbifold acts by quotienting the $U(1)$ fiber of the fibration $S^7 \sim S^1 \hookrightarrow \mathbb{P}^3$. In fact, in the large k limit, the fiber shrinks and the geometry is better understood as the IIA $AdS_4 \times \mathbb{P}^3$ background with suitable fluxes to preserve 24 supersymmetries. From this perspective, the vector of CS levels in gauge group space specifies the $U(1)$ dual to the M-theory circle. Indeed, diagonal monopole operators, charged under this $U(1)$, become the KK states of the reduction, that is, the D0 branes [4].

It is clearly greatly desirable to understand the AdS_4/CFT_3 duality in the generic case, where the M2 branes probe less symmetric spaces X . On general grounds, the radius/energy relation of AdS/CFT requires the manifold X to be a cone over a 7-dimensional base Y ,

that is, $ds^2(X) = dr^2 + r^2 ds(Y)^2$. Then the appropriate 11-dimensional supergravity solution corresponding to N M2 branes located at the tip of X is

$$ds_{11}^2 = h^{-2/3} ds^2(\mathbb{R}^{1,2}) + h^{1/3} ds^2(X), \quad G = d^3x \wedge dh^{-1}, \quad h = 1 + \frac{R^6}{r^6}. \quad (2.1)$$

In the near horizon limit, and upon defining $z = R^2/r^2$, the space becomes a Freund-Rubin product space between AdS_4 , whose metric in Poincare coordinates is

$$ds^2(AdS_4) = \frac{dz^2 + dx(\mathbb{R}^{1,2})^2}{z^2}, \quad (2.2)$$

and the base Y

$$ds_{11}^2 = R^2 \left(\frac{1}{4} ds^2(AdS_4) + ds^2(Y) \right), \quad G = \frac{3}{8} R^3 \text{Vol}(AdS_4). \quad (2.3)$$

Furthermore, the flux quantization condition leads to the relation

$$R = 2\pi\ell_p \left(\frac{N}{6\text{Vol}(Y)} \right)^{1/6}. \quad (2.4)$$

On the other hand, constructing the corresponding dual field theories has proved remarkably difficult. Only in the last few years we have seen big progress along these lines. From the CFT point of view, general field theory arguments, discussed for the 3d case at hand in [9], show that theories with $\mathcal{N} \geq 2$ are of special interest due to the existence of a $U(1)_R$ symmetry. This symmetry endows the moduli space of a graded structure which allows to classify chiral operators according to their R-charge; which equals, in virtue of the superconformal algebra, their scaling dimension. At the same time, it automatically implies that the moduli space has a cone-like structure. We will thus demand $\mathcal{N} \geq 2$, which in turn requires, on general grounds [10], the M2 branes to move in spaces of at most $SU(4)$ holonomy. Following the ABJM example, it is natural to consider Chern-Simons-matter theories as potential SCFT duals. As shown in [11], $\mathcal{N} \geq 3$ fixes the superpotential couplings to be proportional to the CS levels, thus almost ensuring conformal invariance. However, for our purposes we will be mostly interested in the less restrictive but yet tractable (due to the existence of $U(1)_R$) $\mathcal{N} = 2$ case, where the dual geometry is strictly CY_4 (i.e., Y is Sasaki-Einstein), which we will further assume toric. While we refer the reader to the standard literature for a thorough introduction to toric geometry (for a physics related discussion, see, e.g., [12]), let us briefly highlight, for completeness, the basic ideas. The cone $\mathcal{C}(Y)$ is *toric* if it can be seen as a $U(1)^4$ fibration over a polyhedral cone in \mathbb{R}^4 . This polyhedral cone defined as the convex set of the form $\cap\{\mathbf{x} \cdot \mathbf{v}_\alpha \geq 0\} \subset \mathbb{R}^4$, where $\mathbf{v}_\alpha \in \mathbb{Z}^4$ are integer vectors. The Calabi-Yau condition implies that, with a suitable choice of basis, we can write $\mathbf{v}_\alpha = (1, \mathbf{w}_\alpha)$, with $\mathbf{w}_\alpha \in \mathbb{Z}^3$. If we plot these latter points in \mathbb{R}^3 and take their convex hull, we obtain the *toric diagram*. In fact, the toric diagram contains all the relevant information about the CY_4 geometry.

As shown in [13–15] and briefly reviewed in Section 4, toric manifolds naturally arise as moduli space of $\mathcal{N} = 2$ CS-matter quiver gauge theories with toric superpotentials whose

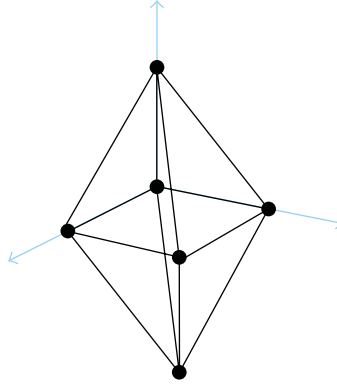


Figure 1: The toric diagram for $C(Q^{111})$.

levels add up to zero. (By toric W we mean a W where each field appears exactly twice, one time in a monomial with $+$ sign, another time in a monomial with sign $-$.) Furthermore, very much like in ABJM, the CS level vector in gauge space selects the M-theory circle, which at generic level is quotiented. Thus, the actual moduli space of these $\mathcal{N} = 2$ Chern-Simons-matter theories is a certain \mathbb{Z}_k quotient of the toric CY_4 . In Section 4 we will study in more detail one such example, conjectured to be dual to the cone over Q^{111} , whose toric diagram we show in Figure 1.

We should note that, as opposed to the ABJM case, in the $\mathcal{N} = 2$ cases this circle generically collapses as one moves on the base of the cone. This motivates the recently appeared proposals [16, 17] involving fundamental matter as well as bifundamental fields, as, on general grounds, associated to these collapsing loci there can be extra flavor branes in the IIA reduction.

Yet one more warning note is in order. While the construction [13–15] yields to toric CY_4 classical abelian moduli spaces, it yet remains to be understood whether at the nonabelian quantum level these theories are indeed SCFT's. Only very recently a manageable criterion to determine whether a 3d theory flows to an IR fixed point, which amounts to the minimization of the partition function \mathcal{Z} , has been proposed in [18] (see also [19]). One particular example where to put this at practice is the HVZ theory [20]. While at the classical abelian level the moduli space is $\mathbb{C}^2/\mathbb{Z}_k \times \mathbb{C}^2$, a more careful analysis [21] shows that the chiral ring (studied at large k to avoid subtleties with monopole operators) contains completely unexpected nonabelian branches while there is no trace of the necessary $SO(4)_R$ symmetry of the generically $\mathcal{N} = 4$ orbifold. In fact, as shown in [22], the superconformal index fails to meet the gravity expectations. Indeed, as briefly discussed in the appendix, when the \mathcal{Z} -minimization is applied to the HVZ theory it suggests that for no k it can be dual to the ABJM model. In [23] a variant of the theory with explicit $\mathcal{N} = 3$ SUSY and no extra branches in the chiral ring was considered, finding however, that the index computation was still in disagreement with the expectations.

3. Global Symmetries in AdS_4/CFT_3 and Their Spontaneous Breaking

We have so far discussed generic aspects of the AdS_4/CFT_3 duality. As described, the cases of interest are those where a stack of M2 branes probes a CY_4 cone. In turn, these

cones generically have a nontrivial topology, in particular containing $b_2(Y) \neq 0$ 2 cycles. This allows the fluctuations of the supergravity potentials to wrap on them yielding to vector fields on AdS_4 . In fact, due to Poincare duality $\dim H_5(Y) = \dim H_2(Y) = b_2(Y)$. We can then introduce a set of dual harmonic five-form $\alpha_1, \dots, \alpha_{b_2(Y)}$ and consider 6-form potential fluctuations of the form

$$\delta C_6 = \frac{2\pi}{T_5} \sum_{I=1}^{b_2(Y)} \mathcal{A}_I \wedge \alpha_I. \quad (3.1)$$

Upon KK reduction, this gives rise to $b_2(Y)$ massless gauge fields \mathcal{A}_I in AdS_4 . These fields sit in certain multiplets, known from the supergravity point of view as *Betti multiplets* (see, e.g., [24]).

In the context of the AdS_5/CFT_4 , these Betti symmetries correspond to global baryonic symmetries on the field theory side. In fact, these arise from the $U(1)$ factors inside the $\prod U(N)$ total gauge group, which in 4d are IR free. It is possible to show that indeed the b_2 nonanomalous such $U(1)$'s—which appear as global baryonic symmetries—are identified with these Betti multiplets (see, e.g., [7] and references therein for a comprehensive discussion).

In turn, in the AdS_4/CFT_3 case the role of these symmetries must be different. This can be inferred from general field theory arguments, as they clearly cannot arise from decoupled $U(1)$ factors, which are not IR free in 3 dimensions. Nevertheless, due to their origin, similar to the AdS_5 case, we will still refer to them as baryonic symmetries. (When referring to the ABJM theory the difference $U(1)$ gauge field is sometimes also called baryonic $U(1)$, mirroring the Klebanov-Witten terminology—recall that ABJM is described by the same quiver and superpotential as the Klebanov-Witten theory, only in one dimension less and adding CS for the gauge groups. We stress that our baryonic symmetries are very different from this one, which is basically the M-theory circle.) Since on general grounds global symmetries are of much help in classifying the spectrum of a gauge theory, the study of such baryonic-like $U(1)$'s is indeed of much interest. Let us now turn to the supergravity side to extract as much information as possible about these symmetries and their implication in the dual field theory.

Let us note that while the CY_4 might have other types of cycles, only 2 cycles (and the Poincare-dual 5 cycles) are relevant for our discussion. As discussed in [5], the toric CY_4 of interest can typically have additional 6 cycles, which manifest themselves as internal points in the toric diagram. Nevertheless, it is clear that these will not lead to vector fields in AdS_4 upon KK reduction of SUGRA p -forms on them, and so their role must be different than that of 2 and 5 cycles. In fact, as briefly discussed in [5], it appears that these 6 cycles can yield to nonperturbative corrections to superpotentials, as euclidean 5-branes can be wrapped on them. Since we will be mostly concerned with global baryon-like symmetries, we will not touch upon these 6 cycles and focus for the rest of the contribution on 2 and 5 cycles.

Finally, making use of results in [5, 25] it was argued that the number of such two cycles is given by $b_2(Y) = d - 4$, with d being the number of external points in the toric diagram. While this result is strictly valid only for isolated singularities, we note that it coincides with the conjecture in [26, 27]. We note that, as discussed above, internal points, being related to 6 cycles over which no SUGRA p -form yields an AdS_4 vector upon KK reduction, are not related to baryonic symmetries. Conversely, the $d - 4$ number of such symmetries does not depend on the number of internal points.

3.1. Gauge Fields in AdS_4

The $b_2(Y)$ vector fields satisfy, at the linearized level, Maxwell equations in AdS_4 . (The vector fields arising from KK reduction correspond to abelian bulk gauge fields, and thus will correspond to global/gauged $U(1)$ boundary symmetries. In fact, as discussed in the main text, wrapped branes behave as sources of this abelian theory. Thus, we do not expect any nonabelian enhancement.) Note that this argument is strictly applicable to isolated singularities. Furthermore, these $b_2(Y)$ copies of 4d E & M generically contain both electric and magnetic point like sources in AdS_4 . From the 11-dimensional point of view, these point like electrons and monopoles will become wrapped branes, and their role will be crucial in the following.

Let us analyze more in detail E and M in AdS_4 . In fact, we will keep the discussion generic and consider a vector field in AdS_{d+1} . We can set $A_z = 0$ away from the sources. Then, using the straightforward generalization to AdS_{d+1} of the coordinates in (2.2), the bulk equations of motion set

$$A_\mu = a_\mu + j_\mu z^{d-2}, \quad (3.2)$$

where the a_μ, j_μ satisfy the free Maxwell equation in the boundary directions. Furthermore, Lorentz gauge for these is automatically imposed. In fact, this can be naturally interpreted as fixing bulk Coulomb gauge upon regarding z as the time coordinate. The condition $A_z = 0$ away from the source is then the standard radiation gauge in that context.

The AdS/CFT duality requires specifying the boundary conditions for the fluctuating fields in AdS . In particular, and crucially different to AdS_5 , vector fields in AdS_4 admit different sets of boundary conditions [28–30] leading to different boundary CFT's. Coming back to (3.2), it turns out that in $d < 4$ both behaviors have finite action, and thus can be used to define a consistent AdS/CFT duality. Furthermore, the fluctuations a_μ, j_μ are naturally identified, according to the AdS/CFT rules, with a dynamical gauge field and a global current in the boundary, respectively. In accordance with this identification, (3.2) and the usual AdS/CFT prescription shows each field to have the correct scaling dimension for this interpretation: for a gauge field $\Delta(a_\mu) = 1$, while for a global current $\Delta(j_\mu) = 2$.

Let us now concentrate on the case of interest $d = 3$, where both quantizations are allowed. In order to have a well-defined variational problem for the gauge field in AdS_4 we should be careful with the boundary terms when varying the action. In general, we have

$$\delta S = \int \left\{ \frac{\partial \sqrt{\det g} \mathcal{L}}{\partial A_M} - \partial_N \frac{\partial \sqrt{\det g} \mathcal{L}}{\partial \partial_N A_M} \right\} \delta A_M + \partial_N \left\{ \frac{\partial \sqrt{\det g} \mathcal{L}}{\partial \partial_N A_M} \delta A_M \right\}. \quad (3.3)$$

The bulk term gives the equations of motion whose solution behaves as (3.2). In turn, the boundary term can be seen to reduce to

$$\delta S_B = -\frac{1}{2} \int_{\text{Boundary}} j_\mu \delta a^\mu. \quad (3.4)$$

Therefore, in order to have a well-posed variational problem, we need to demand $\delta a_\mu = 0$; that is, we need to impose boundary conditions where a_μ is fixed in the boundary.

On the other hand, since in $d = 3$ both behaviours for the gauge field have finite action, we can consider adding suitable boundary terms such that the action becomes [30]

$$S = \frac{1}{4} \int \sqrt{\det g} F_{AB} F^{AB} + \frac{1}{2} \int_{\text{Boundary}} \sqrt{\det g} A^\mu F_{z\mu} |_{\text{Boundary}}. \quad (3.5)$$

The boundary term is now

$$\delta S_B = \frac{1}{2} \int_{\text{Boundary}} a_\mu \delta j^\mu, \quad (3.6)$$

so that we need to impose the boundary condition $\delta j_\mu = 0$; that is, fix the boundary value of j_μ .

The radiation-like gauge $A_z = 0$ suggests to interpret z as the time direction. Defining then the usual electric and magnetic fields $\vec{B} = (1/2)\epsilon^{\mu\nu\rho} F_{\nu\rho}$ and $\vec{E} = F_{\mu z}$, we have

$$B^\mu = \epsilon^{\mu\nu\rho} \partial_\nu a_\rho + \epsilon^{\mu\nu\rho} \partial_\nu j_\rho z, \quad E^\mu = j^\mu z^2. \quad (3.7)$$

In terms of these, the two sets of boundary conditions correspond, on the boundary, to either setting $E_\mu = 0$ while leaving a_μ unrestricted, or setting $B_\mu = 0$ while leaving j_μ unrestricted. To be more explicit, recalling the *AdS/CFT* interpretation of a_μ, j_μ , the quantization $E_\mu = 0$ is dual to a boundary CFT where the $U(1)$ gauge field is *dynamical*, while the quantization $B_\mu = 0$ is dual to a boundary CFT where the $U(1)$ is ungauged and is instead a *global symmetry*. Furthermore, as discussed in [31] for the scalar counterpart, once the improved action is taken into account the two quantizations are Legendre transformations of one another [6], as can be seen by for example, computing the free energy in each case.

In turn, this has an important consequence for the spectrum of electrons and monopoles in this 4d E & M—which of course come wrapped branes from an 11-dimensional point of view-. Let us consider an M5 brane wrapped in one of the $b_2(Y)$ 5 manifolds $\Sigma_5 \subset Y$. From the *AdS₄* point of view, this brane looks like a pointlike electric charge for the corresponding vector field. On the other hand, the linearized C_6 fluctuation which such brane sources must be of the form $\delta C_6 \sim f(z) dt \wedge \text{Vol}(\Sigma_5)$. Upon reduction this precisely yields to $E_0 \neq 0$ while $B_\mu = 0$. Thus, it follows that wrapped M5 branes are only allowed upon choosing the quantization condition which fixes a_μ . Conversely, dual wrapped M2 branes, though nonSUSY, would only be allowed upon choosing the boundary conditions which fix j_μ . In turn, these boundary conditions do forbid the wrapped M5.

One can consider electric-magnetic duality in the bulk theory, which exchanges $E_\mu \leftrightarrow B_\mu$ thus exchanging the two boundary conditions for the *AdS₄* gauge field quantization. This action translates in the boundary theory into the so-called *S operation* [28]. This is an operation on three-dimensional CFTs with a global $U(1)$ symmetry, taking one such CFT to another. In addition, it is possible to construct a *T operation*, which amounts, from the bulk perspective, to a shift of the bulk θ -angle by 2π . In fact, these two operations generate an $SL(2, \mathbb{Z})$ algebra transforming among the possible generalized boundary conditions [28, 29].

3.1.1. *Wrapped Branes in AdS_4 and Baryonic Operators*

As the gauge symmetries in AdS_4 of interest arise from reduction of the SUGRA potentials, it is clear that no usual KK-state will be charged under them—the converse holds for the dual operators in the CFT side. In turn, as described above, the relevant objects charged under them are M5 branes, which act as electric sources once the appropriate boundary conditions have been selected. Let us discuss these branes in more detail for the toric CY_4 's at hand. In these cases, an M5 brane wrapped on a five-manifold $\Sigma_5 \subset Y$, such that the cone $\mathcal{C}(\Sigma_5)$, is a complex divisor in the Kähler cone $\mathcal{C}(Y)$, is supersymmetric and leads to a BPS particle propagating in AdS_4 . As we argued in the previous subsection, since the M5 brane is a source for C_6 , this particle is electrically charged under the $b_2(Y)$ massless $U(1)$ gauge fields \mathcal{A}_I . One might also consider M2 branes wrapped on two cycles in Y . However, such wrapped M2 branes are not supersymmetric, as there are no calibrating 3 forms for the cone over the Σ_2 submanifold which they would wrap.

For toric manifolds there is a canonical set of wrapped M5 brane states, where $\mathcal{C}(\Sigma_5)$ are taken to be the toric divisors. In fact, the set of vectors defining the toric diagram introduced above is precisely the set of charge vectors specifying the $U(1)$ subgroups of $U(1)^4$ that have complex codimension one fixed point sets, and thus must correspond to the 5 manifolds where to wrap the M5 branes. To make this precise, in the Q^{111} example the toric divisors correspond to the 6 external points in the toric diagram in Figure 1.

The standard rules of the AdS/CFT prescription allow to identify these wrapped M5 branes, whenever the boundary conditions allow for them, with chiral operators in the dual field theory. In fact, as they correspond to nonperturbative states in supergravity, we should expect their scaling dimension to be of order N . In order to check this, we can consider changing to global coordinates for AdS , such that the energy of a particle in AdS in units of $1/R$ is directly the scaling dimension in the field theory. For the wrapped branes under consideration it is straightforward to show that the action reduces to

$$S = T_5 \text{Vol}(\Sigma_5) R^5 \int dt \sqrt{\hat{g}_{tt}}, \quad (3.8)$$

where \hat{g} stands for the AdS_4 metric in global coordinates. Thus, this indeed describes a mass $m = T_5 R^5 \text{Vol}(\Sigma_5)$ particle in global AdS_4 . Thus, through AdS/CFT , the dimension of the dual operator is

$$\Delta(\Sigma_5) = mR = T_5 R^6 \text{Vol}(\Sigma_5) = N \frac{\pi}{6} \frac{\text{Vol}(\Sigma_5)}{\text{Vol}(Y)}. \quad (3.9)$$

As the ratio of the volume of the 5 manifold to the ratio of Y is an $\mathcal{O}(1)$ number, it follows that in fact these wrapped M5 branes must correspond to $\mathcal{O}(N)$ operators.

3.2. *Field Theory Perspective of Betti Symmetries*

In the previous sections we have seen that the KK reduction of supergravity potentials must lead, on the boundary, to either a gauge or a global symmetry, depending on the choice of boundary conditions. This arises as, crucially, both boundary behaviors for gauge fields in AdS_4 are allowed; and it is the choice of boundary conditions that selects whether these

bulk gauge fields correspond to a boundary gauge or global symmetry. Consistently, the choice of boundary conditions also determines which wrapped objects are allowed. Through *AdS/CFT*, as discussed in the previous subsection, these objects correspond to operators of dimension $\mathcal{O}(N)$.

On general grounds, the suitable CFT's dual to the toric geometries of interest will be $\prod U(N)$ gauge theories. These theories will contain a chiral ring consisting on a set of chiral operators with protected dimensions such that in the large N limit they remain $\mathcal{O}(1)$. As their dimensions remain small, these operators must correspond to KK states in the gravity side. On the other hand, if a global baryonic symmetry is present in the theory, we expect baryon-like operators with dimensions $\mathcal{O}(N)$. The natural form of these operators is $\mathcal{B} = \det X$, with X being a certain field charged under the corresponding baryonic symmetry. Conversely, these $\mathcal{O}(N)$ dimension operators must correspond to wrapped branes in the gravity dual, that is, the M5 branes wrapped on toric divisors we have just discussed. In turn, from the gravity analysis above, we learn that these branes are allowed once the suitable boundary conditions have been chosen, namely, those fixing a_μ on the boundary and leaving a dynamical j_μ , which has the correct properties for a global symmetry current. On the other hand, the set of boundary conditions which do not allow for the wrapped M5 branes must correspond to a theory where the baryonic symmetry is gauged (instead of global). Consistently, the boundary a_μ is dynamical, which in fact has the correct features to be identified with a gauge field. In turn, being the $U(1)_B$ a gauged symmetry, the baryon-like operators would be forbidden because of gauge noninvariance; thus reflecting the lack of wrapped M5's. Therefore, for each baryonic symmetry we should expect two *different* dual CFTs, each associated to a choice of boundary conditions, where the baryonic $U(1)$ symmetries are either gauged or global. We stress that these theories are different CFTs, related though by the gauging/ungauging of the $U(1)_B$'s. In fact, the gravity dual allows us to be more precise. As reviewed above, the exchange of the boundary conditions stands for the electric-magnetic duality of the AdS_4 E & M. It is possible to enhance this action with yet another transformation so that we have an $SL(2, \mathbb{Z})$ action. Following [28] (see also [29]), these bulk actions translate in a precise way to the boundary CFT. Starting with a three-dimensional CFT with a global $U(1)$ current j^μ , one can couple this global current to a background gauge field A resulting in the action $S[A]$. The \mathcal{S} operation then adds a BF coupling of A to a new background field B and at the same time promotes A to a dynamical gauge field by introducing the functional integral over it, while the \mathcal{T} operation instead adds a CS term for the background gauge field A :

$$\mathcal{S} : S[A] \longrightarrow S[A] + \frac{1}{2\pi} \int B \wedge dA, \quad \mathcal{T} : S[A] \longrightarrow S[A] + \frac{1}{4\pi} \int A \wedge dA. \quad (3.10)$$

As shown in [28], these two operations generate the group $SL(2, \mathbb{Z})$. (Even though we are explicitly discussing the effect of $SL(2, \mathbb{Z})$ on the vector fields, since these are part of a whole Betti multiplet we expect a similar action on the other fields of the multiplet. We leave this investigation for future work.) In turn, as discussed above, the \mathcal{S} and \mathcal{T} operations have the bulk interpretation of exchanging $E_\mu \leftrightarrow B_\mu$ and shifting the bulk θ -angle by 2π , respectively. It is important to stress that these actions on the bulk theory change the boundary conditions. Because of this, the dual CFTs living on the boundary are different.

3.3. Spontaneous Symmetry Breaking

We have seen that the choice of boundary conditions where we fix the boundary value of the bulk vectors arising from KK reduction of the supergravity potentials lead, on the CFT side, to global symmetries. On general grounds, we might then consider their spontaneous breaking to further test the consistency of the picture. In turn, generically, we should expect spontaneous symmetry breaking to correspond, in the gravity side, to Calabi-Yau resolutions of the cone [31] where an S^2 —of radius b —is blown up.

Upon resolution, the CY_4 will only be asymptotically conical. In fact, the first correction to the asymptotic cone-like metric generically goes like r^{-2} , which leads to the following behavior for the warp factor

$$h \sim \frac{R^6}{r^6} \left(1 + \frac{b}{r^2} + \dots \right). \quad (3.11)$$

Recalling the relation between the cone radial coordinate and the appropriate AdS_4 radial coordinate, according to the standard AdS/CFT rules the subleading correction $\mathcal{O}(z^{-1})$ must be dual to a dimension 1 operator which acquires a VEV proportional to b . In fact, the natural candidate is the scalar component \mathcal{U} in the global current multiplet, whose dimension is protected by supersymmetry to be 1. This operator is roughly the moment map of the $U(1)_B$ action and is of the form

$$\mathcal{U} = \frac{1}{N} \sum_{\text{charged fields}} \text{Tr } q_{X_i} X_i X_i^\dagger. \quad (3.12)$$

It is then clear that spontaneous symmetry breaking, triggered by a VEV of a scalar with charge q_{X_i} under the $U(1)_{B'}$, will give a VEV to \mathcal{U} . Furthermore, this VEV must trigger an RG flow to a different fixed point. In turn, in the gravity side, much like in [32], upon using the appropriate radial coordinate, close to the branes the space develops an AdS_4 throat which stands for the IR fixed point.

3.3.1. The Order Parameter for SSB

The baryonic $U(1)_B$ symmetry is broken whenever a field X charged under it takes a VEV. In particular, the \mathcal{U} operator discussed above signals such breaking. However, a natural operator to consider is the associated baryon $\mathcal{B} = \det X$, which, as discussed above, corresponds to a BPS particle in AdS_4 arising from a wrapped M5 brane on Σ_5 . From the gravity perspective we can compute its VEV by considering the action S_E of an euclidean brane which wraps the cone over Σ_5 —the so-called baryonic condensate. Indeed, the AdS/CFT dictionary allows to identify

$$\langle \mathcal{B} \rangle = e^{-S_E}. \quad (3.13)$$

Let us concentrate on the modulus of the VEV, which comes from the exponential of the DBI action of the euclidean brane. Quite remarkably, as shown in [5], this contribution, which amounts to the warped volume of the cone over Σ_5 , can be computed generically for the

toric CY_4 of interest. Such warped volume is divergent, and it is then necessary to regulate it cutting off the integral at some large r_c . We refer to [5] for the details of the computation. For the time being, let us quote the most relevant aspect of the result, namely, that the modulus of the VEV is proportional to

$$\langle \mathcal{B} \rangle \sim z^{-\Delta(\Sigma_5)}. \quad (3.14)$$

This result from supergravity can be seen as a prediction for the field theory dual. Indeed, if the expected dual operator is $\langle \det X \rangle$, we would expect its scaling dimension to be $N\Delta(X)$, so that $\Delta(X) = N^{-1}\Delta(\Sigma_5)$, in agreement with (3.9).

3.3.2. The Emergence of the Goldstone Particle and the Global String

In the preceding section we concentrated on the modulus of the VEV of the baryonic operator obtaining nontrivial expectations for the dual field theory. However, a complete picture of spontaneous symmetry breaking must involve the identification of the associated Goldstone boson. On general grounds, field theoretic spontaneous symmetry breaking can lead to cosmic strings around which such Goldstone boson would have a nontrivial monodromy. In fact, following the AdS_5 example [33], in the gravity dual these strings can be easily identified as M2 branes wrapping the blown-up 2 cycles. Remarkably, these branes remain of finite tension at the bottom of the cone in the warped geometry (2.1) where $ds^2(X)$ is replaced by the resolved cone metric.

The finite tension M2 branes wrapped on the blown-up cycle appear as a pointlike object in the Minkowski directions. In fact, in 3-dimensions they correspond to cosmic “strings”. In order to complete this picture, we must find the Goldstone boson winding around them. To that matter, we consider a 3-form linearized fluctuation [5]

$$\delta C_3 = A \wedge \beta, \quad (3.15)$$

where β is a 2 forms which, in the bottom of the cone, becomes the volume of the blown-up 2 cycles. Furthermore, 11-dimensional supergravity demands it to obey

$$d\beta = 0, \quad d(h\star_8\beta) = 0; \quad (3.16)$$

where the \star_8 is the Hodge-dual with respect to the 8-dimensional resolved cone metric. Following [33] it is possible to argue for the existence of such β . First, in the unwarped case β is just a harmonic two forms. Furthermore, in the warped case the equations above can be seen to arise from an action, thus satisfying a minimum principle.

On the other hand, the 1-form A can be conveniently dualized into a scalar in the 3-dimensional field theory directions. In fact, the Hodge dual of the above 3-form potential involves

$$\delta G_7 = \star_3 dA \wedge h\star_8\beta. \quad (3.17)$$

Defining $\star_3 dA = dp$, we can write the above field strength fluctuation as

$$\delta G_7 = dp \wedge h \star_8 \beta. \quad (3.18)$$

Thus, making use of the equations of motion above, we see that we can take $\delta C_6 = ph \star_8 \beta$. As β is proportional, in the bottom of the cone, to the volume form of the blown-up cycle, its dual precisely goes through the Σ_5 cycle. Thus, this supergravity fluctuation couples to the baryonic condensate described above through the Wess-Zumino part of the euclidean brane action. In fact, this provides the phase of the \mathcal{B} VEV, so that schematically

$$\langle \mathcal{B} \rangle \sim z^{-\Delta(\Sigma_5)} e^{ip} \quad (3.19)$$

which shows that p must be identified with the Goldstone boson of symmetry breaking. Indeed, we could use a different gauge for the δG_7 field strength such that asymptotically

$$\delta C_6 \sim z dp \wedge \text{Vol}(\Sigma_5) \quad (3.20)$$

which implies $\langle J_\mu^{\mathcal{B}} \rangle \sim \partial_\mu p$ for the boundary theory.

4. An Example: The Cone Over Q^{111}

We have so far kept the discussion generic. Let us put the previous machinery at work in a particularly interesting example: the cone over Q^{111} . This is a toric CY_4 manifold, whose toric diagram we anticipated in (2.1). Its isometry group is $SU(2)^3 \times U(1)_R$, and in local coordinates the explicit metric is

$$ds^2(Q^{111}) = \frac{1}{16} \left(d\psi + \sum_{i=1}^3 \cos \theta_i d\phi_i \right)^2 + \frac{1}{8} \sum_{i=1}^3 \left(d\theta_i^2 + \sin^2 \theta_i d\phi_i^2 \right). \quad (4.1)$$

Here (θ_i, ϕ_i) are standard coordinates on three copies of $S^2 = \mathbb{CP}^1$, $i = 1, 2, 3$, and ψ has period 4π . The two Killing spinors are charged under ∂_ψ , which is dual to the $U(1)_R$ symmetry. The metric (4.1) shows very explicitly the regular structure of a $U(1)$ bundle over the standard Kähler-Einstein metric on $\mathbb{CP}^1 \times \mathbb{CP}^1 \times \mathbb{CP}^1$, where ψ is the fibre coordinate and the Chern numbers are $(1, 1, 1)$.

We now consider a stack of N M2 brane at the tip of this cone. The near horizon geometry is the standard Freund-Rubin type $AdS_4 \times Q^{111}$. Since $b_2(Q^{111}) = 2$, according to the general discussion above, we should expect two vector fields in AdS_4 arising from KK reduction on the dual 5 cycles of C_6 fluctuations.

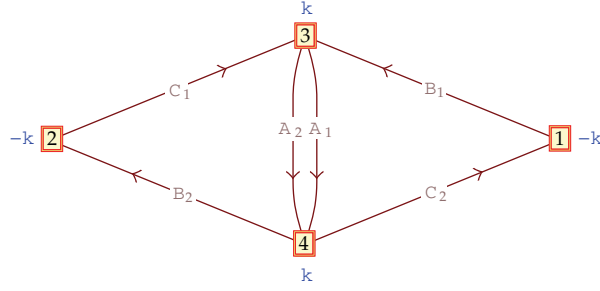


Figure 2: The toric diagram for $\mathcal{C}(Q^{111})$.

4.1. Two Versions for the Same Theory

From the toric diagram in Figure 1 we can immediately read the minimal gauged linear σ -model (GLSM) realizing the variety. It contains 6 fields whose charges under the $U(1)_I \times U(1)_{II}$ gauge symmetries are

$$\begin{array}{c|cccccc} & a_1 & a_2 & b_1 & b_2 & c_1 & c_2 \\ \hline U(1)_I & -1 & -1 & 1 & 1 & 0 & 0 \\ U(1)_{II} & -1 & -1 & 0 & 0 & 1 & 1 \end{array} \quad (4.2)$$

Following the ABJM example, we look for a Chern-Simons matter theory where to embed this minimal GLSM. As shown in [34], we can succinctly encode such theory in the quiver shown in Figure 2.

We assume all the nodes to come with an $\mathcal{N} = 2U(N)$ Chern-Simons action with the level indicated in Figure 2. Furthermore, the superpotential reads

$$W = \text{Tr}\left(C_2 B_1 A_i B_2 C_1 A_j e^{ij}\right). \quad (4.3)$$

It can be shown [34] that this theory indeed contains, at $k = 1$, the desired GLSM, where $a_i \leftrightarrow A_i$, $b_i \leftrightarrow B_i$, $c_i \leftrightarrow C_i$. Let us give a flavor on the proof by describing the generic construction associated to $\mathcal{N} = 2$ toric Chern-Simons-matter quiver theories (see [13–15] for more details). For a start, we note that $\mathcal{N} = 2$ SUSY in 3 dimensions can be thought as the dimensional reduction along, say, x^3 of 4-dimensional $\mathcal{N} = 1$. In particular, upon gauge fixing, the 3-dimensional vector supermultiplet contains two scalars D , σ arising, respectively, from the 4-dimensional D scalar and A_3 component of the gauge field. Crucially, it turns out that both scalars are auxiliary fields for Chern-Simons matter theories (see, e.g., [11]) and thus must be integrated out. The resulting F and (generalized) D flatness conditions turn out to be

$$\partial_{X_{ab}} W = 0, \quad -\sum_{b=1}^G X_{ba}^\dagger X_{ba} + \sum_{c=1}^G X_{ac} X_{ac}^\dagger = \frac{k_a \sigma_a}{2\pi}, \quad \sigma_a X_{ab} - X_{ab} \sigma_b = 0, \quad (4.4)$$

where latin indices run to the G gauge groups (in the case at hand four) and X_{ab} is a $(U(N)_a, U(N)_b)$ bifundamental.

The last equation in (4.4) is automatically satisfied upon diagonalizing our fields and taking $\sigma_a = \sigma I_N \forall a$. Thus, the theory breaks into N copies of the $U(1)$ version. Furthermore, assuming $\sum k_a = 0$ it is easy to see that the equations setting $\mu_a = 0$ reduce to $G - 2$ independent equations. On the other hand, it is a standard result that for toric W the set of F -flat configurations the so-called *master space*, see, for example, [35] is of dimension $G + 2$. Thus, out of this $G + 2$ -dimensional master space and after imposing the $G - 2$ generalized D terms, we finally have a 4-dimensional toric manifold as moduli space. One can verify that for the case at hand, at $k = 1$, this manifold is indeed the cone over Q^{111} . Let us stress that this computation merely focuses on the abelian moduli space. In fact, at the abelian level the W vanishes. A more detailed analysis requires the study of the chiral ring at the nonabelian level, which on general grounds must match the coordinate ring of the variety. Generically, this is a very difficult task, as we *a priori* expect crucial nonperturbative effects associated to monopole operators. In order to simplify the problem, we can consider the large k limit, as the dimension of such monopole operators should scale with k thus decoupling. In that limit, the chiral ring is composed out of standard gauge invariant operators, that is, closed loops in the quiver modulo F -terms. Conversely, the $k \neq 1$ moduli space is indeed an orbifold of the $k = 1$ variety. As shown in [36], it is possible to exactly match the coordinate ring of this orbifolded variety to the nonabelian chiral ring of the theory above, in particular explicitly checking the W structure. We refer to [36] for a complete discussion.

Let us note that the orbifold action breaks the original $SU(2)^3$ down to the single $SU(2)$ present in the superpotential. This action in fact has fixed points away from the tip of the cone. This motivated the authors [16, 17] to propose alternative theories containing fundamental matter associated to the flavor branes, from a IIA perspective, to which these singularities lead. We refer to these works, as well as to [37], for further details.

Being the gauge group of the theory we have just discussed $U(N)^4$, it cannot accommodate for gauge invariant baryon-like operators. It must then correspond to a choice of boundary conditions in the gravity dual where the 2 vector fields in AdS_4 arising from KK reduction on the $b_2(Q^{111}) = 2$ 2 cycles have $j_\mu = 0$; that is, they are dual to boundary gauge symmetries. As discussed above, the field theory dual to changing these boundary conditions can be found by acting with the $\{\mathcal{T}, \mathcal{S}\}SL(2, \mathbb{Z})$ generators, as these correspond to swapping boundary conditions. In order to further proceed, let us strip off the abelian part of the gauge symmetry and denote the corresponding generators \mathcal{A}_i . We define

$$\begin{aligned} \mathcal{B}_k &= \mathcal{A}_1 + \mathcal{A}_2 - \mathcal{A}_3 - \mathcal{A}_4, & \mathcal{B}_d &= \mathcal{A}_1 + \mathcal{A}_2 + \mathcal{A}_3 + \mathcal{A}_4, \\ \mathcal{A}_+ &= \mathcal{A}_1 - \mathcal{A}_2, & \mathcal{A}_- &= \mathcal{A}_3 - \mathcal{A}_4. \end{aligned} \quad (4.5)$$

It is not hard to show that the full action at $k = 1$ can be written as (we focus on the bosonic content)

$$S = \frac{1}{4\pi} \int \mathcal{A}_+ \wedge d\mathcal{A}_+ - \frac{1}{4\pi} \int \mathcal{A}_- \wedge d\mathcal{A}_- + S_{SU}, \quad S_{SU} = \frac{1}{4\pi} \int \mathcal{B}_k \wedge d\mathcal{B}_k + S_R, \quad (4.6)$$

where S_R collects the remaining terms from the original Lagrangian and in particular contains \mathcal{A}_\pm through the covariant derivatives of the fields. In fact, let us consider the theory defined by this action *per se*. We note that this is an $SU(N)^4 \times U(1)_k \times U(1)_d$ theory, where the abelian factors are given by the $\mathcal{B}_k, \mathcal{B}_d$ fields above.

Starting from S_{SU} alone, we can think of the \mathcal{A}_\pm as background nondynamical gauge fields. Thus, we are in the situation described in [28], where we can act with the generators $\{\mathcal{S}, \mathcal{T}\}$. (We will follow a slightly different path as in [5]. We thank C. Closset and S. Cremonesi for discussions on this topic.) Let us now act with the \mathcal{S} generator by adding new background gauge fields \mathcal{C}_\pm

$$S_{SU}[\mathcal{A}_+, \mathcal{A}_-] \longrightarrow S_{SU}[\mathcal{A}_+, \mathcal{A}_-] + \frac{1}{2\pi} \int \mathcal{C}_+ \wedge d\mathcal{A}_+ + \frac{1}{2\pi} \int \mathcal{C}_- \wedge d\mathcal{A}_-. \quad (4.7)$$

While we will not write it explicitly, the \mathcal{S} operation also introduced a functional integral over \mathcal{A}_\pm . We can act again with the \mathcal{S} generator on the newly generated background gauge symmetries \mathcal{C}_\pm , so that we find, grouping terms

$$S_{SU}[\mathcal{A}_+, \mathcal{A}_-] + \frac{1}{2\pi} \int \mathcal{C}_+ \wedge d(\mathcal{A}_+ + \mathfrak{D}_+) + \frac{1}{2\pi} \int \mathcal{C}_- \wedge d(\mathcal{A}_- + \mathfrak{D}_-). \quad (4.8)$$

Again, we stress that a functional integration, this time over \mathcal{C}_\pm has been introduced. Acting now with the \mathcal{T} generator on the new background gauge symmetries \mathfrak{D}_\pm we find

$$\begin{aligned} S_{SU}[\mathcal{A}_+, \mathcal{A}_-] + \frac{1}{2\pi} \int \mathcal{C}_+ \wedge d(\mathcal{A}_+ + \mathfrak{D}_+) + \frac{1}{2\pi} \int \mathcal{C}_- \wedge d(\mathcal{A}_- + \mathfrak{D}_-) \\ + \frac{1}{4\pi} \int \mathfrak{D}_+ \wedge d\mathfrak{D}_+ - \frac{1}{4\pi} \int \mathfrak{D}_- \wedge d\mathfrak{D}_-. \end{aligned} \quad (4.9)$$

The functional integration over \mathcal{C}_\pm leads to a functional δ setting $\mathfrak{D}_\pm = -\mathcal{A}_\pm$, thus recovering exactly S_U . Thus, from this perspective, we can consider the theory defined by S_{SU} as the dual to the background with boundary conditions fixing a_μ in the boundary. In turn, these boundary conditions allow for wrapped M5 branes and must be dual to a theory with global baryonic symmetries. Conversely, upon considering the S_{SU} theory, we no longer need to demand gauge invariance with respect to the \mathcal{A}_\pm gauge symmetries. Thus, operators such as, for example, $\det A_i$ become gauge-invariant and are the natural candidates for duals to the wrapped M5 branes.

We can understand the previous procedure in yet a different manner. The M5 branes corresponding to baryonic operators are in one-to-one correspondence with the divisors, encoded in the toric diagram arising from the GLSM charge matrix (4.2). Thus, that particular combination of $U(1)$'s naturally encodes the baryonic charges necessary to describe all baryonic operators. In turn, the Chern-Simon-matter theory described above contains precisely this GLSM. In fact, the sequence of $\{\mathcal{T}, \mathcal{S}\}$ operations above amount to ungauged precisely these two $U(1)$'s (which are nothing but $\mathcal{A}_+ \pm \mathcal{A}_-$).

4.2. Spontaneous Symmetry Breaking

As discussed, spontaneous symmetry breaking amounts to resolution in the gravity dual. In [5] a comprehensive algebraic analysis of the cone over Q^{111} was performed, paying attention in particular to the space of Kahler parameters which account for the resolutions. From the point of view of the GLSM above, by turning on Fayet-Iliopoulos parameters we can achieve

every possible resolution of the geometry. In turn, for each of the resolutions of $\mathcal{C}(Q^{111})$, there is a corresponding Ricci-flat Kähler metric that is asymptotic to the cone metric over Q^{111} . More precisely, there is a unique such metric for each choice of Kähler class, or equivalently FI parameter $\zeta_1, \zeta_2 \in \mathbb{R}$. Roughly speaking, these parameters correspond to the volumes of the 2 cycles which can be blown up. Denoting the radii of these blown-up S^2 's by (a, b) , the resolved Calabi-Yau metric is given by

$$ds^2(X) = \kappa(r)^{-1} dr^2 + \kappa(r) \frac{r^2}{16} \left(d\psi + \sum_{i=1}^3 \cos \theta_i d\phi_i \right)^2 + \frac{(2a+r^2)}{8} (d\theta_2^2 + \sin^2 \theta_2 d\phi_2^2) + \frac{(2b+r^2)}{8} (d\theta_3^2 + \sin^2 \theta_3 d\phi_3^2) + \frac{r^2}{8} (d\theta_1^2 + \sin^2 \theta_1 d\phi_1^2), \quad (4.10)$$

where

$$\kappa(r) = \frac{(2A_- + r^2)(2A_+ + r^2)}{(2a + r^2)(2b + r^2)}, \quad (4.11)$$

a and b are arbitrary constants determining the sizes of the blown-up S^2 's; and we have also defined

$$A_{\pm} = \frac{1}{3} \left(2a + 2b \pm \sqrt{4a^2 - 10ab + 4b^2} \right). \quad (4.12)$$

We are interested in studying supergravity backgrounds corresponding to M2 branes localized on one of these resolutions of $\mathcal{C}(Q^{111})$. If we place N spacetime-filling M2 branes at a point $y \in X$, we must then solve the following equation for the warp factor:

$$\Delta_x h[y] = \frac{(2\pi\ell_p)^6 N}{\sqrt{\det g_X}} \delta^8(x-y), \quad (4.13)$$

where Δ is the scalar Laplacian on the resolved cone. In order to simplify the problem, let us analyse the case in which we partially resolve the cone, setting $a = 0$ and $b > 0$. With no loss of generality, we put the N M2 branes at the north pole of the blown-up S^2 parametrized by (θ_3, ϕ_3) . We then find

$$h(r, \theta_3) = \sum_{l=0}^{\infty} H_l(r) P_l(\cos \theta_3), \quad (4.14)$$

$$H_l(r) = C_l \left(\frac{8b}{3r^2} \right)^{3(1+\beta)/2} {}_2F_1 \left(-\frac{1}{2} + \frac{3}{2}\beta, \frac{3}{2} + \frac{3}{2}\beta, 1 + 3\beta, -\frac{8b}{3r^2} \right),$$

where P_l denotes the l th Legendre polynomial,

$$\beta = \beta(l) = \sqrt{1 + \frac{8}{9}l(l+1)}, \quad (4.15)$$

and the normalization factor C_l is given by

$$C_l = \frac{3\Gamma((3/2) + (3/2)\beta)^2}{2\Gamma(1 + 3\beta)} \left(\frac{3}{8b}\right)^3 (2l + 1)R^6, \quad (4.16)$$

$$R^6 = \frac{(2\pi\ell_p)^6 N}{6\text{vol}(Q^{111})} = \frac{256}{3}\pi^2 N\ell_p^6.$$

In the field theory this solution corresponds to breaking one combination of the two global $U(1)$ baryonic symmetries, rather than both of them. As discussed in general above, the resolution of the cone can be interpreted in terms of giving an expectation value to a certain operator \mathcal{M} in the field theory. This operator is contained in the same multiplet as the current that generates the broken baryonic symmetry and couples to the corresponding $U(1)$ gauge field in AdS_4 . Since a conserved current has no anomalous dimension, the dimension of \mathcal{M} is uncorrected in going from the classical description to supergravity [31]. According to the general AdS/CFT prescription [31], the VEV of the operator \mathcal{M} is dual to the subleading correction to the warp factor. For large r one can show

$$h(r, \theta_3) \sim \frac{R^6}{r^6} \left(1 + \frac{18b \cos \theta_3}{5r^2} + \dots\right). \quad (4.17)$$

In terms of the AdS_4 coordinate $z = r^{-2}$ we have that the leading correction is of order z , which indicates that the dual operator \mathcal{M} is dimension 1. This is precisely the expected result, since this operator sits in the same supermultiplet as the broken baryonic current, and thus has a protected dimension of 1. Furthermore, its VEV is proportional to b , the metric resolution parameter, which reflects the fact that in the conical (AdS) limit in which $b = 0$ this baryonic current is not broken, and as such $\langle \mathcal{M} \rangle = 0$.

Furthermore, we can compute, following the steps described for the general case, the VEV of the baryonic condensate as the volume of an euclidean brane wrapping the cone over Σ_5 . While the details of the computation can be seen in [5], here we content ourselves with quoting the result

$$e^{-S(r_c)} = e^{7N/18} \left(\frac{8b}{3r_c^2}\right)^{N/3} \left(\sin \frac{\theta_3}{2}\right)^N, \quad (4.18)$$

where r_c is the radial cutoff. From (4.18) we can read off the dimension of the associated baryonic operator $\Delta(\mathcal{B}) = N/3$, which suggests that if $\mathcal{B} = \det X$, then $\Delta(X) = 1/3$. In fact, in accordance with the results in [38], a similar computation shows that all baryonic operators must have the same scaling dimension. In turn, in the context of the Chern-Simons-matter quiver gauge theory described in the previous subsection, this implies that all fields have the same $\Delta = 1/3$ scaling dimension, and hence $R = 1/3$. This is in fact consistent with the sextic superpotential, as this assignation of R charges ensures it to be marginal at the putative fixed point. In fact, in view of these results it would be very interesting to apply the recently discovered techniques of [18] along the lines of the appendix for the Q^{111} theory to confirm or disprove its potential agreement. We leave this as an open question for future work.

5. Conclusions

Global symmetries are important tools in studying the spectrum of a gauge theory. In the context of the AdS/CFT duality a particularly important set of such symmetries are those which arise from KK reduction of the supergravity p -forms in nontrivial cycles yielding to AdS vectors. Following the terminology of the AdS_5 case, we dubbed such symmetries as baryonic. These symmetries appear as particularly interesting and important in the AdS_4/CFT_3 case, as they behave much differently from the AdS_5 case. In particular, on the gravity side, the two possible fall-offs are admissible, thus leading to two possible AdS_4/CFT_3 dualities depending on the chosen boundary conditions. In turn, in the field theory side, these correspond to a choice of gauged versus global baryonic symmetry.

As briefly mentioned, the CY_4 's of interest can also potentially contain 6 cycles. While they are not directly related to the baryonic symmetries we discussed—as they do not yield to vectors in AdS_4 upon KK reduction of p -forms, it would be very interesting to clarify their role as they might lead to nonperturbative, instantonic, corrections to the superpotentials. We refer to [5] for a first study along these lines.

While a lot has been learned recently about the $AdS_4 \times CFT_3$ duality, much remains yet to be clarified, specially from the field theory perspective in the $\mathcal{N} = 2$ case. In particular, the gravity analysis briefly reviewed above following [5] must yield to important consistency checks. As we described, in the particular $\mathcal{C}(Q^{111})$ case described, the gravity predictions are in fact consistent with the expectations for the theory proposed in [34]. Nevertheless, it still remains to perform a conclusive \mathcal{Z} minimization analysis in the spirit of that in the appendix. Very recently a series of very refined checks involving the superconformal index have been performed in [39, 40]. While flavored theories appear better behaved, the full picture yet remains to be clarified. We leave such analysis as an open problem for the future.

Appendix

\mathcal{Z} -Minimization for HVZ

Following [18], the properties of the putative fixed point of a 3d theory are encoded in the minimization of the modulus squared of the partition function regarded as a function of the trial R-charges (which in 3d are equal, at the SCFT point, to the scaling dimensions). As the theories which we consider do not break the parity symmetry, the partition function itself is real, and thus it is enough to minimize it. Following the localization procedure in [18, 19], one can check that for a generic quiver theory with gauge group $U(N)^G$ and a number of bifundamental fields X in the $(\square_{\alpha_X}, \overline{\square}_{\beta_X})$ under the α_X, β_X factors and with trial scaling dimension Δ_X , the partition function on the S^3 can be written as

$$\mathcal{Z} = \frac{(-1)^{NG}}{N!^G} \int \prod_{g=1}^G \prod_{\alpha_g} du_{\alpha_g}^g e^{i\pi k_g (u_{\alpha_g}^g)^2} \prod_{\alpha_g < \beta_g} \sinh^2 \left(\pi \left(u_{\alpha_g}^g - u_{\beta_g}^g \right) \right) \prod_X \prod_{\alpha_X, \beta_X} e^{\ell(1-\Delta_X+i(u_{\alpha_X}^i - u_{\beta_X}^f))}. \quad (\text{A.1})$$

Let us now compare the HVZ and the ABJM theories. In order to simplify the computations, let us just focus on the $U(2) \times U(2)$ case. After some algebra, the ABJM partition function

reads (we refer to [18, 19] as well to the pioneering papers on 3d localization [41, 42] for the definition of the special function ℓ)

$$\mathcal{Z}_{ABJM}^{U(2)} = \frac{1}{4k} \int dx dy e^{i2\pi k(x^2-y^2)} \sinh^2(2\pi x) \sinh^2(2\pi y) e^{f(x,y)}, \quad (\text{A.2})$$

with

$$f(x, y) = 2 \sum_{s_1=\pm, s_2=\pm} \ell(\Delta + s_1(x + s_2 y)) + \ell(1 - \Delta + s_1(x + s_2 y)). \quad (\text{A.3})$$

In order to obtain these expressions we made use of the constraints imposed by the superpotential, which allows to express all dimensions as a function of a single one Δ . As expected, the partition function is minimized at $\Delta = 1/2$, which leads to

$$\mathcal{Z}_{ABJM}^{U(2)} = \frac{1}{2^{10}k} \int dx dy e^{i2\pi k(x^2-y^2)} \frac{\sinh^2(2\pi x) \sinh^2(2\pi y)}{\cosh^4(\pi(x+y)) \cosh^4(\pi(x-y))}. \quad (\text{A.4})$$

On the other hand, for HVZ, we obtain

$$\mathcal{Z}_{HVZ}^{U(2)} = \frac{1}{4k} \int dx dy e^{i2\pi k(x^2-y^2)} \sinh^2(2\pi x) \sinh^2(2\pi y) e^{f(x,y)}, \quad (\text{A.5})$$

with

$$f(x, y) = 2 \sum_{s_1=\pm} \sum_{s_2=\pm} \ell(1 - \Delta + i s_1(x + s_2 y)) + 4\ell(\Delta) + 2 \sum_{s=\pm} \ell(\Delta + i 2s x). \quad (\text{A.6})$$

While this expression is very similar to the ABJM expression, it is not quite the same. In fact, while it is minimized at $\Delta = 1/2$, leading to the R-charge assignation guessed in [21], the final expression becomes

$$\mathcal{Z}_{HVZ}^{U(2)} = \frac{1}{2^{10}k} \int dx dy e^{i2\pi k(x^2-y^2)} \frac{\sinh^2(2\pi x) \sinh^2(2\pi y)}{\cosh^2(\pi(x+y)) \cosh^2(\pi(x-y)) \cosh^2(\pi x)}, \quad (\text{A.7})$$

which is just different from the ABJM result (A.4) for all k . We note, however, that the same computation for $U(1) \times U(1)$ indeed gives the same answer for the two theories.

Acknowledgments

The author would like to thank AHEP and the guest editors, specially Yang-Hui He, of the special issue on *Computational Algebraic Geometry in String and Gauge Theory* for the invitation to write this contribution. The author is supported by the Israel Science Foundation through Grant 392/09. He wishes to thank N. Benishti, A. Hanany, S. Franco, I. Klebanov, J. Park and J. Sparks for many discussions and explanations, as well as for very enjoyable collaborations. He also would like to thank C. Closset and S. Cremonesi for enlightening discussions.

References

- [1] J. M. Maldacena, "The large N limit of superconformal field theories and supergravity," *Advances in Theoretical and Mathematical Physics*, vol. 2, pp. 231–252, 1998.
- [2] A. Gustavsson, "Algebraic structures on parallel M2 branes," *Nuclear Physics B*, vol. 811, no. 1-2, pp. 66–76, 2009.
- [3] J. Bagger and N. Lambert, "Comments on multiple M2 branes," *Journal of High Energy Physics*, vol. 2008, no. 02, 105, 2008.
- [4] O. Aharony, O. Bergman, D. L. Jafferis, and J. Maldacena, " $N = 6$ superconformal Chern-Simons-matter theories, M2-branes and their gravity duals," *Journal of High Energy Physics*, vol. 2008, no. 10, 091, 2008.
- [5] N. Benishti, D. Rodriguez-Gomez, and J. Sparks, "Baryonic symmetries and M5 branes in the AdS_4/CFT_3 correspondence," *Journal of High Energy Physics*, vol. 2010, no. 07, 024, 2010.
- [6] I. R. Klebanov, S. S. Pufu, and T. Tesileanu, "Membranes with topological charge and AdS_4/CFT_3 correspondence," *Physical Review D*, vol. 81, no. 12, Article ID 125011, 25 pages, 2010.
- [7] D. Martelli and J. Sparks, "Symmetry-breaking vacua and baryon condensates in AdS/CFT correspondence," *Physical Review D*, vol. 79, no. 6, Article ID 065009, 51 pages, 2009.
- [8] M. Benna, I. Klebanov, T. Klose, and M. Smedbäck, "Superconformal Chern-Simons theories and AdS_4/CFT_3 correspondence," *Journal of High Energy Physics*, vol. 2008, no. 09, 072, 2008.
- [9] D. Berenstein and J. Park, "The BPS spectrum of monopole operators in ABJM: towards a field theory description of the giant torus," *Journal of High Energy Physics*, vol. 2010, no. 06, 073, 2010.
- [10] B. S. Acharya, J. M. Figueroa-O'Farrill, C. M. Hull et al., "Branes at conical singularities and holography," *Advances in Theoretical and Mathematical Physics*, vol. 2, pp. 1249–1286, 1999.
- [11] D. Gaiotto and X. Yin, "Notes on superconformal Chern-Simons-matter theories," *Journal of High Energy Physics*, vol. 2007, no. 08, 056, 2007.
- [12] D. Martelli and J. Sparks, "Toric geometry, Sasaki-Einstein manifolds and a new infinite class of AdS/CFT duals," *Communications in Mathematical Physics*, vol. 262, no. 1, pp. 51–89, 2006.
- [13] D. L. Jafferis and A. Tomasiello, "A simple class of $N = 3$ gauge/gravity duals," *Journal of High Energy Physics*, vol. 2008, no. 10, 101, 2008.
- [14] D. Martelli and J. Sparks, "Moduli spaces of Chern-Simons quiver gauge theories and AdS_4/CFT_3 ," *Physical Review D*, vol. 78, Article ID 126005, 26 pages, 2008.
- [15] A. Hanany and A. Zaffaroni, "Tilings, Chern-Simons theories and M2 Branes," *Journal of High Energy Physics*, vol. 2008, no. 10, 111, 2008.
- [16] D. L. Jafferis, "Quantum corrections to $N = 2$ Chern-Simons theories with flavor and their AdS_4 duals," <http://arxiv.org/abs/0911.4324>.
- [17] F. Benini, C. Closset, and S. Cremonesi, "Chiral flavors and M2-branes at toric CY_4 singularities," *Journal of High Energy Physics*, vol. 2010, no. 02, 036, 2010.
- [18] D. L. Jafferis, "The exact superconformal R-symmetry extremizes Z ," <http://arxiv.org/abs/1012.3210>.
- [19] N. Hama, K. Hosomichi, and S. Lee, "Notes on SUSY gauge theories on three-sphere," *Journal of High Energy Physics*, vol. 2011, no. 3, 127, 2011.
- [20] A. Hanany, D. Vegh, and A. Zaffaroni, "Brane tilings and M2 branes," *Journal of High Energy Physics*, vol. 2009, no. 03, 012, 2009.
- [21] D. Rodriguez-Gomez, "M5 spikes and operators in the HVZ membrane theory," *Journal of High Energy Physics*, vol. 2010, no. 03, 039, 2010.
- [22] J. Choi, S. Lee, and J. Song, "Superconformal indices for orbifold Chern-Simons theories," *Journal of High Energy Physics*, vol. 2009, no. 03, 099, 2009.
- [23] S. Kim and J. Park, "Probing AdS_4/CFT_3 proposals beyond chiral rings," *Journal of High Energy Physics*, vol. 2010, no. 08, 069, 2010.
- [24] R. D'Auria and P. Fre, "On the spectrum of the $N = 2SU(3) \otimes SU(2) \otimes U(1)$ gauge theory from $D = 11$ supergravity," *Classical and Quantum Gravity*, vol. 1, no. 5, article 003, pp. 447–468, 1984.
- [25] E. Lerman, "Homotopy groups of K-contact toric manifolds," *Transactions of the American Mathematical Society*, vol. 356, no. 10, pp. 4075–4083, 2004.
- [26] J. Davey, A. Hanany, N. Mekareeya, and G. Torri, "Phases of M2-brane theories," *Journal of High Energy Physics*, vol. 2009, no. 06, 025, 2009.
- [27] J. Davey, A. Hanany, N. Mekareeya, and G. Torri, "Higgsing M2-brane theories," *Journal of High Energy Physics*, vol. 2009, no. 11, 028, 2009.

- [28] E. Witten, "SL(2,Z) action on three-dimensional conformal field theories with Abelian symmetry," <http://arxiv.org/abs/hep-th/0307041>.
- [29] R. G. Leigh and A. C. Petkou, "SL(2,Z) action on three-dimensional CFTs and holography," *Journal of High Energy Physics*, vol. 2003, no. 12, 020, 2003.
- [30] D. Marolf and S. F. Ross, "Boundary conditions and dualities: vector fields in AdS/CFT," *Journal of High Energy Physics*, vol. 2006, no. 11, 085, 2006.
- [31] I. R. Klebanov and E. Witten, "AdS/CFT correspondence and symmetry breaking," *Nuclear Physics B*, vol. 556, no. 1-2, pp. 89–114, 1999.
- [32] I. R. Klebanov and A. Murugan, "Gauge/gravity duality and warped resolved conifold," *Journal of High Energy Physics*, vol. 2007, no. 03, 042, 2007.
- [33] I. R. Klebanov, A. Murugan, D. Rodriguez-Gomez et al., "Goldstone bosons and global strings in a warped resolved conifold," *Journal of High Energy Physics*, vol. 2008, no. 05, 090, 2008.
- [34] S. Franco, A. Hanany, J. Park et al., "Towards M2-brane theories for generic toric singularities," *Journal of High Energy Physics*, vol. 2008, no. 12, 110, 2008.
- [35] D. Forcella, A. Hanany, Y.-H. He, and A. Zaffaroni, "The master space of $N = 1$ gauge theories," *Journal of High Energy Physics*, vol. 2008, no. 08, 012, 2008.
- [36] S. Franco, I. R. Klebanov, and D. Rodriguez-Gomez, "M2-branes on orbifolds of the cone over $Q^{1,1,1}$," *Journal of High Energy Physics*, vol. 2009, no. 08, 033, 2009.
- [37] S. Cremonesi, "Type IIB construction of flavoured ABJ(M) and fractional M2 branes," *Journal of High Energy Physics*, vol. 2011, no. 01, 076, 2011.
- [38] D. Fabbri, P. Fré, L. Gualtieri et al., "3D superconformal theories from Sasakian seven-manifolds: new non-trivial evidences for AdS_4/CFT_3 ," *Nuclear Physics B*, vol. 577, no. 3, pp. 547–608, 2000.
- [39] Y. Imamura, D. Yokoyama, and S. Yokoyama, "Superconformal index for large N quiver Chern-Simons theories," <http://arxiv.org/abs/1102.0621>.
- [40] S. Cheon, D. Gang, S. Kim, and J. Park, "Refined test of AdS_4/CFT_3 correspondence for $N = 2, 3$ theories," <http://arxiv.org/abs/1102.4273>.
- [41] A. Kapustin, B. Willett, and I. Yaakov, "Exact results for Wilson loops in superconformal Chern-Simons theories with matter," *Journal of High Energy Physics*, vol. 2010, no. 03, 089, 2010.
- [42] A. Kapustin, B. Willett, and I. Yaakov, "Nonperturbative tests of three-dimensional dualities," *Journal of High Energy Physics*, vol. 2010, no. 10, 013, 1010.

Review Article

A Simple Introduction to Gröbner Basis Methods in String Phenomenology

James Gray

Rudolf Peierls Centre for Theoretical Physics, University of Oxford, Oxford OX1 3NP, UK

Correspondence should be addressed to James Gray, jamesgrayphysics@gmail.com

Received 3 February 2011; Accepted 13 February 2011

Academic Editor: Yang-Hui He

Copyright © 2011 James Gray. This is an open access article distributed under the Creative Commons Attribution License, which permits unrestricted use, distribution, and reproduction in any medium, provided the original work is properly cited.

I give an elementary introduction to the key algorithm used in recent applications of computational algebraic geometry to the subject of string phenomenology. I begin with a simple description of the algorithm itself and then give 3 examples of its use in physics. I describe how it can be used to obtain constraints on flux parameters, how it can simplify the equations describing vacua in 4D string models, and lastly how it can be used to compute the vacuum space of the electroweak sector of the MSSM.

1. Introduction

There is currently a great deal of interest in applying the methods of computational algebraic geometry to string phenomenology and closely related subfields of theoretical physics. For some examples of recent work see [1–23, 14] and references therein. These papers utilise advances in algorithmic techniques in commutative algebra to study a wide range of subjects including various aspects of globally supersymmetric gauge theory [1–9, 6], finding flux vacua in string phenomenology [10–16], studying heterotic model building on smooth Calabi-Yau in non-standard embeddings [17, 18], and more besides [19–23].

Despite the wide range of physical problems which have been addressed within this context, the computational tools which are being used are all based, finally, on the same algorithm. The Buchberger algorithm [24, 25] is at once what lends these methods their power and also the rate limiting step—placing bounds on the size of problem that can be dealt with. The recent burst of activity in this field has been fueled, in part, by the advent of freely available, efficient implementations of this algorithm [26, 27]. There are also interfaces available between the commutative algebra program [27] and Mathematica [11–14, 28], with

[11–14] being particularly geared towards physicist’s needs. The aim of this paper is to give an elementary introduction to the Buchberger algorithm and some of its recent applications.

In order to give an idea of how one simple algorithm can make so much possible, I will present the Buchberger algorithm and then show how it may be applied to physics in 3 elementary examples. Firstly, I will describe how it can be used to obtain constraints on the flux parameters in four-dimensional descriptions of string phenomenological models which are necessary and sufficient for the existence of certain types of vacuum [11–14]. Secondly, I will describe how the Buchberger algorithm can be used to simplify the equations describing the vacua of such systems making problems of finding minima much more tractable [11–14]. Finally, I will describe how the same simple algorithm can be used to calculate the supersymmetric vacuum space geometry of the electroweak sector of the MSSM [1, 2].

The remainder of this paper is structured as follows. In Section 2, I take a few pages to explain the algorithm and the few mathematical concepts that we will require. In the three sections following that, I then describe the three examples mentioned above. I will conclude by making a few final comments about the versatility and scaling of the Buchberger algorithm.

2. A Tiny Bit of Commutative Algebra

Two pages of simple mathematics will suffice to achieve all of the physical goals mentioned in the introduction. First of all we define the notion of a polynomial ring. In this paper we will call the fields of the physical systems we study ϕ^i and any parameters present, such as flux parameters, a^α . The polynomial rings $\mathbb{C}[\phi^i, a^\alpha]$ and $\mathbb{C}[a^\alpha]$ are then simply the infinite set of all polynomials in the fields and parameters and the infinite set of all polynomials in the parameters, respectively.

Another mathematical concept we will require is that of a monomial ordering. This is simply an unambiguous way of stating whether any given monomial is formally bigger than any other given monomial. We may denote this in a particular case by saying $m_1 > m_2$, where $m_1, m_2 \in \mathbb{C}[\phi^i, a^\alpha]$ are monomials in the fields and parameters. It is important to say what is *not* meant by this. We are not saying that we are taking values of the variables such that the monomial m_1 is numerically larger than the monomial m_2 . We are rather saying that, in our formal ordering, m_1 is considered to come before m_2 .

For our purposes we will require a special type of monomial ordering called an elimination ordering. This means that our formal ordering of monomials has the following property:

$$P \in \mathbb{C}[\phi^i, a^\alpha], \quad \text{LM}(P) \in \mathbb{C}[a^\alpha] \implies P \in \mathbb{C}[a^\alpha]. \quad (2.1)$$

In words this just says that if the largest monomial in P according to our ordering, $\text{LM}(P)$, does not depend on ϕ^i , then P does not depend on the fields at all. The monomial ordering classes all monomials with fields in them as being bigger than all of those without such constituents.

Given this notion of monomial orderings, we can now present the one algorithm we will need to use—the Buchberger algorithm [24, 25]. The Buchberger algorithm takes as its input a set of polynomials. These may be thought of as a system of polynomial equations by the simple expedient of setting all of the polynomials to zero. The algorithm returns a new

set of polynomials which, when thought of as a system of equations in the same way, has the same solution set as the input. The output system, however, has several additional useful properties as we will see.

The Buchberger Algorithm

- (1) Start with a set of polynomials call this set \mathcal{G} .
- (2) Choose a monomial ordering with the elimination property described above.
- (3) For any pair of polynomials $P_i, P_j \in \mathcal{G}$, multiply by monomials, and form a difference so as to cancel the leading monomials with respect to the monomial ordering:

$$S = p_1 P_i - p_2 P_j \quad \text{s.t. } p_1 \text{LM}(P_i), p_2 \text{LM}(P_j) \text{ cancel.} \quad (2.2)$$

- (4) Perform polynomial long division of S with respect to \mathcal{G} ; that is, form $\tilde{h} = S - m_3 P_k$, where m_3 is a monomial and $P_k \in \mathcal{G}$ such that $m_3 \text{LM}(P_k)$ cancels a monomial in S . Repeat until no further reduction is possible. Call the result h .
- (5) If $h = 0$, then consider the next pair. If $h \neq 0$, then add h to \mathcal{G} and return to step (3).

The algorithm terminates when all S -polynomials which may be formed reduce to 0. The final set of polynomials is called a Gröbner basis.

As mentioned above, the resulting set of polynomials has several nice properties. The feature which is often taken as defining is that polynomial long division with respect to this new set of polynomials always gives the same answer—it does not matter in which order we divide the polynomials out by.

For us, however, the important point about our Gröbner basis \mathcal{G} is that it has what is called the elimination property. The set of all polynomials in \mathcal{G} which depend only upon the parameters, $\mathcal{G} \cap \mathbb{C}[a^\alpha]$, gives a complete set of equations on the a^α which are necessary and sufficient for the existence of a solution to the set of equations we started with. The reason why this is so is actually very straightforward. Our elimination ordering says that any monomial with a field in it is greater than any monomial only made up of parameters. Looking back at step (3) of the Buchberger algorithm we see that we are repeatedly canceling off the leading terms of our polynomials—those containing the fields—as much as we can. Thus, if it is possible to rearrange our initial equations to get expressions which do not depend upon the fields ϕ^i , then the Buchberger algorithm will do this for us. Clearly, while we have interpreted the a^α as parameters and the ϕ^i as fields in the above, as this is what we will require for Section 3, this was not necessary. The Buchberger algorithm can be used to eliminate any unwanted set of variables from a problem, in the manner we have described.

This completes all of the mathematics that we will need for our entire discussion, and we may now move on to apply what we have learnt.

3. Constraints

The first physical question we wish to answer is the following. Given a four-dimensional $\mathcal{N} = 1$ supergravity describing a flux compactification, what are the constraints on the flux

parameters which are necessary and sufficient for the existence of a particular kind of vacuum? This question can be asked, and answered [11–14], for any kind of vacuum, but in the interests of concreteness and brevity let us restrict ourselves to the simple case of supersymmetric Minkowski vacua.

Here is the superpotential of a typical system, taken from [29]. It describes a nongeometric compactification of type IIB string theory

$$\begin{aligned}
W = & a_0 - 3a_1\tau + 3a_2\tau^2 - a_3\tau^3 + S(-b_0 + 3b_1\tau - 3b_2\tau^2 + b_3\tau^3) \\
& + 3U(c_0 + (\hat{c}_1 + \check{c}_1 + \tilde{c}_1)\tau - (\hat{c}_2 + \check{c}_2 + \tilde{c}_2)\tau^2 - c_3\tau^3).
\end{aligned} \tag{3.1}$$

This system has some known constraints on its parameters which are necessary for the existence of a permissible vacuum. These come from, for example, tadpole cancellation conditions:

$$\begin{aligned}
a_0b_3 - 3a_1b_2 + 3a_2b_1 - a_3b_0 &= 16, \\
a_0c_3 + a_1(\check{c}_2 + \hat{c}_2 - \tilde{c}_2) - a_2(\check{c}_1 + \hat{c}_1 - \tilde{c}_1) - a_3c_0 &= 0, \\
c_0b_2 - \tilde{c}_1b_1 + \hat{c}_1b_1 - \check{c}_2b_0 &= 0, & c_0\tilde{c}_2 - \check{c}_1^2 + \tilde{c}_1\hat{c}_1 - \hat{c}_2c_0 &= 0, \\
\check{c}_1b_3 - \hat{c}_2b_2 + \tilde{c}_2b_2 - c_3b_1 &= 0, & c_3\tilde{c}_1 - \check{c}_2^2 + \tilde{c}_2\hat{c}_2 - \hat{c}_1c_3 &= 0, \\
c_0b_3 - \tilde{c}_1b_2 + \hat{c}_1b_2 - \check{c}_2b_1 &= 0, & c_3c_0 - \check{c}_2\hat{c}_1 + \tilde{c}_2\check{c}_1 - \hat{c}_1\tilde{c}_2 &= 0, \\
\check{c}_1b_2 - \hat{c}_2b_1 + \tilde{c}_2b_1 - c_3b_0 &= 0, & \hat{c}_2\tilde{c}_1 - \tilde{c}_1\check{c}_2 + \check{c}_1\hat{c}_2 - c_0c_3 &= 0.
\end{aligned} \tag{3.2}$$

We also have the same constraints with the hats and checks switched around. In this example the fields, which we have been calling ϕ^i , are S , τ , and U , and everything else is a “flux” parameter, or an a^a in our notation.

In total, the equations which must be satisfied if a supersymmetric Minkowski vacuum is to exist are $W = 0$, $\partial_S W = 0$, $\partial_\tau W = 0$, $\partial_U W = 0$, and the constraints on the flux parameters given above. To extract a set of constraints solely involving the parameters which are necessary and sufficient for the existence of a solution to these equations, we simply follow the procedure outlined in the previous section.

We can carry out this calculation trivially in Stringvacua [11–14] and, in fact, this example is provided for the user in the help system. The result is as follows:

$$\begin{aligned}
0 &= \tilde{c}_1 = \tilde{c}_2 = \hat{c}_1 = \hat{c}_2 = \check{c}_1 = \check{c}_2 = c_0 = c_3, \\
0 &= 16 + a_3b_0 - 3a_2b_1 + 3a_1b_2 - a_0b_3, \\
0 &= 16a_3^2b_0^2 - 96a_2a_3b_0b_1 - 288a_2^2b_1^2 + 432a_1a_3b_1^2 + 54a_2^3b_1^3 - 81a_1a_2a_3b_1^3 + 27a_0a_3^2b_1^3 \\
&\quad + 432a_1a_3b_0b_2 - 27a_2^2a_3b_0^2b_2 + 48a_1a_3^2b_0^2b_2 - 288a_0a_3b_1b_2 - 18a_1a_2a_3b_0b_1b_2 - 45a_0a_3^2b_0b_1b_2 \\
&\quad - 54a_1a_2^2b_1^2b_2 + 81a_1^2a_3b_1^2b_2 - 27a_0a_2a_3b_1^2b_2 + 54a_0a_2a_3b_0b_2^2 + 27a_0a_1a_3b_1b_2^2 - 27a_0^2a_3b_2^3
\end{aligned}$$

$$\begin{aligned}
& -288a_1a_2b_0b_3 - 32a_0a_3b_0b_3 + 27a_2^3b_0^2b_3 - 45a_1a_2a_3b_0^2b_3 + 432a_0a_2b_1b_3 - 27a_1a_2^2b_0b_1b_3 \\
& + 54a_1^2a_3b_0b_1b_3 + 48a_0a_2a_3b_0b_1b_3 + 18a_0a_2^2b_1^2b_3 - 81a_0a_1a_3b_1^2b_3 - 144a_0a_1b_2b_3 \\
& + 27a_1^2a_2b_0b_2b_3 - 54a_0a_2^2b_0b_2b_3 - 51a_0a_1a_3b_0b_2b_3 + 27a_0a_1a_2b_1b_2b_3 + 45a_0^2a_3b_1b_2b_3 \\
& - 27a_0a_1^2b_2^2b_3 + 27a_0^2a_2b_2^2b_3 + 16a_0^2b_3^2 - 27a_1^3b_0b_3^2 + 45a_0a_1a_2b_0b_3^2 + 27a_0a_1^2b_1b_3^2 \\
& - 48a_0^2a_2b_1b_3^2 + 3a_0^2a_1b_2b_3^2.
\end{aligned} \tag{3.3}$$

The reader will note that the result is a somewhat lengthy set of equations. In principle one has to find quantized solutions to these expressions, an obviously intractable Diophantine problem, and therefore it might be asked why this result is of any use. In fact, knowledge of such constraints on the flux parameters is hugely useful for a number of reasons.

- (i) Firstly, we note that, while the full result of this process is often complex, some of the constraints can give us simple information about the system. In the current case, for example, it can be seen that $\tilde{c}_2 = 0$ is required for the existence of a supersymmetric Minkowski vacuum.
- (ii) Secondly, if one is scanning over a range of flux parameters and trying to numerically solve the equations to find vacua, one can speed up one's analysis by first substituting any given set of flux parameters into the constraints we have obtained. If the constraints are not satisfied, then vacua do not exist and there is no point in searching numerically for a solution. This turns what would be a time-consuming numerical process giving inconclusive results (no solution was found) into a quick analytic conclusion (no solution exists).
- (iii) Lastly, knowledge of such constraints can greatly speed up algebraic approaches to finding vacua such as those outlined in [11–14].

4. Simplifying Equations for Vacua

Another use for the mathematics we learnt in Section 2 is the so-called “splitting tools” used in work such as [11–14]. The physical idea here is simple. Consider trying to solve the equations $\partial V/\partial\phi^i = 0$ to find the vacua, including those which spontaneously break supersymmetry, of some supergravity theory. These equations are often extremely complicated. One way of viewing why this is so is that the equations for the turning points of the potential contain a *lot* of information. They describe not only the isolated minima of the potential which are of interest but also lines of maxima, saddle points of various sorts, and so forth. A useful tool to have, therefore, would be an algorithm that takes such a system as an input and returns a whole series of separate sets of equations, each individually describing fewer turning points. Since each separate equation system would then contain less information, one might expect them to be easier to solve. It would be beneficial to choose a division of these equations which has physical interest. The choice we will make here, and which programs like Stringvacua implement [11–14], is to split up the equations for the turning points according to how they break supersymmetry—that is, according to which F -terms vanish when evaluated on those loci.

The ability that packages such as Stringvacua have to split up equations in this manner is based upon the following splitting tool (see [30] for a nice set of more detailed notes on this kind of mathematical technique). Say that one of the F -terms of our theory is called F . Then we can split the equations describing turning points of the potential into two pieces:

$$\frac{\partial V}{\partial \phi^i} = 0, \quad F = 0, \quad (4.1)$$

$$\frac{\partial V}{\partial \phi^i} = 0, \quad F \neq 0. \quad (4.2)$$

The first of these expressions is a set of equations which is easier to solve, in general, than $\partial V/\partial \phi^i = 0$ alone. We can use the F -term to simplify the equations for the turning points of the potential. On the other hand, expression (4.2) is not even a set of equations—it contains an inequality. We can convert (4.2) into a system purely involving equalities by making use of the mathematics we learned in Section 2.

Consider the following set of equations, including a dummy variable t :

$$\frac{\partial V}{\partial \phi^i} = 0, \quad Ft - 1 = 0. \quad (4.3)$$

The second equation in (4.3) has a solution if and only if $F \neq 0$, simply $t = 1/F$. If $F = 0$, then the equation reduces to $-1 = 0$ which clearly has no solutions. Equations (4.3), then, have a solution whenever the set of equalities and inequalities (4.2) do. Unfortunately they also depend upon one extra, and unwanted, variable— t . This is not a problem as we already know how to remove unwanted variables from our equations. We can simply eliminate them, as we did the fields in Section 2. This will leave us with a necessary and sufficient set of equations in ϕ^i and a^α for a solution to (4.3) and thus to (4.2).

So we can split the equations for the turning points of our potential into two simpler systems. One describes the turning points of V for which $F = 0$ and the other, those for which $F \neq 0$. We can of course perform such a splitting many times—once for each F -term! In fact, using additional techniques from algorithmic algebraic geometry [11–14, 31–33], which are essentially based upon the same trick, one can go much further. One can split the equations for the turning points up into component parts gaining one set of equations for every separate locus. Because we know which F -terms are nonzero on each of them, these are classified according to how they break supersymmetry. The researcher interested in a certain type of breaking can therefore select the equations describing the vacua of interest and throw everything else away.

The above process of splitting up the equations for the vacua of a system can be very simply carried out in Stringvacua. Numerous examples can be found in the Mathematica help files which come with the package [11–14]. Here, let us consider the example of M-theory

compactified on the coset $(SU(3) \times U(1))/ (U(1) \times U(1))$. The Kähler and superpotential for this coset, which has $SU(3)$ structure, has been presented in [34]

$$K = -4 \log(-i(U - \bar{U})) - \log(-i(T_1 - \bar{T}_1)(T_2 - \bar{T}_2)(T_3 - \bar{T}_3)),$$

$$W = \frac{1}{\sqrt{8}} [4U(T_1 + T_2 + T_3) + 2T_2T_3 - T_1T_3 - T_1T_2 + 200]. \quad (4.4)$$

Even this, relatively simple, model results in a potential of considerable size. Defining $T_i = -it_i + \tau_i$ and $U = -ix + y$, we find

$$V = \frac{1}{256t_1t_2t_3x^4} \left(40000 + t_3^2\tau_1^2 - 400\tau_1\tau_2 - 4t_3^2\tau_1\tau_2 + 4t_3^2\tau_2^2 + \tau_1^2\tau_2^2 - 400\tau_1\tau_3 + 800\tau_2\tau_3 \right)$$

$$+ 2\tau_1^2\tau_2\tau_3 - 4\tau_1\tau_2^2\tau_3 + \tau_1^2\tau_3^2 - 4\tau_1\tau_2\tau_3^2 + 4\tau_2^2\tau_3^2 - 24t_2t_3x^2 + 4t_3^2x^2 - 24t_1(t_2 + t_3)x^2$$

$$+ 4\tau_1^2x^2 + 8\tau_1\tau_2x^2 + 4\tau_2^2x^2 + 8\tau_1\tau_3x^2 + 8\tau_2\tau_3x^2 + 4\tau_3^2x^2 + 1600\tau_1y - 8t_3^2\tau_1y$$

$$+ 1600\tau_2y + 16t_3^2\tau_2y - 8\tau_1^2\tau_2y - 8\tau_1\tau_2^2y + 1600\tau_3y - 8\tau_1^2\tau_3y + 16\tau_2^2\tau_3y - 8\tau_1\tau_3^2y \quad (4.5)$$

$$+ 16\tau_2\tau_3^2y + 16t_3^2y^2 + 16\tau_1^2y^2 + 32\tau_1\tau_2y^2 + 16\tau_2^2y^2 + 32\tau_1\tau_3y^2 + 32\tau_2\tau_3y^2 + 16\tau_3^2y^2$$

$$+ t_1^2(t_2^2 + t_3^2 + \tau_2^2 + 2\tau_2\tau_3 + \tau_3^2 + 4x^2 - 8\tau_2y - 8\tau_3y + 16y^2)$$

$$+ t_2^2(4t_3^2 + \tau_1^2 - 4\tau_1(\tau_3 + 2y) + 4(\tau_3^2 + x^2 + 4\tau_3y + 4y^2)).$$

To find the turning points of this potential we naively need to take eight different derivatives of (4.5) and solve the resulting set of intercoupled equations in eight variables. This is clearly prohibitively difficult. Using the techniques described in this section, however, Stringvacua can separate off parts of the vacuum space for us with ease. Consider, for example, the vacua which are isolated in field space and for which the real parts of all of the F -terms are nonzero, with the imaginary parts vanishing. To find these, the package tells us, we need only to solve the equations

$$9x^2 - 500 = 0, \quad 5t_1 - 2x = 0, \quad t_2 - x = 0, \quad t_3 - x = 0, \quad \tau_1 = \tau_2 = \tau_3 = y = 0. \quad (4.6)$$

Because they only describe a small subset of all of the turning points of the full potential, these equations are extremely simple in form and may be trivially solved. For this particular example the physically acceptable turning point that results is a saddle—something which can be readily ascertained once its location has been discovered.

5. Geometry of Vacuum Spaces

As a final example of what we can do with the simple techniques introduced in Section 2, we will show how to calculate the vacuum space of a globally supersymmetric gauge theory. It is a well-known result (see [35] and references therein) that the supersymmetric vacuum space

Table 1: The set of elementary gauge invariant operators for the electroweak sector of the MSSM.

Type	Explicit sum	Index	Number
LH	$L_\alpha^i H_\beta e^{\alpha\beta}$	$i = 1, 2, 3$	3
$H\bar{H}$	$H_\alpha \bar{H}_\beta e^{\alpha\beta}$		1
LLe	$L_\alpha^i L_\beta^j e^k e^{\alpha\beta}$	$i, j = 1, 2, 3; k = 1, \dots, j-1$	9
$L\bar{H}e$	$L_\alpha^i \bar{H}_\beta e^{\alpha\beta} e^j$	$i, j = 1, 2, 3$	9
ν	ν^i	$i = 1, 2, 3$	1

of such a theory, with gauge group G , can be described as the space of holomorphic gauge invariant operators (GIOs) built out of F -flat field configurations. What does this space look like? Consider a space, the coordinates of which are identified with the GIOs of the theory. If there were no relations amongst the gauge invariant operators, then this space would be the vacuum space. However, there frequently are relations because of the way in which the GIOs are built out of the fields. For example, if we have three gauge invariant operators S^1 , S^2 , and S^3 which are built out of the fields as $S^1 = (\phi^1)^2$, $S^2 = (\phi^2)^2$, $S^3 = \phi^1 \phi^2$, then we have the relation $S^1 S^2 = (S^3)^2$. If we take these GIOs to be built out of the F -flat field configurations, then there will be still further relations among them. The vacuum space of the theory is the subspace defined by the solutions of these equations describing relations amongst the gauge invariant operators, once F -flatness has been taken into account.

How can we calculate such a thing? The holomorphic gauge invariant operators of a globally supersymmetric gauge theory are given in terms of the fields

$$S^I = f^I(\phi^i). \quad (5.1)$$

Here S^I are our GIOs, and the f^I are the functions of the fields that define them. Let us write the F -terms of the theory as F^i . Consider the following set of equations:

$$F^i = 0, \quad S^I - f^I(\phi^i) = 0. \quad (5.2)$$

These equations have solutions whenever the S^I are given by functions of the fields in the correct way and when those field configurations which are being used are F -flat. However, according to the proceeding discussion, we wish to simply have equations in terms of the GIOs to describe our vacuum space. As in previous sections, we can eliminate the unwanted variables in our problem, in this case, the fields ϕ^i , using the algorithm of Section 2 to obtain the equations describing the vacuum space.

As a simple example, let us take the electroweak sector of the MSSM [1, 2] (with right-handed neutrinos). Given the field content of the left-handed leptons, L_α^i , the right-handed leptons, e^i and ν^i , and the two Higgs, H and \bar{H} , one can build the elementary GIOs given in Table 1. The indices i, j run over the 3 flavours, and the indices α, β label the fundamental of $SU(2)$.

Gröbner basis can be found in [36]. If d is the largest degree found in your original set of equations, then this bound is

$$2\left(\frac{d^2}{2} + d\right)^{2^{n-1}}, \quad (6.1)$$

where n is the number of variables. This *worst case* bound is therefore scaling doubly exponentially in the number of degrees of freedom. These very high-degree polynomials are an indication that the problem is becoming very complex and thus computationally intensive. Despite this, physically useful cases can be analysed using this algorithm quickly, as demonstrated in this paper and in the references. This scaling does mean that one is not likely to gain much by putting one's problem on a much faster computer. One good point about (6.1) is that if you can find a way, using physical insight, to simplify the problem under study, then what you can achieve may improve doubly exponentially. Such a piece of physical insight was one of the keystones of the application of these methods to finding flux vacua [11–14].

We finish by commenting that the methods of computational commutative algebra which we have discussed here are extremely versatile. We have been able to perform three very different tasks simply utilizing one algorithm in a very simple manner. These methods are of great utility in problems taken from the literature, and their implementation in a user friendly way in Stringvacua means that they may be tried out on any given problem with very little expenditure of time and effort by the researcher. Many more techniques from the field of algorithmic commutative algebra could be applied to physical systems than those described here or indeed in the physics literature. We can therefore expect that this subject will only increase in importance in the future.

Acknowledgments

The author is funded by STFC and would like to thank the University of Pennsylvania for generous hospitality while some of this document was being written. In addition he would like to thank the organisers of the 2008 Vienna ESI workshop “Mathematical Challenges in String Phenomenology,” where the talk upon which these notes are based was first given. The author would like to offer heartfelt thanks to his collaborators on the various projects upon which this paper is based. These include Lara Anderson, Daniel Grayson, Amihay Hanany, Yang-Hui He, Anton Ilderton, Vishnu Jejjala, André Lukas, Noppadol Mekareeya, and Brent Nelson.

References

- [1] J. Gray, Y. H. He, V. Jejjala, and B. D. Nelson, “Exploring the vacuum geometry of $N = 1$ gauge theories,” *Nuclear Physics B*, vol. 750, no. 1-2, pp. 1–27, 2006.
- [2] J. Gray, Y. H. He, V. Jejjala, and B. D. Nelson, “Vacuum geometry and the search for new physics,” *Physics Letters. Section B*, vol. 638, no. 2-3, pp. 253–257, 2006.
- [3] S. Benvenuti, B. O. Feng, A. Hanany, and Y. H. He, “Counting BPS operators in gauge theories: quivers, syzygies and plethystics,” *Journal of High Energy Physics*, vol. 2007, no. 11, article 050, 2007.
- [4] B. Feng, A. Hanany, and Y. H. He, “Counting gauge invariants: the plethystic program,” *Journal of High Energy Physics*, vol. 2007, no. 3, article no. 090, 2007.

- [5] D. Forcella, A. Hanany, Y. -H. He, and A. Zaffaroni, "The master space of $N = 1$ gauge theories," *Journal of High Energy Physics*, vol. 2008, no. 8, article 012, 2008.
- [6] J. Gray, Y. -H. He, A. Hanany, N. Mekareeya, and V. Jejjala, "SQCD: A geometric aperçu," *Journal of High Energy Physics*, vol. 2008, no. 5, article 099, 2008.
- [7] A. Hanany and N. Mekareeya, "Counting gauge invariant operators in SQCD with classical gauge groups," *Journal of High Energy Physics*, vol. 2008, no. 10, article 012, 2008.
- [8] A. Hanany, N. Mekareeya, and G. Torri, "The Hilbert series of adjoint SQCD," *Nuclear Physics B*, vol. 825, no. 1-2, pp. 52–97, 2010.
- [9] F. Ferrari, "On the geometry of super Yang-Mills theories: phases and irreducible polynomials," *Journal of High Energy Physics*, vol. 2009, no. 1, article no. 026, 2009.
- [10] J. Distler and U. Varadarajan, "Random polynomials and the friendly landscape," <http://arxiv.org/abs/hep-th/0507090>.
- [11] J. Gray, Y. H. He, A. Ilderton, and A. Lukas, "STRINGVACUA. A Mathematica package for studying vacuum configurations in string phenomenology," *Computer Physics Communications*, vol. 180, no. 1, pp. 107–119, 2009.
- [12] J. Gray, Y. H. He, A. Ilderton, and A. Lukas, "A new method for finding vacua in string phenomenology," *Journal of High Energy Physics*, vol. 2007, no. 7, article no. 023, 2007.
- [13] J. Gray, Y. H. He, and A. Lukas, "Algorithmic algebraic geometry and flux vacua," *Journal of High Energy Physics*, vol. 2006, no. 9, article no. 031, 2006.
- [14] "The Stringvacua Mathematica package," <http://www-thphys.physics.ox.ac.uk/projects/Stringvacua/>.
- [15] A. Font, A. Guarino, and J. M. Moreno, "Algebras and non-geometric flux vacua," *Journal of High Energy Physics*, vol. 2008, no. 12, article no. 050, 2008.
- [16] A. Guarino and G. J. Weatherill, "Non-geometric flux vacua, s-duality and algebraic geometry," *Journal of High Energy Physics*, vol. 2009, no. 2, article 042, 2009.
- [17] L. Anderson, Y.-H. He, and A. Lukas, "Monad bundles in heterotic string compactifications," *Journal of High Energy Physics*, vol. 2008, no. 7, article 104, 2008.
- [18] L. B. Anderson, Y. H. He, and A. Lukas, "Heterotic compactification, an algorithmic approach," *Journal of High Energy Physics*, vol. 2007, no. 7, article no. 049, 2007.
- [19] P. Kaura and A. Misra, "On the existence of non-supersymmetric black hole attractors for two-parameter Calabi-Yau's and attractor equations," *Fortschritte der Physik*, vol. 54, no. 12, pp. 1109–1141, 2006.
- [20] S. Raby and A. Wingerter, "Can string theory predict the Weinberg angle?" *Physical Review D*, vol. 76, no. 8, Article ID 086006, 2007.
- [21] V. Braun, T. Brelidze, M. R. Douglas, and B. A. Ovrut, "Calabi-Yau metrics for quotients and complete intersections," *Journal of High Energy Physics*, vol. 2008, no. 5, article 080, 2008.
- [22] V. Braun, T. Brelidze, M. R. Douglas, and B. A. Ovrut, "Eigenvalues and eigenfunctions of the scalar Laplace operator on Calabi-Yau manifolds," *Journal of High Energy Physics*, vol. 2008, no. 7, article 120, 2008.
- [23] P. Candelas and R. Davies, "New Calabi-Yau manifolds with small Hodge numbers," *Fortschritte der Physik*, vol. 58, no. 4-5, pp. 383–466, 2010.
- [24] B. Buchberger, *An algorithm for finding the bases elements of the residue class ring modulo a zero dimensional polynomial ideal*, Ph.D. thesis, University of Innsbruck, Austria, 1965.
- [25] B. Buchberger, "An algorithmical criterion for the solvability of algebraic systems of equations," *Aequationes Mathematicae*, vol. 4, no. 3, pp. 374–383, 1970 (German).
- [26] D. Grayson and M. Stillman, "Macaulay 2, a software system for research in algebraic geometry," <http://www.math.uiuc.edu/Macaulay2/>.
- [27] G.-M. Greuel, G. Pfister, and H. Schönemann, "Singular: a computer algebra system for polynomial computations," Centre for Computer Algebra, University of Kaiserslautern, 2001, <http://www.singular.uni-kl.de/>.
- [28] M. Kauers and V. Levandovskyy, "Singular.m," <http://www.risc.uni-linz.ac.at/research/combinat/software/Singular/>.
- [29] J. Shelton, W. Taylor, and B. Wecht, "Nongeometric flux compactifications," *Journal of High Energy Physics*, no. 10, pp. 2057–2080, 2005.
- [30] M. Stillman, "Tools for computing primary decompositions and applications to ideals associated to Bayesian networks," in *Solving Polynomial Equations: Foundations, Algorithms, and Applications*, A. Dickenstein and I. Z. Emiris, Eds., Springer, Berlin, Germany, 2005.

- [31] P. Gianni, B. Trager, and G. Zacharias, "Gröbner bases and primary decomposition of polynomial ideals," *Journal of Symbolic Computation*, vol. 6, pp. 149–167, 1988.
- [32] D. Eisenbud, C. Huneke, and W. Vasconcelos, "Direct methods for primary decomposition," *Inventiones Mathematicae*, vol. 110, no. 1, pp. 207–235, 1992.
- [33] T. Shimoyama and K. Yokoyama, "Localization and primary decomposition of polynomial ideals," *Journal of Symbolic Computation*, vol. 22, no. 3, pp. 247–277, 1996.
- [34] A. Micu, E. Palti, and P. M. Saffin, "M-theory on seven-dimensional manifolds with SU(3) structure," *Journal of High Energy Physics*, vol. 2006, no. 5, article 048, 2006.
- [35] M. A. Luty and W. Taylor, "Varieties of vacua in classical supersymmetric gauge theories," *Physical Review D*, vol. 53, no. 6, pp. 3399–3405, 1996.
- [36] H. M. Möller and F. Mora, "Upper and lower bounds for the degree of Gröbner bases," in *Proceedings of the International Symposium on Symbolic and Algebraic Computation (EUROSAM '84)*, Lecture Notes in Comput. Sci. 174, pp. 172–183, Cambridge, UK, 1984.

Research Article

Del Pezzo Singularities and SUSY Breaking

Dmitry Malyshev

*Center for Cosmology and Particle Physics, NYU, Meyer Hall of Physics, 4 Washington Place,
New York, NY 10003, USA*

Correspondence should be addressed to Dmitry Malyshev, dm137@nyu.edu

Received 5 December 2010; Accepted 28 February 2011

Academic Editor: Yang-Hui He

Copyright © 2011 Dmitry Malyshev. This is an open access article distributed under the Creative Commons Attribution License, which permits unrestricted use, distribution, and reproduction in any medium, provided the original work is properly cited.

An analytic construction of compact Calabi-Yau manifolds with del Pezzo singularities is found. We present complete intersection CY manifolds for all del Pezzo singularities and study the complex deformations of these singularities. An example of the quintic CY manifold with del Pezzo 6 singularity and some number of conifold singularities is studied in detail. The possibilities for the “geometric” and ISS mechanisms of dynamical SUSY breaking are discussed. As an example, we construct the ISS vacuum for the del Pezzo 6 singularity.

1. Motivation

Recently, there has been a substantial progress in Model building involving the D-branes at the singularities of noncompact Calabi-Yau manifolds. On the one hand, the singularities provide enough flexibility to find phenomenologically acceptable extensions of the Standard Model [1, 2] and solve some problems such as finding metastable susy breaking vacua [3, 4]. On the other hand, the presence of the singularity eliminates certain massless moduli, such as the adjoint fields on the branes wrapping rigid cycles [1, 5].

The main purpose of this paper is to study the del Pezzo and conifold singularities on compact CY manifolds that may be useful for the compactifications of dynamical SUSY breaking mechanisms. The stringy realizations of metastable SUSY breaking vacua have been known for some time [6, 7]. We will focus on the two recent approaches to the dynamical SUSY breaking: on the “geometrical” approach of [8, 9] and on the ISS construction [10]. One of the main goals will be to study the topological conditions for the compactification of the above constructions.

An important topological property of “geometrical” mechanism is the presence of several homologous rigid two-cycles. This is not difficult to achieve in the case of conifold singularities. For example, in the geometric transitions on compact CY manifolds [11, 12],

several conifolds may be resolved by a single Kahler modulus, that is, the two-cycles at the tip of these conifolds are homologous to each other. However, this is not always true for the del Pezzo singularities, that is, the two-cycles in the resolution of del Pezzo singularity may have no homologous rigid two-cycles on the compact CY. In the paper, we explicitly construct a compact CY manifold with del Pezzo 6 singularity and a number of conifolds such that some two-cycles on the del Pezzo are homologous to the two-cycles of the conifolds. This construction opens up the road for the generalization of geometrical SUSY breaking in the case of del Pezzo singularities, where one may hope to use the richness of deformations of these singularity for phenomenological applications.

A more direct way towards phenomenology is provided by the ISS mechanism. The realization of ISS construction for del Pezzo 5 and 8 singularities was considered in [4]. As an example, we find an ISS vacuum for the del Pezzo 6 singularity. The del Pezzo 6 surface can be embedded in \mathbb{P}^3 by a degree 3 polynomial. This is one of the most simple analytical representations of del Pezzo surfaces, which enables us to find an analytical embedding of the corresponding del Pezzo 6 singularity in a compact Calabi Yau manifold, the quintic CY embedded in \mathbb{P}^4 by a degree 5 polynomial.

A nice feature of the del Pezzo singularities is that they are isolated. Thus, the fractional branes, that one typically introduces in these models, are naturally stabilized against moving away from the singularity. But, for example, in the models involving quotients of conifolds [3, 13], the singularities are not isolated and one needs to pay special attention to stabilize the fractional branes against moving along the singular curves.

Apart from the application to SUSY breaking, the construction of compact CY manifolds with del Pezzo singularities may be useful for the study of deformations of these singularities. In particular, we will be interested in the D-brane interpretation of deformations.

In general, a singularity can be smoothed out in two different ways, it can be either deformed or resolved (blown up). The former corresponds to the deformations of the complex structure, described by the elements of $H^{2,1}$; the latter corresponds to Kähler deformations given by the elements of $H^{1,1}$ [14–16]. In terms of the cycles, the resolution corresponds to blowing up some two-cycles (four-cycles), while the complex deformations correspond to the deformations of the three-cycles. For example, the conifold can be either deformed by placing an S^3 at the tip of the conifold or resolved by placing an S^2 [17]. The process where some three-cycles shrink to form a singularity and after that the singularity is blown up is called the geometric transition [11, 12]. For the conifold, the geometric transition has a nice interpretation in terms of the branes. The deformation of the conifold is induced by wrapping the D5-branes around the vanishing S^2 at the tip [18]. The resolution of the conifold corresponds to giving a vev to a baryonic operator, that can be interpreted in terms of the D3-branes wrapping the vanishing S^3 at the tip of the conifold [19].

The example of the conifold encourages to conjecture that any geometric transition can be interpreted in terms of the branes. The nonanomalous (fractional) branes produce the fluxes that deform the three-cycles. The massless/tensionless branes correspond to baryonic operators whose vevs are interpreted as the blow-up modes.

However, there are a few puzzles with the above interpretation. In some cases, there are less deformations than nonanomalous fractional branes; in the other cases there are deformations but no fractional branes, The quiver gauge theory on the del Pezzo 1 singularity has a nonanomalous fractional brane; moreover, it has a cascading behavior [20] similar to the conifold cascade. But it is known that there are no complex deformations of the cone over

dP_1 [21–23]. The relevant observation [24] is that there are no geometric transitions for the cone over dP_1 . From the point of view of gauge theory, there is a runaway behavior at the bottom of the cascade and no finite vacuum [25].

On the other side of the puzzle, there are more complex deformations of higher del Pezzo singularities, than there are possible fractional branes. It is known that the cone over del Pezzo n surface has $c^\vee(E_n) - 1$ complex deformations [24], where $c^\vee(E_n)$ is the dual Coxeter number of the corresponding Lie group. For instance, the cone over dP_8 has 29 deformations. But there are only 8 nonanomalous combinations of fractional branes [1].

We believe that these puzzles can be managed more effectively if there were more examples of compact CY manifolds with local del Pezzo singularities. The advantage of working with compact manifolds is that they have finite a number of deformations and well-defined cohomology (there are no noncompact cycles).

The organization of the paper is as follows. In Section 2, we study the singularities on compact CY manifolds using the quintic CY manifold as an example. We restrict our attention to isolated singularities that admit crepant resolution, that is, their resolution does not affect the CY condition. There are two types of primitive isolated singularities on CY 3-folds: small contractions or conifold singularities, and del Pezzo singularities [26, 27]. We will study the example of del Pezzo 6 singularity and some number of conifolds on the quintic. The presence of conifold singularities is important if we want to put fractional branes at the del Pezzo singularity. Without conifolds, the nonanomalous two-cycles on del Pezzo (i.e., the ones that do not intersect the canonical class) are trivial within the CY manifold. It is impossible to put the fractional branes on such “cycles”, because the corresponding RR fluxes have “nowhere to go.” In the presence of conifolds, some of the two-cycles on del Pezzo may become homologous to the two-cycles of the conifolds (this will be the case in our example). Then we can put some number of D5-branes on the two-cycles of del Pezzo and some number of anti-D5-branes on the two-cycles of the conifolds. Such configuration of branes and antibranes is a first step in the geometrical SUSY breaking [8, 28]. Also the possibility to introduce the fractional branes will be crucial for the D-brane realizations of ISS construction.

In Section 3, we discuss the compactification of the geometrical SUSY breaking and the ISS model and find an ISS SUSY breaking vacuum in a quiver gauge theory for the dP_6 singularity.

In Section 4, we formulate the general construction of compact CY manifolds with del Pezzo singularities and discuss the complex deformations of these singularities. We observe that the number of deformations depends on the global properties of the two-cycles on del Pezzo that do not intersect the canonical class and have self-intersection (-2) . Suppose all such cycles are trivial within the CY, then the singularity has the maximal number of deformations. This will be the case for our embeddings of del Pezzo 5, 6, 7, and 8 singularities and for the cone over $\mathbb{P}^1 \times \mathbb{P}^1$. In the case of $dP_0 = \mathbb{P}^2$ and dP_1 singularities, we do not expect to find any deformations. In the case of del Pezzo 2, 3, and 4, our embedding leaves some of the (-2) two-cycles nontrivial within the CY; accordingly, we find less complex deformations. This result can be expected, since it is known that the del Pezzo singularities for $n \leq 4$ in general cannot be represented as complete intersections [27, 29]. In our case, the del Pezzo singularities are complete intersections but they are not generic. Specific equations for embedding of del Pezzo singularities and their deformations are provided in the appendix.

Section 5 contains discussion and conclusions.

2. Del Pezzo 6 and Conifold Singularities on the Quintic CY

The CY manifolds can have two types of primitive isolated singularities: conifold singularities and del Pezzo singularities [26, 27]. Correspondingly, we will have two types of geometric transitions.

- (1) Type I, or conifold transitions: several \mathbb{P}^1 's shrink to form conifold singularities and then these singularities are deformed.
- (2) Type II, or del Pezzo transition: a del Pezzo shrinks to a point and the corresponding singularity is deformed.

In order to illustrate the geometric transitions, we will study a particular example of transitions on the quintic CY. The example is summarized in the diagram in Figure 1. The type I transitions are horizontal, whereas the type II transitions are vertical. It is known [24] that the maximal number of deformations of a cone over dP_6 is $c^\vee(E_6) - 1 = 11$, where $c^\vee(E_6) = 12$ is the dual Coxeter number of E_6 . Going along the left vertical arrow we recover all complex deformations of the cone over dP_6 . In this case, all the two-cycles that do not intersect the canonical class on dP_6 are trivial within the CY.

For the CY with both del Pezzo and conifold singularities, the deformation of the del Pezzo singularity has only 7 parameters (right vertical arrow). The del Pezzo surface is not generic in this case. It has a two-cycle that is nontrivial within the full CY and does not intersect the canonical class inside del Pezzo. As a general rule, the existence of nontrivial two-cycles reduces the number of possible complex deformations.

The horizontal arrows represent the conifold transitions. In our example, we have 36 conifold singularities on the quintic CY. These singularities have 35 complex deformations. In the presence of dP_6 singularity, there will be only 32 conifolds that have, respectively, 31 complex deformations. (It may seem puzzling that we need exactly 36 or 32 conifolds. One can easily find the examples of quintic CY with fewer conifold singularities. But it is impossible to blow up these singularities unless we have a specific number of them at specific locations. In the example considered in [11, 12], the quintic CY has 16 conifolds placed at a \mathbb{P}^2 inside the CY.)

In general, the del Pezzo singularity and the conifold singularities are away from each other but they still affect the number of complex deformations, that is, the presence of conifolds reduces the number of deformations of del Pezzo singularity and vice versa. The diagram in Figure 1 is commutative, and the total number of complex deformations of the CY with the del Pezzo singularity and 32 conifold singularities is 42. But the interpretation of these deformations changes whether we first deform the del Pezzo singularity or we first deform the conifold singularities.

Before we go to the calculations, let us clarify what we mean by the deformations of the del Pezzo singularity. We will distinguish three kinds of deformations. The deformations of the shape of the cone, the deformations of the blown up del Pezzo with fixed canonical class and deformations that smooth out the singularity.

The first kind of deformations corresponds to the general deformations of del Pezzo surface at the base of the cone. Recall that the dP_n surface for $n > 4$ has $2n - 8$ deformations that parameterize the superpotential of the corresponding quiver gauge theory [5].

The second kind of deformations is obtained by blowing up the singularity and fixing the canonical class on the del Pezzo. In this case, the deformations of del Pezzo n surface can be described as the deformations of E_n singularity on the del Pezzo [30]. The deformations of this singularity have n parameters, corresponding to the n two-cycles that do not intersect

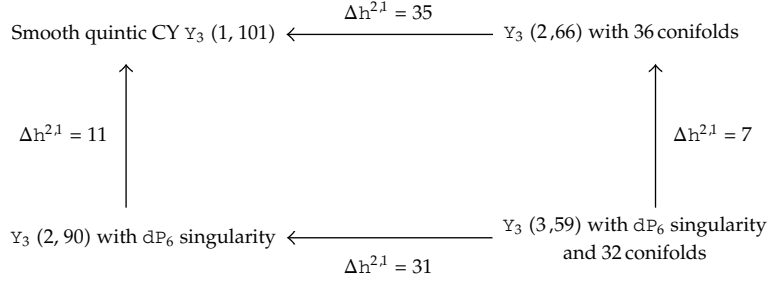


Figure 1: Possible geometric transitions of quintic CY. The numbers in parentheses denote the dimensions $(h^{1,1}, h^{2,1})$.

the canonical class. Note that the intersection matrix of these two-cycles is (minus) the Cartan matrix of E_n . The E_n singularity on the del Pezzo is an example of du Val surface singularity [31] (also known as an ADE singularity or a Kleinian singularity). A three-dimensional singularity that has a du Val singularity in a hyperplane section is called compound du Val (cDV) [26, 31]. The conifold is an example of cDV singularity since it has the A_1 singularity in a hyperplane section. The generalized conifolds [32, 33] also have an ADE singularity in a hyperplane section, that is, from the 3-dimensional point of view they correspond to some cDV singularities. In terms of the large N gauge/string duality, the deformation of the E_n generalized conifold singularity corresponds to putting some combination of fractional branes on the zero size two-cycles at the singularity. Hence, the deformation of cDV singularity that restricts to E_n singularity on the del Pezzo can be considered as a generalized type I transition.

We will be mainly interested in the the third type of deformations that correspond to smoothing of del Pezzo singularities. These deformations make the canonical class of del Pezzo surface trivial within the CY. If we put some number of nonanomalous fractional D-branes at the singularity, then the corresponding geometric transition smooths the singularity [24]. But not all the deformations can be described in this way.

In order to get some intuition about possible interpretations of these deformations, we will consider the del Pezzo 6 singularity. It is known that the dP_6 singularity has 11 complex deformations [21, 34] but there are only 6 nonanomalous fractional branes in the corresponding quiver gauge theory and there are only 6 two-cycles that do not intersect the canonical class [24]. It will prove helpful to start with a quintic CY that has 36 conifold singularities. The del Pezzo 6 singularity can be obtained by merging four conifolds at one point. There are 7 deformations of del Pezzo 6 singularity that separate these four conifolds (right vertical arrow). The remaining 4 deformations of dP_6 cone correspond to 4 deformations of the four “hidden” conifolds at the singularity. Note that the total number of deformations is 11 (left vertical arrow).

2.1. Quintic CY

The description of the quintic CY is well known [16]. Here, we repeat it in order to recall the methods [16] of finding the topology and deformations that we use later in more difficult situations.

The quintic CY manifold Y_3 is given by a degree five equation in \mathbb{P}^4

$$Q_5(z_i) = 0, \quad (2.1)$$

where $(z_0, z_1, z_2, z_3, z_4) \in \mathbb{P}^4$. The total Chern class of this manifold is

$$c(Y_3) = \frac{(1+H)^5}{1+5H} = 1 + 10H^2 - 40H^3 \quad (2.2)$$

and the first Chern class $c_1(Y_3) = 0$.

Let us calculate the number of complex deformations. The complex structures are parameterized by the coefficients in (2.1) up to the change of coordinates in \mathbb{P}^4 . The number of coefficients in a homogeneous polynomial of degree n in k variables is

$$\binom{n+k-1}{n} = \frac{(n+k-1)!}{n!(k-1)!}. \quad (2.3)$$

In the case of the quintic in \mathbb{P}^4 , the number of coefficients is

$$\binom{9}{5} = \frac{9!}{5!4!} = 126. \quad (2.4)$$

The number of reparametrizations of \mathbb{P}^4 is equal to $\dim Gl(5) = 25$. Thus, the dimension of the space of complex deformations is 101.

The number of complex deformations of CY threefolds is equal to the dimension of $H^{2,1}$ cohomology group

$$h^{2,1} = h^{1,1} - \frac{\chi}{2}, \quad (2.5)$$

where $h^{1,1}$ can be found via the Lefschetz hyperplane theorem [16, 35]

$$h^{1,1}(Y_3) = h^{1,1}(\mathbb{P}^4) = 1 \quad (2.6)$$

and the Euler characteristic is given by the integral of the highest Chern class over Y_3

$$\chi = \int_{Y_3} c_3 = \int_{\mathbb{P}^4} -40H^3 \wedge 5H = -200, \quad (2.7)$$

here, we have used that $5H$ is the Poincare dual class to Y_3 inside \mathbb{P}^4 . Consequently, $h^{2,1} = 101$ which is consistent with the number of complex deformations found before.

2.2. Quintic CY with dP_6 Singularity

Suppose that the quintic equation is not generic but has a degree three zero at the point $(w_0, w_1, w_2, w_3, w_4) = (0, 0, 0, 0, 1)$,

$$P_3(w_0, \dots, w_3)w_4^2 + P_4(w_0, \dots, w_3)w_4 + P_5(w_0, \dots, w_3) = 0, \quad (2.8)$$

where P_n 's denote degree n polynomials. The shape of the singularity is determined by $P_3(w_0, \dots, w_3)$ (we will see that this polynomial defines the del Pezzo at the tip of the cone). The deformations that smooth out the singularity correspond to adding less singular terms to (2.8), that is, the terms that have bigger powers of w_4 .

The resolution of the singularity in (2.8) can be obtained by blowing up the point $(0, 0, 0, 0, 1) \in \mathbb{P}^4$. Away from the blowup, we can use the following coordinates on \mathbb{P}^4 :

$$(w_0, \dots, w_3, w_4) = (tz_0, \dots, tz_3, s), \quad (2.9)$$

where $(s, t) \in \mathbb{P}^1$ and $(z_0, \dots, z_3) \in \mathbb{P}^3$. The blowup of the point at $t = 0$ corresponds to inserting the \mathbb{P}^3 instead of this point. Hence, the points on the blown up \mathbb{P}^4 can be parameterized globally by $(z_0, \dots, z_3) \in \mathbb{P}^3$ and $(s, t) \in \mathbb{P}^1$. The projective invariance $(s, t) \sim (\lambda s, \lambda t)$ corresponds to the projective invariance in the original \mathbb{P}^4 . In order to compensate for the projective invariance of \mathbb{P}^3 , we need to assume that locally the coordinates on \mathbb{P}^1 belong to the following line bundles over \mathbb{P}^3 , $s \in \mathcal{O}$ and $t \in \mathcal{O}(-H)$. Thus, the blowup of \mathbb{P}^4 at a point is a \mathbb{P}^1 bundle over \mathbb{P}^3 obtained by projectivization of the direct sum of $\mathcal{O}_{\mathbb{P}^3}$ and $\mathcal{O}_{\mathbb{P}^3}(-H)$ bundles, $\tilde{\mathbb{P}}^4 = P(\mathcal{O}_{\mathbb{P}^3} \oplus \mathcal{O}_{\mathbb{P}^3}(-H))$ (for more details on projective bundles see, e.g., [36, 37]). In working with projective bundles, we will use the technics similar to [37].

Using parametrization (2.9), we can write the equation on the blown up \mathbb{P}^4 as

$$P_3(z_0, \dots, z_3)s^2 + P_4(z_0, \dots, z_3)st + P_5(z_0, \dots, z_3)t^2 = 0. \quad (2.10)$$

This equation is homogeneous of degree two in the coordinates on \mathbb{P}^1 and degree three in the z_i 's. Note that $t \in \mathcal{O}(-H)$, that is, it has degree (-1) in the z_i 's and $s \in \mathcal{O}$ has degree zero.

Let us prove that the manifold defined by (2.10) has vanishing first Chern class, that is, it is a CY manifold. Let H be the hyperplane class in \mathbb{P}^3 and G the hyperplane class on the \mathbb{P}^1 fibers. Let $M = P(\mathcal{O}_{\mathbb{P}^3} \oplus \mathcal{O}_{\mathbb{P}^3}(-H))$ denote the \mathbb{P}^1 bundle over \mathbb{P}^3 . The total Chern class of M is

$$c(M) = (1 + H)^4(1 + G)(1 + G - H), \quad (2.11)$$

where $(1 + H)^4$ is the total Chern class of \mathbb{P}^3 , $(1 + G)$ corresponds to $s \in \mathcal{O}_{\mathbb{P}^3}$, and $(1 + G - H)$ corresponds to $t \in \mathcal{O}_{\mathbb{P}^3}(-H)$. Note that $G(G - H) = 0$ on this \mathbb{P}^1 bundle and, as usual, $H^4 = 0$ on the \mathbb{P}^3 .

Let Y_3 denote the surface embedded in M by (2.10). Since the equation has degree 3 in z_i and degree two in (s, t) , the class Poincare dual to $Y_3 \subset M$ is $3H + 2G$ and the total Chern class is

$$c(Y_3) = \frac{(1 + H)^4(1 + G)(1 + G - H)}{1 + 3H + 2G}. \quad (2.12)$$

Expanding $c(Y_3)$, it is easy to check that $c_1(Y_3) = 0$.

The intersection of Y_3 with the blown up \mathbb{P}^3 at $t = 0$ is given by the degree three equation $P_3(z_0, \dots, z_3) = 0$ in \mathbb{P}^3 . The surface B defined by this equation is the del Pezzo 6 surface [16, 35]. The total Chern class and the Euler character of B

$$c(B) = \frac{(1+H)^4}{1+3H} = 1 + H + 3H^2, \quad (2.13)$$

$$\chi(B) = \int_B c_2(B) = \int_{\mathbb{P}^3} 3H^2 \wedge 3H = 9. \quad (2.14)$$

In the calculation of $\chi(B)$, we have used that $3H$ is the Poincare dual class to B inside \mathbb{P}^3 .

It is known that the normal bundle to contractable del Pezzo in a CY manifold is the canonical bundle on del Pezzo [38]. Let us check this statement in our example. The canonical class is minus the first Chern class that can be found from (2.13) (Slightly abusing the notations, we denote by H both the class of \mathbb{P}^3 and the restriction of this class to $B \in \mathbb{P}^3$.)

$$K(B) = -H. \quad (2.15)$$

The coordinate t describes the normal direction to B inside Y_3 . Since $t \in \mathcal{O}_{\mathbb{P}^3}(-H)$, restricting to B we find that t belongs to the canonical bundle over B . Hence locally, near $t = 0$, the CY threefold Y_3 has the structure of the CY cone over the del Pezzo 6 surface.

The smoothing of the singularity corresponds to adding less singular terms in (2.8). These terms have 15 parameters, but also we get back 4 reparametrizations (now, we can add w_4 to the other coordinates). Hence, smoothing of the singularity corresponds to 11 complex structure deformations that is the maximal expected number of deformations of dP_6 singularity.

In view of applications in Section 4, let us describe the geometric transition between the CY with the resolved dP_6 singularity and a smooth quintic CY in more details. As we have shown above, the CY with the blown up dP_6 singularity can be described by the following equation in the \mathbb{P}^1 bundle over \mathbb{P}^3 :

$$P_3(z_0, \dots, z_3)s^2 + P_4(z_0, \dots, z_3)st + P_5(z_0, \dots, z_3)t^2 = 0. \quad (2.16)$$

This equation can be rewritten as

$$P_3(tz_0, \dots, tz_3)s^2 + P_4(tz_0, \dots, tz_3)s + P_5(tz_0, \dots, tz_3) = 0. \quad (2.17)$$

Next, we note that, being a projective bundle, M is equivalent [35, 36] to $P(\mathcal{O}_{\mathbb{P}^3}(H) \oplus \mathcal{O}_{\mathbb{P}^3})$, where locally s and t are sections of $\mathcal{O}_{\mathbb{P}^3}(H)$ and $\mathcal{O}_{\mathbb{P}^3}$, respectively. We further observe that tz_i , $i = 0 \dots 3$ are also sections of $\mathcal{O}_{\mathbb{P}^3}(H)$ and the equivalence $(t, s) \sim (\lambda t, \lambda s)$ induces the equivalence $(tz_0, \dots, tz_i, s) \sim (\lambda tz_0, \dots, \lambda tz_i, \lambda s)$. Consequently, if we blow down the section $t = 0$ of M , then $(tz_0, \dots, tz_i, s) \in \mathbb{P}^4$. Now, we define $(w_0, \dots, w_3, w_4) = (tz_0, \dots, tz_3, s)$ and rewrite (2.17) as

$$P_3(w_0, \dots, w_3)w_4^2 + P_4(w_0, \dots, w_3)w_4 + P_5(w_0, \dots, w_3) = 0. \quad (2.18)$$

Not surprisingly, we get back (2.8).

Above we have found that there are 11 complex deformations of the dP_6 singularity embedded in the quintic CY manifold. In the view of further applications, let us rederive the number of complex deformations by calculating the dimension of $H^{2,1}$.

Expanding (2.12), we get the third Chern class

$$c_3(Y_3) = -2G^3 - 13HG^2 - 17H^2G - 8H^3. \quad (2.19)$$

The Poincare dual class to $Y_3 \in M$ is $3H + 2G$ and

$$\chi(Y_3) = \int_{Y_3} c_3(Y_3) = \int_M c_3(Y_3) \wedge (3H + 2G). \quad (2.20)$$

In calculating this integral, one needs to take into account that $G(G - H) = 0$ on M . Finally, we get

$$\begin{aligned} \chi(Y_3) &= -176, \\ h^{2,1} &= h^{1,1} - \frac{\chi}{2} = 90. \end{aligned} \quad (2.21)$$

The number of complex deformations of the del Pezzo singularity is $101 - 90 = 11$, which is consistent with the number found above.

2.3. Quintic CY with 36 Conifold Singularities

In this subsection, we use the methods of geometric transitions [11, 12, 16] to find the quintic CY with conifold singularities, that is, we describe the upper horizontal arrow in Figure 1. Consider the system of two equations in $\mathbb{P}^4 \times \mathbb{P}^1$

$$\begin{aligned} P_3u + R_3v &= 0, \\ P_2u + R_2v &= 0, \end{aligned} \quad (2.22)$$

where $(u, v) \in \mathbb{P}^1$ and P_n, R_n denote polynomials of degree n in \mathbb{P}^4 .

Suppose that at least one of the polynomials $P_3, R_3, P_2,$ and R_2 is nonzero, then we can solve for u, v and substitute in the second equation, where we get

$$P_3R_2 - R_3P_2 = 0, \quad (2.23)$$

a nongeneric quintic in \mathbb{P}^4 . The points where $P_3 = R_3 = P_2 = R_2 = 0$ (but otherwise generic) have conifold singularities. There are $3 \cdot 3 \cdot 2 \cdot 2 = 36$ such points. The system (2.22) describes the blowup of the singularities, since every singular point is replaced by the \mathbb{P}^1 and the resulting manifold is non singular.

Let H be the hyperplane class of \mathbb{P}^4 and G by the hyperplane class of \mathbb{P}^1 , then the total Chern class of Y_3 is

$$c = \frac{(1+H)^5(1+G)^2}{(1+3H+G)(1+2H+G)}, \quad (2.24)$$

since $c_1 = 0$, Y_3 is a CY.

By Lefschetz hyperplane theorem $h^{1,1}(Y_3) = h^{1,1}(\mathbb{P}^4 \times \mathbb{P}^1) = 2$, there are only two independent Kahler deformations in Y_3 . One of them is the overall size of Y_3 and the other is the size of the blown up \mathbb{P}^1 's. Thus, the 36 \mathbb{P}^1 's are not independent but homologous to each other and represent only one class in $H_2(Y_3)$. If we shrink the size of blown up \mathbb{P}^1 's to zero, then we can deform the singularities of (2.23) to get a generic quintic CY. In this case, the 35 three chains that were connecting the 36 \mathbb{P}^1 's become independent three cycles. Thus, we expect the general quintic CY to have 35 more complex deformations than the quintic with 36 conifold singularities.

Calculating the Euler character similarly to the previous subsections, we find

$$h^{2,1} = 66. \quad (2.25)$$

Recall that the smooth quintic has 101 complex deformations. Thus, the quintic with 36 conifold singularities has $101 - 66 = 35$ less complex deformations than the generic one.

2.4. Quintic CY with dP_6 Singularity and 32 Conifold Singularities

The equation for the quintic CY manifold with the blown up dP_6 singularity was found in (2.10). Here, we reproduce it for convenience

$$P_3(z_i)s^2 + P_4(z_i)st + P_5(z_i)t^2 = 0. \quad (2.26)$$

This equation describes an embedding of the CY manifold in the \mathbb{P}^1 bundle $M = P(\mathcal{O}_{\mathbb{P}^3} \oplus \mathcal{O}_{\mathbb{P}^3}(-H))$. As before, $(z_0, \dots, z_3) \in \mathbb{P}^3$ and (s, t) are the coordinates on the \mathbb{P}^1 fibers over \mathbb{P}^3 .

In order to have more Kahler deformations, we need to embed (2.26) in a space with more independent two-cycles. For example, we can consider a system of two equations in the product (\mathbb{P}^1 bundle over \mathbb{P}^3) $\times \mathbb{P}^1$

$$\begin{aligned} (P_1s + P_2t)u + (Q_1s + Q_2t)v &= 0, \\ (R_2s + R_3t)u + (S_2s + S_3t)v &= 0, \end{aligned} \quad (2.27)$$

where (u, v) are the coordinates on the additional \mathbb{P}^1 . Let G , H , and K be the hyperplane classes on the \mathbb{P}^1 fibers, on the \mathbb{P}^3 , and on the additional \mathbb{P}^1 , respectively. Then, the total Chern class of Y_3 is

$$c = \frac{(1+H)^4(1+G)(1+G-H)(1+K)^2}{(1+H+G+K)(1+2H+G+K)}, \quad (2.28)$$

and it is easy to see that the first Chern class is zero.

For generic points on the \mathbb{P}^1 bundle over \mathbb{P}^3 , at least one of the functions in front of u or v is nonzero. Thus, we can find a point (u, v) and substitute it in the second equation, which becomes a nongeneric equation similar to (2.26)

$$(P_1S_2 - Q_1R_2)s^2 + (P_1S_3 + P_2S_2 - Q_1R_3 - Q_2R_2)st + (P_2S_3 - Q_2R_3)t^2 = 0. \quad (2.29)$$

The CY manifold defined in (2.27) has the following characteristics:

$$\begin{aligned} \chi &= \int_{Y_3} c_3 = -112, \\ h^{1,1} &= 3, \\ h^{2,1} &= h^{1,1} - \frac{\chi}{2} = 59. \end{aligned} \quad (2.30)$$

Recall that the number of complex deformations on the quintic with the del Pezzo 6 singularity is 90. Since we lose 31 complex deformations, we expect that the corresponding three-cycles become the three chains that connect 32 \mathbb{P}^1 's at the blowups of the singularities in (2.29). These singularities occur when all four equations in (2.27) vanish

$$\begin{aligned} R_2s + R_3t &= 0, \\ S_2s + S_3t &= 0, \\ P_1s + P_2t &= 0, \\ Q_1s + Q_2t &= 0. \end{aligned} \quad (2.31)$$

The number of solutions equals the number of intersections of the corresponding classes $\int_M (2H + G)^2 (H + G) = 32$, where M is the \mathbb{P}^1 bundle over \mathbb{P}^3 and $G(G - H) = 0$.

The right vertical arrow corresponds to smoothing of del Pezzo singularity in the presence of conifold singularities. Before the transition, the CY has $h^{2,1} = 59$ deformations and after the transition it has $h^{2,1} = 66$ deformations. Hence, the number of complex deformations of dP_6 singularity is $66 - 59 = 7$ which is less than $c^\vee(E_6) - 1 = 11$. This is related to the fact that the del Pezzo at the tip of the cone is not generic. The equation of the del Pezzo can be found by restricting (2.27) to $t = 0, s = 1$ section

$$\begin{aligned} P_1u + Q_1v &= 0, \\ R_2u + S_2v &= 0. \end{aligned} \quad (2.32)$$

This del Pezzo contains a two-cycle α that is nontrivial within the full CY and does not intersect the canonical class inside dP_6 .

In the rest of this subsection, we will argue that α is homologous to four \mathbb{P}^1 's at the tip of the conifolds. The heuristic argument is the following. The formation of dP_6 singularity on the CY manifold with 36 conifolds reduces the number of conifolds to 32. Let us show that the deformation of the del Pezzo singularity that preserves the conifold singularities corresponds

to separating 4 conifolds hidden in the del Pezzo singularity. The CY that has a dP_6 singularity and 32 resolved conifolds can be found from (2.27) by the following coordinate redefinition $(w_0, \dots, w_3, w_4) = (tz_0, \dots, tz_3, s)$ (compare to the discussion after (2.17)):

$$\begin{aligned} (P_1 w_4 + P_2)u + (Q_1 w_4 + Q_2)v &= 0, \\ (R_2 w_4 + R_3)u + (S_2 w_4 + S_3)v &= 0. \end{aligned} \tag{2.33}$$

If we blow down the \mathbb{P}^1 , then we get the quintic CY with 32 conifold singularities and a dP_6 singularity. For a finite size \mathbb{P}^1 , the conifold singularities and one of the two-cycles in the dP_6 are blown up. The deformations of dP_6 singularity correspond to adding terms with higher power of w_4 . After the deformation, the degree two zeros of R_2 and S_2 will split into four degree one zeros that correspond to the four conifolds “hidden” in the dP_6 singularity. The blown up two-cycle of dP_6 is homologous to the two-cycles on the four conifolds. (Formally, we can prove this by calculating the corresponding Poincaré dual classes. The Poincaré dual of \mathbb{P}^1 on the blown up conifold is $H^3 G$ —this is the \mathbb{P}^1 parameterized by (u, v) . The Poincaré dual of the canonical class on dP_6 is $(G - H)(H + K)(2H + K)(-H)$, where $(G - H)$ restricts to $t = 0$ section of the \mathbb{P}^1 bundle, $(H + K)(2H + K)$ restricts to dP_6 in (2.32), while the restriction of $(-H)$ is the canonical class on dP_6 (see (2.15)). The class that does not intersect $(-H)$ inside dP_6 is dual to $(G - H)(H + K)(2H + K)(2H - 3G) = 4H^3 G$, q.e.d.)

3. SUSY Breaking

In this paper, we compare two mechanisms for dynamical SUSY breaking: the “geometrical” approach of Aganagic et al. [8] and a more “physical” approach of ISS [10].

In both approaches, there is a confinement in the microscopic gauge theory leading to the SUSY breaking in the effective theory. But the particular mechanisms and the effective theories are quite different. In the “geometrical” approach the effective theory is a non-SUSY analog of Veneziano-Yankielowicz superpotential [39] for the gaugino bilinear field S . This potential has an interpretation as the GVW superpotential [40] for the complex structure moduli of the CY manifold. The original Veneziano-Yankielowicz potential [39] is derived for the pure YM theory without any flavors. It has a number of isolated vacua and no massless fields. This is a nice feature for the (meta) stability of the vacuum but, since all the fields are massive, the applications of this potential in the low-energy effective theories are limited (see, e.g., the discussion in [41]).

In the ISS construction, the number of flavors is bigger than the number of colors $N_c < N_f < 3/2 N_c$ (and probably $N_f = N_c$). After the confinement, the low-energy effective theory contains classically massless fields that get some masses only at 1 loop. Hence, this theory is a more genuine effective theory but the geometric interpretation is harder to achieve [3]. Moreover, the geometric constructions similar to [3] generally have D5-branes wrapping vanishing cycles. In any compactification of these models, one has to put the O-planes or anti D5-branes somewhere else in the geometry, that is, the analysis of [8, 9] becomes inevitable.

In summary, it seems that the ISS construction is more useful for immediate applications to SUSY breaking in the low-energy effective theories, whereas more global geometric analysis of [8, 9] becomes inevitable in the compactifications.

In the previous section, we constructed the compact CY with del Pezzo 6 singularity and some number of conifold singularities. We have shown that it is possible to make some

two-cycles on del Pezzo homologous to the two-cycles on the conifolds. This is the first step in the geometric analysis of [8]. In the next subsection, we show how the ISS story can be represented in the del Pezzo 6 quiver gauge theories.

3.1. ISS Vacuum for the dP_6 Singularity

Consider the quiver gauge theory for the cone over dP_6 represented in Figure 2. This quiver can be found by the standard methods [1] from the three-block exceptional collection of sheaves [42]. But, in order to prove the existence of this quiver, it is easier to do the Seiberg dualities on the nodes 4, 5, 6, and 1 and reduce it to the known dP_6 quiver [2].

In the compact CY manifold, one can put the D5-branes only on cycles that are nontrivial globally. A deformation of the dP_6 singularity in (2.33) leaves four conifold singularities. We will assume that after joining the 4 conifolds to form a dP_6 singularity the two-cycles remain nontrivial. We also expect that these two-cycles are represented by the four two-cycles on del Pezzo that have self-intersection (-2) and do not intersect with each other. Note that the total number of nonanomalous fractional branes and the number of (-2) two-cycles is 6, but there are only 4 two-cycles that do not intersect with each other and with the canonical class. (It is interesting to note the similarity between the branes wrapping the non intersecting cycles on dP_6 and the deformation D-branes in [3, 23].)

Let A_i denote the two-cycle corresponding to the D5-brane charge [1] of the bound state of branes at the i th node in Figure 2. Then, the four non intersecting (-2) two-cycles can be chosen as A_2-A_3 , A_4-A_5 , A_6-A_7 , and A_8-A_9 . Now, we would like to add K fractional branes to A_4-A_5 and N fractional branes to A_6-A_7 and to A_8-A_9 . The corresponding quiver is depicted in Figure 3.

The gauge groups at the nodes 6 and 8 have $N_f = N_c$. Consider the Seiberg duality in the strong coupling limit of these gauge groups. The moduli space consists of the mesonic and the baryonic branches [43, 44]. Suppose we are on the baryonic branch. For the generic Yukawa couplings, the two mesons $\Phi = BC$ couple linearly to the fields A and become massive together with two of the A fields.

An important question is whether the baryons for the gauge groups in nodes 6 and 8 remain massless. The baryons are charged under the baryonic $U(1)_B$ symmetries. In the noncompact setting, these $U(1)_B$ symmetries are global [45]. If the baryons get vevs, then the symmetries are broken spontaneously and there are massless goldston bosons. But for the compact CY manifold the $U(1)_B$ symmetries are gauged and the goldstone bosons become massive [13, 45] through the Higgs mechanism. Integrating out the massive fields, we get the quiver in Figure 4.

Next, we assume that the strong coupling scale for the gauge group $SU(N + K)$ at node 4 is bigger than the scale for the $SU(2N)$. This assumption does not include a lot of tuning especially if $K \lesssim N$. The number of flavors for the gauge group $SU(N + K)$ is $N_f = 2N > N_c = N + K$. Consequently, we can assume that the mesons do not get VEVs after the confinement of $SU(N + K)$ and remain massless. The corresponding quiver is shown in Figure 5. The subscripts of the bifundamental fields denote the gauge groups at the ends of the corresponding link. The subscript $k = 2, 3$ labels the two $U(N)$ gauge groups on the left. For example, A_{k1} denotes both the field A_{21} going from the node 2 to the node 1 and A_{31} going from 3 to 1.

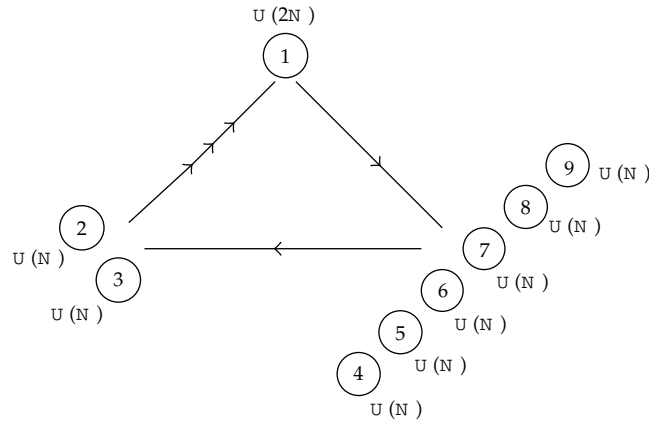


Figure 2: Quiver gauge theory for the cone over dP_6 .

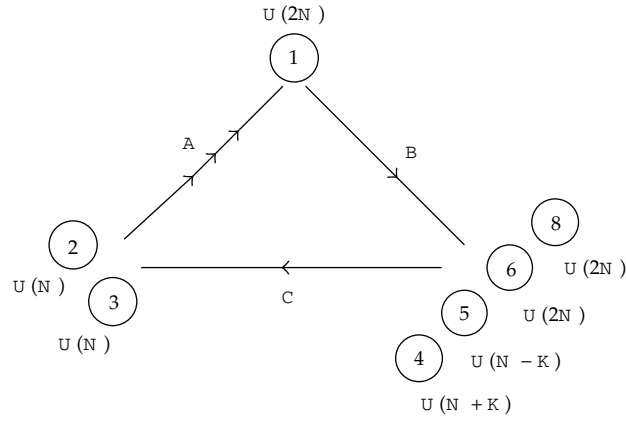


Figure 3: Quiver gauge theory for the cone over dP_6 after adding the fractional branes.

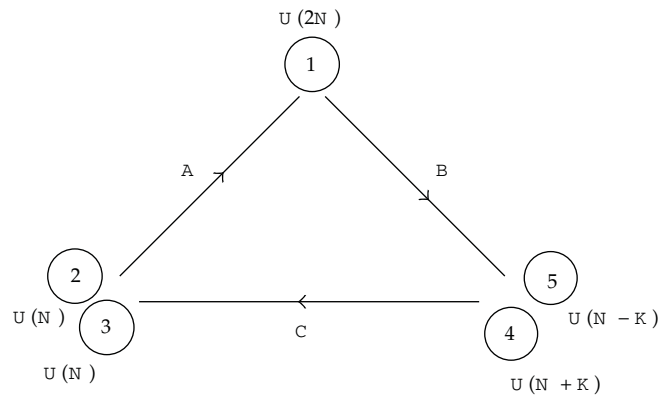


Figure 4: Quiver gauge theory for the cone over dP_6 after confinement of nodes 6 and 8.

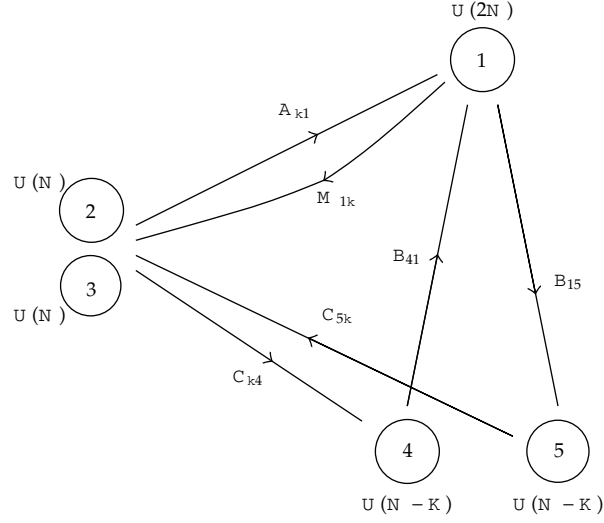


Figure 5: Quiver gauge theory for the cone over dP_6 after Seiberg duality on node 4.

The superpotential of the quiver gauge theory in Figure 5 has the form

$$\begin{aligned}
 W = & \text{Tr}(mA_{21}M_{12} + mA_{31}M_{13}) \\
 & + \text{Tr}\left(\lambda M_{12}\tilde{C}_{24}\tilde{B}_{41} + \lambda A_{21}B_{15}C_{52} + \lambda M_{13}\tilde{C}_{34}\tilde{B}_{41} + \lambda A_{31}B_{15}C_{53}\right).
 \end{aligned} \tag{3.1}$$

In order to make the notations shorter, we do not write the subscripts of the couplings. (The couplings are different but have the same order of magnitude.)

If Λ_1 for the $SU(2N)$ gauge group at node 1 is close to Λ_4 for $SU(N+K)$ at node 4 in Figure 4, then it is natural to assume that for small values of corresponding Yukawa couplings the mass parameters m satisfy $m \ll \Lambda_1$. Now, we note that the $SU(2N)$ gauge group has $N_c = 2N$ and $N_f = 3N - K$, that is, $N_c + 1 \leq N_f < 3/2N_c$. This group is a good candidate for the microscopic gauge group in the ISS construction. After the Seiberg duality, the magnetic gauge group has $\tilde{N}_c = N - K$. The superpotential of the dual theory is

$$\begin{aligned}
 \tilde{W} = & \text{Tr}(mM_{22} + mM_{33}) \\
 & + \text{Tr}\left(\lambda M_{22}\tilde{M}_{21}\tilde{A}_{12} + \lambda M_{33}\tilde{M}_{31}\tilde{A}_{13}\right) \\
 & + \text{Tr}\left(mM_{42}\tilde{C}_{24} + mM_{25}C_{52} + mM_{43}\tilde{C}_{34} + mM_{35}C_{53}\right) \\
 & + \text{Tr}\left(\lambda M_{42}\tilde{M}_{21}\tilde{B}_{14} + \lambda M_{25}\tilde{B}_{51}\tilde{A}_{12} + \lambda M_{43}\tilde{M}_{31}\tilde{B}_{14} + \lambda M_{35}\tilde{B}_{51}\tilde{A}_{13}\right).
 \end{aligned} \tag{3.2}$$

The indices of the meson fields correspond to the two gauge groups under which they transform. In our case, this leads to unambiguous identifications, for example, $M_{22} = A_{21}M_{12}$,

$M_{33} = A_{31}M_{13}$, $M_{42} = \tilde{B}_{41}M_{12}$, and so forth. The mesons M_{22} and M_{33} are in adjoint representation of $SU(N)_2$ and $SU(N)_3$, and their F-term equations read

$$\begin{aligned} m \cdot \mathbf{1} + \lambda \tilde{M}_{21} \tilde{A}_{12} &= 0, \\ m \cdot \mathbf{1} + \lambda \tilde{M}_{31} \tilde{A}_{13} &= 0, \end{aligned} \tag{3.3}$$

where $\mathbf{1}$ is the $N \times N$ identity matrix. The Seiberg dual gauge group at node 1 is $SU(N - K)$; hence the rank of the matrices \tilde{M}_{21} and so forth, is at most $N - K$ and the SUSY is broken by the rank condition of [10]. Classically, there are massless excitations around the vacua in (3.3). In order to prove that the vacuum is metastable, one has to check that these fields acquire a positive mass at 1 loop. Similarly to [10], we expect this to be true, but a more detailed study is necessary.

As a summary, in this section we have found an example of dynamical SUSY breaking in the quiver gauge theory on del Pezzo singularity. An interesting property of this example is that there are massless chiral fields after the SUSY breaking. This behaviour seems to be quite generic, and we expect that similar constructions are possible for other del Pezzo singularities.

4. Compact CY Manifolds with Del Pezzo Singularities

Noncompact CY singularities are useful in constructing local geometries that enable SUSY breaking configurations of D-branes. However, for a consistent embedding of these constructions in string theory, one needs to find compact CY manifolds that possess the corresponding singularities.

The noncompact CY manifolds with del Pezzo singularities are known [27, 29]. The dP_n singularities for $5 \leq n \leq 8$ and for the cone over $\mathbb{P}^1 \times \mathbb{P}^1$ can be represented as complete intersections. (Note that in the mathematics literature, the del Pezzo surfaces are classified by their degree $k = 9 - n$, where n is the number of blown up points in \mathbb{P}^2 .) The CY cones over \mathbb{P}^2 and dP_n for $1 \leq n \leq 4$ are not complete intersections. The compact CY manifolds for complete intersection singularities were presented in [34].

Our construction is different from [34]. It enables one to construct the complete intersection compact CY manifolds for all del Pezzo singularities. This construction does not contradict the statement that for $n \leq 4$ the del Pezzo singularities are not complete intersections. The price we have to pay is that these singularities will not be generic, that is, they will not have the maximal number of complex deformations. Whereas for the del Pezzo singularities with $n \geq 5$ and for $\mathbb{P}^1 \times \mathbb{P}^1$ we will represent all complex deformations in our construction.

4.1. General Construction

At first, we present the construction in the case of dP_6 singularity and, then, give a more general formulation.

The input data is the embedding of dP_6 surface in \mathbb{P}^3 via a degree three equation. The problem is to find a CY threefold such that it has a local dP_6 singularity. The solution has several steps.

- (1) Find the canonical class on $B = dP_6$ in terms of a restriction of a class on \mathbb{P}^3 . Let us denote this class as $K \in H^{1,1}(\mathbb{P}^3)$. K can be found from expanding the total Chern class of B

$$c(B) = \frac{(1+H)^4}{1+3H} = 1 + H + \dots \quad (4.1)$$

Thus, $K = -c_1(B) = -H$.

- (2) Construct the \mathbb{P}^1 fiber bundle over \mathbb{P}^3 as the projectivisation $M = P(\mathcal{O}_{\mathbb{P}^3} \oplus \mathcal{O}_{\mathbb{P}^3}(K))$.
 (3) The Calabi-Yau Y_3 is given by an equation of degree 3 in \mathbb{P}^3 and degree 2 in the coordinates on the fiber. The total Chern class of Y_3 is

$$c(Y_3) = \frac{(1+H)^4(1+G-H)(1+G)}{1+3H+2G} \quad (4.2)$$

This has a vanishing first Chern class. By construction, this Calabi-Yau has a del Pezzo singularity at $t = 0$.

This construction has a generalization for the other del Pezzo surfaces. Let B denote a del Pezzo surface embedded in X as a complete intersection of a system of equations [16]. Assume, for concreteness, that the system contains two equations and denote by L_1 and L_2 the classes corresponding to the divisors for these two equations in X . The case of other number of equations can be obtained as a straightforward generalization.

- (1) First, we find the canonical class of surface $B \subset X$, defined in terms of two equations with the corresponding classes $L_1, L_2 \in H^{1,1}(X)$,

$$c(B) = \frac{c(X)}{(1+L_1)(1+L_2)} = 1 + c_1(X) - L_1 - L_2 + \dots \quad (4.3)$$

Thus, the canonical class of X is obtained by the restriction of $K = L_1 + L_2 - c_1(X)$.

- (2) Second, we construct the \mathbb{P}^1 fiber bundle over X as the projectivisation $M = P(\mathcal{O}_X \oplus \mathcal{O}_X(K))$.
 (3) In the case of two equations, the Calabi-Yau manifold $Y_3 \subset M$ is not unique. Let G be the hyperplane class in the fibers, then we can write three different systems of equations that define a CY manifold: the classes for the equations in the first system are L_1+2G and L_2 , the second one has L_1+G and L_2+G , and the third one has L_1 and L_2+2G (here $L_1, L_2 \in H^{1,1}(M)$ are defined via the pull back of the corresponding classes in $H^{1,1}(X)$ with respect to the projection of \mathbb{P}^1 the fibers $\pi : M \rightarrow X$).

As an example, let us describe the first system. The first equation in this system is given by L_1 in X and has degree 2 in the coordinates on the fibers. The second equation is L_2 in X . The total Chern class is

$$c(Y_3) = \frac{c(X)(1+G+K)(1+G)}{(1+L_1+2G)(1+L_2)} \quad (4.4)$$

Since $K = L_1 + L_2 - c_1(X)$, it is straightforward to check that the first Chern class is trivial.

Let us show how this program works in an example of a CY cone over $B = \mathbb{P}^1 \times \mathbb{P}^1$. The $\mathbb{P}^1 \times \mathbb{P}^1$ surface can be embedded in \mathbb{P}^3 by a generic degree two polynomial equation [16, 35]

$$P_2(z_i) = 0, \quad (4.5)$$

where $(z_0, \dots, z_3) \in \mathbb{P}^3$. (By coordinate redefinition in \mathbb{P}^3 one can represent the equation as $z_0 z_3 = z_1 z_2$. The solutions of this equation can be parameterized by the points $(x_1, y_1) \times (x_2, y_2) \in \mathbb{P}^1 \times \mathbb{P}^1$ as $(z_0, z_1, z_2, z_3) = (x_1 x_2, x_1 y_2, y_1 x_2, y_1 y_2)$. This is the Segre embedding $\mathbb{P}^1 \times \mathbb{P}^1 \subset \mathbb{P}^3$.)

The first step of the program is to find the canonical class of B in terms of a class in \mathbb{P}^3 . Let H be the hyperplane class of \mathbb{P}^3 . Then, the total Chern class of B is

$$c(B) = \frac{(1+H)^4}{1+2H} = 1 + 2H + 2H^2. \quad (4.6)$$

The canonical class is

$$K(B) = -c_1(B) = -2H. \quad (4.7)$$

Next, we construct the \mathbb{P}^1 bundle $M = P(\mathcal{O}_{\mathbb{P}^3} \oplus \mathcal{O}_{\mathbb{P}^3}(K))$ with the coordinates (s, t) along the fibers, where locally $s \in \mathcal{O}_{\mathbb{P}^3}$ and $t \in \mathcal{O}_{\mathbb{P}^3}(-2H)$. The equation that describes the embedding of the CY manifold Y_3 in M is

$$P_2(z_i)s^2 + P_4(z_i)st + P_6(z_i)t^2 = 0. \quad (4.8)$$

This equation is homogeneous in z_i of degree two, since t has degree -2 .

The section of M at $t = 0$ is contractible, and the intersection with the Y_3 is $P_2(z_i) = 0$, that is, Y_3 is the CY cone over $\mathbb{P}^1 \times \mathbb{P}^1$ near $t = 0$.

The total Chern class of Y_3 is

$$c(Y_3) = \frac{(1+H)^4(1+G)(1+G-2H)}{1+2H+2G}. \quad (4.9)$$

It is easy to check that $c_1(Y_3) = 0$.

4.2. A Discussion of Deformations

In this subsection, we will discuss the deformations of the del Pezzo singularities in the compact CY spaces. The explicit description of the singularities and their deformations can be found in the appendix.

The procedure is similar to the deformation of the dP_6 singularity described in Section 2. As before, let $Y_3 \subset M$ be an embedding of the CY threefold Y_3 in M , a \mathbb{P}^1 bundle over products of (weighted) projective spaces. If we blowdown the section of the \mathbb{P}^1 bundle

that contains the del Pezzo, then M becomes a toric variety that we denote by V . After the blowdown, equation for the CY in M becomes a singular equation for a CY embedded in V . The last step is to deform the equation in V to get a generic CY. (In the example of dP_6 singularity on the quintic, the projective bundle is $M = P(\mathcal{O}_{\mathbb{P}^3} \oplus \mathcal{O}_{\mathbb{P}^3}(-H))$, the manifold V , obtained by blowing down the exceptional \mathbb{P}^3 in M , is \mathbb{P}^4 , and the singular equation is the singular quintic in \mathbb{P}^4 .)

Let n denote the number of two-cycles on del Pezzo with self-intersection (-2) . The intersection matrix of these cycles is minus the Cartan matrix of the corresponding Lie algebra E_n .

The maximal number of complex deformations of del Pezzo singularity is $c^\vee(E_n) - 1$, where $c^\vee(E_n)$ is the dual Coxeter number of E_n . These deformations can be performed only if the del Pezzo has a zero size. As a result of these deformations, the canonical class on the del Pezzo becomes trivial within the CY and the del Pezzo singularity is partially or completely smoothed out. In the generic situation, we expect that all (-2) two-cycles on del Pezzo are trivial within the CY, then the number of complex deformations is maximal (this will be the case for $\mathbb{P}^1 \times \mathbb{P}^1$, dP_5 , dP_6 , dP_7 , dP_8). If some of the (-2) two-cycles become nontrivial within the CY, then the number of complex deformations of the corresponding cone is smaller. We will observe this for our embedding of dP_2 , dP_3 , and dP_4 . This reduction of the number of complex deformations depends on the particular embedding of del Pezzo cone. In [8], the generic deformations of the cones over dP_2 and dP_3 were constructed (Tables 1 and 2).

5. Conclusions and Outlook

In this paper, we have constructed a class of compact Calabi-Yau manifolds that have del Pezzo singularities. The construction is analytic, that is, the CY manifolds are described by a system of equations in the \mathbb{P}^1 bundles over the projective spaces.

We argue that this construction can be used for the geometrical SUSY breaking [8] as well as for the compactification of ISS [10]. As an example, we find a compact CY manifold with del Pezzo 6 singularity and some conifolds such that some 2-cycles on del Pezzo are homologous to the 2-cycles on the conifolds, that is, this manifold can be used for the geometrical SUSY breaking. Also we find an ISS vacuum in the quiver gauge theory for dP_6 singularity.

In order to have a consistent string theory representation of the SUSY breaking vacua, one needs to find compact CY manifolds that have the necessary local singularities. In the last section, we present embedding of del Pezzo singularities in complete intersection CY manifolds and study the complex deformations of the singularities. The del Pezzo n surface corresponds to the Lie group E_n . The expected number of complex deformations for the cone over del Pezzo is $c^\vee(E_n) - 1$, where c^\vee is the dual Coxeter number for the Lie group E_n . In the studied examples, the cones over $\mathbb{P}^1 \times \mathbb{P}^1$ and over dP_5 , dP_6 , dP_7 , and dP_8 have generic deformations. But the cones over dP_2 , dP_3 , and dP_4 have less deformations, that is, these cones do not describe the most generic embedding of the corresponding del Pezzo singularities. (It is known that the generic embeddings of del Pezzo n singularities for $n \leq 4$ (or rank $k = 9 - n \geq 5$) cannot be represented as complete intersections [27, 29], in our construction the del Pezzo singularities are nongeneric complete intersections.)

We propose that for the generic embedding the two-cycles on del Pezzo with self-intersection (-2) are trivial within the full Calabi-Yau geometry. The nontrivial two cycles with self-intersection (-2) impose restrictions on the complex deformations. This proposal

Table 1: Some characteristics of del Pezzo surfaces.

Del Pezzo	No. two-cycles	No. (-2) two-cycles	Dynkin's diagram	$c^V - 1$
\mathbb{P}^2	1	0	0	0
$\mathbb{P}^1 \times \mathbb{P}^1$	2	1	A_1	1
dP_1	2	0	0	0
dP_2	3	1	A_1	1
dP_3	4	3	$A_2 \times A_1$	3
dP_4	5	4	A_4	4
dP_5	6	5	D_5	7
dP_6	7	6	E_6	11
dP_7	8	7	E_7	17
dP_8	9	8	E_8	29

Table 2: Complex deformations of del Pezzo singularities studied in the paper.

Del Pezzo	No. (-2) two-cycles	No. trivial (-2) two-cycles	$c^V - 1$	No. complex deforms
\mathbb{P}^2	0	0	0	0
$\mathbb{P}^1 \times \mathbb{P}^1$	1	1	1	1
dP_1	0	0	0	0
dP_2	1	0	1	0
dP_3	3	1	3	1
dP_4	4	3	4	3
dP_5	5	5	7	7
dP_6	6	6	11	11
dP_7	7	7	17	17
dP_8	8	8	29	29

agrees with the above examples of the embeddings of del Pezzo singularities. Also we get a similar conclusion when the CY has some number of conifolds in addition to the del Pezzo singularity. Although the conifolds are away from the del Pezzo and the del Pezzo itself is not singular, it acquires a nontrivial two-cycle and the number of deformations is reduced.

Sometimes the F-theory/orientifolds point of view has advantages compared to the type IIB theory. Our construction of CY threefolds can be generalized to find the 3-dimensional base spaces of elliptic fibrations in F-theory with the necessary del Pezzo singularities. Also we expect this construction to be useful as a first step in finding the warped deformations of the del Pezzo singularities and in the studies of the Landscape of string compactifications.

Appendix

A List of Compact CY with Del Pezzo Singularities

In the appendix, we construct the embeddings of all del Pezzo singularities in compact CY manifolds and describe the complex deformations of these embeddings. This description follows the general construction in Section 4.

In the following, B denotes the two-dimensional del Pezzo surface and X denotes the space where we embed B . The space X will be either a product of projective spaces or a

weighted projective space. For example, if $B \subset X = \mathbb{P}^n \times \mathbb{P}^m \times \mathbb{P}^k$, then the coordinates on the three projective spaces will be denoted as (z_0, \dots, z_n) , (u_0, \dots, u_m) , and (v_0, \dots, v_k) , respectively. The hyperplane classes of the three projective spaces will be denoted by H , K , R , respectively.

A polynomial of degree q in z_i , degree r in u_j , and degree s in v_l will be denoted by $P_{q,r,s}(z_i; u_j; v_l)$.

If there are only two or one projective space, then we will use the first two or the first one projective spaces in the above definitions.

For the weighted projective spaces, we will use the notations of [30]. For example, consider the space $W\mathbb{P}_{11pq}^3$ where $p, q \in \mathbb{N}$. The dimension of this space is 3, the subscripts $(1, 1, p, q)$ denote the weights of the coordinates with respect to the projective identifications $(z_0, z_1, z_2, z_3) \sim (\lambda z_0, \lambda z_1, \lambda^p z_2, \lambda^q z_3)$.

The \mathbb{P}^1 bundles over X will be denoted as $M = P(\mathcal{O}_X \oplus \mathcal{O}_X(K))$, where K is the class on X that restricts to the canonical class on B . The coordinates on the fibers will be (s, t) so that locally $s \in \mathcal{O}_X$ and $t \in \mathcal{O}_X(K)$. The hyperplane class of the fibers will be denoted by G , it satisfies the property $G(G + K) = 0$ for $M = P(\mathcal{O}_X \oplus \mathcal{O}_X(K))$. In the construction of the \mathbb{P}^1 bundles, we will use the fact that $K(B) = -c_1(B)$ and will not calculate $K(B)$ separately.

The deformations of some del Pezzo singularities will be described via embedding in particular toric varieties. We will call them generalized weighted projective spaces. Consider, for example, the following notation:

$$\begin{array}{l} \text{GW}\mathbb{P}^5 \\ 11100002 \\ 00011001 \\ 00000111 \end{array} \quad (\text{A.1})$$

The number 5 is the dimension of the space. This space is obtained from \mathbb{C}^{8*} by taking the classes of equivalence with respect to three identifications. The numbers in the three rows correspond to the charges under these identifications

$$\begin{aligned} (z_1, z_2, z_3, z_4, z_5, z_6, z_7, z_8) &\sim (\lambda_1 z_1, \lambda_1 z_2, \lambda_1 z_3, z_4, z_5, z_6, z_7, \lambda_1^2 z_8), \\ (z_1, z_2, z_3, z_4, z_5, z_6, z_7, z_8) &\sim (z_1, z_2, z_3, \lambda_2 z_4, \lambda_2 z_5, z_6, z_7, \lambda_2 z_8), \\ (z_1, z_2, z_3, z_4, z_5, z_6, z_7, z_8) &\sim (z_1, z_2, z_3, z_4, z_5, \lambda_3 z_6, \lambda_3 z_7, \lambda_3 z_8). \end{aligned} \quad (\text{A.2})$$

$$(1) B = \mathbb{P}^2 \subset X = \mathbb{P}^3.$$

The equation for B

$$P_1(z_i) = 0. \quad (\text{A.3})$$

The total Chern class of B

$$c(B) = (1 + H)^3 = 1 + 3H + 3H^2. \quad (\text{A.4})$$

The \mathbb{P}^1 bundle is $M = P(\mathcal{O}_X \oplus \mathcal{O}_X(-3H))$. The equation for the Calabi-Yau threefold Y_3

$$P_1(z_i)s^2 + P_4(z_i)st + P_7(z_i)t^2 = 0. \quad (\text{A.5})$$

The embedding space $V = W\mathbb{P}_{11113}^4$ has the coordinates $(z_0, \dots, z_3; w)$ and the singular CY is

$$P_1(z_0, \dots, z_3)w^2 + P_4(z_0, \dots, z_3)w + P_7(z_0, \dots, z_3) = 0. \quad (\text{A.6})$$

This is already the most general equation, that is, there are no additional complex deformations.

$$(2) B = \mathbb{P}^1 \times \mathbb{P}^1 \subset X = \mathbb{P}^3.$$

The equation for B

$$P_2(z_i) = 0. \quad (\text{A.7})$$

The total Chern class of B

$$c(B) = \frac{(1+H)^4}{1+2H} = 1 + 2H + 2H^2. \quad (\text{A.8})$$

The \mathbb{P}^1 bundle is $M = P(\mathcal{O}_X \oplus \mathcal{O}_X(-2H))$. The equation for the Calabi-Yau threefold Y_3

$$P_2(z_i)s^2 + P_4(z_i)st + P_6(z_i)t^2 = 0. \quad (\text{A.9})$$

The embedding space $V = W\mathbb{P}_{11112}^4$ has the coordinates $(z_0, \dots, z_3; w)$ and the singular CY is

$$P_2(z_i)w^2 + P_4(z_i)w + P_6(z_i) = 0. \quad (\text{A.10})$$

This equation has one deformation kw^3 , and the spaces M and V have the same number of coordinate redefinitions. Thus, the space of complex deformations is one dimensional.

$$(3) B = dP_1 \subset X = \mathbb{P}^2 \times \mathbb{P}^1.$$

The equation defining B has degree one in z_i and degree one in u_j

$$P_1(z_i)u_0 + Q_1(z_i)u_1 = 0. \quad (\text{A.11})$$

The total Chern class of B

$$c(B) = \frac{(1+H)^3(1+K)^2}{1+H+K} = 1 + 2H + K + H^2 + 3HK. \quad (\text{A.12})$$

The \mathbb{P}^1 bundle is $M = P(\mathcal{O}_X \oplus \mathcal{O}_X(-2H - K))$. The equation for the Calabi-Yau threefold Y_3 is

$$P_{1,1}(z_i; u_j)s^2 + P_{3,2}(z_i; u_j)st + P_{5,3}(z_i; u_j)t^2 = 0. \quad (\text{A.13})$$

The embedding space $V = GW\mathbb{P}^4_{\substack{111002 \\ 000111}}$ has the coordinates $(z_0, z_1, z_2; u_0, u_1; w)$ and the singular CY is

$$P_{1,1}(z_i; u_j)w^2 + P_{3,2}(z_i; u_j)w + P_{5,3}(z_i; u_j) = 0. \quad (\text{A.14})$$

There are no complex deformations of this equation.

(4) $B = dP_2 \subset X = \mathbb{P}^2 \times \mathbb{P}^1 \times \mathbb{P}^1$.

The del Pezzo surface is defined by a system of two equations. The first equation has degree one in z_i and degree one in u_k . The second equation has degree one in z_i and degree one in v_k

$$\begin{aligned} P_1(z_i)u_0 + Q_1(z_i)u_1 &= 0, \\ R_1(z_i)v_0 + S_1(z_i)v_1 &= 0. \end{aligned} \quad (\text{A.15})$$

The total Chern class of B

$$c(B) = \frac{(1+H)^3(1+K)^2(1+R)^2}{(1+H+K)(1+H+R)} = 1 + 2H + K + R + 2H(K+R) + KR. \quad (\text{A.16})$$

The \mathbb{P}^1 bundle is $M = P(\mathcal{O}_X \oplus \mathcal{O}_X(-2H - K - R))$. The system of equations for the Calabi-Yau threefold Y_3 can be written as

$$\begin{aligned} P_{1,1,0}(z_i; u_k; v_k)s^2 + P_{3,2,1}(z_i; u_k; v_k)st + P_{5,3,2}(z_i; u_k; v_k)t^2 &= 0, \\ Q_{1,0,1}(z_i; u_k; v_k) &= 0. \end{aligned} \quad (\text{A.17})$$

The space $V = GW\mathbb{P}^5_{\substack{11100002 \\ 00011001 \\ 00000111}}$ has the coordinates $(z_0, z_1, z_2; u_0, u_1; v_0, v_1; w)$, and the singular CY is

$$\begin{aligned} P_{1,1,0}(z_i; u_k; v_k)w^2 + P_{3,2,1}(z_i; u_k; v_k)w + P_{5,3,2}(z_i; u_k; v_k) &= 0, \\ Q_{1,0,1}(z_i; u_k; v_k) &= 0. \end{aligned} \quad (\text{A.18})$$

There are no complex deformations of this equation. This is in contradiction with the general expectation of one complex deformation, that is, the embedding is not the most general. This is connected to the fact that all the two-cycles on the del Pezzo are nontrivial within the CY.

$$(5) B = dP_3 \subset X = \mathbb{P}^1 \times \mathbb{P}^1 \times \mathbb{P}^1.$$

The del Pezzo surface is defined by an equation of degree one in z_i , degree one in u_j and degree one in v_k

$$P_{1,1,1}(z_i; u_j; v_k) = 0. \quad (\text{A.19})$$

The total Chern class of B

$$c(B) = \frac{(1+H)^2(1+K)^2(1+R)^2}{(1+H+K+R)} = 1 + (H+K+R) + 2(HK+HR+KR), \quad (\text{A.20})$$

where H , K , and R are the hyperplane classes on the three \mathbb{P}^1 's. The \mathbb{P}^1 bundle is $M = P(\mathcal{O}_X \oplus \mathcal{O}_X(-H-K-R))$. The equation for the Calabi-Yau threefold Y_3 is

$$P_{1,1,1}(z_i; u_j; v_k)s^2 + P_{2,2,2}(z_i; u_j; v_k)st + P_{3,3,3}(z_i; u_j; v_k)t^2 = 0. \quad (\text{A.21})$$

The embedding space $V = GW\mathbb{P}^4$ has the coordinates $(z_0, z_1; u_0, u_1; v_0, v_1; w)$, and the singular CY is

$$P_{1,1,1}(z_i; u_j; v_k)w^2 + P_{2,2,2}(z_i; u_j; v_k)w + P_{3,3,3}(z_i; u_j; v_k) = 0. \quad (\text{A.22})$$

This equation has one deformation kw^3 , and the spaces M and V have the same number of reparameterizations. Consequently, there is one complex deformation of the cone. This is related to the fact that 3 out of 4 two-cycles on dP_3 are independent within the CY and there is only one (-2) two-cycle on dP_3 that is trivial within the CY.

$$(6) B = dP_4 \subset X = \mathbb{P}^2 \times \mathbb{P}^1.$$

Equation defining B has degree two in z_i and degree one in u_j

$$P_2(z_i)u_0 + Q_2(z_i)u_1 = 0. \quad (\text{A.23})$$

The total Chern class of B

$$c(B) = \frac{(1+H)^3(1+K)^2}{1+2H+K} = 1 + H + K + H^2 + 3HK, \quad (\text{A.24})$$

where H and K are the hyperplane classes on \mathbb{P}^2 and \mathbb{P}^1 , respectively. The \mathbb{P}^1 bundle is $M = P(\mathcal{O}_X \oplus \mathcal{O}_X(-H-K))$. The equation for the Calabi-Yau threefold Y_3 is

$$P_{2,1}(z_i; u_j)s^2 + P_{3,2}(z_i; u_j)st + P_{4,3}(z_i; u_j)t^2 = 0. \quad (\text{A.25})$$

The embedding space $V = GW_{\substack{111001 \\ 000111}}\mathbb{P}^4$ has the coordinates $(z_0, z_1, z_3; u_0, u_1; w)$, and the singular CY is

$$P_{2,1}(z_i; u_j)w^2 + P_{3,2}(z_i; u_j)w + P_{4,3}(z_i; u_j) = 0. \quad (\text{A.26})$$

The deformations of the singularity have the form of degree one polynomial in z_0, z_1, z_2 times w^3 . Consequently, there are three deformation parameters and the spaces V and M have the same reparameterizations. In this case, we have three complex deformations and three (-2) two-cycles on dP_4 that are trivial within CY.

$$(7) B = dP_5 \subset X = \mathbb{P}^4.$$

The del Pezzo surface is defined by a system of two equations. Both equation have degree 2 in z_i

$$\begin{aligned} P_2(z_i) &= 0, \\ R_2(z_i) &= 0. \end{aligned} \quad (\text{A.27})$$

The total Chern class of B

$$c(B) = \frac{(1+H)^5}{(1+2H)^2} = 1 + H + 2H^2. \quad (\text{A.28})$$

The \mathbb{P}^1 bundle is $M = P(\mathcal{O}_X \oplus \mathcal{O}_X(-H))$. The system of equations for the first possible Calabi-Yau threefold Y_3 is

$$\begin{aligned} P_2(z_i)s^2 + P_3(z_i)st + P_4(z_i)t^2 &= 0, \\ R_2(z_i) &= 0. \end{aligned} \quad (\text{A.29})$$

It has the following characteristics:

$$\begin{aligned} \chi(Y_3) &= -160, \\ h^{1,1}(Y_3) &= 2, \\ h^{2,1} &= 82. \end{aligned} \quad (\text{A.30})$$

Now we find the deformations of this cone over dP_5 . The \mathbb{P}^1 bundle M is, in fact, the \mathbb{P}^5 blown up at one point. By blowing down the $t = 0$ section of M , we get \mathbb{P}^5 . The CY three-fold with the dP_5 singularity is embedded in \mathbb{P}^5 by the system of two equations

$$\begin{aligned} P_2(z_i)w^2 + P_3(z_i)w + P_4(z_i) &= 0, \\ R_2(z_i) &= 0. \end{aligned} \tag{A.31}$$

The deformations of the singularity correspond to taking a general degree four polynomial in the first equation. This general CY has

$$\begin{aligned} \chi &= -176, \\ h^{1,1}(\mathcal{Y}_3) &= 1, \\ h^{2,1} &= 89. \end{aligned} \tag{A.32}$$

Since the system (A.31) has only the dP_5 singularity and the general CY manifold has $89 - 82 = 7$ more complex deformations, we interpret these extra 7 deformations as the deformations of the cone over dP_5 . This number is consistent with the general expectation, since $c^\vee(D5) - 1 = 7$, where $c^\vee(D5) = 8$ is the dual Coxeter number for $D5$.

The second CY with the dP_5 singularity is described by

$$\begin{aligned} P_2(z_i)s + P_3(z_i)t &= 0, \\ R_2(z_i)s + R_3(z_i)t &= 0. \end{aligned} \tag{A.33}$$

Using the same methods as for the first CY, one can show that this singularity also has 7 complex deformations.

(8) $B = dP_6 \subset X = \mathbb{P}^3$.

The case of dP_6 was described in details in Section 2; here we just repeat the general results.

The equation defining $dP_6 \subset \mathbb{P}^3$

$$P_3(z_i) = 0. \tag{A.34}$$

The \mathbb{P}^1 bundle is $M = P(\mathcal{O}_X \oplus \mathcal{O}_X(-H))$.

The equation for the Calabi-Yau threefold \mathcal{Y}_3

$$P_3(z_i)s^2 + P_4(z_i)st + P_5(z_i)t^2 = 0. \tag{A.35}$$

The total Chern class of \mathcal{Y}_3

$$c(\mathcal{Y}_3) = \frac{(1+H)^4(1+G)(1+G-H)}{1+3H+2G}. \tag{A.36}$$

The Euler number and the cohomologies for the CY with the dP_6 singularity are

$$\begin{aligned}\chi &= -176, \\ h^{1,1} &= 2, \\ h^{2,1} &= 90.\end{aligned}\tag{A.37}$$

The deformation of this singularity is a quintic in \mathbb{P}^4 , that has

$$h^{2,1} = 101\tag{A.38}$$

complex deformations. The difference between the number of complex deformations is $101 - 90 = 11$, which is consistent with $c^\vee(E6) - 1 = 11$.

$$(9) \ B = dP_7 \subset X = W\mathbb{P}_{1112}^3.$$

The equation defining B is homogeneous of degree four in z_i 's

$$P_4(z_i) = 0.\tag{A.39}$$

The \mathbb{P}^1 bundle is $M = P(\mathcal{O}_X \oplus \mathcal{O}_X(-H))$. The equation for the Calabi-Yau threefold Y_3

$$P_4(z_i)s^2 + P_5(z_i)st + P_6(z_i)t^2 = 0.\tag{A.40}$$

The total Chern class of Y_3

$$c(Y_3) = \frac{(1+H)^3(1+2H)(1+G)(1+G-H)}{1+4H+2G}.\tag{A.41}$$

The Euler number and the cohomologies for the CY with the dP_6 singularity are

$$\begin{aligned}\chi &= -168, \\ h^{1,1} &= 2, \\ h^{2,1} &= 86.\end{aligned}\tag{A.42}$$

Blowing down the $t = 0$ section of M , we get $V = W\mathbb{P}_{11112}^4$. The general CY is given by the degree six equation in V . The total Chern class of this CY is

$$c = \frac{(1+H)^4(1+2H)}{(1+6H)}.\tag{A.43}$$

And the number of complex deformations

$$h^{2,1} = 103. \quad (\text{A.44})$$

The difference $103 - 86 = 17$ is equal to $c^\vee(E7) - 1 = 17$, where $c^\vee(E7) = 18$ is the dual Coxeter number of $E7$. Consequently, we can represent all complex deformations of dP_7 singularity in this embedding.

$$(10) \ B = dP_8 \subset X = W\mathbb{P}_{1123}^3.$$

The equation defining B has degree six

$$P_6(z_i) = 0. \quad (\text{A.45})$$

The \mathbb{P}^1 bundle is $M = P(\mathcal{O}_X \oplus \mathcal{O}_X(-H))$. The equation for the Calabi-Yau threefold Y_3

$$P_6(z_i)s^2 + P_7(z_i)st + P_8(z_i)t^2 = 0. \quad (\text{A.46})$$

The total Chern class of Y_3

$$c(Y_3) = \frac{(1+H)^2(1+2H)(1+3H)(1+G)(1+G-H)}{1+6H+2G}. \quad (\text{A.47})$$

The problem with this CY is that for any polynomials P_6 , P_7 , and P_8 , it has a singularity at $s = z_0 = z_1 = z_2 = z_3 = 0$ and $z_4 = 1$. As a consequence, the naive calculation of the Euler number gives a fractional number

$$\chi = -150\frac{2}{3}. \quad (\text{A.48})$$

The good feature of this singularity is that it is away from the del Pezzo; thus one can argue that, this singularity should not affect the deformation of the dP_8 cone. In order to justify that we will calculate the number of complex deformations of the CY manifold with dP_8 singularity by calculating the number of coefficients in the equation minus the number of reparameterizations of M . The result is

$$h^{2,1} = 77. \quad (\text{A.49})$$

Blowing down the $t = 0$ section of M , we get $V = W\mathbb{P}_{11123}^4$. The general CY is given by the degree eight equation in V . The number of coefficients minus the number of reparameterizations of $V = W\mathbb{P}_{11123}^4$ is

$$h^{2,1} = 106. \quad (\text{A.50})$$

The difference $106 - 77 = 29$ is equal to $c^\vee(E8) - 1 = 29$, where $c^\vee(E8) = 30$ is the dual Coxeter number of $E8$. Thus, all complex deformations of dP_8 singularity can be realized in this embedding.

Acknowledgments

The author is thankful to Herman Verlinde, Igor Klebanov, Nikita Nekrasov, Matt Buican, Sebastian Franco, Sergio Benvenuti, and Yuji Tachikawa for their valuable discussions and comments. The work is supported in part by Russian Foundation of Basic Research under Grant no. RFBR 06-02-17383.

References

- [1] H. Verlinde and M. Wijnholt, "Building the standard model on a D3-brane," *Journal of High Energy Physics*, vol. 2007, no. 1, p. 106, 2007.
- [2] M. Wijnholt, "Geometry of particle physics," *Advances in Theoretical and Mathematical Physics*, vol. 13, no. 4, pp. 947–990, 2009.
- [3] R. Argurio, M. Bertolini, S. Franco, and S. Kachru, "Metastable vacua and D-branes at the conifold," *Journal of High Energy Physics*, vol. 2007, no. 6, p. 17, 2007.
- [4] D.-E. Diaconescu, B. Florea, S. Kachru, and P. Svrček, "Gauge-mediated supersymmetry breaking in string compactifications," *Journal of High Energy Physics*, vol. 2006, no. 2, p. 20, 2006.
- [5] M. Wijnholt, "Large volume perspective on branes at singularities," *Advances in Theoretical and Mathematical Physics*, vol. 7, no. 6, pp. 1117–1153, 2003.
- [6] S. Kachru, J. Pearson, and H. Verlinde, "Brane/flux annihilation and the string dual of a non-supersymmetric field theory," *Journal of High Energy Physics*, vol. 2002, no. 6, p. 21, 2002.
- [7] S. Kachru, R. Kallosh, A. Linde, and S. P. Trivedi, "de Sitter vacua in string theory," *Physical Review D*, vol. 68, no. 4, Article ID 046005, 10 pages, 2003.
- [8] M. Aganagic, C. Beem, J. Seo, and C. Vafa, "Geometrically induced metastability and holography," *Nuclear Physics B*, vol. 789, no. 1-2, pp. 382–412, 2008.
- [9] M. R. Douglas, J. Shelton, and G. Torroba, "Warping and supersymmetry breaking," <http://arxiv.org/abs/0704.4001>.
- [10] K. Intriligator, N. Seiberg, and D. Shih, "Dynamical SUSY breaking in meta-stable vacua," *Journal of High Energy Physics*, vol. 2006, no. 4, p. 21, 2006.
- [11] P. Candelas, P. S. Green, and T. Hübsch, "Rolling among Calabi-Yau vacua," *Nuclear Physics B*, vol. 330, no. 1, pp. 49–102, 1990.
- [12] B. R. Greene, D. R. Morrison, and A. Strominger, "Black hole condensation and the unification of string vacua," *Nuclear Physics B*, vol. 451, no. 1-2, pp. 109–120, 1995.
- [13] R. Argurio, M. Bertolini, S. Franco, and S. Kachru, "Gauge/gravity duality and meta-stable dynamical supersymmetry breaking," *Journal of High Energy Physics*, vol. 2007, no. 1, p. 83, 2007.
- [14] P. Candelas and X. C. de la Ossa, "Moduli space of Calabi-Yau manifolds," *Nuclear Physics B*, vol. 355, no. 2, pp. 455–481, 1991.
- [15] M. B. Green, J. H. Schwarz, and E. Witten, *Superstring Theory*, Cambridge University Press, Cambridge, UK, 1987.
- [16] T. Hübsch, *Calabi-Yau Manifolds. A Bestiary for Physicists*, World Scientific, River Edge, NJ, USA, 1991.
- [17] P. Candelas and X. C. de la Ossa, "Comments on conifolds," *Nuclear Physics B*, vol. 342, no. 1, pp. 246–268, 1990.
- [18] I. R. Klebanov and M. J. Strassler, "Supergravity and a confining gauge theory: duality cascades and chiralSB-resolution of naked singularities," *The Journal of High Energy Physics*, vol. 2000, no. 8, p. 52, 2000.
- [19] I. R. Klebanov and E. Witten, "AdS/CFT correspondence and symmetry breaking," *Nuclear Physics B*, vol. 556, no. 1-2, pp. 89–114, 1999.
- [20] C. P. Herzog, Q. J. Ejaz, and I. R. Klebanov, "Cascading RG flows from new Sasaki-Einstein manifolds," *Journal of High Energy Physics*, vol. 2005, no. 2, p. 9, 2005.
- [21] K. Altman, "The versal deformation of an isolated toric Gorenstein singularity," *Inventiones Mathematicae*, vol. 128, no. 3, pp. 443–479, 1997.

- [22] M. Gross, "Deforming Calabi-Yau threefolds," *Mathematische Annalen*, vol. 308, no. 2, pp. 187–220, 1997.
- [23] S. Franco, A. Hanany, F. Saad, and A. M. Uranga, "Fractional branes and dynamical supersymmetry breaking," *Journal of High Energy Physics*, vol. 2006, no. 1, p. 11, 2006.
- [24] F. Cachazo, B. Fiol, K. Intriligator, S. Katz, and C. Vafa, "A geometric unification of dualities," *Nuclear Physics B*, vol. 628, no. 1-2, pp. 3–78, 2002.
- [25] K. Intriligator and N. Seiberg, "The runaway quiver," *Journal of High Energy Physics*, vol. 2006, no. 2, p. 31, 2006.
- [26] P. M. H. Wilson, "The Kähler cone on Calabi-Yau threefolds," *Inventiones Mathematicae*, vol. 107, no. 3, pp. 561–583, 1992.
- [27] M. Gross, "Deforming Calabi-Yau threefolds," *Mathematische Annalen*, vol. 308, no. 2, pp. 187–220, 1997.
- [28] J. J. Heckman, J. Seo, and C. Vafa, "Phase structure of a brane/anti-brane system at large N ," *Journal of High Energy Physics*, vol. 2007, no. 7, p. 73, 2007.
- [29] M. Reid, "Canonical 3-folds," in *Journées de Géométrie Algébrique d'Angers*, A. Beauville, Ed., pp. 273–310, Sijthoff and Noordhoff, Alphen aan den Rijn, The Netherlands, 1980.
- [30] R. Friedman, J. Morgan, and E. Witten, "Vector bundles and F theory," *Communications in Mathematical Physics*, vol. 187, no. 3, pp. 679–743, 1997.
- [31] M. Reid, "Young person's guide to canonical singularities," in *Algebraic Geometry, Bowdoin, 1985 (Brunswick, Maine, 1985)*, Vol. 1, S. Bloch, Ed., vol. 46 of *Proceedings of Symposia in Pure Mathematics*, pp. 345–414, American Mathematical Society, Providence, RI, USA, 1987.
- [32] S. S. Gubser, N. Nekrasov, and S. Shatashvili, "Generalized conifolds and four-dimensional $N = 1$ superconformal theories," *The Journal of High Energy Physics*, vol. 1999, no. 5, p. 3, 1999.
- [33] R. Corrado and N. Halmagyi, " $N = 1$ field theories and fluxes in IIB string theory," *Physical Review D*, vol. 71, no. 4, Article ID 046001, 17 pages, 2005.
- [34] G. Kapustka and M. Kapustka, "Primitive contractions of Calabi-Yau threefolds I," *Communications in Algebra*, vol. 37, no. 2, pp. 482–502, 2009.
- [35] P. Griffiths and J. Harris, *Principles of Algebraic Geometry*, John Wiley & Sons, New York, NY, USA, 1994.
- [36] D. R. Morrison and C. Vafa, "Compactifications of F-theory on Calabi-Yau threefolds. I," *Nuclear Physics B*, vol. 473, no. 1-2, pp. 74–92, 1996.
- [37] B. Andreas, " $N = 1$ heterotic/F-theory duality," *Fortschritte der Physik*, vol. 47, no. 6, pp. 587–642, 1999.
- [38] M. Buican, D. Malyshev, D. R. Morrison, H. Verlinde, and M. Wijnholt, "D-branes at singularities, compactification, and hypercharge," *Journal of High Energy Physics*, vol. 2007, no. 1, p. 107, 2007.
- [39] G. Veneziano and S. Yankielowicz, "An effective lagrangian for the pure $N = 1$ supersymmetric Yang-Mills theory," *Physics Letters B*, vol. 113, no. 3, pp. 231–236, 1982.
- [40] S. Gukov, C. Vafa, and E. Witten, "CFT's from Calabi-Yau four-folds," *Nuclear Physics B*, vol. 584, no. 1-2, pp. 69–108, 2000, Erratum in: *Nuclear Physics B*, vol. B608, pp. 477–478, 2001.
- [41] K. Intriligator, R. G. Leigh, and N. Seiberg, "Exact superpotentials in four dimensions," *Physical Review D*, vol. 50, no. 2, pp. 1092–1104, 1994.
- [42] B. V. Karpov and D. Y. Nogin, "Three-block exceptional collections over del Pezzo surfaces," *Izvestiya Mathematics*, vol. 62, no. 3, pp. 429–463, 1998.
- [43] N. Seiberg, "Exact results on the space of vacua of four-dimensional SUSY gauge theories," *Physical Review D*, vol. 49, no. 12, pp. 6857–6863, 1994.
- [44] K. Intriligator and N. Seiberg, "Lectures on supersymmetric gauge theories and electric-magnetic duality," *Nuclear Physics B*, vol. 45, no. 2-3, pp. 1–28, 1996.
- [45] S. S. Gubser, C. P. Herzog, and I. R. Klebanov, "Symmetry breaking and axionic strings in the warped deformed conifold," *Journal of High Energy Physics*, vol. 2004, no. 9, p. 36, 2004.